8-32-63-1 • MARCH 1963

8-32-63-1

FACILITY FORM 602
X65 13071
(ACCESSION NUMBER)
486
(PAGES)
CR 51297
(NASA CR OR TMX OR AD NUMBER)
(THRU)
2D
(CODE)
30
(CATEGORY)

MANNED INTERPLANETARY MISSION STUDY

SUMMARY REPORT-VOLUME 1

NASA CR 51297



George C. Marshall
Space Flight Center
Huntsville, Alabama
Contract NAS 8-5024

LOCKHEED
MISSILES & SPACE COMPANY
A GROUP DIVISION OF LOCKHEED AIRCRAFT CORPORATION
SUNNYVALE, CALIFORNIA

8-32-63-1 • MARCH 1963 486 p refs

8-32-63-1

SUMMARY REPORT

EARLY MANNED INTERPLANETARY MISSION STUDY,

VOLUME 1

(NASA CR-51297)

by the following principal contributors:

SECTION	AUTHOR(S)	SECTION	AUTHOR(S)
1.	R. V. Ragsac M. G. Ross L. F. Koehler Z. A. Taulbee	6.	J. A. Carson
		7.	E. I. Curtis
		8.	F. V. Bischof G. E. Rich C. M. Bennett
2.	J. F. McLaughlin		
3.	G. C. Vliet	9.	J. Zoszak
4.	R. R. Titus	10.	L. B. Stark
5.	R. S. Thomas (See Sect. 5 title page)	11.	S. M. Vuscovich

APPROVED

C J Liddell, Jr

C. J. Liddell, Jr.
Manager, Space Systems

APPROVED

B P Martin

B. P. Martin
Project Leader

Prepared under (NASA) Contract No. NAS 8-5024
for the George C. Marshall Space Flight Center, Huntsville, Ala.
by

LOCKHEED MISSILES & SPACE COMPANY 5240700

A GROUP DIVISION OF LOCKHEED AIRCRAFT CORPORATION

SUNNYVALE, CALIFORNIA

[redacted]

FOREWORD

The studies reported herein were prepared by Lockheed Missiles & Space Company for the George C. Marshall Space Flight Center, Huntsville, Ala., under Contract No. NAS 8-5024. The results of the Early Manned Interplanetary Mission Study are reported in two volumes. Volume 1 contains the unclassified portion of the studies and Volume 2 presents the classified (CRD) studies relating to orbital escape propulsion systems.

CONTENTS

Section		Page
	FOREWORD	iii
	ILLUSTRATIONS	ix
	TABLES	xvii
	GENERAL SUMMARY	xix
1	MISSION ANALYSIS AND REQUIREMENTS	1-1
	1.1 Study Scope	1-1
	1.2 Technical Approach	1-6
	1.3 Summary of Results	1-13
	1.4 Technical Discussion	1-26
	1.5 References	1-84
2	ORBIT LAUNCH VEHICLES AND OPERATIONS	2-1
	2.1 Orbit Launch Vehicles	2-2
	2.2 Orbit Launch Operations	2-20
	2.3 References	2-30
3	CRYOGENIC PROPELLANT STORAGE REQUIREMENTS	3-1
	3.1 Introduction and Summary	3-1
	3.2 Propellant Tank Design	3-2
	3.3 Insulation	3-3
	3.4 Environmental Considerations	3-5
	3.5 Results	3-6
	3.6 Conclusions	3-32
	3.7 Recommendations	3-33

Section		Page
4	EARTH ENTRY SYSTEMS	4-1
	4.1 Summary	4-1
	4.2 General Philosophy	4-3
	4.3 Definition of Parameters	4-4
	4.4 Comparison of Entry Systems	4-6
	4.5 Significance of Entry Systems in Interplanetary Role	4-8
	4.6 Trajectory Mode	4-8
	4.7 Deceleration Limits	4-11
	4.8 Drag Brake Configuration	4-11
	4.9 Parametric Analysis	4-30
	4.10 Integration of Parametric Analysis	4-30
	4.11 Entry Heating Analysis	4-36
	4.12 Conclusions	4-48
	4.13 Symbols for Section 4	4-50
	4.14 References	4-51
5	CREW UTILIZATION AND REQUIREMENTS	5-1
	5.1 Summary	5-1
	5.2 Introduction	5-4
	5.3 Human Engineering	5-6
	5.4 Atmosphere Selection and Gas Supply	5-25
	5.5 Carbon Dioxide Removal	5-47
	5.6 Trace Contamination Control	5-49
	5.7 Thermal Control	5-53
	5.8 Diet and Metabolism	5-66
	5.9 Biological Regneration	5-70
	5.10 Physico-Chemical Regeneration	5-72
	5.11 Weightlessness, Artifical g and Coriolis	5-77
	5.12 Meteoritic Phenomena	5-78
	5.13 Ionizing Radiation	5-84
	5.14 Pressure Suits	5-91

Section		Page
	5.15 Acceleration Stress	5-91
	5.16 Sound and Vibration	5-92
	5.17 Waste Handling and Microbial Contamination	5-92
	5.18 Sensors and Warnings	5-93
	5.19 Crew Support Equipment	5-94
	5.20 Research and Development Areas	5-94
	5.21 References	5-99
6	GUIDANCE AND CONTROL	6-1
	6.1 Summary	6-1
	6.2 Introduction	6-2
	6.3 Navigation and Guidance Accuracy Requirements	6-3
	6.4 Guidance Mechanization	6-15
	6.5 Guidance Error Equations	6-24
	6.6 Physical Characteristics	6-36
	6.7 References	6-39
7	RECONNAISSANCE AND SCIENTIFIC INSTRUMENTATION	7-1
	7.1 Scope and Summary	7-1
	7.2 Mission Considerations	7-2
	7.3 Potential Functions	7-5
	7.4 Trajectory Considerations	7-8
	7.5 High Resolution Optics	7-11
	7.6 Advantages of Orbiter for Reconnaissance	7-25
	7.7 Total Flyby Reconnaissance System	7-29
	7.8 Future Reconnaissance/Scientific Study Requirements	7-35
	7.9 References	7-38
8	POWER SYSTEMS	8-1
	8.1 Summary	8-1
	8.2 Nuclear Power Systems	8-1
	8.3 Solar Dynamic Power Systems	8-11
	8.4 Conclusions	8-15
	8.5 Recommendations	8-15

Section		Page
9	VEHICLE CONCEPTS	9-1
	9.1 Summary	9-1
	9.2 Discussion	9-4
	9.3 Configuration Description	9-9
	9.4 Zero-Gravity Spacecraft	9-23
	9.5 Spacecraft Weight Summary	9-27
	9.6 Stability	9-27
	9.7 References	9-29
10	DEVELOPMENT PLANNING	10-1
	10.1 Summary	10-1
	10.2 Introduction	10-2
	10.3 Planning Premises	10-2
	10.4 Related National Space Programs	10-5
	10.5 Manned Interplanetary System Development Program Plans	10-6
	10.6 Program Planning Conclusions	10-14
11	COST AND FUNDING SCHEDULE	11-1
	11-1 Summary	11-1
	11-2 Analysis	11-1

ILLUSTRATIONS

Figure		Page
1-1	High-Energy Nonstop Flyby Past Mars	1-3
1-2	Low-Energy Nonstop Flyby Past Mars	1-4
1-3	Nonstop Interplanetary Missions	1-7
1-4	Stopover Interplanetary Missions	1-8
1-5	Flyby Mission Requirements for Various Years (Chemical Escape – Retro Earth Entry)	1-14
1-6	Flyby Mission Requirements for Various Years (Chemical Escape – Drag-Brake Earth Entry)	1-15
1-7	Flyby Mission Requirements for Various Years (Nuclear Escape – Retro Earth Entry)	1-16
1-8	Flyby Mission Requirements for Various Years (Nuclear Escape – Drag-Brake Earth Entry)	1-17
1-9	Mission Requirements for 1972 Conjunction Venus Ten-Day Stopover (Chemical Escape – Drag-Brake Earth Entry) (Nuclear Escape – Drag-Brake Earth Entry)	1-18
1-10	Mission Requirements for Various Oppositions – Mars Ten-Day Stopover (Chemical Escape – Drag-Brake Earth Entry) (Nuclear Escape – Drag-Brake Earth Entry)	1-19
1-11	Nonstop Flyby Past Venus	1-27
1-12	Venus Flyby Passage Distance – Velocity Contours	1-28
1-13	Influence of Passage Distance on Venus Flyby Requirements	1-30
1-14	Mission Requirements for Various Systems Venus Lightside Flyby	1-32
1-15	Distribution of Subsystems for Mass on Parking Orbit	1-34
1-16	Mars Flyby Passage Distance – Velocity Contours	1-36
1-17	Trip Selection Criteria	1-37
1-18	Influence of Passage Distance on Mars Flyby Requirements (Chemical Escape)	1-39

Figure		Page
1-19	Mass Reduction Using Drag Brake Entry	1-40
1-20	Distribution of Subsystems for Mars Cool Flyby	1-42
1-21	Two-Planet Flyby 1970–1972	1-45
1-22	Three-Planet Flyby 1970–1972	1-46
1-23	Effect of Trip Selection Venus 1972 Ten-Day Stopover	1-52
1-24	Venus 1972 Ten-Day Stopover	1-54
1-25	Mission Requirements for Various Oppositions, Mars Ten-Day Stopover	1-56
1-26	Mars 1973 Ten-Day Stopover Chemical Earth Escape, Probe Weight 2.3 Metric Tons	1-57
1-27	Mars Ten-Day Stopover Reentry Velocity Requirements	1-59
1-28	Extended Orbital Stopover Requirements Mars 1973	1-60
1-29	Mars Capture Mission with Ten-Day Stopover	1-62
1-30	Comparison of Arrival Conditions at Mars	1-65
1-31	Martian Atmospheric Density Models	1-72
1-32	Martian Satellite Orbit Lifetimes	1-74
1-33	Periods of Martian Satellite Orbits	1-75
1-34	Rotation Rate of Line-of-Apsides for Elliptic Orbits Around Mars, 300 nm Periapsis Altitude	1-78
1-35	Nodal Regression Rates of Elliptic Orbits Around Mars	1-79
1-36	Nodal Regression Rates for Circular Orbits Around Mars	1-80
1-37	Flow Chart of Mission Analysis Computer Program	1-82
1-38	Flow Chart of Mission Analysis Computer Program	1-83
2-1	Performance of Orbit Launch Booster Using Single J-2 Engine	2-5
2-2	Performance of Orbit Launch Booster Using 1,500 Mw Engine	2-6
2-3	Performance of Orbit Launch Booster Using 4,000 Mw Engine	2-7
2-4	Performance of Orbit Launch Booster Using 10,000 Mw Engine	2-8
2-5	Performance of Orbit Launch Booster Using Single J-2 Engine	2-10
2-6	Performance of Orbit Launch Booster Using 1,500 Mw Engine	2-13
2-7	Comparison of Nuclear Orbit Launch Vehicle Performance	2-15
2-8	Nuclear Orbit Launch Vehicle Mission Capabilities	2-16

Figure		Page
2-9	Estimated Effect of Orbit Altitude on Saturn C-5 Performance	2-22
2-10	Departure Right Ascension and Declination for 1972 Venus Flyby	2-24
2-11	Estimated Effect of Launch Azimuth on Saturn Orbital Performance	2-26
3-1	Effect of Tank Diameter and Capacity on Percent Boiloff for the Vented Design	3-8
3-2	Optimum Insulation Weight as a Function of Tank Diameter and Initial Propellant Weight for the Vented Design	3-9
3-3	Effect of Tank Diameter and Capacity on the Percent Boiloff for the Vented Design	3-11
3-4	Effect of Tank Diameter on Optimized Insulation Weight for the Vented Design	3-13
3-5	Effect of Mars Orbit Duration on Percent Boiloff and Insulation Thickness for the Vented Design	3-14
3-6	Tank and Support Configuration	3-16
3-7	Effect of Insulation Thickness on Final Tank Pressure for the Non-Vented Design	3-20
3-8	Effect of Initial Liquid H_2 Subcooling on Insulation Weight for Tank Capacity and Final Tank Pressure as Parameters	3-21
3-9	Effect of Insulation Thickness on Total Tank Weight for the Non-Vented Design	3-24
3-10	Effect of Final Tank Pressure on Total Tank for the Non-Vented Design	3-25
3-11	Effect of Final Tank Pressure on Total Tank Weight for the Non-Vented Design with Subcooling	3-26
3-12	Effect of Initial Liquid Hydrogen Subcooling on Insulation Weight with Final Pressure a Parameter	3-28
3-13	Effect of Insulation Thickness and Initial State of Hydrogen of Final Tank Pressure for Non-Vented Design; Heat Leaks Included	3-29
3-14	Effect of Initial State of Hydrogen on Insulation Weight for the Non-Vented Design with Final Tank Pressure a Parameter	3-31

Figure		Page
4-1	Definition of Parameters	4-5
4-2	Weight Comparison of Earth Entry Systems	4-7
4-3	Entry System Concept	4-9
4-4	Trajectory Phasing	4-10
4-5	Acceleration Tolerances	4-12
4-6	Earth Entry (h_{PO} = 260,000 ft)	4-14
4-7	Earth Entry (h_{PO} = 270,000 ft)	4-15
4-8	Earth Entry (h_{PO} = 280,000 ft)	4-16
4-9	Earth Entry (h_{PO} = 290,000 ft)	4-17
4-10	Earth Entry (h_{PO} = 300,000 ft)	4-18
4-11	Mass-Deceleration Relationships	4-20
4-12	Entry System Mass vs. Pullout Velocity	4-21
4-13	Optimum Pullout Deceleration vs. Pullout Velocity	4-22
4-14	Frontal Area vs. Pullout Velocity	4-23
4-15	Propellant Mass vs. Pullout Velocity	4-24
4-16	Entry Ballistic Factor vs. Pullout Velocity	4-25
4-17	Total Pullout Deceleration vs. Pullout Velocity	4-27
4-18	Acceleration Summary	4-28
4-19	Thrust Time History	4-29
4-20	Earth Entry Parameters	4-31
4-21	Entry-to-Pullout Velocity Loss (W/C_DA = 4.0 psi)	4-32
4-22	Entry-to-Pullout Velocity Loss	4-33
4-23	Entry vs. Pullout Velocities	4-34
4-24	Entry System Mass	4-35
4-25	Regimes of Radiation Phenomena	4-39
4-26	Energy Radiated Toward Body	4-41
4-27	Integrated Luminous Front Intensity	4-42
4-28	Nonequilibrium Radiation Intensity	4-43
4-29	Stagnation Point Heating Rate Summary	4-47
4-30	Stagnation Temperatures	4-49

Figure		Page
5-1	Three Man Crew Activities During a Typical 24-hour Period of Outbound or Inbound Phase of Mission	5-17
5-2	Proportion of 24-hour Day Spent in Various Activities by Crew Members During Outbound and Inbound Phases of Mission	5-18
5-3	Partial Pressure of Oxygen Required to Provide Various P_{A_2}'s as a Function of Barometric Pressure (P_b)	5-28
5-4	Partial Pressure of Oxygen Required to Provide Various $P_{A_{O_2}}$'s as a Function of Barometric Pressure (P_b)	5-29
5-5	Alveolar Gas Pressure at Various Altitudes (Air Pressure) Exposure and After Acclimitization	5-30
5-6	Time of Useful Consciousness After Sudden Decompression Breathing Air (540 Torr) and Oxygen (200 Torr)	5-35
5-7	Leakage Rate as a Function of Leakage Area for Isothermal Flow	5-37
5-8	Cabin Pressure Decay vs. Time	5-38
5-9	Total Mission Leakage vs. Mission Space Duration	5-42
5-10	Contaminant Buildup with High Leakage Rates	5-51
5-11	Contaminant Buildup with Low Leakage Rates	5-52
5-12	Effect of Near Ultraviolet Radiation in Vacuum on the Solar Absorptance α_s, of Candidate White Surfaces	5-57
5-13	Rotating Vehicle Equilibrium Temperatures for Venus Mission	5-62
5-14	Metabolic Supplies vs. Mission Duration for 3 Men	5-73
5-15	Nearly Closed Life Support System	5-76
5-16	Meteoroid Flux vs. Mass (In the Vicinity of Earth)	5-79
5-17	Meteorite Flux vs. Single Sheet Aluminum Shielding Thickness	5-82
5-18	Radiation Hazard	5-88
5-19	Probability of Receiving > 200 Rads Aggregate to Blood-Forming Organs from Solar Flare Protons	5-89

Figure		Page
6-1	Initial-Terminal Error Coefficients	6-5
6-2	Effect of Velocity Errors on Midcourse Position	6-7
6-3	Effect of Injection Velocity Error on Δv Requirements for Midcourse Correction (Ref. 6)	6-8
6-4	Error Characteristic for Miss Distance (Ref. 6-6)	6-10
6-5	Error Characteristic for Position Deviation at Arrival (Ref. 6-6)	6-10
6-6	Position Loci Determined by a Single Angle Measurement	6-16
6-7	Spacecraft G & C System for Performance Analysis	6-19
6-8	Navigation Optical Sighting Geometry	6-25
7-1	The Manned Blyby Reconnaissance Role	7-3
7-2	Advantages and Limitations of Mars Manned Flyby	7-6
7-3	Earth/Mars Orbital Geometry and Physical Data (1971)	7-9
7-4	Hyperbolic Approach – Departure Trajectory	7-10
7-5	Rotation Rate of True Anomaly vs. Radial Distance in Hyperbolic Approach to Mars as a Function of Periapsis Distance	7-12
7-6	Total Flight Time Between Equivalent Radial Distances from Mars Center as a Function of Periapsis Height, for Two Values of Hyperbolic Excess Speed	7-13
7-7	Sample High Resolution Optics	7-14
7-8	Simplified Resolution Geometry	7-16
7-9a	Circle of Diffraction	7-18
7-9b	Image Intensity vs. Distance from Focal Point/Wavelength	7-18
7-10	Payload Performance Capability Manned Mars Flyby Reconnaissance	7-31
8-1	Nuclear Power Plant – Rotating Vehicle Configuration	8-4
8-2	Nuclear Power Plant – Zero G Vehicle Configuration	8-5
8-3	SNAP 2 Flight System Schematic	8-6
8-4	Proposed 8 Kw Power System Schematic	8-7
8-5	Shield Weight vs. Total Integrated Dose and Separation Distance	8-8
8-6	Solar Space Power System	8-12
8-7	Rubidium k-Kw Solar Turbogenerator	8-13

Figure		Page
9-1	Manned Interplanetary Spacecraft	9-10
9-2	Launch Configuration	9-11
9-3	Erection Sequence	9-13
9-4	Erection Sequence (Continued)	9-14
9-5	Service Module	9-19
9-6	Rotating Configuration Nuclear Power Supply	9-22
9-7	Zero-G Configuration Solar Power Supply	9-24
9-8	Zero-G Configuration Nuclear Power Supply	9-26
10-1	Typical Early Venus Flyby – Single Launch Vehicle Development Program	10-7
10-2	Typical Venus Flyby – Nuclear Upper Stage System Development Program Plan	10-12

TABLES

Table		Page
1-1	System Design Assumptions	1-10
1-2	Sample Early Venus Flyby Mission	1-33
1-3	Mars Cool Flyby	1-43
1-4	Multi-Planet Flyby Mass Summary	1-47
1-5	Grand Tour 1970	1-48
1-6	Grand Tour 1972	1-49
1-7	Three-Planet Flyby	1-50
1-8	1975 Manned Stopover Trips to Mars and Phobos	1-63
3-1	Heat Leak Analysis	3-15
3-2	Comparison of Boiloff with and Without Heat Leaks	3-17
5-1	Crew Utilization and Requirements	5-2
5-2	Mass and Power Summary for Life Support and Crew Protection System for Three Men (kg)	5-3
5-3	Threshold Altitudes and Physiologic Limits for Unacclimatized Individuals	5-32
5-4	Effect of Atmosphere on Blower Power	5-43
5-5	Gas Requirements (Without Containers)(kg)	5-46
5-6	Gas Supply System Weights (kg)	5-46
5-7	Candidate Solar-Reflector Thermal Control Surface Systems	5-55
5-8	Activity Spectrum and Metabolism	5-66
5-9	Metabolic Consumption and Production	5-67
5-10	Water Balance (gm)	5-68
5-11	Mass Blance (gm)	5-68
5-12	Probabilities of Solar Proton Events	5-87

Tables		Page
6-1	Values Assumed in Reference Case, Friedland & Harry (Ref. 6-6)	6-11
6-2	Estimated Guidance Accuracy Requirements and Resulting Errors (Earth-Mars Trip Model, Refs. 6-4, 6-6, 6-7)	6-14
6-3	Guidance and Control Physical System Characteristics Summary	6-37
6-4	Optical Instrument Characteristics and Performance	6-38
6-5	Examples of Time Reference Equipment	6-40
7-1	Maximum Frame Rate at Periapsis and Parameter Altitude	7-23
7-2	Maximum Data Collection Rate and Transmission Bandwidth Requirements High-Resolution Orbiter – (0.6° Mars Surface Per Frame)	7-28
7-3	Manned Flyby Potential Payload Reconnaissance & Scientific Instrumentation	7-30
7-4	Mars Onboard Manned Flyby Hypothetical Reconnaissance Sensor Package	7-32
7-5	Mars & Venus Onboard Manned Flyby Hypothetical Scientific Instrument Package (Extension of Mariner-Centaur)	7-34
7-6	Manned Flyby Mars Probe Instrumentation Candidates (After Mariner B)	7-36
8-1	Performance Objectives for Space Power Systems	8-2
8-2	Solar Dynamic Power System	8-11
9-1	Spacecraft Weight Summary	9-28
10-1	Comparison of Development Program Requirements, Initial and Advanced Nuclear Escape Stage Systems	10-16
11-1	Cost Estimates for Early Manned Interplanetary Missions Chemical or Nuclear Upper Stage	11-6

GENERAL SUMMARY

MISSION ANALYSIS AND REQUIREMENTS

Planning the effective utilization of the manned interplanetary flybys in relation to an overall exploration program requires a relationship among the three general parameters of the transportation system mass to be placed on Earth parking orbit, the year in which the mission is to be launched and the duration of the flight. This tack will initially provide sufficient information for establishing the most efficient mission-vehicle system combination in relation to surface launch booster capabilities, advantageous launch year, and subsequent contributions to manned capture missions. It is with these final objectives in mind, that the analyses of the flyby mission requirements were undertaken.

The basic parameter assumed for these studies was the transportation system mass on Earth parking orbit. This was computed for numerous nonstop round trips to Mars and Venus using various transportation system designs compatible with the 1970–1975 time period. These system analyses yield a set of vehicle requirements as a function of the mission duration for any launch year in the time period of interest. A nuclear escape propulsion system or its all-chemical (O_2/H_2) counterpart were the major design variations analyzed. The importance of the Earth entry system mode on mass requirements is presented in combination with the two types of escape propulsion systems. What is considered as an early entry system employing solid propellant retro-rockets is compared in several aspects with a sophisticated light-weight aerodynamic drag brake which represents a technology state subsequent to the retro-rocket. The final results are displayed as curves corelating mass requirements with mission duration and launch year.

To aid in placing the flyby mission and its general requirements in perspective, manned orbital stopover missions at Mars and Venus for various years were studied. Sufficient information is presented so that estimates may be made on the requirements of surface launch vehicles, orbital escape stages, and associated systems. These may be related in a gross sense to the corresponding information in the flybys. In addition to a summary of the general flyby and stopover mission requirements, a technical discussion is presented which elaborates on the method of analysis.

Closely related to the planetary capture mission are the orbital operations in the vicinity of the planet. Of particular interest is the possibility of utilizing Mars' closest satellite, Phobos, as a stopover station from which the mission could combine gathering Martian surface and atmospheric data (by employing orbiting and landing probes) with actual direct manned contact with a part of the Martian system, namely its moon Phobos. A preliminary study was conducted to estimate the requirements of a direct landing on Phobos or of using an eccentric orbit about Mars to intercept its moon. These requirements are compared with a direct stopover mission employing a low-altitude orbit about Mars.

The nature of orbital operations in the vicinity of a planet is obviously affected by the atmospheric environment of the planet. Because the low Martian gravitation yields a low rate of atmospheric density reduction with altitude, a study of drag life as a function of orbit altitude and eccentricity was included. Results show that the 500-km altitude assumed for orbital stopover missions is sufficiently high and, in fact, could be somewhat reduced. Another factor important to orbital stopover missions is the effect on return propulsion requirements of orbital perturbations during stay time. Rates of nodal regression and apsidal rotation were computed as a function of orbit altitude and eccentricity.

ORBIT LAUNCH VEHICLES AND OPERATIONS

An analysis was made of the sizing and operation requirements for orbit launch vehicles used for the interplanetary flyby and stopover missions. The requirements were then matched with the capabilities of current or projected NASA programs.

The Saturn C-5 is considered incapable of orbiting sufficient mass in one launch for a manned mission to Mars; however, a manned flyby past Venus may be possible using a nuclear OLV (orbit launch vehicle). The S-IVB, as an OLV, is capable of launching Venus flybys only, but Earth orbit rendezvous is required. The S-II has potential capability, with rendezvous and LOX tanking, to permit flybys to both planets. The presently conceived operational RIFT vehicle will permit flybys to Venus for any conjunction and to Mars only under special circumstances.

The analysis further showed that nuclear OLV capability can be increased by enlarging the propellant tank capacity over those of anticipated programs (which will also involve orbit transfer of liquid hydrogen if the Saturn C-5 is used as ground-to-orbit booster) and by increasing the nuclear engine power. A substantial performance gain is obtained by increasing the NERVA power level to 4000 Mw. For flyby missions using C-5 technology, little (if any) additional capability is obtained with power levels above 4000 Mw. However, levels of the order of 10,000 Mw will be more efficient for launching stopover missions.

It appears that no post-Saturn C-5 vehicle should be acquired that has an orbit delivery capability of less than 450 to 700 metric tons (1 to 1.5 million pounds). Even with this capability, Earth orbit rendezvous will be necessary for any ambitious landing missions.

Finally, the analysis showed that a nuclear escape stage equivalent to several RIFT stages will be required to make any planetary stopovers possible. Serious thought should be given to on-orbit clustering of RIFT stages as a technique for accumulating sufficient initial mass for these missions.

CRYOGENIC PROPELLANT STORAGE

For those missions involving manned stopovers at the planets, a significant reduction in the transportation system mass requirements may be realized if cryogenic chemical or nuclear propulsion stages can be utilized instead of the storable liquid or solid systems

assumed in this contract study. These cryogenic systems may be employed either for escape from the planet or to brake the vehicle on its approach trajectory. For the interplanetary missions of interest, employment of cryogenic propellants entails proficient design of storage tanks subjected to a variety of thermal environments.

Accordingly, the study of extended cryogenic storage included the investigation of the problems involved in storing liquid hydrogen for long term missions and to provide solutions and recommendations where possible. The parameters of primary interest are initial propellant state (saturated, subcooled, or solid), and tank volume and shape for both vented and non-vented designs. The relation of heat leaks, as governed by tank support design and structure material, to the overall heat transfer to the liquid is considered. The consequences of propellant tank orientation, artificial gravity, volume, shape, and interface structure were analyzed to some extent.

The practicality of storing hydrogen for space missions was demonstrated. Initially subcooling or freezing the propellant will significantly reduce the weight penalty for either a vented or non-vented tank design.

EARTH ENTRY SYSTEMS

An Earth entry system is presented which involves no advancment in the state-of-the-art in materials development or technology. It consists of an Apollo-type capsule fitted with a drag brake and propulsive lift system.

The initial entry is ballistic to pull-out, where the propulsion system then maintains the vehicle at a near-constant altitude until Apollo entry velocity is reached. The drag brake and spent propulsion system are then jettisoned, allowing a normal Apollo descent to the landing site.

The drag brake concept provides a relatively lightweight system compared to others analyzed. These consisted of exospheric retro-braking of an Apollo capsule to its

design entry velocity; a lifting, Apollo-type, blunt ablative configuration; and a small nose radius, conical ablative vehicle designed to minimize the maximum total heating rates. A minimum weight system requirement arises from the gross entry system influence on the total planetary transportation system mass.

The thermodynamic analysis considers convective, equilibrium and non-equilibrium heating, involving the complicated phenomena of dissociation, ionization and interaction between convection and radiation.

The phenomenon of "collision limiting," coupled with the radiation cooled structure, greatly reduces the total radiative heating and yields stagnation temperatures consistent with the assumed drag brake material.

CREW UTILIZATION AND REQUIREMENTS

Systems are sized on the basis of three men for 365 and 600 days. A two-gas cabin atmosphere is recommended, 180 torr O_2 and 180 torr N_2. Atmospheric water, urine, and carbon dioxide regeneration by physico-chemical means is preferred over an open or biological regeneration system. Metabolic supplies are calculated on the basis of an average metabolism of 2,820 kcal day^{-1}. Radiation shielding weights are based on a 0.001 probability of receiving 200 rads to the blood-forming organs from all sources of radiation throughout the mission.

Meteoroid shielding is based on Whipple's 1962 distribution and Summers' hypervelocity penetration equation. Because artificial gravity may be required a rotating vehicle was assumed to provide a gravitational acceleration of some 0.3 to 0.85 g. Thermal control is based upon space radiators and circulating liquid coolants. A large number of areas requiring further research and development are defined.

GUIDANCE AND CONTROL

The guidance and control study for Empire has been directed to determining first order accuracy requirements, investigating suitable self-contained measurement techniques, and synthesizing a guidance system. The most promising measurement techniques for both midcourse and planet approact guidance position fixes, using self-contained instruments, involve optically metered angles. These include range determination by stadiametric angles for the planet approach phase.

Alternative mechanizations have been discussed prior to selection of starlock angle trackers for the midcourse, and a wide field scan telescope for the planet approach guidance. Inertial instruments (gyroscopes and accelerometers) have been included for use during corrective velocity impulses, or for temporary attitude references when optical instruments are in the search mode. Earth-based angle tracking and ranging is recommended for the post-injection correction, and as a back-up guidance mode. Several functions to be performed by the human navigator in augmenting the spacecraft guidance system have been discussed, including: repairing or replacing defective components; performing instrument calibrations; and programming or initiating automatic sequences.

Although the selected mechanization is based on midcourse and planet approach guidance requirements, the major components essential to boost phase and reentry guidance are included. Total system weight is 122 kg and maximum power usage is 380 watts, estimated for 1970 state-of-the-art. During quiescent periods the power required will drop to about 50 watts.

RECONNAISSANCE AND SCIENTIFIC INSTRUMENTATION

Properly instrumented, the manned flyby mission may serve an important reconnaissance function in collecting landing site detail to implement future precision manned landings. To do this may require ground resolution an order better than achieved by prior unmanned missions. Two factors contribute to this performance potential: large payload

capability and the presence of man onboard to guide a close planetary approach. The reconnaissance section of this report reviews a preliminary high-resolution optical study aimed at providing 1.5 meter (5-foot) ground resolution at the point of closest approach to Mars. The hypothetical system developed includes a trajectory of 0.2 Earth-mean-orbital-speed hyperbolic excess velocity and 463-kilometer pericenter altitude, a 120-inch focal-length camera with f/8 optics, 4-millisecond frame time, 0.1 milliradian-per-second stability, and 100 lines-per-millimeter operational resolution. Estimated film ASA rating requirements vary from 15 to 20,000 for the range of light conditions examined. Development of the optical system lies within the present state-of-the-art. The most severe film speed requirements may be attainable with research films using direct positive processing. However, further data and analysis are required relative to operational light conditions and the tradeoffs between standard film, electrostatic, and other storage techniques.

Comparing the flyby and orbiting mission as high-resolution reconnaissance tools indicates that the orbiter is vastly superior in feasibility of high-performance instrumentation, uniformity of data scale, and volume of collectible data. Radar, infrared, and other techniques for reconnaissance and scientific data collection are also reviewed.

SPACE POWER SYSTEMS

Two general classes of space power systems that show promise of fulfilling the EMPIRE program requirements are the nuclear and the solar dynamic conversion systems (the SNAP-2 nuclear reactor-turbogenerator and the solar concentrator-turbogenerator system). Each of these systems is capable of producing the indicated requirements of 5 to 6 kw(e) and can be installed in either the rotating or the zero-g class of configurations presented in this report.

The currently estimated system weights for the 8 kw(e) version of SNAP 2 (unshielded value) and the 6 kw(e), Biphenyl, version of the Solar Dynamic system are 727 kg and 340 kg respectively. Both require radiators over 20 m^2 in area.

VEHICLE CONCEPTS

Several spacecraft configurations were generated for the early manned interplanetary flyby missions. These spacecraft were configured to be launched with their three-man crew by a single booster, erected and checked out in Earth orbit, then injected into the interplanetary orbit. The Apollo command module was used as a major component of the spacecraft and as the final Earth reentry body. Current state-of-the-art and projected Apollo technology were used throughout. The rotating (gravity) configuration received the major emphasis primarily because of man in the system. The missions under consideration will require from 330 – 600 days and man may not survive a zero-g field for this length of time.

The rotating spacecraft consists of two modules (command and service), connected by rigid structure, and rotated about a central hub section. One crewman is stationed in the command module at all times, the others are in the service module. The hub section has the power supply unit attached at one end, the midcourse propulsion at the other, and has the "storm cellar" solar flare shelter mounted inside. Midcourse corrections are applied while the spokes are in the extended position. The spacecraft has an 82-ft (25 m) spin radius to the floor of the end modules. At this radius and with a 0.4 rad/sec angular velocity, the crew experiences a 0.4 g field in the end modules.

Several zero-g configurations were examined with a nuclear power supply and with a solar power supply to establish weight savings over the rotating, gravity-providing configuration. The zero-g configuration proved to be about 12 percent lighter than the rotating configuration. A weight summary is included for both a Mars and a Venus flyby mission for three different configurations. The sum of the weights of the life support system and the solar flare shelter are about the same for any mission even though these weights vary significantly between missions. The life support system is heavier for the longer Mars mission, while the solar flare shelter is heavier for the Venus mission which comes closer to the sun and encounters a higher proton flux. The total weight for any given configuration is about the same for either the Mars or the Venus flyby.

DEVELOPMENT PLANNING

The development planning analyses and results are initially defined as to scope and objectives. In scope, development program plans were restricted for this first contract period to two systems concepts for early manned Venus flyby missions. Consideration was given solely to systems utilizing a single launch mode of operation, Saturn C-5 launch vehicle hardware and technology, and an early operational nuclear stage evolving from the RIFT and NERVA programs.

Master development program plans are presented, based on specifically stated groups of premises, for an all chemical propulsion vehicle system (although a Venus flyby appears doubtful or marginal at present with an all chemical system utilizing a C-5 and a single launch) and a composite chemical propulsion Earth launch vehicle – nuclear injection stage system. Major program areas for the required developments, including the related application of major National Space programs are presented in the master plans (Figs. 11-1 and 11-2).

Major program planning conclusions are summarized for both the all-chemical propulsion and composite chemical-nuclear propulsion systems concepts. Further planning conclusions of significant importance are presented for the areas of nuclear engine development, advanced launch vehicles, and critical applied research and development problem areas.

COST AND FUNDING SCHEDULE

A cost analysis of the Early Manned Interplanetary Mission concept has been conducted. Although this study was extremely cursory, it seems apparent that the cost will run between $1.4 and $1.9 billion, depending upon the requirements for a nuclear upper stage. This cost was based upon 10 interplanetary missions (5 to Venus and 5 to Mars) during the period 1970 – 1979. It must be emphasized that the cost estimates were developed from concept information only and design data required for a comprehensive cost analysis is unavailable at this time.

Section 1

MISSION ANALYSIS AND REQUIREMENTS

by

R. V. Ragsac
M. G. Ross
L. F. Koehler
Z. A. Taulbee

Section 1
MISSION ANALYSIS AND REQUIREMENTS

The discussion on mission analysis and requirements is divided into four parts: Study Scope, Technical Approach, Summary of Results, and Technical Discussion. The first two parts discuss the types of interplanetary flyby and short stopover missions which were analyzed, and present the basic assumptions used in the transportation system design. The final results of the entire analyses are given in the summary, wherein the transportation system mass required on Earth parking orbit is presented as a function of year and of total trip time for various vehicle subsystem designs. Additional supporting information and technical details are discussed in Subsection 1.4.

1.1 STUDY SCOPE

It is the purpose of the mission studies to determine the system requirements as manifested by the vehicle mass that must be placed on a near Earth parking orbit (200 km). By using the transportation system mass as the predominant parameter, it is possible to establish trends caused by changes in launch year, in vehicle subsystem design, and in total mission duration. A relation among these three causes will form a basis from which a rational evaluation may be made of the manned planetary flyby mission with respect to an overall space program. This methodology assures optimum trip selection, isolates the importance of major vehicle design parameters, establishes the magnitude of payload capability for future surface launch vehicles, and leads to efficient utilization of each flyby reconnaissance in relation to the multitude available. Sufficient information is generated from which more detailed and extensive analyses may be initiated.

The major assumption utilized in these studies is in the design and makeup of the model transportation system. It is recognized that certain other assumptions in this regard will change the mass requirements somewhat. However, an attempt was made to

anticipate these eventualities by introducing different major propulsion systems and Earth reentry modes. The final system mass values obtained should provide a valid basis for a relative comparison of the numerous trips and should demonstrate the effects of changing various related parameters.

A major portion of the investigation was devoted to analyzing flyby (or nonstop) round trips to Venus or Mars in the years 1970 through 1975. The effects of passage distance, in terms of planetary radius, were included in most of the trips and although this influence in some cases cannot be neglected, it is not shown for all the trips analyzed. Passage on the lightside or darkside of the planet was taken into account in the Mars trips, while only lightside flybys of Venus were considered. In the darkside passage, the planet lies between the vehicle and the Sun at the time of closest approach, and in the light side case the reverse is true.

Labeling a trip as either a lightside or darkside passage follows this definition and should not be taken as a dichotomous classification since there are trips which pass along or through the terminator at the time of closest approach. In this study, where the objective is to establish general mission requirements, it was considered premature to determine the actual planetary illumination with respect to the spacecraft at passage.

Two types of Mars flybys were studied, these being a high-energy and a low-energy class with the former group further qualified by a dark or lightside passage. In the succeeding sections these trips will be referred to as a darkside or lightside flyby, with the understanding that they are of the high-energy class. The low-energy class (labeled as such) is a lightside flyby although its trajectory is quite different from the former class. Figures 1-1 and 1-2 display sample mission profiles from the two Mars trip categories. The high-energy class of trajectories all dip within Earth's orbit and perform about one and a half solar circuits during each complete trip. This class of trajectory is sometimes referred to as the "hot" trips in a solar radiation since it passes nearest the Sun. The aphelion distance occurs at passage and for different opposition periods these contacts will occur at different radial distances from the Sun,

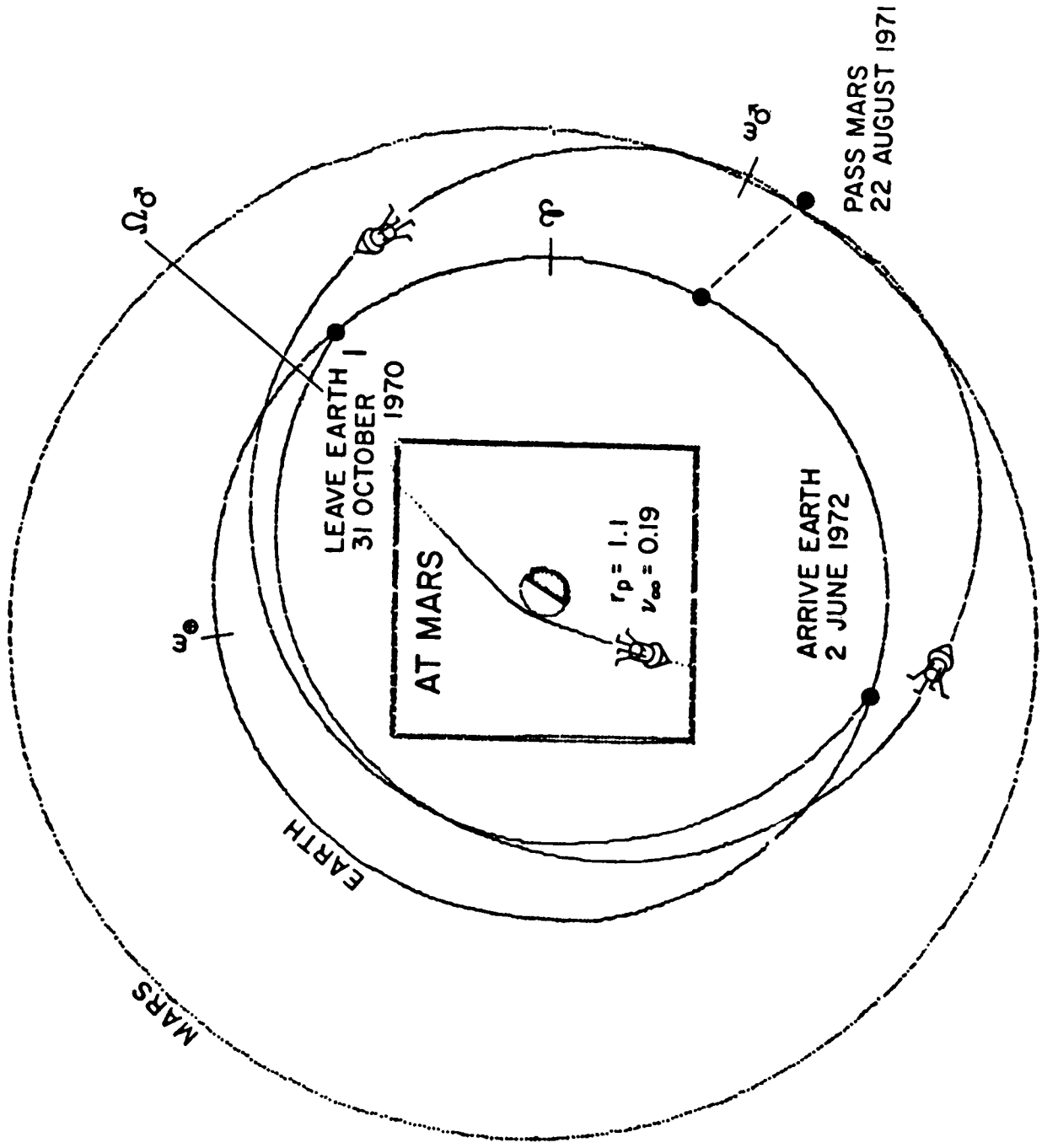


Fig. 1-1 High-Energy Nonstop Flyby Past Mars

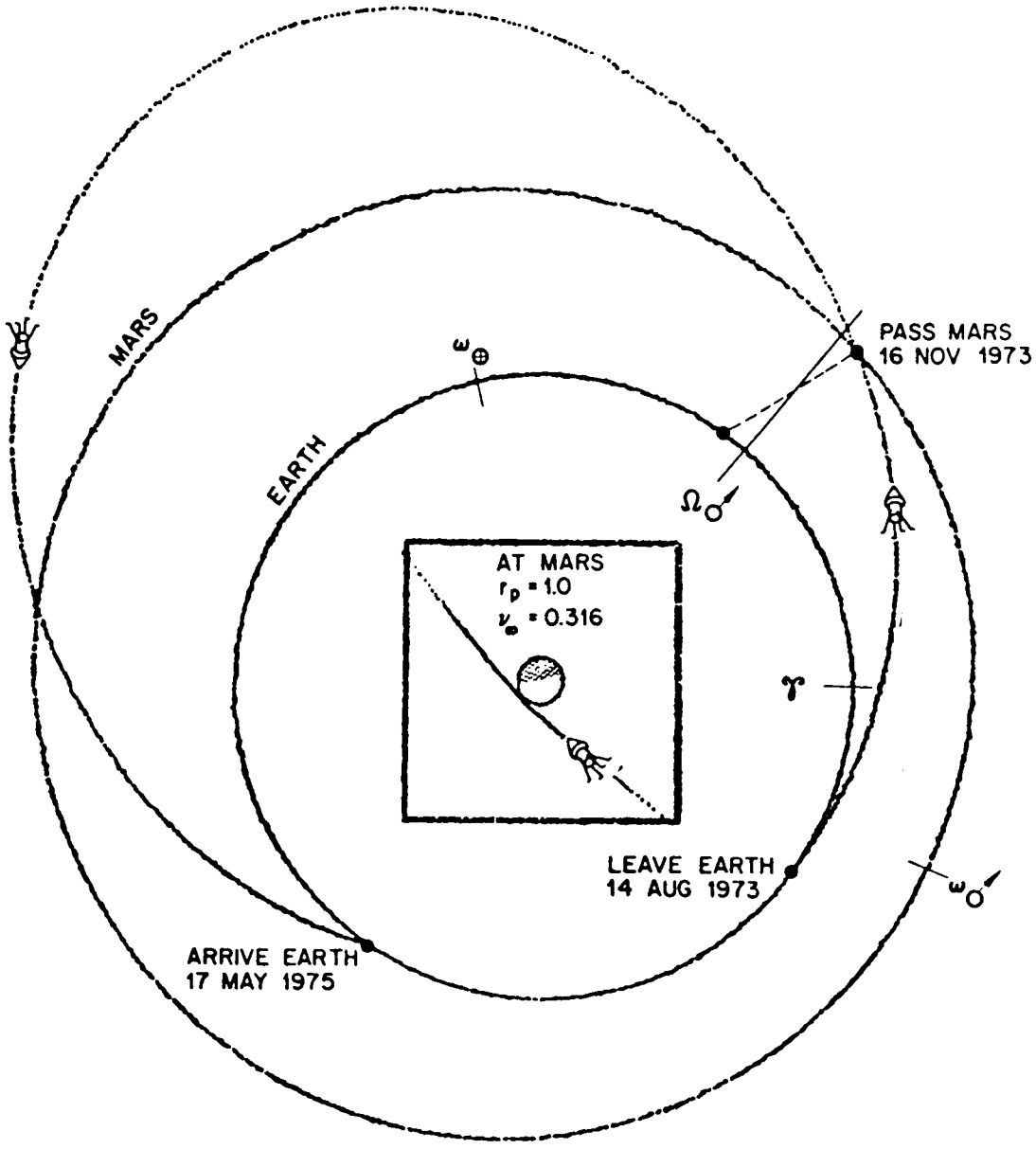


Fig. 1-2 Low-Energy Nonstop Flyby Past Mars

due to Mars' appreciable orbit eccentricity. As will be seen, this variation in radial distance is reflected in wide launch mass fluctuations over the various opposition years. The low energy trips never pass inside Earth's orbit and thus may possibly possess advantages in terms of shielding requirements against solar flares. Because of this, the low energy trips are occasionally termed "cool" trips. From the nature of this type of trajectory, it appears to be relatively insensitive to Mars' orbital eccentricity. This comparison will be evident when the different years are compared in terms of the mission requirement.

An unusual type of flyby mission, possessing enormous potential for planetary reconnaissance, is the multiplanet flyby, or interplanetary grand tour. On these missions, the spacecraft passes both Mars and Venus on the same trip. The necessary planet-vehicle trajectory alignment for each type of grand tour is repetitive every 2338 days (6.4 years), however the mission requirements will not be the same due to the eccentricity of Mars' orbit. An important consideration, which will be amplified later, is that both planets may be reconnoitered for essentially the same requirements as a Mars nonstop trip. This means that the amount of information obtainable per trip is greatly increased at little or no expense in launch weight or trip duration.

Three promising grand tours were studied for their requirements. The first yields the lowest total trip time compared with any other trajectory which passes Mars only; the second passes both planets on the lightside but displays lower velocity requirements than any available lightside passage of Mars alone, although at the expense of slightly longer trip times; and the third trip passes Venus, Mars and Venus again with the lowest velocity requirements found so far, even for the Venus flybys, however its corresponding total trip time is highest of all the flyby trips.

During the early part of the next decade the nonstop missions can be used as the first phase in a program leading to manned exploration. To place this phase in perspective with the earliest possible capture missions and to provide data for future launch vehicle and orbital rendezvous systems, short orbiting stopover missions with no manned

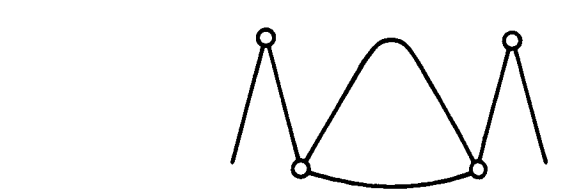
landings were investigated for Mars and Venus. In this study a stopover of ten days was assumed as an adequate period for completing all planetary observations and experiments while in the capture orbit. Shorter stay times are possible although it appears to nullify the observational utility especially when compared to the vehicle system mass necessary. Longer stay times of up to two months are briefly studied for their influence on the mission requirements and on the optimum trip selection.

The entire study of both flyby and stopover missions utilized realistic, joined-conic trajectory data (Ref. 1-1) which include the effects of terminal planetary perturbations, orbital eccentricities and inclinations. The technique of optimum trip selection for the stopover missions in this current study is given in Ref. 1-2.

1.2 TECHNICAL APPROACH

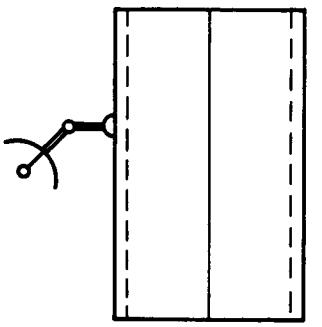
The values of vehicle system mass on Earth parking orbit computed for each trip were based on a model transportation system selected as one representative of numerous possible designs that may be conceived for the early 1970 time period. The basic system employed here is not to be taken as the promising approach for manned interplanetary flight, but rather as one which possesses all the necessary subsystems and components important in performing the mission successfully, in maintaining the psychophysiological wellbeing of the crew, in providing safeguards against the space environment, and in recovering the spacecraft upon return.

Insofar as the values of mass are concerned, each subsystem is accounted for in terms of its weight, before and after staging, with some allowance made for housing and structurally tying together the various major components. Figures 1-3 and 1-4 depict the major vehicle systems for the flyby and stopover missions. The arrangements are not intended to be a packaging of the systems but as an aid in locating subsystem components and equipment will respect to the entire vehicle. The field of astronautical human engineering has not advanced to the point that reliable design data regarding the man-mission relationship are available to the system analyst. In light of these



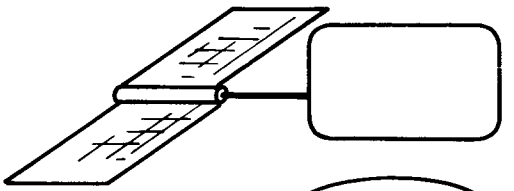
Command Module
(Transition Phase Duty Station)

- Drag Brake
- Entry Capsule
- Life Support (minor)
- Attitude Control & Stabilization
- Electronics



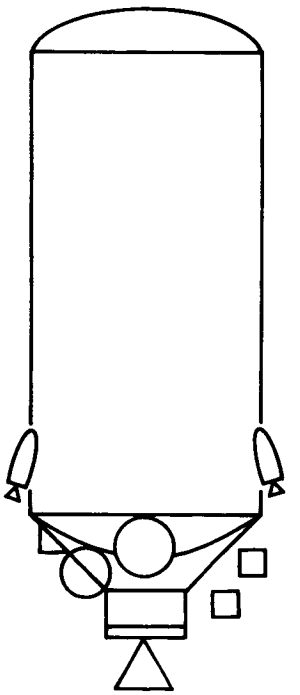
Mission Module
(Normal Duty Station)

- G & C, Navigation
- Communications
- Life Support (Major)
- Living Quarters
- Observatory (Scientific Probes)
- Attitude Control & Stabilization
- Aux. Power Supply
- Structure & Tie-ins
- Storm Cellar



Power Supply

- SNAP Reactor/Solar Boiler
- Conversion Equipment
- Radiator



Earth Escape Propulsion

- Propellant (Cryogenic)
- Engine ($0_2/H_2$ or Nuclear)
- Feed System
- Structure

Fig. 1-3 Nonstop Interplanetary Missions

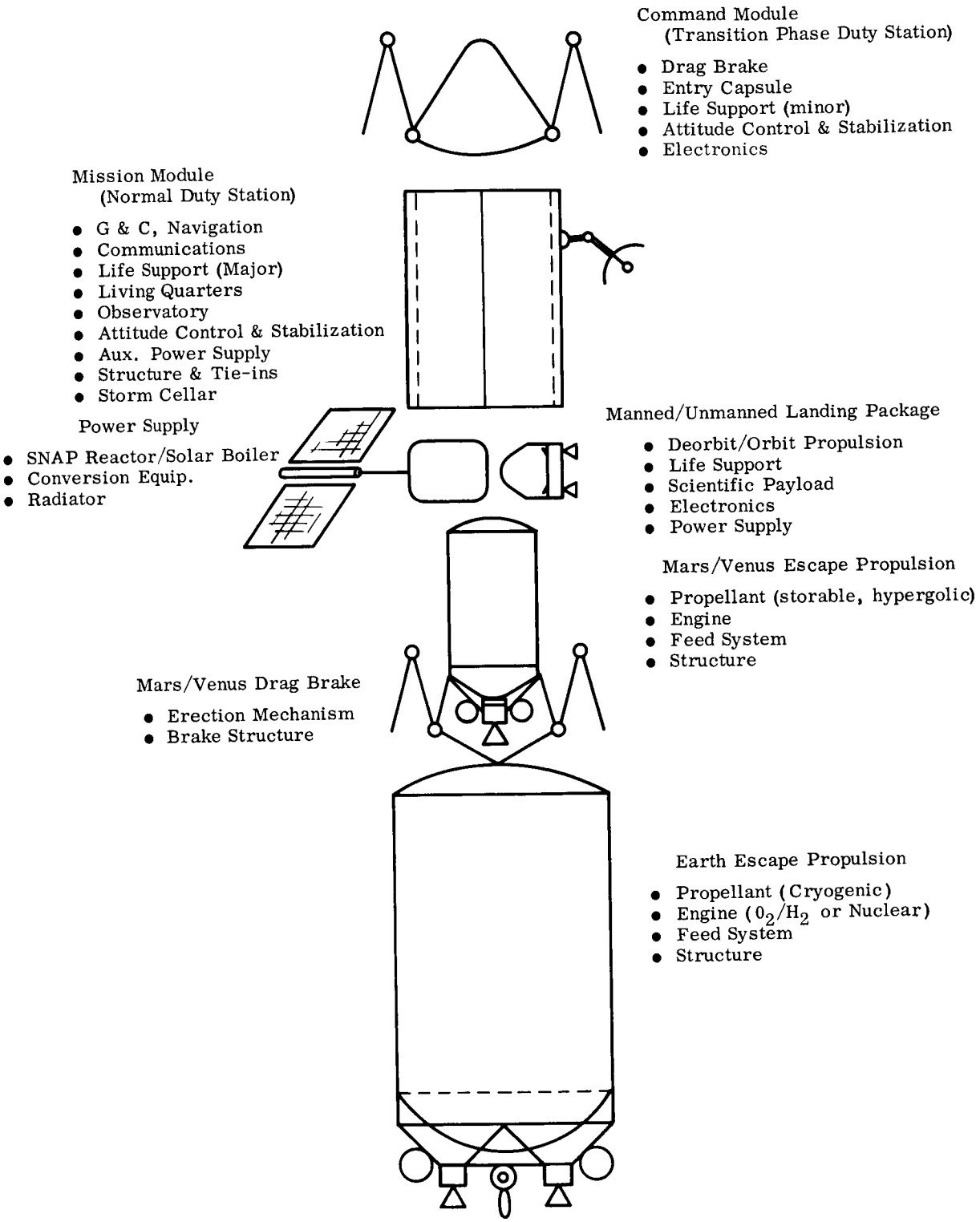


Fig. 1-4 Stopover Interplanetary Missions

uncertainties, the assumptions regarding confinement duration, radiation hazard and protection, artificial gravity, etc., and their effects on spacecraft design (especially volume enclosed) were made as reasonable as possible.

The command module is the crew's primary duty station, from which spacecraft control is exerted. This Apollo-type three-man module is occupied by the crew during the acceleration periods of escape and capture, but during the major portion of the journey, the non-primary duty hours are spent in the mission module. This latter unit is sized to provide sufficient space for individual quarters and in addition, to house the life support system, instrumentation, and on-board mission equipment. A weight estimate of such a module was placed at 9 metric tons (20,000 lb), but is dependent on the spacecraft configuration being either rotating or zero-g, and on the crew size. A rotating spacecraft was assumed here.

Of course, as more detailed transportation system design and analysis are performed and definitive requirements on each of the subsystems are established, the weights as well as dimensions of the subsystems will change and consequently so will the computed vehicle system mass. An additional influence, the advance in the state of technology, may possibly replace or integrate separate subsystems and their functions. With these considerations in mind, the system design assumptions of Table 1-1 are presented for spacecraft in the flyby and orbital stopover missions.

These assumptions are considered to be on the level of technological accomplishment not much advanced beyond the Apollo system. The crew size is restricted to three men on all missions since the Earth entry system consists of a modified Apollo command module integrated with a reentry system. An early operational reentry system uses a solid propellant retrorocket (250 Isp) arrangement to decelerate the vehicle from its approach speed down to parabolic speed, after which the command module ablative heat shield absorbs the final reentry phase. A more sophisticated technique much more efficient of weight, utilizes an aerodynamic drag brake to attain parabolic speed. This is discussed in more detail elsewhere in this report.

Table 1-1

SYSTEM DESIGN ASSUMPTIONS

Subsystem	Flyby Missions	Orbital Stopovers
Crew*	3 Men	3 Men
Life Support	Semiclosed system (3 men) Mass (kg) = 10.3 × trip time + 1590	Semiclosed system (3 men) Mass (kg) = 10.3 × trip time + 1590
Radiation Shielding	Storm cellar, 55 gm/cm^2	Storm cellar, 55 gm/cm^2
Command Module	Modified Apollo + Reentry System	Modified Apollo + Reentry System
Earth Entry	Solid propellant retro-rocket or Aerodynamic drag brake + lift (17 km/sec limit)	Aerodynamic drag brake + lift control (17 km/sec limit)
Mission Module	Living quarters, life support, on-board mission equipment	Living quarters, life support on-board mission equipment
Earth Escape	Chemical (430 sec Isp) Nuclear (830 sec Isp)	Chemical (430 sec Isp) Nuclear (830 sec Isp)
Midcourse Correction	Storable chemical (330 sec Isp) 0.6 km/sec to heliocentric payload	Storable chemical (330 sec Isp) 0.8 km/sec to mass on planet orbit
Capture at Planet	–	Aerodynamic braking + lift control (12 km/sec limit)
Planetary Escape	–	Storable chemical (330 sec Isp)
Probes & Scientific Equipment	4.5 metric tons	2.3 metric tons
Power Supply	Solar boiler or SNAP II type	Solar boiler or SNAP II type

*Artificial gravity provided by spacecraft rotation

A semi-closed cycle ecology system is used and a variable life support allotment of about 10 kg/day is adopted for the three man crew. The weight of this system was analyzed in some detail for trip durations of 330 and 550 days. For other durations, a linear interpolation was employed. Radiation shielding is provided partly by a "storm cellar" and partly by a judicious arrangement of instrumentation, equipment, water and food so that the effective shielding is equivalent to an area density of about 55 gm/cm^2. The effectiveness of a given area density in protecting the crew against radiation hazard is discussed in Section 5 of this report.

Observational equipment, small sounding probes, scientific experiments are alloted a total of 4.5 and 2.3 metric tons for the flyby and stopover missions respectively. Midcourse correction, spacecraft attitude control, and orbit stabilization are provided by a restartable, hypergolic, storable propellant propulsion system. The system is sized to deliver a specified incremental velocity to the mass injected into the heliocentric transfer orbit.

The Earth escape stages considered were an oxygen/hydrogen propulsion system having a delivered specific impulse of 430 sec and a nuclear system with specific impulse of 830 sec. Both impulse values are believed to be reasonable for the early 1970 time period, although in the case of the nuclear propulsion system, the stated impulse relies heavily on the current engine development tests. Hence for 1970 at least, 830 sec is probably optimistic. A storable hypergolic propellant system is employed as the planetary escape propulsion not only because of its storability for extended periods, but also for its reliable ignition to insure return of the spacecraft. Furthermore, the survivability of a storable stage during the capture maneuver is more favorable compared to a cryogenic stage.

The computation of system mass is not affected by the thrust levels of any of the propulsion stages but rather by the ratio of step inert-weight to the step loaded-weight, and thrust-to-weight ratio. To include the effects of thrust-to-weight ratio which are important in terms of losses during the escape phase, the incremental velocity requirements were upgraded a few percent. An estimated value of eight percent was assessed

against both propulsion systems during the Earth escape maneuver and a value of five percent was used for planetary escape losses.

A change in the assumed crew size may be dictated by later experimentation in training flights and by Earth satellite studies on the comprehensive psycho-physiological aspects of extended isolation and group interaction. Furthermore, shielding requirements will undoubtedly experience changes as new knowledge is gained in establishing the dosage allowance and in the radiation environment for any year. Therefore, it must be understood that the system mass requirements as presented in the accompanying figures are, at worst, minimal for the mission in question. It is believed nevertheless, that these values are representative of the various missions, and if taken in a relative sense, they present a fairly accurate picture of the relationship among requirements, launch year, and mission duration.

An additional premise that affects vehicle mass is the use of probes which are sent into the planet's atmosphere and possibly landed on the surface. Different probe weight values will merely change the vehicle mass on parking orbit, hence this was not considered a parameter in the mission analysis and requirements.

To allow machine computation of the propulsion stage sizes, a brief analysis was performed on the dependence of step inert-weight fraction on thrust-to-weight ratio and on the amount of impulse propellant, for various rocket engine systems using O_2/H_2, nuclear (H_2), and storable propellants (e.g., N_2O_4/N_2H_4). With these graphs it was possible to derive three equations for the step inert weight which could be used in the computer program. Obviously such general relationships, even taking into account propellant and engine type, cannot be accurate over such large ranges of impulse propellant encountered in the study. However, in the mission analysis, the trips requiring the lowest mass on orbit generally require an amount of propellant essentially within the region from which the equations were derived.

1.3 SUMMARY OF RESULTS

The major results are presented in Figs. 1-5 through 1-10 and are separated into the two major missions studied: nonstop and short orbiting capture. Figures 1-5 through 1-8 display the flyby mission requirements for different years as a function of trip duration, and are in sequence according to the Earth escape stage/reentry system combination:

- Chemical/retro rocket
- Chemical/drag brake
- Nuclear/retro rocket
- Nuclear/drag brake

Figures 1-9 and 1-10 present the requirements for the 10-day orbiting stopover missions for Venus, then Mars. Comparisons between the chemical and nuclear escape systems are given in each figure. In all of the stopover analyses, a drag brake Earth entry system was assumed. For most of the curves presented, only those computed data points in the region of minimum system mass are plotted in order to prevent the closely grouped curves from crossing others or doubling over on themselves.

It should be remembered that the mass requirements are computed assuming a continuous relationship between the trajectory parameters and the vehicle designed to these parameters. Hence each point on the curve represents a system designed specifically for that one trip. This of course, holds true for the entire mission studies.

1.3.1 Flyby Missions

The requirements in the Venus missions change slightly with conjunction year, since the orbits of Venus and Earth are nearly circular and coplanar. Although there appears to be a small increase above the 1970 trips, it can be seen that in the region of minimum mass, the requirements will be essentially the same for all conjunction years in which flyby missions will be of interest. Reductions on total trip time up to twenty days are available with relatively small increase in requirements. The penalties for even lower trip times are evident from the graph.

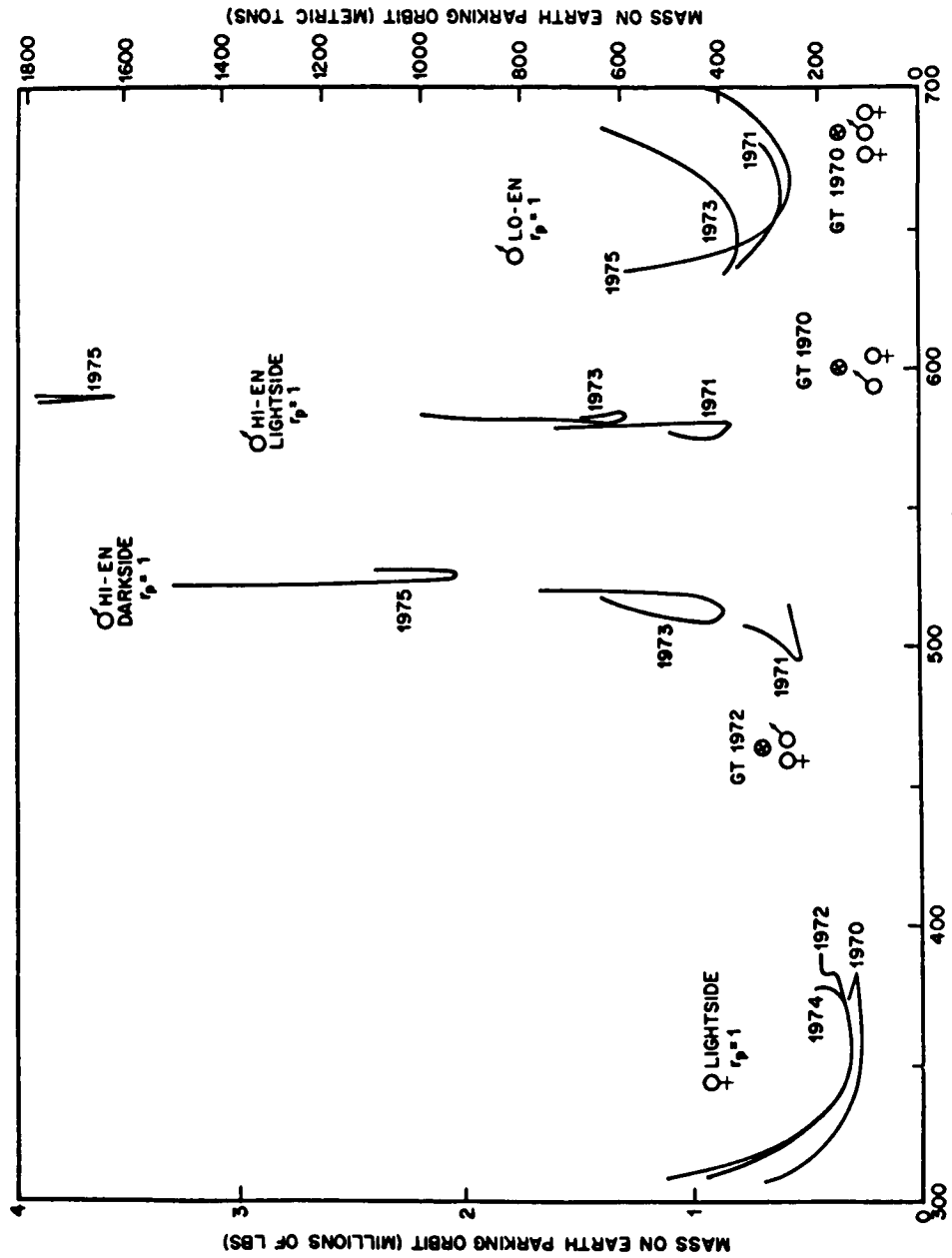


Fig. 1-5 Flyby Mission Requirements for Various Years (Chemical Escape – Retro Earth Entry)

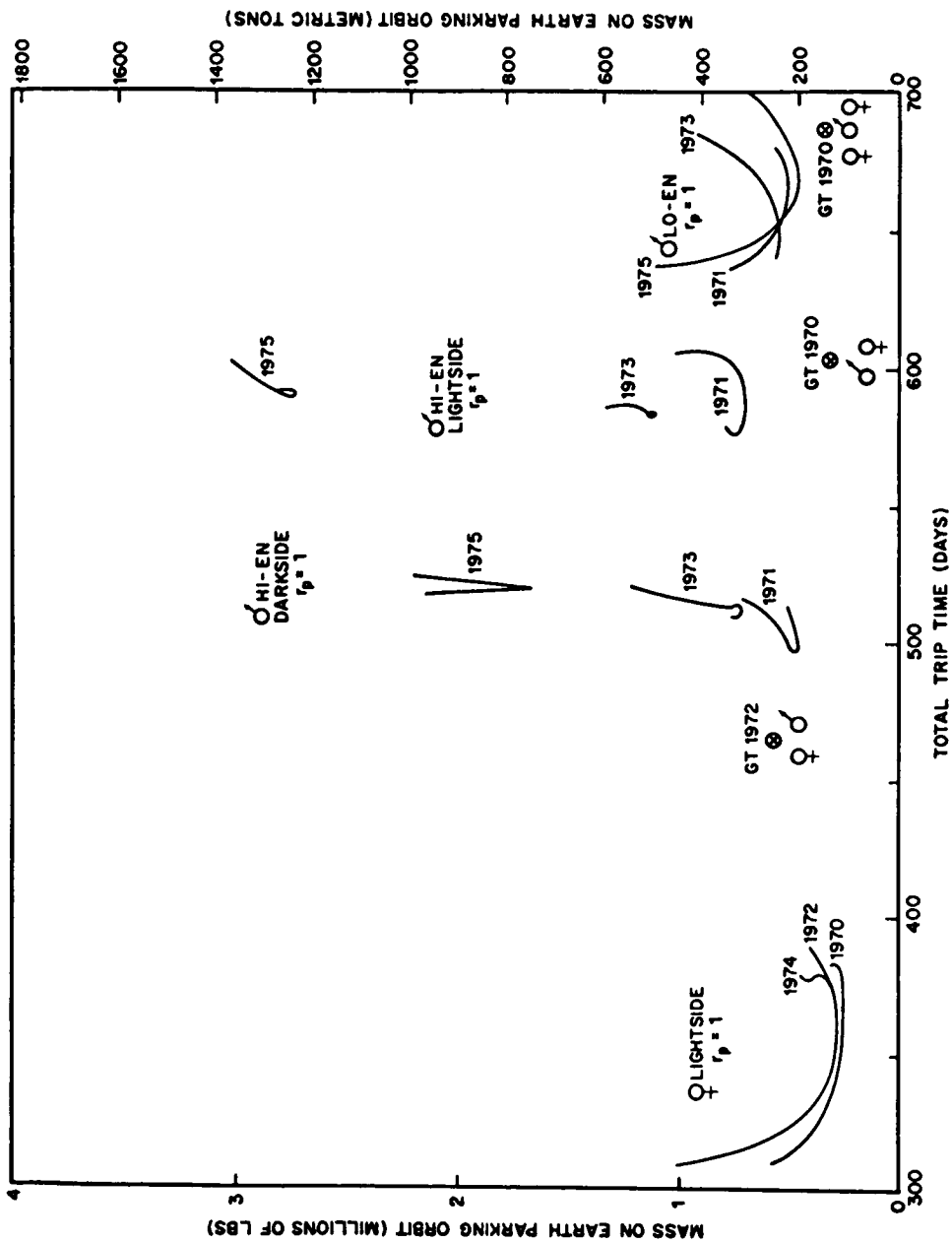


Fig. 1-6 Flyby Mission Requirements for Various Years (Chemical Escape – Drag-Brake Earth Entry)

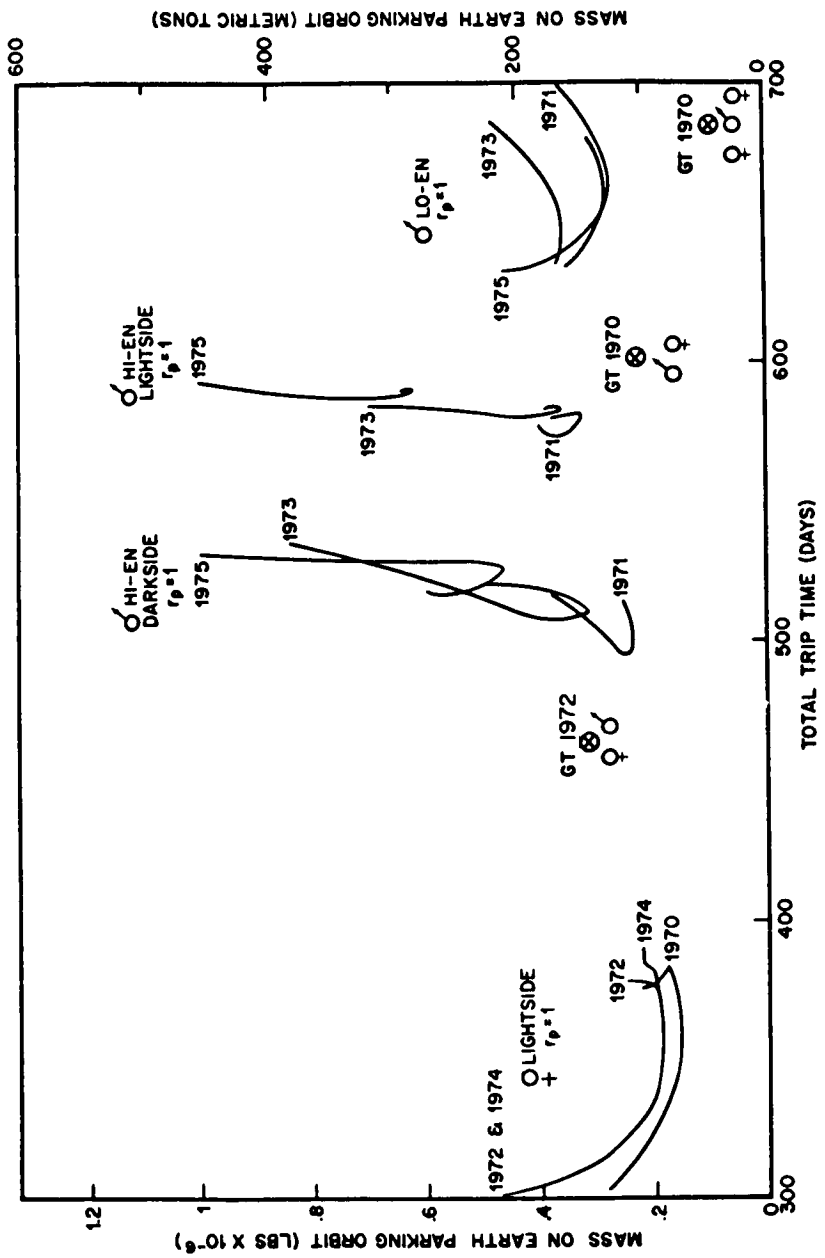


Fig. 1-7 Flyby Mission Requirements for Various Years (Nuclear Escape – Retro Earth Entry)

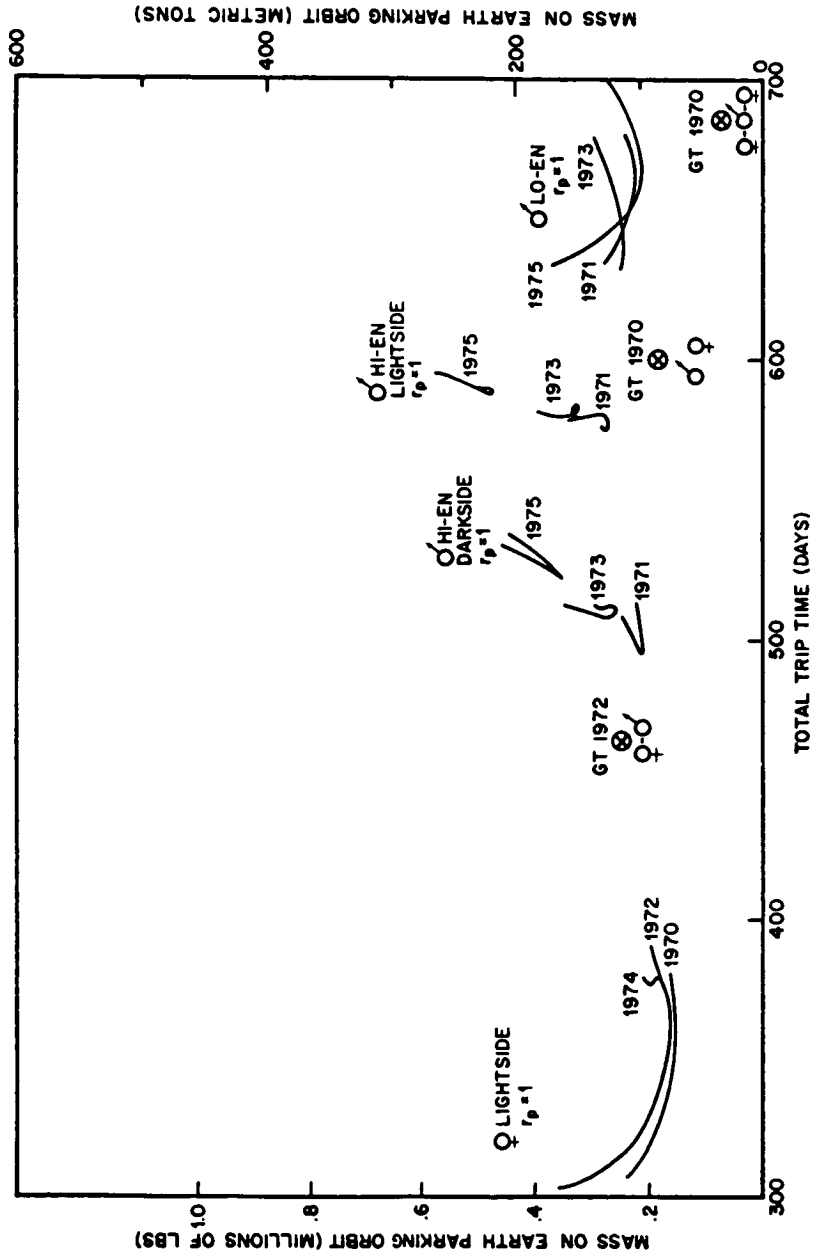


Fig. 1-8 Flyby Mission Requirements for Various Years (Nuclear Escape – Drag-Brake Earth Entry)

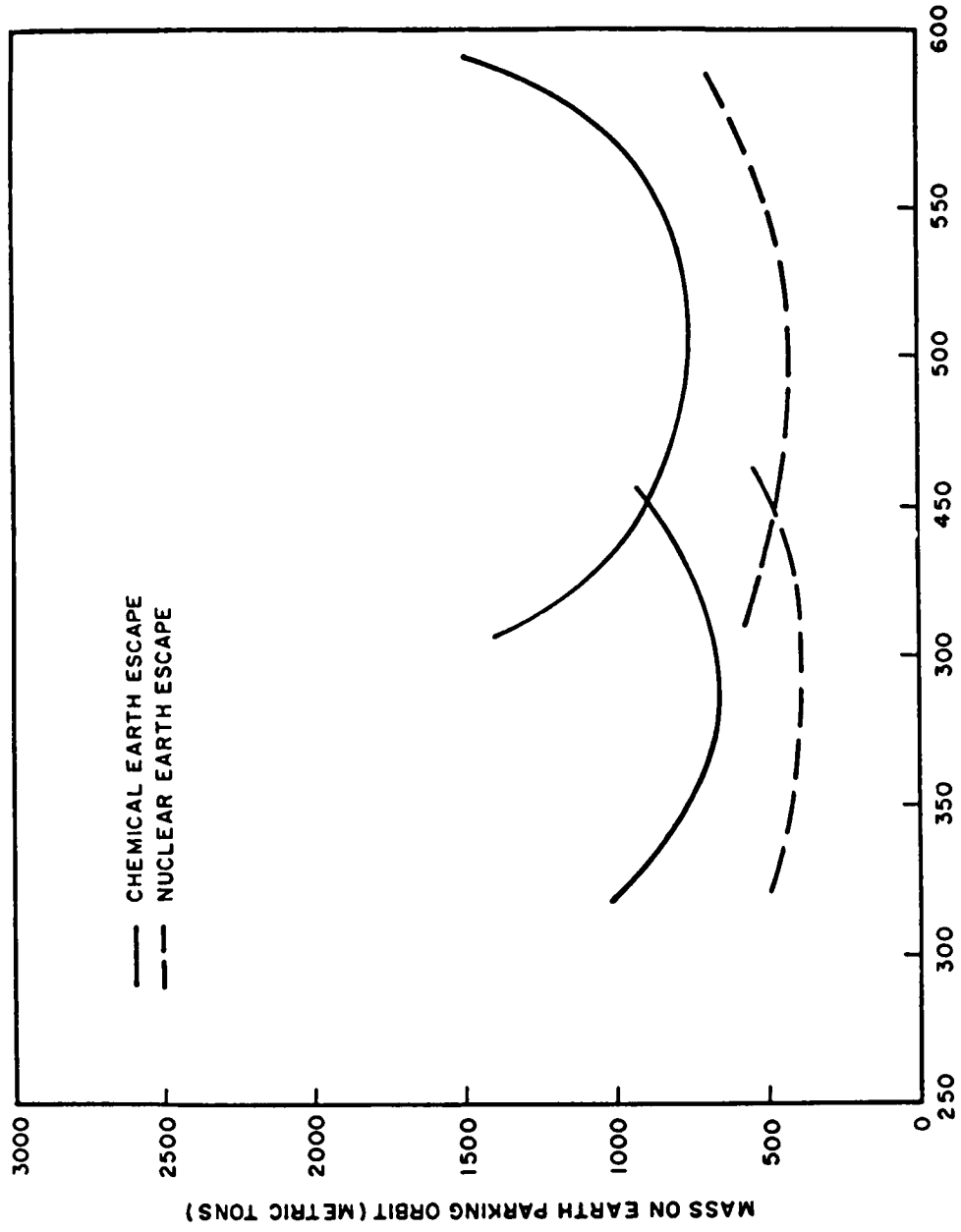


Fig. 1-9 Mission Requirements for 1972 Conjunction, Venus Ten-Day Stopover (Chemical Escape – Drag-Brake Earth Entry) (Nuclear Escape – Drag-Brake Earth Entry)

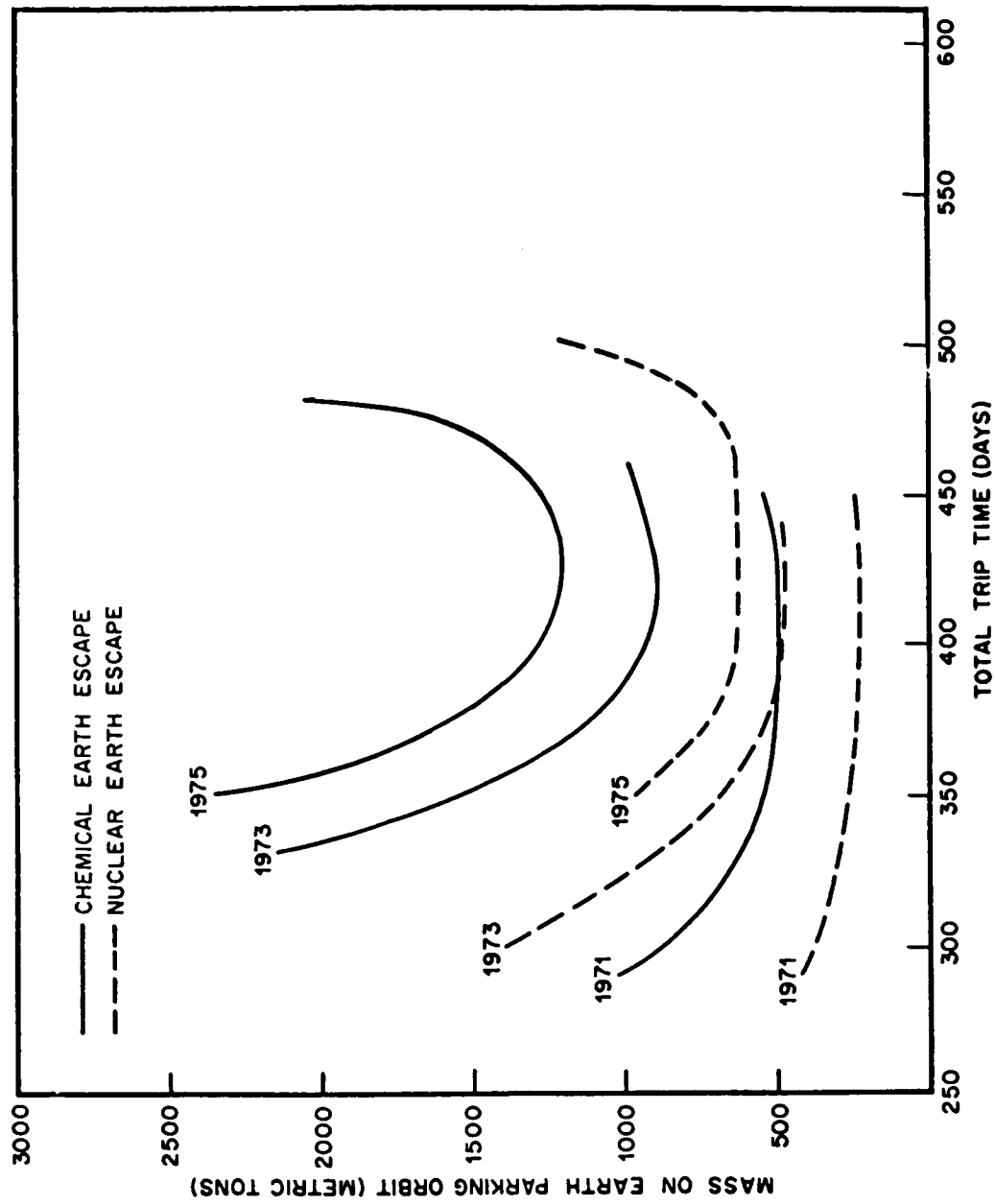


Fig. 1-10 Mission Requirements for Various Oppositions – Mars Ten-Day Stopover (Chemical Escape – Drag-Brake Earth Entry) (Nuclear Escape – Drag-Brake Earth Entry)

The minimum mass required (140 metric tons) in the chemical escape system is just above the capability of a single Saturn C-5, under the assumptions used for the transportation system. Utilization of a drag brake entry system reduces the requirements somewhat so that it is about 10 metric tons above the C-5 capability. This mission is easily within a single launch if a nuclear escape stage is used. The requirements in this case are sufficiently lowered, that additional mass may be included in the heliocentric payload, for example in the form of increased mission module size, more radiation protection and other contingencies.

The three types of Mars flyby trips discussed previously are represented in Figs. 1-5 through 1-8 by curves each grouped vertically according to the opposition year. The low energy lightside and high energy darkside and lightside trips may be conveniently compared with respect to opposition year and requirements in each of the figures.

The most striking feature to be noted is that for the later oppositions the system requirements increase rapidly in the high energy class of trips. For the chemical system, these changes range from 50 to 60 percent between 1971 and 1973, and from 140 to 180 percent between 1973 and 1975. The curves are more closely clustered if a nuclear stage is used, although the relative increases are still quite significant. For example, in the lightside flyby an increase of 13 percent is necessary in 1973 compared to 1971; and 72 percent in 1975 over 1973. The desirability of these high energy trips lies primarily in the relatively lower trip times, although in each year there is practically no choice in the mission duration.

At the expense of a trip of at least 100-day duration, the low energy missions offer less sensitivity to year. For both types of escape stages, the requirements increase by approximately 30 percent between 1971 and 1973. However in 1975, the mass on orbit is of the same order as 1971. Thus, the later year is available for a lightside flyby of Mars for essentially no penalty, the only drawback being its extended flight time.

In an overall comparison of the Mars flyby missions, the three important parameters of total trip time, mass on Earth orbit, and opposition year must be considered in planning these flights. The high energy darkside trips offer the lowest trip times; however because it passes on the darkside of the planet, the effectiveness of the reconnaissance may be lessened. For approximately three more trip-time months and somewhat higher requirements, lightside flybys are available. From the growth in requirements with year, these trips are essentially unavailable after 1971. Low sensitivity to year is offered by the low energy trips with requirements through all the years approximately the same as the high energy class in 1971. Reductions in trip time of up to twenty days may be effected for increased mass, nevertheless the durations involved are still greater than 1.5 years.

Within the time period chosen, technology can affect only one of the mission parameters, viz., transportation system mass, by utilizing an efficient nuclear escape stage. In this event, all the flyby missions through 1975 may be accomplished with less than 200 metric tons (Fig. 1-7 and 1-8). The availability of these large nuclear systems now becomes important in view of current engine technology projected for the early 1970's.

It is with this background of information on the nonstop explorations that the multiple-planet flybys or interplanetary grand tours offer the most effective means of reconnoitering the neighboring planets. Three grand tours were studied: one which possesses the lowest trip duration, another which requires minimum system mass, and finally, a three planet flyby which passes by Venus, then Mars and Venus again. In all of these trips the spacecraft passes on the sunlit side of each planet with distances of less than three planetary radii. A more intensive analysis of the analysis of the heliocentric trajectories for the grand tours will alter the velocities, passage distances and trip times somewhat, however the values as indicated on the figures are representative of this class of trips. These multi-legged trips are executed in purely ballistic fashion using terminal planetary perturbations and bending to adjust the subsequent leg so as to pass the next planet. No additional propulsion other than the midcourse system, is necessary for these types of flybys.

The grand tours are available approximately every 6.4 years, which means we can expect them again in about 1976–77, but with generally increased velocity requirements. Thus the 1970 Venus-Mars trips although early in terms of transportation system development, are quire attractive with requirements of only 160 and 100 tons respectively for the chemical and nuclear escape systems. This early date coupled with a trip time of 600 days should be evaluated with respect to the single Mars or Venus flybys which require about the same mass in 1971. The 1970 trip remarkably enough passes Mars' lightside only 98 days after opposition, and Venus' lightside only 11 days before conjunction. For an approximate increase in requirements of 100 percent in the chemical case and 50 percent in the nuclear, the trip may be delayed to 1972 with an attendant lower duration of 460 days. Note that in comparison to high and low energy Mars trips this 1972 grand tour requires lower trip times and essentially the same mass. Consequently the 1970 and 1972 grand tours are potentially more productive and less demanding in the manned flyby planetary reconnaissance role not only because of the comparatively reasonable values of system mass necessary, but because both planets may be scanned on a single trip.

In the search for the multiplanet flybys it was found possible to join the various planetary legs of the heliocentric trajectory so that Venus, Mars, then Venus are passed on the same trip. This can be done using pure ballistic flight without major propulsive maneuvers other than the usual midcourse guidance corrections and orientations. As before, slight changes may be made in this type of trajectory, but in essence the requirements on velocity and trip time and hence system mass are approximately as depicted in the figures.

This trip requires little more mass than the 1970 two-planet flyby, however the trip duration is close to two years. In this respect the three-planet tour is not as attractive as the two-planet flybys discussed previously. A more valid comparison requires further definition of the importance of trip time to the crew especially in regard to the psycho-physiological balance of each individual member and further, the influence this aspect has on transportation system design. This however, generally applies to all of the trips analyzed.

The importance of weight reduction in the Earth return system, especially as higher entry speeds are encountered, is depicted in Figs. 1-6 and 1-8 wherein a large aerodynamic drag brake instead of a retrorocket system is utilized. Comparisons may be made for specific trips and it can be seen that considerably more savings in mass requirements due to the entry system are available in the chemical system than in the nuclear case. This is primarily due to the already drastic reductions obtained through the use of the nuclear stage.

The light weight drag brake method can be advantageously employed in marginal cases such as the Venus flyby. As stated previously, the chemical escape system which requires 140 tons is slightly beyond the capability of a single Saturn C-5 booster. Sufficient savings in mass may be realized with a drag brake system so that now the required mass is just about at the single boost capability. So close in this case, that it appears more intensive study should be made to determine whether a manned Venus flyby can indeed be accomplished with a single C-5. A detailed technical study of an Apollo integrated aerodynamic drag brake has established the feasibility of such a system for the early 1970's. This is treated in other parts of the report.

As high energy trips are attempted at the later opposition years larger savings in system mass are obtainable through the use of the drag brake system. One may expect that any weight reduction in the heliocentric payload becomes more important as the higher velocity trips are attempted. This is illustrated for example by the high energy lightside Mars trips in which the reduction in required mass is 13 percent for 1971, 16 percent for 1973 and 24 percent for 1975 (Figs. 1-6, 1-8).

1.3.2 Orbiting Stopover Missions

The system requirements depicted in Figs. 1-9 and 1-10 for a ten day orbital stopover at Venus and Mars respectively, were obtained by the optimizing method of Ref. 1-2. Briefly, this technique establishes a locus of minimum mass on Earth parking orbit by systematically analyzing the parametric effects of inbound and outbound leg duration,

total trip time and departure and arrival velocities at both Earth and the destination planet. This integrated approach, though requiring numerous calculations of transportation system mass, eliminates arbitrary selection of an interplanetary trip from the multitude available.

As stated before, the orbital eccentricities and inclinations of Venus and Earth are such that system requirements do not change significantly with conjunction. This fact was shown graphically in the preceding figures. For this reason, the Venus orbiting stopover was investigated in only one conjunction year, 1972. The requirements for succeeding years will be essentially as indicated for 1972.

Because the orbits of Venus and Earth are not exactly coplanar, two general departure regions are available, each distinguished by the resultant range in total trip time. In Fig. 1-9 this effect is shown by the two curves for a given Earth escape stage. All possible departure and arrival regions were studied and only those two yielding lower system mass and reasonable trip time are presented in the figure. The two curves may be made to join together smoothly by applying a midcourse plane change, which will cause the two departure regions to unite. This technique was not used here, for, as will be seen in more detail later, one departure region yields a distinctly lower mass minima with corresponding shorter mission duration.

From Fig. 1-9, the best trip for each escape system occurs at about 390 days total duration with the requirement of 660 metric tons for the chemical system and 400 metric tons for the nuclear case. The chemical system exhibits a sharper minimum compared to the nuclear case. This means that for a given reduction in trip time, the chemical system will require a larger increase in mass than that of the nuclear case. For example, if an off-optimum selection were made for a trip duration of 320 days, the chemical requirements increase by about 50 percent whereas the nuclear system changes by 25 percent. Therefore, as expected, utilization of a nuclear escape stage not only decreases the mass necessary on orbit but in addition, tends to flatten the requirements curve so that shorter trips are available at a reasonable price.

In the study of Mars capture missions, the large eccentricity of the planet's orbit necessitates analysis of each possible opposition-year for its effect on the required mass. This was done for three opposition years, the range of which was believed to be of use in evaluating the relationship of flyby missions to short orbital captures. Again as in the Venus study, two possible departure regions were analyzed without recourse to a midcourse plane change.

The important result to be noted in Fig. 1-10 is the considerable increase in the minimum required mass as flights are attempted in later years. In 1971, opposition occurs at nearly the perihelion passage of Mars and consequently this year is the most favorable of all the oppositions. This fortunate set of events does not recur until about 1989. Thus insofar as Mars is concerned, trips attempted in the late 1970's will be on the forward slope of the steeply rising velocity requirements curve. It is these circumstances that are characterized in Fig. 1-10.

The effect of later years may be quantitatively evaluated by comparing each of the minima. The 1971 trip requires approximately 500 metric tons on orbit; however, a 400 metric ton increase is necessary if this mission were to be executed in 1973. A 300 metric ton increase over the 1973 value of 900 metric tons is required for the 1975 time period. These values when compared to the single flyby requirements, especially for Mars, suggest that if a booster or rendezvous capability for flybys were developed in the 1975 period, it may be economically feasible in terms of the overall interplanetary exploration program to plan instead for short orbiting stopovers.

A second important point is that for the chemical escape stage the curves yield a more pronounced minimum as the years progress. There is then less chance of decreasing the mission duration without incurring undue increases in required mass. In 1971, the curve is quite flat over a range of 100 days, whereas in 1973 and 1975 the curves are insensitive only over 60 and 30 days respectively.

The importance of the nuclear escape stage for these stopover missions is clearly demonstrated in Fig. 1-10. The higher specific impulse system is not very sensitive

to changes in velocity requirements, therefore the nuclear stage will not be as significantly affected by opposition year compared to the chemical system. This can become important in terms of surface launch vehicle capability and in terms of multiple rendezvous and on-orbit assembly. An additional observation is that the system requirements do not change considerably with decreasing total trip time.

1.4 TECHNICAL DISCUSSION

This section discusses in technical detail the analysis performed in obtaining the final mission requirements presented in the Summary of Results. For convenience the section is broken down into five topics: Venus flybys, Mars flybys, multi-planet flybys, short orbiting stopovers and the computer program. The subsections describe the corresponding trajectory information and the form in which it is used. Sample trips of optimum mass are given with a preliminary weight summary for the required transportation system. Also presented is the influence of periplanet passage distance on system requirements. The computation of mass requirements for the multitude of trips analyzed could only be accomplished by a machine program with sufficient flexibility to include several desirable options. This computer program is outlined in the last section.

1.4.1 Venus Mission Requirements

Figure 1-11 is a pictorial display of a one year, non-stop round trip, leaving in the conjunction period of 1970. It is possible to obtain such a plot for all possible trips of interest in any conjunction year along with the corresponding trajectory information of departure and arrival at Earth and of planetary passage. A systematic analysis of this type of transfer trajectory (Ref. 1-3) yields a set of velocity contour charts on which lines of constant planetary passage distances are drawn. Such a chart is depicted in Fig. 1-12 for the conjunction of 10 November 1970, with lines of passage distance r_p equal to 1, 2, and 5. The velocities are given as hyperbolic excess speeds normalized with respect to Earth's mean orbital speed (EMOS) and are indicated as

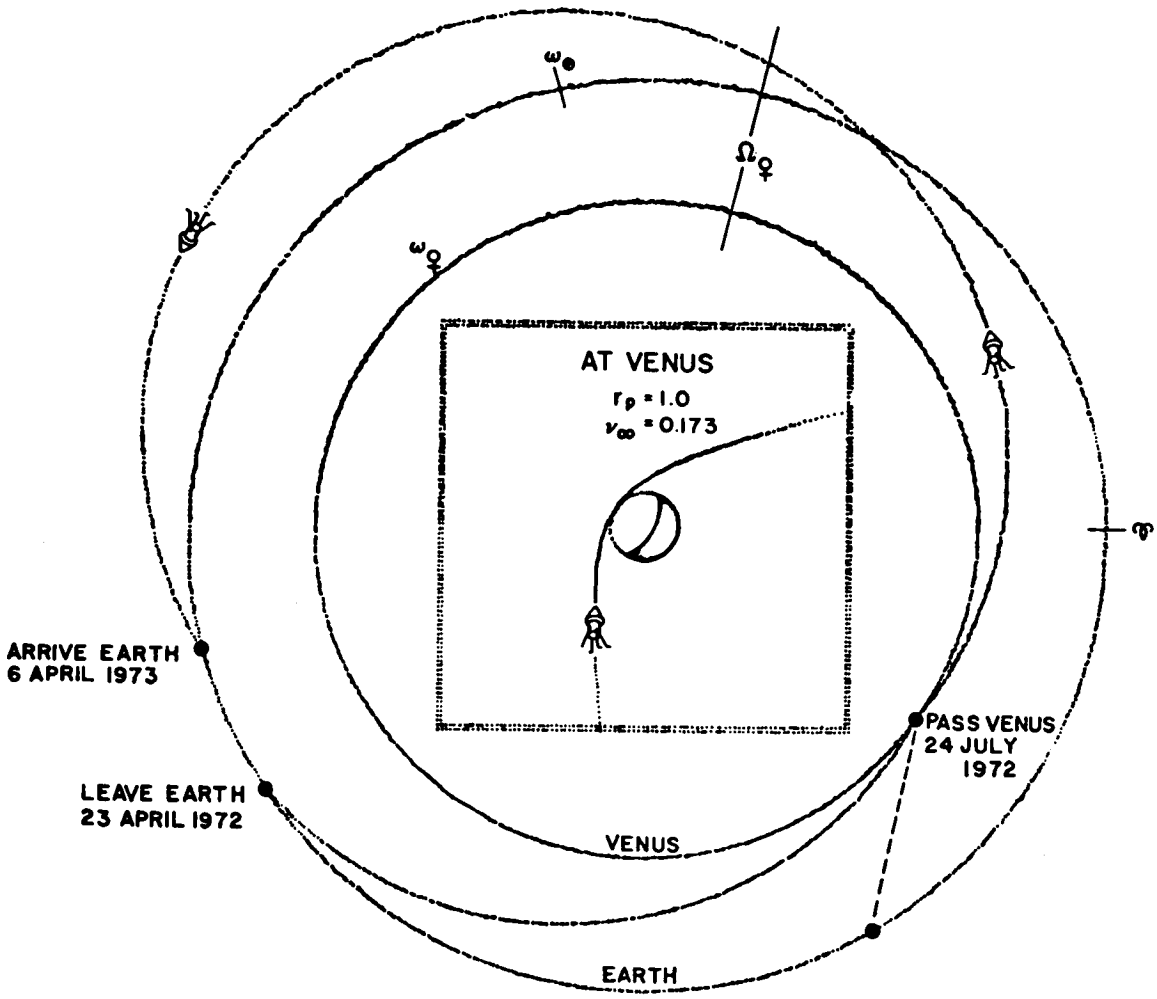


Fig. 1-11 Nonstop Flyby Past Venus

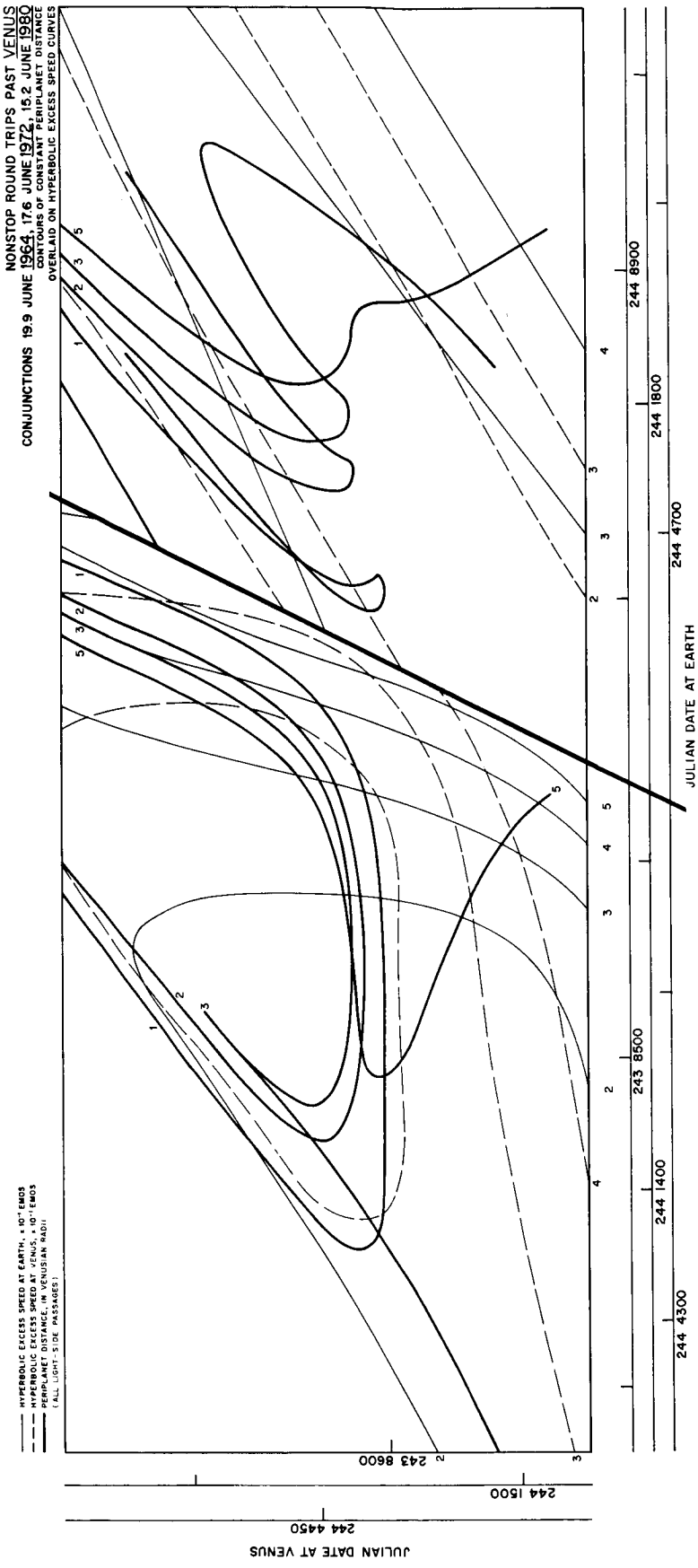


Fig. 1-12 Venus Flyby Passage Distance – Velocity Contours

departure or arrival by a solid or dotted curve respectively. The diagonal line divides the chart into the outbound conditions on the left and the homebound conditions on the right. To identify a trip, one selects an r_p and an Earth departure date which immediately gives the Julian date of arrival at Venus. This Julian date located on the homebound region along with the given r_p yields the arrival date at Earth. The difference in the Julian dates at Earth is, of course, the total mission duration. The hyperbolic excess speeds of departure and arrival are indicated by the corresponding contour and the intersection of a Julian date and r_p line. Note that the speed arriving at Venus must equal the speed leaving Venus since these are all flyby trips. Only trips passing on the illuminated side of Venus were considered, with passage distances of 1, 3, and 5 planetary radii.

The mission analysis and trip selection could have easily been done by selecting the point on an r_p line which has the lowest Earth departure velocity contour. This approach does not in general assure minimum system mass, as the effect of the accompanying Earth entry speed and consequently the entry system is not reflected in the vehicle requirements. This approach, furthermore, does not show the penalties for attempting shorter mission times or the influence of passage distance. These objections may be overcome by selecting several points along on r_p line and computing the required system mass.

Figure 1-13 shows a particular result of the computations for a chemical and nuclear escape system. For clarity, in some cases, the entire curve is not shown. The effect of increasing passage distance is seen to incur an increase in system requirements, although for the nuclear system the effect is not as pronounced due to the higher specific impulse. An optimum mass is established in each case which when considered with non-integer r_p's determines an envelope of minimum requirements. This region is bounded on one side by the physical limitation of one radius passage and on the other by the locus of minima. It is expected that the limiting case of infinite passage distance would be approached asymptotically by the locus of minima.

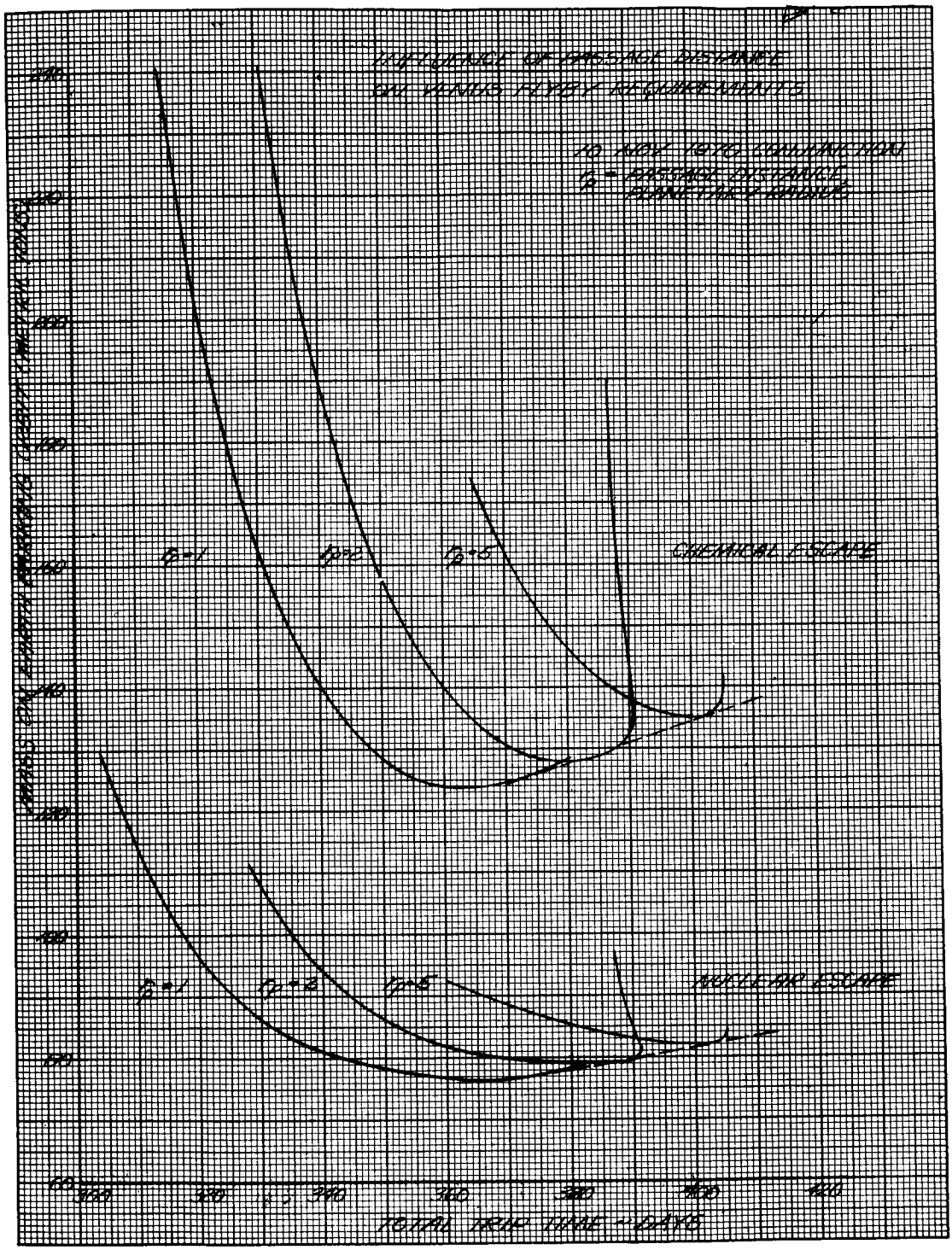


Fig. 1-13 Influence of Passage Distance on Venus Flyby Requirements

The tradeoff between shorter trip time and system mass on parking orbit is quite appreciable for reductions of about one month. For an r_p of one in the chemical case, this entails about a 25 percent increase in the mass requirements. Of course, even shorter trips are available but at a prohibitive cost. Note that at an r_p of 2 and a trip time of 390 days, several trips are available which if not selected properly could result in very high system mass. In this instance, identification of the best trip is accomplished by plotting the requirements against Julian departure date.

The mission requirements for the various transportation system types are presented in Fig. 1-14, for three conjunction years. Significant savings may be realized with a drag brake system in the years after 1970, although in an overall sense the requirements do not fluctuate greatly through the years. Each combination of escape propulsion and Earth entry system may be considered as indicative of a period in the state of technology; this would attach more meaning to the surface launch vehicles required to place the corresponding mass on orbit. A chronological arrangement would list a chemical escape/retro rocket combination as an early system, followed by one using a drag brake, and finally a nuclear system coupled with a drag brake. The first system is considered a "safe" one since it employs a reliable, low performing (250 Isp) solid propellant retro-rocket to decelerate the command module. The third system is the most desirable as its mass requirements are well within the single boost capability of the Saturn C-5. Furthermore, it reduces the differences between years allowing essentially the same size escape stage for any conjunction year.

Table 1-2 presents a summary of an early (1970) Venus flyby obtained from the optimum points of Fig. 1-13. The values in the mass breakdown should be viewed in light of the system design assumptions presented earlier.

By referring to Fig. 1-15 it can be seen where the major system growth lies. As expected, the escape step dominates the entire transportation system requirements, whereas the heliocentric payload is virtually unaffected by trip time. This latter point generally holds for the Venus non-stop trips in any conjunction year.

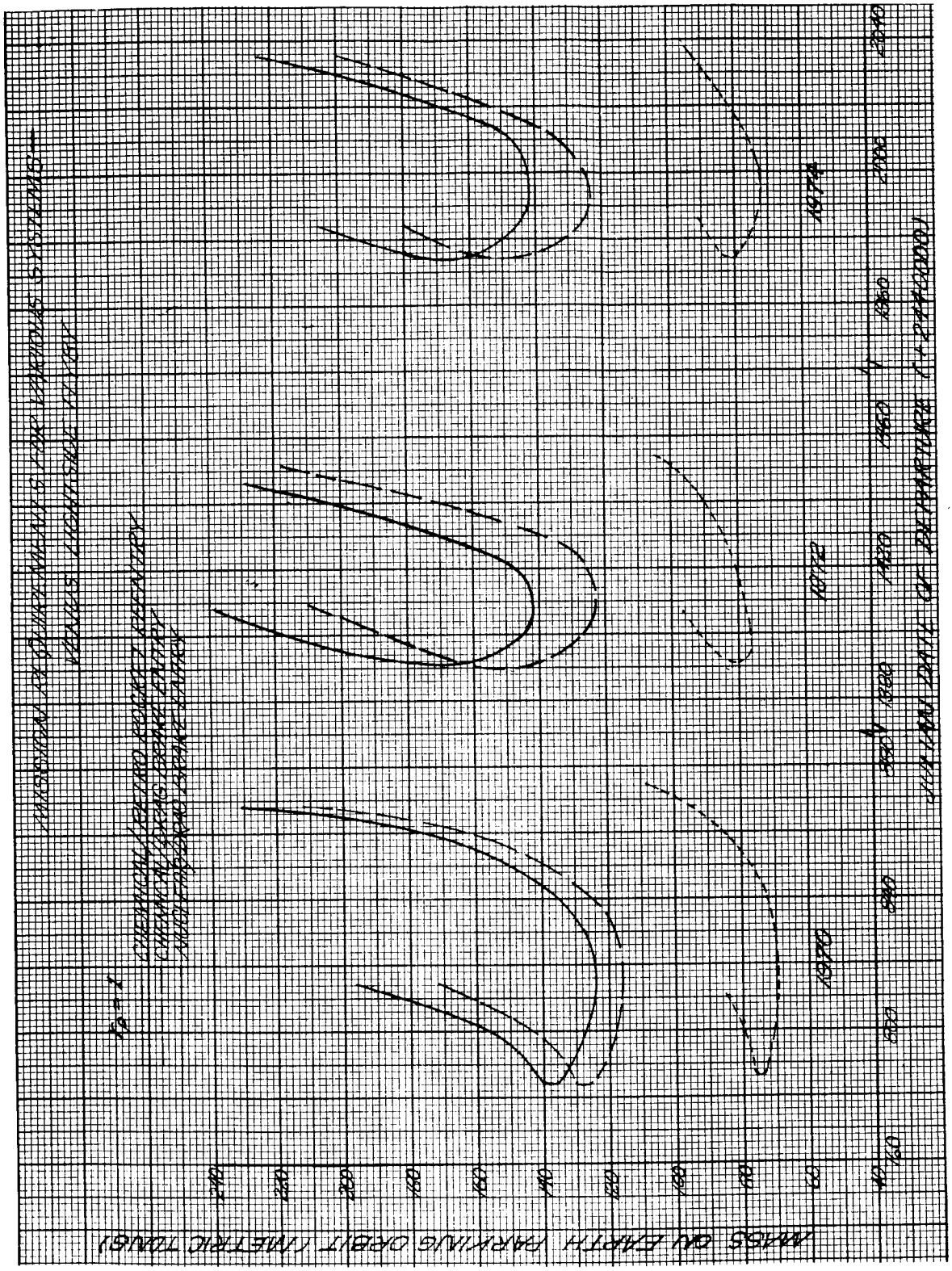


Fig. 1-14 Mission Requirements for Various Systems – Venus Lightside Flyby

Table 1-2

SAMPLE EARLY VENUS FLYBY MISSION

Lv ⊕	Aug 1970	EMOS 0.0977	Incremental velocity, 3.6 km/sec
Ar ♀	Dec 1970	0.1847	Passage distance, 1.0 radius
Lv ♀	Dec 1970	0.1847	
Ar ⊕	Aug 1971	0.2377	Arrival velocity, 13.2 km/sec

Mass Summary (metric tons)	Retro-Rocket Earth Capture	Drag-Brake Earth Capture
Mass on Heliocentric Orbit	36	34
Probes & Scientific Equipment	4	4
Mass on Earth Parking Orbit		
Chemical Escape	125	115
Nuclear Escape	76	73

LOCKHEED MISSILES & SPACE COMPANY

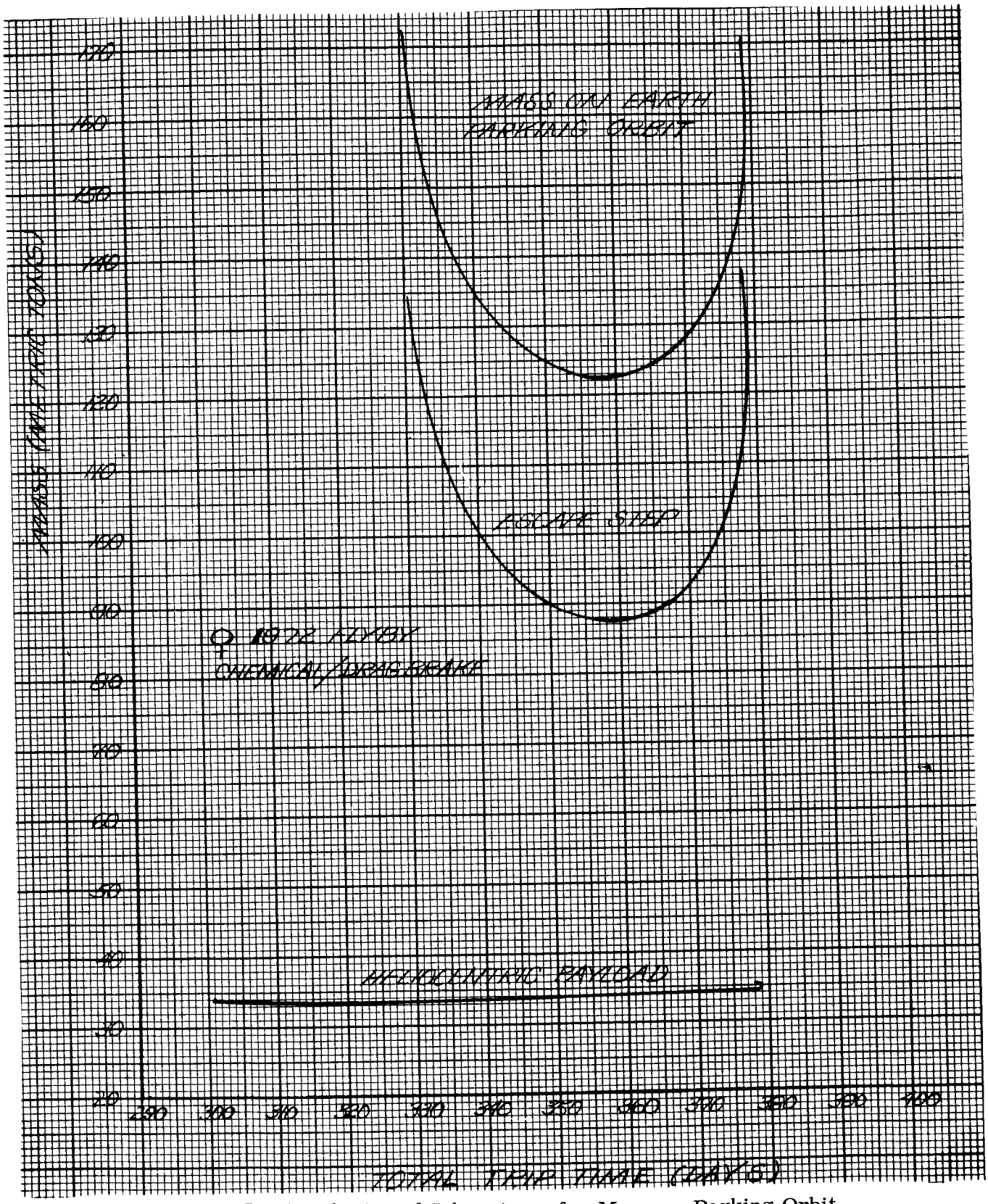


Fig. 1-15 Distribution of Subsystems for Mass on Parking Orbit

1.4.2 Mars Mission Requirements

The high and low energy classes of nonstop trips to Mars mentioned in the Study Scope, yield the trips of practical interest to the flyby mission for the early 1970 time period. In each opposition year and for each trajectory class a velocity contour-passage distance chart such as Fig. 1-16 may be obtained. This chart is a valuable aid in gaining insight into the interrelationship between hyperbolic excess speed, passage type and distance, and Julian date, and their effects on mission requirements. In addition, the chart lends coherence to the computed mass curves by noting the location of each data point on a given r_p line. Thus the curves of Figs. 1-5 through 1-8 in the high energy case will cross themselves if all the data were plotted; however, each trip is distinct by the manner in which it was taken from the chart. From Fig. 1-16 it can be observed that as one moves along an outbound r_p line the variation in total trip time is small if the horizontal distance to the corresponding homebound line is somewhat constant. This is indeed the case for the high energy class and partially explains why the curves in Figs. 1-5 through 1-8 display such small sensitivity to mission duration. Therefore no matter what the choice is for passage distance and departure date, once the illumination condition at approach is selected, the total mission duration is essentially the same.

The mission analysis approach used in this study utilizes the system mass required on Earth parking orbit as the major parameter for the evaluation of trip selection and vehicle tradeoffs. As noted previously, trip selection could easily use the minimum departure velocity as an indicator. In the case of Mars such a selection criteria does not produce the lowest mass, especially for the later opposition years as can be seen in Fig. 1-17. In 1973, the minimum departure speed yields a vehicle of 680 metric tons on orbit compared to the computed minimum of 590 tons at a slightly higher velocity. This is approximately a 15 percent increase. The comparison is even higher in 1975, where minimum speed requires 1840 tons to the computed 1540 tons, an increase of about 20 percent.

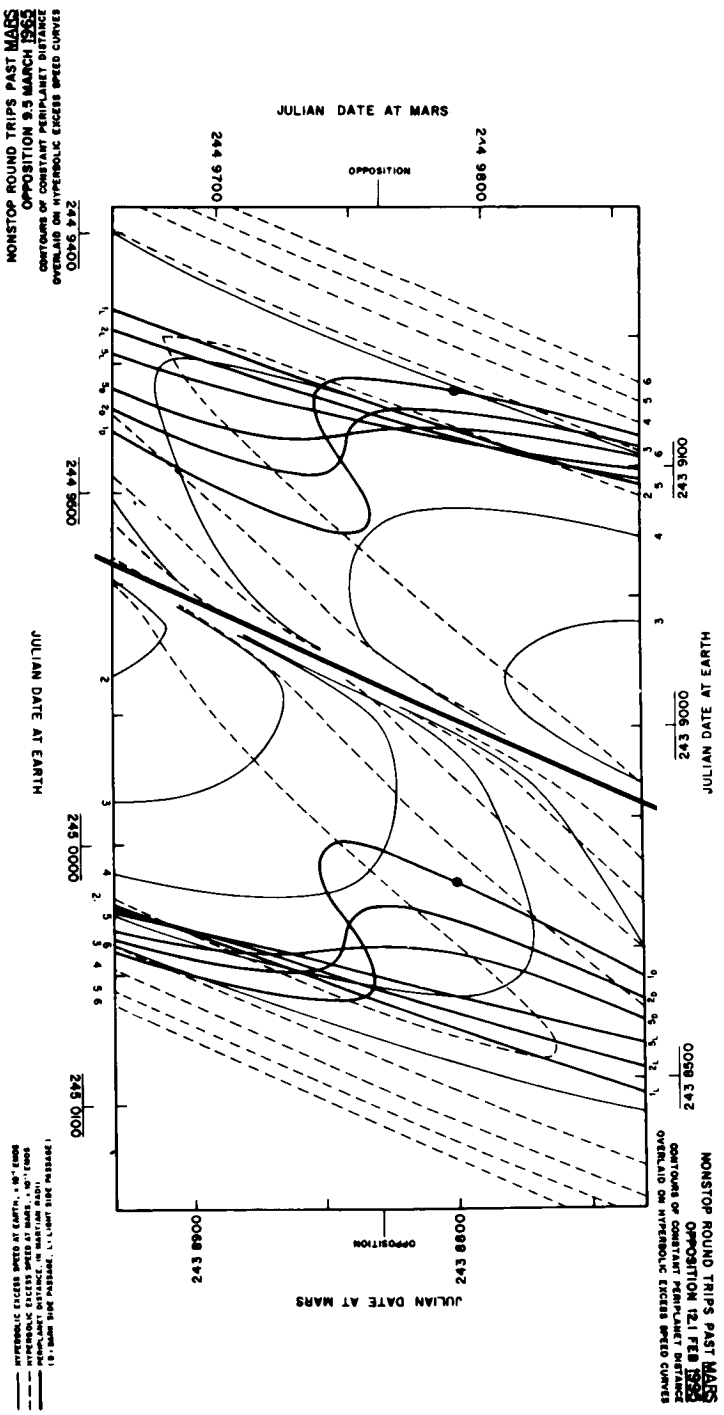


Fig. 1-16 Mars Flyby Passage Distance – Velocity Contours

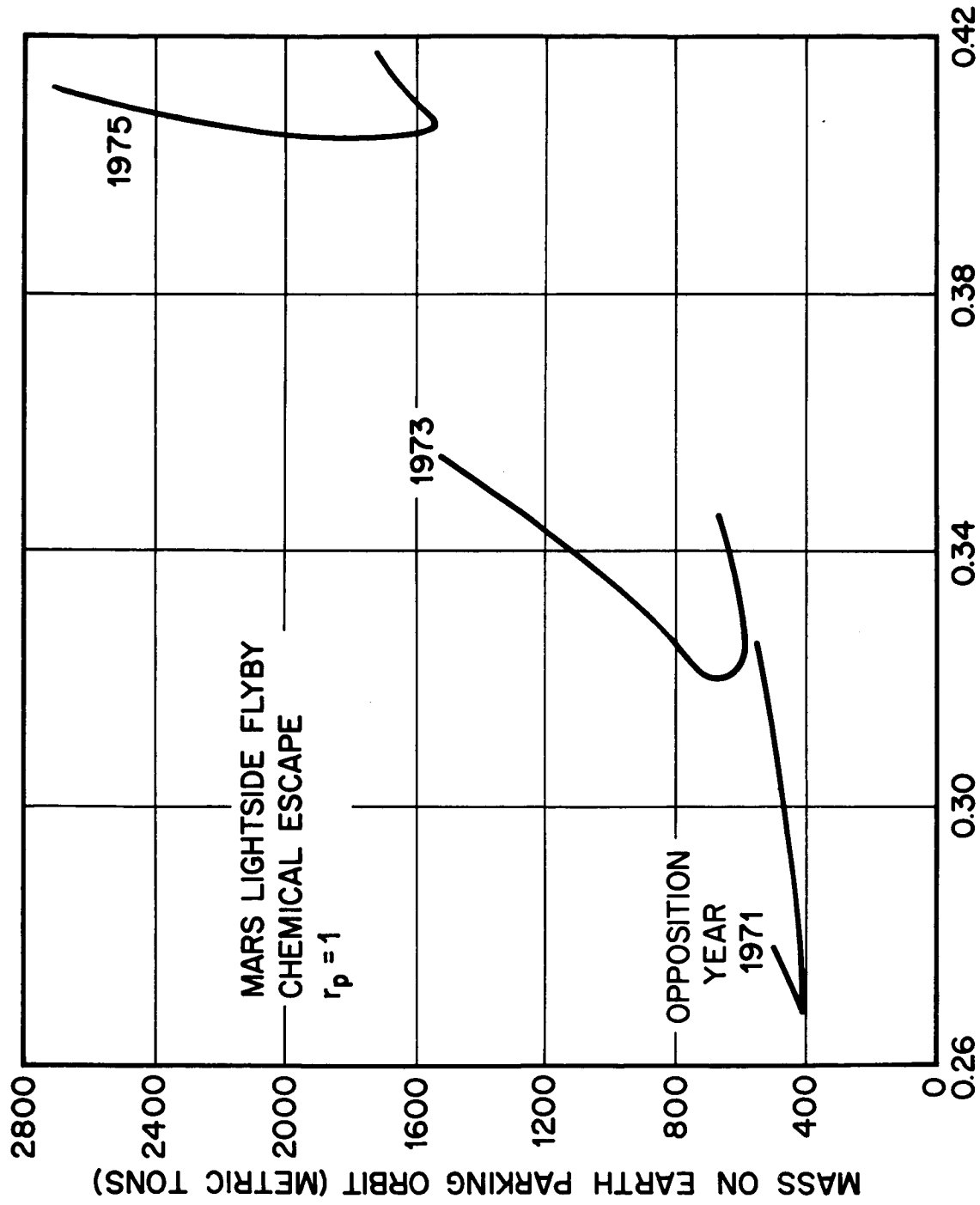


Fig. 1-17 Trip Selection Criteria

The influence of passage distance on system requirements depends on the type of trajectory being executed. This can be seen in Fig. 1-18 wherein lightside flybys are compared between the high and low energy classes. From the trajectory profiles of Figs. 1-1 and 1-2 it can be surmised that decreasing the lightside passage distance will tend to lower the trajectory requirements. Because the high energy trips barely graze Mars' orbit, passing further away from the planet on its illuminated side will cause mass decreases until the limiting case is reached where the spacecraft passes at the uninteresting distance of infinity. On the other hand, the low energy trips reduce the requirements less for each increase in r_p, which implies that infinite passage is reached asymptotically. From the trajectory information, any r_p past five achieves this limiting case insofar as the system mass is concerned. To maintain a common basis for comparing the numerous trips and the several vehicle systems considered, the distance of closest approach was fixed at one planetary radius.

These comparisons are conveniently presented in Fig. 1-19 for the high energy lightside flyby as an example. Utilization of a drag brake entry is seen to be important, especially as trips of later oppositions are attempted. The effect of year is quite pronounced in the chemical system for this type of trajectory, whereas a nuclear escape stage used in conjunction with a drag brake is practically insensitive to opposition year. The high energy class of trajectories although requiring relatively lower trip durations, do not appear to be desirable when viewed in light of booster and/or orbital rendezvous techniques. As pointed out before, the low energy class compares favorably in this respect.

The payload placed on the heliocentric trajectory by the escape propulsion system varies slightly with year, any variation being due primarily to the higher reentry speeds and its consequent effect on the Earth entry system. The largest effect on the required system mass is brought about by the escape step which is sized to the higher velocity requirements for the later years. It follows that although the heliocentric payload is approximately the same in weight, differing only in makeup, the orbital escape booster would be of major concern especially with regard to multiple surface launches and rendezvous. These problems do not arise in the low energy trips.

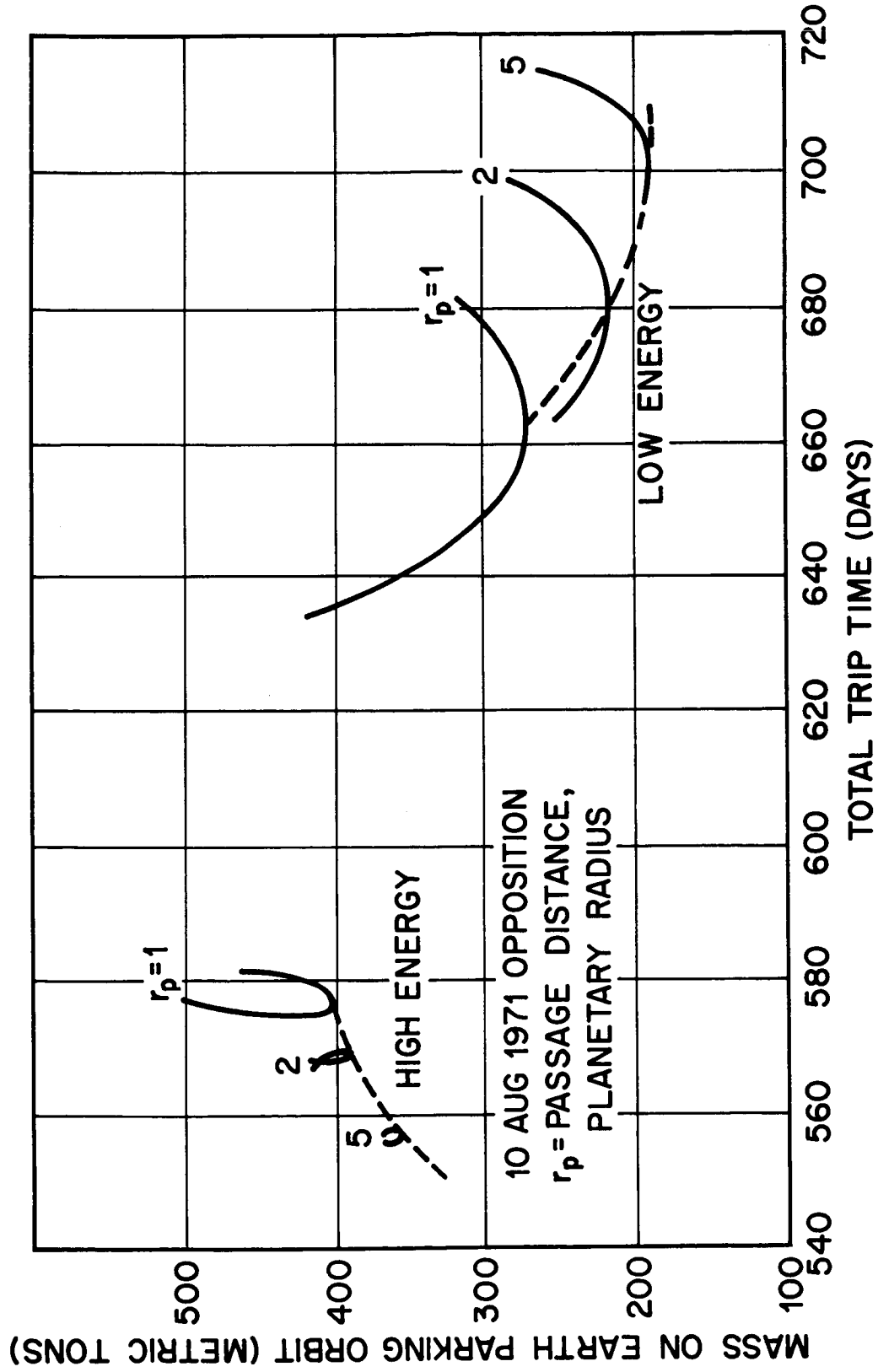


Fig. 1-18 Influence of Passage Distance on Mars Flyby Requirements (Chemical Escape)

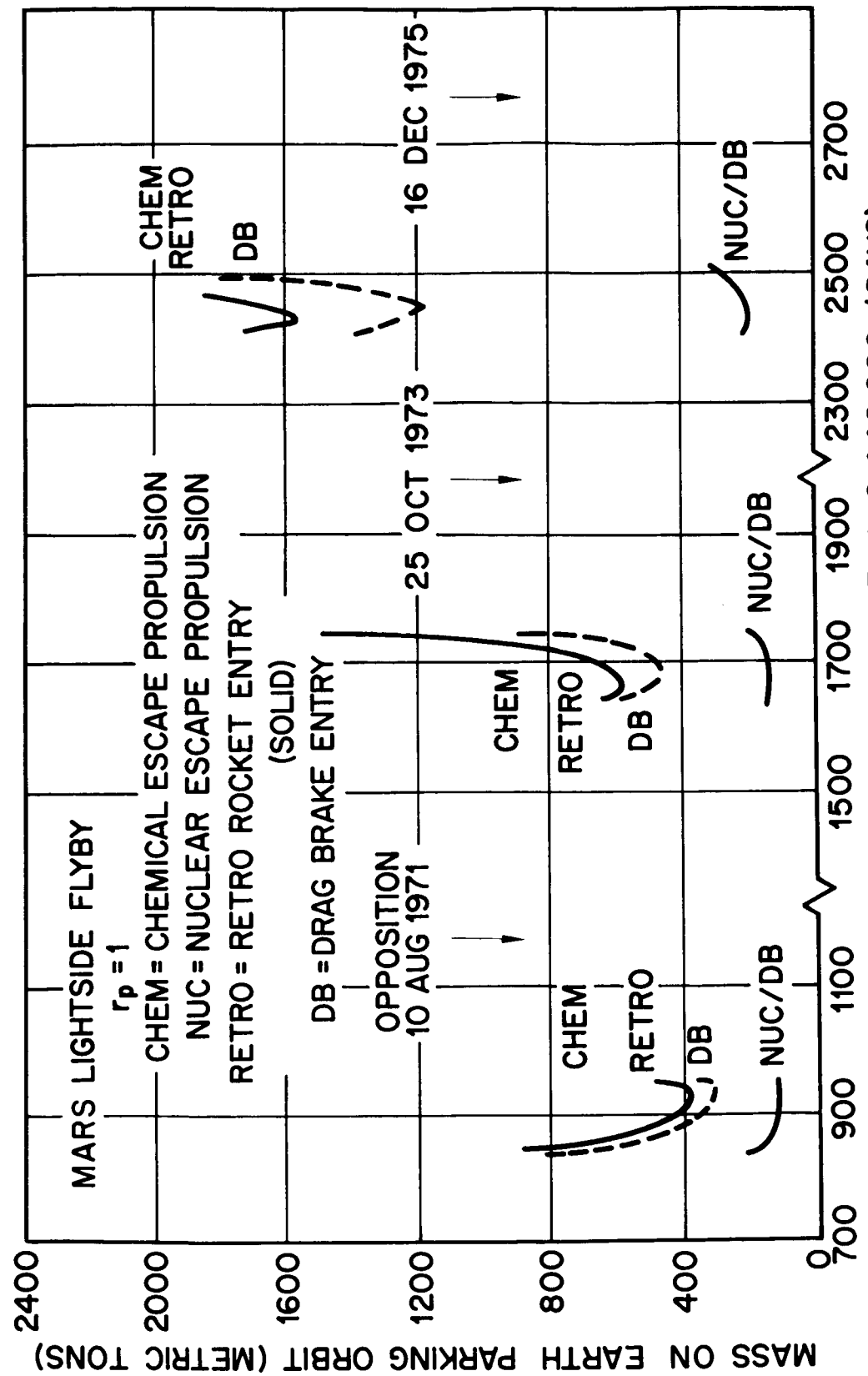


Fig. 1-19 Mass Reduction Using Drag Brake Entry

This fact is brought out clearly by Fig. 1-20 which presents a major weight breakdown of the transportation systems for each year. Essentially the same heliocentric payload is required for each year and in addition, the necessary size of the escape booster is seen to decrease with each year. Thus a single chemical escape step may be selected for the Mars flyby mission which can be applied to trips in later oppositions.

For example, if an illuminated flyby of Mars is to be scheduled for 1973, the spacecraft to be placed on the heliocentric trajectory is about 40 metric tons which requires an escape booster of 200 tons and a trip duration of 647 days. By designing the escape step to the size indicated by the intersection of the 1973 and 1975 curves several alternatives become available. First, if for some reason this trip cannot be executed in 1973, it may still be attempted in 1975 by a system using the original escape step for practically no change in trip time because the required payload does not change. Or, since this escape booster is over-designed for the 1975 optimum mission, a heavier payload may be injected into the heliocentric trajectory for only an 18 day increase in trip duration. Obviously, practically the identical transportation system may be used for Mars reconnaissance in both years provided the trip indicated by the intersection is employed. Finally, a 200 ton escape booster will admirably serve the Venus missions (cf. Fig. 1-15) either by allowing heavier payloads or by reducing the trip time markedly (Fig. 1-13). Note further that if flyby missions are scheduled for as early as 1971, similar conclusions may be obtained from the intersection of the 1971 and 1973 escape step curves.

An estimated weight summary is presented in Table 1-3 for a 1973–1975 equivalent transportation system to be used in a 650 day nonstop trip to Mars.

1.4.3 Multiple Planet Flybys

To completely analyze the potential of the multiple planet reconnaissance requires an exhaustive search throughout the time period in which planetary flybys are of importance to the manned capture and landings. In general, any grand tour subsequent to

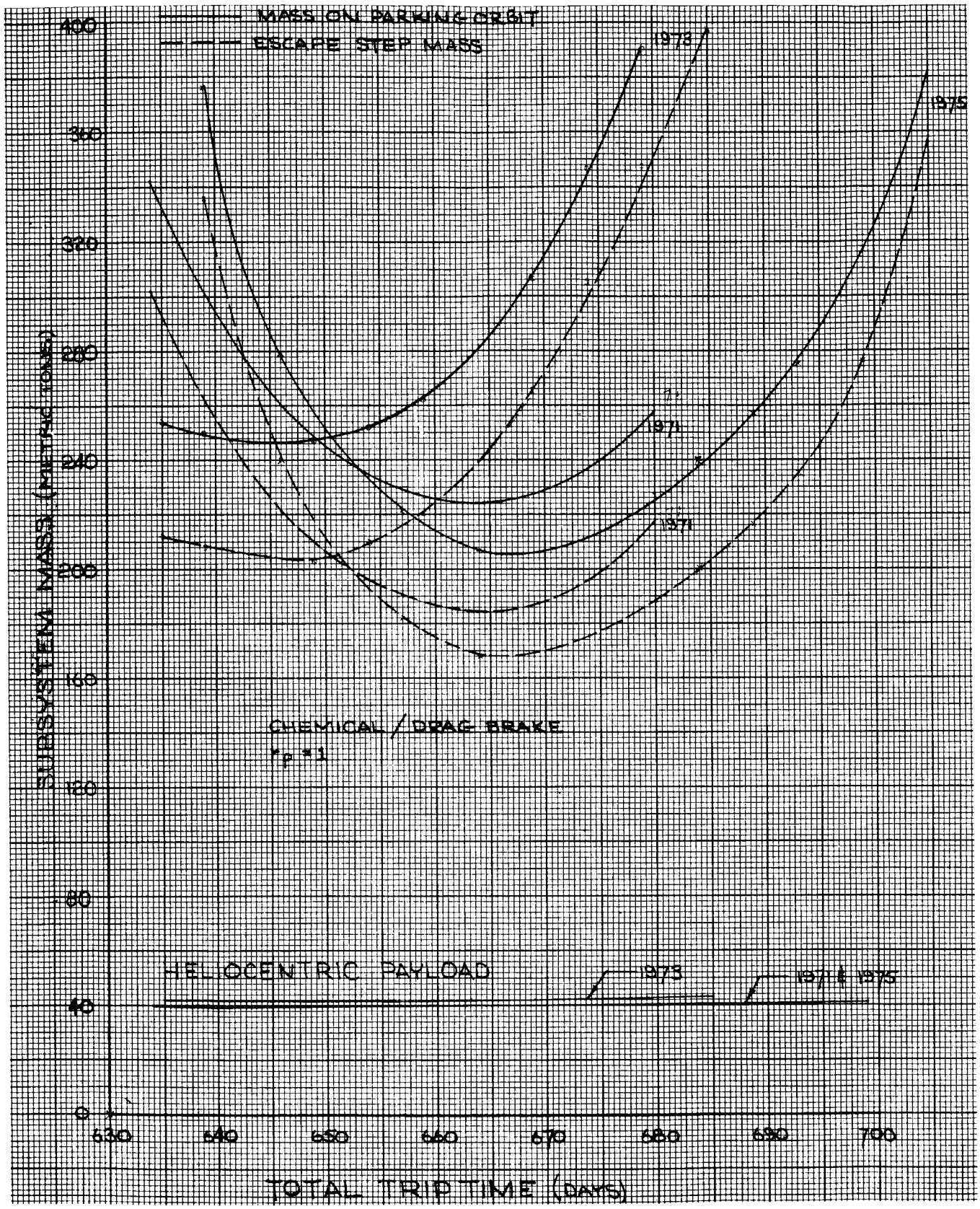


Fig. 1-20 Distribution of Subsystems for Mars Cool Flyby

Table 1-3

MARS COOL FLYBY

Identical Chemical Escape Step for 1973 and 1975

1973				1975			
Lv ⊕ 244	1896	EMOS = 0.2219		Lv ⊕ 244	2700	EMOS = 0.2356	
Ar ♂	1996	r_p = 1.0	0.3214	Ar ♂	2815	r_p = 1.0	0.2863
Ar ⊕	2546		0.3785	Ar ⊕	3350		0.3225

Mass Summary (Metric Tons)	1973	1975
Reentry System (Drag Brake)	10.81	9.24
Life Support	8.32	8.32
Mission Module	9.09	9.09
Contingency	2.27*	0.00
Probes & Scientific Equip.	4.54	4.54
Midcourse Correction	9.64	8.18
Escape Payload	44.67	39.37
Escape Propulsion	219.0	219.0
Propellant	(192.1)	(192.1)
Inert	(26.9)	(26.9)
Mass on Parking Orbit	263.7	258.4

*2.27 mt contingency available through use of 1975 escape booster

those presented here will have increased velocity requirements. It should be remembered that these journeys have a long repetition cycle; if they are not performed at the times indicated, the next opportunities for such easy missions will not present themselves for about thirteen years. The three grand tours presented herein are indicative of the types of early flybys that are available. Within a given trip some freedom may be exercised when matching each incoming planetary leg with an outgoing one; however such refinements do not alter the trajectory requirements markedly.

The trajectory of each interplanetary grand tour was extensively analyzed so that a scaled plot of each leg may be drawn to include the effects of planetary bending at the time of passage. Figures 1-21 and 1-22 present trajectory plots for two types of grand tours, along with the dates of the several events. The three grand tours considered in the study are identified according to the minimum system mass required, the lowest duration so far found, and finally the three planet flyby. Not shown is the 1972 grand tour which exhibits the lowest mission duration. Although the three planet tour does give the lowest mass it is not directly comparable to that given in Fig. 1-21 since the latter is only a two planet flyby. The three grand tours may be compared by reference to Table 1-4, wherein trajectory data as well as a major system breakdown are presented.

Tables 1-5, 1-6, and 1-7 present a more detailed summary of each grand tour. In a strict sense mass comparisons cannot be directly made as different weight allowances were assumed for contingencies, probes and scientific equipment. The estimated values for the system mass in each case should be viewed with this in mind.

1.4.4 Planetary Stopover Missions

The investigation of manned orbiting stopover missions involved three major study areas. In order of presentation they are 1) capture of the vehicle into a circular orbit of the planet by use of aerodynamic drag brake, 2) the use of Mars' large satellite, Phobos, as a stopover station for the interplanetary vehicle and 3) drag lifetimes of orbits about Mars including effects of perturbations on the orbit by the planet.

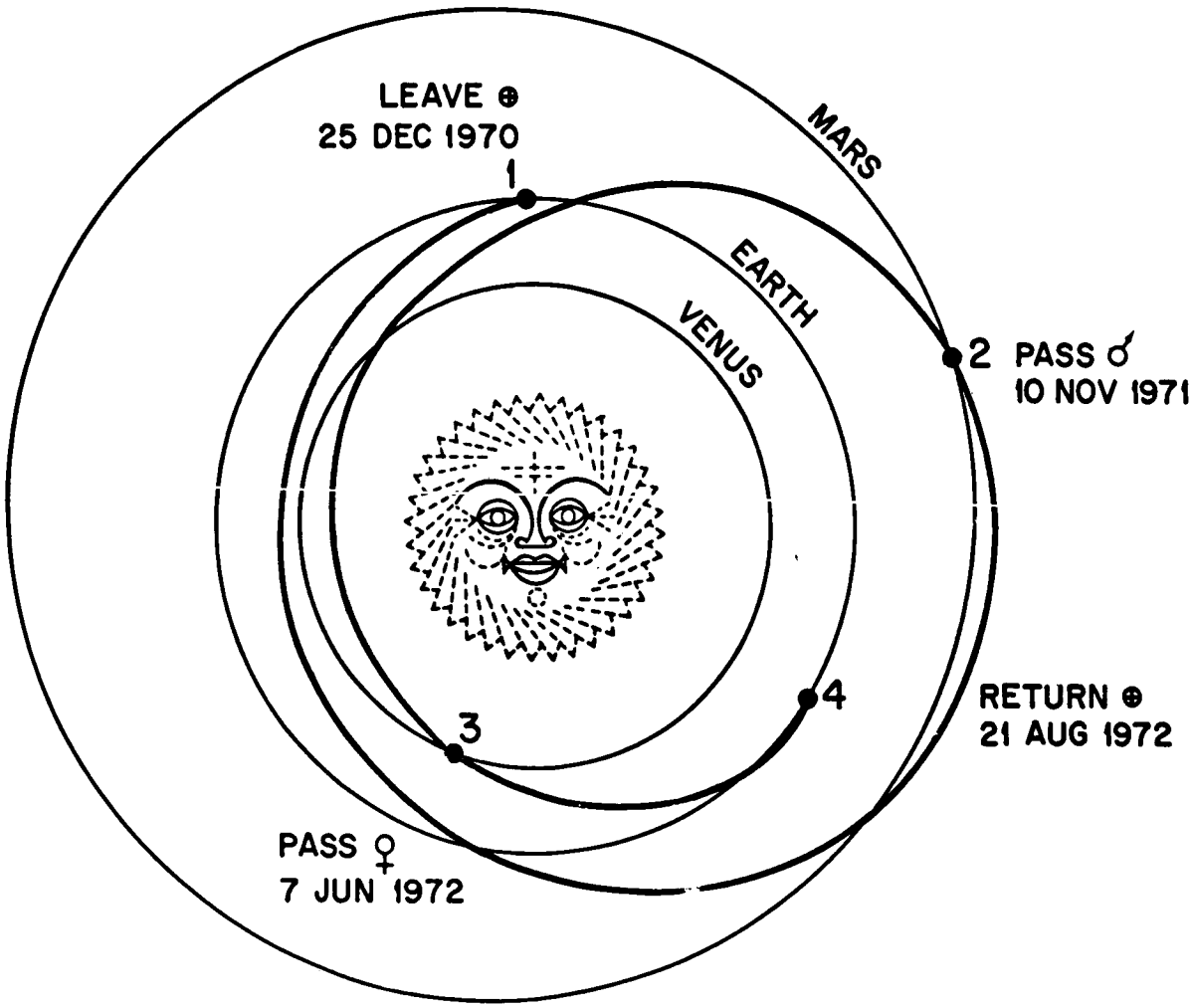


Fig. 1-21 Two-Planet Flyby 1970–1972

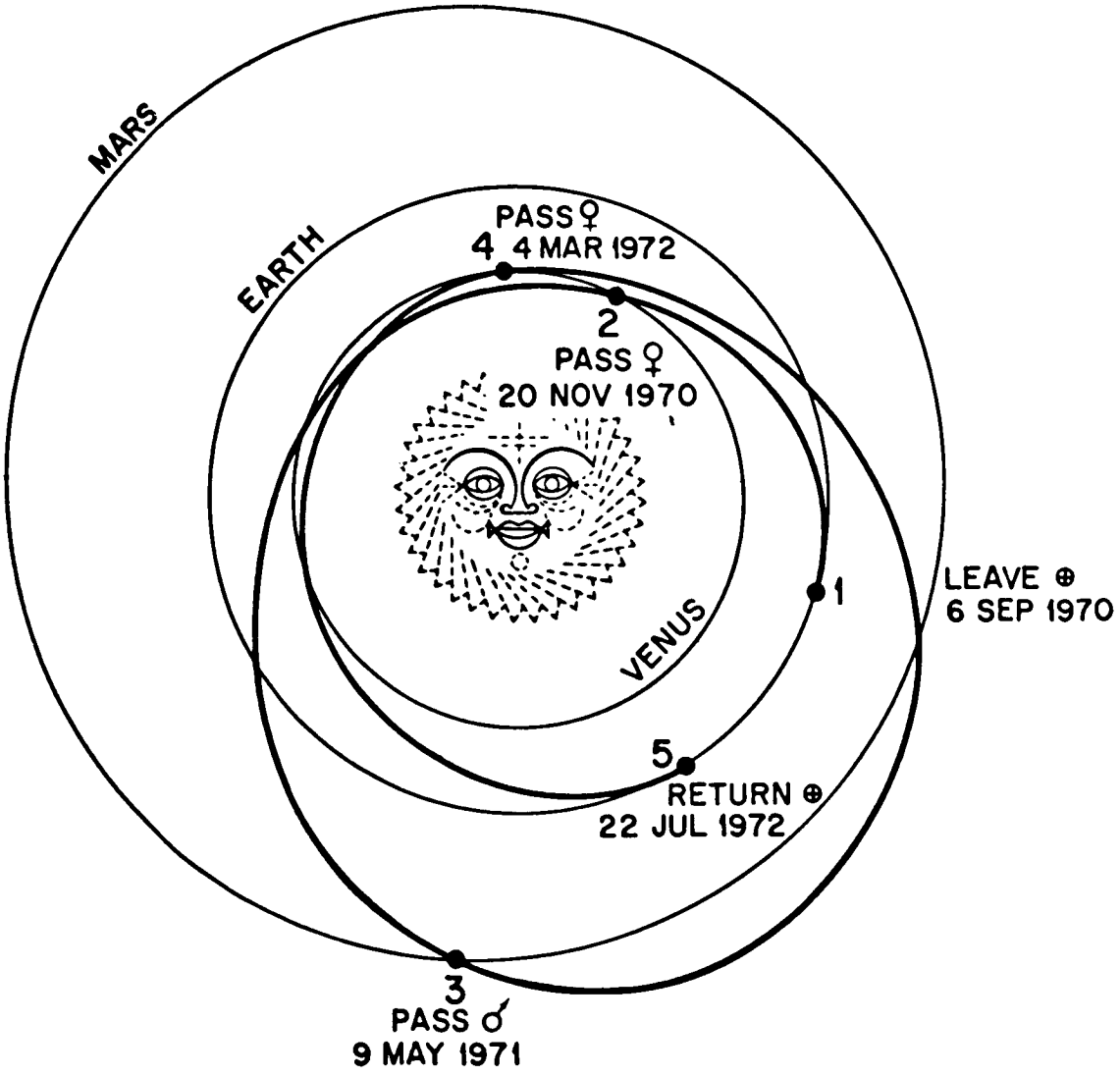


Fig. 1-22 Three-Planet Flyby 1970—1972

Table 1-4

MULTI-PLANET FLYBY MASS SUMMARY

	Minimum Mass			Minimum Trip Time			3 Planet Flyby		
	Date	Pass Dist.	EMOS	Date	Pass Dist.	EMOS	Date	Pass Dist.	EMOS
Lv ⊕	Sept. 1970		0.1267	Aug 1972		0.2377	Sep 1970		0.1577
Ar ♀	Dec 1970	3	0.2295		1.5		Nov 1970	1.2	–
Ar ♂	Jul 1971	1.6	0.1909		1.0		May 1971	1.2	–
Ar ♀	–		–	–			Mar 1972	1.7	–
Ar ⊕	May 1972		0.2882	Nov 1973		0.3357	Jul 1972		0.1552
Mass on Earth Parking Orbit (Metric Tons)									
Chemical Escape									
Retro-Rocket Earth Capture		164			316			165	
Drag Brake Earth Capture		142			248			–	
Nuclear Escape									
Retro-Rocket Earth Capture		101			145			90	
Drag Brake Earth Capture		88			115			–	

LOCKHEED MISSILES & SPACE COMPANY

Table 1-5

GRAND TOUR 1970

Minimum Mass on Parking Orbit

	Julian Date	Calendar Date		EMOS
Lv ⊕	244 0839	10 Sep 1970		0.1267 (11.7 km/sec)
Ar ♂	0925	5 Dec 1970	$r_p = 3.0$	0.2295
Ar ♀	1145	13 Jul 1971	$= 1.6$	0.1909
Ar ⊕	1440	3 May 1972		0.2882 (14.0 km/sec)

Mass Summary
(metric tons)

Reentry System (Retro-Rocket)		13.50
Life Support		7.81
Power Supply		0.68
Shielding		2.27
Structure & Equipment		2.50
Service Module		3.64
Contingency		2.27
	Chemical	Nuclear
Probes & Scientific Equipment	2.27	4.54
Midcourse Correction (Storable)	9.36	9.91
Escape Payload	44.3	47.1
Escape Propulsion	119.8	53.6
(Propellant)	(102.8)	(40.3)
(Inert)	(17.0)	(13.3)
Mass on Parking Orbit		
Retro-Rocket	164.1	100.7
Drag Brake (8.18)	141.5	88.2

Table 1-6

GRAND TOUR 1972

Minimum Trip Time 464 Days

	Julian Date	Calendar Date		EMOS
Lv ⊕	244 1540	11 Aug 1972		0.2377 (13.1 km/sec)
Ar ♀	1675	24 Dec 1972	r_p = 1.5	0.4165
Ar ♂	1932	7 Sep 1973	= 1.0	0.3100
Ar ⊕	2004	18 Nov 1973		0.3357 (14.9 km/sec)

MASS SUMMARY
(metric tons)

Reentry System (Retro-Rocket)	19.52	
Life Support	6.36	
Power Supply	0.68	
Shielding	2.27	
Structure & Equipment	2.50	
Service Module	3.64	
Contingency	2.27	
	Chemical	Nuclear
Probes & Scientific Equipment	2.27	4.54
Midcourse Correction (Storable)	10.45	11.00
	50.0	52.8
Escape Propulsion	266.0	91.9
(Propellant)	(234.5)	(73.1)
(Inert)	(31.5)	(18.8)
Mass on Parking Orbit		
Retro-Rocket	316.0	144.7
Drag Brake (9.41)	247.5	114.9

Table 1-7

THREE PLANET FLYBY

Trip Time 685 Days

	Julian Date	Calendar Date		EMOS
Lv ⊕	244 0835	6 Sep 1970		0.1577 (12.02 km/sec)
Ar ♀	0910	20 Nov 1970	r_p = 1.2	
Ar ♂	1080	9 May 1971	= 1.2	
Ar ♀	1380	4 Mar 1972	= 1.7	
Ar ⊕	244 1520	22 Jul 1972		0.1552 (12.00 km/sec)

MASS SUMMARY
(metric tons)

Reentry System (Retro-Rocket)		5.95
Life Support		8.68
Power Supply		0.68
Shielding		2.27
Structure & Equipment		2.50
Service Module		3.64
Contingency		4.54
Probes & Scientific Equipment		2.27
Midcourse Correction (Storable)		8.36
Escape Payload		38.9
	Chemical	Nuclear
Escape Propulsion	126.2	51.4
(Propellant)	(108.6)	(38.4)
(Inert)	(17.6)	(13.0)
Mass on Parking Orbit	165.1	90.3

Manned Orbital Capture. The analysis of short orbiting capture missions for Mars and Venus utilized the optimization technique of Ref. 1-2. A knowledge of this method and of the basic aid, the velocity contour charts, is presumed in the following discussion. There are several advantages to using this approach in the study of interplanetary stopover missions. First, for each conjunction or opposition year there is found a unique trip which will minimize the transportation system mass, and because of the procedure involved, this mass and any off-optimum mass will be known. A second consideration is that sufficient information is generated to permit comprehensive evaluation of alternatives such as: the year and planet for which the mission is scheduled, the penalties for shortening the trip duration, the effect of proportioning the outbound and homebound legs, and the importance of Julian date to estimate overall launch window requirements. Finally, by systematically exploring all the trip possibilities within the limitations of vehicle technology assumed, no promising trips will be inadvertently omitted.

With this general approach, mission requirement curves similar to those of Fig. 1-23 may be generated for each planet at the promising year. Only this figure is shown in its entirety for illustration. Usually, just the curves demonstrating lowest system mass, e.g., curve II-B, are used in the mission requirement studies.

In the investigation of Venus requirements, one combination of outbound and inbound regions (II-B, Fig. 1-23) was found to provide the lowest system mass on parking orbit for both the chemical and nuclear escape systems. This is expected to be valid for the 1970 and 1974 conjunctions due to the nearly circular and coplanar orbits of Venus and Earth. The mission requirements will vary but slightly with year. A comparison of the requirements for the chemical and nuclear systems is shown in Fig. 1-23, where also the favored regions are depicted by the miniature velocity contour chart. Note that if one is concerned with the overall effects of total trip time and further, it is required that each trip of a given duration be of optimum mass, then the regions I-A should not be considered. This may be observed from the figure where trip times between 250 and 600 days may be attained for minimum mass by following the curves

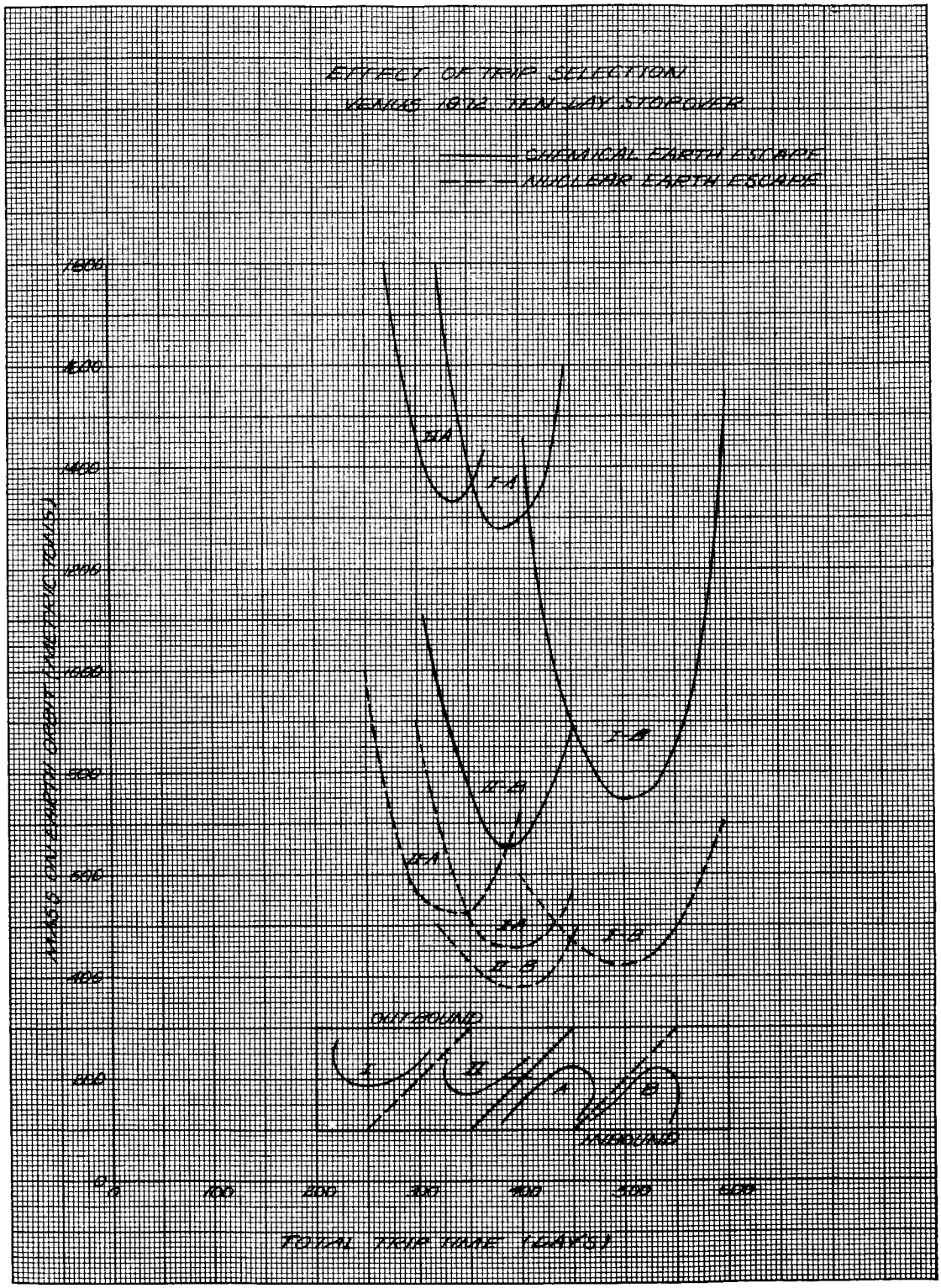


Fig. 1-23 Effect of Trip Selection Venus 1972 Ten-Day Stopover

II-A and I-B. Consequently, this indicates when to change regions, and hence, what the dates are for the optimum mass trip. It must be remembered that each curve is a locus of minimum mass points.

Complete trip information for each region may be plotted for either of the escape systems studied. Figure 1-24 presents such a graph for the II-B region in which the system uses chemical escape step. The Earth entry speed is not given in this figure as all the values encountered were well within the technological limit (50,000 fps) assumed for a drag brake in that year. The entry speed is a major factor to be considered in mission planning and trip selection. As will be seen later in the case of Mars, the entry limit is exceeded in most of the minimum mass trips.

Specification of Julian departure date, inbound leg duration and mission trip time uniquely determines the mission; and from the curves (Fig. 1-24), the required system mass becomes known. This type of display presents all the relevant information sufficient for initial planning purposes. Note that the inbound leg corresponding to a trip duration implies the proper division of the entire mission duration including the orbital stay time.

The conjunction of 1972 occurs on 18 June 1972 (2441486). Using the minimum mass point, the spacecraft leaves Earth at 2441415 with an inbound leg of 275 days and a total trip time of 384 days. Hence passage occurs at 2441514, which means that during the most communications dependent portion of the voyage, the distance between the spacecraft and Earth is essentially the distance to Venus at conjunction. Planetary capture occurring nearer conjunction is possible by selecting trips of lower trip time. For example, a trip of 340 days will produce an earlier arrival date by ten days, however, the reduction in communications distance is insignificant, in view of the much higher required system mass.

The desirable Mars stopover trips were discussed in the summary and the results presented in Fig. 1-10. In these cases, only those trips deemed favorable from a

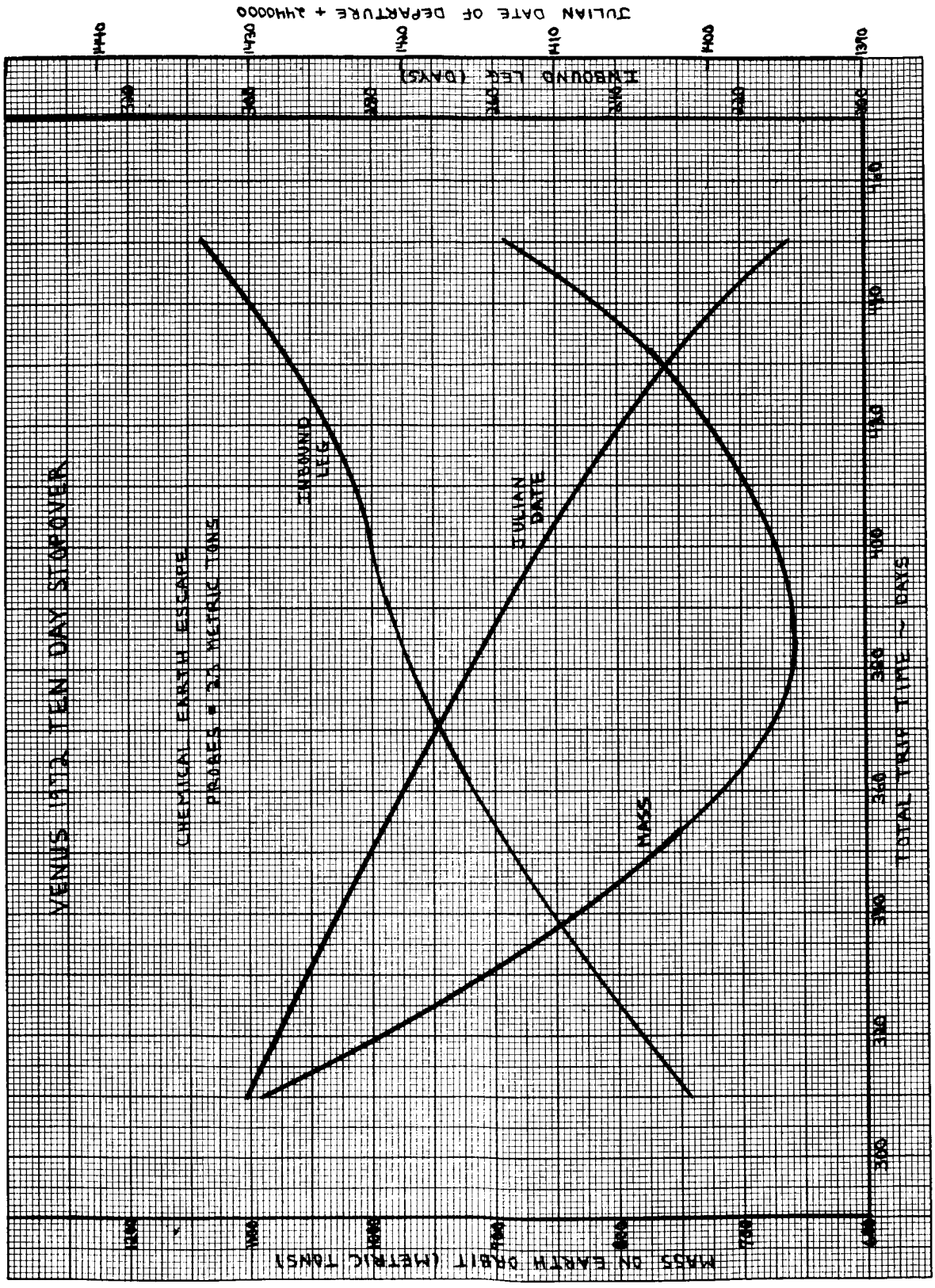


Fig. 1-24 Venus 1972 Ten-Day Stopover

mass-trip time standpoint were given as representative of the indicated opposition years. However, additional trip selection is available by considering other combinations of outbound and inbound regions (see Fig. 1-23, small velocity contour chart). The results are depicted in Fig. 1-25 for 1975 using the I-B and II-B regions which were found to yield the lower mass requirements.

In the case of the chemical escape system, the desirable trips are obvious. Comparing the two selected regions of 1975, it can be seen that II-B requires one-third less mass and 100 days less mission duration. One would reasonably expect this desirable set of trips to be applicable to the nuclear system. There is in this case, a saving of approximately 25 percent which can be obtained by increasing the trip time 100 days, thereby utilizing trips in the I-B regions. This noncoincidence of favorable trip regions between the two types of escape propulsion systems was found to occur only in 1975. It is expected that in the oppositions through 1980, wherein all the velocities are much higher, the difference between the regions for each of the escape systems will become greater. Notice that this phenomenon amplifies the point that trip selection for interplanetary stopover missions should be based on the integrated analysis of trajectory data and vehicle design technology.

A summary of the relevant mission data is presented in Fig. 1-26 for the 1973 opposition using a chemical escape system. The three parameters considered important for mission planning are trip time, mass requirements, and Earth entry velocity. Although the analysis initially assumed a maximum Earth entry velocity of 15 km/sec (50,000 ft/sec), it was discovered during the optimizing procedure that the velocities corresponding to the minimum mass trips are somewhat higher. Rather than redefine a new system for these higher velocities, it was felt in view of the promising results from the reentry system analyses that the current vehicle may be reasonable extended to a maximum of 18 km/sec (60,000 ft/sec). From Fig. 1-26 the entry speed corresponding to the overall optimum mass point is above 17 km/sec. This may be lowered to above 15 km/sec by choosing a trip requiring 370 days, but at the expense of increas- the mass requirements 20 percent. If further decreases in entry speed are sought,

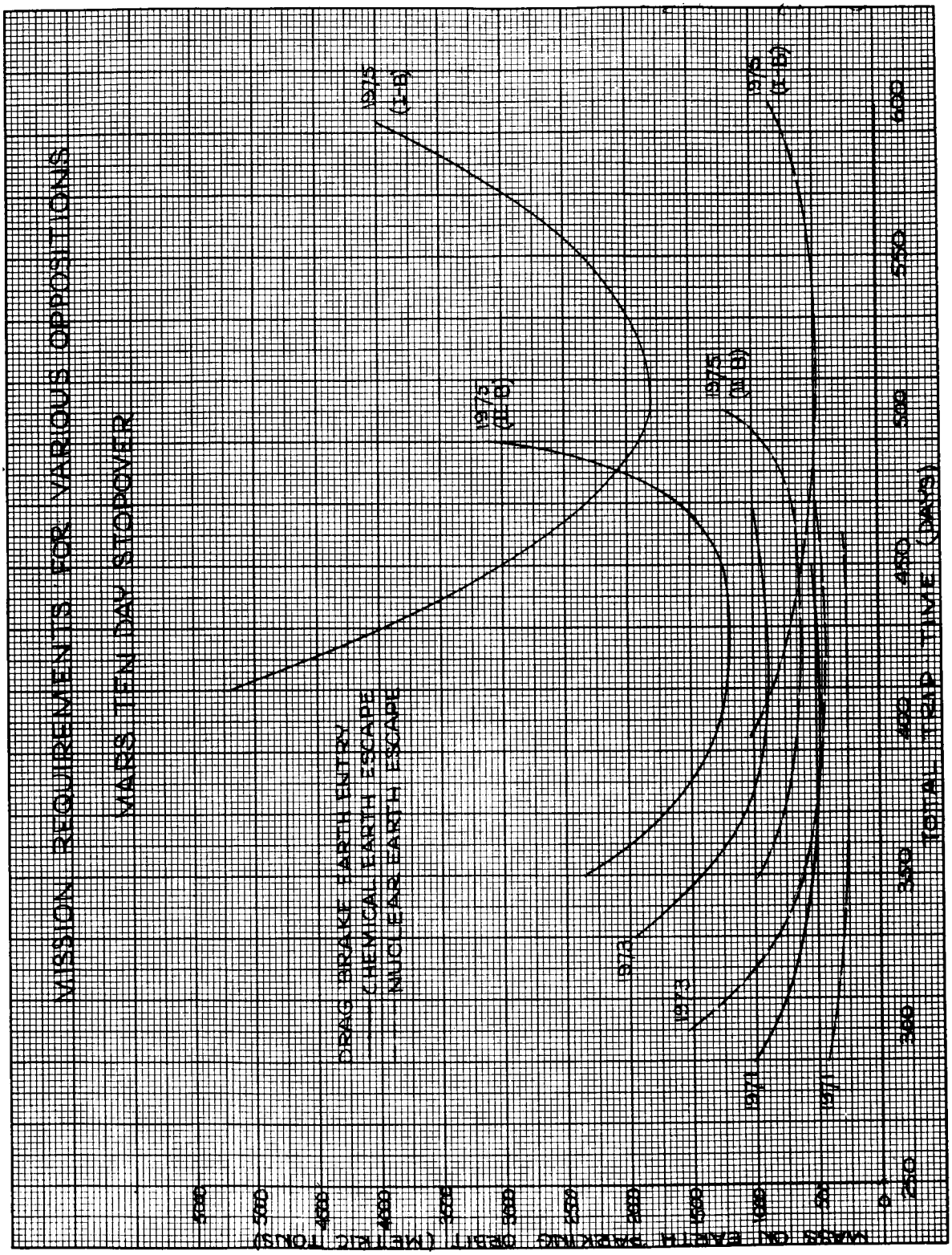


Fig. 1-25 Mission Requirements for Various Oppositions, Mars Ten-Day Stopover

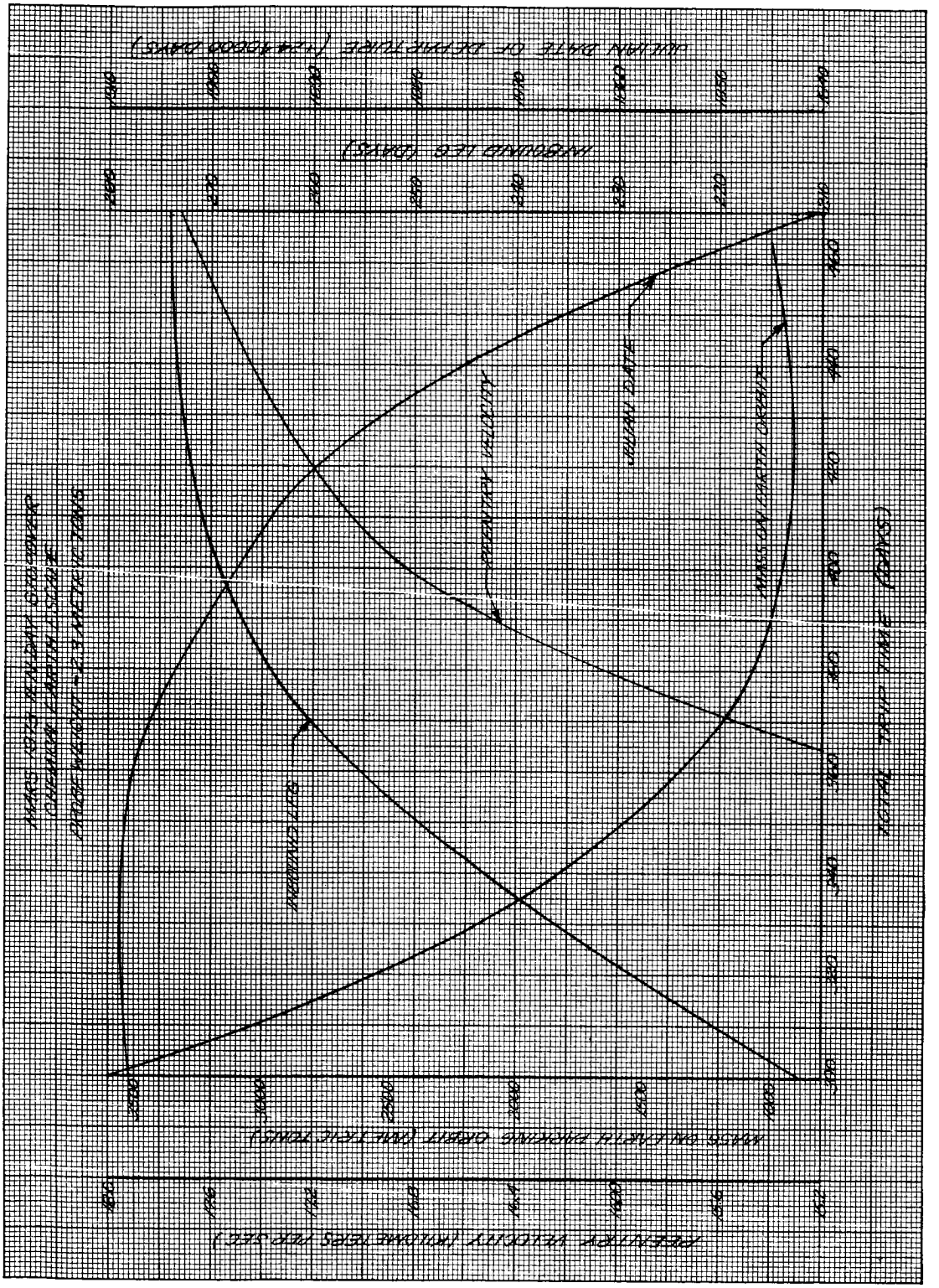


Fig. 1-26 Mars 1973 Ten-Day Stopover Chemical Earth Escape. Probe Weight 2.3 Metric Tons

the given mass curve (locus of minimum) must be followed; otherwise, even higher mass values than those indicated will result.

Optimum trips occurring in later years will require Earth entry velocities much higher than those of the earlier years, 1971 and 1973. Figure 1-27 shows this comparison between 1973 and 1975. From Fig. 1-10, the minimum mass trips for these two years occur at a trip time of about 420 days, regardless of the escape system used. The accompanying entry speeds are observed to be higher for the chemical system compared to the nuclear case, and further, the trips of 1975 are 15 percent higher in speed over the corresponding 1973 trips. Thus, not only do the trips in later years suffer in terms of mass required on orbit, but also in terms of the generally higher entry speeds which become even higher for the oppositions through 1980. Earth capture systems possessing capability beyond the aerodynamic braking technique will become of primary importance along with system mass, otherwise the "safe" but weightwise expensive approach must be used. This means applying the drag brake method as assumed here, but using shorter trip times, or by utilizing retro-rockets to absorb the additional velocity over the capability of the drag brake.

The stopover time of ten days selected for both the Venus and Mars mission was believed to be of sufficient length to perform all the experiments and observations necessary from the capture orbit. The effect of extended stay times was briefly investigated for the optimum chemical Mars trip of 1973. New optimum requirements were calculated for stopovers of up to two months, using the same inbound and outbound regions as determined in the 10-day case. The increase in transportation system mass on Earth orbit was found to be almost linear with stopover time, with, as expected, the nuclear system being least affected (Fig. 1-28). Staying over 60 days instead of 10 approximately doubles the mass requirements in the chemical case, whereas only a 50-percent increase is experienced in the nuclear system. It may be concluded that the system mass necessary for the various trips computed will not change significantly with orbital stay times between 5 and 15 days.



Fig. 1-27 Mars Ten-Day Stopover Reentry Velocity Requirements

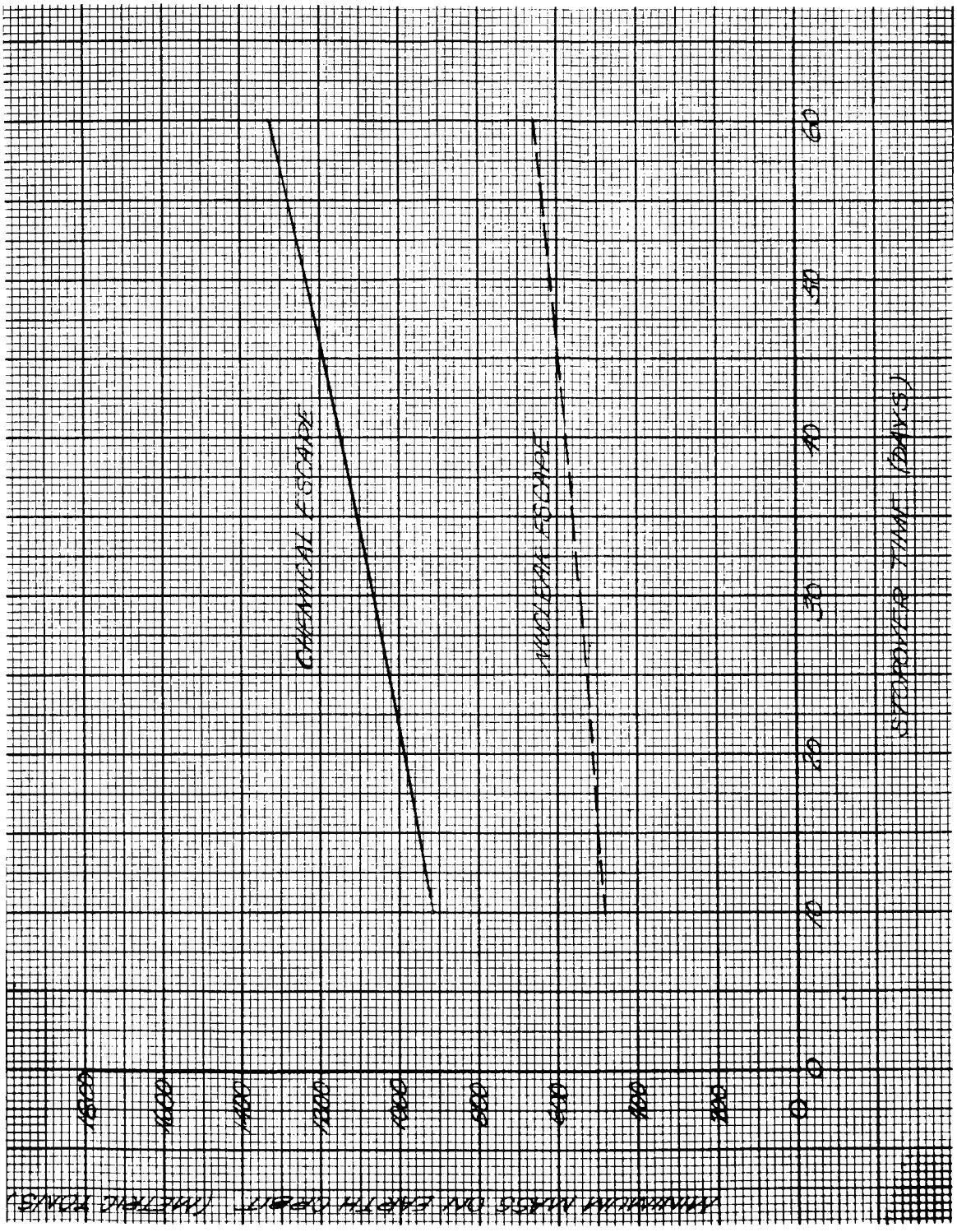


Fig. 1-28 Extended Orbital Stopover Requirements Mars 1973

A sample mission profile is depicted in Fig. 1-29 for a 1971 Mars 10-day stopover using a chemical escape propulsion system. This profile is typical of the trajectory executed in most of the promising stopover trips, regardless of year or system selected, although the actual speed and mass requirements will very markedly from mission to mission. The distance between Earth and the planet at the time of spacecraft capture is indicated and is seen to be reasonable for the heavy communications traffic expected at this time.

Phobos Stopover Missions. Mars' largest and closest satellite, Phobos, appears to offer certain advantages as a stopover station for the interplanetary vehicle. To identify the major requirements for such a mission, a preliminary investigation of a particular set of Mars orbital excursions was conducted. The mission was assumed to occur during the opposition of 15 December 1975.

Three types of stopover missions were considered and compared:

- Direct landing on Phobos
- Orbit 500 km above Mars – land on Mars
- Establish eccentric orbit about Mars – land on Phobos

In each case the same interplanetary trajectory from Earth to the vicinity of Mars was employed. With these constraints it is possible to establish preliminary propellant and drag brake requirements for comparison among these trips.

Comparative evaluation is made through the "remaining mass fractions" listed in Table 1-8. The term "remaining mass fraction" as used here refers to the percent of mass that is left after the expenditure or discarding of a portion of mass. The initial mass for each phase is the mass remaining after a previous use of propellant or discard of mass. All values listed in Table 1-8 are for remaining mass fractions after propellant has been used except when followed by the notation (Drag Brake).

A trajectory (Table 1-8) for use in this analysis was selected from the charts and computed data prepared at LMSC for round-trip excursions to Mars (Ref. 1-1).

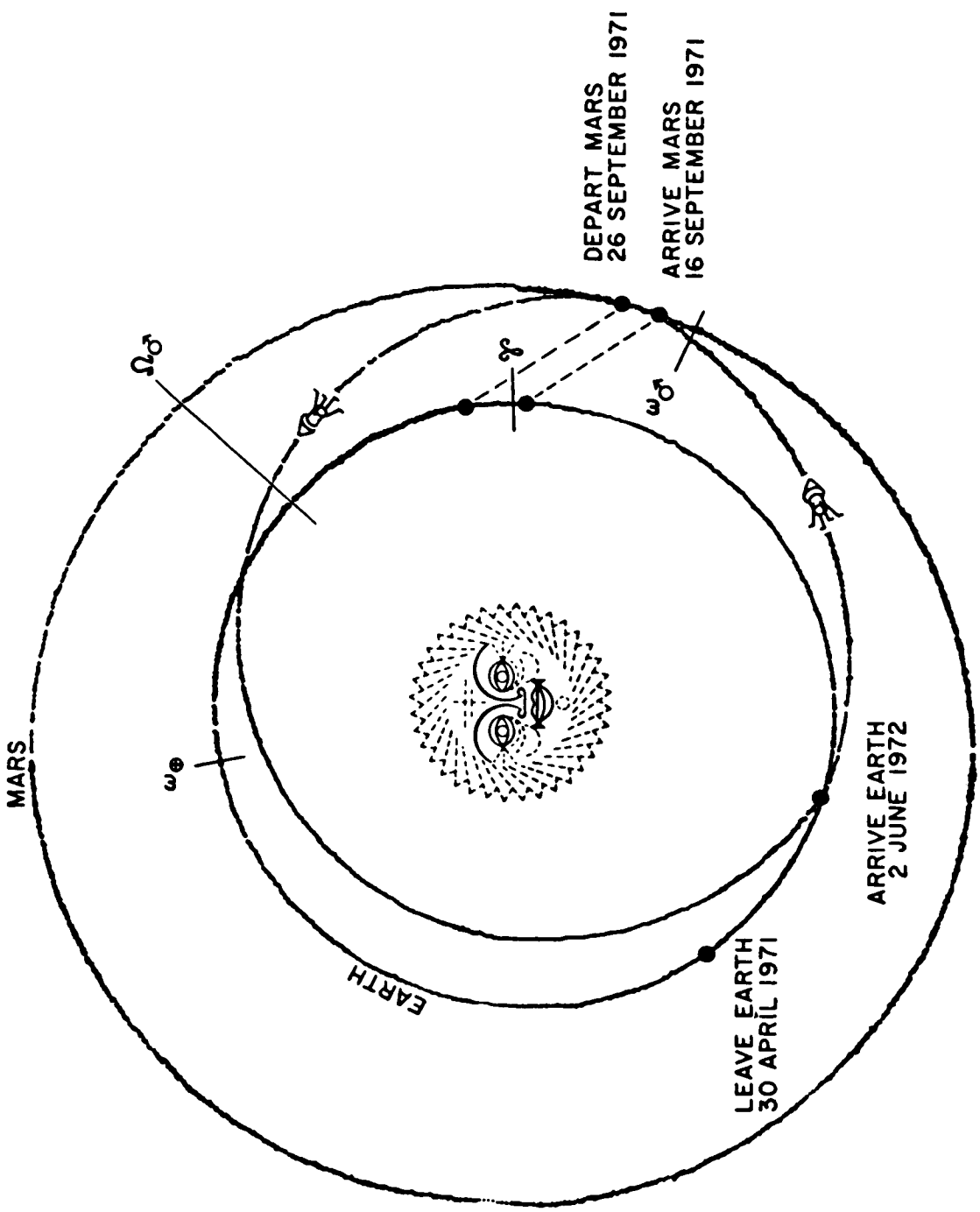


Fig. 1-29 Mars Capture Mission with Ten-Day Stopover

Table 1-8

1975 MANNED STOPOVER TRIPS TO MARS AND PHOBOS

TRIP		Julian Date	Cal. Date	Dur. Days	Total Days	V_{HE} (*EMOS)	V_p (km/sec)	Decl. (deg)	Remain. Mass Fraction	
CASE I	LV ⊕	2442410	12-29-74	–	–	0.4252	16.79	-20.63	0.120	
	AR PH	2660	9-5-75	250	–	0.2265	7.40	+ 1.67	0.200	
	LV PH	2670	9-15-75	10	–	0.1719	5.95	- 0.32	0.312	
	AR ⊕	2900	5-2-76	230	490	0.1349	11.81	-53.84	0.833	(Drag Brake)
CASE II	LV ⊕	2442410	12-29-74	–	–	0.4252	16.79	-20.63	0.120	
	AR ♂	2660	9-5-75	250	–	0.2265	8.35	+ 1.67	0.725	(Drag Brake)
	Circularize Orbit 500 km Above Mars								0.985	
	LV ♂	2670	9-15-75	10	–	0.1719	6.96	- 0.32	0.332	
	AR ⊕	2900	5-2-76	230	490	0.1349	11.81	-53.84	0.833	(Drag Brake)
CASE III	LV ⊕	2442410	12-29-74	–	–	0.4252	16.79	-20.63	0.120	
	AR ♂	2660	9-5-75	250	–	0.2265	8.35	+ 1.67	0.797	(Drag Brake)
	RENDEZ. PHOBOS	2660	9-5-75	–	–	–	–	–	0.850	
	LV PH & ♂	2670	9-15-75	10	–	0.1719	5.95	- 0.32	0.312	
	AR ⊕	2900	5-2-76	230	490	0.1349	11.81	-53.84	0.833	(Drag Brake)

*EMOS = Earth Mean Orbital Speed = 29.8 km/sec

The criteria by which the trajectory was chosen were that propulsion requirements at planetary approaches be minimized and that angles of declination at approach to and departure from Mars be small; if possible, equal to the inclination of the orbital plane of Phobos with respect to the equatorial plane of Mars.

Figure 1-30 depicts the arrival phase at Mars and Phobos of the three trips and pertinent data concerning them are tabulated in Table 1-8.

The chosen trajectory prescribes that the vehicle: (1) departs from Earth on Julian Date 2442410 (29 Dec 1974) at hyperbolic excess velocity of 0.4252 EMOS; (2) arrives in vicinity of Mars after 250 days with hyperbolic excess speed of 0.2265 EMOS with respect to Mars; (3) remains in vicinity of Mars for 10 days; (4) departs at hyperbolic excess velocity of 0.1719 EMOS with respect to Mars; and (5) arrives after 230 days in the vicinity of Earth with hyperbolic excess velocity of 0.1349 EMOS on Julian Date 2442900 (2 May 1976). The entire trip time is 490 days.

It is assumed in this analysis that Earth departure, arrival, and the interplanetary portions of the three trips are identical and that the only variations occur in the vicinity of Mars and Phobos.

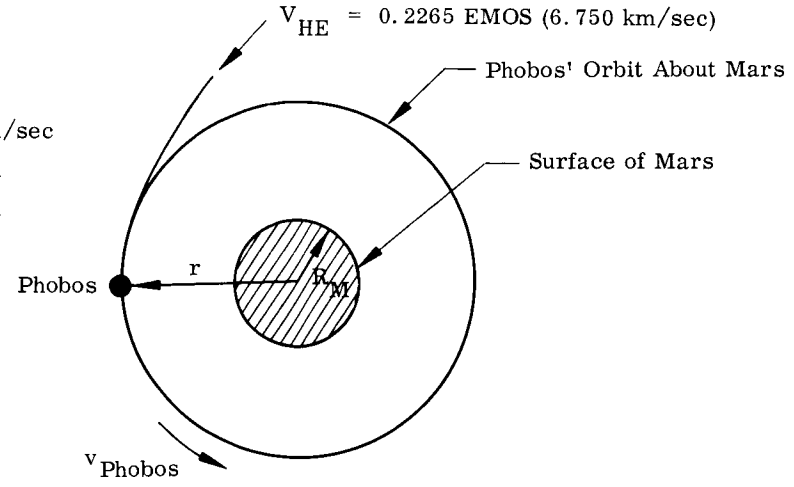
The hyperbolic pericenter velocity, V_p, is computed for each phase of each trip and is recorded in Table 1-8. It is defined by the equation,

$$V_p^2 = V_{HE}^2 + V_{Escape}^2$$

In each case the vehicle is assumed to depart from a 200-km parking orbit above Earth's surface with hyperbolic excess velocity of 0.4252 EMOS (12.67 km/sec). The velocity of escape from Earth at 200 km is 11.01 km/sec, therefore, on the outbound portion all trips will leave at the same departure speed of 16.79 km/sec.

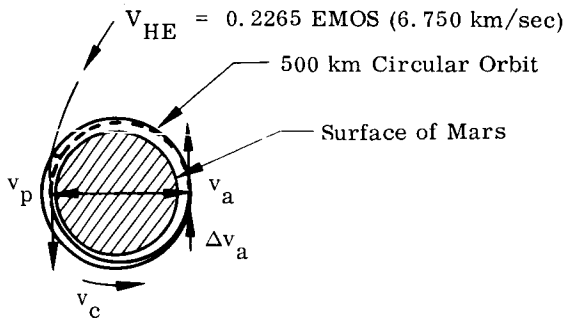
Case I

v_{Phobos} = 2.132 km/sec
r = 9,350 km
R_M = 3,375 km



Case II

v_c = 3.333 km/sec
r_p = 3575 km
r_a = 3875 km
v_p = 3.539 km/sec
v_a = 3.265 km/sec
Δv_a = 0.068 km/sec



Case III

r_p = 3575 km
r_a = 9350 km
v_p = 4.173 km/sec
v_a = 1.596 km/sec
v_{Phobos} = 2.132 km/sec
Δv_a = 0.536 km/sec

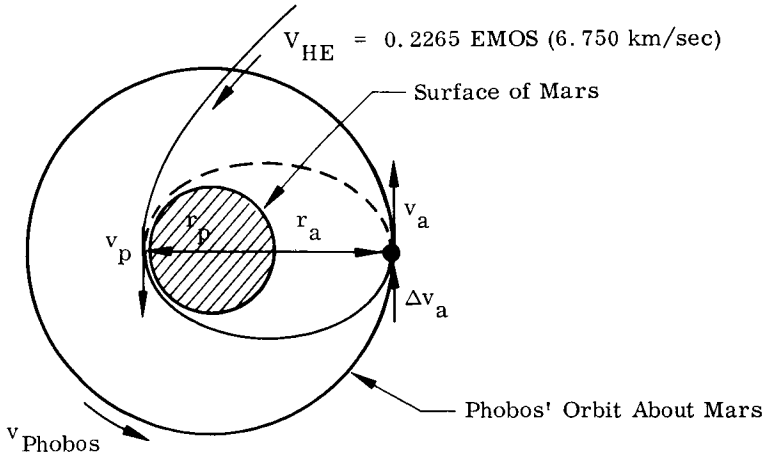


Fig. 1-30 Comparison of Arrival Conditions at Mars

At return to Earth the approach speed is 11.81 km/sec at 100 km. Adequate deceleration for reentry from this speed is possible by the use of an Apollo Drag Brake type of capture system at no mass penalty for propellant. However, it is estimated that the mass penalty for such a drag brake system is of the order of 20 percent of the mass being decelerated.

The orbital plane of Phobos is inclined at an angle of 0° 57' to the equatorial plane of Mars. The trajectory angles of declination of +1.67° at arrival and -0.32° at departure from Mars are assumed to differ negligibly from the required angle of 0° 57'; thus orbital plane change requirements were not included in this investigation.

In Case I the vehicle is assumed to make a direct landing on Phobos by "slipping" into the orbit of Phobos about Mars, so oriented as to require no plane change. To rendezvous with Phobos the velocity of the vehicle must be decreased from an approach speed of 7.40 km/sec to 2.132 km/sec, the orbital speed of Phobos about Mars. Retro-rockets are required to effect this change and if, as was assumed, the propellants are storable chemicals (I_{sp} = 333 sec), the mass fraction remaining after retardation will be 0.200 or only 1/5 of the mass of the vehicle that approached Phobos.

To return from Phobos the velocity must be increased to meet the trajectory constraint of an excess of 5.123 km/sec (0.1719 EMOS). Assuming that the vehicle leaves Phobos at 9,350 km from the center of Mars, Phobos' mean distance from Mars, the departure velocity will be 5.95 km/sec, the escape velocity is 3.015 km/sec and the additional increment required is 3.82 km/sec. The mass fraction remaining on hyperbolic orbit is now 0.312 as 68.8 percent of the mass leaving Phobos is consumed as propellant.

In Case II it is assumed that on approach to Mars the vehicle is decelerated to near-circular velocity by a drag brake and that a 500-km circular orbit is established. This maneuver is accomplished by decreasing the approach speed of 8.345 km/sec (0.2265 EMOS) to 3.539 km/sec at 200 km. The orbit now is an ellipse with periapsis at 200 km and apoapsis at 500 km above the surface of Mars. The drag brake required

to effect the necessary velocity change is approximately 27.5 percent of the total mass approaching Mars. At 500 km the elliptical velocity is 3.265 km/sec and the circular velocity is 3.333 km/sec; 1.5 percent of the remaining mass on orbit will be required to circularize the orbit by the addition of a velocity increment of 0.068 km/sec.

To leave the circular orbit at 500 km and have hyperbolic excess velocity of 5.123 km/sec (0.1719 EMOS), the departure speed with respect to Mars is 6.961 km/sec; the circular and escape velocities are respectively 3.333 km/sec and 4.713 km/sec. To provide the needed additional velocity, 66.8 percent of the mass leaving the orbit will be required as propellant leaving a mass fraction on hyperbolic orbit of 0.332.

In Case III, the vehicle is assumed to be decelerated aerodynamically also, but to a velocity that permits the establishment of an elliptical orbit about Mars with periapsis at 200 km and apoapsis at 6,040 km above the surface. This latter number corresponds to the mean distance of Phobos from the center of Mars of 9,350 km. The drag brake penalty in this case is 20.3 percent of the mass. At 6,040 km a velocity increment of 0.536 km/sec is supplied to effect rendezvous with Phobos on its orbit about Mars. The propellant required for this maneuver is 15 percent of the mass on elliptical orbit thus there is a remaining mass fraction of 0.85 to land on Phobos. The return from Phobos to Earth will be identical to that described for Case I.

From this preliminary investigation the following conclusions are apparent.

- Direct retro-rocket landings on Phobos require excessive propellant, and precise timing of arrival of the vehicle to permit rendezvous with the satellite.
- Preliminary drag brake capture in an eccentric orbit about Mars permits sending unmanned one-way probes to the surface of Mars, leaving unmanned capsules in parking orbit around Mars, and landing manned vehicles on Phobos with very little retro-propulsion and easy rendezvous.

- Returning to Earth from Phobos and from a Mars 500-km parking orbit require approximately the same propulsion capability.
- The manned landing on Phobos in a typical case requires 13 percent more propellant mass at Mars than stopping in a parking orbit at Mars. However, landing on Phobos requires much less propulsion capability than landing on Mars, unless water is found on Mars.

Martian Orbit Lifetimes and Perturbations. Many manned interplanetary missions now envisioned require that the interplanetary space vehicle be placed in a parking orbit around the alien planet while the voyagers glide to the surface of the planet in a landing craft, complete their exploration, and return to the mother-ship in the parking orbit. The altitude of the parking orbit must be great enough to give the mother-ship a lifetime in orbit sufficient for the surface mission to be completed and the explorers returned before orbital decay becomes excessive. This lifetime is affected mainly by the atmospheric drag on the orbiting space vehicle. Therefore, some knowledge of the atmospheric density at various altitudes is necessary. In this study approximate Martian atmospheric density-altitude models were used to produce approximate figures on Martian satellite orbit lifetimes.

More is known about Mars than any other of our neighboring planets, but the information remains scarce and varied. Four different atmospheric models are presented and two are used to calculate orbit lifetimes. Earth's density model is presented for comparison.

Yanow Model. The first density model is due to Gilbert Yanow (Ref. 1-4) and is based on a proposed photochemistry of the Martian ionosphere. The Yanow model uses the following assumptions: The Martian atmosphere is composed of 95 percent N_2 and 5 percent CO_2; the surface density is 1.94×10^{-4} slug/ft^3; the surface temperature is 273°K; the ionospheric photochemistry is based on two body molecular recombination.

The method of analysis was to consider the Martian atmosphere completely insulated from radiation so that only molecular carbon dioxide and nitrogen would exist. This insulated atmosphere was assumed to be isothermal and to follow the customary density relation:

$$\rho = \rho_o \exp\left\{ - \frac{mg_o}{kT} \cdot \frac{ah}{a + h} \right\}$$

where

ρ_o = surface density

m = mean molecular mass of gas

g_o = surface acceleration of gravity

k = Boltzman constant

T = Absolute temperature

a = radius of the planet

h = altitude above surface

Solar radiation was then introduced and the density distribution, as given by the above relation, was assumed to be the only criterion for the possible photochemical reactions. The resulting reactions caused the temperature in the particular density layer to change and the perfect gas law was employed to calculate the new density assuming only the temperature had changed. The entire calculation of the photochemistry was repeated based on the new density. Energy transmitted to the next lower density increment was used to calculate the photochemistry of this layer. This iteration process was used to numerically integrate the model from 650 km to 250 km.

Mr. Yanow admits that the results are preliminary and the data speculative, but the analysis appears plausible. The results do suggest the existence of a multi-layered, high altitude Martian ionosphere.

Extreme Model. The second model was designed to be the maximum density profile for the Martian atmosphere. The model was fashioned after the Earth's profile with the largest gradient of slopes that seems plausible. Both the ratio of the gravitational acceleration of Mars to that of Earth, and the ratio of the slopes of the Rand model (Ref. 1-5) and the Yanow model to the slope of the Earth are examined to find the largest gradient of slopes.

Comparing only the gravitational accelerations of the two planets indicates that the slope of the Earth model should approximately be 2.6 times the slope of the Martian model. Comparing the slope of the Rand model (which is the same as the slope of the Yanow model extrapolated to surface conditions) and the slope of the low altitude straight line portion of the Earth model indicates that the slope of the Earth model should be approximately 3.0 times the slope of the Martian model. Therefore, the extreme model was constructed with a slope one third that of the Earth model at the same density level.

Rand Model. The third model is extrapolated from a curve given in a Rand Corporation Report (Ref. 1-6). This model extends only to an altitude of 50 nautical miles and extrapolation to the area of interest at several hundred miles altitude was not used for orbit lifetime calculations.

1959 ARDC Earth Model. The fourth model is a plot of the 1959 ARDC Earth Atmospheric model (Ref. 1-7) which is presented for comparison with the various Martian models. This model also helps in the construction of the extreme Martian model for the orbit lifetime calculations.

Schilling Model. The fifth model is due to G. F. Schilling of the Rand Corporation (Ref. 1-8). This report was designed for the purpose of studying deceleration and heating during atmospheric entry and is concerned with lower altitudes than are useful for orbit lifetime calculations. Schilling proposed both an upper and lower limit and stated that the reliability of enclosing the Martian atmospheric model between his two limits is due chiefly to their wide extremes. Although no quantitative statements may be made, it can be said that qualitatively the extension of the Schilling upper limit model agrees quite well with the high altitude extreme model proposed above.

Comparison of Models. Figure 1-31 shows all the models for comparison. It can be seen that a small extrapolation of the Yanow profile causes it to cross the Earth model at an altitude of approximately 650 km. Although the lower limit model proposed by Schilling follows the Earth profile rather closely, it is believed that the higher altitude Yanow model approaches the minimum density limit. The actual Martian atmosphere is believed to lie somewhere between the Yanow model and the extreme model, and probably the actual case is nearer to the extreme than to the Yanow model.

Orbital Lifetime Calculations. Based on the two most probable models, calculations of the orbit lifetime and rate of decrease of orbital period were made for various orbit eccentricities and perigee altitudes. Also, the periods of the respective orbits were calculated. The results of these calculations are presented in graphical form.

The total number (N) of orbital revolutions completed before the satellite encounters the planetary surface is given by

$$N = \frac{B}{a_o \rho(h_p)} \quad \frac{f(\beta)}{4\pi k a_o}$$

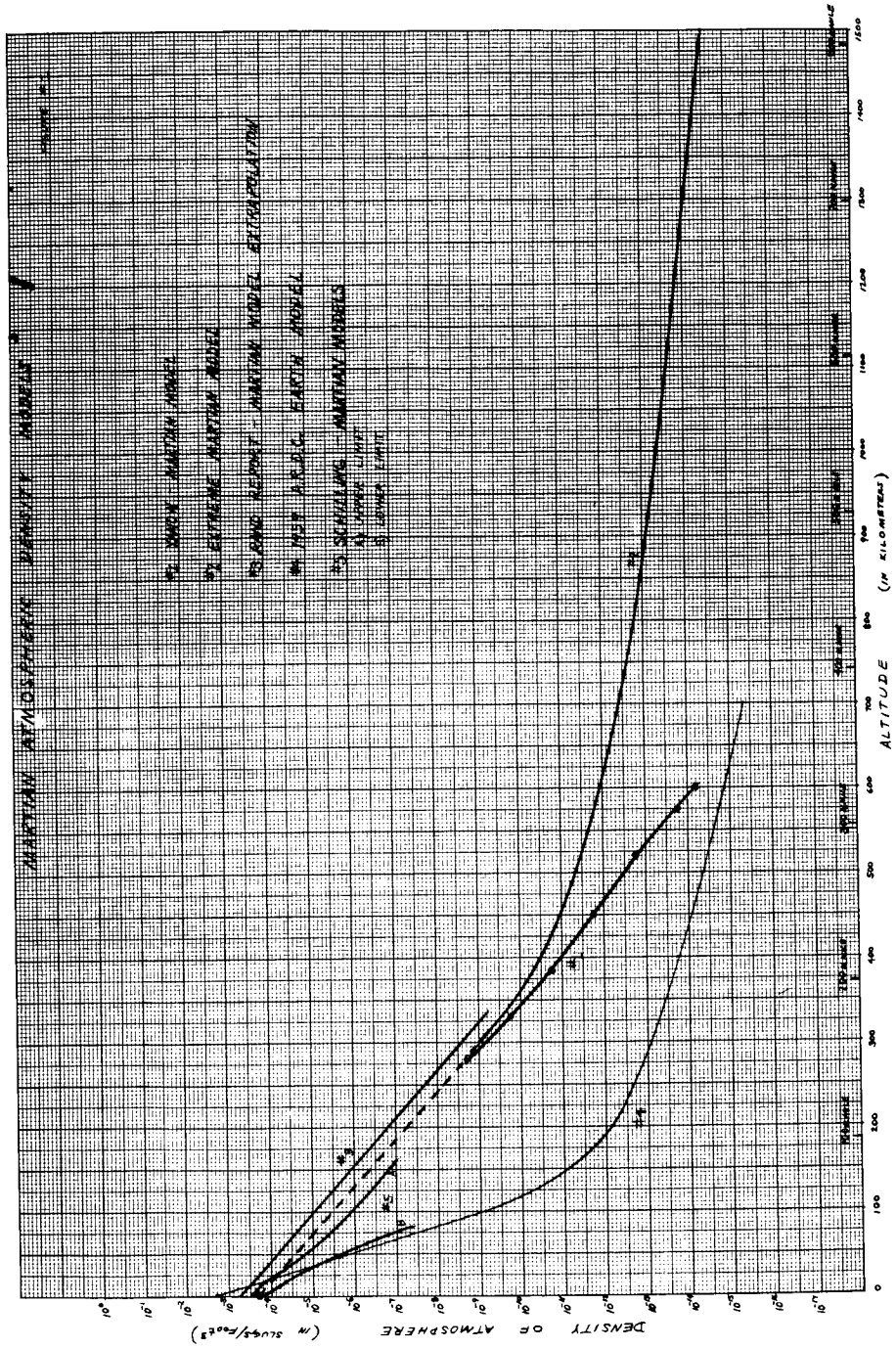


Fig. 1-31 Martian Atmospheric Density Models

where

$B = 1/2(C_D A/M)$ satellite drag function

M satellite mass

C_D satellite drag coefficient

A reference projected area of satellite

a_o initial semi-major axis of orbit

(h_p) atmospheric density at initial perigee altitude h_p

$$f(\beta) = \frac{\beta \epsilon^{\beta}}{2I_o(\beta)}$$

$\beta = a_o ek$

$I_o(\beta)$ modified Bessel function

$$k = -\frac{d}{dh}(\ln \rho)$$

e initial orbit eccentricity

The above equation for N was derived under the assumption of a constant k, but it may be shown (Ref. 1-9) that the relation may be more generally used if k is taken to be the actual value in the region of the initial perigee altitude. Figure 1-32 presents a graphical comparison of the lifetimes resulting from use of the Extreme Martian and Yanow atmospheric models. Figure 1-33 shows the periods of the orbits in the range of consideration. A gravitational constant of 4.2617×10^3 km^3/sec^2 and a planetary radius of 3408 km was assumed.

Discussion of Results

It is easily seen that the different density models have a great effect on the orbit lifetimes. At an altitude of four hundred nautical miles, for example, the Yanow model atmosphere would give a satellite in a circular orbit a lifetime of approximately one

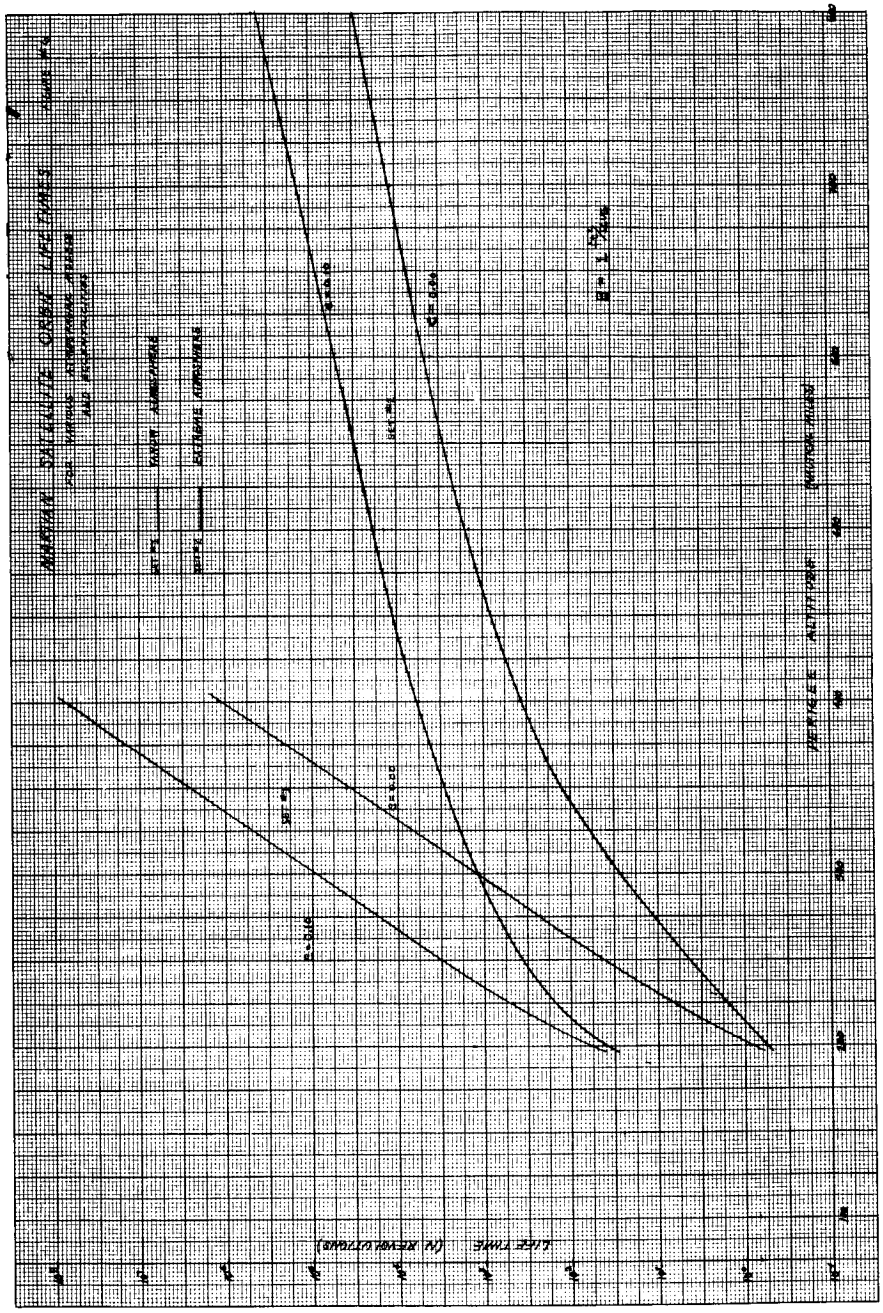


Fig. 1-32 Martian Satellite Orbit Lifetimes

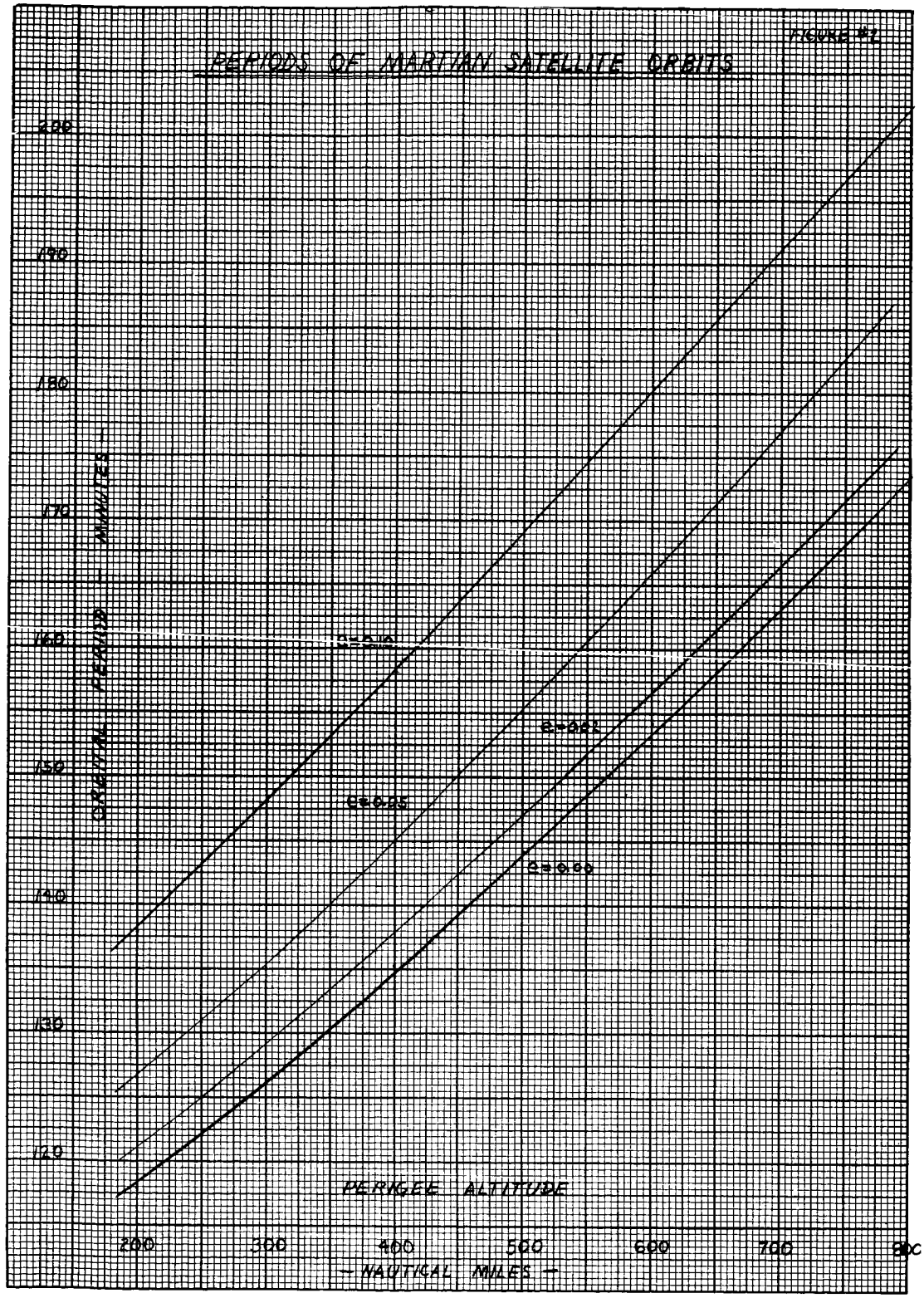


Fig. 1-33 Periods of Martian Satellite Orbits

million revolutions while the Extreme atmosphere results in a lifetime of approximately four hundred revolutions. All the results in this report were calculated using a satellite drag function of one square foot per slug. $B = C_D A/2M = 1\ ft^2/slug$. If the actual satellite drag function differs from one square foot per slug, the lifetime of the actual satellite may be found by dividing the respective quantities from the graph by the actual satellite drag function.

The orbital period calculations indicate that for a given altitude the period of the Mars satellite is 1.25 times the period for an Earth satellite.

The entire reliability of the orbit calculations depends on the choice of the atmospheric density profile. The results of this study may easily be in error by several orders of magnitude. Calculations of this type will remain speculative in nature until more accurate information is available on the high altitude properties of the atmosphere of Mars.

Orbital Perturbations of Martian Satellites. In the analysis of orbit operations about Mars, it will be essential to account for the effects of the perturbations on the orbit by the planet. Calculations of these perturbations to a first order of magnitude were made and the results are presented in the following figures.

The calculation of the rotation rate of the line-of-apsides was made using the equation

$$\frac{d\omega}{dN} = \frac{2\pi J R^2}{a^2\left(1 - e^2\right)^2}\left[2 - \frac{5}{2}\sin^2(i)\right]$$

while the equation

$$\frac{d\Omega}{dN} = -\frac{2\pi J R^2}{a^2\left(1 - e^2\right)^2}\cos i$$

resulted in the nodal regression rate, where

- R Equatorial radius of Mars (1830 nm)
- e Eccentricity of orbit
- a Semi-major axis of orbit
- J Coefficient of second harmonic in gravitational potential (2.925×10^{-3})
- i Inclination angle of orbit plane

Orbital eccentricities ranged from 0 to 0.5. An orbit with periapsis at 300 nm and apoapsis corresponding to the orbit of Phobos results in an eccentricity of approximately 0.4.

The results of these calculations are presented in Fig. 1-34 through 1-36. Figure 1-34 shows the rotation rate of the line-of-apsides for given elliptic orbits all with a 300 nm periapsis. Figure 1-35 shows the nodal regression rates of eccentric orbits for a 300 nm periapsis. Figure 1-36 presents the nodal regression rates of circular orbits at various altitudes as a function of orbit inclination.

1.4.5 Computer Program

The machine program used in all of the mission analysis studies performs detailed computations of escape step sizes, heliocentric payload, life support requirements, midcourse propulsion and transportation system mass. The program is sufficiently flexible to allow analysis of trips to both Mars and Venus which employ either a nuclear or a chemical Earth escape system. These trips may be either flyby missions or orbiting stopovers at the destination planet. The option is available in either type of mission for including an instrumented probe which is to be released at the planet. Each value for such a probe, of course, will result in a separate transportation system computation and hence, a different value of required mass on parking orbit.

Figures 1-37 and 1-38 illustrate the flow chart for the computer program in its entirety. The various choices which are inputs to the program are listed in the Decision Data box.

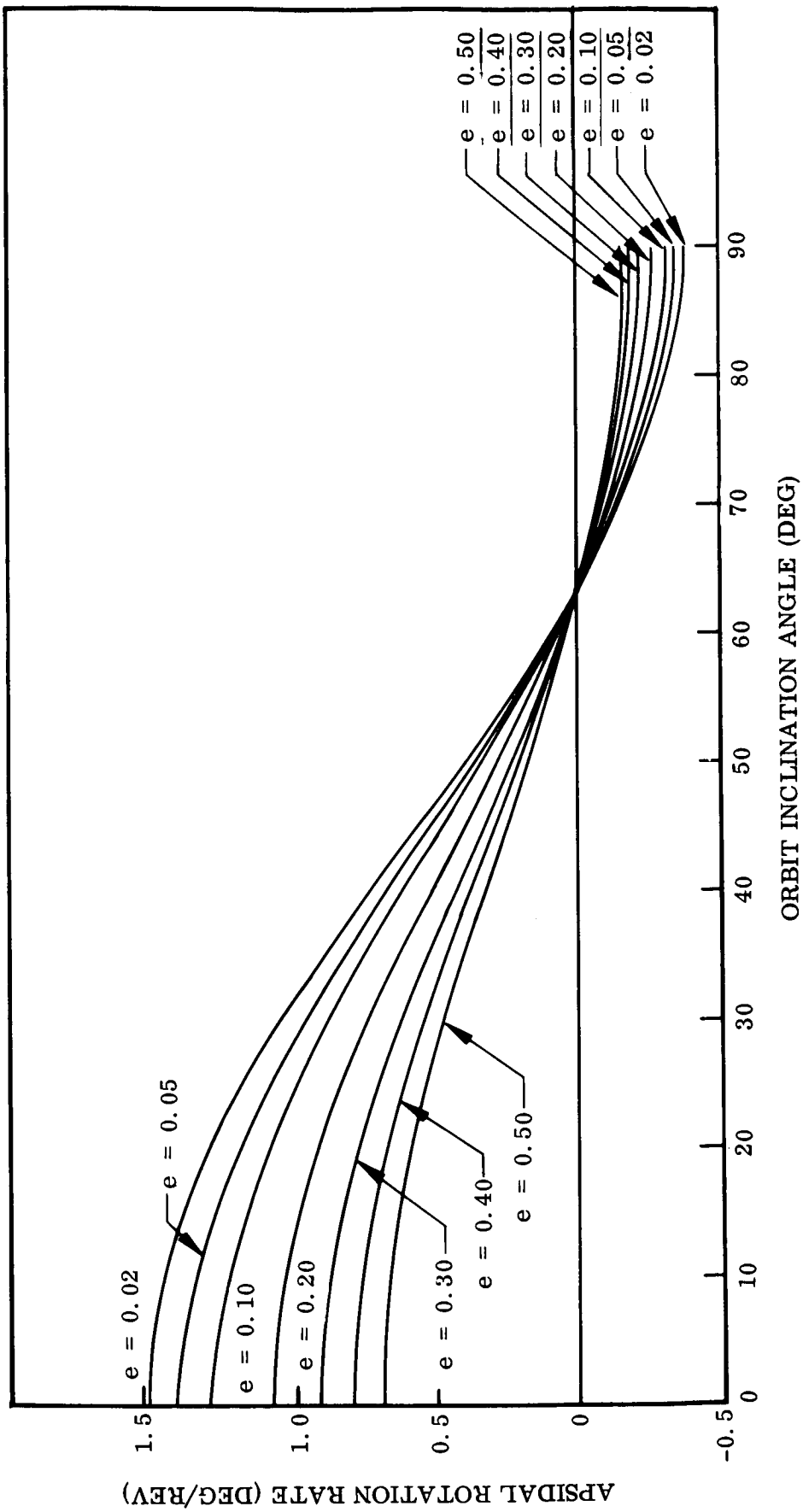


Fig. 1-34 Rotation Rate of Line-of-Apsides for Elliptic Orbits Around Mars, 300 nm Periapsis Altitude

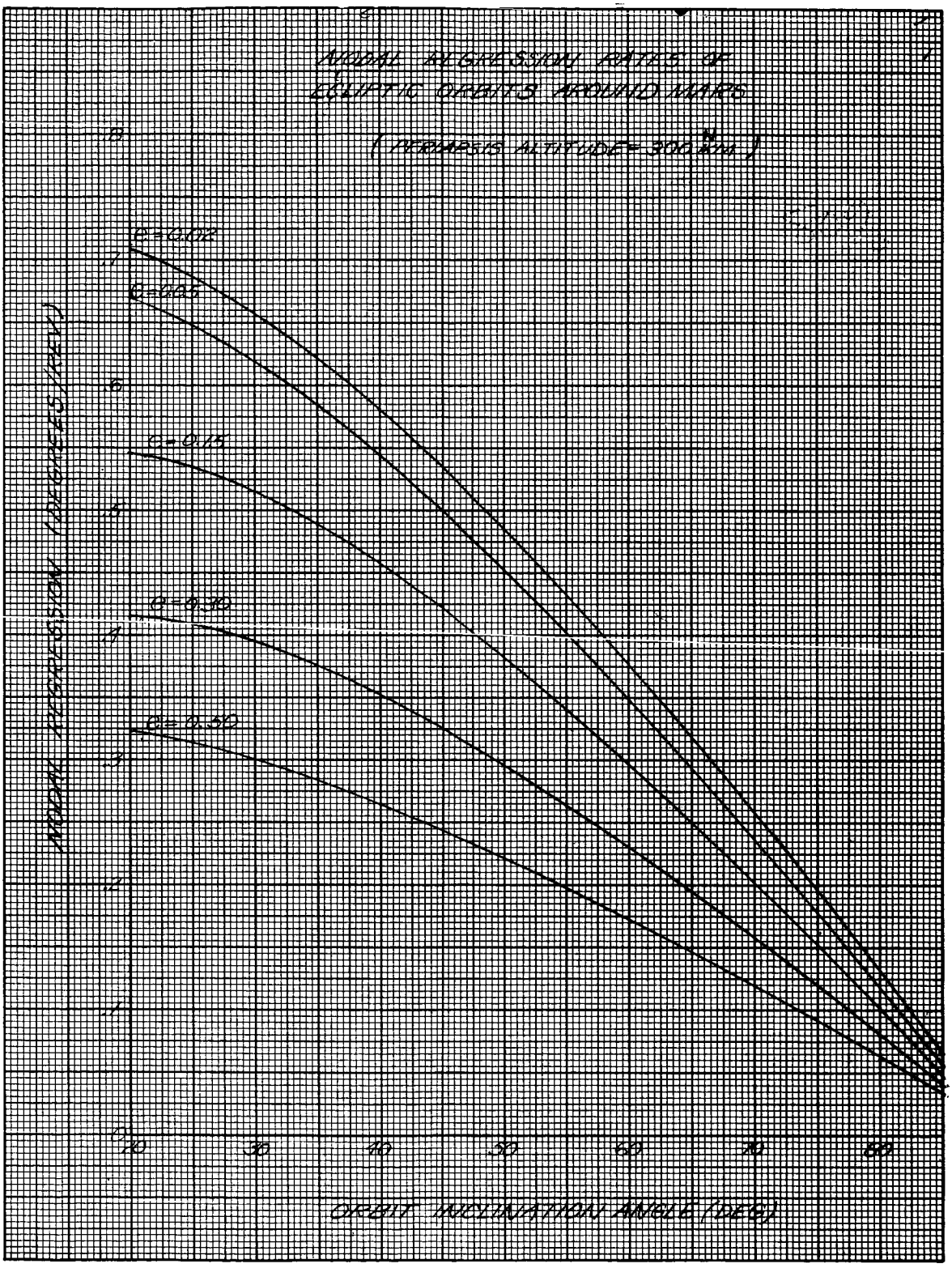


Fig. 1-35 Nodal Regression Rates of Elliptic Orbits Around Mars

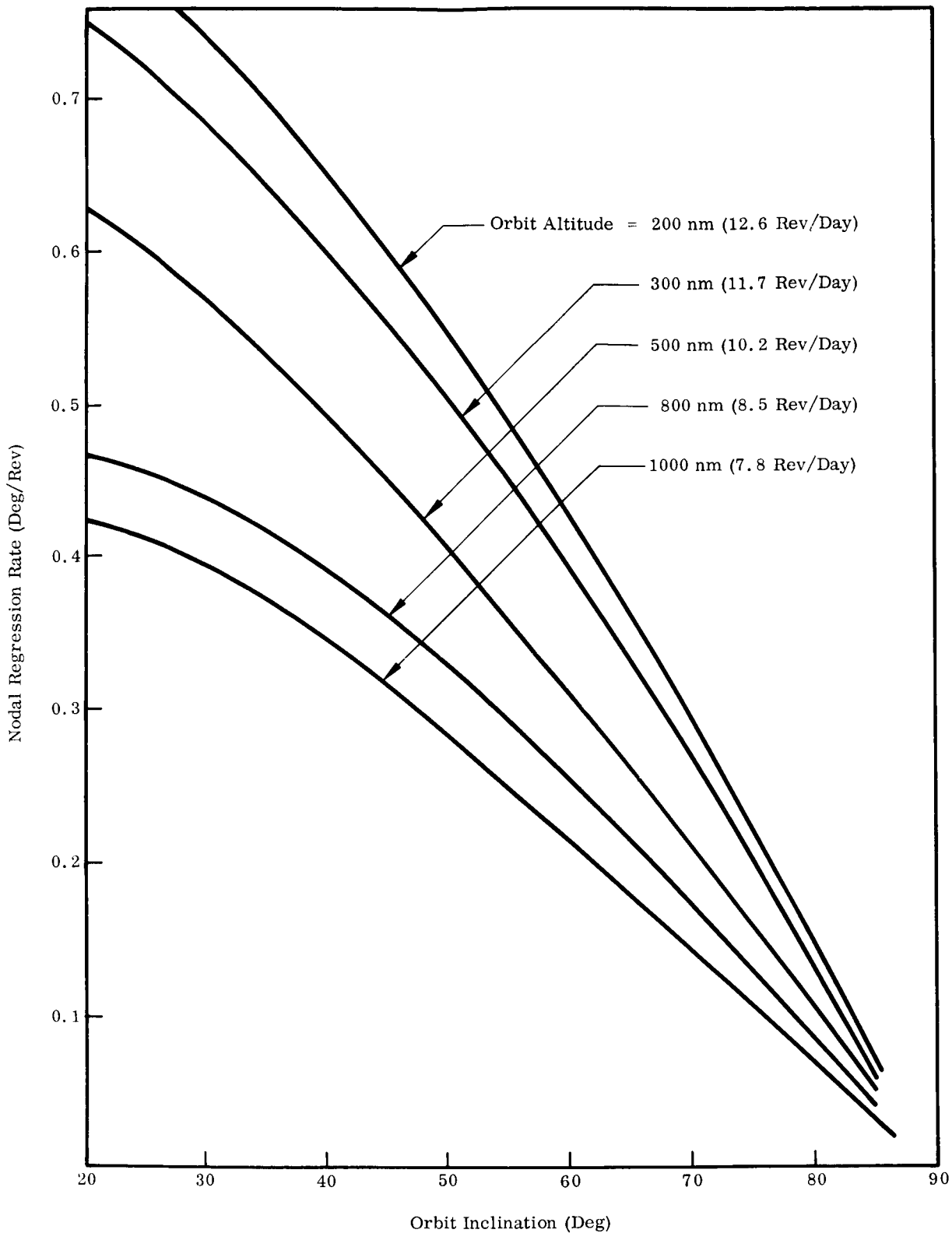


Fig. 1-36 Nodal Regression Rate for Circular Orbits Around Mars

The equations for the drag brake and retro-rocket Earth entry systems and the drag brake at the planets are fitted curves to data from the entry system analyses. A brief analysis of the inert weight requirements for each propulsion step established the relationship of structual factor (ratio of step inert weight to step loaded weight) to the weight and type of impulse propellant. It is these equations that are used in the Iteration Process for estimating the size of the propulsion step. The weight of the life support system was assumed to be linear with trip time between the values actually estimated for 330 and 550 days. Since a semi-closed ecology system was assumed, allowance was made for loss in mass due to waste and leakage dumped overboard.

The essential trajectory parameters required for the program include the Julian dates of departure from Earth, arrival and departure (or passage) at the planet, arrival at Earth, and the corresponding hyperbolic excess velocities for each event. The passage distance for flyby missions is included for easy reference in the mission printout. For any mission, either a drag brake system or retro-rocket system can be chosen as the Earth entry mode. The mass of the basic mission module may be changed through the use of a contingency allowance which is added directly to the module.

In the resultant analysis of a mission, a single transportation system appears on each printout page. This includes a detailed presentation of the trajectory parameters, vehicle subsystem weights, and propulsion systems data. Each such system is clearly identified with the destination planet, opposition year, type of trip (non-stop or stopover), the duration of the trip, and the value of the probe or landing weight. The trajectory is completely identified in overall terms by the Julian dates, the hyperbolic excess velocities in both feet per second and in EMOS, the orbit altitude leaving and arriving Earth, the orbiting or passage distance at the planet, and the incremental velocities leaving Earth and the planet.

The resultant transportation system mass on Earth orbit is listed for both the nuclear and chemical escape systems. A major breakdown of the vehicle mass is given which includes the reentry system, life support, basic mission module, probe or landing

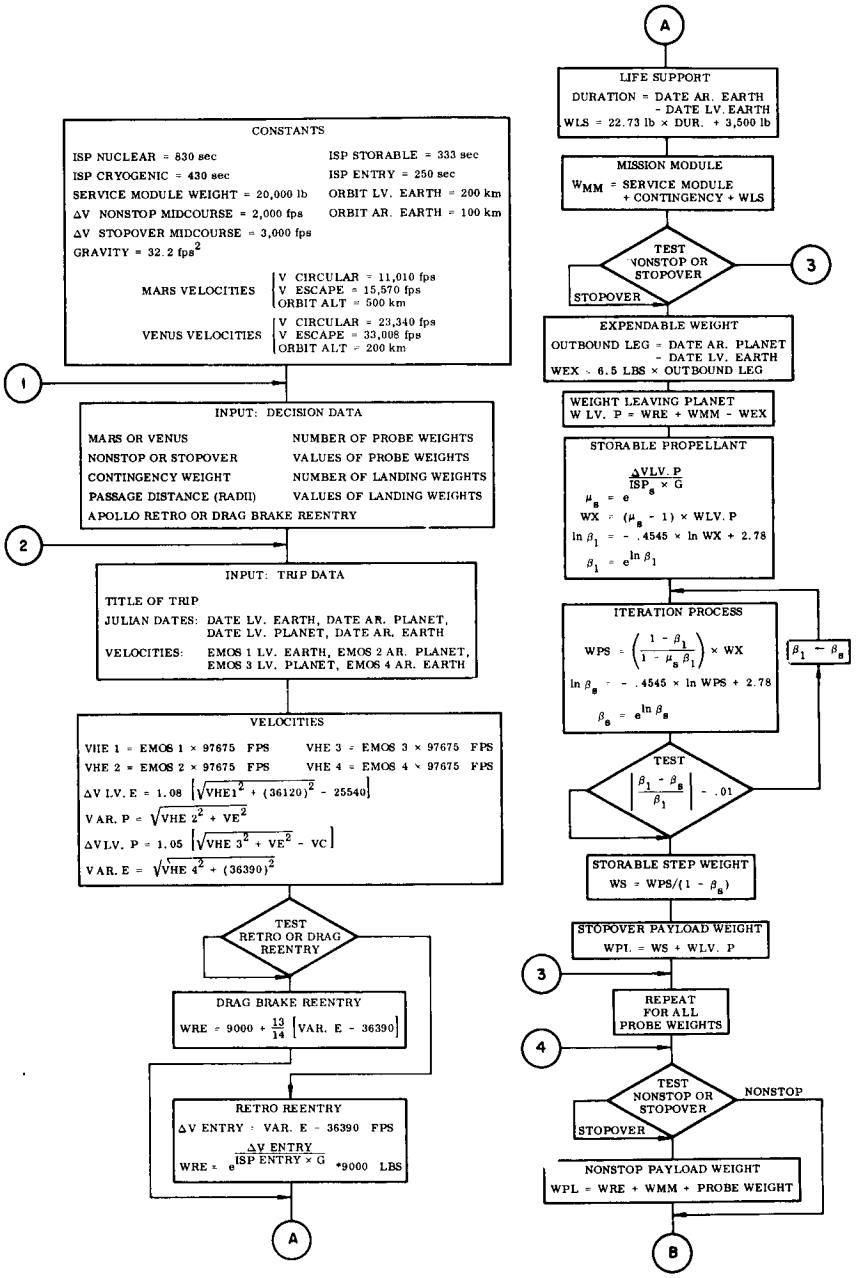


Fig. 1-37 Flow Chart of Mission Analysis Computer Program

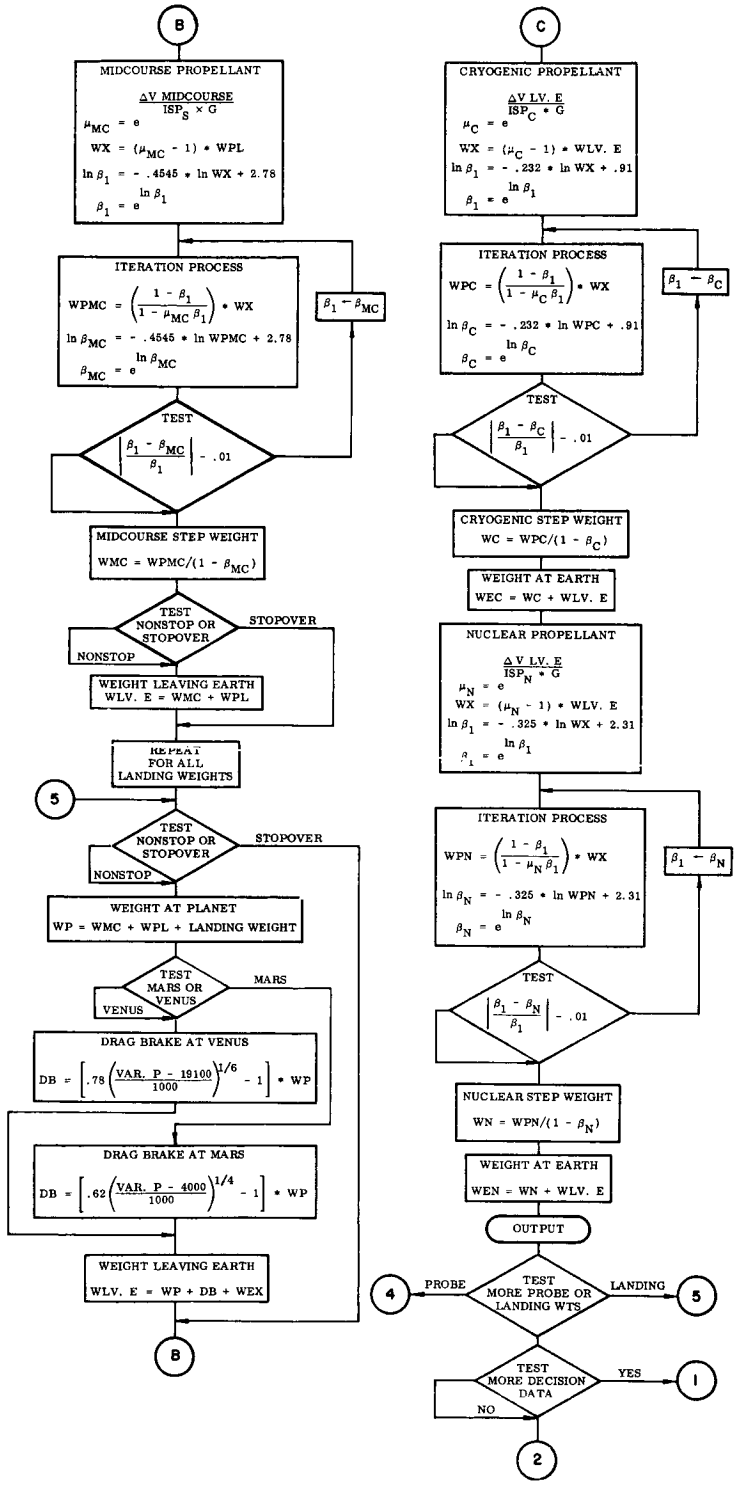


Fig. 1-38 Flow Chart of Mission Analysis Computer Program (Cont'd)

package, and the payload injected onto the heliocentric transfer trajectory. For the stopover missions, the mass placed on the planetary parking orbit is listed. The propulsion parameters used in sizing the stages of the midcourse, storable, nuclear and chemical systems are also given. Included in this list are the step weights, propellant weights, structural factors and mass ratios of the four systems.

The formulation of this machine program is based entirely upon the transportation system design assumptions discussed in the Technical Approach. The sequence of operations delineated above is determined solely by the objective of estimating the mass of the vehicle system required on Earth orbit for each choice listed in the Decision Data. Thus the program, although appearing to be quite flexible in terms of the options available, is somewhat restricted because of the basic transportation subsystem makeup. If totally different or exotic systems were employed so as to change this basic makeup, then of course the program parameters are computational sequence would have to be rewritten.

The relationships between each subsystem and their final effect on the overall system mass was assumed continuous with the varying input conditions. Only in a general overall sense is this true, and insofar as machine computation is concerned such assumptions are necessary. Obviously, if an attractive trip were identified and further information is required on the vehicle system design, a "point" design investigation would be necessary. Further one must remember, as pointed out previously, that in this study best trips are established by the required system mass, and if systems "radically" different from those assumed here are introduced, the best trips themselves will change. This is indicated to some extent by the comparison between chemical and nuclear escape propulsion stages.

REFERENCES

1-1. "Interplanetary Trajectory Handbook," to be released as a NASA Technical Note approximately April 1963. Work performed by LMSC for Marshall Space Flight Center under NASA contract NAS 8-2469

1-2. R. V. Ragsac and R. R. Titus, "Optimization of Interplanetary Stopover Missions," ARS preprint No. 2725-62. Presented to 17th Annual Meeting, American Rocket Society, Los Angeles, Calif., Nov 1962

1-3. S. E. Ross, "A Systematic Approach to the Study of Nonstop Interplanetary Round Trips," Presented to 9th Annual Meeting, American Astronautical Society, Los Angeles, Calif., Jan 1963

1-4. G. Yanow, "A Study of the Martian Upper Atmosphere and Ionosphere," The Journal of the Astronautical Sciences, Vol. VIII, No. 4, Winter 1961

1-5. G. F. Schilling, "Two Extreme Model Atmospheres for Mars," Rand Corporation Report No. RM-2782-JPL

1-6. Rand Corporation Report No. RM-2289-RC, 1958.

1-7. R. Minzner, K. Champion, H. Pond, "The ARDC Model Atmosphere," 1959, AFCRC-TR-59-267, Air Force Surveys in Geophysics No. 115

1-8. G. R. Schilling, "Limiting Model Atmospheres for Mars," Rand Corporation Report No. R-402-JPL

1-9. J. V. Breakwell and L. F. Koehler, "Elliptical Orbit Lifetimes," Advances in Astronautical Sciences, Vol. 3 (Proc. Western Regional Meeting of AAS, 1958)

Section 2

ORBIT LAUNCH VEHICLES AND OPERATIONS

by

J. F. McLaughlin

Section 2
ORBIT LAUNCH VEHICLES AND OPERATIONS

This section presents the results of an analysis of orbit launch vehicle and operation requirements for the early manned interplanetary mission. Some of the tentative conclusions obtained from this study:

- One Saturn C-5 appears incapable of orbiting sufficient mass in one launch for a manned mission to Mars. A manned flyby past Venus using one shot appears possible provided a nuclear booster, about the size of a proposed Saturn Nuclear Stage (SN), is used for the orbit launch vehicle.
- The S-IVB, as an orbit launch vehicle (OLV), is capable of launching Venus flybys. However, Earth orbit rendezvous of at least two Saturn-boosted vehicles is necessary. A single S-IVB is incapable of launching any manned payloads to Mars.
- Rendezvous of two C-5's provides more than sufficient mass on orbit for a manned Venus flyby regardless of OLV. For Mars, many 22-month low energy lightside flybys, some 17-month high energy darkside flybys, and 19-month high energy lightside flybys in 1971 and 1988 are also possible provided a nuclear OLV is used. Most of these Mars missions, however, require nuclear stages larger than presently planned hardware.
- The S-II has possible applicability as an orbit launch vehicle making flyby missions possible past both Mars and Venus. It appears feasible to orbit an S-II, fully loaded with liquid hydrogen, with one Saturn C-5 and then rendezvous LOX tankers and payload vehicles as needed.
- A substantial gain in nuclear OLV performance is obtained by going from present NERVA power levels up to 4000 Mw. For flyby missions using Saturn C-5 technology, little (if any) additional capability is obtained by going to reactor power levels above 4000 Mw. However, levels of the order of 10,000 Mw will be more efficient for launching planetary stopover missions.

- It appears that no post-Saturn C-5 vehicle should be acquired that has an orbit delivery capability of less than 450 to 700 metric tons (1 to 1.5 million pounds).
- A nuclear escape stage equivalent to several SN stages will be required to make any stopover missions possible. Serious thought should be given to on-orbit clustering of SN stages as a technique for accumulating sufficient initial mass.
- Almost all discussion of orbit operations and rendezvous techniques in the current literature appears applicable to the interplanetary mission.
- The directional variation of the Earth departure hyperbolic asymptote will play a major role in the selection of a launch date for a favorable launch window.

These conclusions are explained in detail in the following pages.

2.1 ORBIT LAUNCH VEHICLES

A study was undertaken to provide definitive information on sizes of orbit launch boosters required for early manned missions to Mars and Venus. The scope of the study, the systems examined, the approach, the results, and the conclusions are explained in detail. In addition, the applicability of presently planned booster and propulsion systems to the interplanetary mission is discussed.

2.1.1 Scope of Analysis

This study of orbit launch vehicles had three prime objectives:

- Determine the capabilities of certain boost systems to place payloads on heliocentric orbit
- Match those capabilities with requirements needed for the various interplanetary missions
- Ascertain the applicability of presently conceived propulsion systems and orbit launch boosters to the mission requirements

It was decided to limit the scope of the study in the following ways:

- Consider only LOX/LH and nuclear boost systems
- Use projected state-of-the-art technology for the 1970's
- Consider launch from low Earth orbit
- Consider hyperbolic excess speeds from zero to 0.30 EMOS (~ 9 km/sec)
- Limit consideration to those missions requiring no more than 700 metric tons on Earth orbit or more than 1 hour of engine burn time (whichever came first)
- Consider only the J-2 engine for LOX/LH propellant systems

2.1.2 Definition of Propulsion Systems

Both LOX/LH and nuclear propelled vehicles were examined in the study. The LOX/LH system utilized one J-2 engine; four nuclear systems were analyzed. The power levels selected were 1100, 1500, 4000, and 10,000 Mw. The detailed system characteristics and reasons for their selection, as well as a discussion of applicable nuclear propulsion technology, is presented in Volume II.

2.1.3 Method of Approach

The study of escape stage booster performance was approached in the following manner. Using the specific impulse values and thrust transients described in Volume II, mass ratios required to reach various hyperbolic excess speeds were calculated as a function of thrust-to-initial-mass ratio. The calculations involved integration of the equations of tangential (i.e., "gravity turn") motion in Earth's gravity gradient utilizing an IBM 7090 computer.

Meanwhile, calculations were made of inert weights for the various booster systems as a function of propellant loading. The values for the nuclear systems were generated

during RIFT sizing studies and under NASA/MSFC contract No. NAS 8-1601 (Ref. 2-1). The structural material for tank and skirt structure was assumed to be 5456 aluminum for the nuclear boosters and 2219-T87 for the LOX/LH vehicles. Propulsion system weights were obtained from existing data. Allowances were made for guidance and control equipment, batteries, wiring, separation devices, and miscellaneous weights. For each data point, that amount of propellant capable of producing an extra 2 percent ΔV was added to the above inert mass values. Then, 5 percent of this sum was added on to account for design growth and additional nuclear shielding. This method is believed to have yielded realistic inert weight values for each propellant loading.

It was now possible to take a total mass on orbit and, for each desired hyperbolic excess speed (normalized to Earth's mean orbital speed), determine the burnout mass. Then, the propellant loading and estimated booster inert mass were determined. Subtraction of the inert mass from the burnout mass yielded net payload (including interstage) at the desired hyperbolic excess speed. Burn time could be determined from the trajectory output.

2.1.4 Study Results

Results of this escape booster study are plotted in Figs. 2-1 through 2-4. These graphs show the calculated net payload at injection (including spacecraft/booster interstage) vs the calculated impulse propellant expended for constant initial mass and desired hyperbolic excess speeds (normalized to Earth's mean orbital speed – 29.8 km/sec or 18.5 mi/sec).

With these graphs, one can take a given propulsion system and, by determining the payload desired at some required hyperbolic excess speed, obtain:

- The total initial orbit launch vehicle (OLV) mass on Earth orbit
- The propellant expended
- The estimated inert mass of the orbit launch booster (total mass less propellant and payload masses)

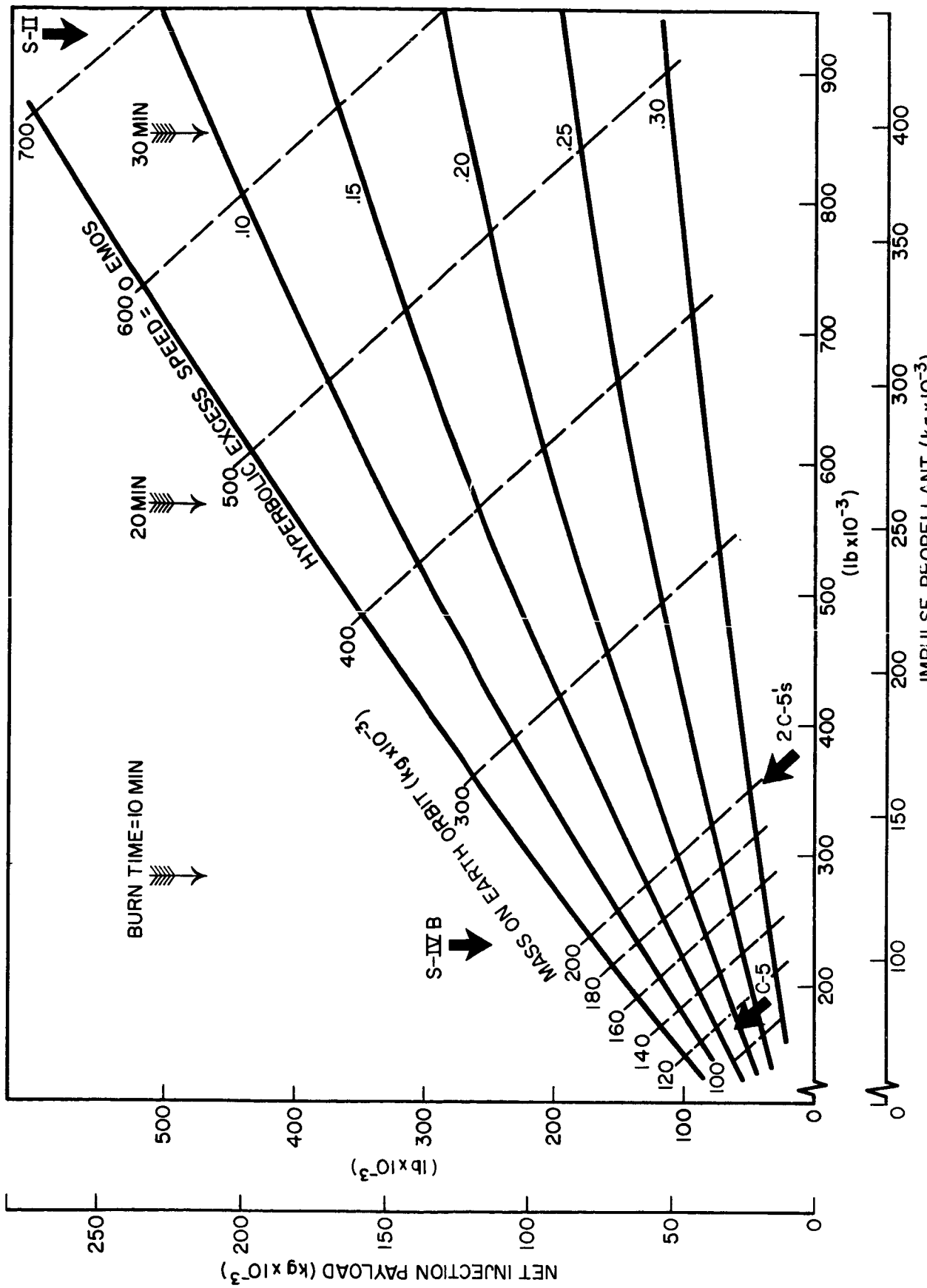


Fig. 2-1 Performance of Orbit Launch Booster Using Single J-2 Engine

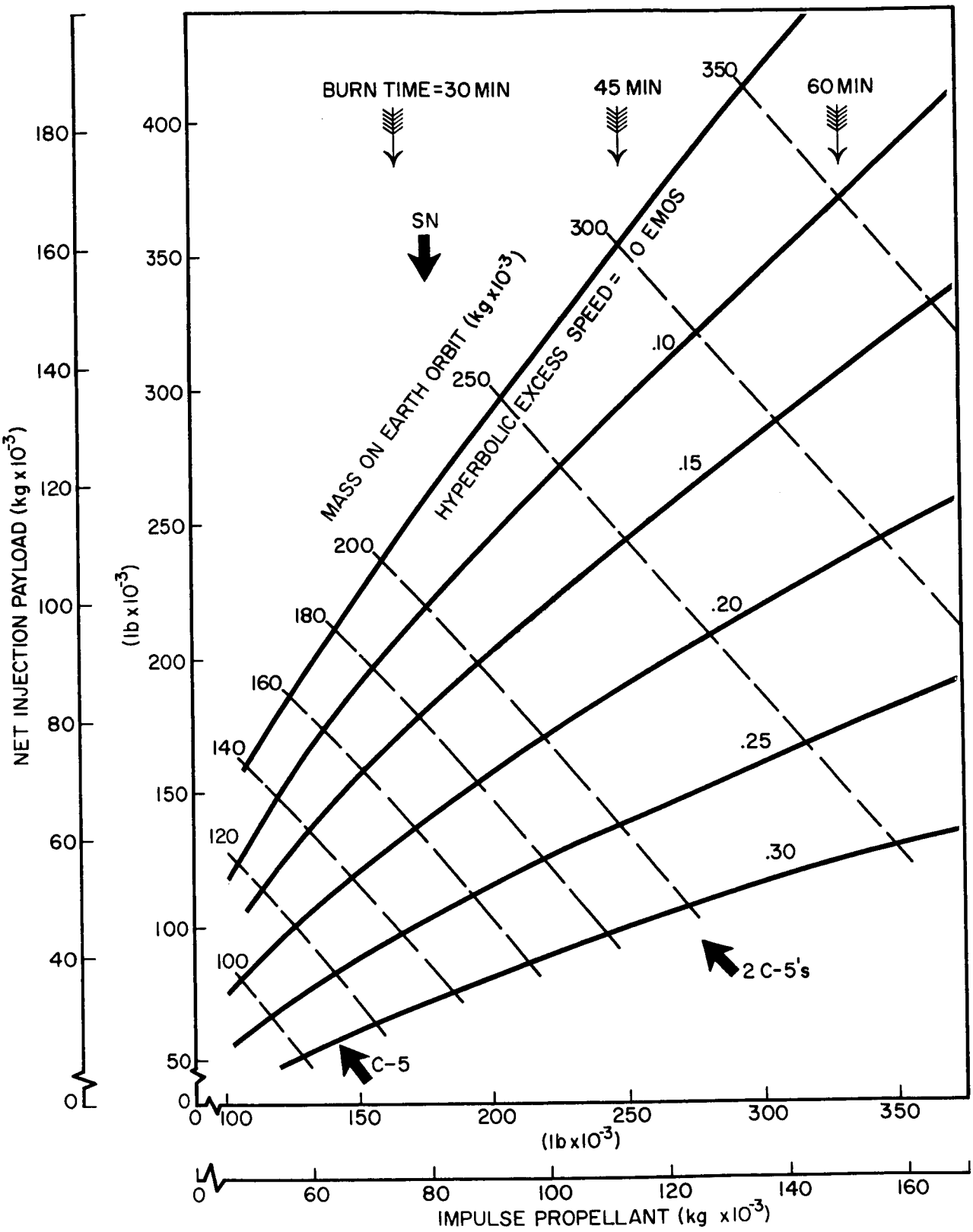


Fig. 2-2 Performance of Orbit Launch Booster Using 1500 Mw Engine

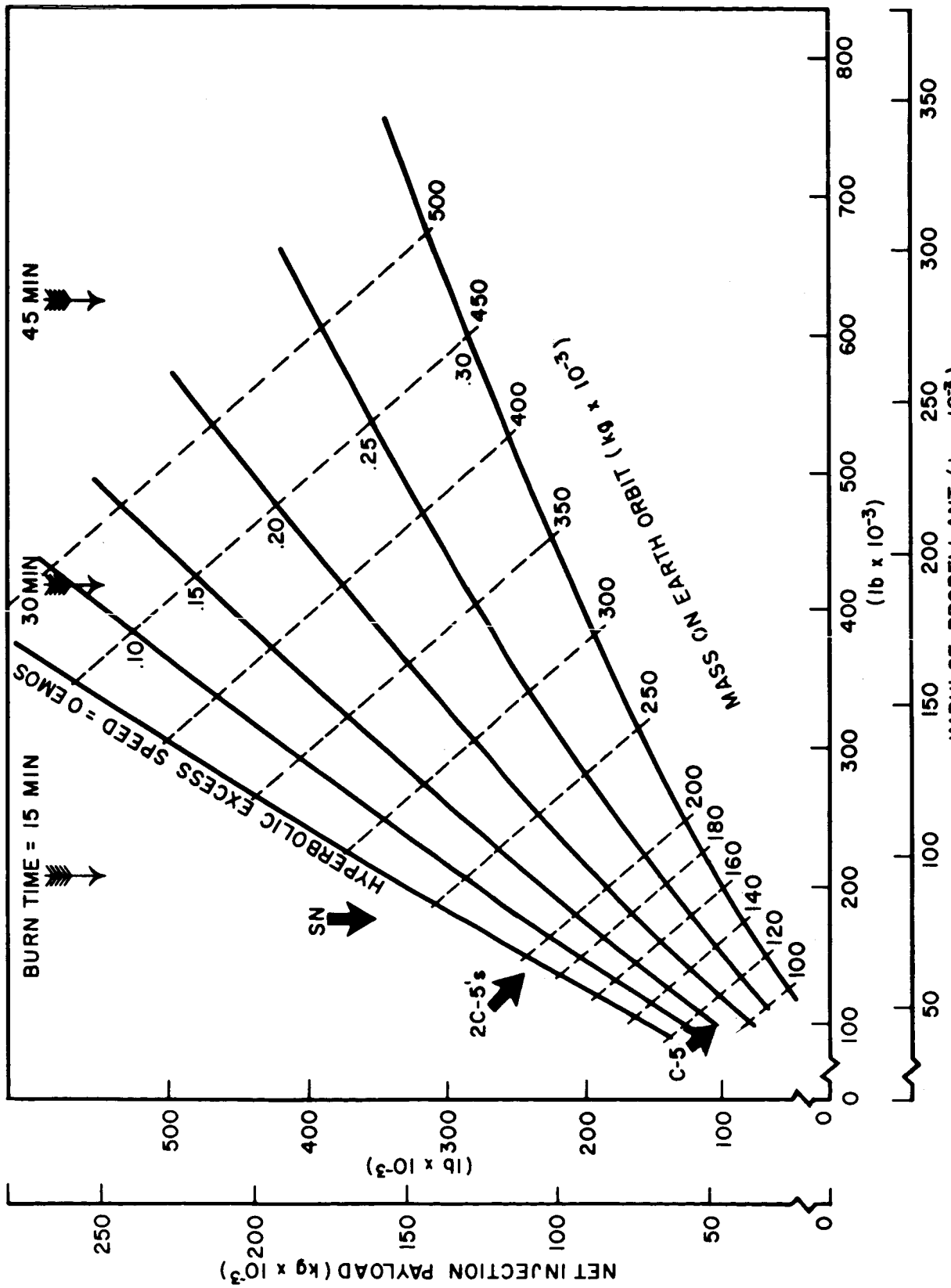


Fig. 2-3 Performance of Orbit Launch Booster Using 4000 Mw Engine

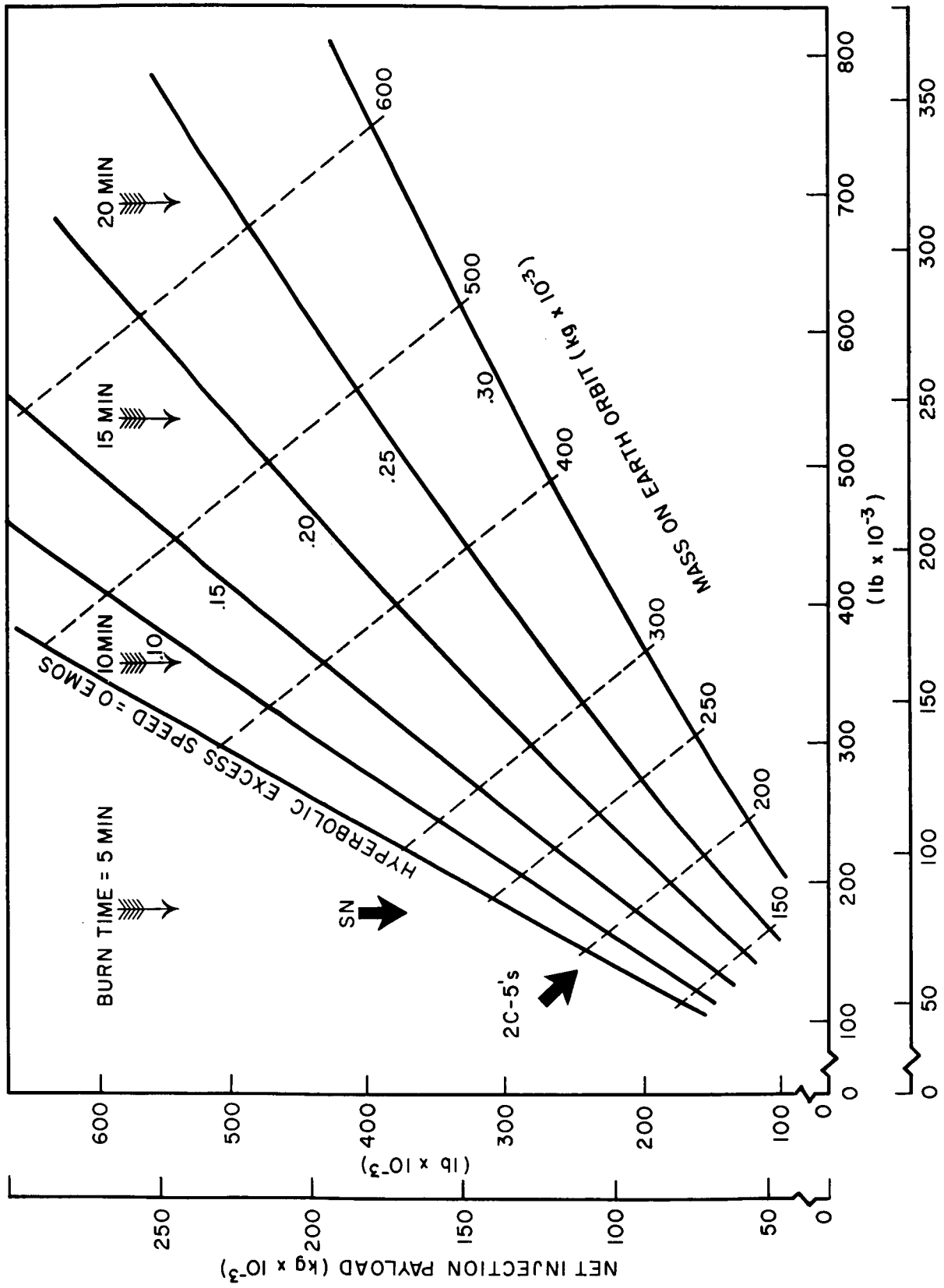


Fig. 2-4 Performance of Orbit Launch Booster Using 10,000 Mw Engine

- Orbit launch booster gross mass (total mass less payload)
- Approximate burn time

Likewise, one can obtain a realistic estimate of:

- The payload injected at various byperbolic excess speeds by a given orbit launch booster (by going down vertical lines of constant propellant load)
- The division of a given initial OLV mass between booster stage and payload as a result of variations in injection hyberbolic excess epeed (by following parallel to the dashed diagonal lines)
- The maximum payload injected at various hyperbolic excess speeds for a given maximum burn time (by ignoring starting transients and going down vertical lines of constant propellant associated with that burn time)
- The increase of mass in Earth orbit and required orbit launch booster mass per pound of payload increase for a given mission (by following constant hyperbolic excess velocity line)
- The increase of mass in Earth orbit and required orbit launch booster mass resulting from a change in mission for a given payload (by following the horizontal constant payload line)

To aid in the interpreting of the graphs, arrows indicate the approximate mass on Earth orbit for one C-5 and rendezvous of 2 C-5's. Other arrows indicate the approximate capacity of known and applicable upper stages. The quoted SN tank capacity yields approximately the largest nuclear stage that can be orbited by a single Saturn C-5.

2.1.5 Conclusions

In order to draw any meaningful conclusions, the capability graphs must be compared with mission requirements. Sample comparisons are made for two selected systems in Figs. 2-5 and 2-6,by the addition of partial mission envelopes.

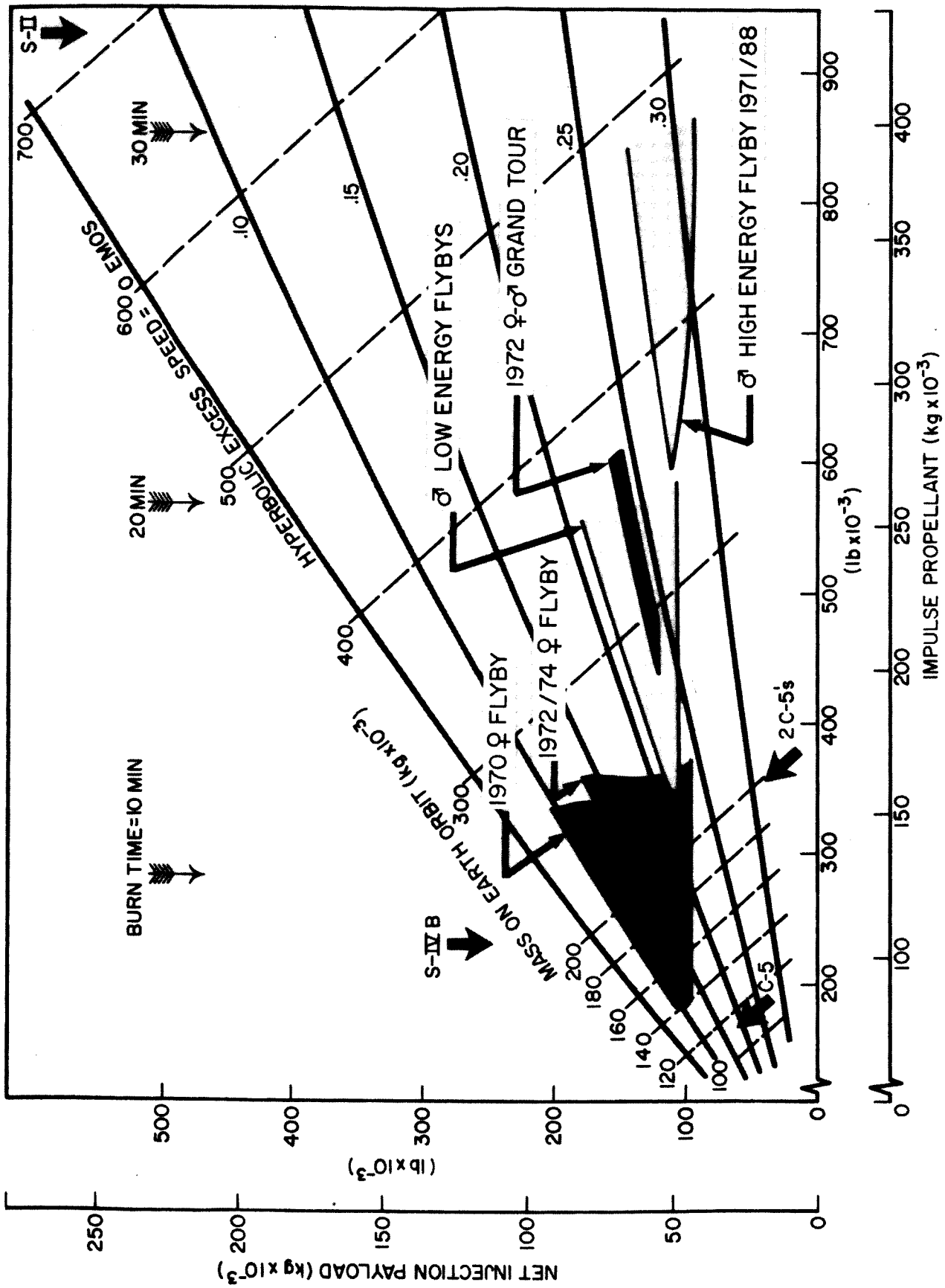


Fig. 2-5 Performance of Orbit Launch Booster Using Single J-2 Engine

Figure 2-5 is identical to Fig. 2-1 except that several partial mission envelopes have been added. The bottom boundary of each envelope is established by an estimation of the minimum injected payload with which the mission can be accomplished. Propulsive retro to planetary entry speeds is assumed. The left hand boundary is obtained by the calculation of the minimum hyperbolic excess departure speed allowed by the inter-planetary trajectory. The rough result is a wedge-shaped area with one side along a line of constant hyperbolic excess speed and the other along a line of minimum estimated injection payload. With the exception of the multi-planet flybys, no bound is placed on the maximum hyperbolic excess speed and the maximum injection payload because, theoretically, there are no such bounds. A determination of this type would have to be completely arbitrary. The cutoffs in this figure are arbitrarily inserted for overall graph clarity.

LOX/LH System

The shaded envelopes in Fig. 2-5 should be interpreted in this manner: trajectory calculations and preliminary spacecraft estimates indicate that, within the boundaries of the envelope, it appears quite feasible to accomplish the stated mission.

One must take care not to read more into the envelopes than they are intended to convey. For example, one might interpret the overlays as saying that minimum hyperbolic excess departure velocity always results in minimum mass on orbit. As pointed out earlier in this report, one finds this is not the case for all planet passage distances. Also, it may be possible to reduce the minimum injection payload below the value shown by developing a drag brake for atmospheric entry. Although a thorough mission analysis must still be made to determine the acceptability of any particular point within an envelope, the envelopes do cover areas of sound technical interest.

With the aid of Fig. 2-5, we can draw several conclusions concerning the applicability of chemical systems to early interplanetary missions:

- One Saturn C-5 appears incapable of orbiting sufficient mass in one shot to allow a manned mission to be accomplished with a chemical

orbit launch vehicle (OLV). However, its capability is close to that required for a Venus flyby. Further study of this interesting possibility would be warranted.

- The S-IVB as an OLV appears capable of launching Venus flybys, especially for the 1970 conjunction. However, Earth orbit rendezvous of Saturn vehicles will be needed to accumulate sufficient initial mass.
- A single S-IVB is incapable of launching any manned payloads to Mars.
- The rendezvous of two Saturn C-5's is more than sufficient for a Venus flyby, but appears very marginal for any Mars mission. Even if a Mars mission were feasible, an OLV larger than a single S-IVB would be required.
- The important possibilities of using the S-II as an OLV deserve careful consideration. It makes certain flybys past both planets possible. The addition of other J-2 engines would cut the burn time and velocity losses, further increasing the capability shown in Fig. 2-5. Moreover, one S-II, fully loaded with liquid hydrogen, appears feasible as a vehicle to be orbited by the Saturn C-5. However, as many as two to four other C-5 launches would be required to complete the on-orbit LOX tanking and payload assembly.

1500 Mw Nuclear System

Because of 1500 Mw reactor propulsion system is a distinct possibility in the early 1970's and as an aid to later discussion, mission requirement envelopes for this system are presented in Fig. 2-6. The minimum payloads and hyperbolic excess speeds making up the envelope boundaries are the same as those in Fig. 2-5 and the same constraints apply. Further information on nuclear propulsion systems can be obtained from Volume II of this contract report.

Examination of Fig. 2-6 reveals the following:

- A 1500 Mw propulsion system should be capable of performing Venus flybys with one Saturn C-5 launch using a SN-type stage provided the injected payload does not exceed approximately 45,000 kg (100,000 lb)

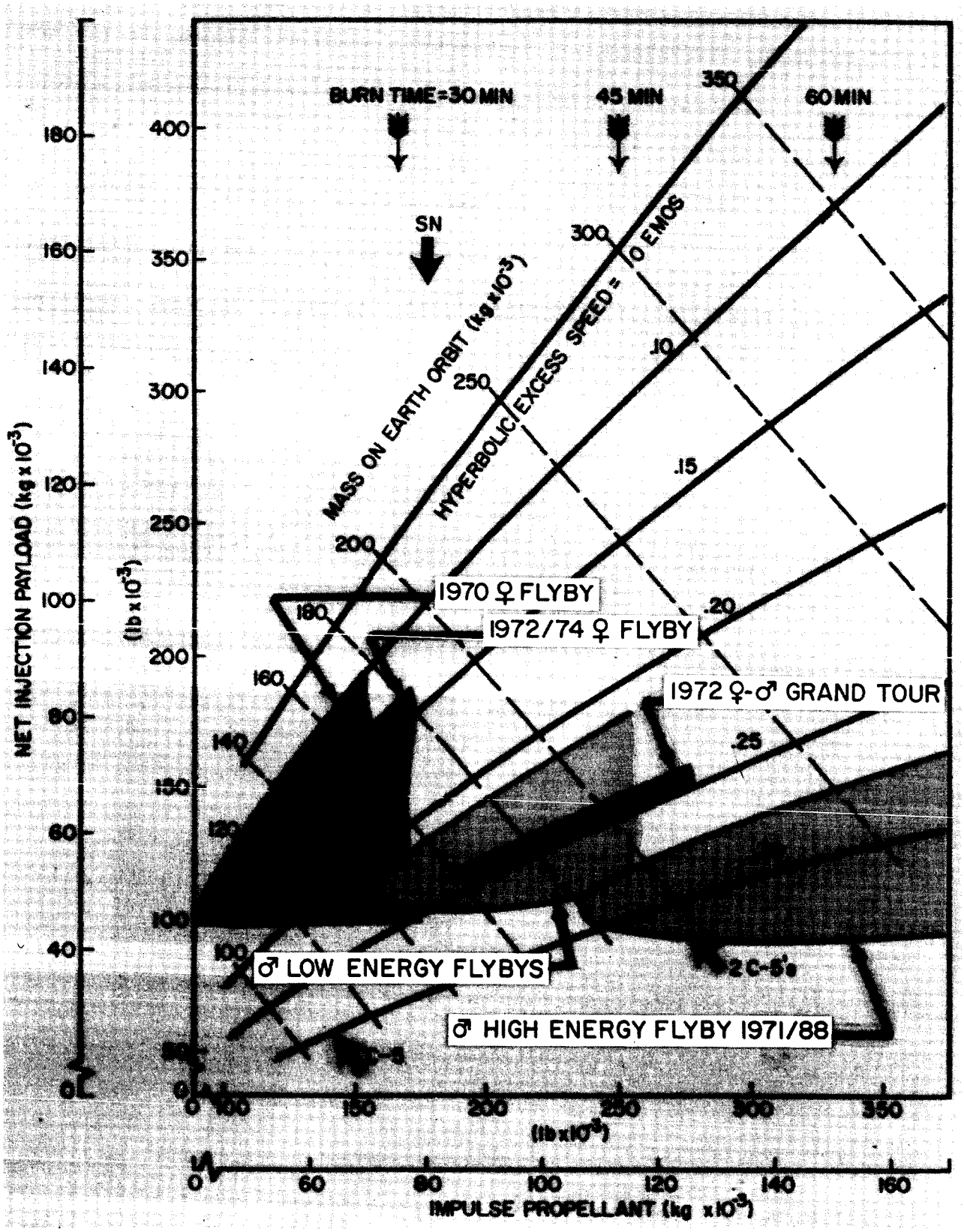


Fig. 2-6 Performance of Orbit Launch Booster Using 1500 Mw Engine

- With rendezvous capability up to two C-5's, Venus flybys, Mars low energy lightside trips, Mars high-energy lightside trips in 1971 or 1988, and certain multi-planet flybys (such as a 1972 Earth-Venus-Mars-Earth mission) appear possible. However, for some of these missions a stage larger than the illustrated operational SN is required. For these cases, some form of liquid hydrogen transfer would also be required if the rendezvous vehicles are launched by C-5's.
- Increasing SN propellant size from 79,000 kg (176,000 lb) appears to yield little more in mission capability (no new mission envelopes are encountered) until about 110,000 kg (240,000 lb) capacity is reached.

Other Nuclear Systems

Finally, Fig. 2-7 was prepared to compare the results obtained from the analysis of the various nuclear systems. It was obtained by taking the 0.15 EMOS (4.47 km/sec) and the 0.30 EMOS (8.94 km/sec) lines from Fig. 2-2 through 2-4 and for the 1100 Mw system and plotting them using common coordinates. The points on each of these lines resulting in one hour burning time were connected by constant burn time lines. Then composite mission envelopes were laid out on top of this. The result (Fig. 2-8) is a busy chart, but it tells an interesting story.

Great care and caution must be exercised in the interpretation of this chart because the envelopes now cover the capabilities of four propulsion systems. Thus, the entire envelope is generally applicable to the 10,000 Mw system, but only certain portions are good for the lower power systems. For example, a Mars high energy lightside trip in 1971 or 1988 cannot be done for a hyperbolic excess speed of less than about 0.27 EMOS. However, by looking at the position of the left hand boundary of the corresponding envelope in Fig. 2-8 (about 0.27 EMOS for the two higher powered systems), one might erroneously say that, for the 1100 Mw system, the trip can be made for an excess speed of ~ 0.20 EMOS. To help resolve this difficulty, one can refer to Fig. 2-6 to get an idea of those portions of the envelopes in Fig. 2-8 that are applicable to the lower power systems.

If we keep this condition in mind, there are numerous important conclusions that can be drawn from Figs. 2-7 and 2-8:

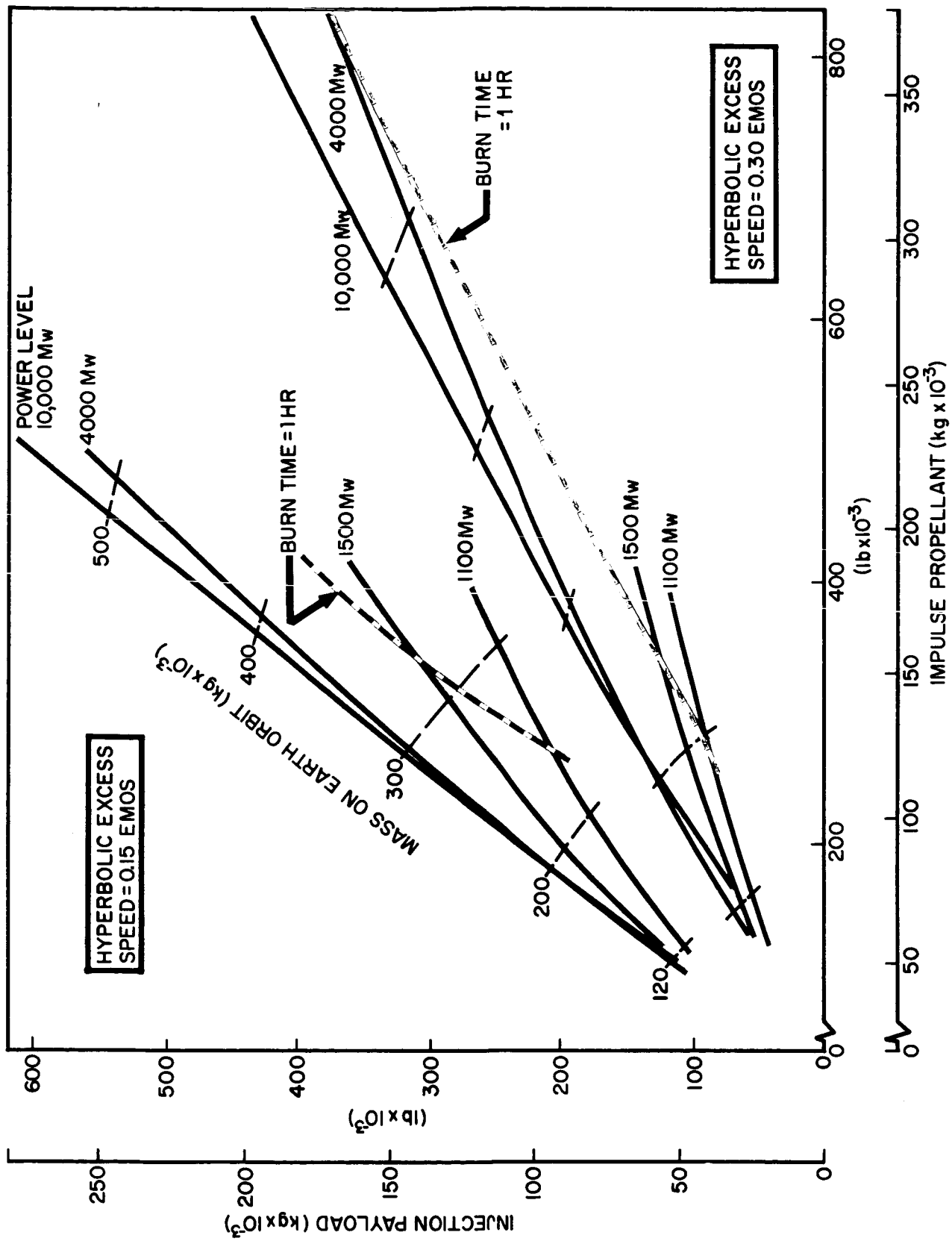


Fig. 2-7 Comparison of Nuclear Orbit Launch Vehicle Performance

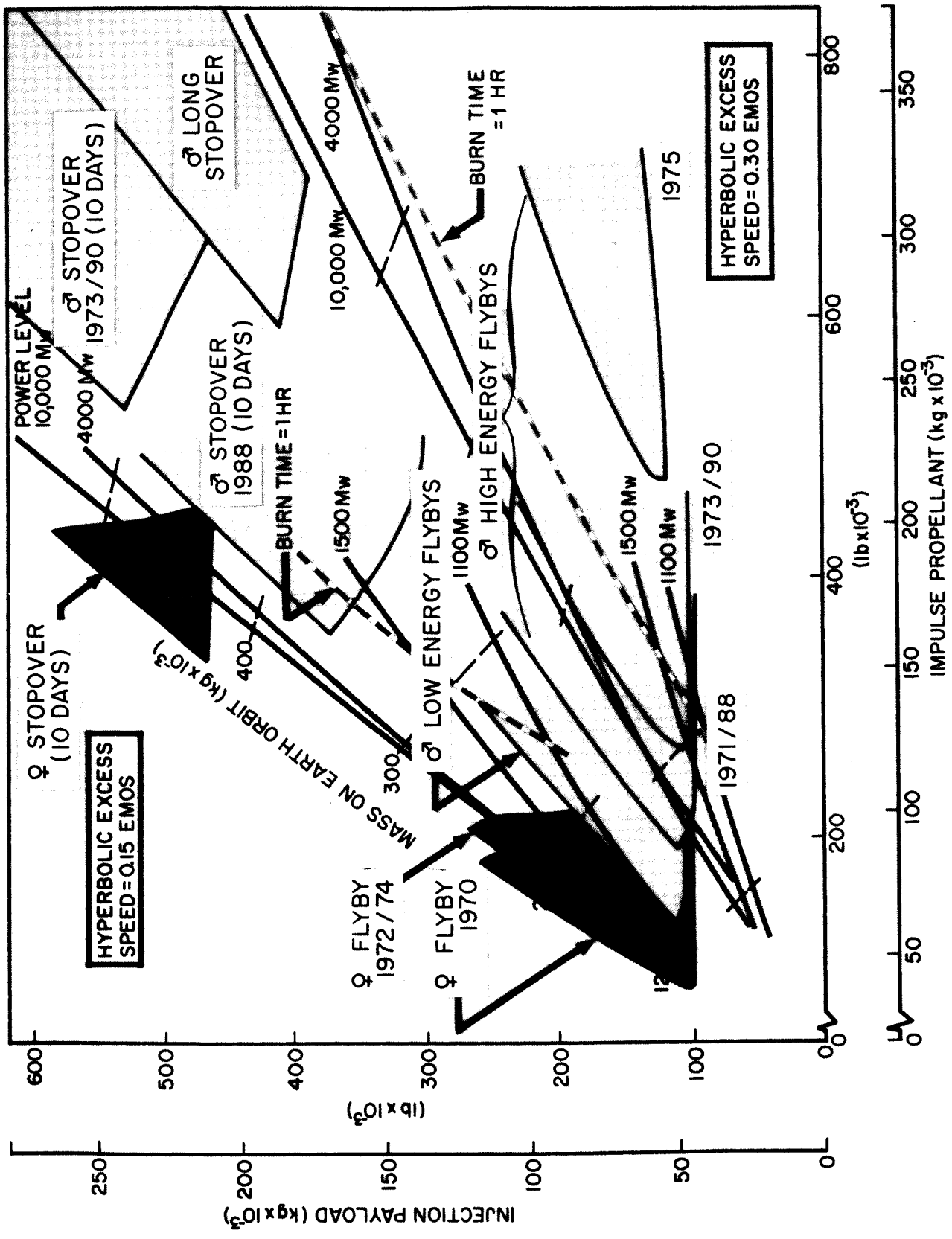


Fig. 2-8 Nuclear Orbit Launch Vehicle Mission Capabilities

- A substantial performance gain is achieved by going from the low power propulsion system to the 4000 Mw system. This is true in terms of
  (1) Greater injected payload (~ 20 percent) for a given mass on orbit;
  (2) Substantial reduction (up to about 30 percent) in orbit launch booster size required for a given mission;
  (3) Much shorter engine burn time for a given mission.
- For early manned flyby missions using Saturn C-5 technology, very little is gained by going to any power level above 4000 Mw. In fact, there appears to be definite crossover points between the various systems. The exact point is a function of the method of determining booster inert masses, but, as the total vehicle mass decreases, it seems logical that any propulsion advantages inherent in the higher powered system would be wiped out by the higher engine mass.
- It appears that no post-Saturn C-5 vehicle should be acquired that has an orbit delivery capability of less than 450 to 700 metric tons (1 to 1.5 million pounds).
- As pointed out before, Venus flybys using a single Earth launch appear within the capabilities of presently planned booster programs (C-5 and SN) provided the payload mass is kept below 45,000 kg (100,000 lb)
- Rendezvous of two C-5's seems to open up some high energy Mars flybys in 1971 and 1988 or low energy lightside Mars flybys during most other oppositions provided technology will permit these 22-month trips. Figure 2-8 shows that the propellant required for most of these trips is greater than the capacity of the largest fully-loaded nuclear booster that can be orbited by one Saturn C-5. Thus, liquid hydrogen transfer in orbit would be necessary.
- A nuclear escape stage equivalent to several SN stages will be required to make any stopover missions possible. Serious thought should be given to on-orbit clustering of fully-loaded SN stages as a means of accumulating a large enough OLV for an interplanetary mission. If this technique

were used with the Saturn C-5, however, six or more launches (including the orbiting of 4 SN stages) would be the minimum needed for a Mars stopover; as low as four launches (including the orbiting of 2 SN stages) for a minimum Venus stopover (no landing and drag braking to orbit).

- Although they have not been seriously studied yet, Fig. 2-8 shows that long Mars stopovers (leaving Earth during one Mars opposition and returning the next) may allow landings and orbital stopovers between 1973 and 1986 without requiring monstrous launch vehicles. The envelope shown here assumes a 36,000 kg (80,000 lb) basic living module, an 18,000 kg (40,000 lb) short stay landing craft, a 23,000 kg (50,000 lb) Mars entry system, hypergolic propellant propulsion system for Mars escape, and near-parabolic Earth entry.

It should be emphasized again that the nuclear reactors listed here are of the thermal, carbon-core type. Fast spectrum, metallic-core reactors (especially around 4000 Mw) would show even better performance capability over the low power systems depicted in Fig. 2-7. Such a comparison had not been made at the time of this writing.

2.1.6 Applicability of Current Booster and Propulsion Systems

As a result of the analysis reported in the preceding pages, what can be said about the applicability to early interplanetary missions of current or projected space booster and propulsion systems? In a brief summary, the following may be concluded:

- Saturn C-5
  - (1) May allow Venus flyby with one launch using nuclear OLV
  - (2) Lowest energy Venus flyby appears to be just out of the reach of a single C-5 using S-IVB
  - (3) Rendezvous of two C-5's should assure a Venus flyby with S-IVB OLV
  - (4) Rendezvous of two C-5's allows possible 22-month Mars low energy lightside flybys for most oppositions and some 19-month high energy

flybys in 1971 and 1988 provided a nuclear OLV is used. However, most of these missions would require on-orbit transfer of liquid hydrogen to the nuclear stage.

(5) Four C-5 launches (including 2 C-5/SN's) appear to be the minimum required for a Venus stopover; a minimum of six launches (including 4 C-5/SN's) for a Mars stopover. Both of these would not allow landings and would require a nuclear engine of at least 4000 Mw.

- Saturn C-1B

  (1) Rendezvous between a C-1B and C-5 may allow the accumulation of sufficient vehicle mass to make a Venus flyby possible using an S-IVB OLV.

  (2) C-1B can perhaps be used to orbit the flight crew following unmanned rendezvous of an interplanetary vehicle.

- Nova

  (1) Flyby missions appear to be within the range of Saturn C-5 rendezvous operations. Stopovers and planetary landings will require orbital payloads measured in millions of kilograms.

  (2) Any Nova (i.e., post-Saturn C-5) booster should not have an orbit capability less than 450 to 700 metric tons (1 to 1.5 million pounds).

- S-IVB

  (1) As an orbit launch vehicle, it appears capable of launching payloads for a manned Venus flyby. However, Earth orbit rendezvous of Saturn C-5's is required.

  (2) A single S-IVB is incapable of launching any manned payloads to Mars.

- S-II

  (1) The S-II has sufficient propellant capacity to be an orbit launch vehicle for certain types of flybys past both planets.

  (2) Orbiting one S-II, fully loaded with liquid hydrogen, via Saturn C-5 seems feasible. Thus, on-orbit propellant tanking could be limited to liquid oxygen only.

- Saturn Nuclear Stage (SN)

  (1) May be capable of launching a Venus flyby with one Saturn C-5 launch.

  (2) Can be considered incapable of launching manned missions to Mars with a single C-5 launch unless the required payload mass is drastically reduced.

  (3) Earth orbit rendezvous allows an SN stage to launch certain types of flybys past both planets.

  (4) On-orbit clustering of SN stages should be considered as a means of accumulating sufficient booster sizes to launch planetary stopovers.

- NERVA engine

  (1) The low-powered NERVA engines will find only limited use for interplanetary missions (some Venus flybys).

  (2) Any NERVA power uprating will distinctly improve mission capability.

- Second Generation Nuclear Systems

  (1) Substantial performance gain is achieved by increasing the nuclear engine power to 4000 Mw.

  (2) For early manned flyby missions using Saturn C-5 technology, little is gained by increasing power level beyond 4000 Mw.

  (3) Power levels up to and beyond 10,000 Mw may be needed for OLV's for stopover missions.

- J-2 Engine

  Single engines or a small cluster should be sufficient to power all but very huge LOX/LH orbit launch vehicles.

- M-1 Engine

  Appears to have little applicability for propelling orbit launch vehicles.

2.2 ORBIT LAUNCH OPERATIONS

The large number of factors which affect orbit launch operations have been studied in considerable detail in recent months. Swanson and Soule (Ref. 2-2) list over 160

papers concerned with rendezvous guidance technology alone. No attempt will be made here to summarize the knowledge and insight so recently gained in this vast field. It is sufficient to say that practically every discussion and technique thus far presented has some applicability to interplanetary missions. There are, however, several items which deserve special attention.

2.2.1 Orbit Altitude Selection

During the preparation of the orbital launch booster sizing analysis presented in this section, the effect of orbital altitude (up to 500 nm) was studied. It was found in this range that, for a given total initial mass on orbit, the payload delivered by a LOX/LH orbit launch booster on a hyperbolic trajectory increases roughly 1 percent for every 100 miles of initial parking orbit altitude over the nominal 100 nm. However, the capability of an Earth launch booster to place payloads into increasing orbit altitude drops very rapidly.

These altitude relationships are shown in Fig. 2-9 using the Saturn C-5 as an example. The lowest line shows the very rapid drop in two-stage direct ascent capability with increasing altitude. This is relieved by the use of Hohmann transfer from 185 km as shown in the second curve. The top curve, meanwhile, shows the mass needed in a higher orbit to deliver the same payload on a low energy interplanetary trajectory that was delivered from a 185 km orbit. Thus, while the mission mass required on orbit decreases slightly as orbit altitude is increased, the rapidly decreasing booster capability indicates the efficiency of operating at lower altitude.

The only serious obstacle to low altitude operation is, of course, the effect of atmospheric drag. This takes the form of lowering the energy of the vehicle in orbit and in distorting the shape of the resulting orbit. Predictability of these effects, especially for some future mission, is difficult because of atmospheric variation due to cyclic and random solar activity, daily changes on the light and dark sides of Earth, inability of forecasting the ballistic factor (M/C_DA) of future spacecraft, and present state of knowledge (Ref. 2-3).

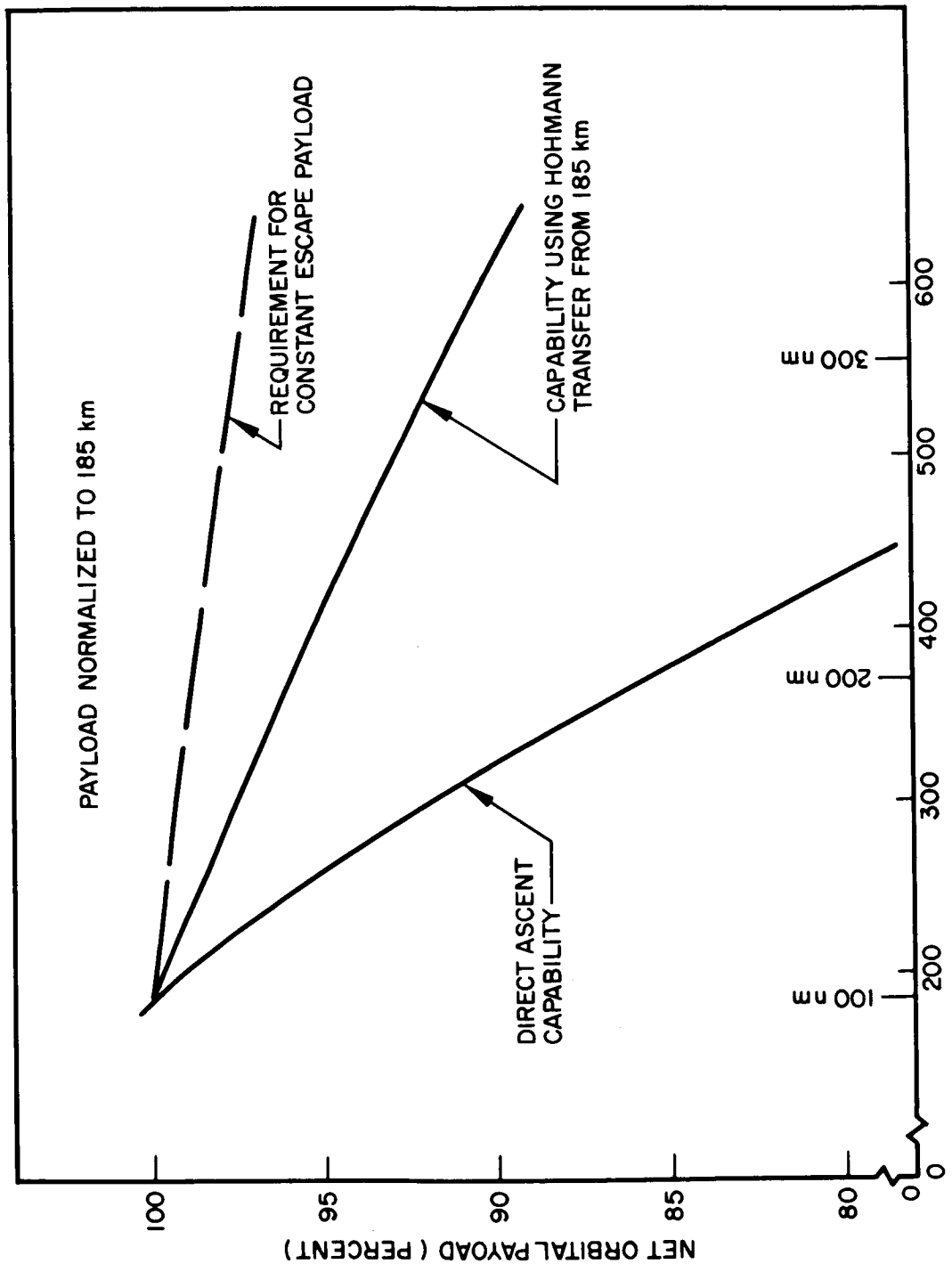


Fig. 2-9 Estimated Effect of Orbit Altitude on Saturn C-5 Performance

For single shot heavy payload LOX/LH boost systems, 100 nm appears to be an acceptable parking altitude. Rendezvous systems, depending on the technique used, must go higher. Use of the promising phasing orbit technique (Ref. 2-4) would result in a vehicle initially at 100 nm rendezvousing with another at between 200−300 nm.

Single shot nuclear systems present different problems because of concern for the satellite lifetime of an inoperable nuclear engine. A longer lifetime would result from separating the engine from the voluminous booster tanks. Estimates of the lifetime for a nuclear engine in random tumbling (Ref. 2-1) increases from a few revolutions at 200 km to 1−2 years at 400 km, to 10−20 years at 550 km depending on assumptions of atmospheric density.

2.2.2 Hyperbolic Asymptote Variation

One of the most important factors in determining the launch and orbit operations timing will be the direction and variation of the departure hyperbolic asymptote. If Earth is visualized as a point mass in the vast heliocentric system, the magnitude and direction of the velocity from Earth needed for a desired interplanetary transfer can be determined (Ref. 2-5). The vector difference between this velocity and Earth's own heliocentric velocity is the required hyperbolic excess velocity. For purposes of this discussion, the hyperbolic asymptote can be thought of as a line segment, beginning at Earth's center, concurrent with the hyperbolic excess velocity vector just determined.

The direction of this asymptote is important because it must lie in or near the vehicle's parking orbit plane. If an angle exists between the asymptote and the orbit plane, some type of plane change maneuver must be accomplished by the vehicle at a cost of propulsion energy. As an example, if the asymptote is 15° out of the plane, roughly 500 to 900 m/sec will be required for plane change alone.

Figure 2-10 will aid the subsequent discussion. It shows the variation of right ascension (angle on the equator measured eastward from the vernal equinox to the meridian

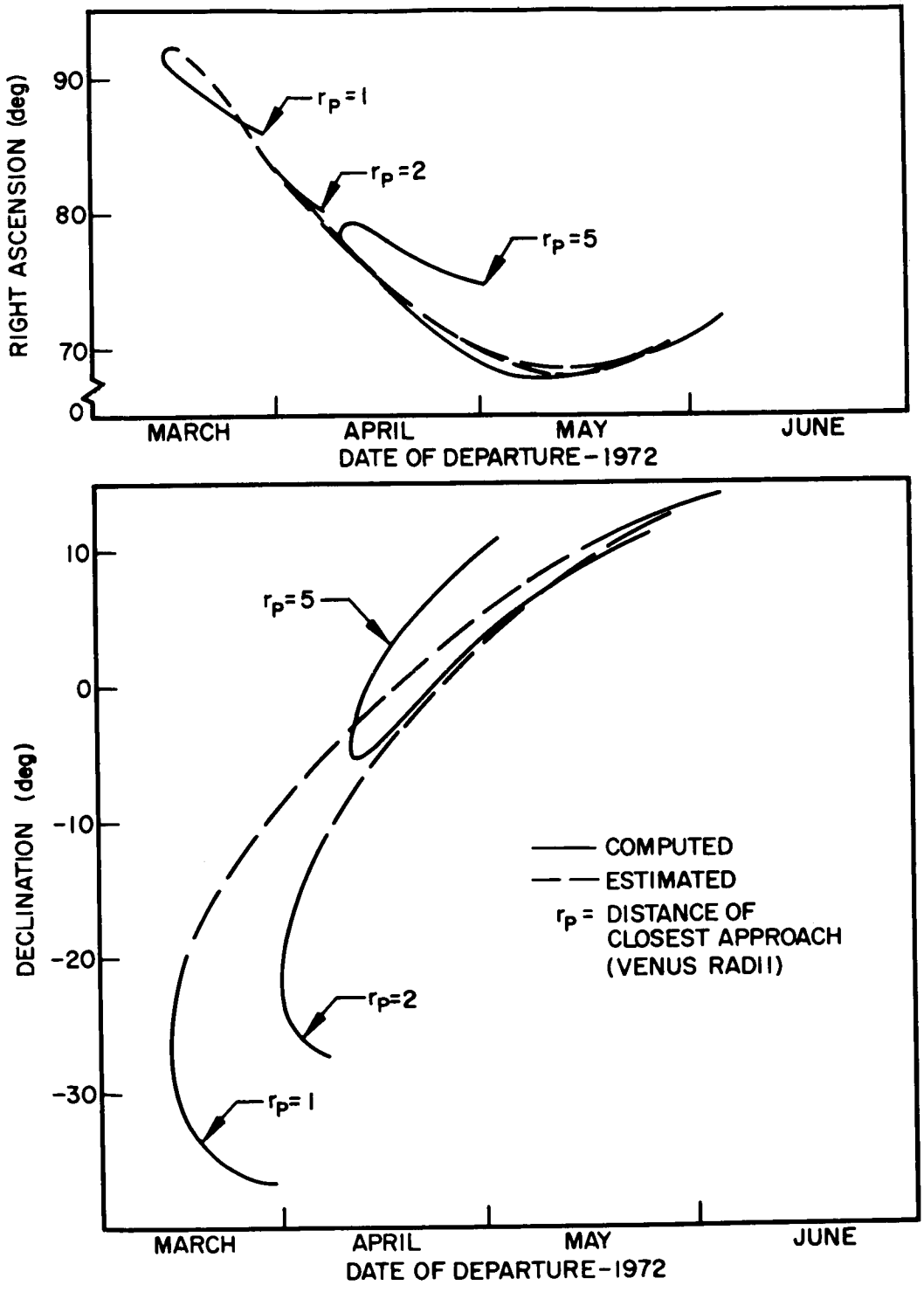


Fig. 2-10 Departure Right Ascension and Declination for 1972 Venus Flyby

of the asymptote) and declincation (angle measured along the asymptote meridian from the equator to the asymptote) as a function of launch date for a 1972 Venus lightside flyby. The solid lines indicate actual values calculated for Ref. 2-6 and under current NASA/MSFC contract (Interplanetary Handbook, NAS 8-2469). A dashed line represents interplanetary trajectories which must pass the planet on the same day in order to return to Earth. Because of the calculation technique, right ascension and declination values were not readily available and were estimated as shown. Where two values of right ascension and declination are shown for a launch date, there exist two possible trajectories upon which the vehicle may depart that day and pass Venus at the desired distance.

Because of the slow variation of passage date, one might expect the mass-on-Earth-orbit requirement to increase as the launch date was delayed. This is indeed the case; the regime of minimum mass occurs near the loop of each curve.

The first consideration that must be examined arises from investigation of the declination curves. As long as the declination remains less than $\pm 28.5°$, it will always be possible to find an orbit that includes the asymptote and still allows an easterly launch from AMR. For the best Mars trajectories, this seems to always be the case. For Venus, the lowest required mass on Earth orbit occurs as the passage distance decreases, and Fig. 2-10 shows that the declination of the $r_p = 1$ curve exceeds $-28.5°$ in the region where minimum mass on Earth orbit occurs. Thus, it was necessary to determine the cost in Earth booster performance that would have to be paid for AMR launch azimuths other than due East in order to achieve the required orbit inclinations.

This can be estimated if one assumes that the booster must make up only what it loses in assistance to orbit from Earth's rotation (a little over 400 m/sec maximum). This can be done by sacrificing payload as the launch azimuth varies. If one further assumes a spherical Earth, an approximation of the resulting orbit inclination can be obtained. These estimates are shown in Fig. 2-11 for both the Saturn C-5 and C-1B. This figure shows that inclinations up to 35° are possible with a loss of only about 1 percent

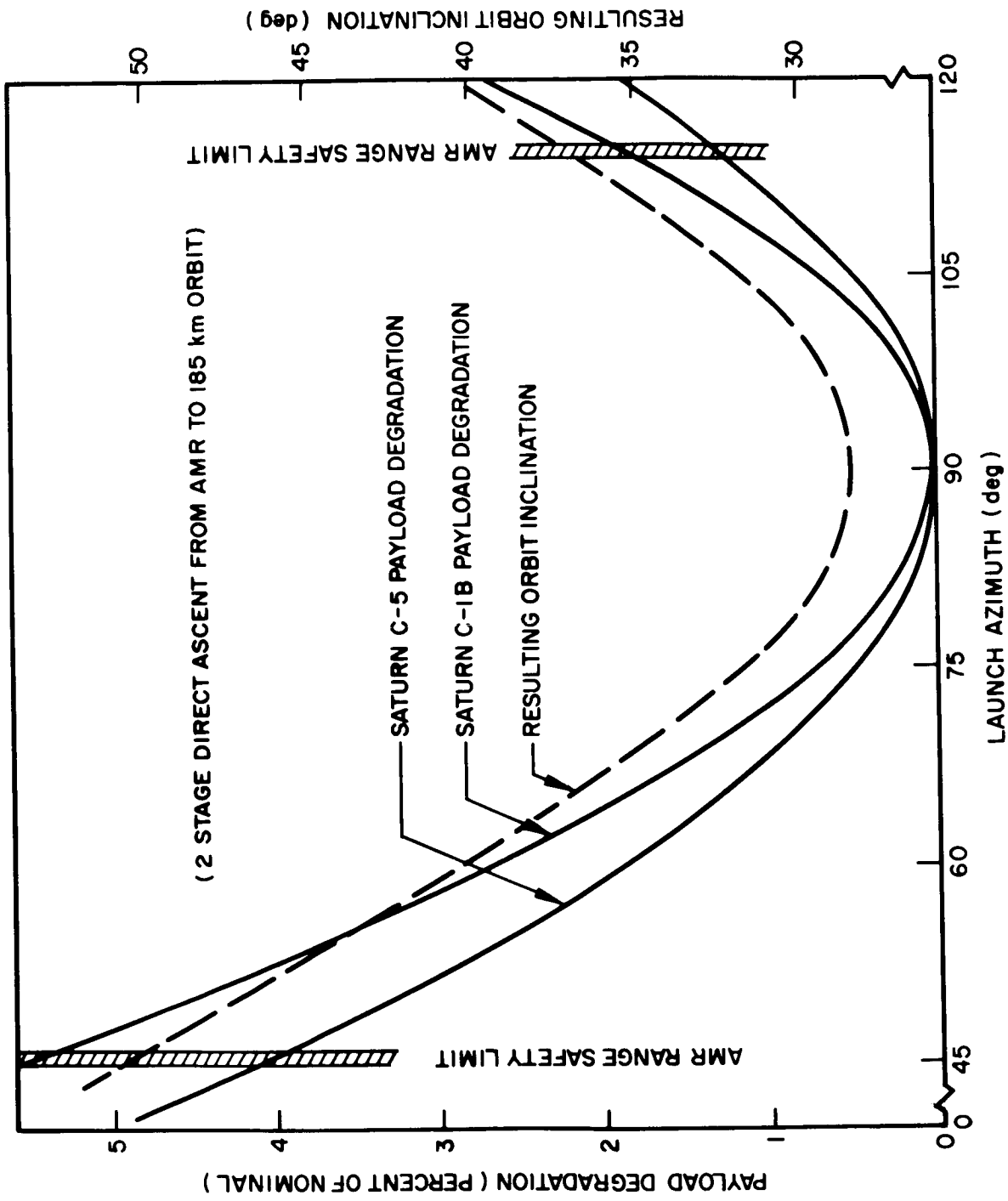


Fig. 2-11 Estimated Effect of Launch Azimuth on Saturn Orbital Performance

in payload. This means that high asymptote declination is a problem only where slight payload decreases would jeopardize the capability to do the mission.

The second, and most important, problem presented by the asymptote is the effect of its daily variation. This problem needs more work, but can, for the moment, be best understood by assuming two planes about Earth. One is the parking orbit plane of our vehicle; the other is a plane at the same inclination, but which moves so as to always include the hyperbolic asymptote. To simplify discussion, the former will be called "orbit plane," and the latter, "asymptote plane."

The motion of the orbit plane for a vehicle in circular orbit, for example, is affected primarily by the various harmonics of Earth's gravitational field resulting in a regression measured at the equatorial line of nodes of approximately 6° to 8° per day. The desirability of keeping the asymptote in or near this orbit plane for as long as possible means that it would initially be worth exploring those areas where the asymptote plane also regresses at nearly the same rate. Assuming a spherical Earth, the motion of the line of intersection of the asymptote plane and Earth's equator is given by

$$\Delta\Omega_N \approx \Delta\Omega_1 \pm \frac{\left(1 + \tan^2 \delta_1\right) \Delta\delta_1}{\sqrt{\tan^2 i - \tan^2 \delta_1}}$$

where

$\Delta\Omega_1$ = small change in asymptote right ascension

$\Delta\delta_1$ = small change in asymptote declination

i = asymptote plane inclination

One can note three things from this equation:

- The asymptote plane regresses one-to-one with a reduction in asymptote right ascension.

- The effect on asymptote plane movement of a change in declination is heavily dependent on the value of declination and its relation to plane inclination. For a 30° inclination, this ranges from ~ 1.7° nodal movement per degree declination change at $\delta_1 = 0$ to 5.7°/day at $\delta_1 = 28°$.
- Examination of the equation reveals that, if the declination is increasing with time, any change of value will cause regression of the asymptote plane provided the asymptote lies on the side of the ascending node. Conversely, a decreasing declination will regress the asymptote plane only if the asymptote lies on the side of the descending node.

Tentative examination of the curves in Fig. 2-10 indicates maximum launch windows would be attained near the looped ends provided the system is launched from AMR so as to pass the asymptote on the ascending phase of the parking orbit.

Examination of departure conditions for a Mars high energy lightside flyby in 1973 indicates that the asymptote plane is always progressing at about 1°/day. This is duc to a relatively stable, low-valued declination and a right ascension increasing at a little over 1°/day throughout the launch period.

The problems presented by hyperbolic asymptote variation will require much more study to obtain meaningful results. This is because our concern is not about movement of an asymptote plane, but movement of the asymptote itself away from the orbit plane. The concept of asymptote plane can lead us to the launch date intervals of most profitable results. The angle between the asymptote and the orbit plane is given by

$$\psi = \sin^{-1}\left[\sin i \sin(\Delta\Omega_T) \sin(\Delta\theta_N)\right]$$

where

$$\Delta\theta_N = \tan^{-1}\left[\frac{\sin \Delta\Omega_T}{\cos i\,(\cos \Delta\Omega_T - 1)}\right] - \sin^{-1}\left[\frac{\sin \delta_1}{\sin i}\right]$$

and

$$\Delta\Omega_T = \Delta\Omega_N - \text{(regression of orbit plane in time interval considered)}$$

At the time of this writing, ψ had not been evaluated for any trips, pending better definition of some of the independent variables.

2.2.3 Orbit Inclination

The effect of hyperbolic asymptote on the desired orbit inclination has been examined in the preceding pages. It was shown that, with a few exceptions (i.e., certain trajectories to Venus), direction of the asymptote did not conflict with the desire for an easterly launch. Thus, other requirements, such as rendezvous launch windows, will establish inclination values.

Straley (Ref. 2-4) details the advantages that accrue by launching into an inclination given by

$$i = \delta_L + \epsilon$$

where

δ_L = launch site latitude

ϵ = allowable angular plane change capability of launch booster

Rendezvous studies (Ref. 2-7) indicate that a turning angle of 2° to 3° results in negligible velocity loss. Straley shows that a latitude of 28.5°, a turning angle of 2°, and a target inclination of 30.5° results in a launch window in excess of 3 hours.

2.3 REFERENCES

2-1 Lockheed Missiles and Space Co., Saturn D Mission Studies, Final Report, Contract No. NAS8-1601, LMSC-B007036, 31 Aug 1962

2-2 R. S. Swanson, P. W. Soule, "Rendezvous Guidance Technology," Proceedings of the National Meeting on Manned Space Flight (IAS), St. Louis, 30 Apr–2 May 1962, p. 106

2-3 B. Billik, "Survey of Current Literature on Satellite Lifetimes," ARS J., Vol. 32, No. 11, Nov 1962, pp. 1641–1650

2-4 W. Straley, "The Phasing Technique in Rendezvous," ARS J., Vol. 32, No. 4, Apr 1962, p. 620–626

2-5 J. V. Breakwell, R. W. Gillespie, S. E. Ross, "Researches in Interplanetary Transfer," ARS J., Vol. 31, No. 2, Feb 1961

2-6 Lockheed Missiles & Space Co., A Study of Interplanetary Transportation Systems, Final Report, Code No. 3-17-62-1, Contract NAS 8-2469, 2 Jun 1962

2-7 Raytheon Company, Rendezvous Guidance and Mechanization for Orbit Launch Operations, Vol. 1, BR-1469A, 20 Dec 1961

Section 3

CRYOGENIC PROPELLANT STORAGE REQUIREMENTS

by

G. C. Vliet

Section 3
CRYOGENIC PROPELLANT STORAGE REQUIREMENTS

3.1 INTRODUCTION AND SUMMARY

Application of either chemical or nuclear propulsion systems using cryogenic propellants is being stressed in proposed early manned interplanetary travel. A typical mission, used in this study as a model, would be an orbital stopover at Mars in which a propulsion system (nuclear or chemical) employing liquid hydrogen is used either to brake the vehicle at the planet or to escape from the capture orbit. Because of the relatively long durations required for these missions the thermal protection of the cryogenic propellant becomes a prime consideration. It is not the intent of the present study to evolve a specific design, but rather to investigate the problems involved in storing liquid hydrogen for long term missions and to provide solutions and recommendations where possible.

Among the many factors influencing the design are the mission duration and orbit stay times. For the present study the mission is assumed to consist of one Earth orbit at 200 km, a transit time of 150 days, and 10 days in a 500 km noon-circular Martian orbit. In addition, the propellant tank orientation, volume, shape, interface structure and pressure design (vented or non-vented), the type of propellant and its initial state (saturated, subcooled, or solid) and the type of insulation are pertinent to the study. For this preliminary analysis, the effects on the cryogenic storage due to the thermal environment associated with drag brake capture at the planet was not investigated. The effects of nuclear energy generation within the propellant in the case of a nuclear propulsion system was also omitted.

The details of the study are principally concerned with storing liquid or solid hydrogen in a cylindrical tank with hemispherical ends which is insulated with a typical super-insulation. The parameters of primary interest are initial propellant state and tank

volume and shape for both the vented and non-vented designs. The relation of heat leaks, as governed by tank support design and structural material, to the overall heat transfer to the liquid is considered. The practicality of using liquid propellants other than hydrogen is also investigated. Results of the study indicate that hydrogen storage for interplanetary missions is feasible.

3.2 PROPELLANT TANK DESIGN

For this study the propellant tank is designed on the basis of a cylindrical section with hemispherical ends, the total volume and diameter being variables. The interface structural support is not defined but estimates of heat leak and recommendations are made in Subsection 3.5.2, below.

The pressure vessel design may be "vented" or "non-vented". By the "vented" design it is implied that all thermal energy entering the propellant is removed as latent heat of vaporization of vented gaseous propellant, and the optimum insultation system is determined by minimizing the effective weight penalty (boiloff weight + insulation weight). The optimization procedure is described below in Section 3.3. In the "non-vented" design, thermal energy which enters the tank appears as sensible energy in the warmer liquid propellant and latent heat in the vaporized propellant which is contained within the vessel and results in a pressure rise. The insulation system is optimized on the basis of minimizing insulation weight plus increased tank weight due to pressure rise. The insulation optimization for the non-vented design is considerably more involved because in determining tank weight as a function of design pressure, the dynamic loads during ascent and many other factors must be considered.

A composite design wherein the tank does not vent until the pressure exceeds a specific value is a third possibility. This design is not treated here but is definitely reasonable and may prove advantageous.

3.3 INSULATION

Types of insulation for a vented design may be evaluated on the basis of weight penalty (W_p) which is equal to boiloff weight + insulation weight:

$$W_p = W_{B0} + W_I$$

$$W_p = \frac{kA\theta(\Delta T)}{\delta L} + \rho \delta A$$

where k, ρ, δ, A and ΔT refer to the insulation thermal conductivity, density, thickness, area and temperature drop respectively, θ to time and L to hydrogen latent heat of vaporization. This equation for the weight penalty assumes: (1) steady state (good for long term missions), (2) $\Delta T \neq f(\delta)$ (good for super insulation), (3) tank area equal to insulation area, and (4) added tank weight to contain lost propellant negligible. Differentiating with respect to δ and setting the result equal to zero to obtain the minimum weight penalty, the optimum insulation thickness is:

$$\delta_{op} = \sqrt{\frac{k\theta\Delta T}{L\rho}}$$

The ratio of weight penalties for two types of insulations based on the optimum values is then:

$$\frac{W_{p,F}}{W_{p,s}} = \sqrt{\frac{k_F \rho_F}{k_s \rho_s}}$$

Comparing a typical foam insulation (F), such as polyurethane*

$$k \approx 0.007 \text{ Btu/hr ft } ^\circ\text{R} \approx 0.01 \text{ kcal/hr m } ^\circ\text{K}; \quad \rho \approx 2.0 \text{ lb/ft}^3 \approx 32 \text{ kg/m}^3$$

*These are the manufacturers quoted values for thermal conductivity.

with a typical super insulation (S), such as Linde SI-4*

$k \approx 2.5 \times 10^{-5}$ Btu/hr ft °R $\approx 3.7 \times 10^{-5}$ kcal/hr m °K; $\rho \approx 4.7$ lb/ft^3 ≈ 75 kg/m^3

applied external to the tank, the weight penalty ratio is:

$$\frac{W_{P,F}}{W_{P,S}} = 11$$

which indicates that the super-insulations are an order of magnitude better than foam insulations. To be effective, super insulations must be evacuated and are therefore particularly appropriate for space applications where they are self evacuating when applied externally. Super insulations do have disadvantages. (1) Proven methods of supporting and protecting the insulations without jeopardizing the effective thermal conductivity are still in the development stage. The manufacturers quoted values of thermal conductivity are theoretical values and are highly optimistic considering the present state-of-the-art of application techniques. (2) For insulating LH_2 tanks, they must be evacuated or purged with helium when under atmospheric pressure on the launch pad. Unless so purged or completely evacuated, oxygen and nitrogen will solidify in the insulation adjacent to the tank wall. Purging with helium increases the thermal conductivity by a factor of approximately 3000 compared to completely evacuated insulation. Evacuation is effective when the pressure is less than approximately one tenth micron of mercury, and complete evacuation of a large system is difficult. Nevertheless super insulation appears to be definitely attractive.

The typical super insulation Linde SI-4, which consists of layers of aluminum foil separated by layers of fiberglass, will be assumed in the following study. The values which are used for its thermal conductivity and density are indicated above, and a protective covering of material of 0.03 inch (0.076 cm) thickness and of 100 lb_m/ft^3 (1600 kg/m^3) density are included in the total insulation weights.

*These are the manufacturers quoted values for thermal conductivity.

3.4 ENVIRONMENTAL CONSIDERATIONS

3.4.1 Acceleration Environment

To provide a gravitational environment for the crew, it is anticipated that the vehicle will be rotated. Artificial gravity is also desirable for the non-vented tank design so that thermal gradients in the propellant are essentially eliminated and maximum tank pressures are therefore minimized. In a truly zero gravity environment, heat transfer in the propellant is by pure conduction. Since the tank pressure corresponds to the vapor pressure of the liquid of maximum temperature, the actual tank pressure for an unmixed propellant could be substantially above the vapor pressure for the propelland if it were completely mixed. This is of greatest importance where there are concentrated heat leaks and the tank is virtually full.

A Rayleigh number

$$Ra = \frac{g \beta (\Delta T) \ell^3 \rho^2 C}{\mu k} \geq 1700$$

indicates the inception of cellular convective flow in the propellant. The symbols μ, k, ρ, c, β, and ΔT refer to liquid viscosity, thermal conductivity, density, specific heat, volumetric coefficient of expansion, and temperature drop respectively, g to acceleration and ℓ to a characteristic length. Assuming $\Delta T \leq 1°R$ (0.55°K) to represent good mixing and hydrogen in a 20-ft (6.1-m) diameter tank ($\ell \approx 10$ ft) (3.05 m) the necessary acceleration to produce the critical Rayleigh number is:

$$g = 7.7 \times 10^{-10} \text{ ft/sec}^2$$
$$= 2.3 \times 10^{-10} \text{ m/sec}^2$$

If the propellant tank is on the axis of the system and the entire system is rotated to provide 1 standard g at 100-ft (30.5-m) radius, the acceleration in the propellant is

of the order 1 to 10 ft/sec^2 which indicates that good mixing will most certainly be assured. In the results which follow for the non-vented design complete mixing is assumed.

3.4.2 Thermal Environment

Accounting for the effects of planet emission and albedo radiation and insolation, the following time-averaged tank surface temperatures were obtained:

Earth Orbit:	T_s = 395°R (220°K)
Transit Phase:	T_s = 360°R (200°K)
Mars Orbit:	T_s = 335°R (186°K)

In determining these surface temperatures it was assumed that the emissivity and absorptivity of the insulation were 0.8 and 0.25 respectively. The insulation conduction was neglibible compared to thermal reradiation for the insulation thicknesses of interest, and therefore the insulative temperature drop was not a function of insulation thickness for the thicknesses considered. It was assumed that the 200-km Earth and 500-km Mars orbits were noon-circular (i.e., passes through the sub-solar point), that the vehicle was rotated on its axis, which was parallel to the surface of the planet, and that the vehicle moved in the nose-forward position. For the transit phase the vehicle was also axially rotated and oriented broadside-to-sun.

For the cases described later in this report where the vehicle is oriented nose-to-sun during the transit phase, a somewhat higher average surface temperature is used for the forward hemisphere.

3.5 RESULTS

The vented and non-vented tank designs are discussed separately below. The effects of tank orientation, initial propellant state, heat leaks, and tank capacity and shape are considered for each design. The major portion of the work which follows considers

only the transit phase of the mission because the duration of Earth and Mars orbit phases are small in comparison.

The two orientations which are considered are the broadside-to-Sun and nose-to-Sun cases. In the former the tank is assumed to be rotated on its axis and the entire tank must be insulated. In the latter the nose only need be insulated during the transit phase. The walls of the tank not exposed to solar radiation may be left uninsulated during transit but must be insulated when in Mars orbit.

3.5.1 Vented Tank Design

For the vented tank design as defined, the performance of the insulation is not affected by liquid subcooling and the results which follow therefore apply to any initial liquid state.

Broadside-to-Sun Orientation. For the 150-day transit time the insulation was optimized for a wide range of tank diameters for the three tank capacities: 100,000; 200,000; and 300,000 lb, (45,400; 90,800;and 136,200 kg respectively). It was found that the optimum insulation thickness was δ = 2.15 in. (5.6 cm) and was independent of tank volume or diameter. Figure 3-1 presents a plot of percent boiloff* as a function of tank diameter and volume based on this optimum insulation thickness. The percent boiloff increases with decreasing tank diameter due to the increases of surface area to volume ratio. The minimum boiloff results for the spherical shape as this represents the minimum A/V ratio, and percent boiloff decreases with increased tank capacity. These values indicate 2-1 to 4-1 percent loss of propellant for all tank capacities where the diameter is greater than 20 ft (6.1 m). Tanks of smaller diameter are poor from structural considerations because of the large L/D ratio.

The optimum insulation weight as a function of tank diameter and capacity is shown in Fig. 3-2, the minimum occurring for the spherical shape. Total weight increases with capacity and with decrease in diameter because of the accompanying higher surface

*Note that heat leaks are not included in these results.

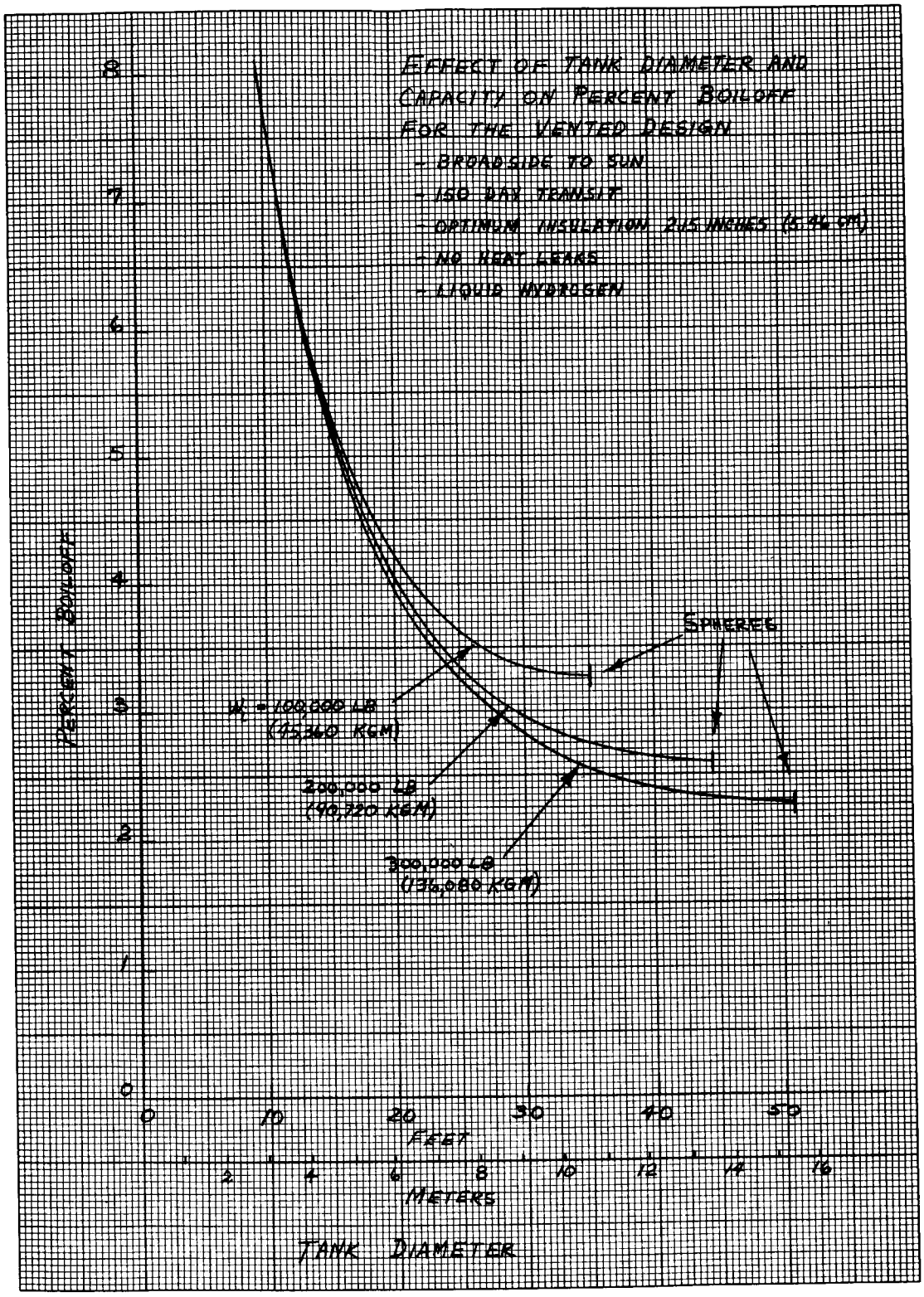


Fig. 3-1 Effect of Tank Diameter and Capacity on Percent Boiloff for the Vented Design

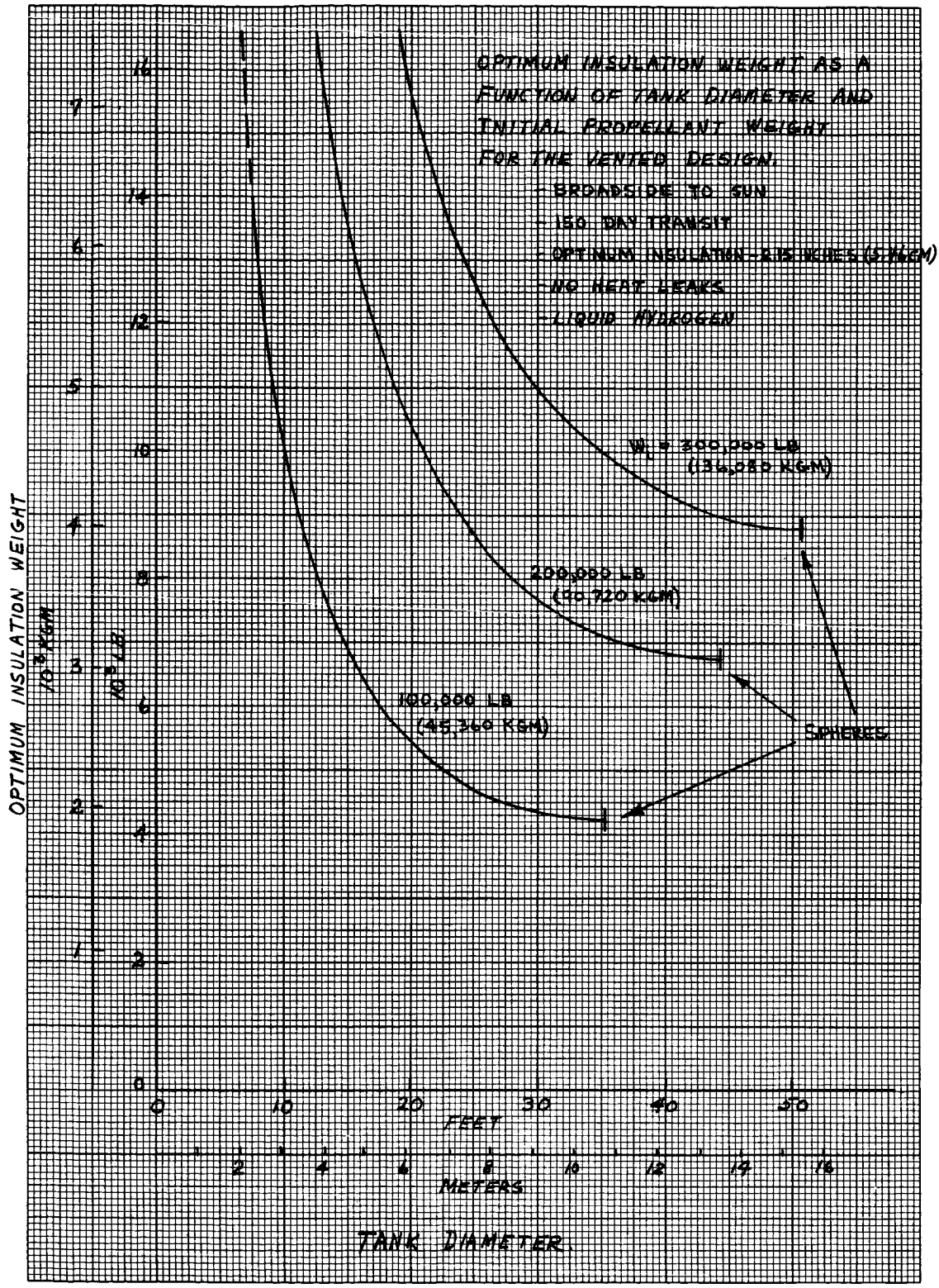


Fig. 3-2 Optimum Insulation Weight as a Function of Tank Diameter and Initial Propellant Weight for the Vented Design

area. The optimum insulation thickness for the entire mission, including the 10-day Mars orbit, would be only 3 percent greater because the optimum thickness varies as the square root of time.

Nose-to-Sun Orientation. If the vehicle can be oriented nose-to-Sun throughout the transit phase, then only the forward hemisphere need be insulated. The optimum insulation thickness covering the forward hemisphere differs from that obtained in the broadside orientation only by the square root of the ratio of the insulation temperature drops. The average surface temperature for the broadside case is 360 °F (200° K) compared to an average forward hemisphere temperature of 383° R (213 °K) for the nose-to-Sun case during the transit phase. Based on a 37 °R LH_2 temperature the increase in optimum insulation thickness is therefore approximately 3.5 percent.

Figure 3-3 presents the percent boiloff* as a function of tank diameter and capacity for the nose-to-Sun orientation and the forward hemisphere covered with the optimum thickness of insulation (2.22 in. or 5.64 cm) based on the 150-day transit time. The solid set of curves represent the case where the bare walls (cylinder and aft hemisphere) radiate to space and the dashed curves correspond to the case where there is no radiation from the walls. An example of the latter would be the case where the insulation on the forward hemisphere is optimized for the 150-day mission and the insulation on the cylinder and aft hemisphere is optimized on the Martian orbit but is in-place for the entire mission. The reason why the solid curves intersect the tank diameter axis at values other than zero is that when radiation from the bare walls is included the actual heat rate to the tank becomes negative for small diameter tanks. The difference in the percent boiloffs for these two cases is greatest at low-tank diameters and decreases with increasing diameter. However, tanks of large L/D ratio (small diameter) have other major disadvantages as discussed below. Therefore the advantage of leaving the walls bare as shown in Fig. 3-3 becomes of less importance for reasonable L/D ratios.

*Note that heat leaks are not included in these results.

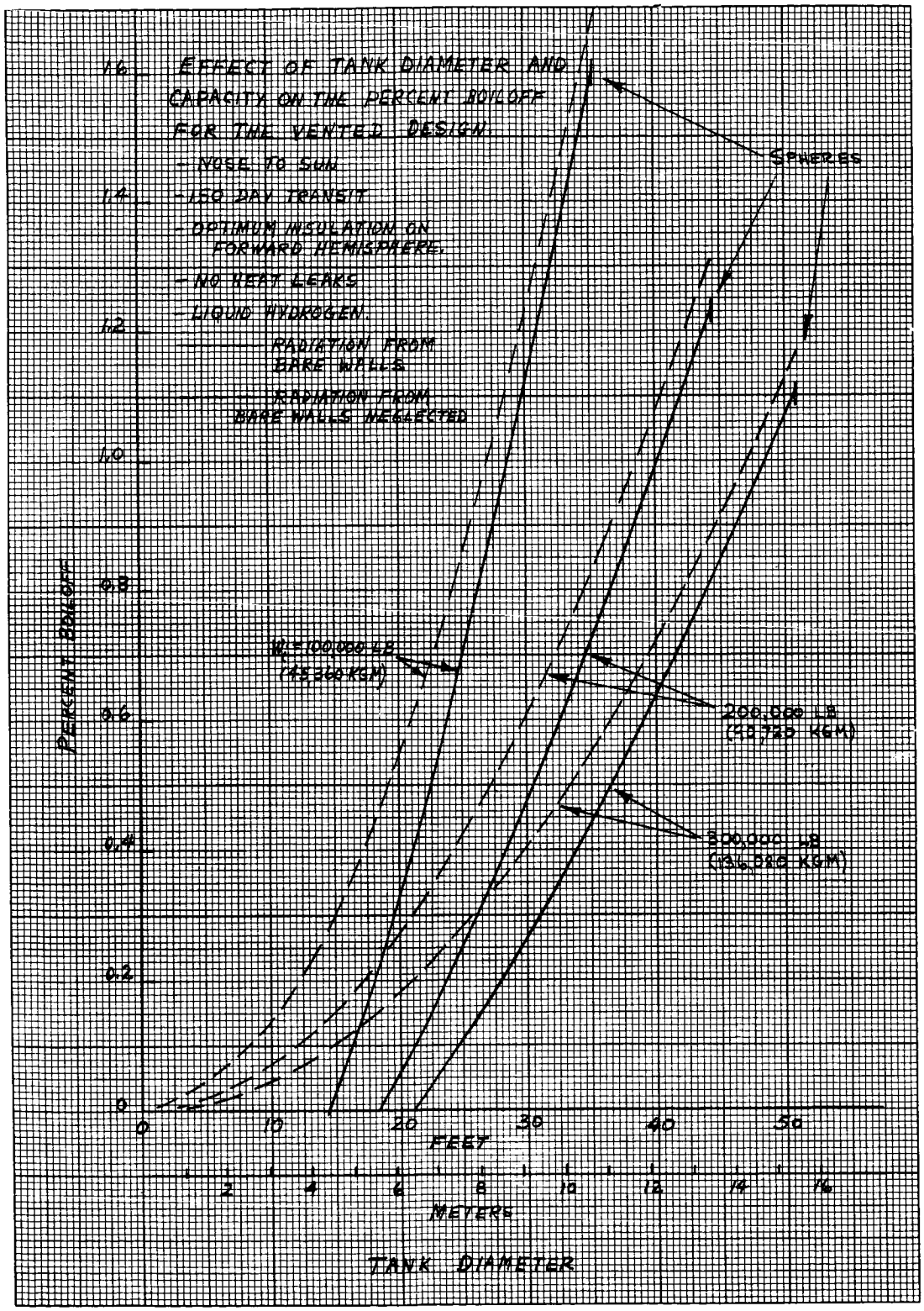


Fig. 3-3 Effect of Tank Diameter and Capacity on the Percent Boiloff for the Vented Design

The optimum insulation weight for the forward hemisphere as a function of tank diameter is shown in Fig. 3-4. The optimum thickness (2.22 in. or 5.64 cm) is independent of tank diameter and the insulation weight therefore varies as the diameter squared since the forward hemisphere surface area varies as D^2.

Insulation for Mars Orbit. If the tank is to be oriented broadside-to-Sun during the transit phase then the transit phase optimized insulation thickness can be increased slightly as discussed above to include the 10 days in Mars orbit. However, if the nose-to-Sun orientation is assumed during transit the walls must be insulated for the duration of the Mars orbit. Possible designs might be an "insulated bag" to be pulled over the tank or a "roll of insulation" to be unrolled and wrapped around the tank while in the vicinity of Mars or to have the Mars optimized insulation "in-place" during transit. Having the cylinder and aft hemisphere insulation in-place initially is advantageous from reliability considerations: there are the problems of attaching the insulation prior to approaching Mars and deviations from exact nose-to-Sun attitude during transit. Furthermore, this provides protection during ascent and earth orbit phases of thc mission. On Fig. 3-5 is presented the percent boiloff as a function of Mars orbit duration with tank capacity as the parameter. This data is based on a vented tank design and the optimum insulation thickness, also shown in Fig. 3-5. It is advantageous to have tanks of low L/D ratio (low area) so that the Mars optimized-insulation weight is minimized.

No Net Heat Rate. If for the nose-to-Sun orientation, the forward hemisphere is insulated such that the heat transfer to the propellant just balances the energy radiated to space from the bare walls, no boiloff will result. Calculations neglecting heat leaks show this method to be impractical due to the resultant large insulation weights, except for longer, slender tanks which are poor for structural reasons.

In addition heat leaks sharply increase insulation weight and may even prevent zero net heat rate from being achieved. In this design, the bare surface must be protected when in the vicinity of either Earth or Mars.

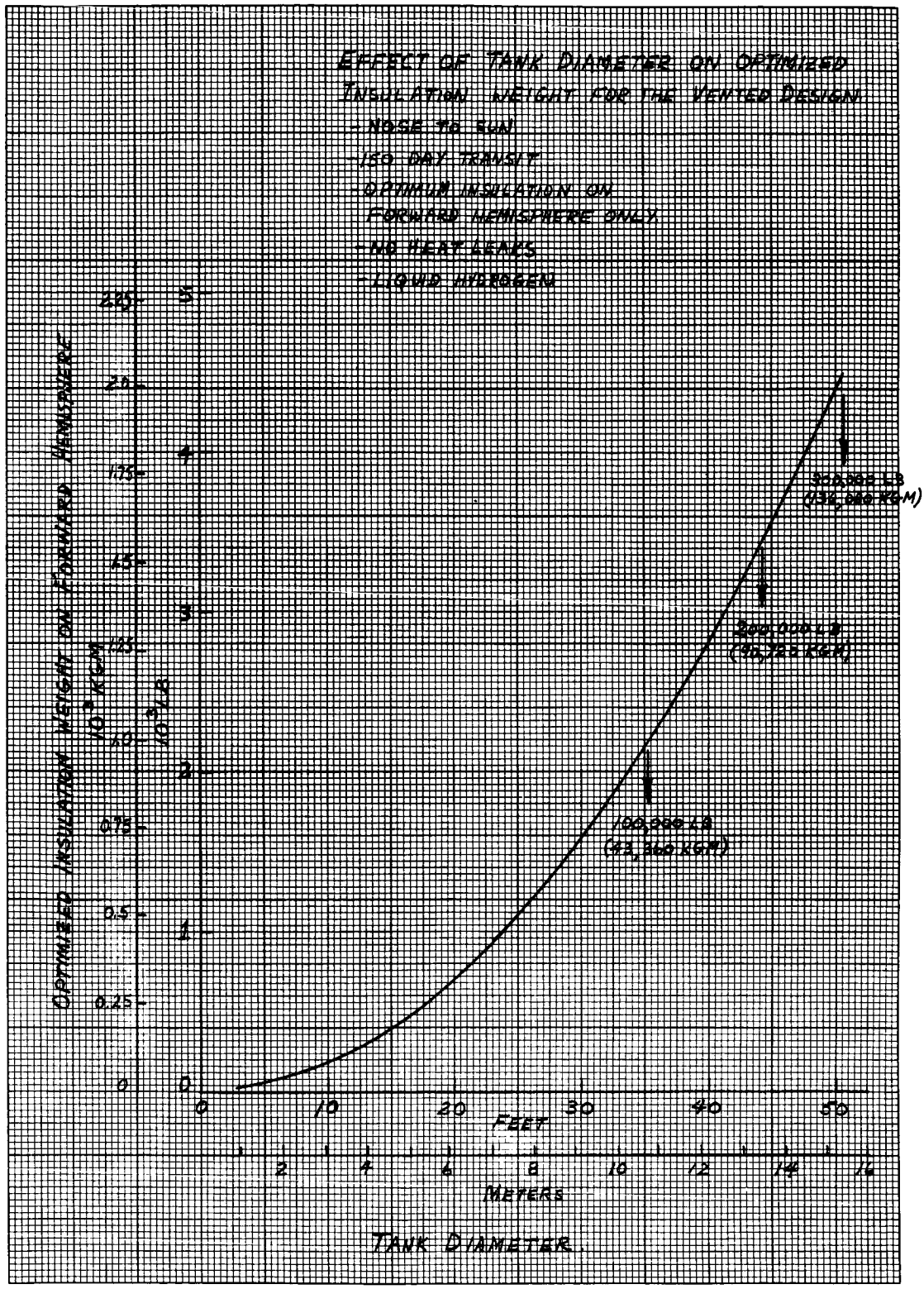


Fig. 3-4 Effect of Tank Diameter on Optimized Insulation Weight for the Vented Design

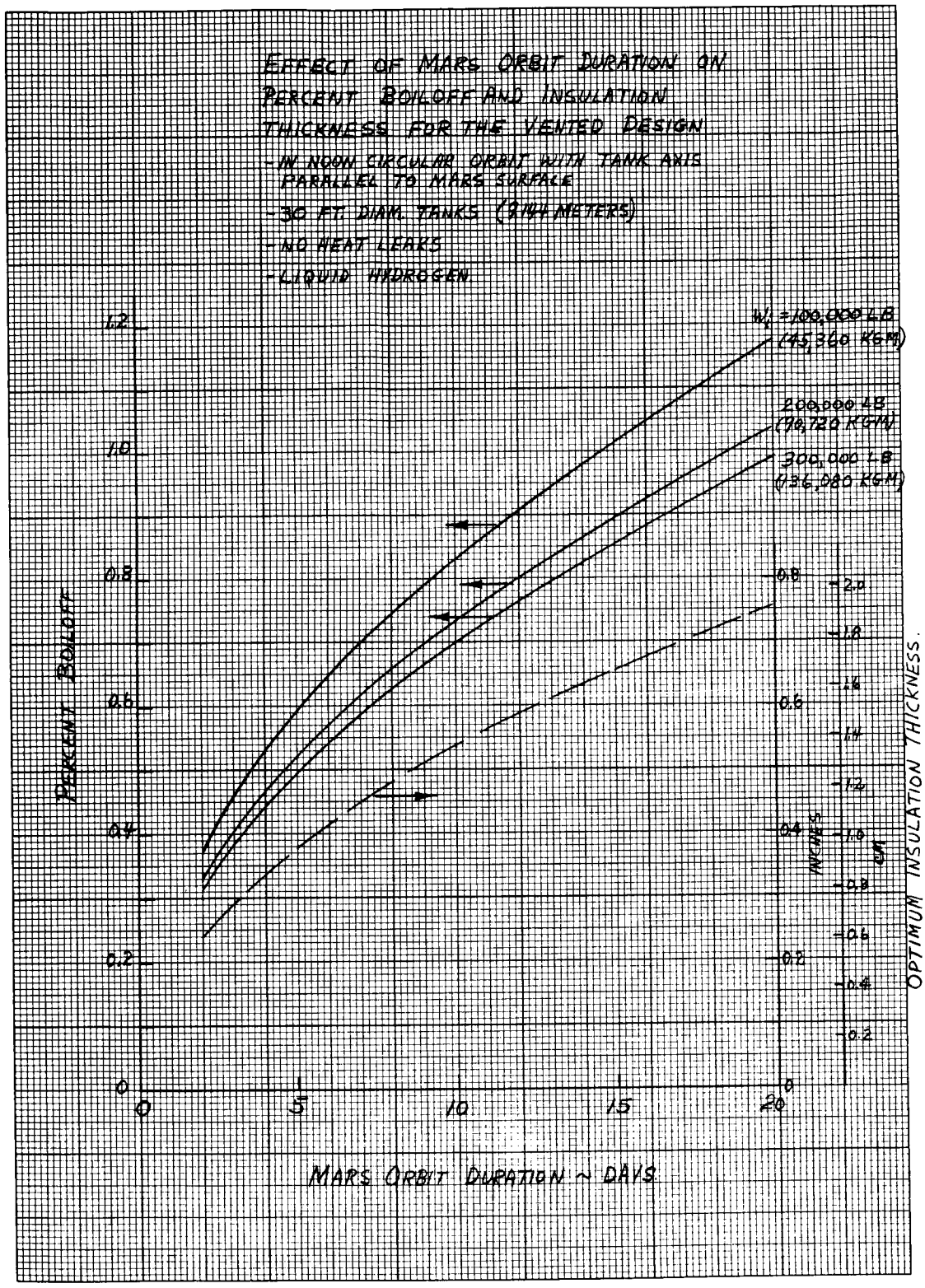


Fig. 3-5 Effect of Mars Orbit Duration on Percent Boiloff and Insulation Thickness For the Vented Design

This concept does not therefore appear attractive, even though the magnitude of reradiation from a vehicle should be considered in any design.

3.5.2 Heat Leaks

Neglected throughout the preceding analyses was the contribution of heat leaks through the tank support structure to the overall heat input to the propellant tank. Because of the uncertainty of tank placement and structural methods to be employed, a basic configuration was assumed for purposes of calculations necessary to estimate the significance of heat leaks. The configuration shown in Fig. 3-6 is a 100,000 lb (45,400 kg) payload supported on the propellant tank by a cylindrical interstage of 35-ft (10.7-m) diameter. The wall thickness necessary to support this payload under an assumed ascent acceleration of 5 standard g's was determined. Consideration was given to both titanium and aluminum as the supporting structure. For the conditions given, the thickness of cylinder wall was found to be 0.25 in. (0.64 cm) and 0.31 in. (0.79 cm) for titanium and aluminum, respectively.

With this data, the heat leak was estimated for two separate orientations, that of nose-to-the-Sun and broadside-to-the-Sun. The length of the forward skirt was assumed to be 10 ft (3.05 m). The results of this analysis are presented in Table 3-1*:

Table 3-1

HEAT LEAK ANALYSIS

Material	Orientation	Heat leak btu/hr	Heat leak kcal/hr
Titanium	Nose to Sun	289	728
	Side to Sun	437	1100
Aluminum	Nose to Sun	1686	4250
	Side to Sun	2710	6830

Because of its considerably lower thermal conductivity, titanium is advantageous in terms of minimizing heat leak.

*It is assumed that the heat leak from the aft interstage, when uncoupled from the booster, can be completely eliminated by insulation.

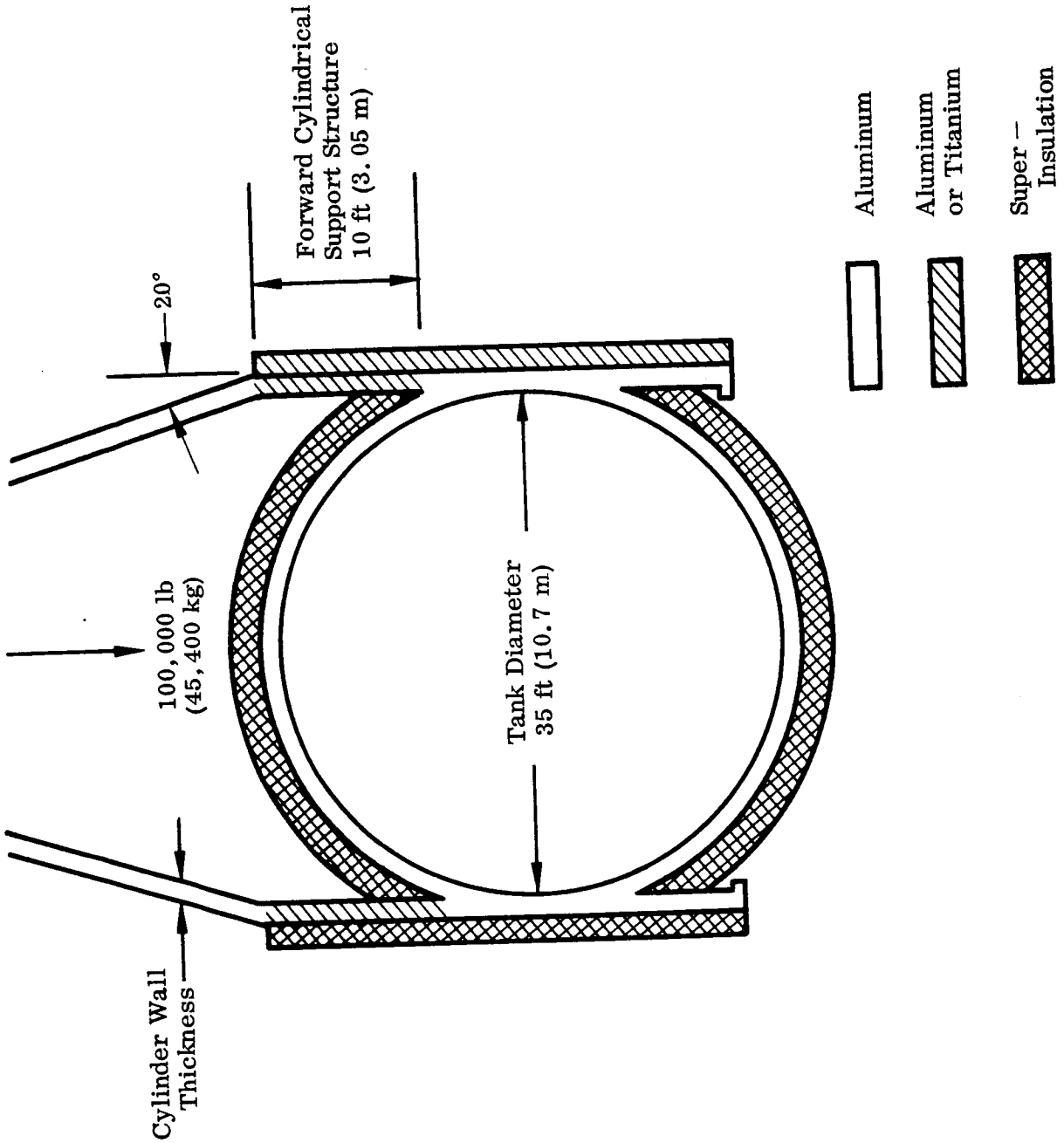


Fig. 3-6 Tank and Support Configuration

Considering again the vented tank design during the transit phase of the mission and adding heat leak (titanium structure) to the previously determined heat flux for the optimized insulation, a comparison of the increase in propellant boiloff is made in Table 3-2 for the 100,000 lb (45,4000 kg) case and a 30 ft (9.15m.) diameter tank. These results indicate that the boiloff, when heat leaks are included, is tolerable.

Table 3-2

COMPARISON OF BOILOFF WITH AND WITHOUT HEAT LEAKS

	Boiloff (%)	
Case	No Heat Leak	With Heat Leak
Side to Sun	3.35	11.50
Nose to Sun	1.24	6.63

It should be noted that the optimum insulation thickness is not affected by the magnitude of the heat leak in the vented tank design. This is because heat leak is essentially independent of insulation thickness and appears as a constant term in the weight penalty. In the non-vented design the weight penalty is the sum of insulation weight and tank weight which is a non-linear function of the sum of heat leak and heat rate through the insulation. The optimum insulation thickness can therefore be influenced by the heat leak. This is particularly so for high degrees of intial subcooling or for initially solidified propellant. The effect of heat leaks on the non-vented design is discussed in Subsection 3.5.3.

Because of the long mission duration and because the vehicle is in a zero-gravity environment during the transit phase as well as the planet orbit phase, it may be practical to thermally isolate the propellant tank from the payload by uncoupling it at the forward interstage. The connection between tank and payload could be in the form of a tow cable or spring mechanism which separates the flanges. If the uncoupling approach is taken to reduce heat transfer to the LH_2 , consideration

must be given to the weight penalty of the uncoupling-recoupling mechanism. While a high degree of uncoupling such as a tow cable would essentially eliminate the heat leak, for this configuration, the recoupling that is necessary for corrective and orbital thrusts is difficult because of realignment problems. It is possible that the complexity of the recoupling system may introduce a prohibitive weight penalty. If springs alone are used to separate the payload and tank, a realignment problem still exists and undesirable oscillations may occur which would have to be damped.

A possible compromise is the use of metal rods for separation that will retain the vehicle alignment and will allow recoupling when thrust is applied. The separation force could be supplied by a spring or the rods could be actuated electrically or hydraulically. For the sake of comparison, the tank and payload are assumed to be separated 24 inches (0.61 m) by three 1-in. (2.54 cm) diameter titanium rods. The total heat leak would be approximately 18 Btu/hr, (38 kcal/hr), which indicates an approximate 25 fold reduction compared to the titanium cylindrical interstage shown in Table 3-1. This heat leak represents only 0.34 percent boiloff during the 150-day transit time, and as can be seen from Table 3-2 is only 1/10 the heat rate through the insulation itself. The total boiloff would therefore be 3.7 percent compared to 11.5 percent for the cylindrical titanium interstage. An uncoupling device of this type therefore represents a large improvement of the overall thermal performance of this system.

3.5.3 Non-Vented Design

In this section it is assumed that the tanks are filled and that perfect mixing of propellant is realized by providing a small artifical acceleration field. For the non-vented design the initial state of the propellant (saturated, subcooled, or solid) is of paramount importance since the liquid temperature dictates the tank pressure.*

*If the vapor pressure of the propellant is less than the minimum tank pressure required during ascent due to structural considerations, an inert pressurant gas (helium) will be required to provide the additional partial pressure.

Broadside-to-Sun Orientation. The effect of insulation thickness on the resulting final tank pressure for the 150 day mission with initially saturated propellant (36.2°R or 20.1°K) at 1 standard atmosphere is shown in Fig. 3-7 for 30 ft (9.15 m) diameter tanks and tank capacity as the parameter. Similar calculations were performed for the two cases of 10°R (5.55°K) initial subcooling (with respect to one standard atmosphere) and initially solid hydrogen (at its melting point), respectively; however the results are not presented here.

The results of Fig. 3-7 should be interpreted as follows: For a particular insulation thickness (i.e., 2.0 in.) and a specific tank capacity (i.e., 100,000 lb) there results a final tank pressure (i.e., 23.4 psia) at the end of the 150-day mission when the LH_2 propellant is initially saturated at 14.7 psia. The results show the rapid increase in pressure at low insulation thicknesses which is due mainly to the inverse variation of heat flux with insulation thickness but also partially to the increase with temperature of the slope of the vapor pressure curve. It should also be noted that these curves are based on 30-ft (9.15 m) diameter tanks in all cases. If the basis had been spheres in each case a more pronounced effect of capacity would be evident.

The results of Fig. 3-7 along with the similar results for initially 10°R subcooled propellant and initially solid propellant are cross plotted and appear as Fig. 3-8. Figure 3-8 should be interpreted as follows: To limit the tinal tank pressure at the end of the 150-day mission to a specific design value (i.e., 20 psia, 1.36 atm) for a particular tank capacity (i.e., 200,000 lb, 91,000 kg) and specific initial LH_2 subcooling (i.e., 6°R) a minimum insulation weight (i.e., 5,000 lb, 2270 kg) is required.

The advantage of subcooling with respect to reducing the weight of insulation for the same design pressure is evident from this figure. Since hydrogen solidifies at 25.13°R or 14°K (corresponding to 11.38°R or 6.31°K subcooling at one standard atmosphere) there is a sharp drop in insulation weight at the freezing point. The reason why there is not a greater difference in insulation weight for solid compared

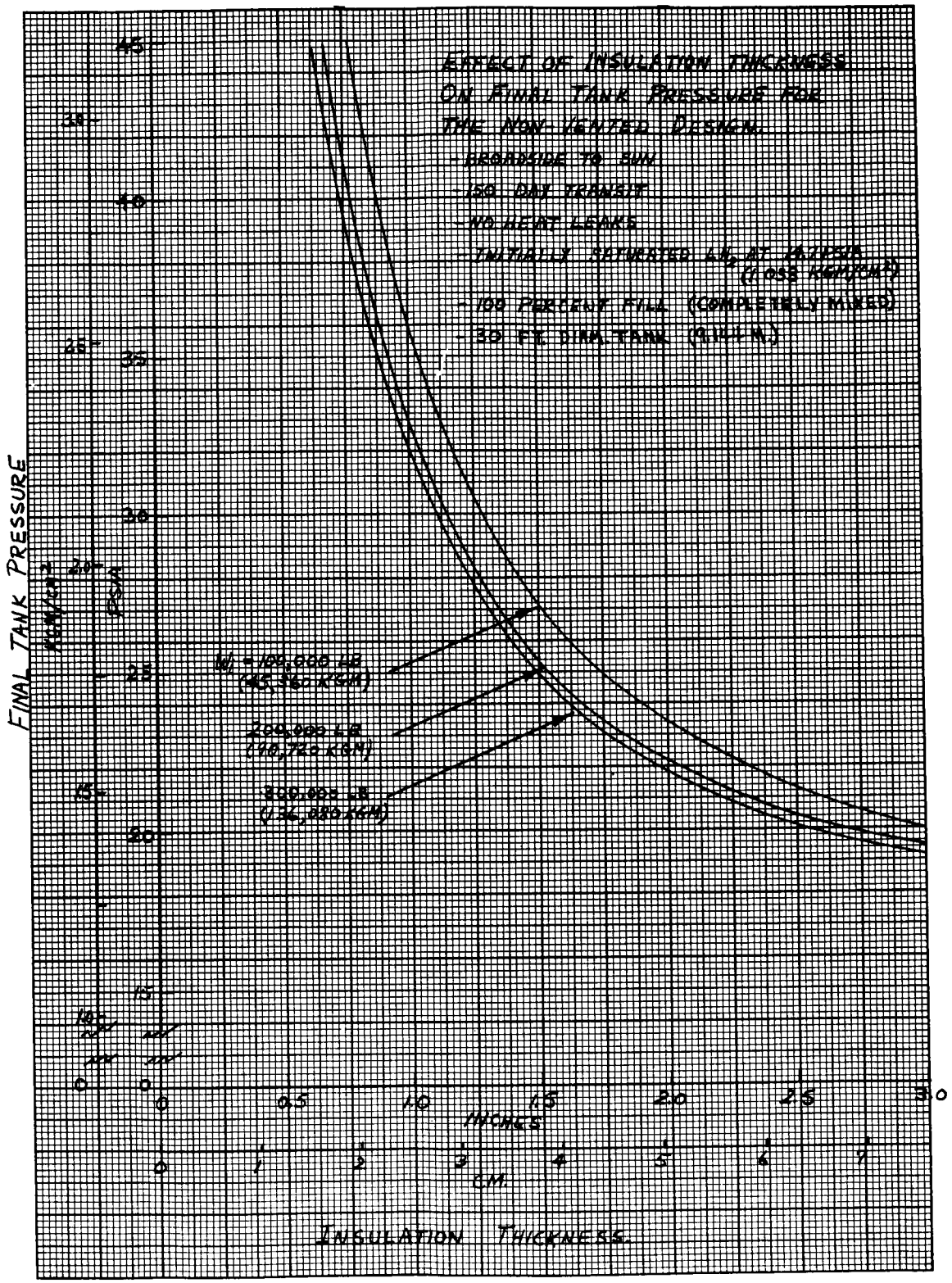


Fig. 3-7 Effect of Insulation Thickness on Final Tank Pressure for the Non-Vented Design

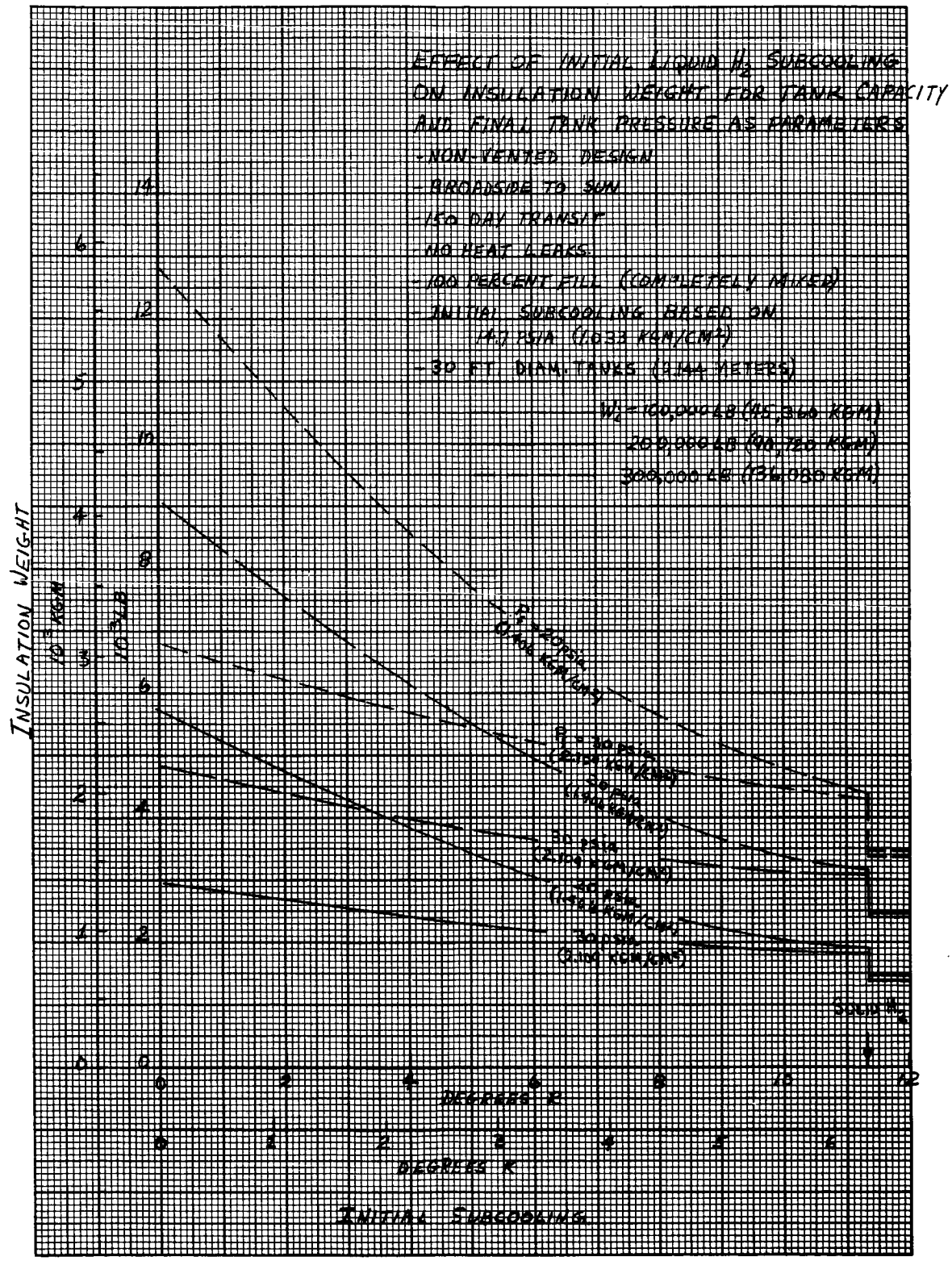


Fig. 3-8 Effect of Initial Liquid H_2 Subcooling on Insulation Weight for Tank Capacity and Final Tank Pressure as Parameters

to LH_2 at the melting point is that although there is a significant reduction in insulation thickness for the solid case, the weight of the covering is constant and is a large portion of the total insulation weight at these small thicknesses. When heat leaks are included the necessary insulation thickness is greater and a greater advantage of subcooling is realized as will be shown below (p. 3-27).

To obtain a more realistic indication of the weight penalty for the non-vented design, the effect of pressure on tank weight must be considered. The tank weight depends on the final tank pressure which in turn depends on the insulation thickness. In reality the tank weight is also affected significantly by the acceleration environment and the payload mass. However in lieu of this latter information, the tank weight will be calculated from the following simple pressure vessel formula,* which refers to a cylindrical vessel capped with hemispherical ends and is constructed of aluminum.

$$W_T = 0.1035\, pV\, \frac{L/D + 1/2}{L/D - 2/3}$$

where

WT	tank weight in lb_m
p	tank pressure in atmospheres
V	tank volume in ft^3
L	tank length in ft
D	tank diameter in ft

In addition the total insulation weight is computed from the following formula:

$$W_I = (0.39\, \delta_I + 0.25)A_I$$

*From "Design Criterion and Analysis for Thin Walled Pressurized Vessels and Interstage Structures," T. J. Hart, LMSD-311623, June 26, 1959.

where

W_I insulation weight in lb_m

δ_I insulation thickness in inches

A_I insulation area in ft^2

and the constants are a result of insulation and covering densities assumed in Section 3.3, above.

The weight penalty or total weight $(W_T + W_I)$ for the non-vented design is plotted against insulation thickness in Fig. 3-9 and against final tank pressure in Fig. 3-10. These figures refer specifically to a 160-day mission (150-day transit plus 10 days in Mars orbit); initially saturated propellant at 1 standard atmosphere; 30-ft (9.14-m) diameter tanks and no heat leaks. The optimum insulation thickness given in the curves of Fig. 3-9 result in the optimum tank final pressures given in Fig. 3-10. For example, the W_i = 100,000 lb case (45,400 kg) gives a minimum total weight of 14,000 lb (6,350 kg) for a final tank pressure of 22 psia (1.55 kg/cm^2) and an insulation thickness of 2.35 in.(6 cm). It is interesting to note that the optimized insulation thickness for the non-vented designs are similar to the optimized thickness (i.e., 2.15 inch) for the vented design.

A similar optimization for the case of 10°R (5.55°K) initial LH_2 subcooling is shown in Fig. 3-11. This figure indicates a large weight reduction with subcooling, but it should be noted that the minimum total weights indicated in Fig. 3-11 are optimistic. This is so because, due to handling requirements and ascent phase considerations (i.e., high accelerations), the tank must be designed for pressures that may be higher than the optimum final pressures obtained using this simplified tank weight versus pressure formula. However, in comparing Figs. 3-10 and 3-11 for higher tank pressure designs, subcooling still significantly reduces total weight.

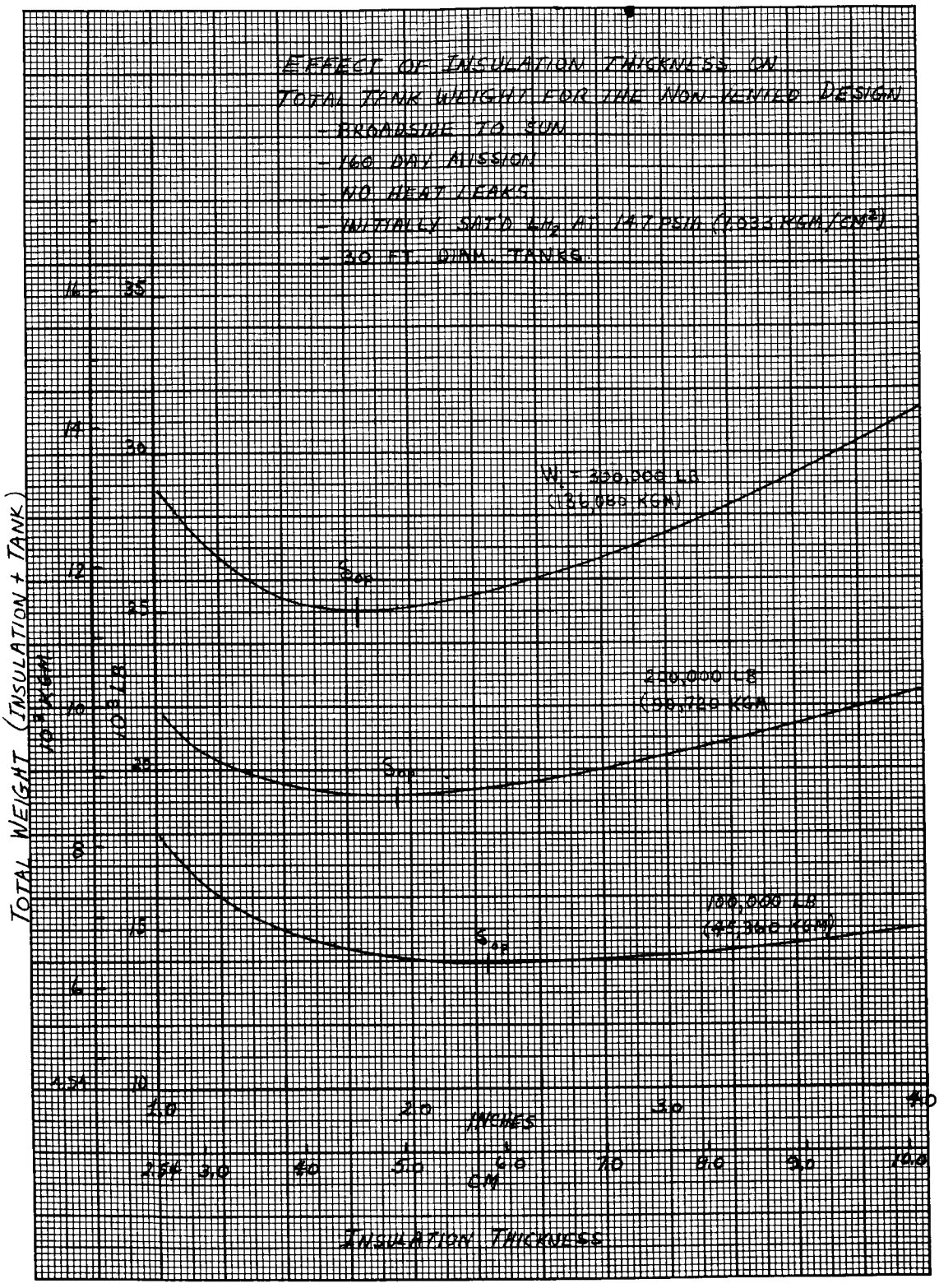


Fig. 3-9 Effect of Insulation Thickness on Total Tank Weight for the Non-Vented Design

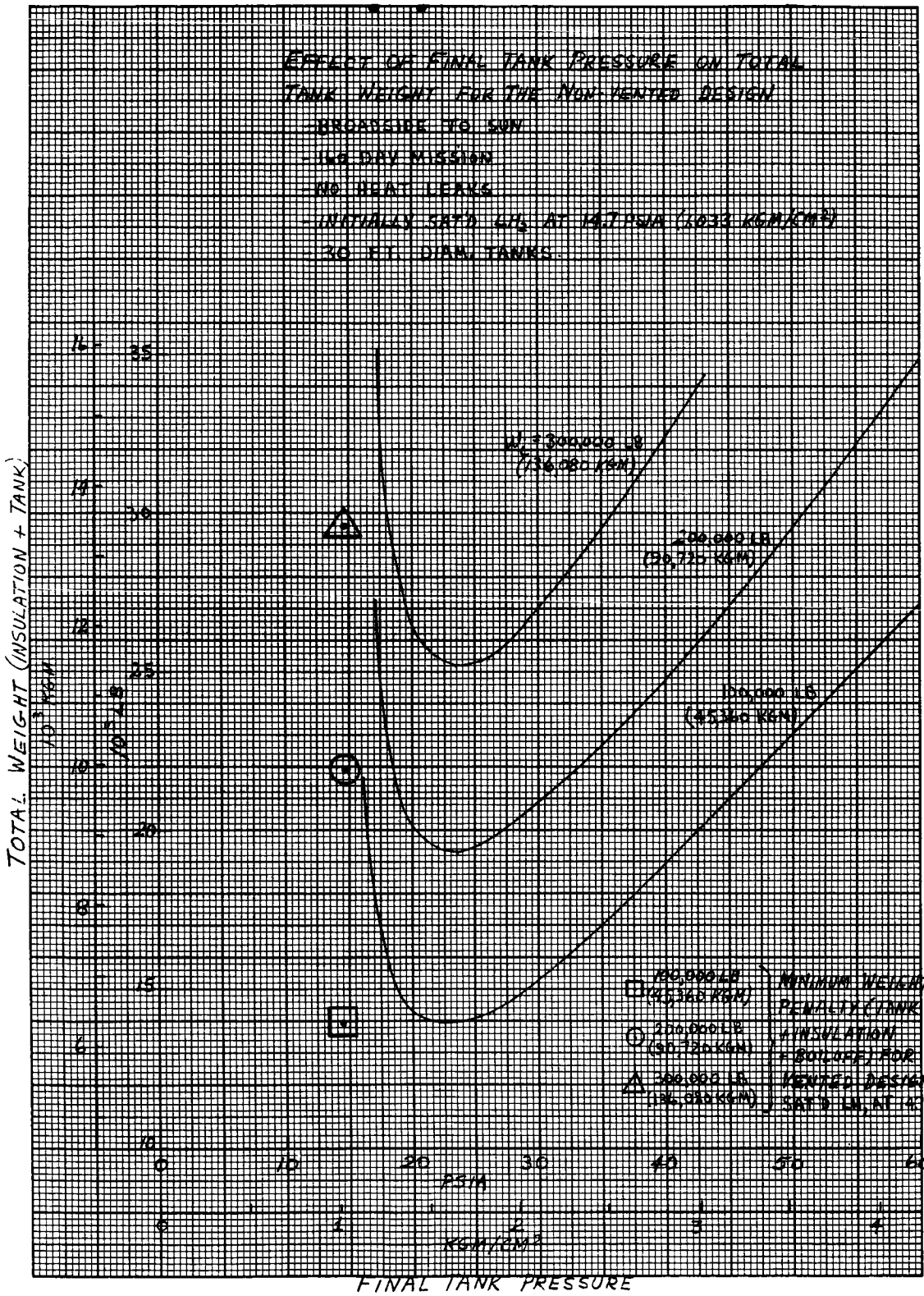


Fig. 3-10 Effect of Final Tank Pressure on Total Tank Weight for the Non-Vented Design

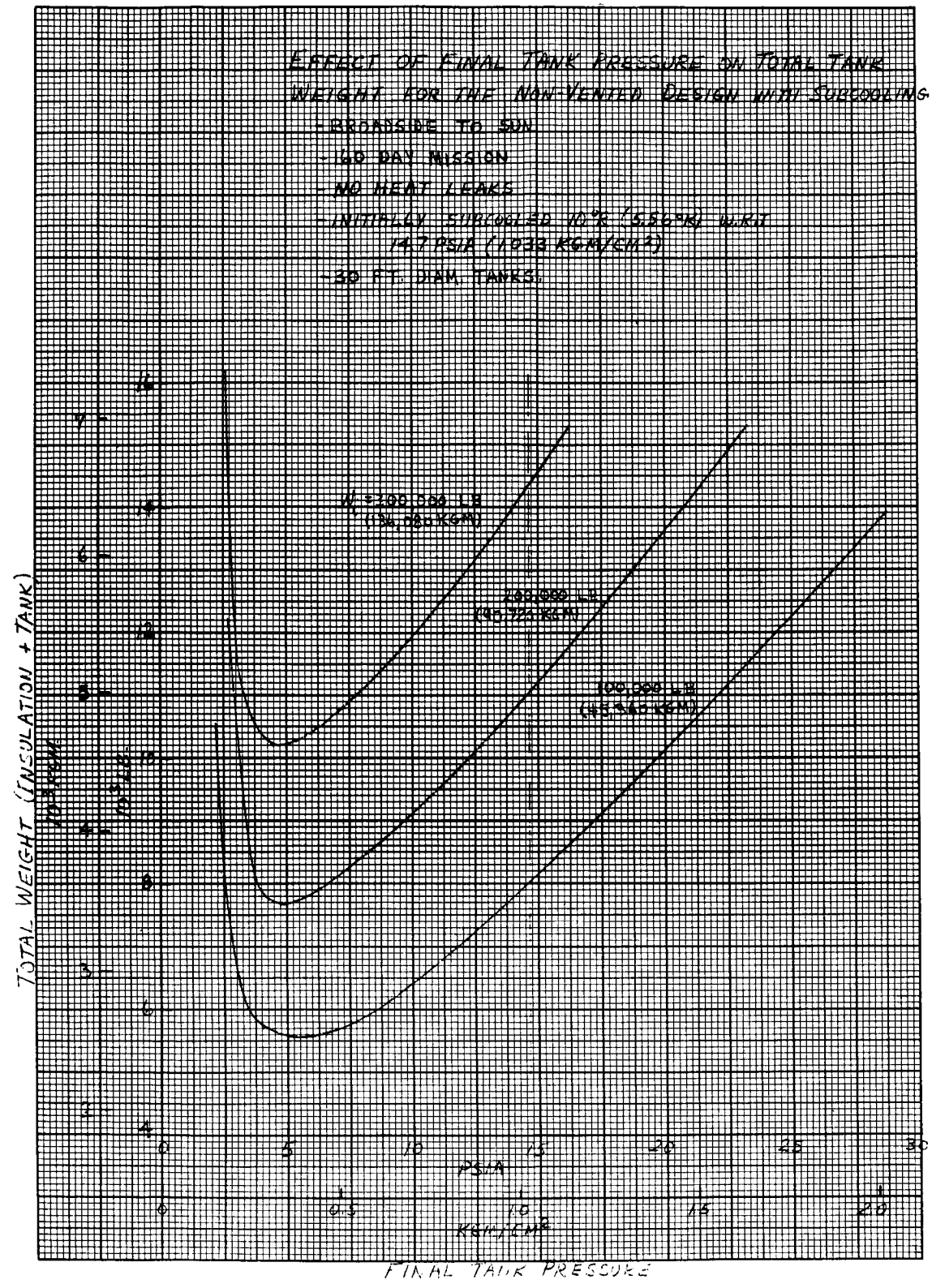


Fig. 3-11 Effect of Final Tank Pressure on Total Tank Weight for the Non-Vented Design With Subcooling

Figure 3-10 also compares the weight penalties of non-vented and vented designs. The symbols indicate the total weight penalties ($W_I + W_T + W_{BO}$) for the vented cases where the tank weight is based on a design pressure of 14.7 psia (1.003 kg/cm^2) and insulation and boiloff weights are based on optimum insulation thickness for the vented design. (See Figs. 3-1 and 3-2.) These results, although not conclusive, indicate that the non-vented design is superior for large tanks.

Nose-to-Sun Orientation. For the nose-to-sun orientation the system can also be designed as non-vented. The effect of forward hemisphere insulation thickness on the final tank pressure for the three tank capacities (100,000; 200,000; and 300,000 lb) and the three initial propellant states (saturated, 10°R, 5.55°K, subcooled, and solid) was computed. These results are not presented here but they are similar to those of Fig. 3-7 for the broadside orientation. Thermal radiation from the uninsulated walls is small compared to the heat rate through the insulated end and is not included in the calculations. Figure 3-12 shows the effect of subcooling and final tank pressure on the necessary insulation thickness for the 200,000 lb (90,800 kg) case. (Similar to Fig. 3-8 for the broadside case.) Subcooling or solidification is of little value with respect to reducing insulation weight because, for the small insulation thicknesses required for the nose-to-sun orientation, the major portion of the insulation weight is in the protective covering.

Effect of Heat Leak (Broadside-to-Sun Orientation). To determine the effect of heat leaks on the non-vented design the estimates determined(Section 3.5.2)for the cylindrical titanium interstage were assumed. Figure 3-13 shows the effect of insulation thickness and initial state of the hydrogen propellant on the final tank pressure for the non-vented design where the estimated heat leaks are included. This figure refers specifically to the broadside-to-sun orientation, a 150-day mission and a 30-ft (9.15-m) diameter tank with 100,000 lb (45,000 kg) capacity.

Using initially saturated LH_2 does not appear to be practical for the magnitude of heat leak considered here. For the nose-to-sun orientation the results for the saturated case would be improved because the heat leaks are reduced, but the significant advantage of subcooling or freezing would still be evident.

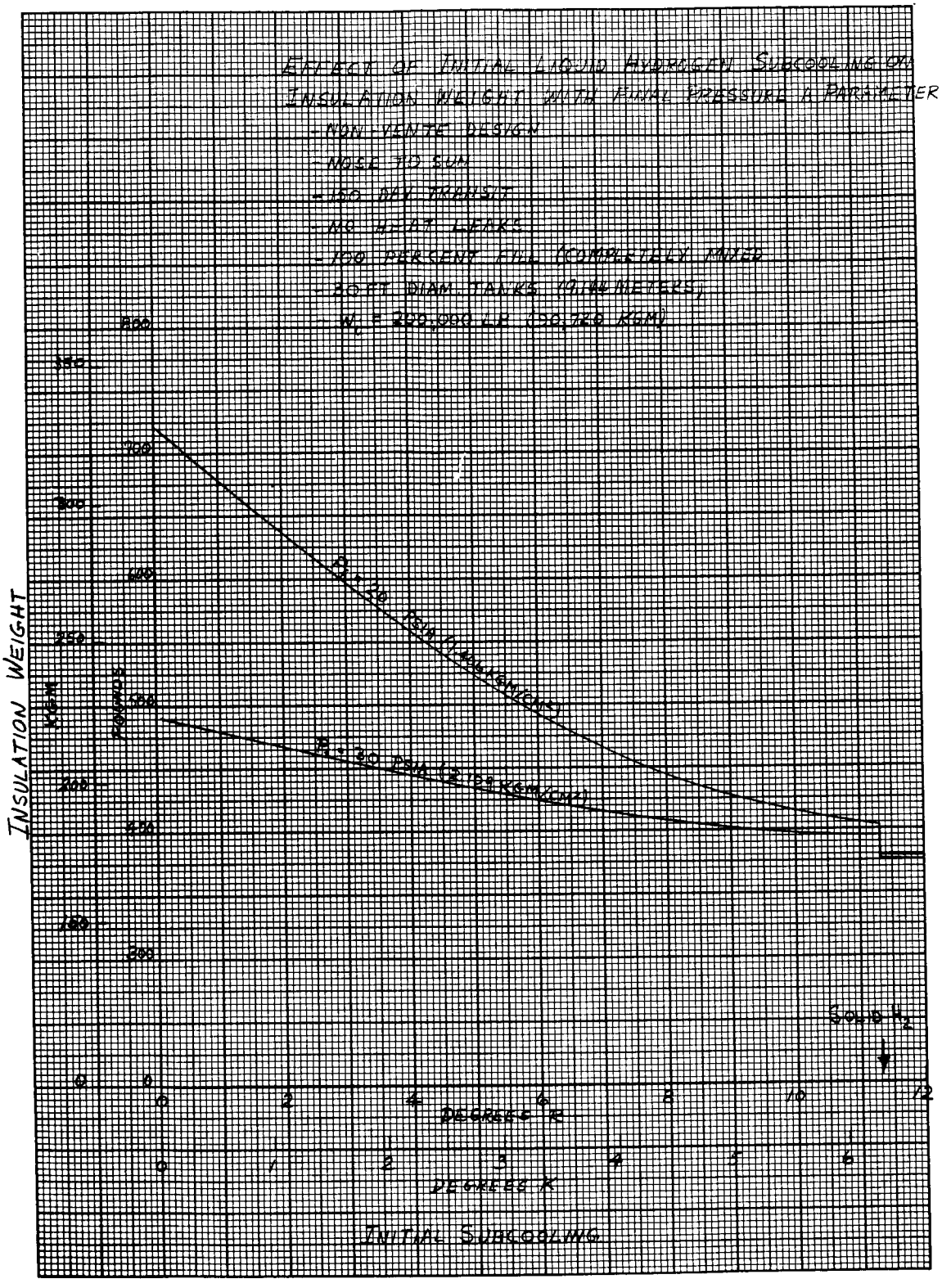


Fig. 3-12 Effect of Initial Liquid Hydrogen Subcooling on Insulation Weight With Final Pressure a Parameter

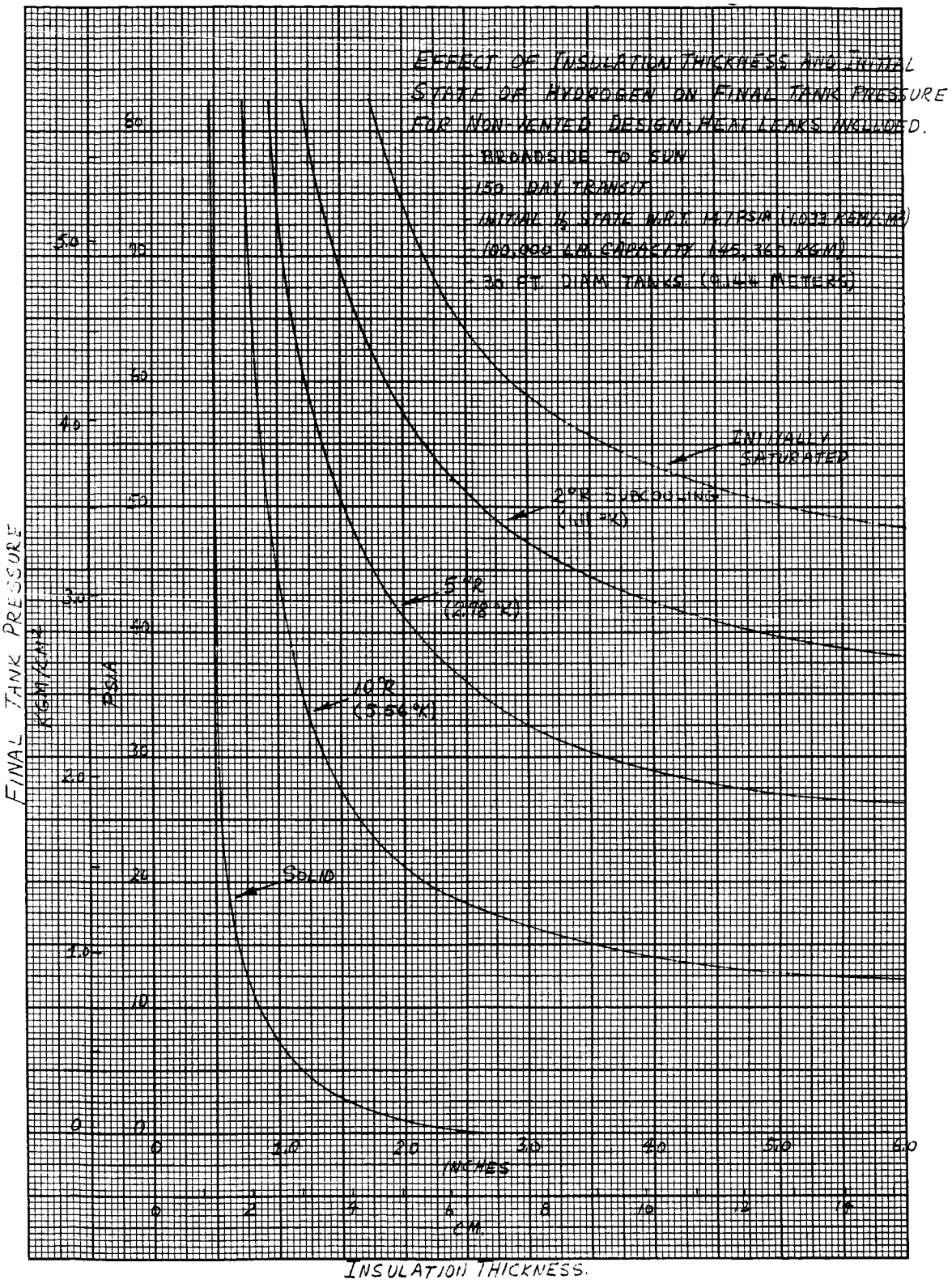


Fig. 3-13 Effect of Insulation Thickness and Initial State of Hydrogen of Final Tank Pressure for Non-Vented Design; Heat Leaks Included

Figure 3-14 is a cross plot of Fig. 3-13 showing the effect of subcooling on the necessary insulation weight to limit the final tank pressure to specific values. The significance of heat leak on the insulation weight for the non-vented design can be seen by comparing Fig. 3-14 with Fig. 3-8.

3.5.4 Other Propellants

It is of interest to examine the advantages of using liquids other than hydrogen as the propellant. A liquid such as propane is of particular interest from a thermal standpoint. With the exception of the boost phase, the vehicle surface temperature for the entire mission varies between approximately 330°R (167°K) and 400°R (222°K). The boiling point of propane is 416°R (231°K) at atmospheric pressure and it freezes at 155°R (86°K). Liquid propane therefore could be stored in an uninsulated tank with boiloff occurring only during the boost phase of the mission.

In present proposed nuclear systems, there is little hydrogen ionization or dissociation. Since the specific impulse varies inversely as the square root of the molecular weight, the ratio of specific impulses for hydrogen and propane in present systems is approximately 4.7. Since the density of liquid propane ratioed to that of hydrogen is 8.4, there is a slight advantage of propane over hydrogen based on propellant tankage requirements; however this advantage is not great. If it were possible to completely dissociate each propellant, the ratio of specific impulses is reduced to 2.0, in which case only twice as much mass of propane compared to hydrogen is required. In this case the volume required to contain the propane is only 24 percent of that for hydrogen.

Thus it appears that the major restriction of using propane, apart from nuclear engine feasibility, is the additional mass required. However, a substantial savings in insulation weight, tank weight and perhaps structural weight for the smaller volume tank is possible.

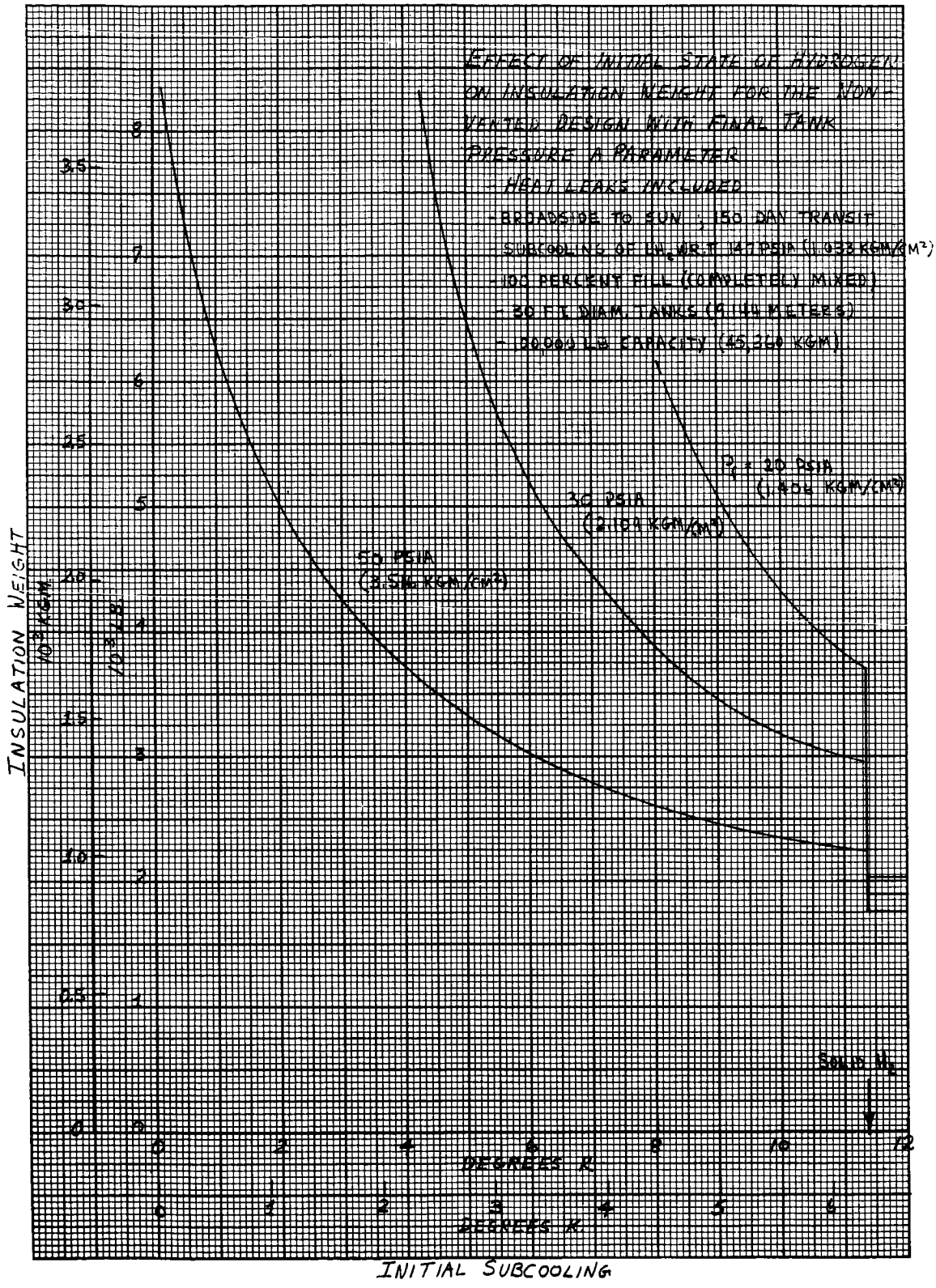


Fig. 3-14 Effect of Initial State of Hydrogen on Insulation Weight for the Non-Vented Design With Final Tank Pressure a Parameter

3.6 CONCLUSIONS

For the transportation and storage of hydrogen propellant on long term missions such as the typical 150-day Martian mission considered in this study, the following conclusions may be drawn:

- Insulation. Use a super-insulation.
- Propellant State. Subcooling or freezing the propellant initially will represent a significant reduction in the weight penalty for either a vented or non-vented tank design.
- Orientation. Orient the vehicle nose-to-sun during the transit phase and optimize the forward hemisphere insulation on the transit phase. The unexposed portions of the tank during transit should be insulated with a Mars orbit optimized insulation. Both because reliability and because the amount of radiation from the unexposed walls is small during transit for practical forward insulation thicknesses and tank shapes, the walls should be insulated for the duration of the mission and not only for the Mars orbit phase. This also meets the need during ascent and earth orbit.
- Vented vs Non-Vented. A comparison of these two designs for the specific case of initially saturated propellant with side-to-sun orientation during transit suggests that the non-vented design is slightely superior weightwise. However this result is not conclusive.
- Tank Shape. Although the transit phase favors a long, slender shape (for the nose-to-sun attitude), the boost phase and Martian orbit phase essentially dictate tanks of low or moderate L/D ratio. From thermal considerations, as few tanks as possible should be used to contain the propellant.
- Heat Leaks. Unless alteration of the tank-payload configuration is made, for long duration missions it appears that the magnitude of heat leaks will be equal to or greater than all other heat rates combined. Separation of tank and payload with long slender rods during the transit phase will however reduce the heat leak to a small fraction of the overall heat rate and still maintain the integrity of the system. Additional unreliability and weight is introduced however.

- Other Propellants. The use of a propellant such as propane, which is liquid in the range of equilibrium space temperatures and which is considerably more dense than LH_2, has definite advantages, but may pose problems too severe when used in a nuclear reactor.

3.7 RECOMMENDATIONS

- Better data on the actual thermal performance of super-insulations when applied to a large vessel is required since the data supplied by the manufacturers is certainly optimistic.
- Further study is recommended in the area of structural configurations since heat leak through structural support members can be a major portion of the overall heat rate.
- Additional insulation optimization studies should be conducted for the non-vented design once adequate information on structure weight as a function of tank pressure is available.
- Consideration should be given to design including various combinations of vented, non-vented and active refrigeration.

Section 4

EARTH ENTRY SYSTEMS

by

R. R. Titus
J. H. Chin

Section 4
EARTH ENTRY SYSTEMS

4.1 SUMMARY

The study of entry into Earth's atmosphere is primarily concerned with entry velocity. The study of return flights from Venus and Mars reveals Earth entry velocities as much as 50 percent higher than those associated with the Apollo program.

The general effect of this is to greatly reduce or eliminate entry corridors and to introduce aerodynamic heating phenomena heretofore of minor significance.

This study presents the analysis of an Earth entry system utilizing aerodynamic braking and propulsive lift which provides entry corridors consistent with expected guidance accuracy and within human tolerance limits on deceleration. This system also operates in a flow regime which reduces the total stagnation point heating to a point where temperatures are in the order of 1600° K or less.

This entry system uses an Apollo-type vehicle, fitted with a large drag brake and a propulsive lift stage.

The basic intent of this study was to establish an entry concept which would be operational in the early 1970 time period. These four concepts were considered:

- An Apollo-type capsule
- An Apollo capsule with exospheric rocket braking to Apollo design speeds
- A conical shaped vehicle using a small nose radius to minimize the stagnation heat rates
- The drag brake system

The latter was chosen on the basis of a minimum weight system and no requirement for materials development nor advanced state-of-the-art. Since one kg reduction in entry system mass may reduce by 20 to 40 kg the mass required on Earth orbit, the saving of many thousands of kg by this system becomes significant.

The drag brake system operates at altitudes between 79.3 km and 91.5 km. The atmospheric entry phase from entry to pull-out is ballistic. The next phase consists of a near constant-altitude deceleration to escape velocity, utilizing propulsion to prevent skip-out and insure single-pass entry. The final phase consists of a normal Apollo entry after discarding the drag brake.

A procedure was used to minimize the mass of the entry system for given entry conditions. This entails a trade-off between the drag brake size and propulsive lift requirements, resulting in an optimum deceleration level for a given entry velocity and pull-out altitude.

The minimum deceleration altitude is then limited by the 10-g limit or a g-time history, defined by a human tolerance limit model.

The flow regime is below the free molecule region and, for this type vehicle, is in the boundary layer regime.

The resulting thermodynamic analysis includes both convective and radiative heating. The latter consists of equilibrium and non-equilibrium phenomena; including the effects of dissociation, ionization, and radiation-convection interaction.

The effect of collision-limiting reduces the total radiation intensity by a factor of six at 79.3 km to sixty at 91.5 km.

The determination of the temperatures on the drag brake includes the assumption of a uniform total heat flux over the surface, since the actual variation of flux is much less than the uncertainties in the total flux itself. The maximum temperature is approximately the initial radiation equilibrium temperature.

The drag brake system provides a solution to hypervelocity Earth entry within the present state-of-the-art and is consistent with an operational time period of the early 1970's.

4.2 GENERAL PHILOSOPHY

The terminal phase of manned interplanetary missions deals with a very complex and somewhat undefined phenomenon: that of entry into Earth's atmosphere. This study is an outgrowth of past entry problems; beginning with missile nose cones, to entry of the Discoverer capsules, to the Mercury program, and the presently proposed Apollo missions. Each in turn has presented new and increasingly difficult problems, especially those entries involving humans. These require major restrictions and design limitations compatible with prescribed human tolerances.

The entry velocities associated with the Mercury program are such that the deceleration levels and aerodynamic heating pulses to which the crew is subjected, are predictable by theory and are substantiated experimentally. The vehicle design is simplified because of the well defined aerodynamic and thermodynamic environment for ballistic entry.

The Apollo program presents additional complications to the entry vehicle. The entry at parabolic velocity tends to subject the crew to higher deceleration forces and also introduces an additional aerodynamic heating phenomenon; that of radiation from the gases behind the bow shock. This effect produces peak heating rates on the order of the convective heating rates; these are difficult to predict accurately either by theory or from test results.

Now we are confronted with the problem of entering at hyperbolic velocities, possibly 50 percent higher than parabolic speed. The entry corridor is now small or non-existent for the ballistic case, and lifting entry is required. Also, the heating definition now includes the very involved phenomenon of non-equilibrium radiation heating, which may be the major contributor. Similarly, the deceleration forces must be closely controlled by entry trajectory selection.

4.3 DEFINITION OF PARAMETERS

The basic independent parameters for this entry study are the entry velocity, entry flight-path angle, and the vehicle ballistic factor, W/C_DA.

The dependent parameters include the pull-out altitude and velocity, deceleration forces, heating flux, and the entry corridor.

Figure 4-1 illustrates the relationships between these parameters. Entry altitude is defined as 122.3 km; the beginning of atmospheric influence on the entry vehicle.

Flight-path angle is measured between the velocity vector and the local horizontal, and is negative when directed below the horizontal.

Pull-out is the point in the trajectory where the flight-path angle becomes zero with respect to the local horizontal, and then becomes positive.

The entry corridor is usually defined in the literature as the difference in perigee altitude between the overshoot and undershoot hyperbolic trajectories, assuming no atmospheric perturbations.

The overshoot boundary is defined as the trajectory corresponding to the minimum entry flight-path angle that will allow a single pass entry.

The undershoot boundary is the maximum allowable flight-path angle consistent with a prescribed deceleration limitation, either absolute magnitude of deceleration forces or a force-time history consistent with defined human tolerances.

During Phase I, the maximum deceleration and heating rates occur near the pull-out point and are defined later in this study. Both are a function of the entry vehicle mass and configuration, or simply its ballistic factor. Ballistic factor is defined as the vehicle weight divided by the product of its zero angle-of-attack drag coefficient and the reference area upon which the drag coefficient is based.

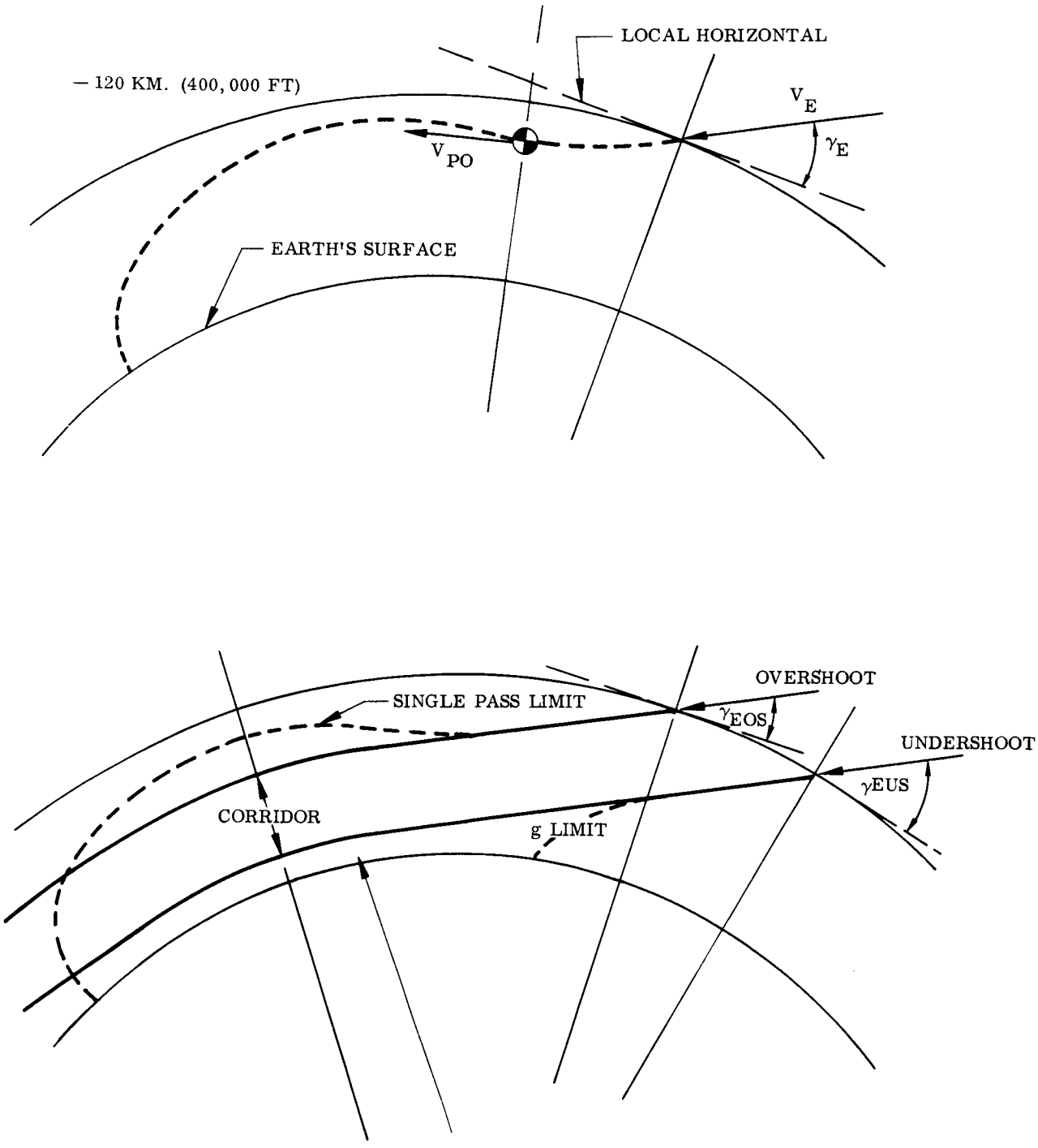


Fig. 4-1 Definition of Parameters

4.4 COMPARISON OF ENTRY SYSTEMS

Initially one must resolve the question of what comprises the entry system, and develop a configuration consistent with the overall interplanetary mission. Figure 4-2 compares four such systems by relating their total mass as a function of entry velocity. These are preliminary estimates and are based on the following type of analyses.

Retaining the Apollo configuration for hyperbolic entry would entail a gross increase in the heat shield mass to survive the increased convective and radiative heat flux. The convective heat flux increases approximately as the third power of the velocity and is inversely proportional to the square root of the nose radius of the vehicle. Likewise, the equilibrium radiative heat flux may increase as much as the 12^{th} or 14^{th} power of the velocity and is directly proportional to the nose radius. It becomes apparent that the additional heat shield requirement for this configuration is prohibitive from a mass standpoint.

Also, one may desire to add a retro-propulsion stage to brake the Apollo vehicle to its design entry velocity. The propulsion stage mass will increase exponentially with the velocity increment. The total mass is dependent upon the specific impulse of the propulsive system and the structural factors used for the inert weights.

A more sophisticated approach is to select a configuration which is consistent with the estimated entry environment. It is possible to design a vehicle which will greatly reduce the total heat flux by determining the nose radius which will minimize the total effect of the convective, equilibrium radiation, and non-equilibrium radiation heating rates. This results in a pointed, conical vehicle as shown in Fig. 4-2. The optimum nose radius becomes very small at high velocities; but for this study, a 15-cm minimum was assumed. It would be desirable to have an ablation rate such that the nose radius is always near optimum as the velocity changes due to vehicle drag. The inherent high W/C_DA values for this type vehicle result in high stagnation temperatures, demanding increased insulation for the crew and probably an ablator material development. This type vehicle possesses good lifting characteristics for trajectory definition.

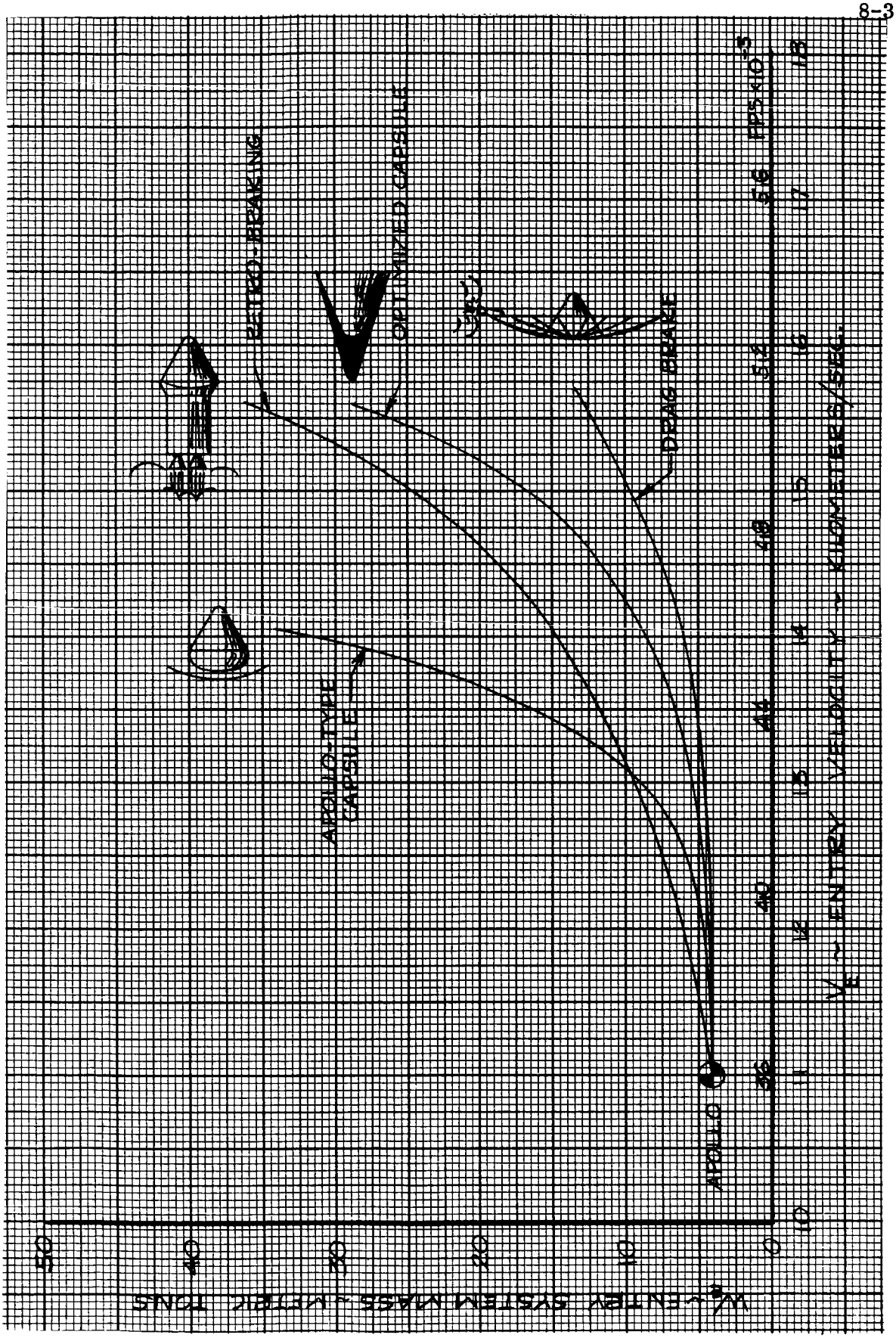


Fig. 4-2 Weight Comparison of Earth Entry Systems

The vehicle design approach described for this study consists of the Apollo capsule fitted with a large, light-weight drag brake to utilize the upper atmosphere for deceleration while greatly reducing the stagnation heat flux due to the low densities. This total mass also includes a propulsion system to provide or supplement the lift vector required for single pass entry. A sketch of this concept is shown in Fig. 4-3.

4.5 SIGNIFICANCE OF ENTRY SYSTEMS IN INTERPLANETARY ROLE

It is very desirable to minimize the total entry system mass due to its influence on the total mission mass requirements.

During the Empire study, it was found that for every kg of entry system mass reduction, the total mass on Earth orbit could be decreased twenty to forty kg. Figure 4-2 illustrates that the drag brake system may save as much as 10 to 20 metric tons over the conical ablator and ratro-brake respectively at 15 km/sec entry. Therefore, this entry concept may save over 500 metric tons on Earth orbit.

This preliminary comparison indicates the drag brake concept may produce a light weight system without relying on an advanced state-of-the-art in materials and ablator technology. It also permits the use of the Apollo capsule, and the technology derived from the lunar program.

4.6 TRAJECTORY MODE

The entry trajectory will consist of four major phases as shown in Fig. 4-4.

- Phase I – Exospheric Hyperbolic Approach. This phase is the near-Earth, hyperbolic approach trajectory and defines the entry velocity and flight path angle.
- Phase II – Initial Entry to Pull-out. This phase incorporates a ballistic entry and terminates when the local flight path angle becomes zero.

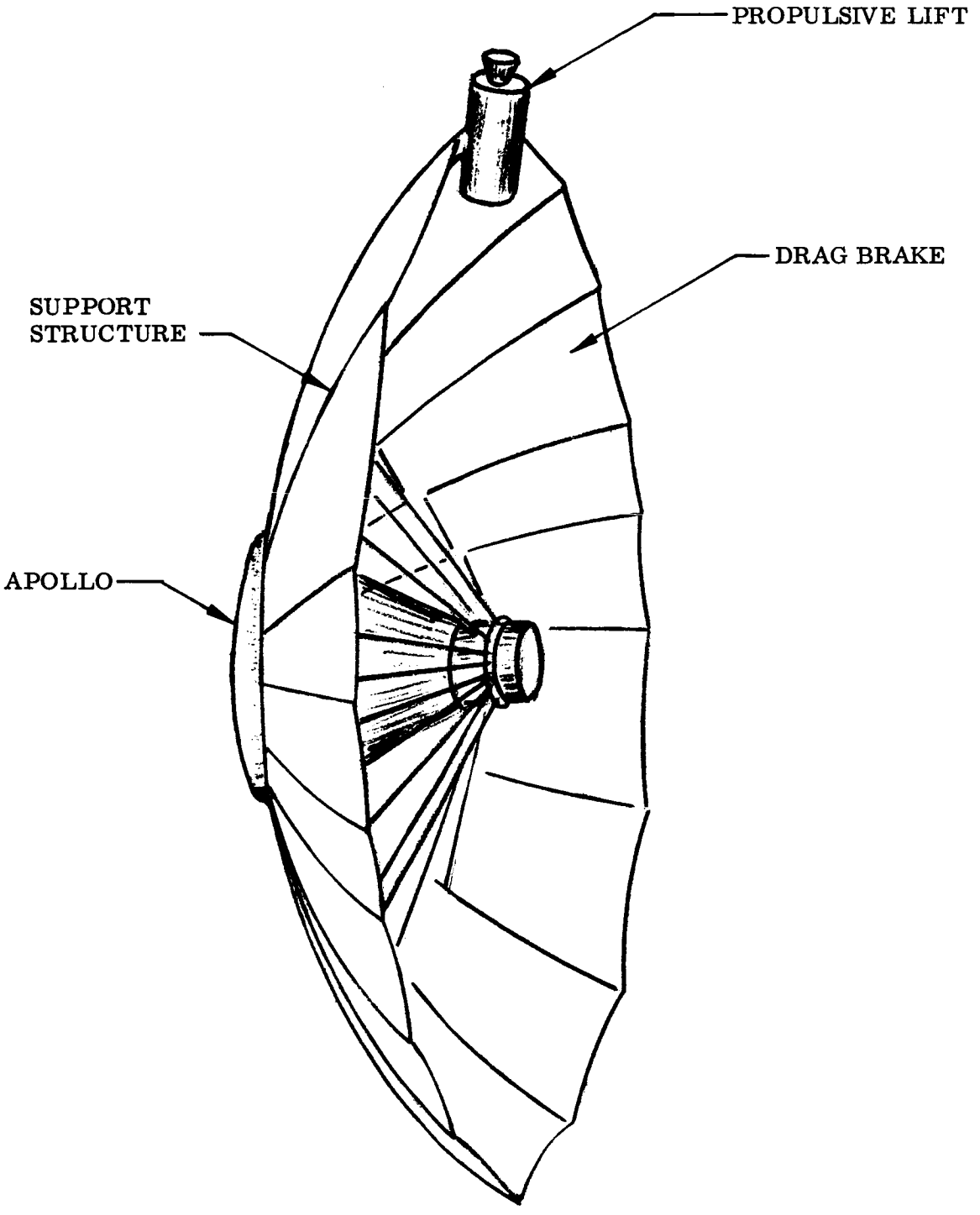


Fig. 4-3 Entry System Concept

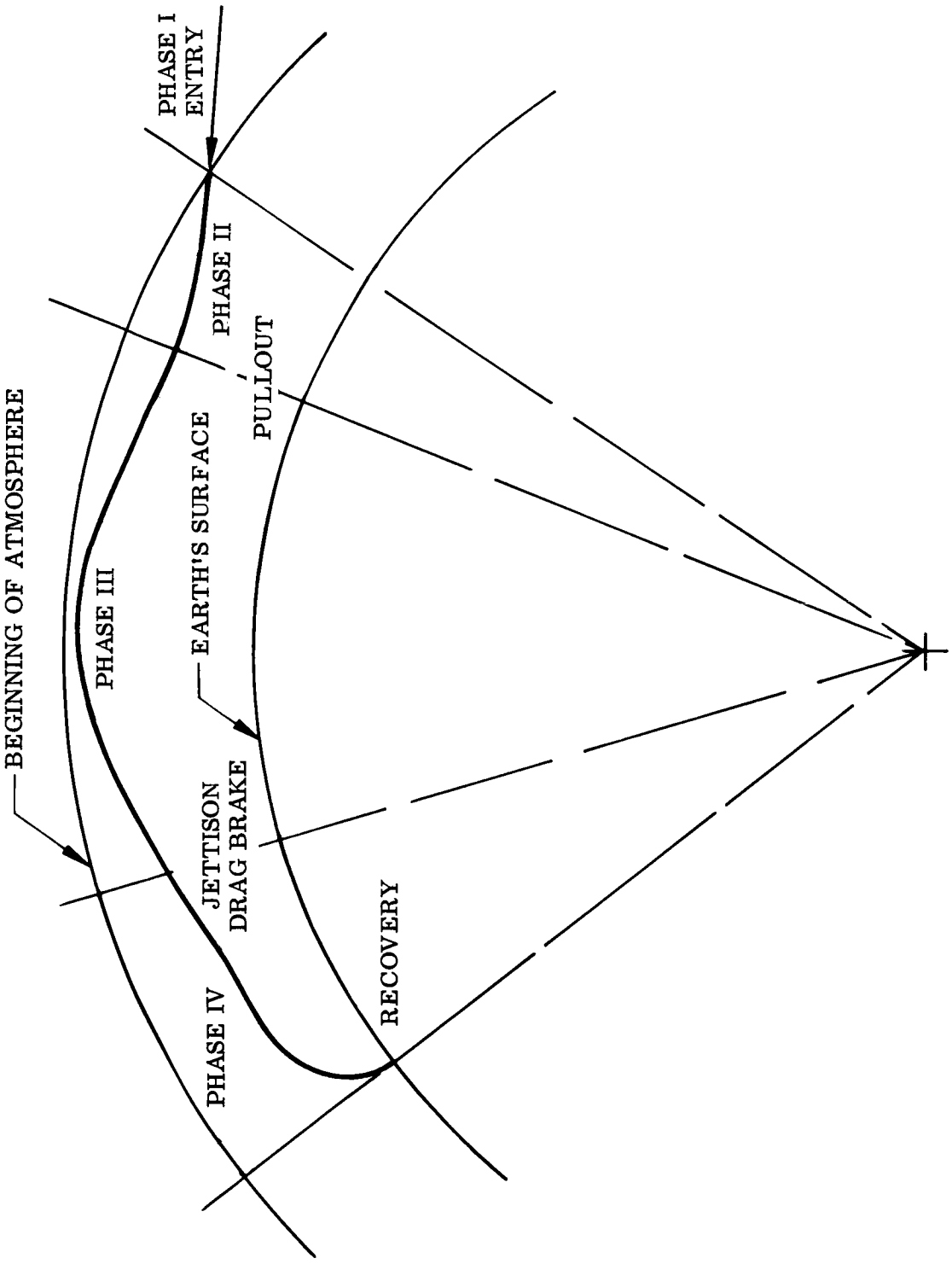


Fig. 4-4 Trajectory Phasing

- Phase III – High Altitude Deceleration. Additional atmospheric braking to parabolic speeds occurs at high altitudes. The propulsive lift system is used to provide a single pass entry. The drag brake is jettisoned at the end of this phase.
- Phase IV – Final Descent and Recovery. An Apollo-type entry is performed.

4.7 DECELERATION LIMITS

The undershoot boundary incorporates maximum deceleration level of 10 g. Equally important is the deceleration-time history.

Human tolerance is also defined by a g level for a finite time. This is important since Phase III tends toward a constant g maneuver. The vehicle mass loss, due to expenditure of propellant, tends to compensate for the drag reduction as the vehicle decelerates. The assumed limits are presented in Fig. 4-5.

4.8 DRAG BRAKE CONFIGURATION

4.8.1 Assumptions

The drag brake weighs 4.9 kg/m^2 including the erection and support structure. The material is a non-porous stainless steel woven cloth and 0.25 mm thick. The basic Apollo capsule weighs 9000 pounds.

The propulsion system has a specific impulse of 300 seconds and provides a constant thrust. Its burning time is consistent with the time for the vehicle to decelerate from the pull-out velocity to parabolic velocity. The thrust level is such that the flight path angle at the end of Phase III is consistent with the ensuing Apollo-type entry. The ARDC 1959 upper atmosphere was used.

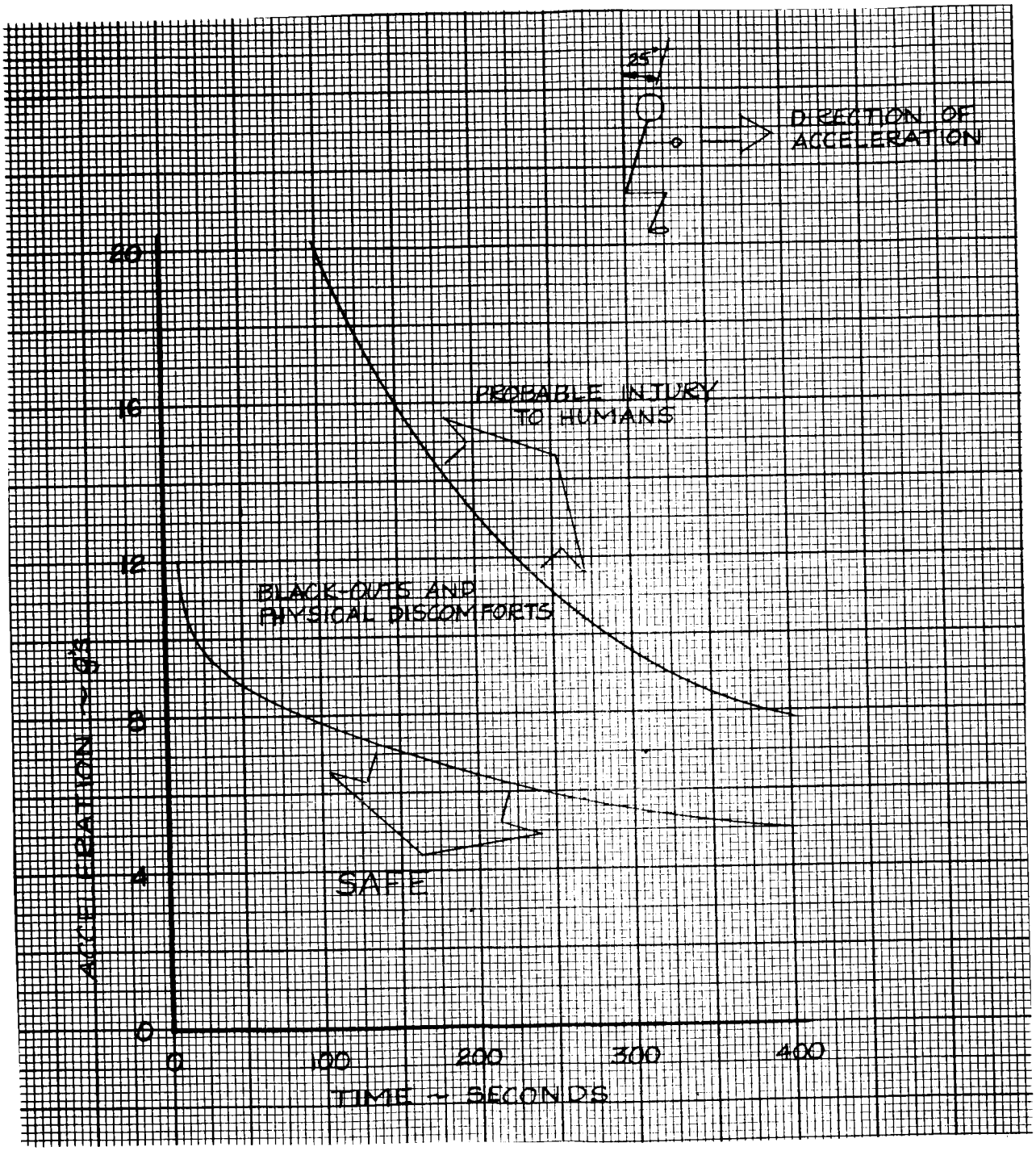


Fig. 4-5 Acceleration Tolerances

4.8.2 Optimization of Drag Brake Configuration

The drag brake analysis is performed for pull-out altitudes of 79.3 to 91.5 km and is initially concerned with Phase III only. To simplify the calculations, this phase is a constant altitude maneuver with no aerodynamic lift. The corresponding lift requirements to maintain altitude dictate the propulsive force required.

Figures 4-6 through 4-10 present the resultant relationships between the ballistic factors at the beginning and end of Phase III for various pull-out altitudes and pull-out velocities. It is now possible to determine a minimum mass configuration for each velocity and altitude by the following method.

The pull-out ballistic factor can be expressed as:

$$(W/C_DA)_{PO} = \frac{\rho_{PO} V_{PO}^2}{2g_{PO}}$$

For a given pull-out deceleration velocity, and altitude; a burn-out ballistic factor can be obtained from Figs. 4-6 through 4-10. Also, the burn-out weight can be expressed as the sum of the Apollo weight and the drag brake weight.

$$W_{BO} = 4100 + W_{DB}$$

Since the drag brake weighs 4.9 kg/m^2, the burn-out weight can also be expressed as $W_{BO} = 4100 + A$. Likewise $W_{BO} = (W/C_DA)_{BO} (C_DA) = (W/C_DA)_{BO} (1.6A)$ since C_D is assumed equal to 1.6.

Therefore: $4100 + A = 1.6A(W/C_DA)_{BO}$ or

$$A = \frac{4100}{1.6(W/C_DA)_{BO} - 1}$$

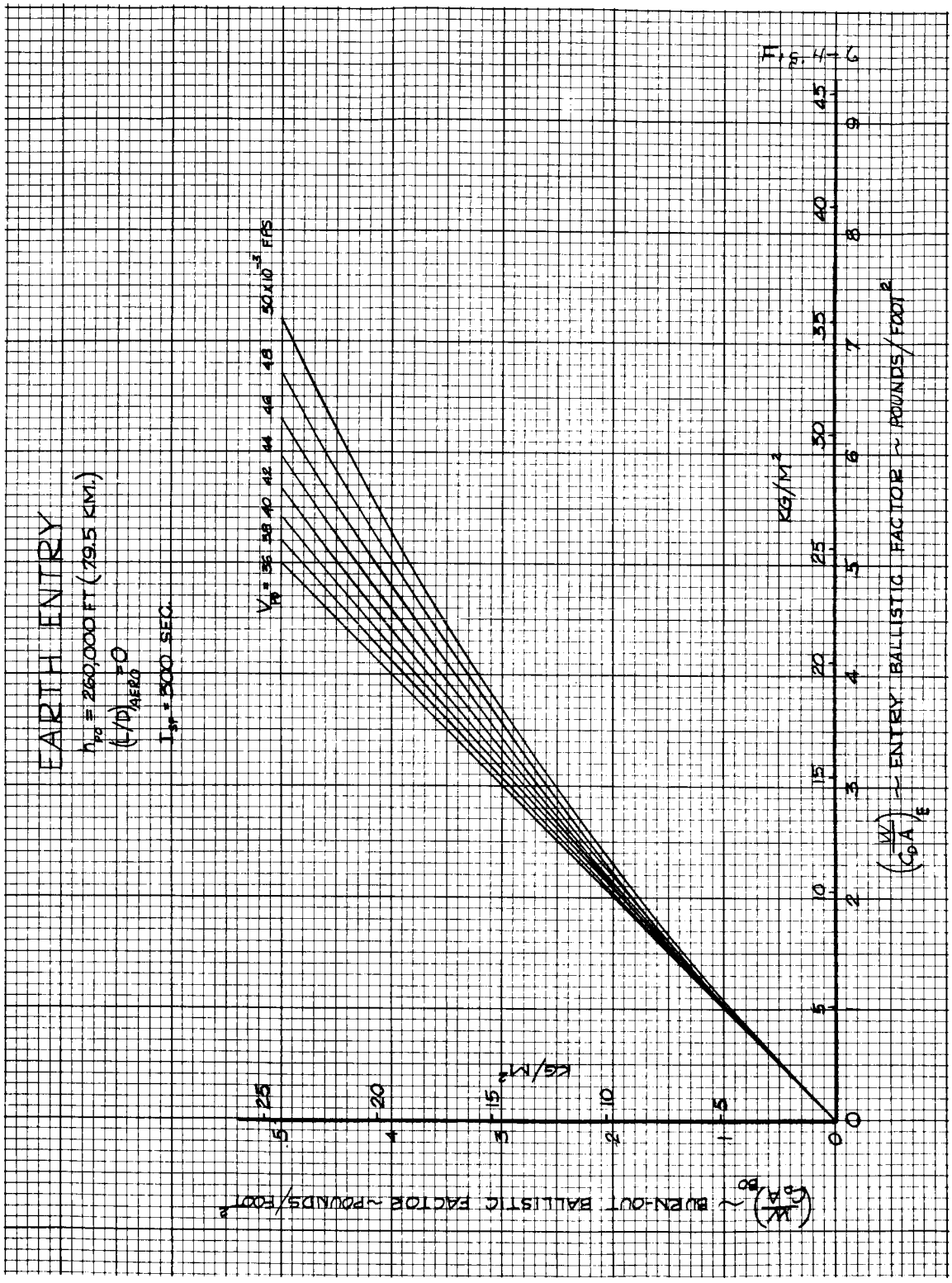


Fig. 4-6 Earth Entry (h_{po} = 260,000 ft)

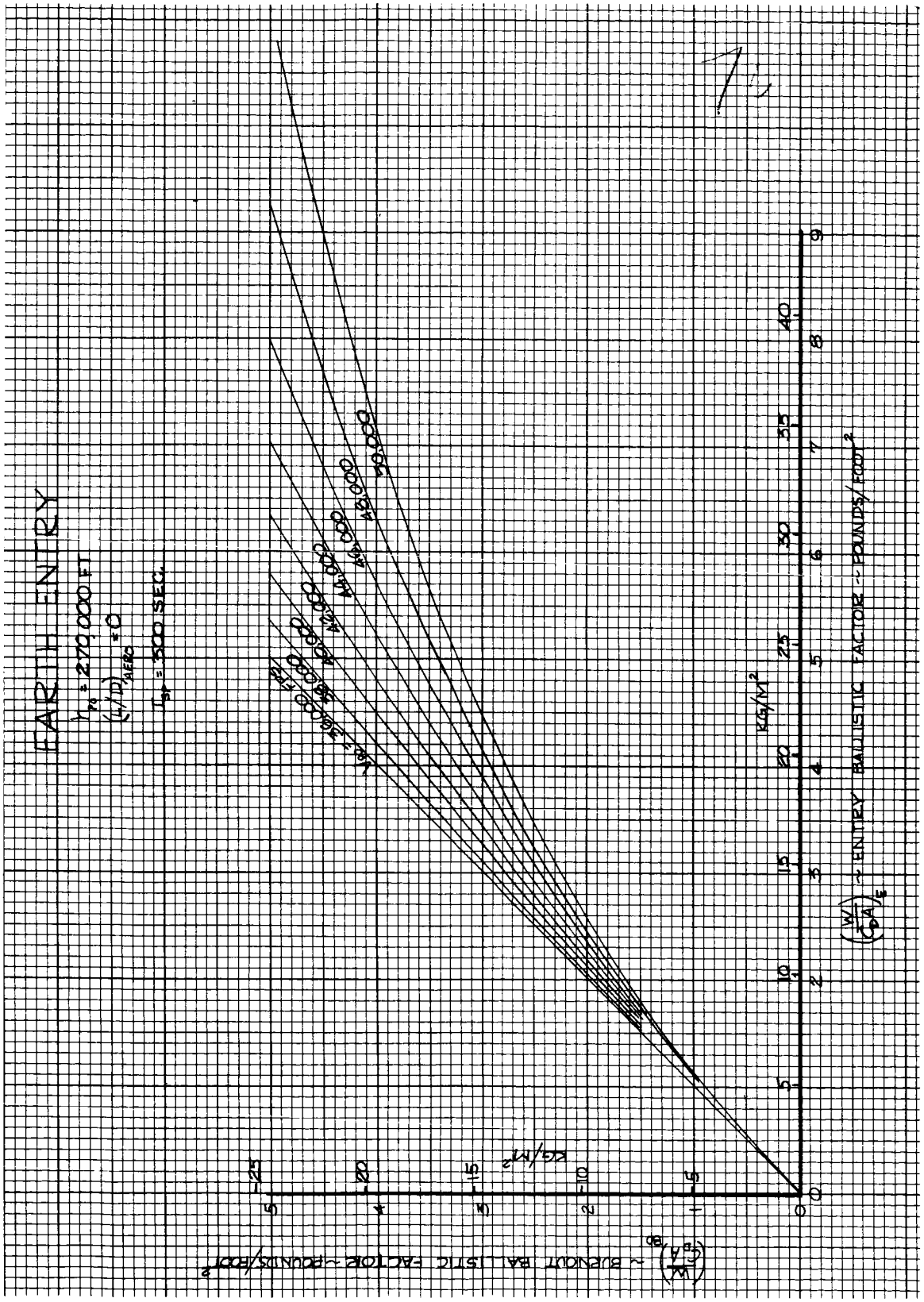


Fig. 4-7 Earth Entry (h_{po} = 270,000 ft)

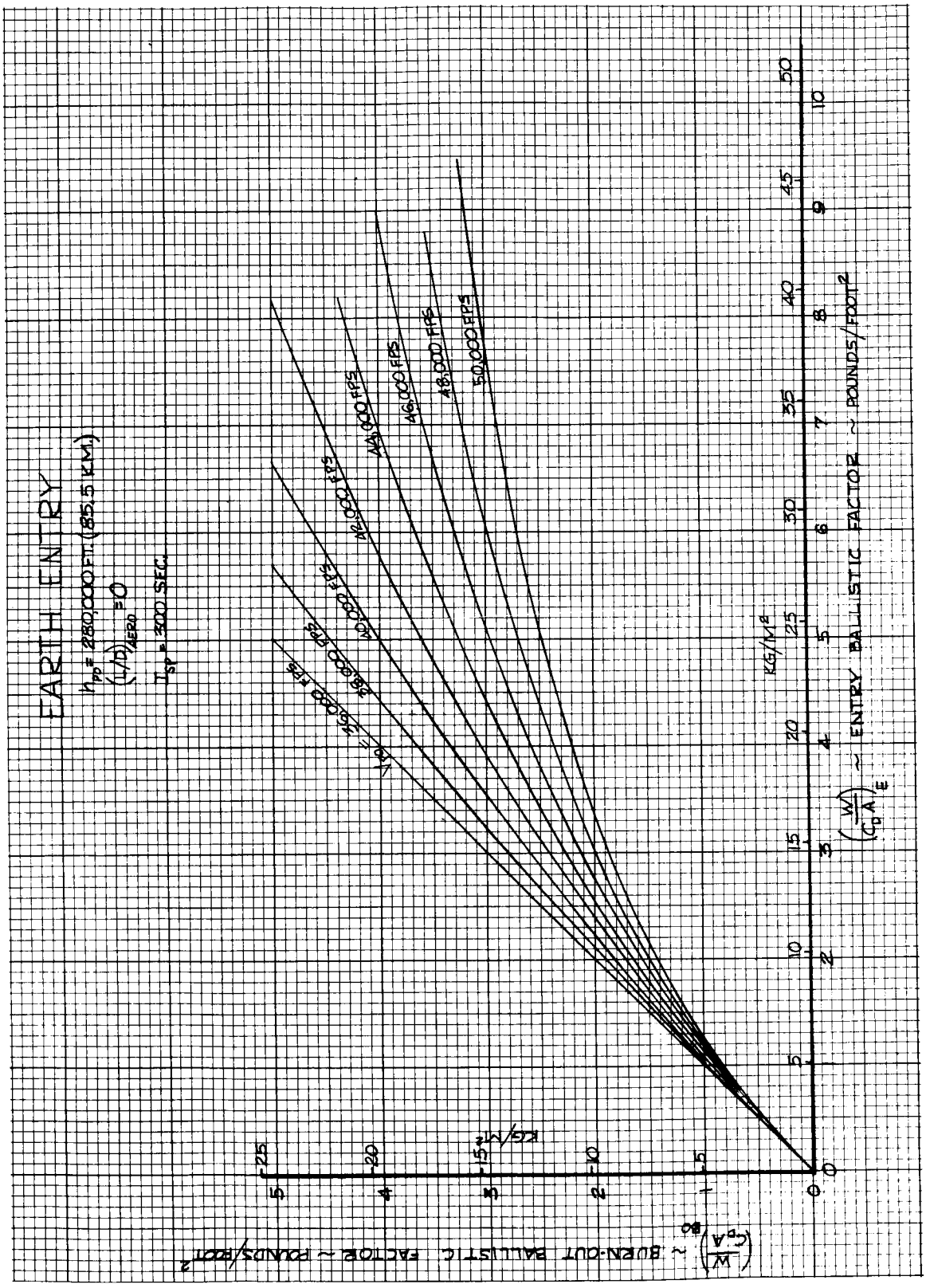


Fig. 4-8 Earth Entry (h_{po} = 280,000 ft)

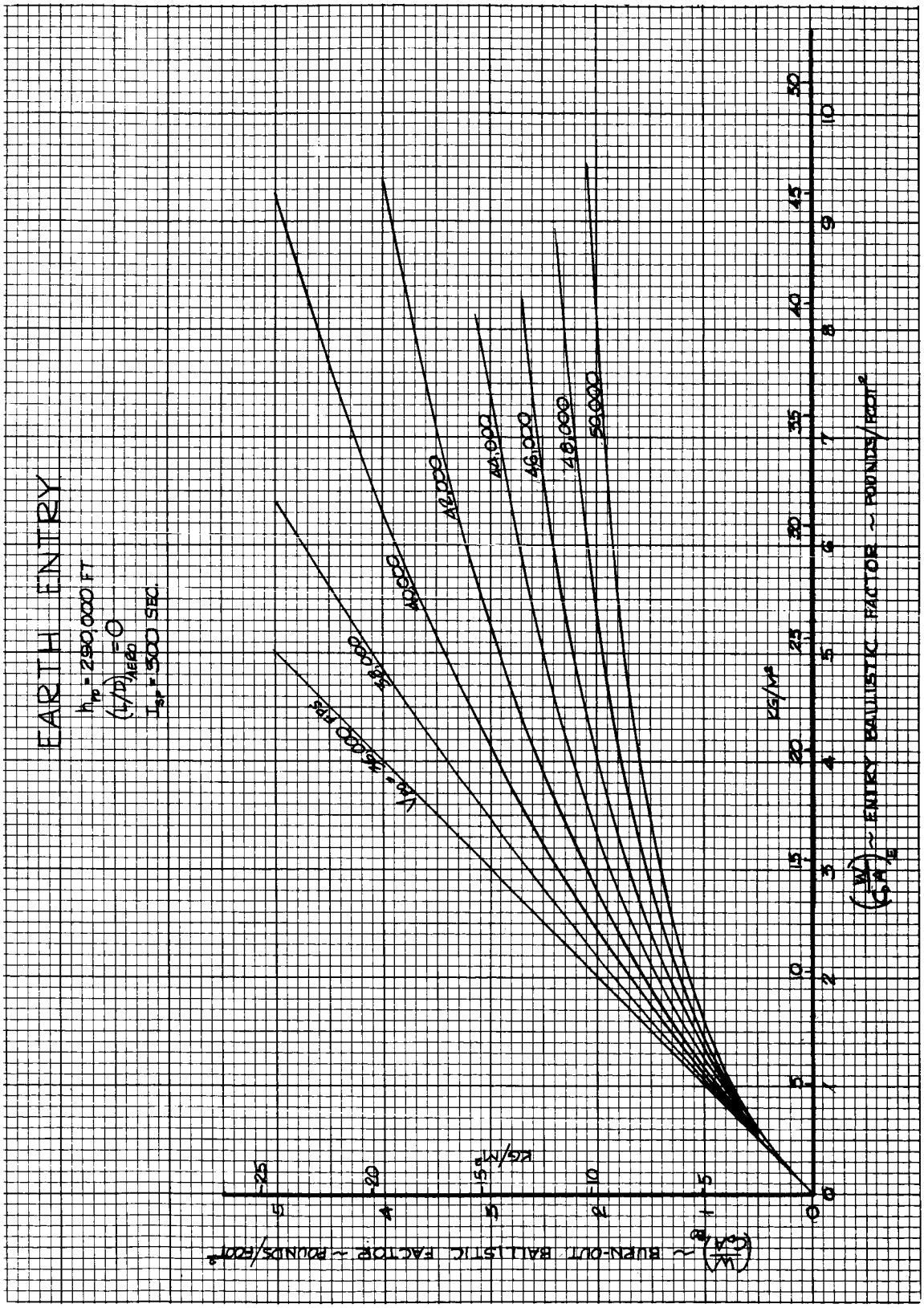


Fig. 4-9 Earth Entry (h_{po} = 290,000 ft)

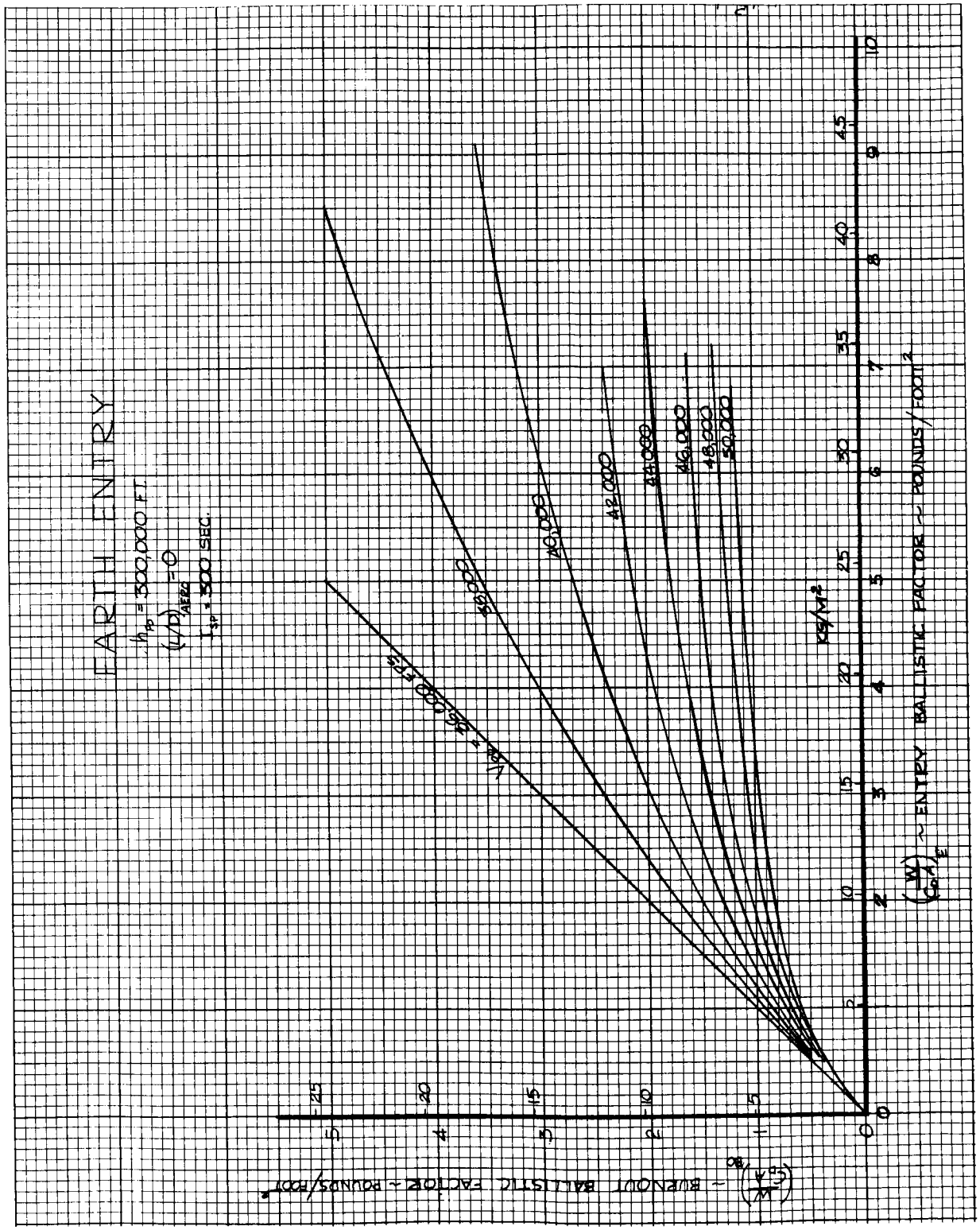


Fig. 4-10 Earth Entry (h_{po} = 300,000 ft)

Once the frontal area is defined, the burn-out weight and ballistic factor can be computed. Then the total pull-out weight can be expressed as:

$$W_{PO} = \frac{(W/C_D A)_{PO}}{(W/C_D A)_{BO}} \quad (W)_{BO}$$

The propulsive weight is then:

$$W_P = W_{PO} - W_{BO}$$

Figure 4-11 shows the resulting pull-out weight versus pull-out g. The resultant minimums constitute potential design points for this system. Figures 4-12 through 4-16 are summary plots presenting the optimum values versus pullout velocity.

It should be noted that the pull-out deceleration of Fig. 4-11 is due only to aerodynamic drag and is not the total g imposed on the crew. To obtain the latter, the thrust (lift) vector must be included, and can be computed as follows. The lift-to-drag ratio required to maintain a given altitude at a given velocity can be expressed as:

$$L/D = \frac{W/C_D A}{1/2\left(\rho V^2\right)} \left[1 - \left(\frac{V}{V_c}\right)^2\right]$$

Since the lift is to be provided by thrust, the pull-out conditions become:

$$(T/D)_{PO} = \frac{(W/C_D A)_{PO}}{1/2\left(\rho_{PO} V_{PO}^2\right)} \left[1 - (V_{PO}/V_C)^2\right]$$

also $D = 1/2\ \rho V^2\ C_D A$ by definition. The thrust required at pull-out is:

$$T_{PO} = W_{PO} \left[1 - (V_{PO}/V_C)^2\right]$$

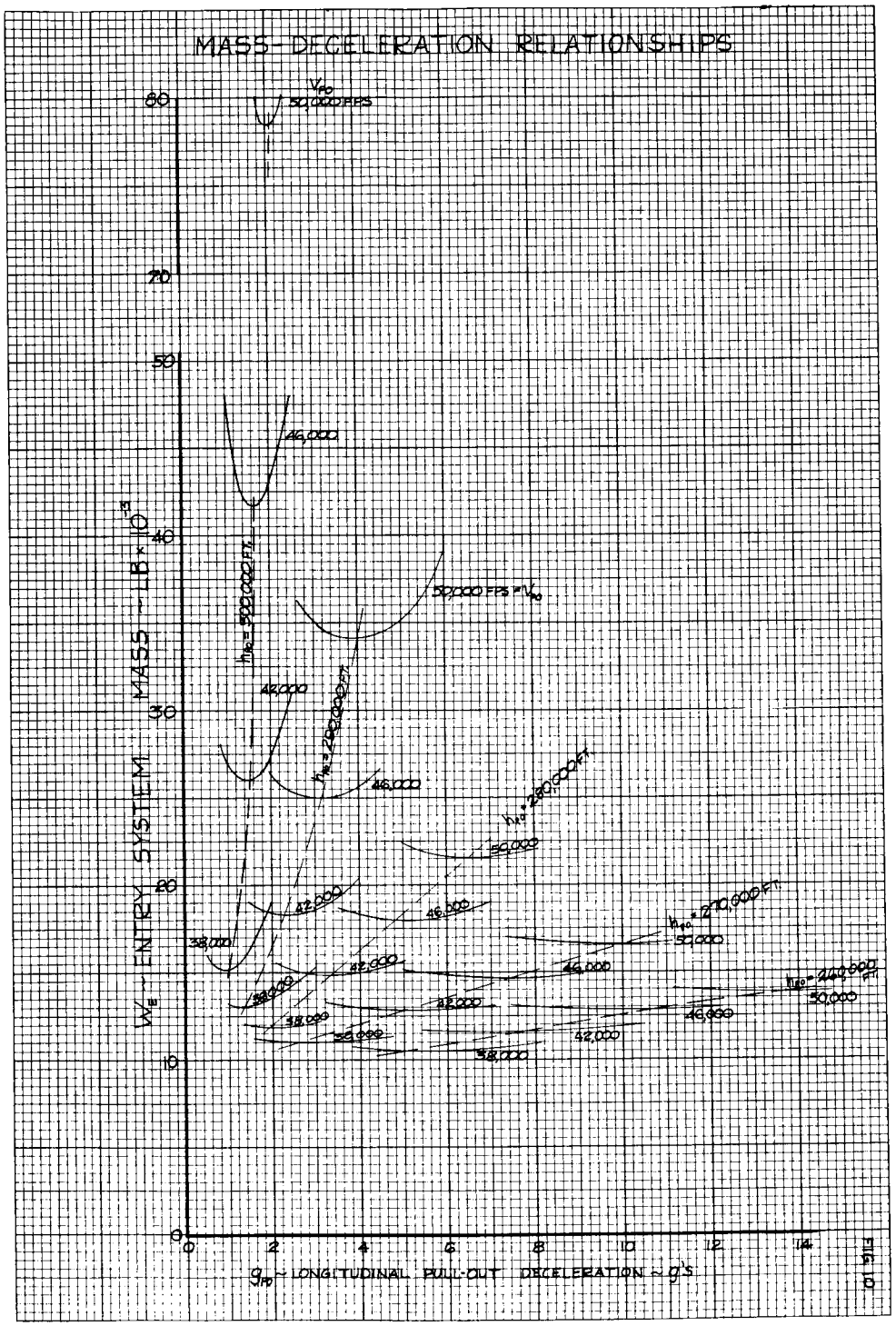


Fig. 4-11 Mass-Deceleration Relationships

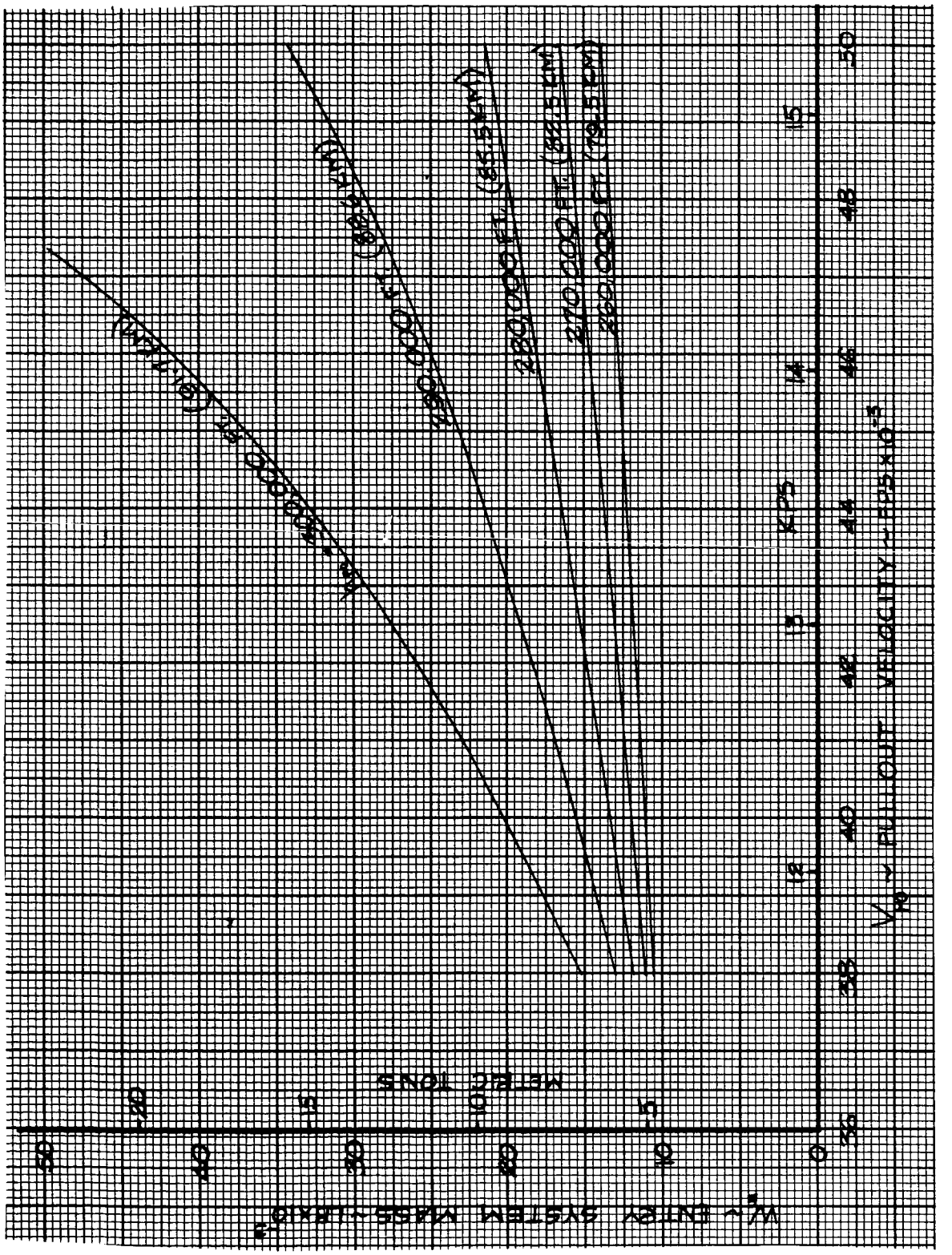


Fig. 4-12 Entry System Mass vs. Pullout Velocity

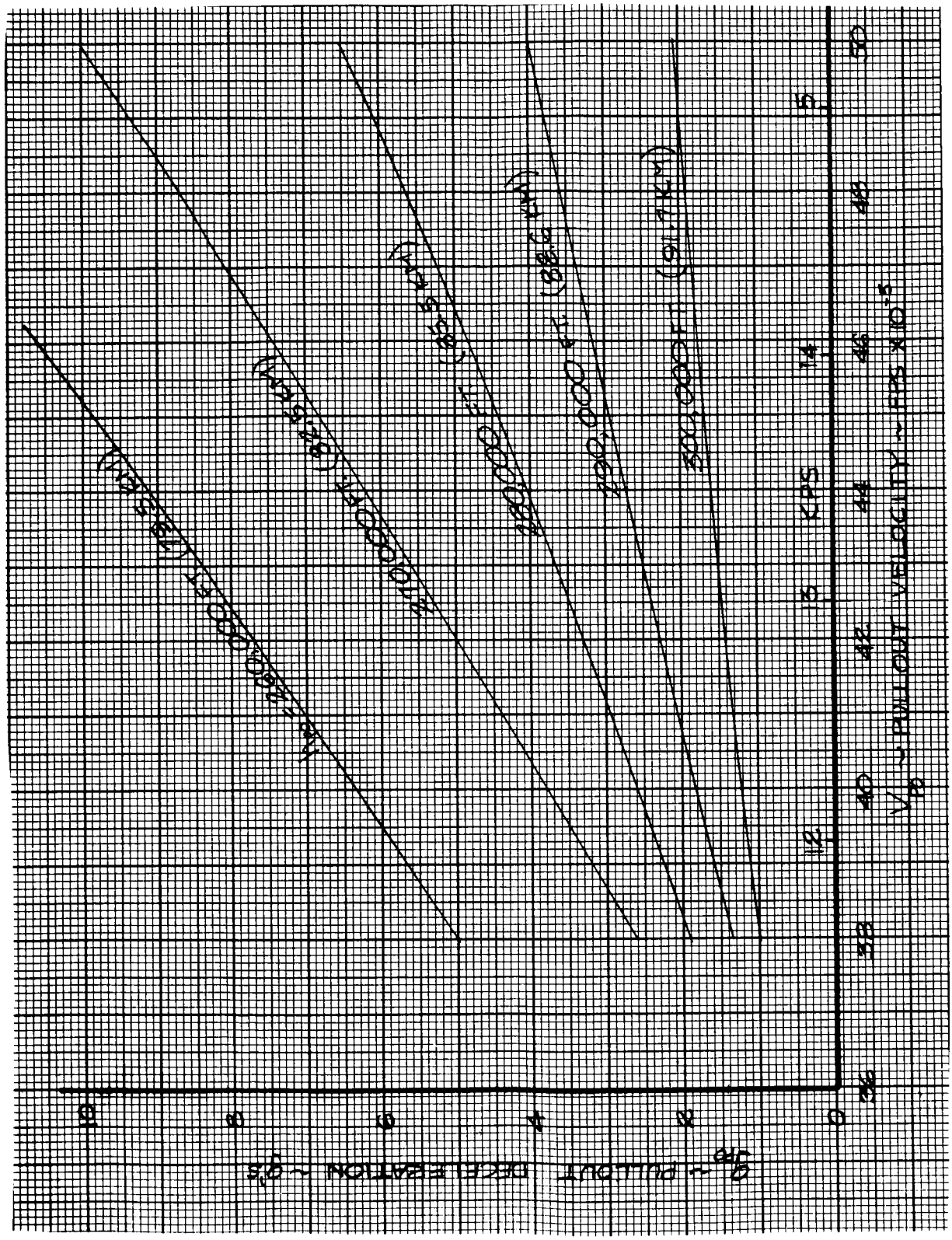


Fig. 4-13 Optimum Pullout Deceleration vs. Pullout Velocity

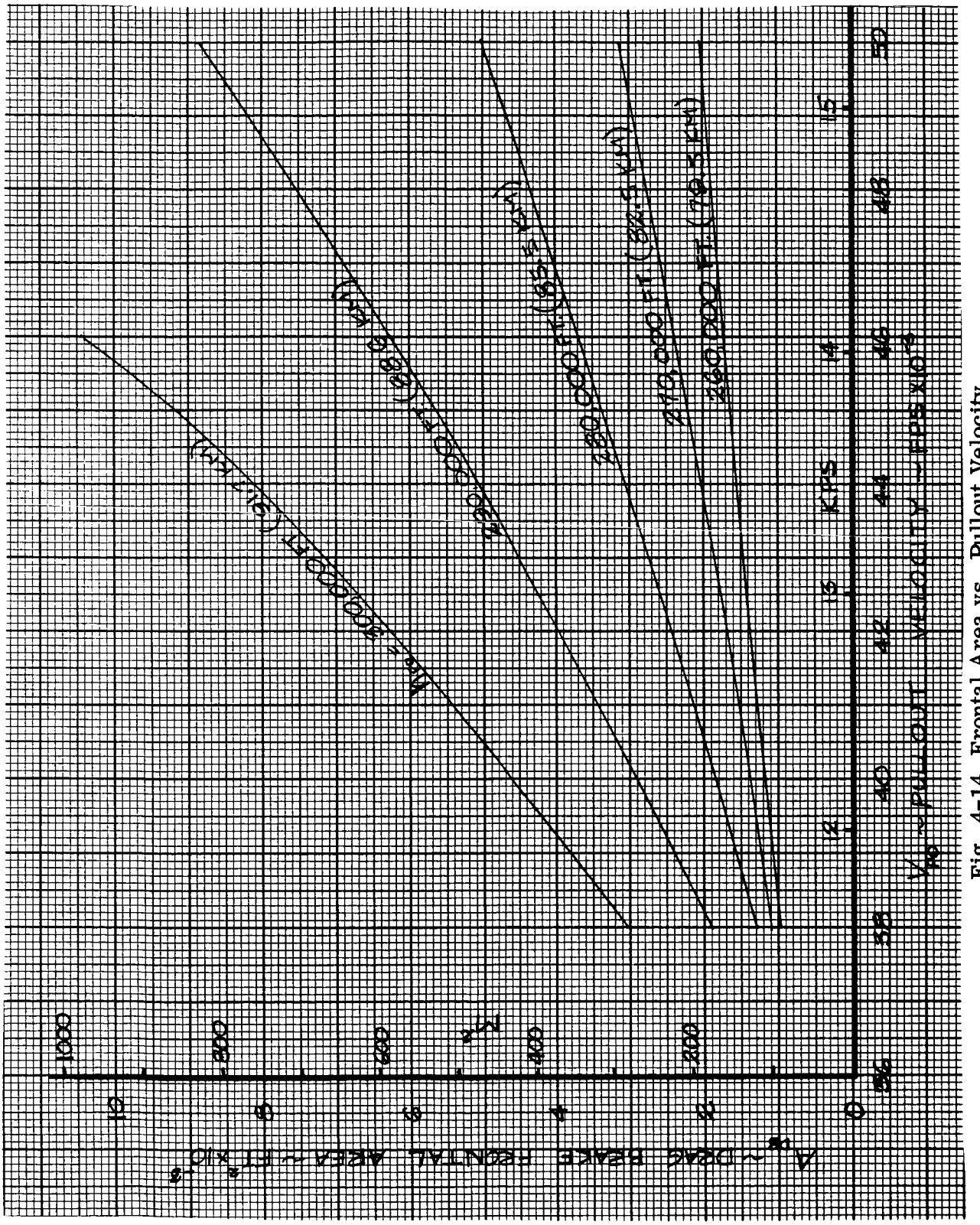


Fig. 4-14 Frontal Area vs. Pullout Velocity

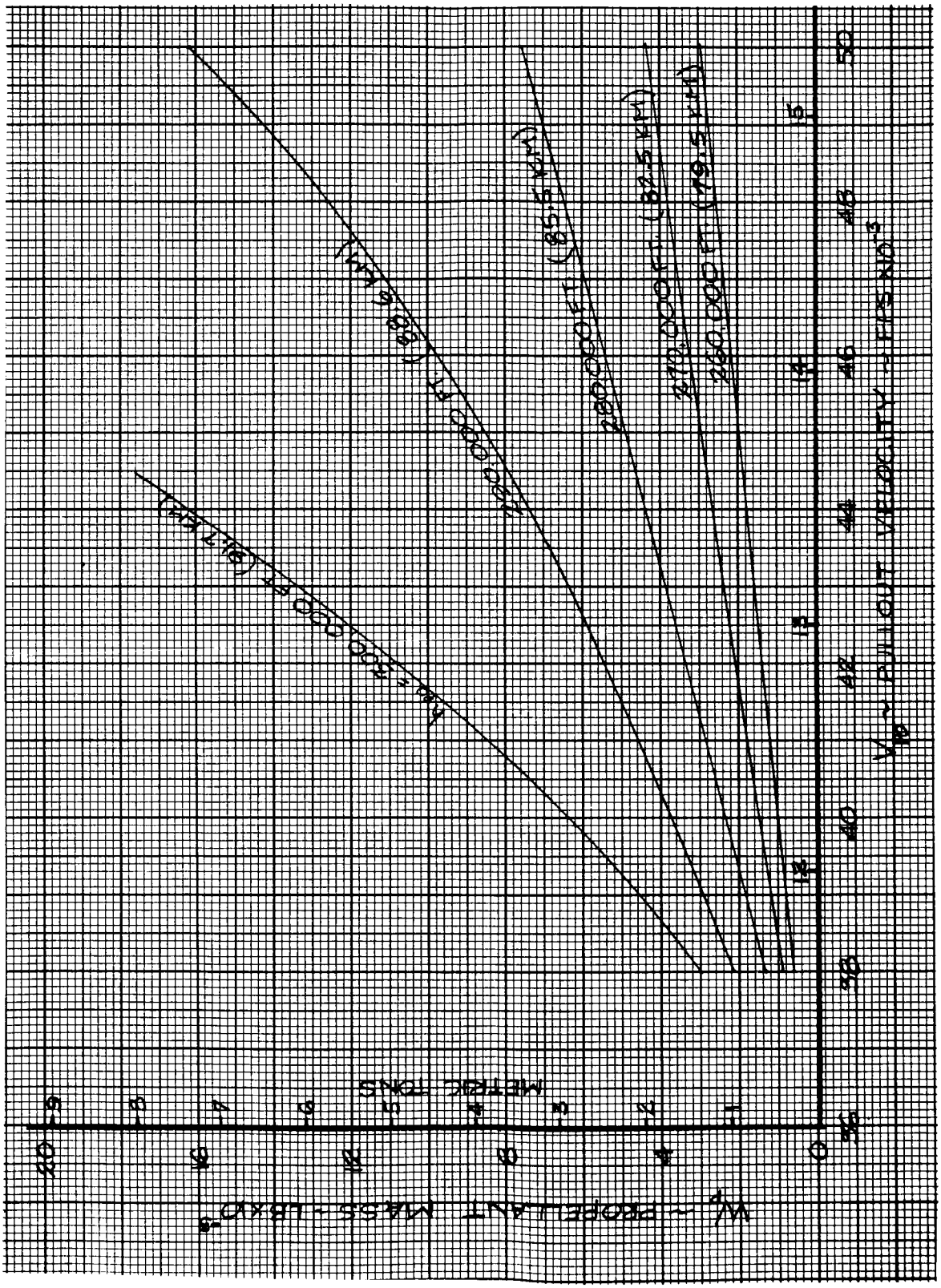


Fig. 4-15 Propellant Mass vs. Pullout Velocity

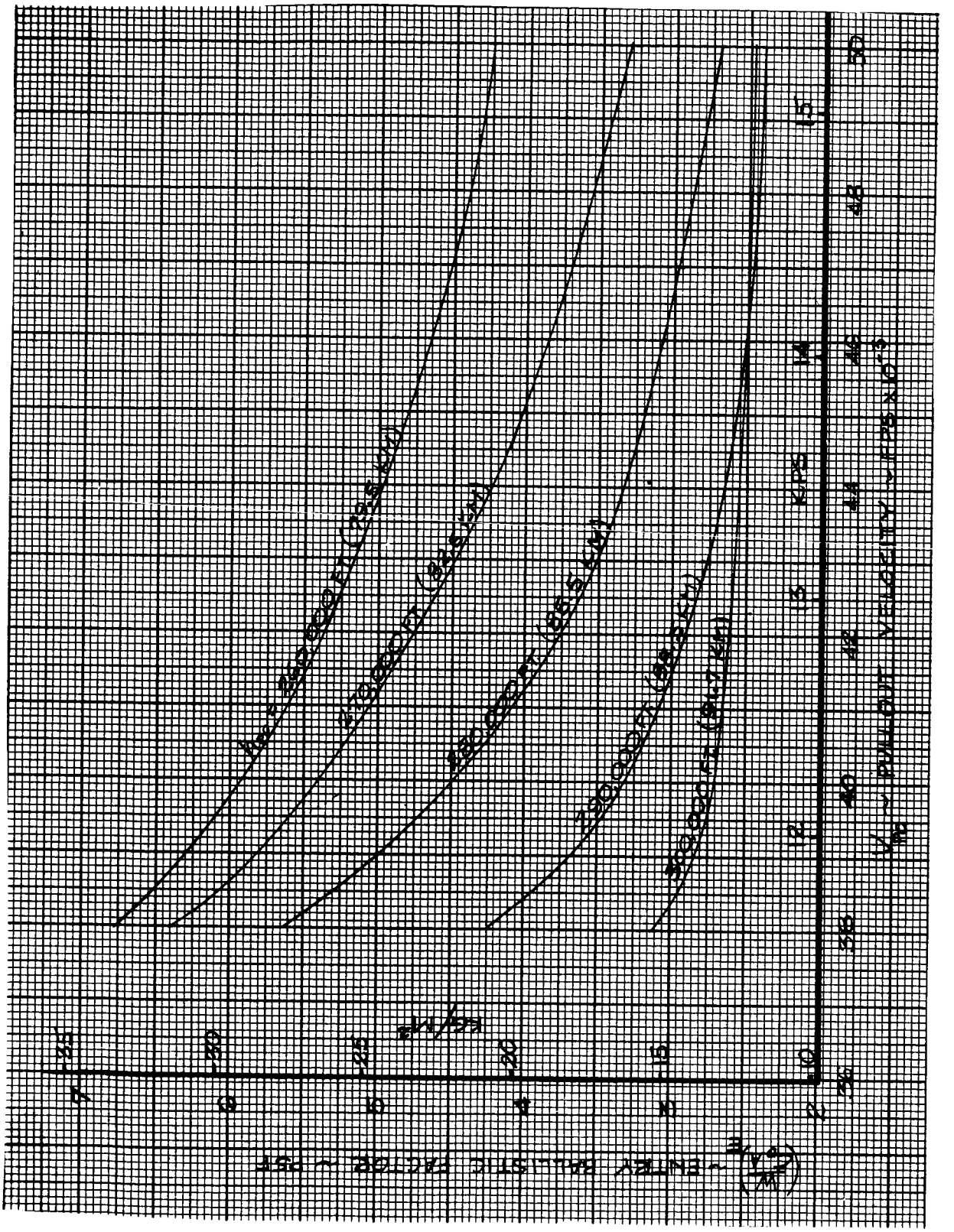


Fig. 4-16 Entry Ballistic Factor vs. Pullout Velocity

The total g at pull-out is then

$$g^*_{PO} = \frac{\left(T^2_{PO} + D^2_{PO}\right)^{1/2}}{D_{PO}} \; g_{PO}$$

or

$$g^*_{PO} = \left\{\left[1 - \left(\frac{V_{PO}}{V_C}\right)^2\right]^2 + g^2_{PO}\right\}^{1/2}$$

Figure 4-17 presents the total pull-out g versus pull-out velocity. The total deceleration envelope is shown in Fig. 4-18. This indicates that the 79.3 km pull-out is limited to an entry velocity of 15.5 km/sec. A 82.5 km pull-out has a 16.2 km/sec limit.

A typical thrust time history required to maintain a given altitude is presented in Fig. 4-19 for the indicated parameters. Such a thrust variation would present throttling problems and grossly complicate the system. The next approach is to choose a constant thrust level and retain the same burning time. This will reduce the pull-out g and more important, will provide a negative flight path angle at burnout to ensure the proper execution of Phase IV. This approximation is shown in Fig. 4-19. Phase III will no longer be a constant-altitude deceleration. Therefore the g time history will vary somewhat.

4.8.3 Use of Aerodynamic Lift

It is possible to reduce the amount of propulsion required by providing aerodynamic lift. This may be accomplished by providing angle-of-attack with an attitude control system or by designing a non-symmetrical drag brake to enable the vehicle to trim at the desired L/D.

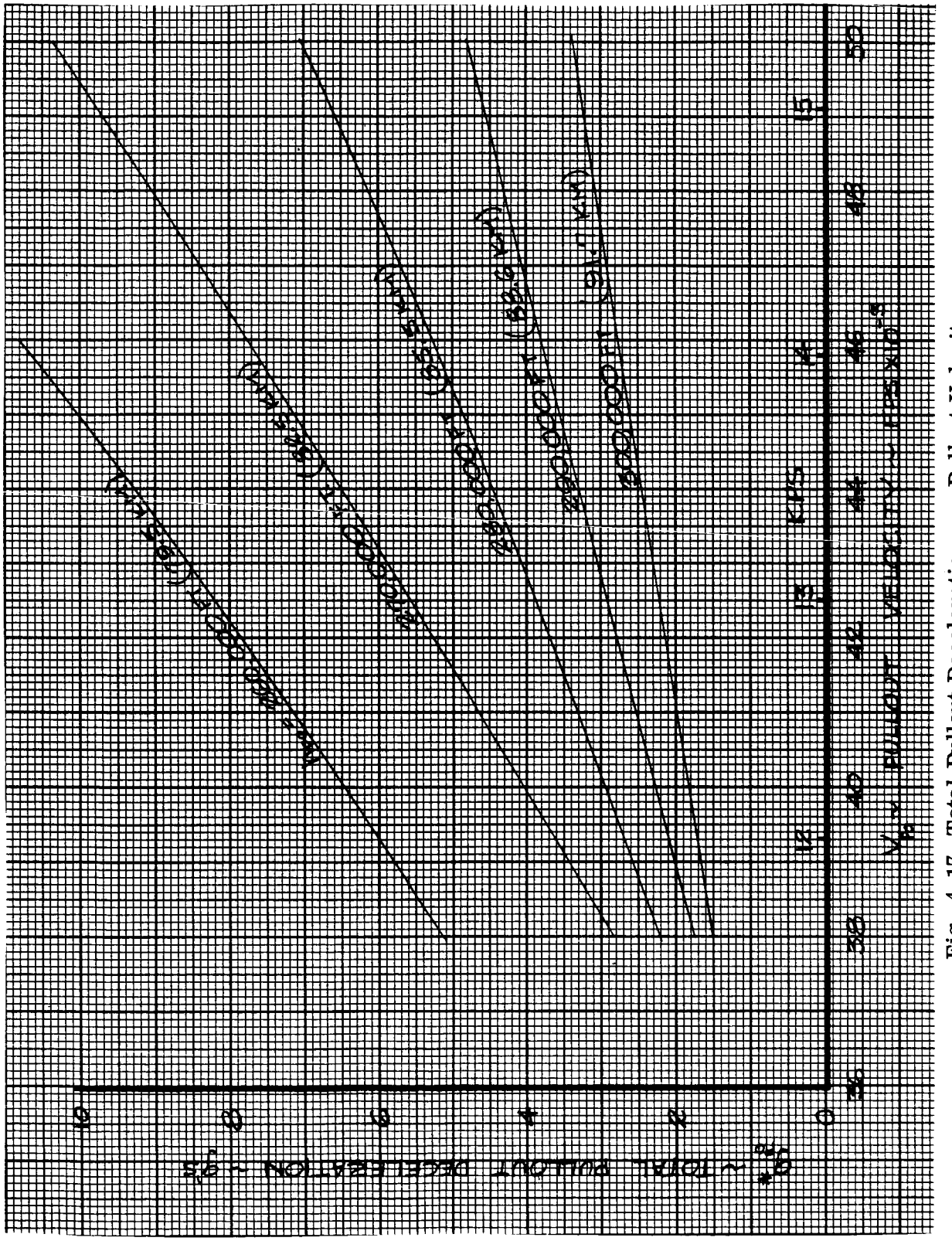


Fig. 4-17 Total Pullout Deceleration vs. Pullout Velocity

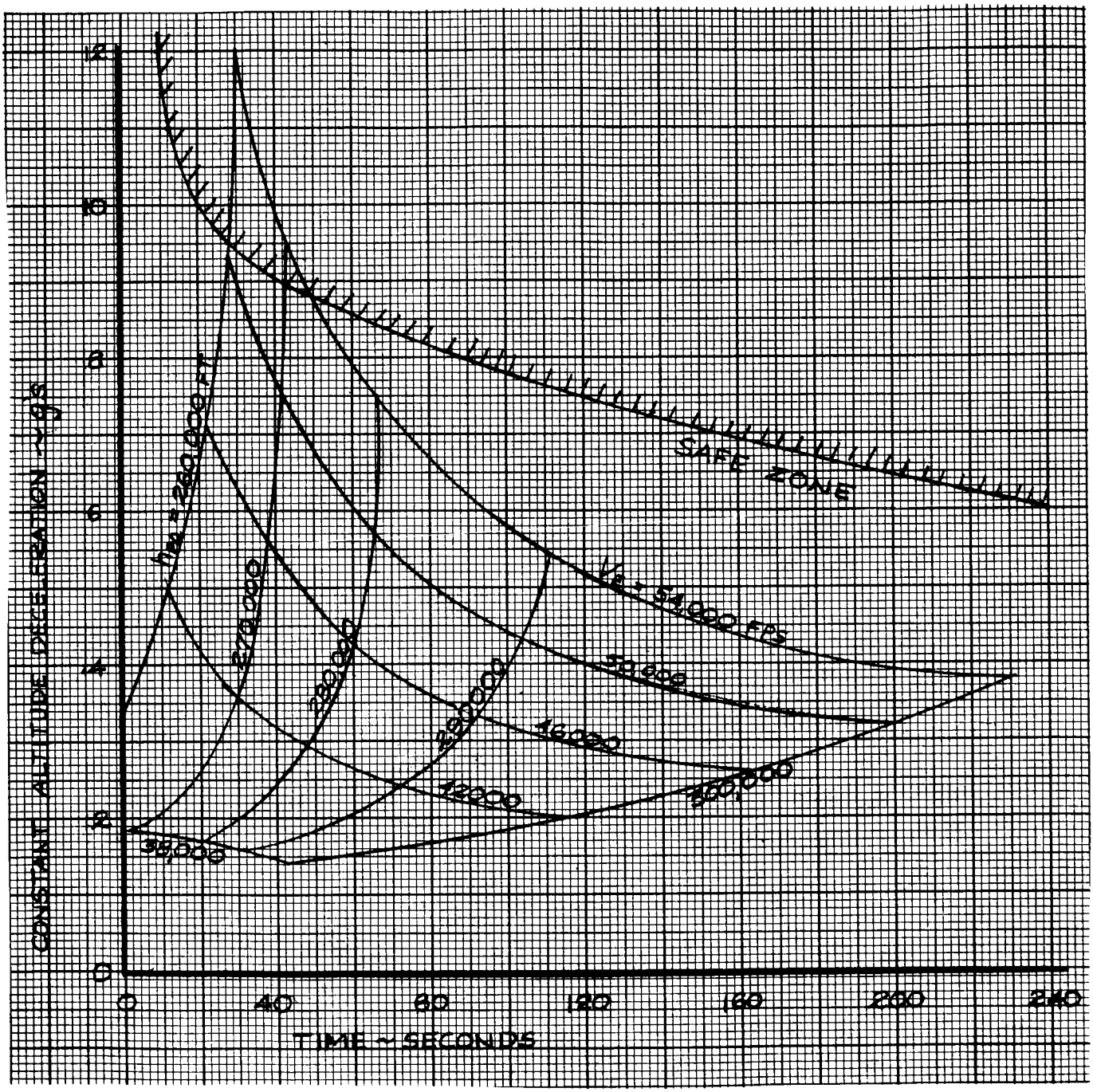


Fig. 4-18 Acceleration Summary

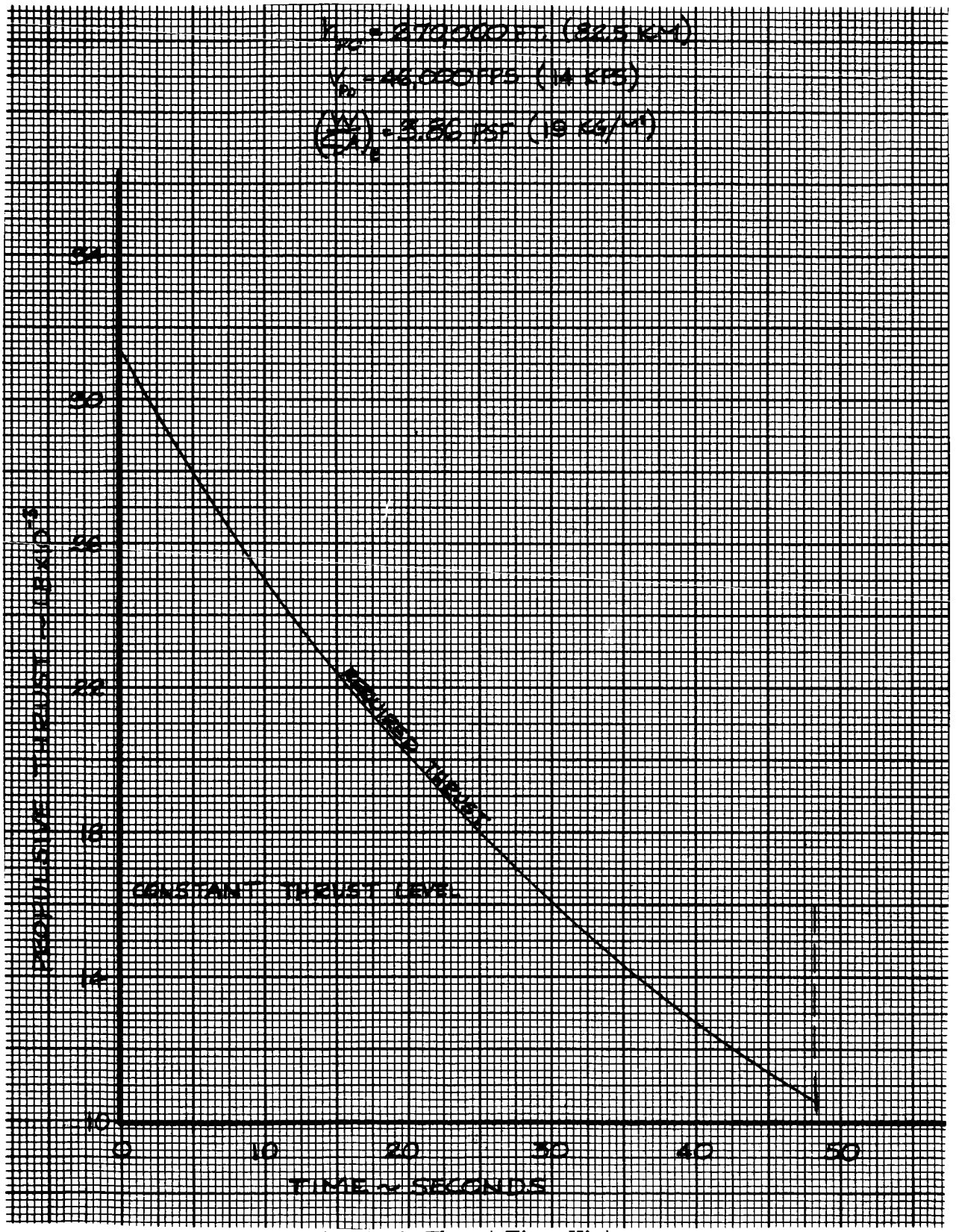


Fig. 4-19 Thrust Time History

High drag configurations are generally not consistent with high lift. However, an L/D of -0.1 to -0.2 may be available without excessive angle-of-attack. The reduced propulsion requirement may reduce the total entry system mass by 10 percent to 20 percent. For this study; the simplicity of design and analysis, resulting from excluding aerodynamic lift, is prevalent.

4.9 PARAMETRIC ANALYSIS

To supplement the drag brake entry study, a general parametric analysis was performed to relate the initial entry conditions to those at pull-out. It was found that pull-out altitude is practically invariant with ballistic factor and only a function of entry velocity and flight path angle. These results are shown in Fig. 4-20.

The velocity loss during Phase II was determined for a wide range of ballistic factors and entry velocities. An example of this variation is shown in Fig. 4-21 for a ballistic factor of 19.6 kg/m^2. By combining Figs. 4-20 and 4-21, lines of constant pull-out altitude are defined. This then indicates the velocity loss is nearly independent of entry velocity for a given altitude. With this approximation, the velocity loss is only a function of ballistic factor and pull-out altitude, as shown in Fig. 4-22.

4.10 INTEGRATION OF PARAMETRIC ANALYSIS

Combining the parametric study with the drag brake detail, will complete the vehicle design and trajectory parameters. The ballistic factor variation of Fig. 4-16 was integrated with Fig. 4-22 to obtain the relationship between entry velocity and pull-out velocity for the entire family of vehicles. This result is presented in Fig. 4-23. Now the total vehicle weights of Fig. 4-12 can be presented as a function of entry velocity, which is an independent parameter of Phase I (Fig. 4-24). Other design parameters can be converted to entry velocity by a similar method.

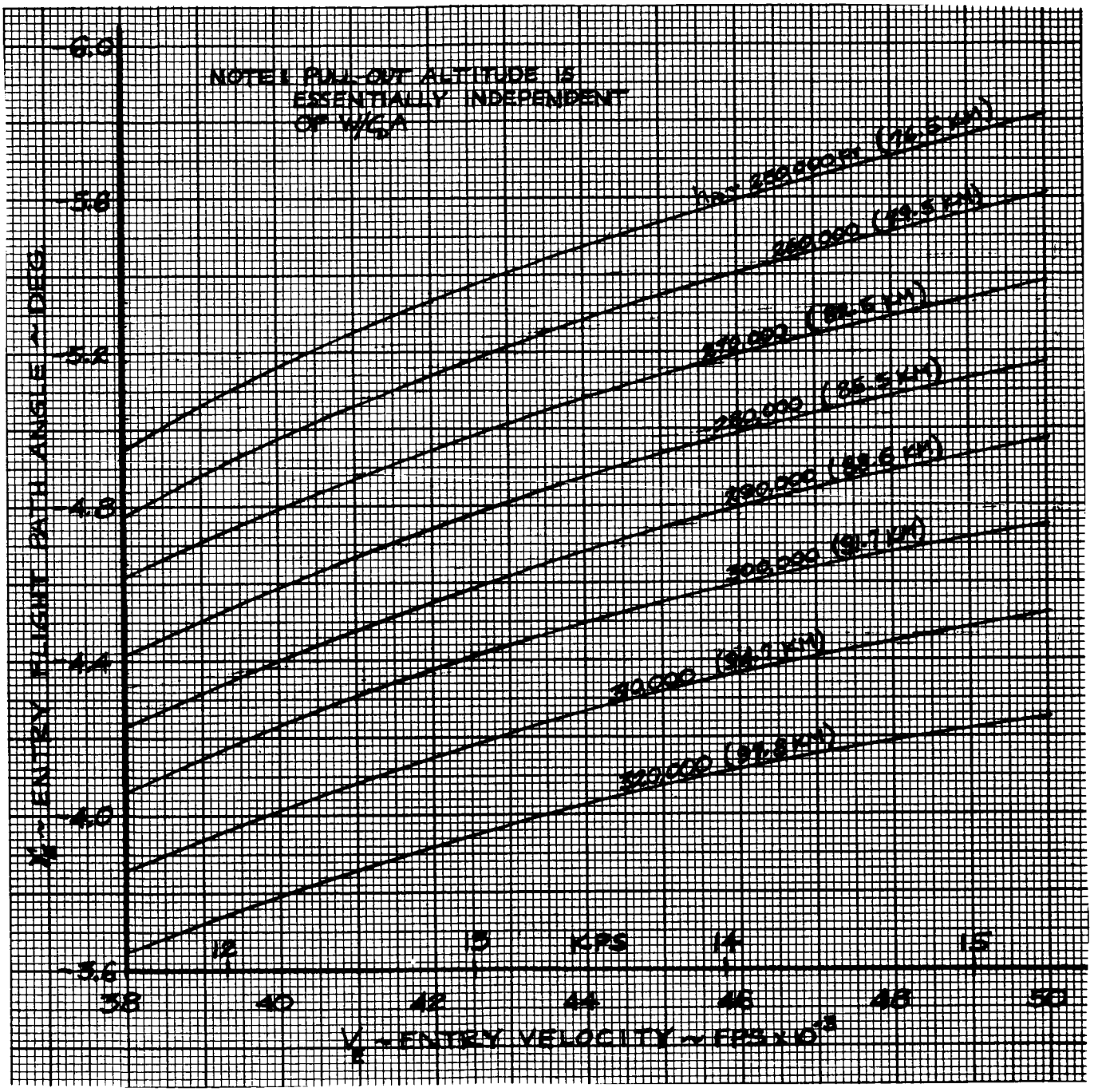


Fig. 4-20 Earth Entry Parameters

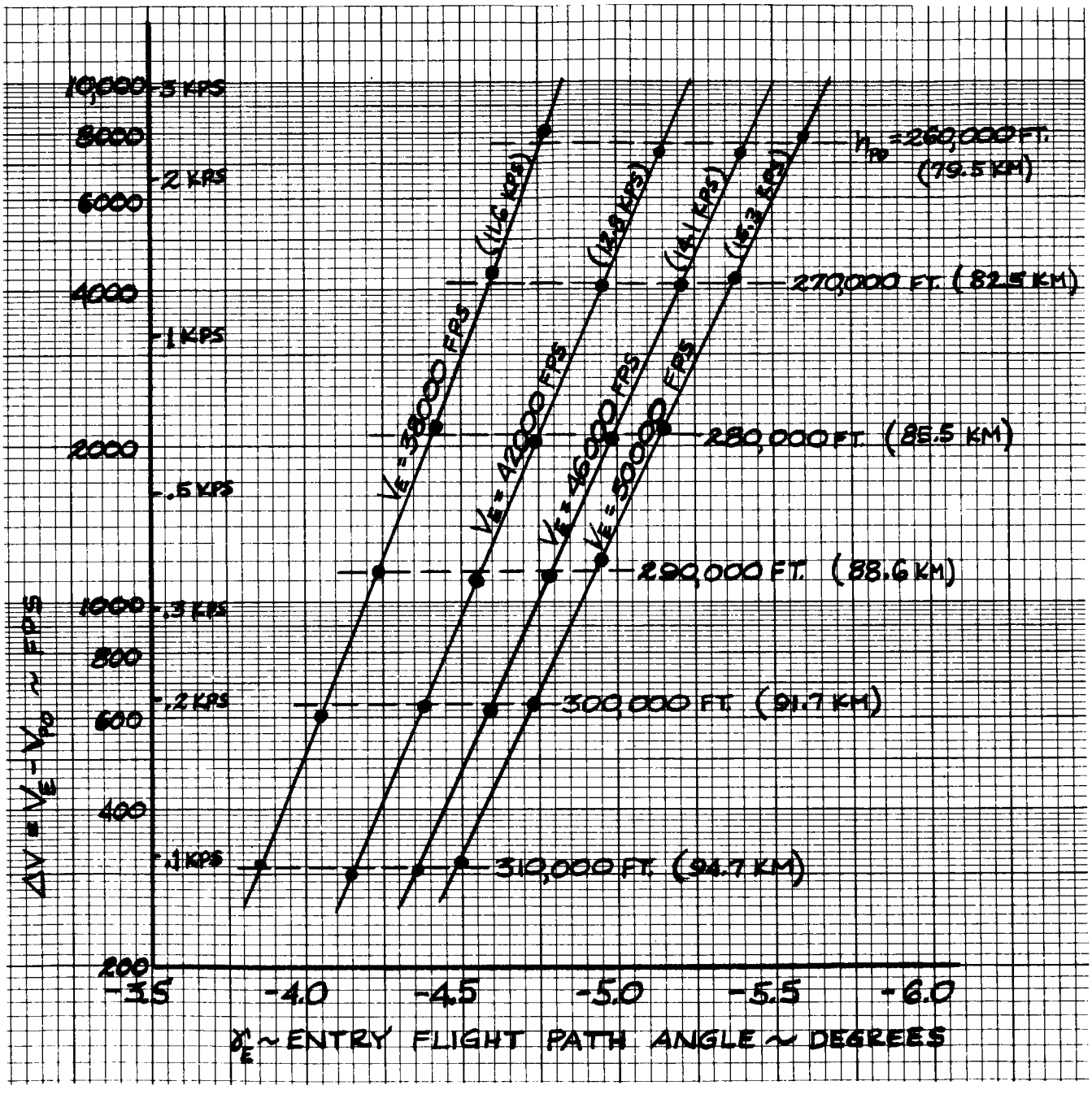
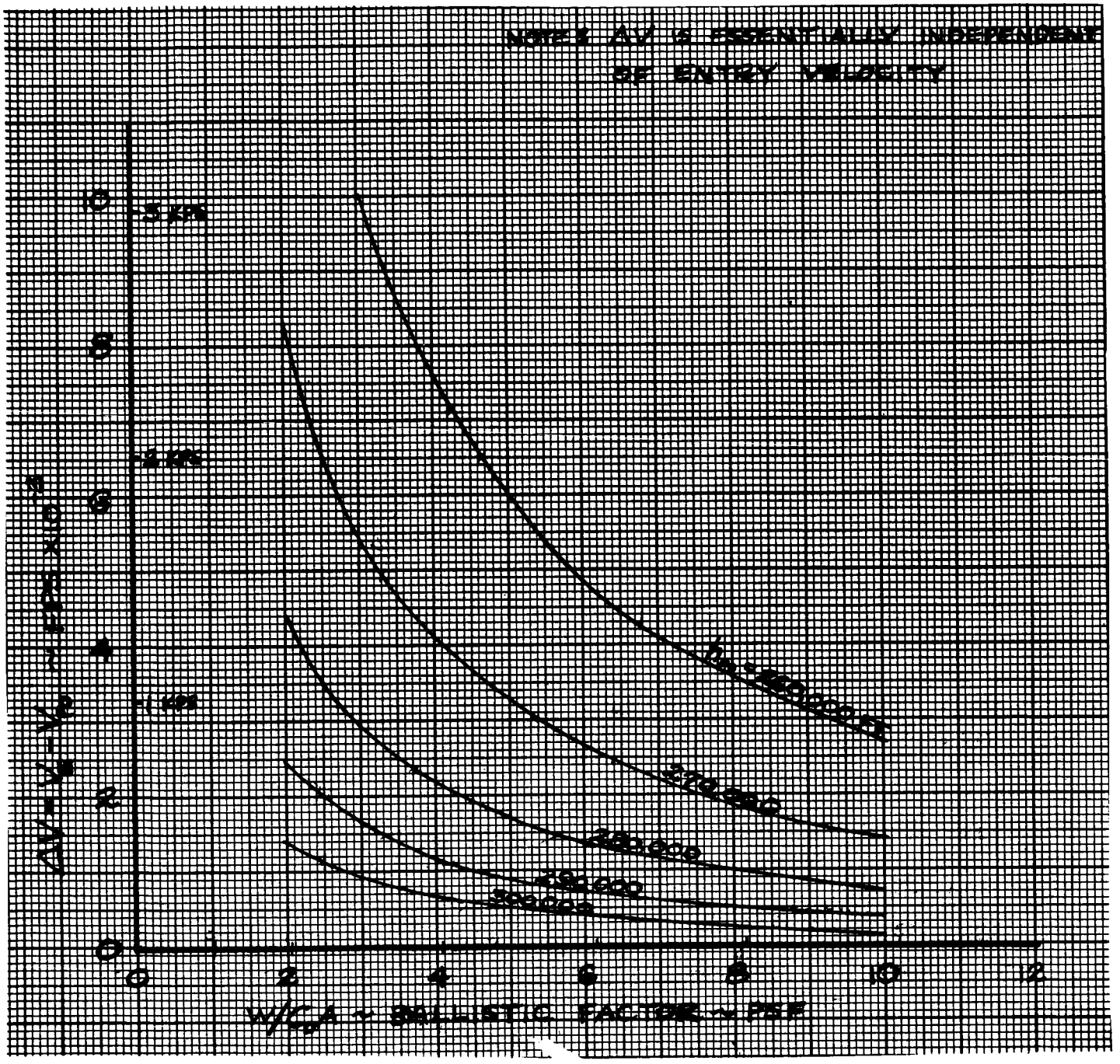


Fig. 4-21 Entry-to-Pullout Velocity Loss (W/C_DA = 4.0 psf)


NOTE: ΔV IS ESSENTIALLY INDEPENDENT OF ENTRY VELOCITY
0 FPS
5
10
15
20
25
30
35
40
45
50
55
60
65
70
75
80
85
90
95
100
105
110
115
120
125
130
135
140
145
150
155
160
165
170
175
180
185
190
195
200

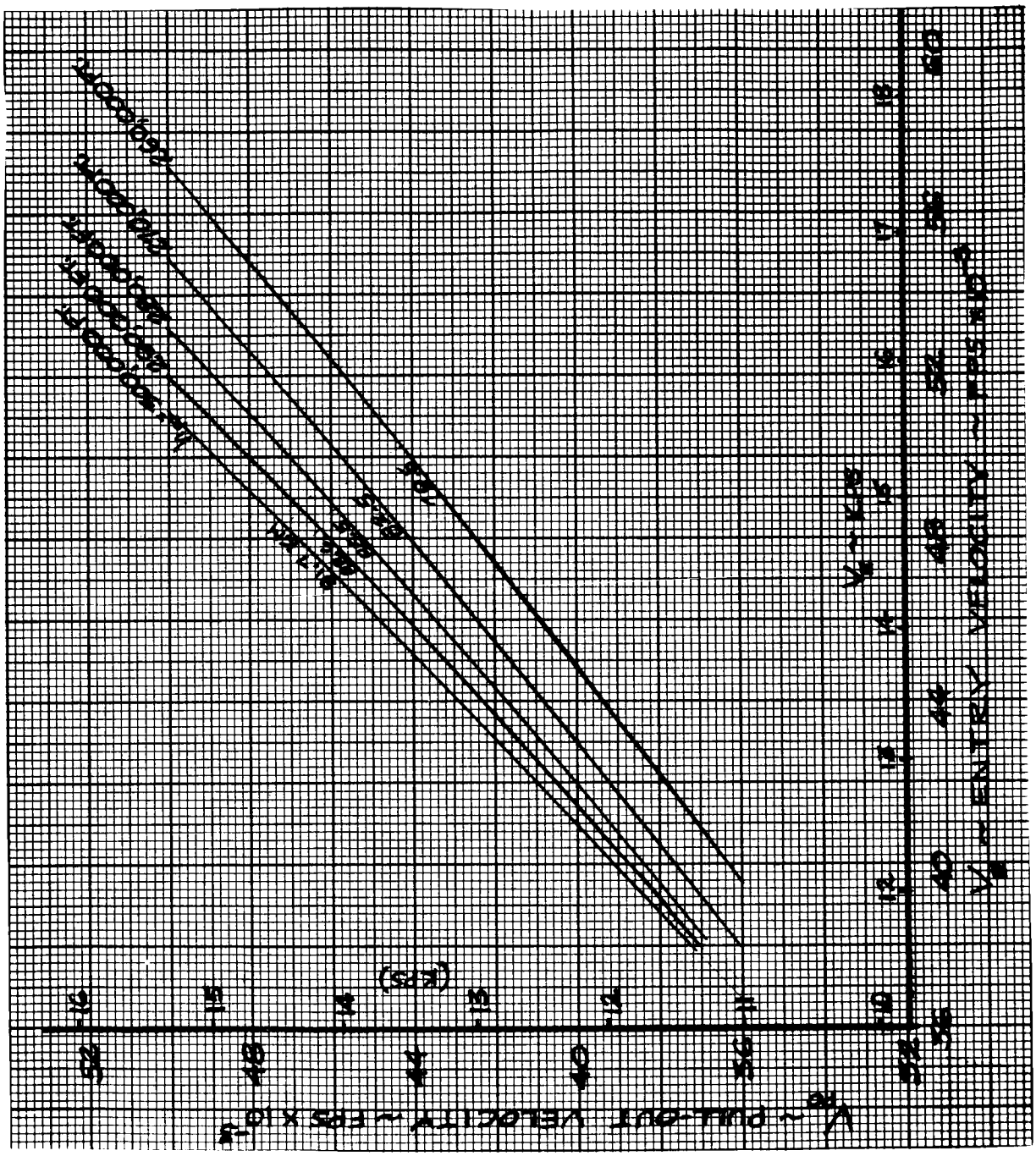


Fig. 4-23 Entry vs. Pullout Velocities

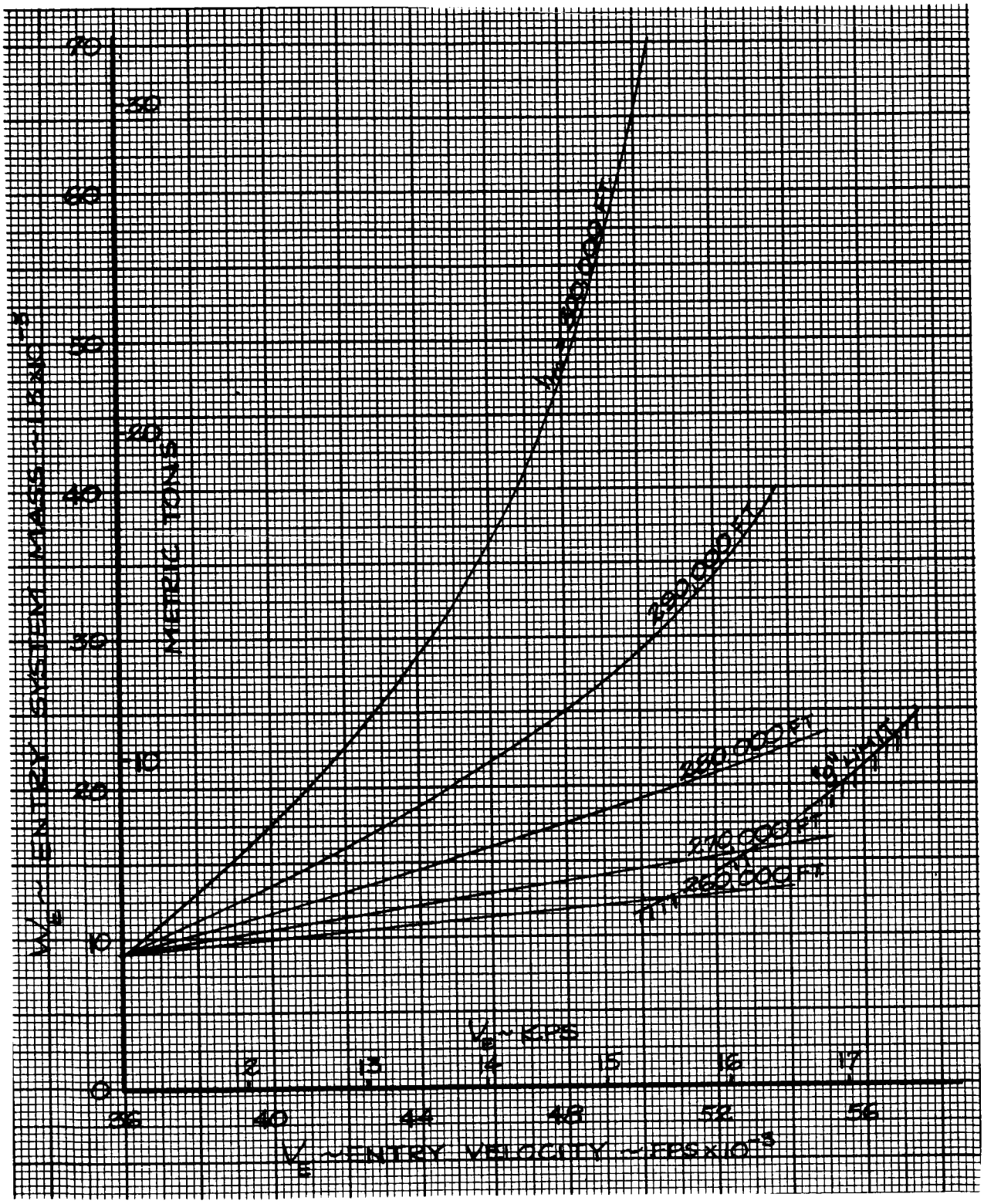


Fig. 4-24 Entry System Mass

It is now possible to define the entry vehicle for any given design entry velocity and desired pull-out altitude. The latter would be a choice consistent with the deceleration environment and the aerodynamic heating, which is discussed in the following section.

4.11 ENTRY HEATING ANALYSIS

The heat transfer phenomena for this entry system involve complicated relaxation processes. First was determined whether the flow is in the free-molecular or the continuum regime. Then the effects of dissociation, ionization, non-equilibrium, and radiation-convection interreaction are examined. Finally, available data are used to obtain the estimation of heat fluxes.

4.11.1 Flow Regime

Reference 4-1 relates the criteria for free molecule flow as:

$$\frac{\lambda_\infty}{R_b} >> \frac{\sqrt{\pi\gamma}}{4}\left(\frac{T_\infty}{T_b}\right)^{1/2} M_\infty$$

If we assume $\gamma = 1.40$; $T_b = T_\infty$ and $>>$ to mean an order of magnitude, the limit is then:

$$\frac{\lambda_\infty}{R_b} = 5.24\ M_\infty$$

For $R_b = 15.3$ meters and $M_\infty = 50$, the mean free path is greater than 3000 meters, corresponding to an altitude of over a 300 kilometers. The conditions of interest are below the free molecule regime.

The basic criterion for continuum flow in the stagnation region of a blunt body is that the mean free path behind the shock be small compared to the shock stand-off distance. Disregarding relaxation phenomenon and using appropriate average equilibrium values, and assuming that:

$$\frac{\Delta}{R_b} \simeq \epsilon \equiv \frac{\rho_\infty}{\rho_S}$$

and

$$\rho_\infty \lambda_C \simeq \rho_S \lambda_S \qquad \text{(hypersonic approximation)}$$

The limits of Ref. 4-1 are as follows:

- Boundary layer $\left(\frac{\lambda_\infty}{R_b} \leq \frac{\epsilon}{10}\right)$
- Viscous layer $\left(\frac{\epsilon}{10} < \frac{\lambda_\infty}{R_b} \leq \frac{\epsilon^{1/2}}{10}\right)$
- Incipient merged layer $\left(\frac{\epsilon^{1/2}}{10} < \frac{\lambda_\infty}{R_b} \leq \frac{1}{10}\right)$
- Fully merged layer $\left(\frac{1}{10} < \frac{\lambda_\infty}{R_b} \leq 1\right)$

For conditions of interest with this vehicle, the flow is within the boundary layer regime.

4.11.2 Convective Heat Flux

Hoshizaki of Ref. 4-2 correlates his theoretical results for convective heat transfer from an ionized layer as:

$$q_{conv} = 2.94 \times 10^4 \sqrt{\frac{\beta R_b \rho_\infty}{V_\infty}} \left(\frac{V_\infty}{10^4}\right)^{3.19} R_b^{-1/2} \ w/cm^2$$

The dimensionless inviscid stagnation point velocity gradient is equal to:

$$(1 - \epsilon) \left(\frac{8}{3} \epsilon\right)^{1/2}$$

from Ref. 4-3.

Using $\beta R_b / V_\infty = (1 - \epsilon) (8/3 \epsilon)^{1/2}$, where $\epsilon = 1/21$ then

$$q_{conv} = 688 \left(\frac{\rho_\infty}{\rho_o}\right)^{1/2} \left(\frac{V_\infty}{10^4}\right)^{3.19} R_b^{-1/2} \ w/cm^2$$

This equation is used for this study.

4.11.3 Radiative Heat Flux

Figure 4-25 shows the radiative heat flux to the stagnation region of a 3 meter radius sphere at a velocity of 7.63 km/sec (Ref. 4-3). At a low altitude, the radiative heat flux is limited by the black body limit when the gas emissivity approaches unity.

At intermediate altitudes, up to about 46 kilometers, the gas behind the shock is in thermodynamic equilibrium and the radiative heat flux is computed by the theories of equilibrium radiation presented in Refs. 4-4, 4-5 and 4-6.

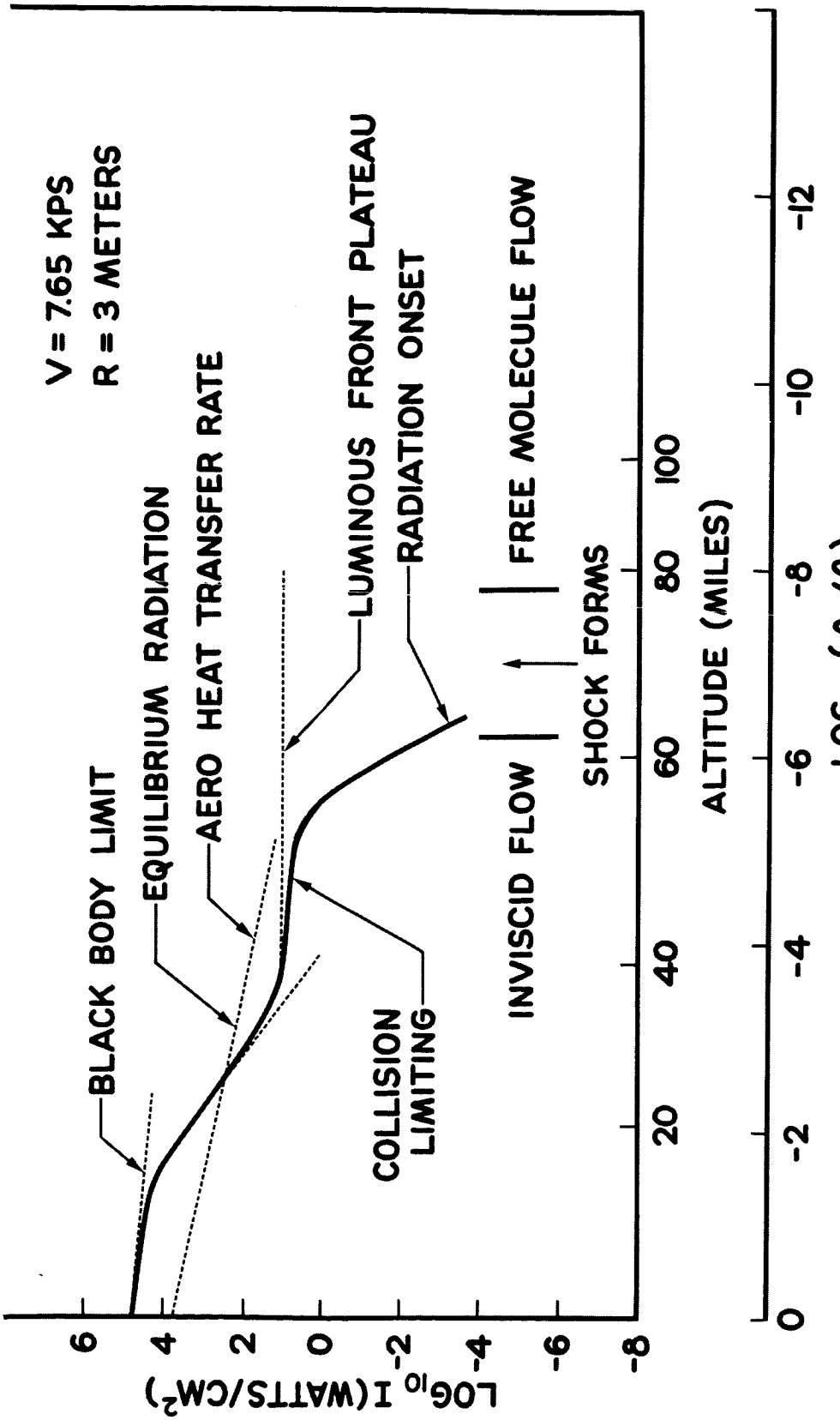


Fig. 4-25 Regimes of Radiation Phenomena

Above this altitude, the non-equilibrium region immediately behind the shock front becomes dominant. The integrated radiative intensity from this region is independent of altitude and is known as the luminous-front plateau. At very low densities, the time required for collisional excitation of molecules is long, compared to the radiative life time. This effect of collision-limiting reduces the radiation intensity because the population of excited states which radiate is not maintained by collision.

The graph of Fig. 4-26 was used to estimate the equilibrium radiative heat flux density to the stagnation region for various velocities and altitudes.

At high velocities and low densities, only the translational and rotational degrees of freedom are excited in the air immediately behind the shock. The effective ratio of specific heat is 1.4. The transformation of the translational-rotational temperature immediately behind the shock front to the final equilibrium temperature involves excitation of vibrational degrees of freedom, dissociation of molecules, and the production of ions, electrons and new molecules. More detailed discussion can be found in Ref. 4-3.

In the non-equilibrium region, almost all of the chemical and excitation processes are binary. Therefore, the intensity of radiation from the region is proportional to the particle density. The thickness of the region is inversely proportional to the density. Consequently, the integrated heat flux from the non-equilibrium region is independent of the particle density as long as the binary mechanisms predominate.

As long as the binary mechanisms predominate and the shock standoff distance is large compared to the non-equilibrium layer behind the shock, the intensity of the "luminous front plateau" will be independent of body radius. Figure 4-27 shows the luminous front intensity for one of the predominant radiating band systems in air. The integrated intensities of other systems must be added for all spectral regions and multiplied by 2π steradians to yield the luminous-front plateau intensity. The estimated total intensity variation with free stream Mach number is shown in Fig. 4-28.

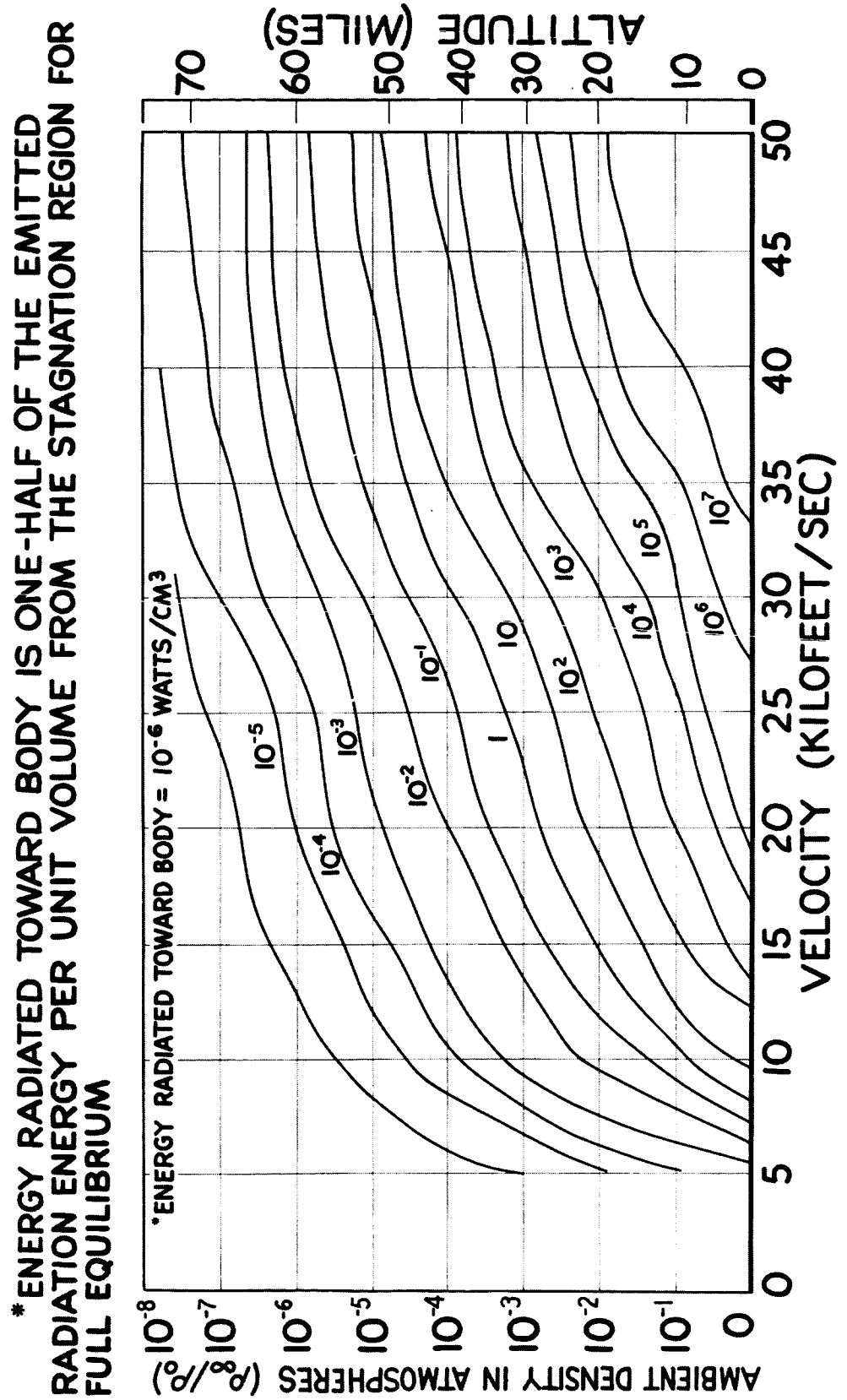


Fig. 4-26 Energy Radiated Toward Body

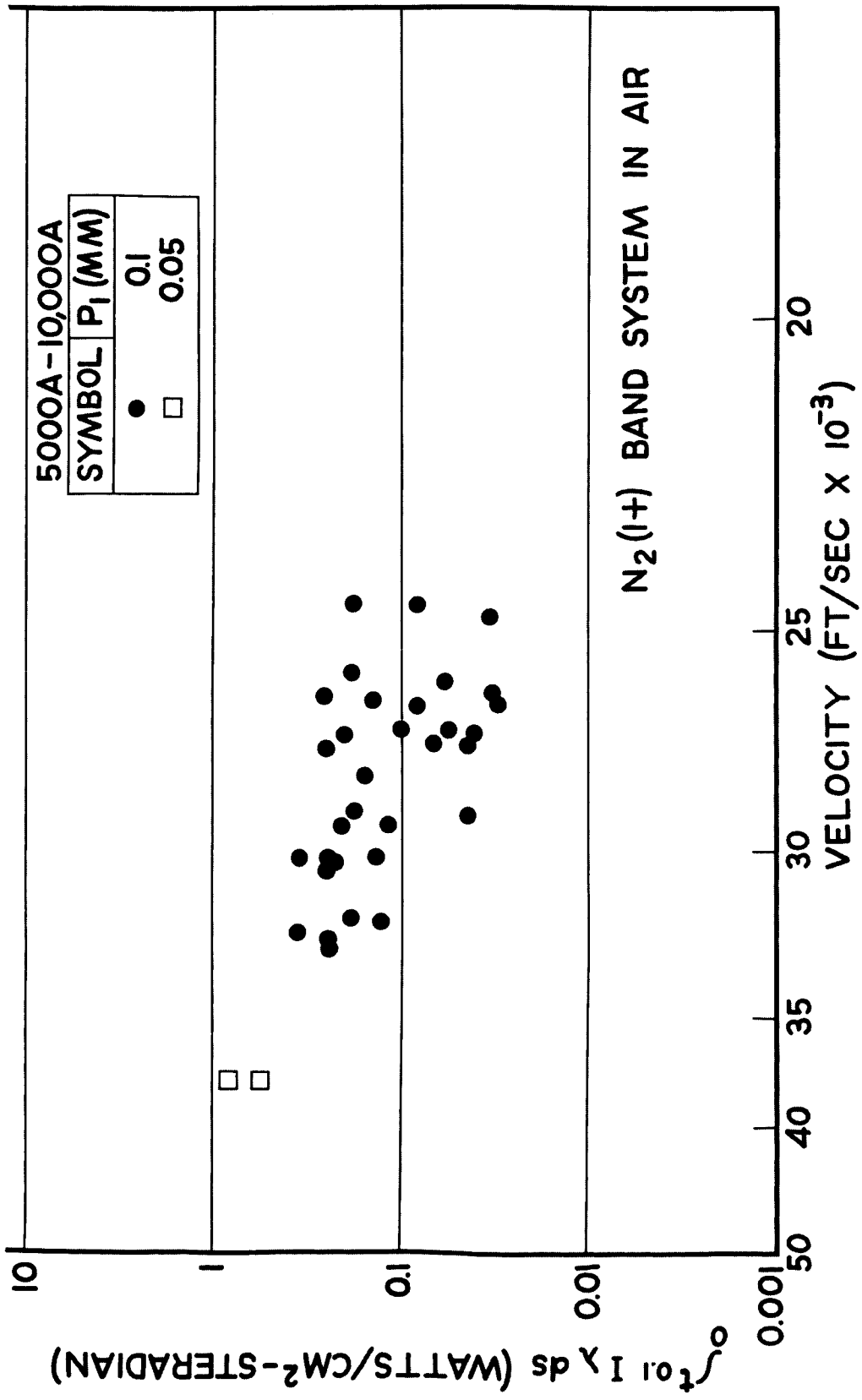


Fig. 4-27 Integrated Luminous Front Intensity

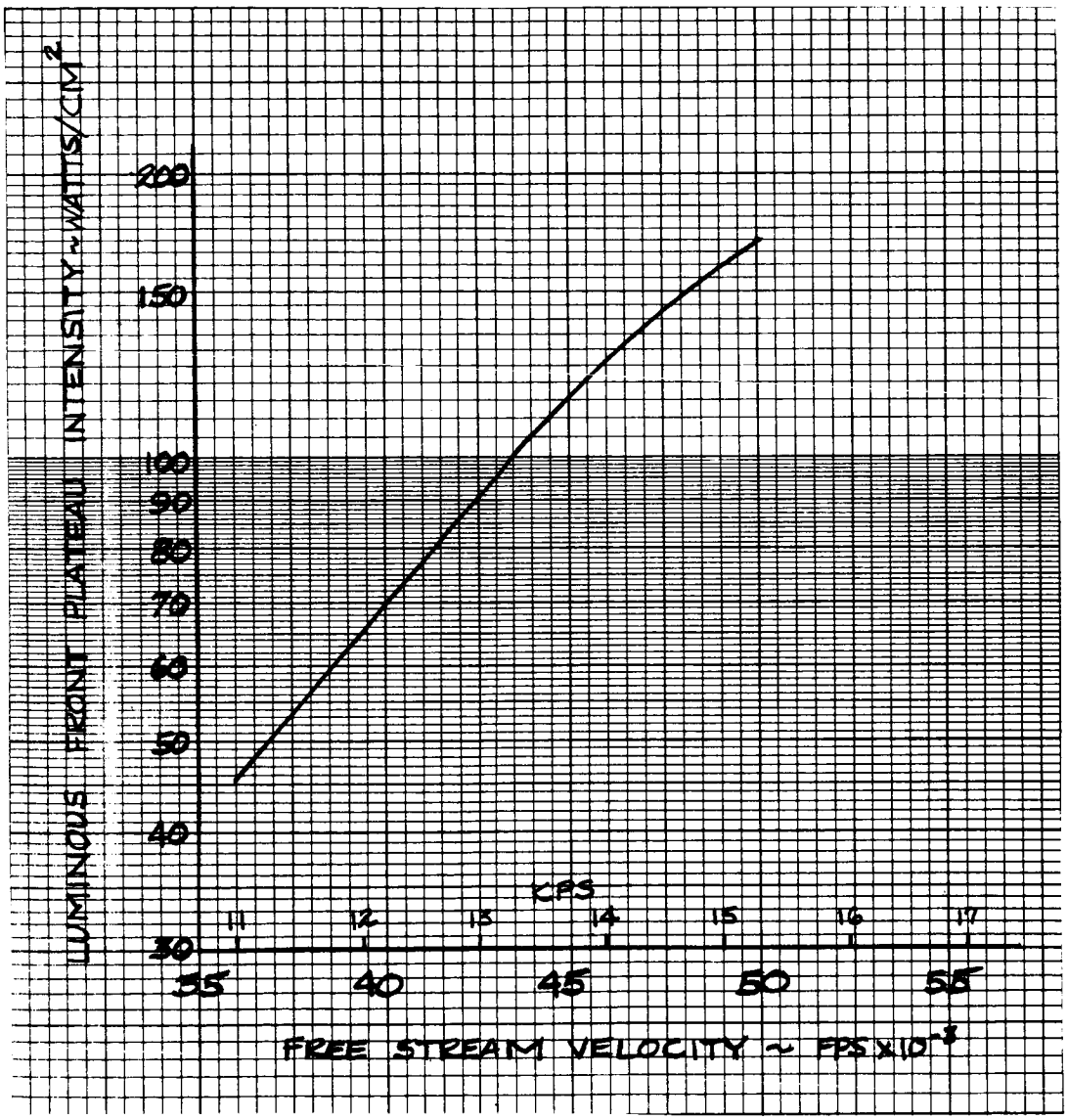


Fig. 4-28 Non-Equilibrium Radiation Intensity

The phenomena of collision-limiting may considerably reduce the radiative heat flux at high altitudes. Consider the excitation and de-excitation of one species in a simple system:

$$A + B \underset{D}{\overset{E}{\rightleftharpoons}} A^* + B$$

De-excitation by emission of a photon:

$$A^* \rightarrow A + h\nu$$

where A^* is the excited state of A, and $h\nu$ is the energy of the photon with frequency ν. The rate equation is:

$$\frac{dA^*}{dt} = k_E BA - k_D BA^* - \frac{A^*}{\tau_R}$$

Where k_E and k_D are the excitation and de-excitation rate constants and τ_R is the radiative life time for the excited state A^*.

The steady state population of the excited state is obtained when $dA^*/dt = 0$ then

$$A^*_{ss} = \frac{\left(A \frac{k_E}{k_D}\right)}{1 + \frac{1}{k_D B \tau_R}}$$

Noting that k_E/k_D is a function of temperature, $K(T)$, and defining a collision time $\tau_C = 1/k_D B$,

$$A^*_{ss} = \frac{AK(T)}{1 + \frac{\tau_C}{\tau_R}}$$

This indicates the radiation intensity is reduced by a factor of $1 + \tau_C/\tau_R$. At low densities, $\tau_C >> \tau_R$ and the radiation intensity may be considerably reduced.

If a critical density ratio, $(\rho/\rho_o)_C$, is defined when $\tau_C \simeq \tau_R$, then

$$\frac{\tau_C}{\tau_R} = \left(\frac{\rho}{\rho_o}\right)_C \left(\frac{\rho_o}{\rho}\right)$$

For the operating regions of this entry system, the density ratio across the shock is nearly constant. It is next assumed that the ambient critical density ratio

$$\left(\frac{\rho_\infty}{\rho_o}\right)_C = \left(\frac{\rho}{\rho_o}\right)_C \left(\frac{\rho_\infty}{\rho}\right) = \text{constant} \quad \left(\frac{\rho}{\rho_o}\right)_C$$

such that "collision limiting" reduces the local equilibrium intensity by a factor of

$$1 + \left(\frac{\rho_\infty}{\rho_o}\right)_C \left(\frac{\rho_o}{\rho_\infty}\right)$$

For this study, $(\rho_\infty/\rho_o)_C = 10^{-4}$ is estimated from the preliminary results of Ref. 4-3.

The shock standoff distance for a sphere, corresponding to the constant density solution, is given as

$$\frac{\Delta}{R_b} = \epsilon \left[1 - \sqrt{8/3\,\epsilon} + 2.6\,\epsilon\right]$$

Since $\epsilon \approx \frac{1}{21}$, $\Delta/R_b \approx 0.0366$

Likewise, the non-equilibrium distance defined previously may be estimated from Ref. 4-3 by the following empirical equation:

$$\Delta_n = 2.5 \times 10^{-6} \left(\frac{\rho_o}{\rho_\infty}\right) e^{\frac{13.7 \times 10^4}{V_\infty}} \quad \text{cm}$$

At 91.5 km, 11 km/sec, and R_b = 12.2 meters, the non-equilibrium distance is larger than the shock stand-off distance. This produces a coupling between the non-equilibrium phenomena and the body size, thereby truncating the radiation profile and further reducing the radiative heat fluxes. For conservatism, this effect is ignored.

The total heat flux to the stagnation region is the sum of the convective and radiative heat fluxes.

The following list summarizes the major assumptions used in this analysis:

- The shock standoff distance is computed according to the constant density solution
- The non-equilibrium distance is computed by an empirical equation derived from Ref. 4-3
- Equilibrium radiation is obtained from Fig. 4-26
- The integrated radiative fluxes from the luminous-front plateau are taken from Fig. 4-28, derived from Ref. 4-3
- Collision-limiting reduces the equilibrium and non-equilibrium radiation values by a factor of $\left(1 + \frac{\rho_o}{\rho_\infty}\ 10^{-4}\right)$ where 10^{-4} is the average critical ambient density ratio
- Stagnation convective heat fluxes are calculated using the correlations of Hoshizaki of Ref. 4-2

This thermal analysis has been applied to the family of entry vehicles. The results are presented in Fig. 4-29. The heating fluxes are normalized with respect to body radius and presented as a function of entry velocity and pull-out altitude.

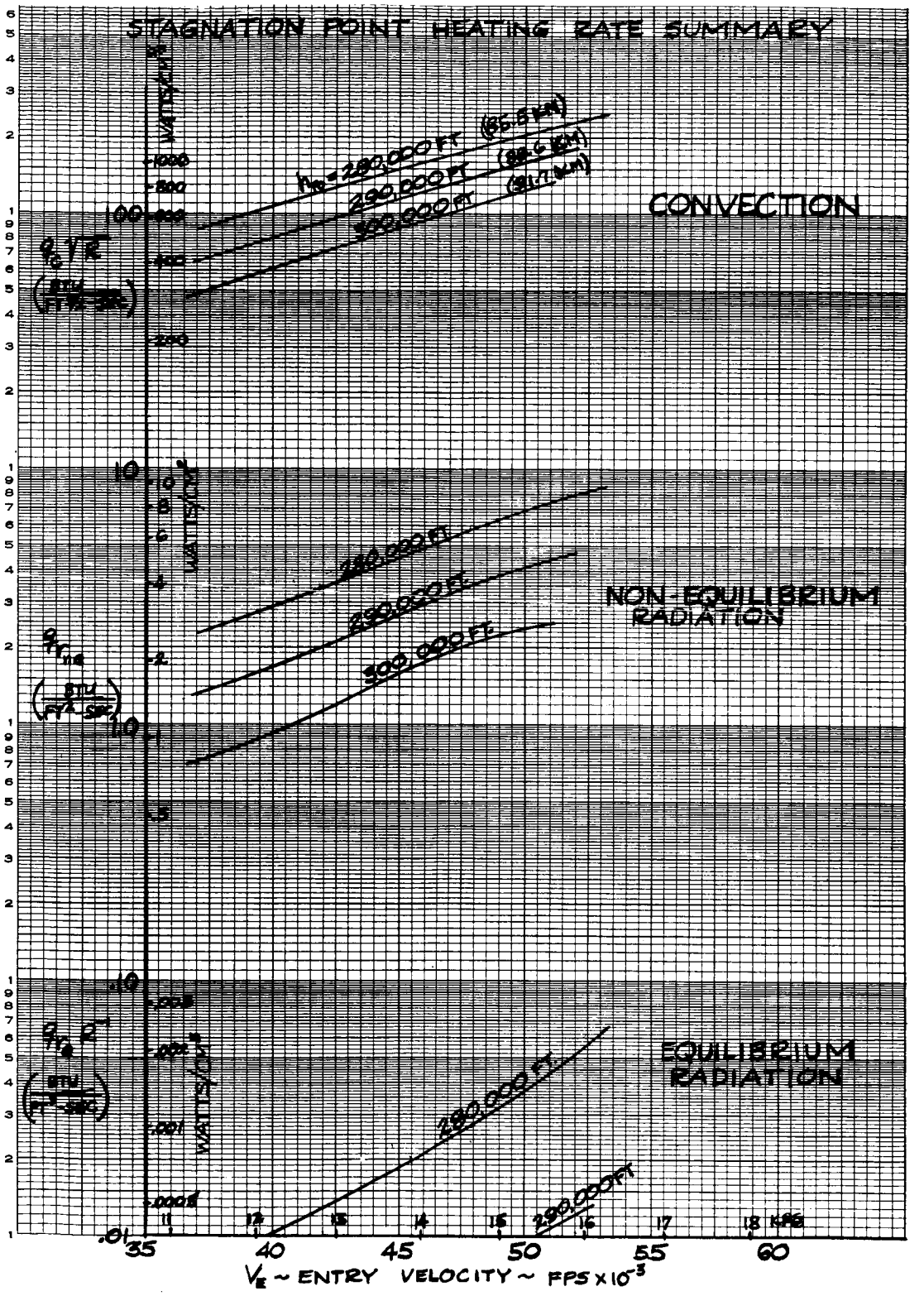


Fig. 4-29 Stagnation Point Heating Rate Summary

4.11.4 Stagnation Temperatures

Since the uncertainty of the total heat flux to the stagnation region is larger than the variation of flux from stagnation to the perimeter of the drag brake, a uniform total heat flux to the frontal surface of the drag brake is assumed.

The heat flux from the wake to the rear surface of the drag brake is expected to be of much smaller magnitude and hence neglected. Transient conduction heat transfer analysis indicates that the skin attains approximately the radiation equilibrium temperatures by radiating the incident, time-dependent, heat fluxes equally from both surfaces. Consequently, the maximum temperature is approximately the initial radiation equilibrium temperature.

The stagnation temperatures are shown in Fig. 4-30 for various pull-out altitudes and entry velocities. The stainless steel cloth appears to be a feasible material and consistent with the temperature environment.

4.12 CONCLUSIONS

The integration of Earth entry systems with planetary mission analyses dictates the necessity for a minimum weight entry system. This system must be consistent with the operational time period and be provided with adequate lead time for development and flight testing. It is also very desirable to use the Apollo capsule as the basic command unit, to fully utilize existing technology.

The drag brake system provides a solution to hyperbolic Earth entry without extensive materials development. Also, the propulsive-lift concept can provide great flexibility to the system and provide corrections to guidance errors, as well as provide adequate entry corridors.

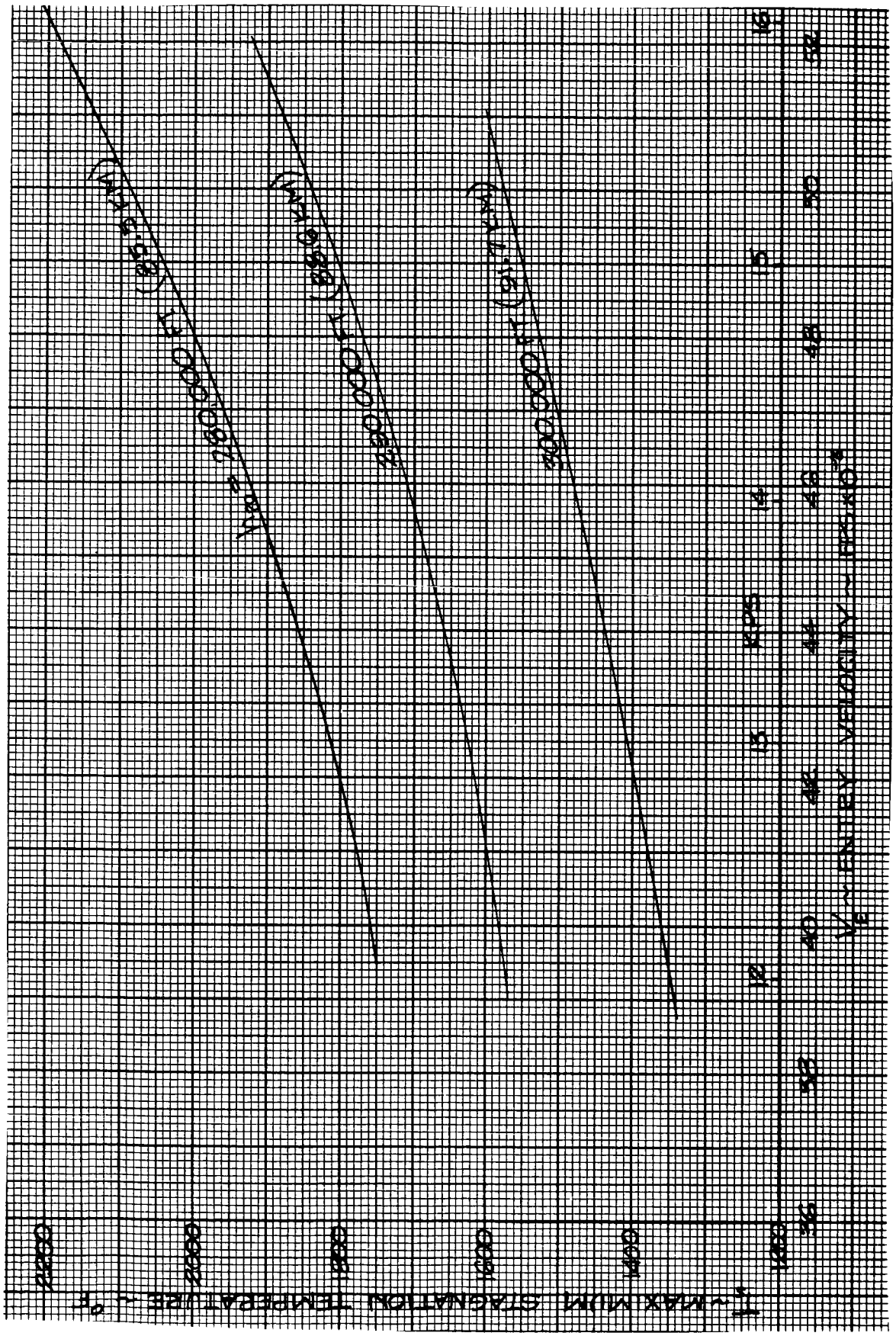


Fig. 4-30 Stagnation Temperatures

An extension of this concept would include different drag brake materials which would allow higher stagnation temperatures and dictate lower pull-out altitudes. This would provide an operational region of better defined atmospheric properties and may reduce the drag brake diameter to a point where it could be fixed, without greatly complicating the design continuity.

4.13 SYMBOLS FOR SECTION 4

V	velocity	fps km/sec	R	radius	ft (cm)
W	weight	lb (kg)	T	absolute temperature	°K
ρ	density	lb-sec^2/ft^4	M	mach number	–
g	deceleration	g	γ	specific heat ratio	–
C_D	drag coefficient	–	γ	flight path angle	deg
A	projected area	ft^2 (m^2)	Δ	shock stand-off distance	ft (cm)
L	lift	lb (kg)	q	heat flux	Btu/ft^2-sec (w/cm^2)
D	drag	lb (kg)	β	stagnation point velocity gradient	–
t	thrust	lb (kg)	ϵ	density ratio across shock front	–
λ	mean free path	ft (cm)	h	altitude	ft (km)

SUBSCRIPTS

PO	pull-out	conv	convective
BO	burn-out	E	entry
DB	drag brake	ne	non-equilibrium
P	propulsion	e	equilibrium
C	circular	r	radiation
b	body	ss	steady state
∞	free stream	os	overshoot
s	behind shock	us	undershoot
		s	stagnation

4.14 REFERENCES

4-1 R. F. Probstein, "Shock Wave and Flow Field Development in Hypersonic Re-entry," ARS J. Vol. 3, No. 1, pp. 185–194, 1961

4-2 H. Hoshizaki, "Heat Transfer in Planetary Atmospheres at Super-Satellite Speeds," ARS Preprint 2173-61, Oct 1961

4-3 J. D. Teare, S. Georgiev, and R. A. Allen, "Radiation from the Non-equilibrium Shock Front," AVCO RR-12, Oct 1961

4-4 B. Kivel and K. Bailey, "Tables of Radiation from High Temperature Air," AVCO RR-21, Dec 1957

4-5 R. E. Meyerott, J. Sokoloff, and R. W. Nicholls, "Absorption Coefficients of Air," Geophysics Research Paper No. 68, AFCRC, 1960

4-6 B. F. Armstrong, J. Sokoloff, R. W. Nicholls, D. H. Holland and R. E. Meyerott, "Radiative Properties of High Temperature Air," J. Quant. Spectrosc. Radiat. Transfer, Vol. 1, pp. 143–162, 1961

Section 5

CREW UTILIZATION AND REQUIREMENTS

by

Thermal Control	R. S. Thomas
Physico-Chemical Regeneration	J. M. Smith
Space Medicine	R. B. Jagow
Radio-Biology	H. W. Rose
Biological Regeneration	O. M. Meredith
Human Engineering	V. H. Lynch
Human Engineering	S. O. Parsons
Nuclear Physics	M. R. Munger
Space Physics	W. H. Harless
Meteoritic Phenomena	R. C. Wentworth
Waste Handling & Microbial Contamination	Y. S. Li
	A. M. Nowitzky

Section 5
CREW UTILIZATION AND REQUIREMENTS

5.1 SUMMARY

Systems are sized on the basis of three men for 365 and 600 days. A two-gas cabin atmosphere is recommended, 180 torr O_2 and 180 torr N_2. Atmospheric water, urine, and carbon dioxide regeneration by physico-chemical means is preferred over an open or biological regeneration system. Metabolic supplies are calculated on the basis of an average metabolism of 2,820 kcal day^{-1}. Radiation shielding weights are based on a 0.001 probability of receiving 200 rads to the blood-forming organs from all sources of radiation throughout the mission.

Meteoroid shielding is based on Whipple's 1962 distribution and Summers' hypervelocity penetration equation. A rotating vehicle is assumed to provide a gravitational acceleration of some 0.3 to 0.85 g. Thermal control is based upon space radiators and circulating liquid coolants. A large number of areas requiring further research and development are defined.

Table 5-1 contains the nominal design values used in the study. Table 5-2 contains a summary of the weight and power levels associated with typical missions of the duration shown.

For the purposes of this study, crew utilization and requirements are defined to include the following:

- Human Engineering
  - Task analysis
  - Schedule of crew activities
  - Confinement factors

Table 5-1

CREW UTILIZATION AND REQUIREMENTS

Nominal Design Values	
Temperature	75°F ± 5°F (24°C ± 3°C)
Relative Humidity	60% ± 20%
Air Velocity	25 ft min^{-1} (12.7 cm-sec^{-1})
Cabin Atmosphere	180 torr O_2 180 torr N_2
Secondary Pressurization System (Suit) Atmosphere	180 torr O_2
Carbon Dioxide Partial Pressure	< 3.8 torr
Methane and Hydrogen Partial Pressures	Well below explosive limits
Angular Velocity of Rotating Vehicle	< 0.4 radians sec^{-1}
Induced g Acceleration	> 0.3 g and < 0.85 g
Probability of One 1 cm Hole from Meteorite Penetration (600-Day Mission)	0.01
Maximum Acute Dose From Relativistic Solar Flare	25 Rad
Maximum Aggregate Dose From All Radiation	200 Rad
Cabin Leakage Area	5×10^{-9} cm^2 per cm^2 os surface
Trace Contaminants – Toxic and Offensive Odors	Well Below Level at Which Effect Observed
Sterilization of Probes	Complete
Acceleration Stress, Sustained	< 4 g
Acceleration Stress, Reentry	< 10 g
Noise Level	< 80 db
Vibration	< 12.7×10^{-2} cm at 10 cps < 12.7×10^{-3} cm at 100 cps

Table 5-2

MASS AND POWER SUMMARY FOR LIFE SUPPORT AND CREW PROTECTION SYSTEM FOR THREE MEN (kg)

	365 Days		600 Days	
	Open	Closed	Open	Closed
Gas Supply	2,330	1,230	3,670	1,850
CO_2 Removal	90	–	90	–
Contamination Control	30	30	50	50
Food and Water	5,810	2,250	9,590	3,500
Crew Support Equipment	70	70	70	70
Temperature and Humidity Control	435	435	435	435
Regeneration Equipment	–	300	–	350
Sterilization	10	10	10	10
Sound and Vibration Control	10	10	10	10
Pressure Suits	100	100	100	100
Utility Water	10,000	200	16,000	200
Radiation Shielding	8,000*	8,000*	6,000*	6,000*
TOTAL	26,885	12,635	36,025	12,575
Power Level (Average)	2.6 kw	4.7 kw	3.1 kw	5.1 kw
Power Level (Peak)	3.9 kw	6.1 kw	4.6 kw	7.6 kw

*Assuming 365-day mission to Venus and 600-day mission to Mars

- Atmosphere Selection and Gas Supply
- Carbon Dioxide Control
- Trace Contamination Control
- Thermal Control
- Diet and Metabolism
- Physico-Chemical Regeneration
- Biological Regeneration
- Weightlessness, Artificial g and Coriolis Effects
- Meteoritic Phenomena
- Ionizing Radiation
- Pressure Suits
- Acceleration Stress
- Sound and Vibration Control
- Waste Handling and Microbial Contamination
- Sensors and Warnings
- Crew Support Equipment
- Research and Development Areas

5.2 INTRODUCTION

The chief purpose of the EMPIRE Mission is assumed to be the gathering of information which contributes to ultimate landings; secondary desiderata are assumed to include the acquisition of exobiological, astrophysical, and planetary data of intrinsic scientific value.

With these objectives in mind, the human tasks necessary and/or desirable for their accomplishment are determined. Various crew sizes and mission durations are postulated. Emphasis is placed upon the early Venus (365 day) and Mars (600 day) flyby mmissions with a minimum crew of three men.*

*No assumption was made that 3 men was an optimum crew. The three-man mission was investigated in the interest of exploring the possibility of utilizing Saturn-type boosters for the earliest possible minimum manned interplanetary missions.

Other factors which strongly influence the choice of systems include trajectory, especially the time history of the distance of the vehicle from the sun, the amount of heat generated aboard, the type of propulsive and auxiliary power available, the power penalty in kg per kw, and, of course, the state of the art during the applicable time period.

The time period of these missions is from 8 to 18 years from now. During this time, intervening explorations both manned and unmanned will probably have demonstrated the existence of hazards now unknown or only suspected and have shown other dangers to be of lesser magnitude than now anticipated.

What is possibly more important, life support hardware will be greatly improved. In order to presently select systems, subsystems, and components, it is necessary to extrapolate reliabilities, weights, volumes, and power requirements of hardware now barely conceived or at best existing in laboratory pilot models to flight qualified equipment which will exist some years from now.

The alternative of selecting a system only from presently available qualified hardware for use in the 1970−1980 time period is so restrictive that the results would be unduly pessimistic and have little usefulness. Regeneration of metabolic wastes would be, for instance, virtually ruled out and nuclear power sources ineligible for consideration.

This study selects a system based on some components which require considerable engineering development. It assumes, however, few if any basic scientific breakthroughs.

In the ensuing analysis, each of the above listed subsystems is considered according to the following organization:

- Determine the requirements upon the subsystem.
- Compare and contrast alternative solutions and select the most feasible systems.
- Determine the approximate mass, volume, and power requirements of the system selected.

5.3 HUMAN ENGINEERING

Assumptions. The interplanetary flyby vehicle consists of a command module, two radial areas, a hub, and a crew living compartment. On the launch pad this vehicle is resting in a folded configuration. During the Earth Parking Orbit phase, rendezvous with another vehicle for the purpose of spacecraft erection and component transfer may or may not be considered. A number of revolutions while in Earth orbit are anticipated prior to injecting the spacecraft into heliocentric orbit. During the Outbound and Inbound Trips some g loading will be developed by spinning the vehicle. Reentry will be accomplished utilizing only the Apollo type command module after separating it from the remaining portions of the vehicle.

The three crew members will all be located in the command module during liftoff, Earth parking orbit, reentry and landing. The crew will be utilized in the system as much as possible especially in the areas of command and decision making, handling low probability events, judgmental diagnosis and correction, variable tasks, configurational recognition, emergency situations, etc. The three crew members will all shift positions frequently, stand watches according to a prescribed work-rest cycle, take navigational fixes and be crosstrained in most of the primary and secondary specialties.

5.3.1 Task Analysis

The following task description is not broken down into duties which will be executed by a specific crew member. Rather, all personnel functions are listed by mission phase.

The required personnel functions have been divided into three major groups; Operation, Maintenance, and Support. Operational functions have been keyed to mission phases in the following listing since such functions are necessary in all phases of the mission. Maintenance and support functions are listed separately since they will probably not be required in all phases of the mission.

Mission Phases. A sequence of major events during the entire mission provides the basis for the following phases:

I Countdown
II Launch
III Earth Parking Orbit
IV Injection to Heliocentric Orbit
V Outbound Trip
VI Planetary Encounter & Maneuver
VII Inbound Trip
VIII Reentry
IX Landing

Operational Functions. The foregoing phases can be further broken down into operational functions comprised of inputs, decisions, and actions as follows:

Input	Decision	Action
Phase I Countdown		
Monitor communication link with Control Center for initiation of countdown	--	Connect space suits to vehicle and fasten restraint devices
Monitor communication link for status of external systems	--	Communicate with Control Center as required
Monitor displays for status of internal systems	Determine Go/No Go condition of systems	Communicate results and descisions to Control Center and crew members

Input	Decision	Action
Phase II Launch		
Monitor systems status on display panel and communication link with Control Center	Determine abort condition if under manual control	Maintain abort readiness Communicate with Control Center as required Voice record subjective and objective report of launch Perform escape tasks in event of abort Initiate separation of escape tower
Phase III Earth Parking Orbit		
Monitor on-board and ground generated position analysis	Determine if spacecraft is in required orbit	Initiate procedural checkout of all systems
Monitor procedural checkout	Determine that all systems are operating within tolerance	Initiate spacecraft erection Perform rendezvous actions if required. May include manual operations in space suits
Monitor spacecraft erection and sectional integrity	Determine that erection process is completed and integrity of craft is assured	Communicate status to Control Center and activate environmental control system for all crew compartments
Monitor status of environmental control systems	Insure that environmental systems are properly operating	Initiate testing of personnel transport systems from command module to living compartments

Input	Decision	Action
Phase III (continued)		
Monitor test of personnel transport system	Determine system is operating properly	Initiate final checkout of all systems prior to injection. Coordinate checkout with Control Center
Monitor display panel and communication link for systems checkout	Determine that all systems are operating within tolerance	Review procedures and initiate injection phase
Phase IV Injection to Heliocentric Orbit		
Monitor on-board and ground generated position computations and analysis	Select transfer orbit	Ignite booster stage for injection into heliocentric orbit, or program ignition
Monitor ignition, burn, and separation of booster	Insure that booster has properly burned and separated	Orient Spacecraft pointing solar collector toward sun Extend arms of spacecraft to final radii Initiate spin-up for G loading
Monitor spacecraft environment	Insure that spacecraft provides safe "shirt-sleeve" environment	Unfasten restraint devices Doff spacesuits Initiate navigation sightings, measurements, and computations
Analyze initial navigation computations	Determine that trajectory is within tolerance	Establish routine work-rest cycles for Outbound phase

Input	Decision	Action
Phase V Outbound Trip		
Monitor on-board and Control Center position analysis	Determine if spacecraft is within required trajectory	Perform navigation sightings, measurements, and computations Compute mid-course corrections as required Activate propulsion system to make midcourse corrections
Monitor communication links to Control Center	--	Record incoming messages Prepare messages as requested or scheduled
Monitor displayed status of spacecraft systems Power Fuel Control Guidance Environmental Communications	Determine that all systems are operating within tolerance	Adjust settings of systems as required Take corrective maintenance action in event of malfunction Switch to emergency operational mode in event of major failure Carry out emergency procedures in event of solar flare
Phase VI Planetary Encounter		
Analyze navigational data	Select final course correction for planetary encounter	Activate propulsion system to effect final course correction

Input	Decision	Action
Phase VI (Continued)		
Analyze photographs, infrared detection data, maps, etc. of planet	Select sites for planetary probes	Compute release points for probes Perform terminal sterilization of probes
Monitor position data	Detect start of planetary encounter	Manually activate cameras and recording devices Fire probes at computed points Voice record subjective data concerning encounter
Monitor position data	Determine termination of useful period of planetary encounter	Terminate data collection activities
Phase VII Inbound Trip		
(Same operational functions as listed under Phase V Outbound Trip.)		
Phase VIII Reentry		
Analyze navigational and position data	Select final course correction for reentry	Activate propulsion system to effect final course correction
Monitor course correction	Evaluate adequacy of correction	Don spacesuits Connect suits to vehicle Fasten restraining devices Initiate separation of command module from spacecraft

Input	Decision	Action
Phase VIII (Continued)		
Monitor module separation, attitude, velocity, and altitude	Select point for activating deceleration system	Activate deceleration system
Monitor module altitude, velocity, and attitude	Select point for activating propulsion system to maintain altitude during deceleration	Activate propulsion system to maintain altitude
Monitor deceleration of module and module attitude	Select point for initiation of reentry attitude maneuvers	Correct attitude of module as required for landing trajectory
Phase IX Landing		
Analyze position data from on-board equipment and Control Center	Select landing point in conjunction with Control Center	Correct attitude for selected landing site Communicate with Control Center
Monitor position and flight data	Select point for release of parachutes (e.g., Rogallo wing)	Release parachutes
Monitor release of chutes, altitude, and velocity	--	Land and egress from module

Inputs	Decision	Action
Maintenance Functions*		
Monitor automatic check-out equipment	Determine that all systems are operating within tolerance and, if not, isolate malfunction to smallest unit possible from console indicators	Take emergency action if required and initiate further troubleshooting with portable test equipment at malfunctioning unit
Analyze results of tests with portable test equipment	Isolate malfunction to replaceable module	Replace malfunctioning module or adjust unit
Monitor check-out equipment	Verify that trouble has been corrected	Resume normal operational mode
Periodically physically inspect units not amenable to automatic check-out such as mechanical devices, spacesuits, shielding, wiring, etc.	Determine that equipment is free of leaks, corrosion, fire hazards, etc.	Repair, adjust, or replace all damaged or defective equipment
Review servicing requirements specified in maintenance schedule	--	Remove sludge from urine regenerator Dispose of carbon from CO_2 regenerator Lubricate mechanical units Clean equipment units

*Maintenance functions will be carried out primarily during Phase V Outbound Trip and Phase VII Inbound Trip. Corrective maintenance of an emergency nature would be carried out whenever it is required.

Support Functions. In addition to the operational functions above, certain support functions will be carried out primarily during Phase V Outbound Trip and Phase VII Inbound Trip. Food preparation and consumption and other necessary activities may be carried out during some of the other phases.

Training

Conduct team training exercises for critical mission activities and emergencies.

Planetary encounter
Reentry
Solar flare
System malfunctions

Conduct crew training exercises for critical crew activities using auto-instructional techniques.

Conduct individual scientific training using auto-instructional techniques.

Food Preparation

Inject water and mix dried foods.
Beat frozen or reconstituted foods.
Dispose of containers and leftovers.
Monitor and control consumption of food supplies.
Monitor and perform technical tasks associated with closed cycle food production.

Recording and Record Keeping

Maintain operational log including unusual events, malfunctions, sightings, position, etc.

Maintain maintenance log including results of tests and checkouts, malfunctions, and corrective action taken.

Maintain environmental log including radiation levels and other environmental parameters recorded periodically. Individual differences among crew members in exposure to radiation, etc. would be recorded.

Maintain records of consumable supplies used against programmed rate of utilization.

Prepare periodic status reports as required for transmission to Control Center or storage for data retrieval after landing.

Scientific Experimentation

Carry out planned experimentation and record and analyze results in following areas.

- Astronomical and astro-physical observations
- Space physics, radiation and meteoritic studies
- Genetics and embryology under conditions of radiation and weightlessness
- Plant physiology
- Human physiology

Modify experimental program and plan new experimentation based on the results of experiments.

Transmit results of critical experiments to Control Center.

Receive data on detailed computer center analyses.

Recreation

Carry out planned recreation program including physical training.

Carry out recreation program selected from available activities.

- Individual training
- Recorded music
- Movies
- Microfilmed books
- Personal diaries
- Games requiring minimal equipment

5.3.2 Schedule of Crew Activities

The entire crew of the spacecraft will be required during a number of the mission phases, such as launch and reentry. During these phases operation of the craft will take precedence over activities such as rest, eating, recreation, etc. The schedule of activities for these phases is, therefore, the schedule of operational functions required.

During the long periods of the outbound and inbound phases of the mission, however, it is necessary to provide scheduling of crew activities to ensure that mission objectives are met, and to provide adequate rest and recreation to the crew.

A suggested typical twenty-four hour schedule for these phases is presented in Fig. 5-1. A summary of the percentage of the day devoted to each type of activity is presented in Fig. 5-2.

The suggested scheduling of activity is based on the assumption that a three-man crew will be utilized for the mission and that a requirement of mission success is that at least one member of the crew is located at the command console at all times for monitoring conditions of the craft and to take emergency or corrective action if required.

The general pattern of the daily schedule for each crew member is: ten hours on duty, two hours off, four hours on duty, and eight hours off. To provide variety during the duty period the ten-hour period is divided among command, maintenance, and scientific experimentation. This division eliminates extended periods of vigilance type tasks associated with command duties.

The schedule has been designed to provide three points during the twenty-four hour period that could be utilized for team training. These three points at which all the crew are awake are indicated in Fig. 5-1 by asterisks. These points could also be used for activities such as briefings and group decision making.

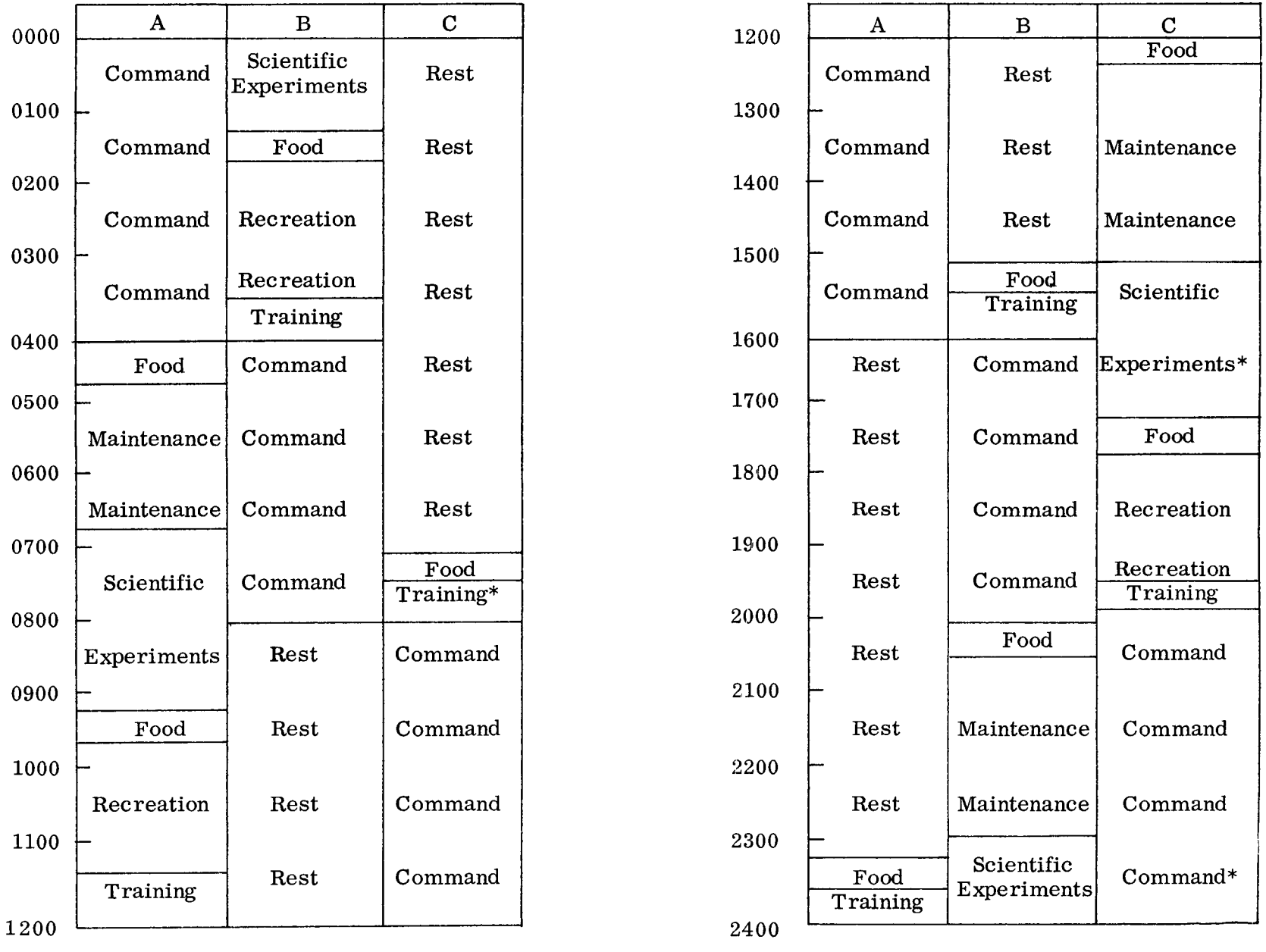


Fig. 5-1 Threeman Crew Activities During a Typical 24-Hour Period of Outbound or Inbound Phase of Mission

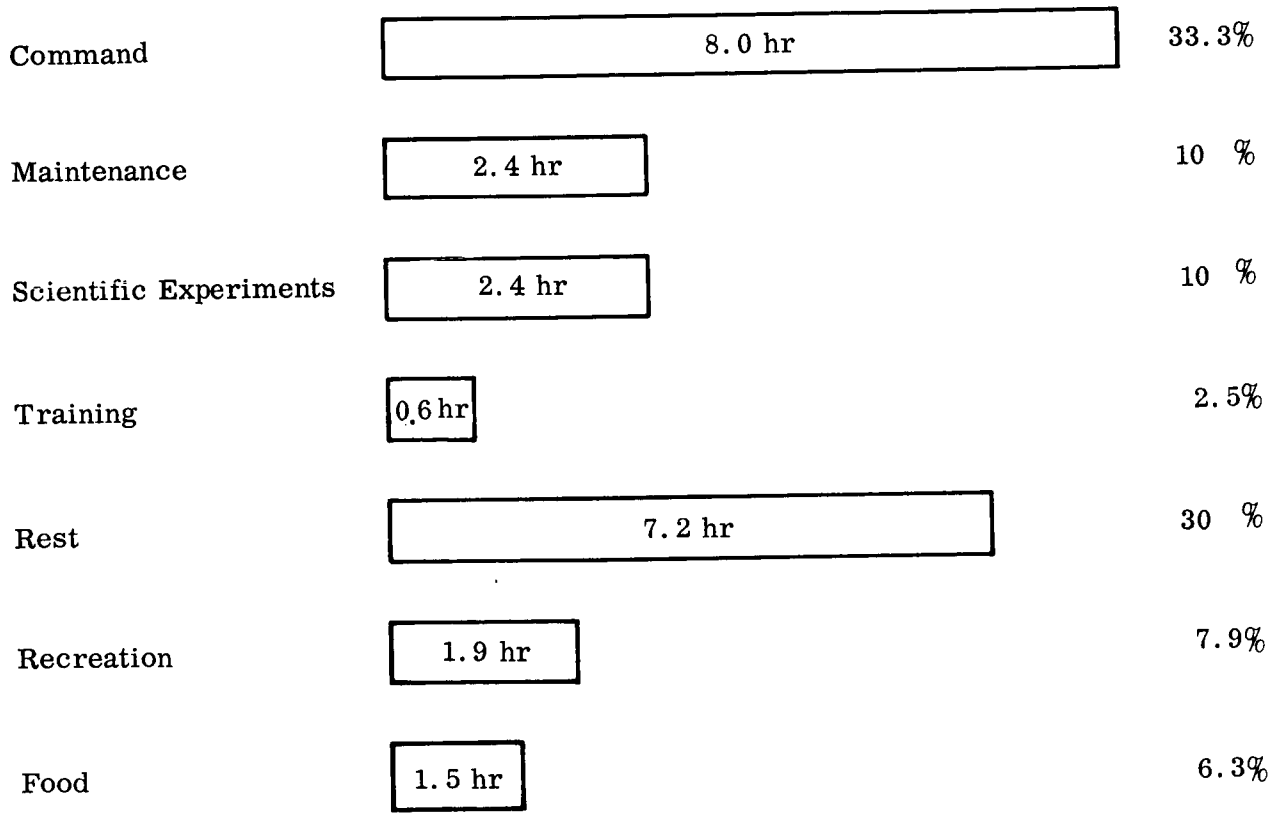


Fig. 5-2 Proportion of 24-Hour Day Spent in Various Activities by Crew Members During Outbound and Inbound Phases of Mission

5.3.3 Confinement Factors

The environment provided by the spacecraft during an interplanetary mission will differ in a number of ways from both Earth based and aircraft based system environments encountered in the past. Some of the parameters of this environment can be dealt with as physical or physiological differences, e.g., weightlessness. Other parameters can best be described as psychological in nature resulting from a summation or interaction of stress-producing physical situations. These parameters can be grouped under the heading of confinement factors.

Confinement factors can be further divided into four major classes:

- Sensory deprivation refers either to a general reduction in the quantity and variety of sensory stimuli, or to the limitation of sensory attention to a restricted field of stimuli as occurs in vigilance or watchkeeping tasks. Both types will be encountered in the spacecraft environment.
- Isolation refers not only to the physical isolation of the spacecraft crew from earth, but also to the detachment from normal behavioral contacts such as with friends and family. This isolation will be offset to some extent due to the fact that there will be a crew or group aboard the craft rather than a single individual.
- Confinement in a limited space restricts the activity pattern of the crew member and reflects the negative aspect of the group situation in that it throws the individual into continual interaction with other members of the crew to a degree not normally encountered.
- Hostile environment of space refers to the potential dangers such as radiation, meteoritic activity, and to the possibility of a malfunction of the spacecraft.

Each of these confinement factors may result in attitudes or behaviors on the part of the crew which may directly or indirectly degrade performance and jeopardize the success of the mission.

Typical attitudes and behaviors resulting from these factors are tabulated below along with suggested remedial action to offset the undesirable effects. The attitudes and behaviors listed represent possible results of the factors. However, a particular individual might manifest none, one, or a number of these behaviors.

A systematic application of the principles contained in the suggested remedial actions both during the design of the mission and equipment and during the mission itself should result in either preventing the development of the negative behaviors or minimize their effect on the success of the mission.

Physical Situation: General Sensory Deprivation

Behaviors or Attitudes: Boredom
Restlessness and Anxiety
Preoccupation with available stimuli such as food and sounds
Regressive Behavior

Remedial Actions:

1. Provide a real time communication link with the Control Center for relay of status information thus increasing the type and variety of audible stimuli.
2. Optimize the stimuli presented by the physical environment through the use of interior coloring, murals, and the elimination of offensive odors and harsh sounds.
3. Provide varied stimuli in recreational activities, e.g. movies, music
4. Include a variety of foods in the diet.
5. Organize work schedules to provide a variety of tasks for each crew member.
6. Design tasks to prevent extended periods of working with limited sensory fields.
7. Increase crew's tolerance for limited environments through adaptation. Some stresses of this type are, however, simply additive and are not relieved by adaptation.

Physical Situation: Sensory Deprivation due to Vigilance

Behaviors or Attitudes: Decreased performance
Failure to detect signals
Perceptual changes or aberrations

Remedial Actions:

1. Use simultaneous presentation of signals in two sensory modes e.g. visual/auditory.
2. Select individuals with demonstrated ability on vigilance tasks.
3. Keep two men on duty at all times for verification of any unusual perceptions.
4. Provide a high signal-to-noise ratio for signals which must be detected.
5. Increase the duration and intensity of signals to be detected.
6. Maintain an optimal temperature and noise level to prevent degradation of vigilance ability.
7. Interpolate other tasks during the period of vigilance to provide variety. These interpolated tasks should not be performed at the same time as the vigilance task.
8. Utilize pharmacological control to enhance vigilance performance during critical phases of the mission.
9. Permit maximum movement of the individual during vigilance consistent with successful task performance.
10. Incorporate immediate feedback displays of actions and status where feasible.

Physical Situation: Isolation

Behaviors or Attitudes: Heightened anxiety
Intense body activity
Depression
Increased muscular tension
Strained emotional environment

Remedial Actions:

1. Screen out emotionally immature, demanding and ego-centric individuals.
2. Utilize high intra-crew interaction during training in a restricted environment to insure group compatibility.
3. Train group members to an equally high level of technical proficiency to eliminate the possibility of group structure based on relative proficiency.
4. Structure group leadership for minimum regimentation with semiautonomous functional responsibility.
5. Train all crew members in semi-skilled and menial tasks so that all members will become personally involved in task success and appreciate relationship of task success to mission success even for menial tasks.
6. Provide cross-training in crew tasks to increase understanding and appreciation of individual functional responsibilities.

Physical Situation: Extended Confinement in Limited Space

Behaviors or Attitudes: Increased irritability
Increased interpersonal conflict and hostility
Lowered morale
Decline in motivation and work satisfaction
Increase in incidence of headaches and other illness
Decreased proficiency

Remedial Actions:

1. Select volunteers with applicable military or civilian training and a strong motivation for space exploration.
2. Select crew members with high biological efficiency and no latent body defects.
3. Provide facilities for physical exercise.
4. Design equipment and work areas to facilitate maintenance and operation in a limited space with particular emphasis on accessibility.
5. Permit each of the crew members to perform part of the voice communication with the Control Center.

6. Maintain an organized schedule of work activities to keep the crew busy on a 12 hour work day, seven day week.
7. Design the living area of the spacecraft to emphasize spaciousness.
8. Provide space in the living area for periodic privacy of individuals.

Physical Situation: Hostile Environment

Behaviors or Attitudes: Apprehension
Anxiety
Sleeping difficulties

Remedial Actions:

1. Insure safety of spacecraft through design for reliability and maintainability.
2. Indoctrinate crew in safety and reliability of spacecraft.
3. Train crew for dealing with emergency procedures e.g., abort, explosion, decompression, etc., during ground training phase of preparation for the mission.
4. Provide facilities and time for continuing emergency drills and training during the mission.
5. Develop procedures which are readily accessible to the crew for dealing with all hazardous situations.
6. Provide expert verbal assistance from the Control Center via the communication link for diagnosing and dealing with unusual or hazardous situations.

5.3.4 Human Engineering Areas for Further Study

Function and Task Analysis. The review of the functions analysis performed during the present study phase with emphasis on the allocation of functions between man and machine based on available experimental and study data on man's capabilities within a spacecraft environment.

Based on the revised functional listing and allocation, the derivation of task requirements for the crew. Although task analysis is a relatively standardized procedure, the present situation has two rather unique features. First, task analytic procedures must be applied to all of the activities of the crew including eating, resting and recreation as well as the work duties. Second, certain tasks, primarily associated with vehicle control, may have to be performed under varying conditions of gravity and acceleration. This means that tasks must be designed that can be performed under varying environmental conditions.

The determination of the impact of various types and levels of malfunction and emergency conditions, that may occur during the mission, upon task requirements and equipment design. This analysis will result in the generation of additional task requirements, such as those associated with solar flares, as well as introduce constraints and modifications on task requirements previously derived.

Cabin Design. Preliminary cabin design considerations and general equipment requirements should be developed based on the following considerations and constraints:

- Task requirements particularly during emergency conditions.
- Environmental constraints imposed directly by the space environment or by the proposed methods for controlling the environment for life support.
- Minimization of the effect of psychological stresses imposed on the crew by the mission environment through design for habitability.

Selection and Training for Long-Term Confinement. The primary problem in this area is the fact that there is really no training or adaptation program possible for the preparation of a space crew to meet the stresses of long-term confinement. This is due to the cumulative nature of such stresses which means that a period of isolation training immediately preceding an actual mission would probably result in a decrease of tolerance to isolation rather than an increased resistance. This situation places the burden of the problem on selection techniques or methods of control of confinement stress effects. The selection of highly motivated men, the maintenance and deepening

of this motivation, will be of great importance to the success of the mission. Further study in this general area should include the following:

- Determination of the tolerance limits for man to long-term confinement. Up to the present time, confinement studies have been limited to one or two weeks in duration with a few extending the period of confinement to a month. Further experimentation is required in this area as well as a systematic review of the experimental and experiential literature.
- Development of predictor techniques for resistance to the stresses of long-term confinement. This would include the identification of personality correlates of confinement tolerance and the exploration of the efficacy of reaction to intense short-term isolation as a predictor of performance under longer time periods of less intense isolation.
- Investigation of adaptation training for the other parameters of the mission environment to develop techniques and regimes for training to meet these other stresses and thus minimize the summation effect of these stresses in combination with confinement stresses.
- Exploration of pharmacological, hypnotic, and conditioned-response techniques as potential methods for controlling the effects of confinement before and during the mission.

5.5 ATMOSPHERE SELECTION AND GAS SUPPLY

5.5.1 Atmosphere Selection

Ideally, the atmosphere selected should:

- Produce minimum physiological stress
- Minimize the danger of decompression sickness
- Maximize the time for action after a puncture
- Minimize fire and meteorite hazards
- Minimize the thermal control problem
- Minimize leakage losses and structure stress
- Simplify the pressure control system

Since no known atmosphere simultaneously does more than two or three of the above, trade-offs are necessary. The known facts under each of the above are marshalled, limiting ranges are determined, effects on total mass noted, and recommendations made.

Minimum Physiological Stress. The ultimate necessity for oxygen is the cells' need to carry on oxidative metabolism. This need is a function partly of the involuntary housekeeping functions of the body, partly of the level of voluntary muscular activity, and partly of diet.

Assuming normal respiration and normal functioning of the oxygen transport system, the body's need for oxygen can be expressed as a requirement for a certain partial pressure of oxygen in the alveoli, i.e., in that part of the lungs containing gases effectively in equilibrium with the arterial blood.

The alveolar partial pressure of oxygen $P_{A_{O_2}}$ is a function, not only of the partial pressure of oxygen in the external environment, but of the total pressure of the external environmental P_b, the respiratory quotient R, and the alveolar partial pressure of carbon dioxide $P_{A_{CO_2}}$. The relationship is the following (Ref. 5-1, p. 804):

$$P_{A_{O_2}} = F_{I_{O_2}}\left(P_b - P_{A_{H_2O}}\right) - P_{A_{CO_2}}\left[F_{I_{O_2}} + \frac{\left(1 - F_{I_{O_2}}\right)}{R}\right] \text{ (torr)}^* \quad (5.1)$$

Where: $F_{I_{O_2}}$ = fractional concentration in inspired dry gas and $P_{A_{H_2O}}$ = 47 torr = the vapor pressure of water at normal body temperature.

Equation (5.1) is an approximation based on the assumption that $P_{I_{CO_2}}$ (partial pressure of carbon dioxide in inspired air) is small relative to $P_{A_{CO_2}}$.

*All pressures in torr.

R is the volume ratio of carbon dioxide produced to oxygen consumed. For a person neither gaining nor losing weight, the steady state R is a function only of the percent of proteins, fats, and carbohydrates in the diet. Most healthy adults in the United States have a respiration quotient between 0.80 and 0.85.

$P_{A_{CO_2}}$ is about 39 torr for adults at sea level. Equation (5.1) is frequently used to determine "physiologically equivalent atmospheres" by assuming R is about 0.82, $P_{A_{CO_2}}$ is about 39 torr, and plotting P_b vs $F_{I_{O_2}}$ for some desired value of $P_{A_{O_2}}$. A family of such curves is plotted in Fig. 5-3. A similar family of curves assuming $P_{A_{CO_2}}$ is 30 torr is plotted in Fig. 5-4. For both curves the vapor pressure of water in the external environment is assumed to be 10 torr.

A $P_{A_{CO_2}}$ of 30 torr is typical of an acclimatized person living at an altitude of 15,000 ft (Ref. 5-2, p. 357). Values of $P_{A_{CO_2}}$ below 25 torr have been observed in trained subjects breathing air at 321 torr (22,000 ft.) for an hour. (Ref. 5-3, p. 152–53). It is doubtful that one would want to presuppose a $P_{A_{CO_2}}$ of less than 30 torr for continuous exposure during a space mission.

In the case of a sudden exposure to hypoxic conditions, R rises to values over 1.0 and $P_{A_{CO_2}}$ falls to values as low as 20, depending on the exposure. Both changes are results of hyperventilation (increased rate and/or volume of respiration) and tend to maintain a higher $P_{A_{O_2}}$. After 45 minutes to an hour at reduced pressure, R returns to its steady state value; $P_{A_{CO_2}}$ continues to fall slowly for several days (Ref. 5-5, pp. 25, 26). Figure 5-5 shows the variation between acclimatized and unacclimatized individuals with R = 0.85. Acute refers to values taken immediately after stabilization of R at the steady state value.

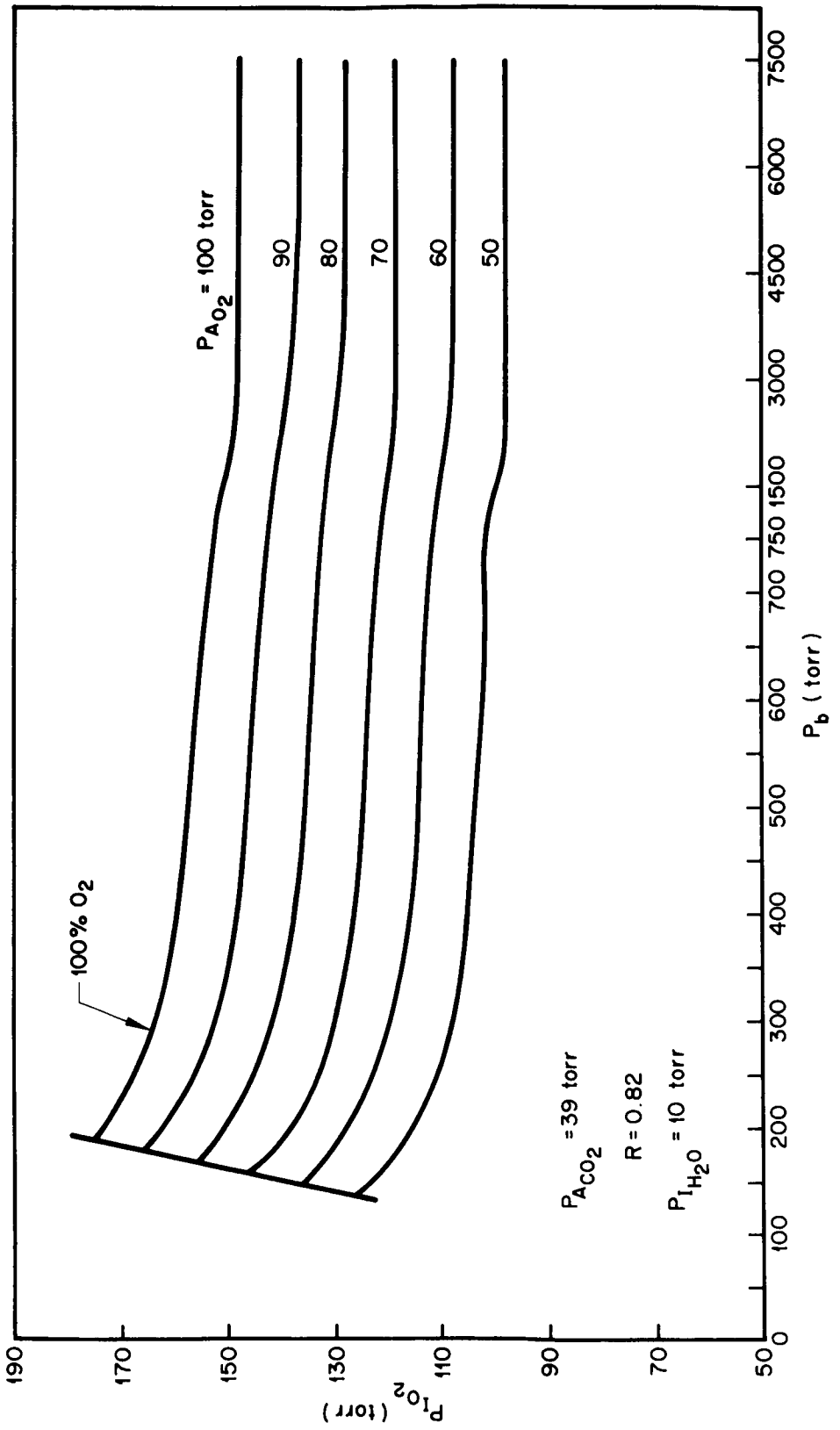


Fig. 5-3 Partial Pressure of Oxygen Required to Provide Various $P_{A_{O_2}}$'s As A Function of Barometric Pressure (P_b)

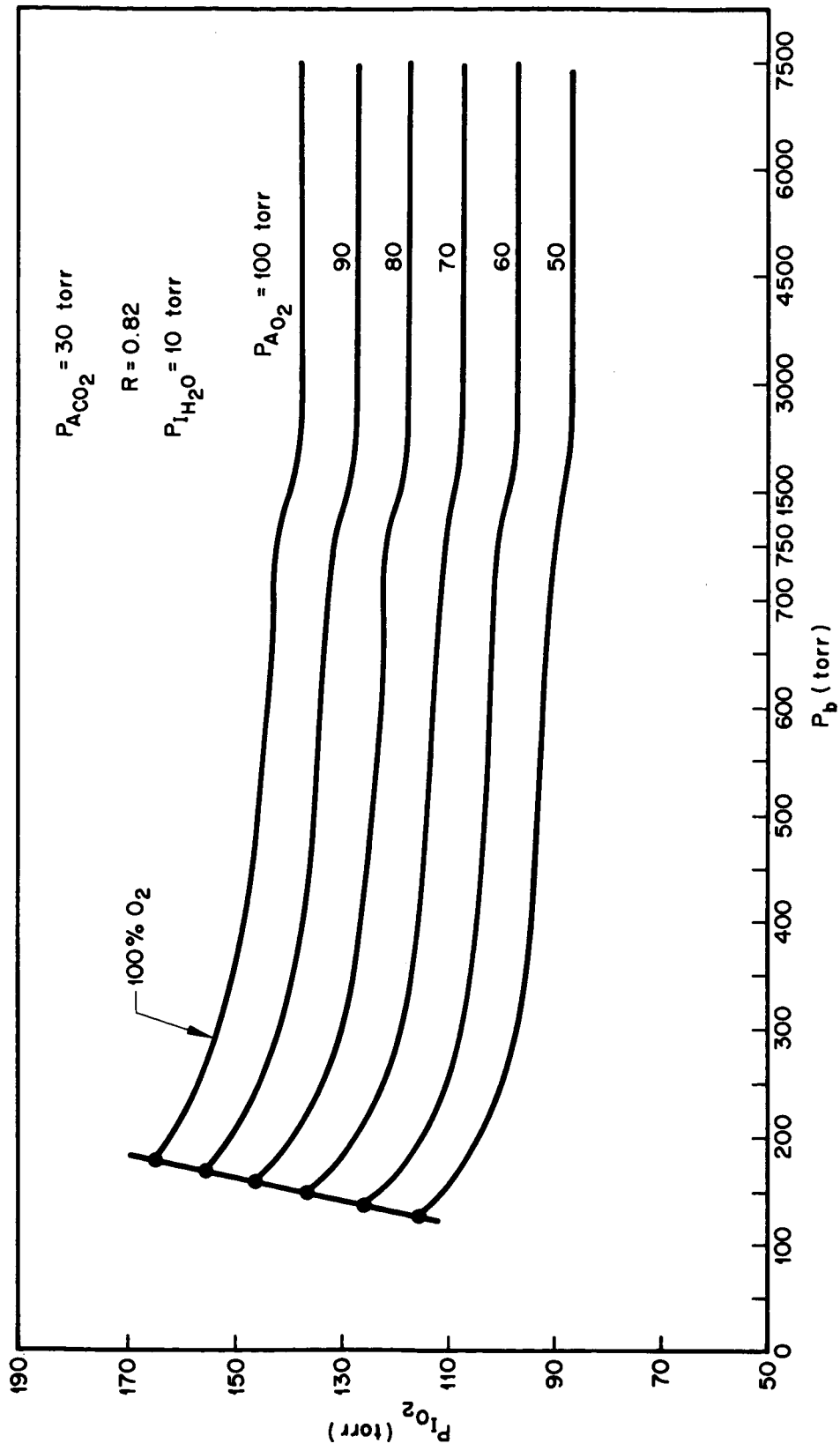


Fig. 5-4 Partial Pressure of Oxygen Required to Provide Various P_{AO_2}'s As A Function of Barometric Pressure (P_b)

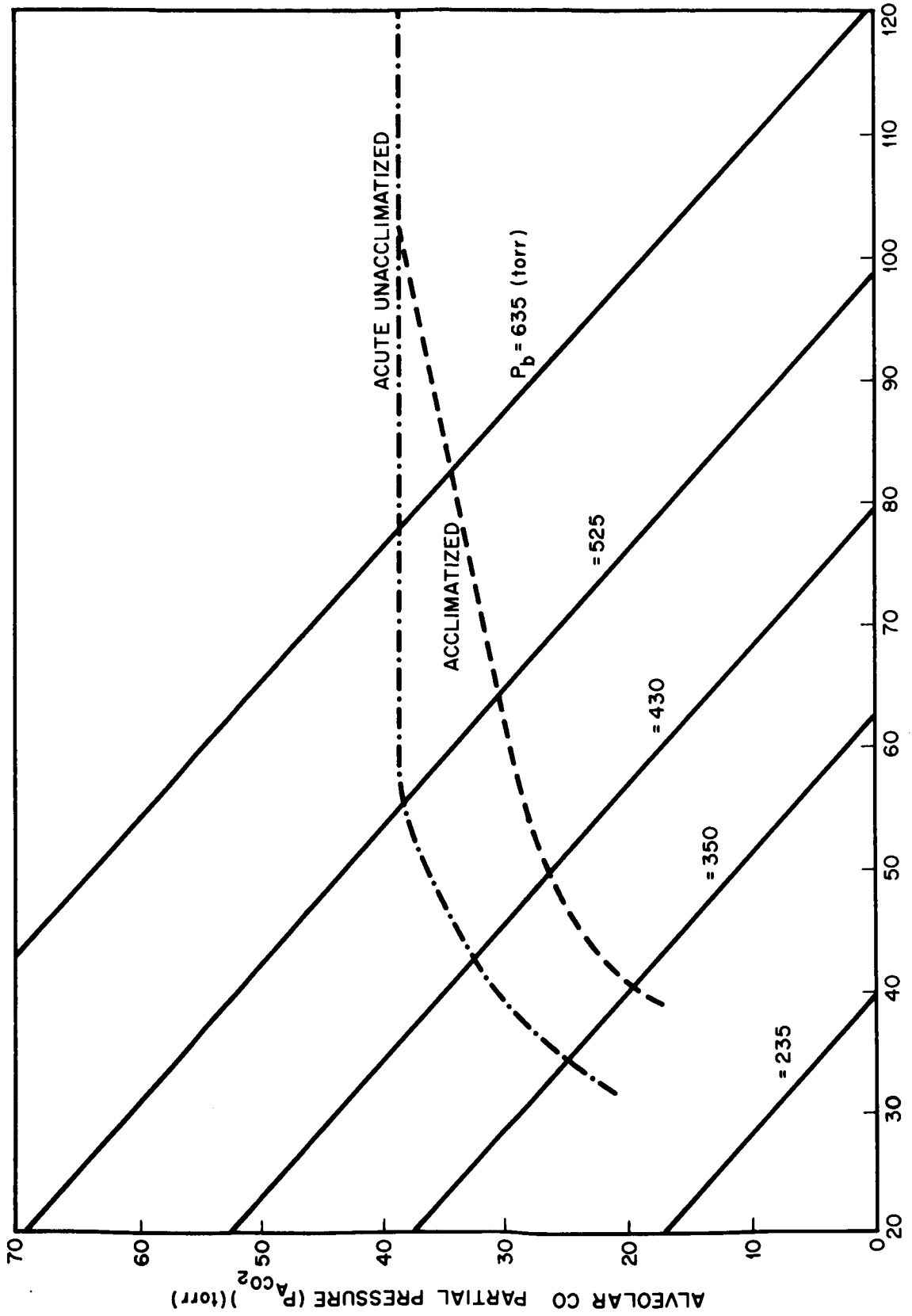


Fig. 5-5 Alveolar Gas Pressures At Various Altitudes (Air Pressure) For Acute Exposure and After Acclimatization

Acclimatization is a complex process involving changes, not only in ventilation rates, but in oxygen dissociation curves, hemoglobin count, pH, and, possibly, basic tissue structure and chemistry (Ref. 5-2). While some of these adaptations take place in minutes, others require weeks. It is possible, indeed probable, that some of the adaptations found in those living their entire lives at elevated altitudes are genetically transmitted and a lifetime would not suffice to induce them in sea level dwelling races.

It has been shown that 6 weeks of altitude plus exercise enables one:

- To be free from hypoxia even while working hard at a $P_{A_{O_2}}$ of 50 torr and less
- To resist decompression sickness much more successfully
- To increase the time to unconsciousness after a decompression from 2 to 30 minutes at 230 torr (air) and from 30 to 90 sec at 140 torr (air). (Ref. 5-5, p. 46)

These advantages are lost in a few weeks unless maintained by breathing low oxygen mixtures for at least an hour per day. (Ref. 5-6, p. 139; Ref. 5-7, p. 160).

Training in deliberate hyperventilation has also been suggested for space crews (Ref. 5-8, p. 4) to avoid the symptoms of hypocapnia usually brought about in untrained subjects by emotional stress or physical stress not associated with hypoxia.

Table 5-3 (Ref. 5-9, p. 192) illustrates physiologic limitations associated with several altitudes. Associated alveolar oxygen pressures are shown to facilitate comparisons with non-air atmospheres where applicable. Decompression sickness limits assume prior breathing of air at sea level.

In addition to the basic physiological requirements for an artificial atmosphere already mentioned, there are a number of other important physiological effects consequent to the use of various artificial environments.

Table 5-3

THRESHOLD ALTITUDES AND PHYSIOLOGIC LIMITS
FOR UNACCLIMATIZED INDIVIDUALS

Altitude	Ambient Pressure (TORR)	*$P_{A_{O_2}}$ (TORR)	Physiologic Limitations
8,000 ft 2.43 km	565 (Air)	65	Max. altitude for prolonged flights without undue fatigue from mild hypoxia
10,000 ft 3.08 km	523 (Air)	57	Max. altitude without supplemental oxygen. The physiologic adjustments mainly respiratory and circulatory, are adequate to compensate for effects of hypoxia. Additional environmental stress or physical exertion may produce decompensation
15,000 ft 4.61 km	427 (Air)	42	The compensatory mechanisms become inadequate, and physical and mental reserves are minimal
20,000 ft 6.16 km	350 (Air)	34	There is mental and physical incapacitation leading to loss of comprehension and posture, convulsions, cessation of respiration and finally cessation of circulation
23,000 ft 7.08 km	308 (Air)		Threshold for occasional symptoms of decompression sickness
25,000 ft 7.69 km	287 (Air)		Threshold for occasional severe manifestations of decompression sickness
30,000 ft 9.22 km	226 (Air)		Critical threshold for high-incidence of decompression sickness
40,000 ft 12.32 km	140 (0_2)	55	Max. altitude breathing pure 0_2 without additional pressure
45,000 ft . 13.85 km	110 (0_2)		Max. altitude for reasonably prolonged emergency pressure breathing of pure 0_2
50,000 ft 15.38 km	87 (0_2)		Max. altitude for brief emergency pressure breathing of pure 0_2 with immediate descent
65,000 ft 20.00 km	54		Body fluids boil

*$P_{A_{O_2}}$ = Alveolar oxygen partial pressure

A $P_{I_{O_2}}$ in excess of 425 torr produces definite toxic affects. Nitrogen and some other proposed diluents have a narcotic effect over 4 or 5 atmospheres (Ref. 5-10). Some indications of atelectasis due to breathing pure oxygen atmospheres are in the literature but this was not noted in the recent School of Aviation Medicine tests (Ref. 5-11) of pure oxygen at 176 torr.* During those tests, however, drying of the upper respiratory passages, a temporary lowering of vital capacity, considerable ear pressure adjustment, and voice alterations were noted.

Such voice alterations are characteristic of any artificial atmosphere. An idea of the relative magnitude of this effect is shown below (Ref. 5-12).

ATMOSPHERE (Torr)			RELATIVE PITCH AIR = 1
$P_{I_{O_2}}$	P_I Diluent	P_b	
167	593 (N_2)	760	1.00
198	370 (N_2)	568	0.98
198	138 (He)	336	1.22
198	370 (He)	568	1.50
258	–	258	0.95
568	–	568	0.95
198	370 (Ne)	568	1.15

The higher thermal conductivities of He and Ne have been said to make people feel colder under otherwise similar thermal conditions than mixtures of O_2 and N_2 of comparable pressures. This could, presumably, be adjusted by variations in wall and gas temperatures, humidity, and ventilation rates. References 5-13 and 5-14 discuss basic respiration in some detail. Reference 5-15 defines the nomenclature of respiration physiology.

*Atelectasis might be more likely, however, under acceleration stress.

Minimizing the Decompression Sickness Danger. When the ambient air pressure is reduced quickly enough and drastically enough from a higher level at which the body has been equilibrated, gas bubbles form in the bloodstream and in the tissues. The resulting syndrome has been called caison disease, compressed air illness, aeroembolism, dysbarism, and decompression sickness. The various names reflect occupation with various conditions of origin and/or symptoms. Decompression sickness will be used throughout this work. The symptoms include diffuse pain in the extremities and chest, itching of skin, and, in severe cases, nausea, paralysis, convulsions, and coma. In the case of very rapid decompression to pressures below 50 torr (63,000 ft), a one minute exposure would be fatal (Ref. 5-9).

Table 5-3 illustrated the decompression sickness symptoms usually associated with several altitudes for unacclimatized men breathing air. Some advantages of acclimatization were indicated. It should be stressed that this table refers only to relatively sudden exposures to the new altitude after breathing air at sea level. The symptoms can be reduced or eliminated by prebreathing gas of lower nitrogen partial pressure and the same total pressure, or gas of both lower nitrogen partial pressure and lower total pressure. Decompression sickness can also be prevented by changing from the higher to the lower pressure gradually by stages, e.g., no symptoms occur if the pressure is reduced from sea level to 47,000 ft in about 10 hours by continuous, and 5 hours by stage decompression. (Ref. 5-16, p. 184.)

Decompression sickness can also be somewhat alleviated by substituting another inert gas for nitrogen, i.e., one which has lower solubility in the tissues and/or a higher diffusion rate. Helium and Neon are such. Argon is somewhat and Xenon and Krypton much worse than Nitrogen with respect to bubble formation.

Figure 5-6 shows the time of useful consciousness following sudden decompression to various altitudes (Ref. 5-6). The times for air and oxygen converge above 15 km to about 15 sec. It is interesting to note that, for exposure to altitudes about 15 km, even when breathing pure O_2, loss of consciousness is unavoidable if the exposure time before recompression exceeds 5 to 6 sec (Ref. 5-9). Recovery is, however, more rapid breathing high oxygen partial pressure mixtures.

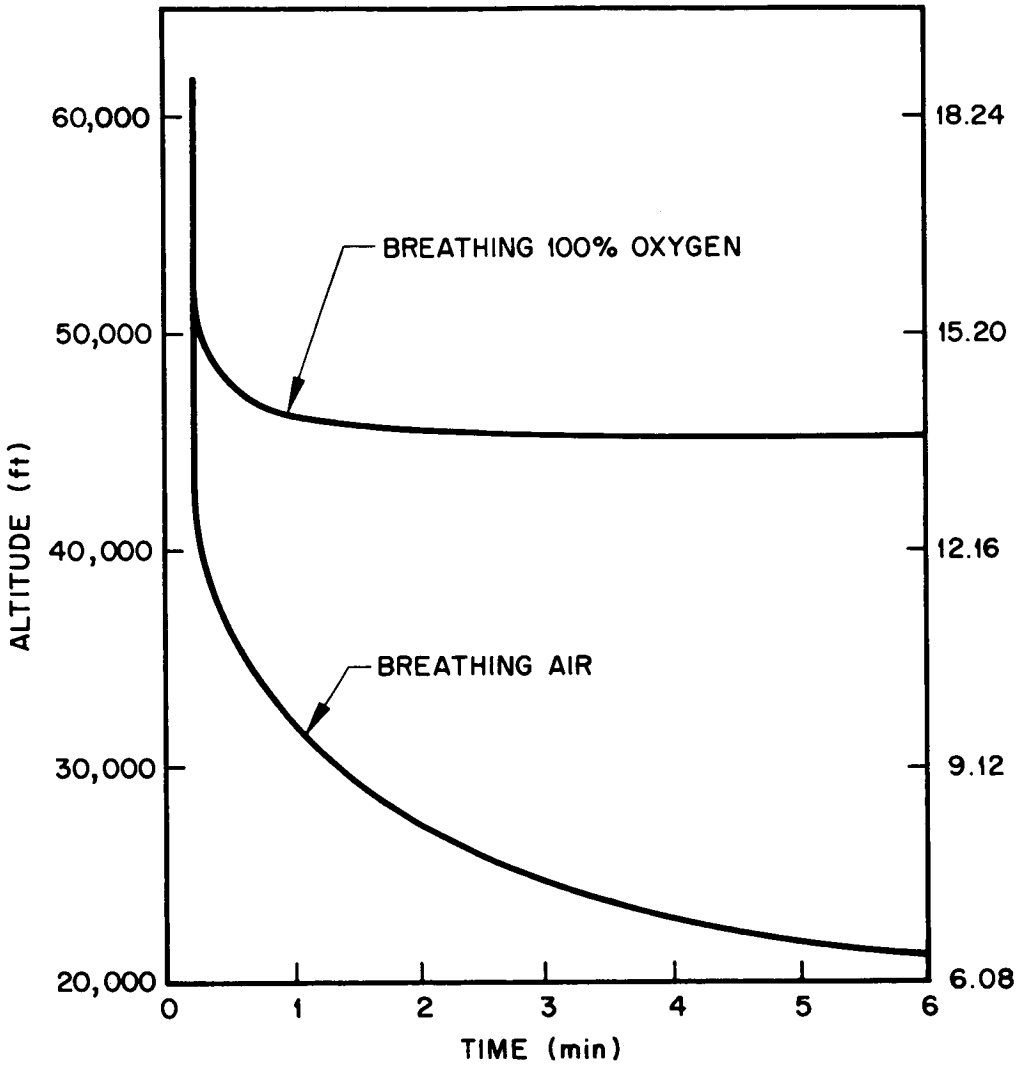


Fig. 5-6 Time of Useful Consciousness After Sudden Decompression Breathing Air (540 Torr) and Oxygen (200 Torr)

Although, as mentioned, a very slow decompression will prevent decompression sickness, Ref. 5-16 (p. 181) indicates no "significant effect on the incidence of serious symptoms" for rates of ascent varying from 150 to 1200 meters per minutes. This corresponds roughly to 10 to 80 torr per minute. This range of values should be kept in mind when referring to Figs. 5-7 and 5-8.

Figure 5-7 (Ref. 5-17) shows cabin leakage as a linear function of leakage area for four different atmospheres. For these curves, it is assumed that delivery of gas is sufficient to maintain cabin pressure at the original values. Under such circumstances the mass flows are approximately proportional to the first power of the pressure and the inverse 1/2 power of the molecular weight of the gas. Figure 5-7 shows that the mass flow for atmospheres of equal mole fractions of oxygen and nitrogen is about 4/3 that of atmospheres of equal mole fractions of oxygen and helium for the same total pressure.

These leakage rates could be extended to normal leakage from the vehicle for holes down to the order of magnitude of the molecular diameter of the gas molecules. At that point, van der Waals forces become important. If leakage is, in fact, mostly from molecular diffusion through the walls, leakage will not be a serious problem.

Figure 5-8 shows the decay of cabin pressure with time for the same 4 atmospheres under the assumption that the gas supply is turned off immediately when the decompression starts. Alternatively, it could be considered to apply after exhaustion of the gas supply.

One could combine Figs. 5-7 and 5-8 in the following manner. From Fig. 5-7 one could determine how long available gas stores could maintain pressure; from Fig. 5-8 one could then see how much additional time would be available for action.

The horizontal arrows in Fig. 5-8 point to the ambient pressure at which the alveolar oxygen pressure ($P_{A_{O_2}}$) equals about 30 torr. The vertical arrows point to the ambient pressure at which symptoms of decompression sickness could be expected.

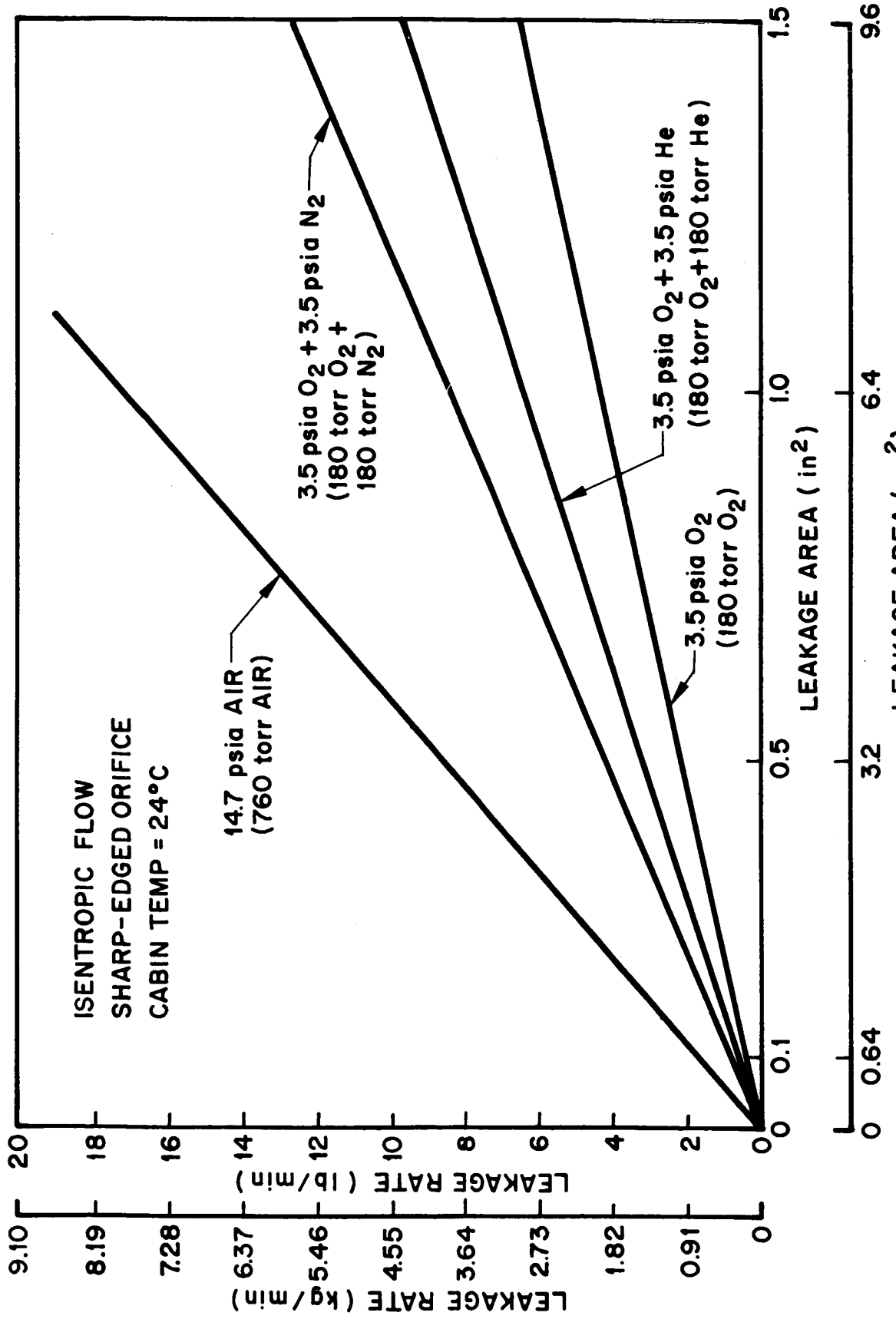


Fig. 5-7 Leakage Rate as a Function of Leakage Area for Isothermal Flow

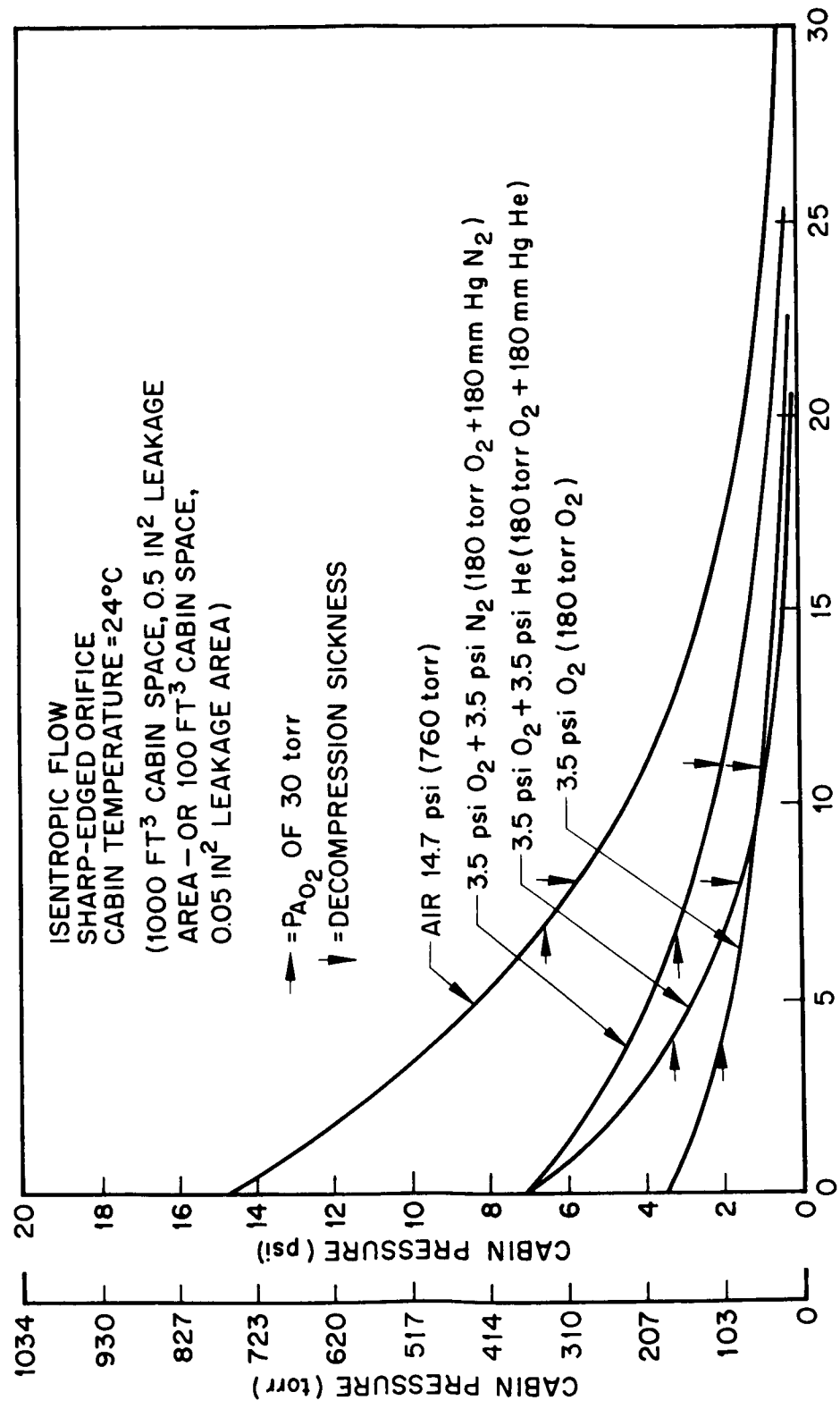


Fig. 5-8 Cabin Pressure Decay Vs Time

Thirty torr is the level at which loss of consciousness is imminent for the "normal unacclimatized man" (Ref. 5-8). The vertical arrows point to the pressure (for the nitrogen and helium mixtures) at which about 50 percent of unacclimatized subjects would have some decompression sickness symptoms. The latter point is subject to considerable variation by age, obesity, physical fitness, and experience and is modified by concurrent exercise and hypoxia. For the pure oxygen atmosphere, decompression sickness would probably occur very little before blood boiling.

Generally, it has been found that decompression sickness symptoms first appear (below one atmosphere) when the ratio of initial pressure to new pressure is about 2.25, regardless of the absolute values of the pressure involved, for air mixtures. Because of the greater mechanical pressure exerted by the higher pressure of the denser bubble upon the elastic restraining forces of the body and the greater amount of gas absorbed in the tissues, symptoms are, in fact, more severe with diving-type than with flying-type decompressions of the same pressure ratio. (Ref. 5-16.)

Figure 5-8 shows that the decompression sickness point comes later than the hypoxia point for all four atmospheres. One could conceive, however, of a mode of temporary emergency action involving the use of an oxygen mask rather than a full pressure suit in which time to reach the minimum ambient pressure for pressure breathing (87 torr) or to reach the pressure at which body fluids boil (47 torr) would be significant.

One of the most important considerations for emergency decompressions does not show up in Fig. 5-8; that is, the problem of abruptly donning a full pressure suit and going from cabin pressure to suit pressure. For purposes of reliability, the suit atmosphere will probably be pure O_2. For purposes of mobility, it will have the lowest possible pressure commensurate with physiological requirements. Assuming suit pressure to be at most 180 torr, it would be impossible to have the cabin pressure over 400 torr (if air) without risking decompressing sickness upon abrupt change to suit pressure. The cabin pressure could be somewhat greater than 400 torr if the nitrogen fraction were reduced or eliminated.

Minimizing the Fire and Meteorite Hazards. In addition to affecting the decompression time after a meteorite penetration, there is some interest in the choice of atmosphere with respect to other meteoritic phenomena. If there is combustion of the meteorite, the combustion will tend to be more complete for higher partial pressures of oxygen for a fixed total pressure and for lower total pressures for a fixed partial pressure of oxygen. The higher the total pressure, the greater the molecular weight and the higher the specific heat of atmospheric gases, the lower will be the temperature rise from a given heat input.

These considerations are marginal. In spite of the fact that at least one experimenter has succeeded in cooking rats in a small enclosure by firing particles into the enclosure at meteorite-like velocities, the total kinetic energy plus energy of combustion of a one gram meteorite (probability of less than 10^{-4} of hitting a 5000 ft^2 cabin in 360 days by Whipple's 1962 distribution) moving at a typical velocity would only raise the temperature of a 1000 ft^3 cabin some 7 degrees C. A smaller cabin and/or the induced burning of other cabin materials could, however, increase the problem.

Further tests need to be made on flammability characteristics of different atmospheres. The problem is complex. Reference 5-18 reports that helium showed little advantage over nitrogen as a diluent. They reach this judgment on the basis of "approximately equal burning rates." Reference 5-19 (p. 355) points out, however, that the data from Ref. 5-18 shows that for 160 torr O_2, about 700 torr N_2 was required to prevent combustion and only 400 torr He; also for a total pressure of 600 torr, the maximum allowable P_{O_2} which would avoid combustion was about 104 torr with N_2 as the diluent and about 218 torr with He. Some theoretical analyses indicate that helium's advantage over nitrogen will be much less in the absence of natural connection.

Reference 5-18 also points out that spontaneous ignition temperatures tend to be higher with pure oxygen atmospheres than with the same P_{O_2} plus diluent, but that a fire once started in the pure oxygen atmosphere burns more vigorously and at a higher temperature.

Generally, atmospheres with low oxygen content moderate the severity of a fire once it starts and in some cases reduce the likelihood of a fire starting. Atmospheres which conduct heat rapidly away from a "hot spot" reduce the likelihood of a fire starting but aid the spread of a fire more than atmospheres with low thermal conductivity. The presence of natural and/or forced convection modifies the problem.

Minimizing Leakage Losses and Structural Stress. Leakage rates are difficult to predict. Very little testing has been done on leakage rates from space cabins exposed to launch vibrations, thermal cycling, vacuum degradation of seals and seal lubricants, and other space stresses for a one to two year mission. In the absence of definitive data, a certain conservatism is requisite.

On the basis of experience at LMSC and elsewhere, a reasonable design objective for an interplanetary vehicle of about 5×10^6 cm^2 surface area seems to be about 2.5×10^{-10} cm^2 of effective leakage area per cm^2 of surface area. Actually, the amount of effective leakage area is not a function of surface area alone but a function of the number and types of seals and joints. Applying this factor to an assumed pressurized area of 5×10^6 cm^2 gives a leakage area of 1.25×10^{-3} cm^2. Using this leakage area and the appropriate mass flows from Fig. 5-7, Fig. 5-9 is constructed.

The leakage shown in Fig. 5-9 assumes a constant leakage rate. In fact, it is expected that initial leakage rates would be lowest and that leakage rates would increase with time. Predictions of the exact variation of leakage rates with time do not seem possible at present.

It is possible to compute the amount of structure necessary to withstand the pressure differential between cabin and space for various atmospheres. This consideration alone would, of course, urge the selection of the lowest possible cabin pressure. If this consideration were, in fact, the chief one in determining structure weight, it would deserve considerable attention. For applications of this type, however, the resistance of launch and re-entry stresses, elastic deformations, internal mechanical

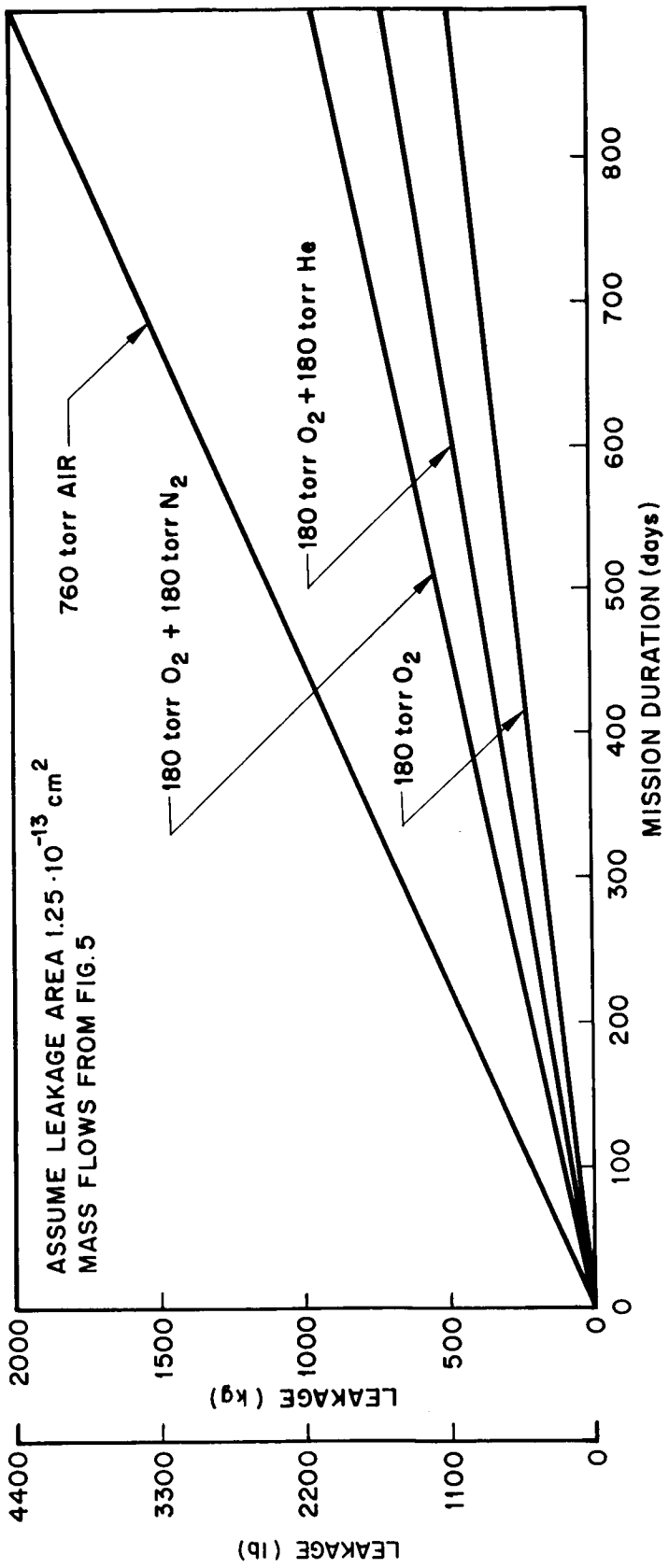


Fig. 5-9 Total Mission Leakage Vs Mission Duration

stresses, and meteorite puncture will require a structure greatly in excess of that dictated by the pressure differential alone. When operations upon the surface of Venus (5 – 10 earth atmospheres) are contemplated, structure mass will indeed be a strong function of internal pressure.

Minimizing the Thermal Control Problem. One of the most important problems in space flight is the elimination of heat generated within the vehicle by crew and equipment. Various methods are possible for conveying the heat from the interior to the outer surface for radiation to space. Most methods rely upon initial removal of heat from crew and equipment by the atmosphere. The pressure and composition of the atmosphere determine the volume and mass flows and the consequent fan power necessary to do the job..

For a given geometry, and constant mass flow, the blower power required is roughly proportional to the inverse square power of the density. Optimization of the geometry and flow rates can sometimes reduce the dependence to the inverse 1.5 or 1.6 power. The approximate variation in power requirements for a fixed geometry is shown in Table 5-4 Two weight penalties more or less bracketing the range considered in the study, i.e., 23 kg/kw for solar-thermionic and 46 kg/kw for nuclear A.P.U's are shown.

Table 5-4

EFFECT OF ATMOSPHERE ON BLOWER POWER

Atmosphere	Blower Power (w)	Weight Penalty (kg) @ 23 kg/kw	Weight Penalty (kg) @ 46 kw/kw
Sea Level Air	400	9.2	18.4
180 Torr O_2 + 180 Torr N_2	1600	36.8	73.6
180 Torr O_2 + 180 Torr He	4400	101.2	202.4
180 Torr O_2	6400	147.2	294.4

The weight differences look insignificant when compared with, e.g., radiation shielding weight, but reducing the power requirements tends to increase the reliability of the system much more than saving an equivalent weight in solid metal.

Simplifying the Pressure Control System. It is much easier to control the total pressure inside a spacecraft than to control the partial pressure of one gas in a multi-gas system. This fact alone may be important enough to cause early brief missions to turn to single gas atmospheres.

Progress in the development of partial pressure sensors has been rapid, however, in the last two years. One person working in the field (Ref. 5-20) predicts a probability of failure of present partial pressure control hardware (partial pressure sensor and associated servomechanisms) of 0.23 for a one year mission and 0.41 for a two year mission. The same observer stresses the importance of "...statistically oriented exploratory testing under extremes of single and combined environmental and functional stresses."

Repair capability would, of course, effectively lower the above probabilities of failure. It seems reasonable to expect considerable improvement in partial pressure sensor systems by the late 1960's.

Summary. One of the most important items determining the choice of atmosphere is the necessity of keeping the suit pressure down to promote mobility. The people working in this area seem to believe this will continue to be of great importance for a number of years. Assuming this to be the case, 180 torr of O_2 is selected as the nominal suit pressure to provide a $P_{A_{O_2}}$ of 100 torr.

It is further assumed that, to avoid decompression sickness, the primary (cabin) pressure should not exceed 360 torr if it contains substantial nitrogen. The 180 torr O_2 + 180 torr N_2 is finally selected over lower pressures to maximize time for action and minimize fire and explosion hazards, and minimize fan power. Helium is neglected

because its known advantages do not seem to outweigh its known disadvantages and its long term physiologic effects are still unknown. If we are ever to operate under conditions such as those previously mentioned as obtaining on the surface of Venus (5 – 10 earth atmospheres), helium may well be the only choice. There is abundant evidence of the success of this technique in deep sea diving.

Although a $P_{A_{O_2}}$ of 100 torr is recommended, a more or less full acclimatization to altitude for the crew is urged to take advantage of reserves thereby built up against hypoxia and decompression sickness. To retain the acclimatization it would be necessary to spend some time each day at lower pressures. The increased trouble and possibly even danger involved in doing this while in flight might out-weigh the advantages, but this should not be assumed summarily.

More experimentation is needed to establish the effect of sudden decompression from an atmosphere such as that recommended for the space cabin of 180 torr O_2 and 180 torr N_2 to that recommended for the space suit of 180 torr O_2. The two factors generally considered responsible for decompression sickness, the difference in partial pressure of nitrogen between the initial and final atmospheres and the ratio of initial and final total pressures, which determines bubble size, both seem to be well under the values for, e.g., the well documented type of decompression from 160 torr O_2 plus 600 torr N_2 to 60 torr O_2 plus 240 torr N_2. Our knowledge of the etiology of this malady is not, however, complete enough to justify complete confidence in such an analogy.

5.4.2 Gas Supply

The density of the atmosphere selected, at 75°F (24°C) is 0.0366 lb/ft^3 (5.85×10^{-4} gm/cm^3). The metabolic oxygen requirement is assumed equal to 825 gm/day per man. The total gas requirements for the two typical missions are summarized on this basis in Table 5-5.

Table 5-5

GAS REQUIREMENTS (WITHOUT CONTAINERS) (kg)

	3 Men – 365 Days			3 Men – 600 Days		
	N_2	O_2	Total	N_2	O_2	Total
Initial pressurization	33	37	70	33	37	70
Leakage and lock losses	196	224	420	327	373	700
Emergency pressurization	165	185	350	264	296	560
Emergency metabolic oxygen	–	50	50	–	50	50
Normal metabolic oxygen*	–	900	900	–	1480	1480
TOTAL	394	1396	1790	624	2236	2860

*

The initial pressurization will be done on the ground presumably and will require no containers. The emergency pressurization and emergency metabolic supply and nitrogen leakage requirement will be presumed to be stored under liquid cryogenic conditions.

At the above leakage rates it will be possible to keep boil-off well below leakage requirements. Normal metabolic oxygen and part of the oxygen leakage requirement will be met by the regeneration of metabolic wastes. Table 5-6 shows the weights of gas plus containers plus valves, tubes, etc., including extra components. (Refs. 5-21, 5-22, 5-23, and 5-24.)

Table 5-6

GAS SUPPLY SYSTEM WEIGHTS (kg)

	3 Men – 365 Days			3 Men – 600 Days		
	N_2	O_2	Total	N_2	O_2	Total
Semi-closed system	580	650	1230	870	980	1850
Open system	580	1750	2330	870	2800	3670

Open system totals assume all gas of Table 5-5 (except initial pressurization) stored by the liquid cryogenic method. The above totals for the semi-closed system do not include the weight of the regenerative equipment. This equipment recovers both oxygen and water and is considered separately under "Physico-chemical Regeneration."

5.5 CARBON DIOXIDE REMOVAL

5.5.1 Requirements

In his review of the subject of carbon dioxide toxicity (Ref. 5-25), Schaefer defines three levels of carbon dioxide concentration with respect to the effects upon the human body:

22.8 torr and above	–	Performance deterioration and alteration in basic physiologic functions
3.8 torr to 22.8 torr	–	No change in performance or basic physiologic functions, but some adaptation over a length of time
Less than 3.8 torr	–	No adaptation observed

The determining experiments did not last longer than 60 days. Since it is assumed that interplanetary missions last 300–700 days, it is felt that a carbon dioxide level well below 3.8 torr should be maintained throughout the trip.

The amount of carbon dioxide presumed (see Section 5.9) produced is 1.01 kg per man per day. For three men this is 1106 kg for 365 days and 1818 kg for 600 days.

5.5.2 System Selection

The 1106 kg and 1818 kg just calculated contain about 800 kg and 1320 kg of chemically bound oxygen respectively. Assuming that throwing away this material necessitates carrying an equal amount of cryogenically stored oxygen (a reasonable assumption considering expected leakage rates), the total effect is to add about 1000 kg and 1650 kg to the 365 day and 600 day missions respectively.

In order to be profitable, carbon dioxide removal-plus-reduction equipment including spare components, delivery, storage equipment, and power penalty must not exceed the above values by more than the weight penalty for simply removing carbon dioxide from the atmosphere and dumping or storing it.

At this time it is very difficult to say how many spare components must be carried to ensure the achievement of a specific reliability for a carbon dioxide reduction device. The high temperatures required of most methods also create a substantial hazard. Incidental heat produced must be removed by the thermal control system.

AiResearch, Hamilton Standard, and American Machine and Foundry all are optimistic about their ability to produce flight qualified carbon dioxide reduction systems within two years from the inception of a major effort. At this time it seems possible to cautiously assume such systems will be available by the time of the earliest manned interplanetary missions. This subject is developed further in Section 5-10.

If carbon dioxide reduction were not included in the system, the recommendations would be a regenerable Hamilton Standard-type alternating silica gel, molecular sieve system vented to space (Ref. 5-26). A rough idea of the weights involved are shown below.

3 Men – 365 Days				3 Men – 600 Days			
CO_2 Vented to Space		CO_2 Reduction		CO_2 Vented to Space		CO_2 Reduction	
Removal system	90 kg	Removal and reduction systems	150 kg	Removal system	90 kg	Removal and reduction systems	150 kg
Power penalty	10	Power penalty	100	Power penalty	10	Power penalty	100
O_2 + container	1000			O_2 + container	1650		
Total	1100 kg		250 kg		1750 kg		250 kg

5.6 TRACE CONTAMINATION CONTROL

5.6.1 Requirements

As the duration of a space mission increases, the hazards associated with trace contamination of the vehicle atmosphere with gaseous and particulate matter increases two ways. Assuming a reasonably leak-proof vehicle, the buildup of such matter will increase faster and be stable at a higher concentration. It is also true of most toxic gases that the severity of symptoms increases with exposure with time as well as with concentration.

Fortunately, however, one cannot be faced with extreme problems with both leakage and trace contamination simultaneously. The basic equation governing the concentration of gases produced at a constant rate and removed at a rate proportional to concentration is an old and familiar differential equation. The equation is simply:

$$\frac{dc}{dt} = k - rc$$

where

- c = concentration
- k = constant production rate
- r = percent of cabin atmosphere leaked per unit time

The solution, assuming the boundary condition that $c = 0$ at time $t = 0$, is

$$\ln \left[1 - \frac{rc}{k}\right] = - rt$$

If one is convinced by mathematical formalisms, the above equation indicates that c cannot exceed $\frac{k}{r}$ and the equation still have meaning. Practically, this just reflects the fact that, at that point, the rate of production just equals the rate of loss.

At the moment, the most sanguine expectation for r is about 0.01 (per day). This means c could not exceed 100k where k is the per day production. Though, formally, the above equation indicates one would never quite arrive at $c = \frac{k}{r}$, calculation shows one can get quite close to this value in a very finite length of time. It is of some interest to plot c (as a multiple of k) as a function of time for several r's. This is done in Figs. 5-10 and 5-11.

The obvious conclusion is, of course, that one might under some circumstances prefer to leak and/or dump atmosphere than try to remove some particularly difficult-to-remove impurities for certain missions. Before comparing the cost of dumping versus the cost of removal it is necessary to know rates of production and permissible levels for continuous exposure to the contaminant of interest.

Considerable uncertainty exists in both of these areas at the moment. The NLDB (NASA Life Science Data Book)(Ref. 5-27), has a very thorough list of substances produced by humans. Other sources include outgassing of materials and equipment, ionizing radiation, high voltage equipment, food handling, and mechanical erosion of surfaces (Ref. 5-28).

The dangers inherent in using industrial toxicity safety standards based (more or less) on exposure for eight hours a day, five days a week have been pointed out sufficiently. Better data, however, is slow in forthcoming.

Hamilton Standard, AiResearch, and Whirlpool are companies that have done considerable work in both sources and removal methods. Reference 4-28 lists a number of works in this field.

5.6.2 System Selection

A better definition of the toxicity problem is badly needed, but it seems that, with leakage rates such as those assumed in this study, the removal of odors for aesthetic reasons may be the most difficult task of the contaminant control subsystem.

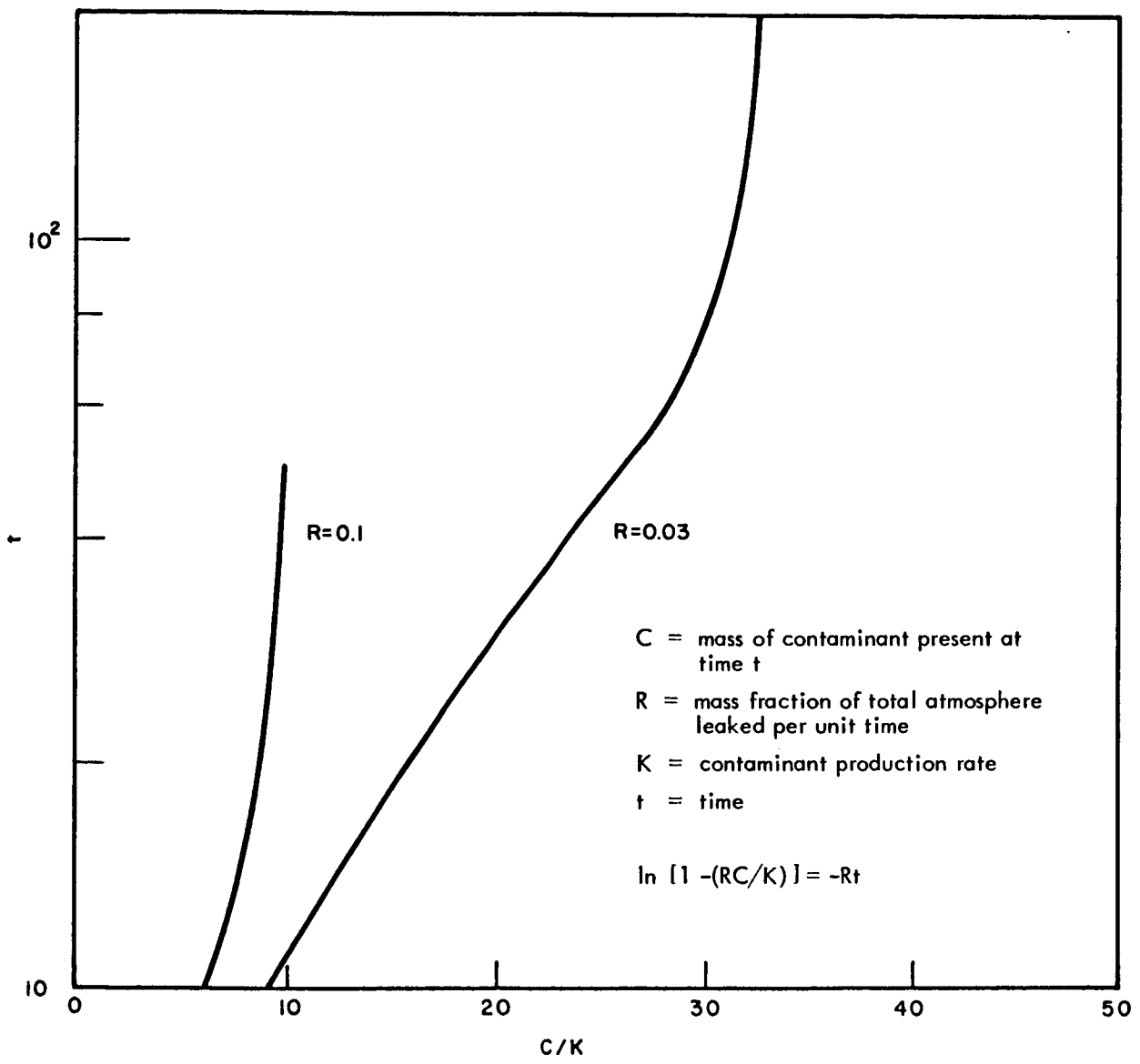


Fig. 5-10 Contaminant Buildup With High Leakage Rates

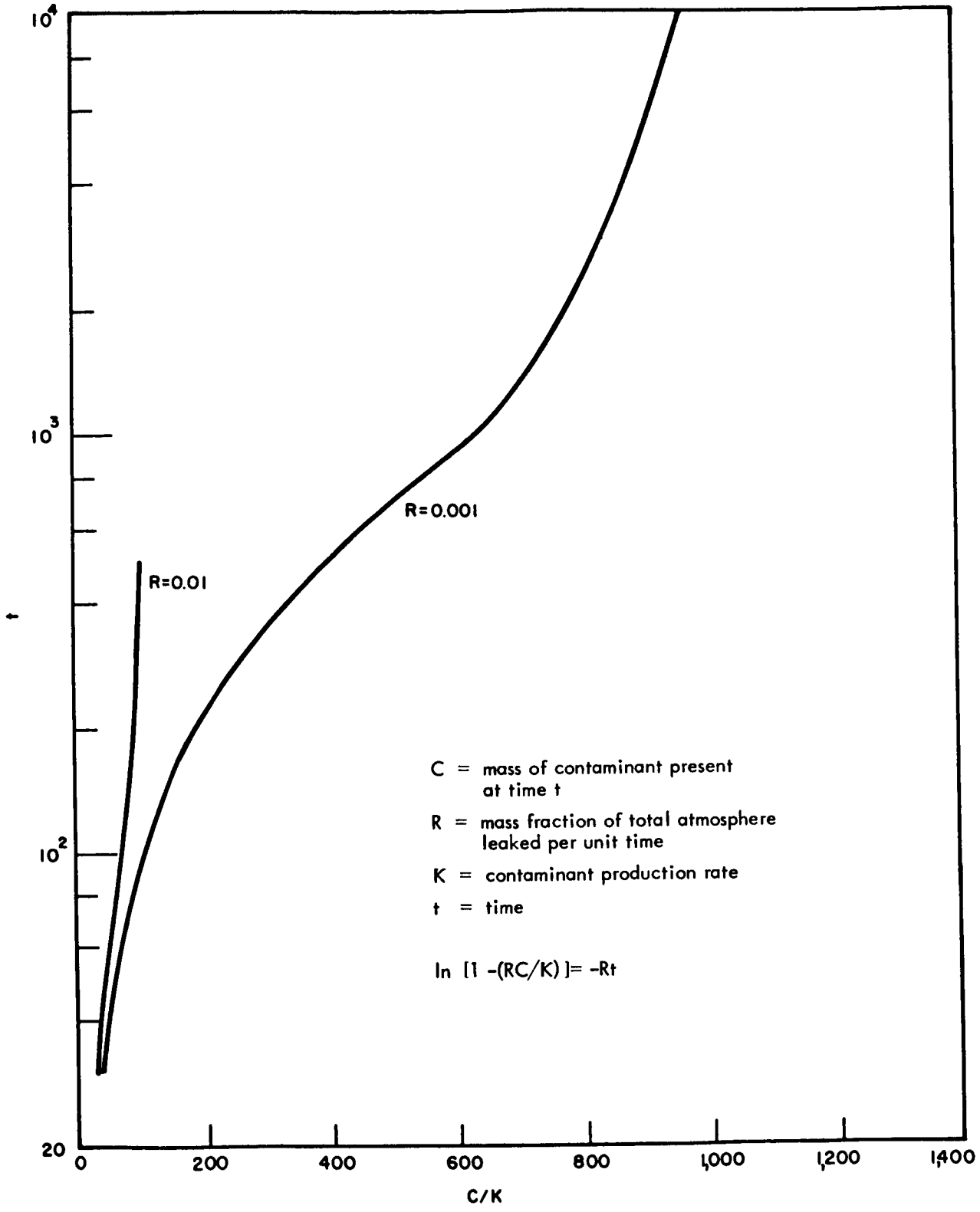


Fig. 5-11 Contaminant Buildup With Low Leakage Rates

It will be necessary also, of course, to maintain such gases as hydrogen and methane below levels which would produce an explosion hazard though these gases are not particularly toxic. It is felt that, even with a much tighter vehicle, a removal system incorporating filters, activated carbon beds, catalytic oxidation at high and low temperatures, and, if proven necessary, grounded screens for ion trapping and one or two more exotic sorbents, e.g., hydrated $CoCl_2$ on pumice for ammonia removal, will suffice to handle the problem. It is expected that such a system would weigh about 30 to 50 kg for three men for 365- to 600-day missions. The power requirement would be about 2 w.

5.7 THERMAL CONTROL

It is assumed that cabin temperature will be maintained at 24°C ± 3°C, the water vapor partial pressure at 10 torr ± 2 torr and that the ventilation rate will be 12.7 cm sec^{-1}.

During entry and exit heat pulses it is assumed than an air ventilated highly reflecting suit will be worn which will enable the crew to resist wall temperatures of 280°C for much longer than the anticipated duration of the heat pulse. The inside wall temperature is, in fact, not expected to reach such a temperature.

The range of heat loads is expected to be from 3 to 10 kw sensible and from 0.15 to 0.60 kw latent. The external flux upon the vehicle will range from the value at Earth to 1.9 times that value at Venus to 0.45 times that value at Mars. If thermal control is being maintained by a cooling system, the vicinity of Venus will provide the greatest challenge. If a heating system is used, the vicinity of Mars will require maximum heating. It is assumed here that a cooling system is of greatest interest for early missions and consequently a Venus mission is analyzed.

The design of the thermal control system must take into account the variations in: (1) internal energy dissipation and, (2) the absorption and rejection of energy by the vehicle exterior surfaces.

The following discussion deals with practically attainable surface characteristics, degradation of these characteristics in the space environment, resulting equilibrium temperatures for a Venus-orbiting vehicle, and systems which might be used to provide the necessary control over the internal temperatures of such a vehicle.

5.7.1 Surfaces

Maximum flexibility in thermal design dictates the achievement of practical surface systems approximating four basic thermal control surfaces; the solar reflector, the solar absorber, the flat reflector, and the flat absorber (Refs. 5-29 and 5-30). In addition, these systems must possess adequate stability in the space environment.

The following discussion will be limited to solar reflectors for two reasons: (1) stable solar reflectors are essential to the operation of spacecraft in the vicinity of the inferior planets due to the increased solar radiation encountered, and (2) of the four basic systems, solar reflectors are most susceptible to environmental damage in space.

Low α_s/ϵ Surfaces

The two basic methods presently in use for achieving solar reflectors, or low α_s/ϵ (solar absorptance/infrared emittance) surfaces are:

- White dielectric high-emittance surfaces (paints, ceramics, and adhesive-backed films)
- Second-surface mirrors

Some examples of these systems are listed in Table 5-7, together with remarks on environmental stability and ease of production. The importance of production problems, and the potentially degrading effects of the pre-launch and ascent environments are discussed in Refs. 5-30, 5-31, and 5-32.

Before reviewing the effects of the space environment, a few comments on mirror-type thermal control surfaces may be of interest. The second-surface mirror consists

Table 5-7

CANDIDATE SOLAR-REFLECTOR THERMAL CONTROL SURFACE SYSTEMS

Class	Material	Initial Values α_s	Initial Values ϵ	Space Stability Ranking	Cure	Remarks
White Organic Paints	Kemacryl Lacquer: White No. M49WC 12 (Sherwin-Williams)	0.27 ±0.04	0.89 ±0.03	3	(1)	In use on LMSC vehicles
White Semiorganic Paints	Fuller 517-W-1 Gloss White Silicone (W.P. Fuller Co.)	0.26 ±0.03	0.84 ±0.04	2	(2)	In use on LMSC vehicles
	Dow-Corning TiO_2-pigmented Silicone Paint	0.21 ±0.03	0.83 ±0.03	1	(1)	Under development by LMSC and Dow-Corning
White Semiorganic Films (adhesive-backed)	Dow-Corning TiO_2-pigmented Silicone Film	0.12 ±0.03	0.86 ±0.04	1	(1)	Under development by LMSC and Dow-Corning
White Inorganic Coatings	LMSC Lithafrax-pigmented Silicate Paint	0.11 ±0.03	0.86 ±0.03	1	(2)	In use on LMSC vehicles; further development on improved formulations underway
Second-Surface Mirrors	1-mm thick sapphire, polished on both faces. Silver vacuum deposited on back by Optical Coating Laboratory, Inc.	0.10 ±0.02	—	1		This data to indicate possible α_s values for the class. Second-surface mirrors are utilized on Mariner II.

(1) Room temperature cure.
(2) Elevated temperature cure

of a material, transparent to solar radiation, with a metallized back surface. Solar radiation is reflected from the carefully prepared and protected metal surface, resulting in a low α_s. With properly chosen materials, and with sufficient thickness for opacity in the far infrared, the solar-transparent material will have an emittance of 0.80 to 0.90.

Environmental Effects

Allowance for the degradation of thermal control surfaces is an extremely important consideration in the design of a thermal control system. A space vehicle encounters a wide variety of environmental conditions; however, only those constituting a probable hazard to thermal control surfaces will be considered here.

Ultraviolet radiation. The most damaging environmental condition which can be adequately evaluated in the laboratory is the near ultraviolet component of solar radiation. This is arbitrarily defined herein as the 2200 to 4000 A band (Ref. 5-30), and is estimated to contain 9 percent of extraterrestrial solar radiation (Ref. 5-33). The effect of this radiation is evaluated by exposing surface specimens in a vacuum of 10^{-6} to 10^{-7} torr to ultraviolet energy from a water-cooled mercury-argon high pressure AH-6 lamp (Ref. 5-34). Measurements of α_s and ϵ are made before and after exposure.

Data showing the exponential nature of the degradation is presented in Fig. 5-12. Data points are not shown in the interest of clarity; the spread of measured α_s for a given exposure is ± 10 percent or less. The dashed lines represent extrapolations which are based on the observed exponential increase of α_s with exposure. A flux density of one "sun" is defined as the total flux density of solar radiation in space at one astronomical unit from the sun, of wavelengths between 2200 and 4000 A, irrespective of spectral distribution within that band.

It should be noted that the time scale of ultra-violet degradation estimated on the basis of this data may be in error by a factor of two or more, due primarily to lack of knowledge of the wavelengths of photons causing the damage. Since the AH-6 lamp

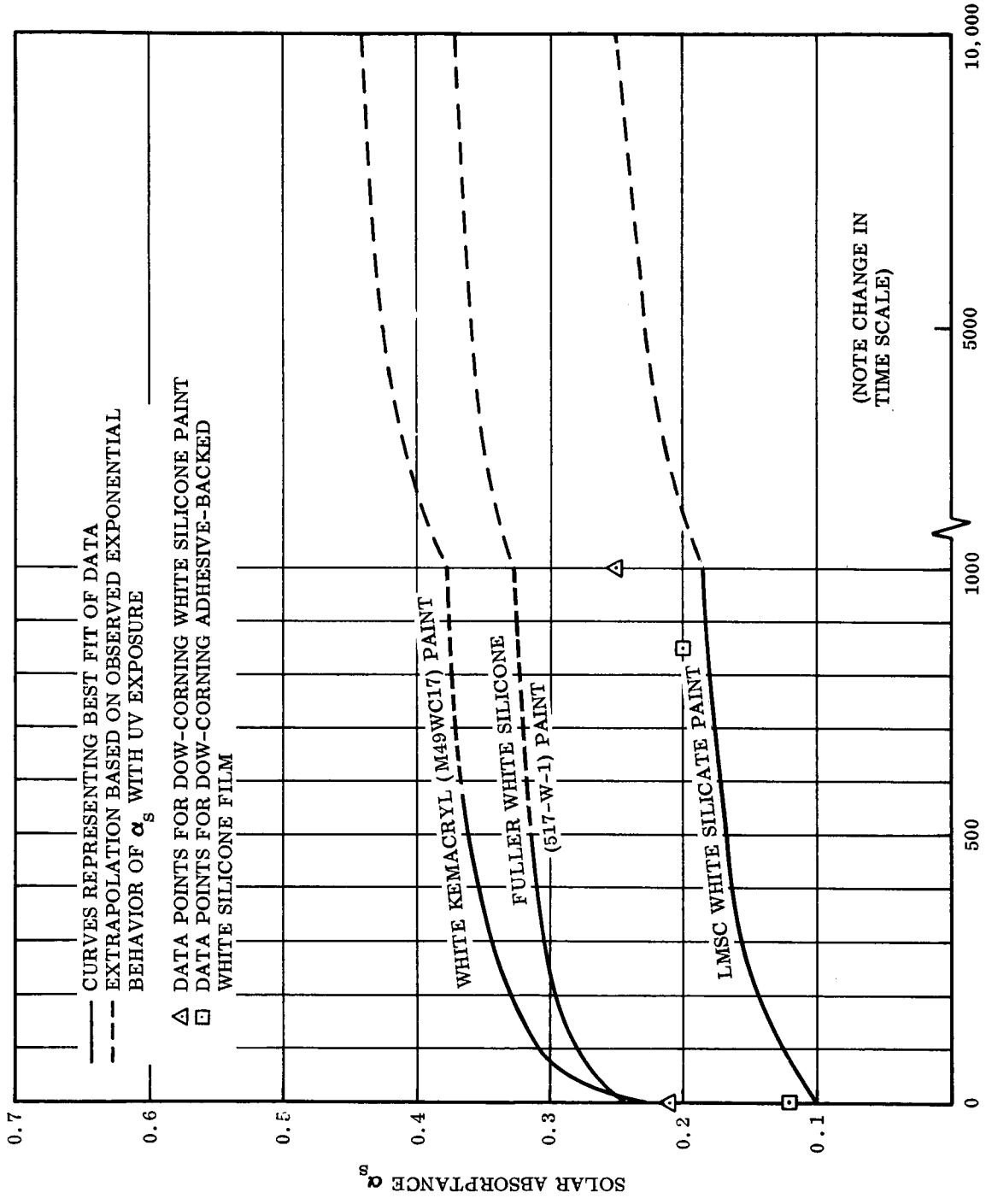


Fig. 5-12 Effect of Near Ultraviolet Radiation in Vacuum on the Solar Absorptance α_s, of Candidate White Surfaces

(or any other intense ultraviolet source) does not duplicate the solar spectrum, information on this wavelength dependence is required for precise prediction of ultraviolet degradation. Investigations are being initiated at LMSC to obtain this data; until this information is available, usage of the admittedly unsatisfactory exposure parameter of "sun-hours" will probably continue.

The damage caused by ultraviolet exposure will be heightened by the increased flux density of solar radiation as the spacecraft travels toward Venus or Mercury. There is experimental evidence of a rate dependence for the ultraviolet damage of some materials (i.e., an exposure to six "suns" for ten hours does not produce the same effect as an exposure to one "sun" for sixty hours). However, generally an error of less than twenty percent in α_s is incurred if one assumes a linear relationship between damage rate $(d\alpha_s/dt)$ and flux density for variations from one to six "suns." The solar flux density at Venus is about 1.9 times that at Earth; at Mercury it is about 6.8 times that at Earth. If precise predictions of damage are required, one must determine the dependence of damage rate upon intensity and take this into account.

In making ultraviolet degradation predictions for calculations in this work both rate-dependences and possible time-scale errors have been ignored.

Penetrating radiation. For thermal control surfaces of the vehicle under consideration, the most important source of penetrating radiation damage is expected to be solar flares. Solar flare protons can cause both radiation damage and sputtering; pertinent data are reviewed in Refs. 4-33 and 4-35. While they are not considered to imperil thermal control surfaces of Earth-satellites, solar flares are worthy of greater attention at the orbits of inferior planets. At the orbit of Venus the flux is estimated to be 2.0 to 2.5 times greater than at the orbit of Earth; at Mercury it is suspected to be 6 to 15 times greater.

The thicknesses of thermal control materials which determine the thermal radiative behavior range from a few microns for metals, from 50 to 250 microns for paints and

ceramics. An exception to this statement is the solar-transparent material of a second-surface mirror, which must maintain its transparency to solar energy; this could be as thick as 1.6 mm in some designs.

All incident particles will have some probability of altering the radiative behavior of the materials, but the largest dose will be from protons of energies less than approximately 20 Mev. These particles can be expected to have a high probability for interaction with thermal control materials within the thicknesses mentioned above. Low energy electrons could represent a greater threat to thermal control surfaces if present in solar flares in large numbers. The fluxes and energy spectral of solar flare electrons are not well-known at present, however (Refs. 5-33, 5-35).

In any case, candidate thermal control surfaces for missions to the inferior planets should be subjected to low energy ($\leq$ 20 Mev) proton bombardment before final approval. It is expected, however, that the damaging effects of ultraviolet radiation will be proved to overshadow degradation caused by penetrating radiation.

Volatilization. Due to the low particle densities in space the potential problem of volatilization must be considered (Ref. 5-32). However, it is our experience at LMSC that materials developed for resistance to the effects of ascent heating, ultraviolet radiation, and penetrating radiation are also generally stable in vacuum.

Thermal stress. The last environmental effects worthy of mention are those of thermal stress and, if appropriate, thermal cycling. Such tests are performed routinely in vacuum at LMSC. In the near future, they are to be combined with the ultraviolet tests mentioned earlier. Such tests should be of particular importance for vehicles orbiting Mercury; surface-substrate systems must not fail due to differential thermal expansion.

5.7.2 Equilibrium Temperatures

Equilibrium temperatures for the various surfaces of a hypothetical vehicle for a Venus-orbiting mission were calculated. Such data are useful in determining what types of thermal control systems might be used.

Mission and Vehicle Data

A Venus mission consisting of a 110-day Earth-to-Venus transfer, 10-day Venus orbit, and a 250-day Venus-to-Earth transfer was selected for study. A rotating interplanetary vehicle comprising a reentry module, an operations module, and a power and control module was assumed. The power and control module acts as the hub of the rotating vehicles with the remaining two modules on the ends of two opposing spokes. The operations module, consisting of a cylindrical section with two hemispherical ends, was the only portion of the vehicle for which equilibrium temperatures were computed. The crew occupies the operations module during the major portion of the mission.

Two orientations were assumed for the transfer periods and for Venus orbit in order to determine the sensitivity of equilibrium temperatures to this parameter. For the transfer periods, the operations module was assumed to be oriented with one hemispherical end continuously facing the sun, or with the axis of the cylinder perpendicular to the solar vector. For Venus orbit, it was assumed that the axis of the cylinder was locally vertical, or locally horizontal and perpendicular to the orbit plane. In all cases the module was assumed to be rotating. The Venus orbit was assumed to be in the ecliptic plane at altitudes of 18,200, 5800, and 270 km.

Assumptions and Calculation Methods

Average equilibrium temperatures were determined by equating the absorbed and emitted energies. The use of average temperatures as a guide is quite reasonable since the vehicle is rotating and temperature-time variations around an orbit do not generally affect the thermal control system significantly.

Solar absorptance values for white silicate paint were taken from Fig. 5-12. The infrared emittance was assumed constant at a value of 0.86. The solar flux was assumed to vary inversely as the square of the distance from the sun.

Transfer periods. During these periods the only absorbed energy is that arising from solar radiation. Solar view factors were determined by taking the ratio of the projected area normal to the solar vector, to the total area of the surface being considered.

Venus orbit. Absorbed fluxes during Venus orbit were determined by the method presented in Ref. 5-29. The solar reflectivity of Venus (0.76) was taken from Ref. 4-36. Venus planetary emission (137 kcal hr^{-1} m^{-2}) was determined from temperature data from Ref. 5-37. Solar, albedo, and planetary-emission view-factors were determined for several positions around an orbit, thereby allowing a determination of the average heat flux absorbed during an orbit.

Calculation results. The resulting equilibrium temperatures, shown in Fig. 5-13, are useful in determining the heat rejection capability of the module surfaces, since at a given temperature:

$$q_r = \sigma \epsilon \left(T_s^4 - T_{eq}^4 \right)$$

where:

q_r	Net heat rejection rate, kcal hr^{-1} m^{-2}
σ	Stefan-Boltzmann constant, kcal hr^{-1} m^{-2} $°K^{-4}$
ϵ	Surface emittance
T_s	Surface temperature, °K
T_{eq}	Surface equilibrium temperature, °K

Throughout the entire mission equilibrium temperatures are sufficiently low that the rejection of sizeable heat loads is possible at reasonable surface temperatures. For example, at an average surface temperature of 289°K the horizontally oriented operations module orbiting at 273 km can reject approximately 17.5 watts m^{-2}. The module could well have a total surface area of 93 m^2, resulting in a total heat rejection capability of approximately 17.5 kw. Heat rejection in the vertical orientation would be slightly greater.

During the transfer periods heat rejection capability would be substantially increased by orienting the module with its axis parallel to the solar vector. However, since the

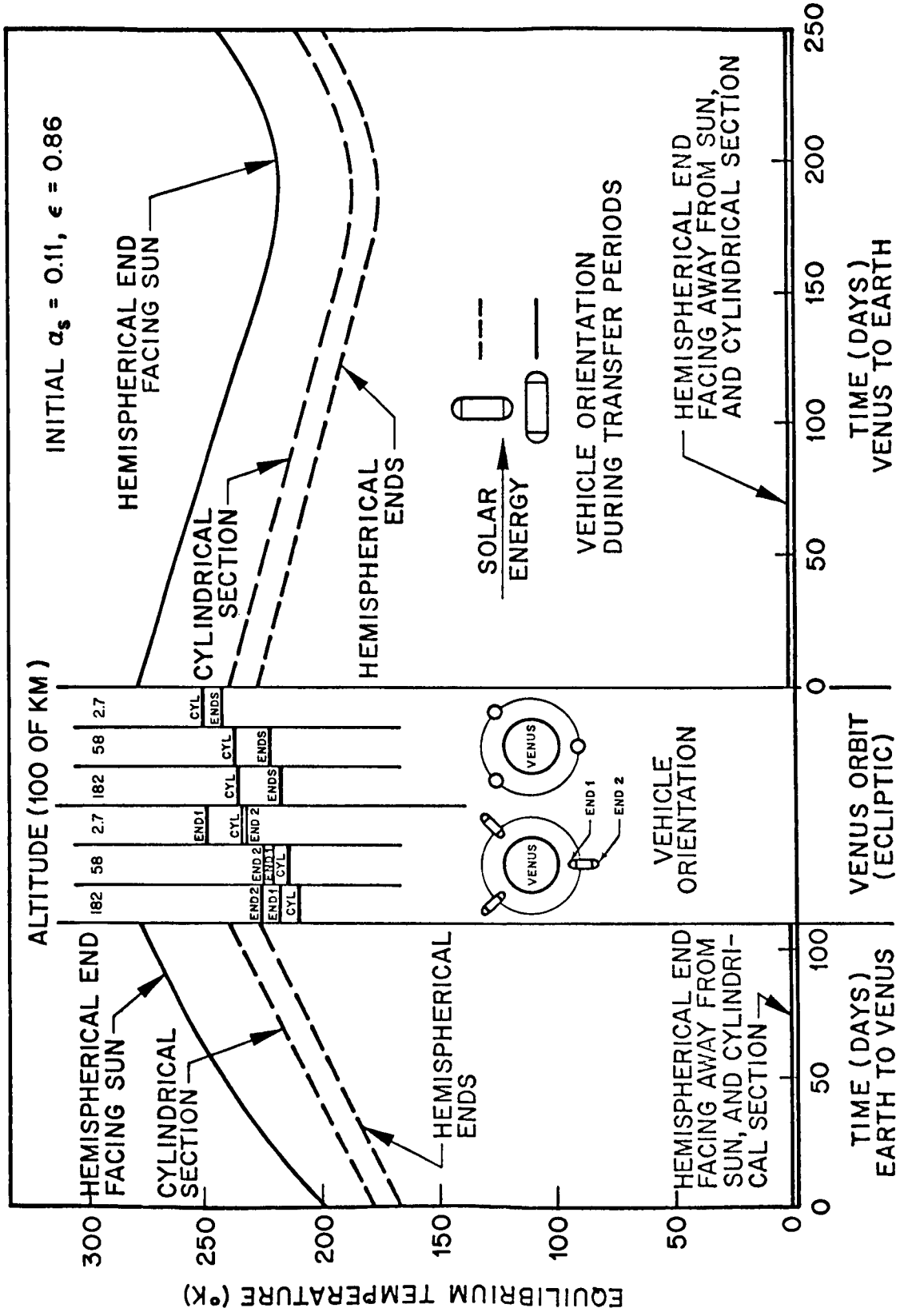


Fig. 5-13 Rotating Vehicle Equilibrium Temperatures for Venus Mission

Venus-orbiting phase is the critical design condition there is nothing to be gained by so restricting the vehicle orientation during the transfer periods.

It should be noted that the calculations were based on nominal values of all parameters, consequently some reduction in heat rejection capability must be considered due to uncertainties in these parameters.

The shape of the curves for Venus-to-Earth transfer results from the assumed trajectory which takes the vehicle nore than one astronomical unit from the sun before it returns to Earth.

5.7.3 Systems

It is possible to specify the exact nature of the thermal control system only after assembling a considerable amount of information on internal loads, allowable temperature variations, equipment locations, etc., and performing the necessary analysis to determine the interrelationship of all the variables. The time variation in vehicle equilibrium temperatures, however, is a useful tool in predicting the general nature of the system which might be used.

If the necessary internal heat loads can be rejected from the vehicle surfaces at sufficiently low temperatures then the problem is one of either (1) properly regulating the flow of energy from the interior of the vehicle to these exterior surfaces or (2) controlling the radiative characteristics of these surfaces. If such a procedure is not possible, as may be the case with large externally absorbed heat fluxes, then evaporative and/or heat pump systems are required.

Evaporative cooling systems, wherein an expendable coolant absorbs the load and is vented to space, have general usefulness for cooling during ascent, emergencies, and reentry, but are not applicable to long-term operation involving substantial heat loads. In cases where heat must be rejected at elevated temperatures for long periods, the heat pump system will provide a weight saving over the evaporative system at some point in time of operation.

Since low altitude manned planetary orbital flights, except around Mercury, can be made without resorting to the use of a heat pump, the following discussion will focus on systems which regulate internal-to-external heat flow, or external radiative characteristics. Such systems include (1) variable external surface properties (α_s and/or ϵ), (2) variable internal-to-external thermal resistance, and (3) controlled internal heating.

Variable α_s and/or ϵ

Systems which vary the solar absorptance and/or infrared emittance of the vehicle exterior can compensate for changes in incident flux and internal heat generation. Examples of these are thermo- and phototropic surfaces, and shutter systems. A detailed treatment of such surfaces and devices is presented in Ref. 5-38. It has been our conclusion, from theoretical analysis, that such systems are not generally applicable to close temperature control of vehicles experiencing significant changes in internal power dissipation.

Variable Internal-to-External Resistance

The internal-to-external thermal resistance can be varied to compensate for changes in internal heat generation and externally absorbed flux. This resistance may be radiative, conductive, convective, or some combination thereof. Examples are: the conduction-radiation switch, infrared radiation shutters, and fluid circulation systems. LMSC has done experimental work on a conduction-radiation switch (Ref. 5-38) and a fluid circulation system (Ref. 5-39). A resistance ratio of approximately 18 to 1 has been achieved with the switch device. Considerably greater resistance ratios can be achieved with the fluid circulation system but with the added complications of a fluid-filled space radiator and a pumping system. This system does, however, represent a present state-of-the-art solution to thermal control for a wide variety of manned interplanetary missions.

Internal Heating

This approach to thermal control involves selection of sufficiently low internal-to-external thermal resistances so that under the combined conditions of maximum internal

heat generation and maximum external flux the internal temperature will not exceed its maximum allowable value. At lower levels of internal heat generation and external heat flux, heat is added internally at a rate sufficient to maintain the internal temperature above its minimum allowable value. Such systems, employing electrical heaters, have been used for satellite thermal control.

An improvement over the electrical heater approach would be the utilization of excess heat from less temperature-sensitive equipment. For example, certain items of equipment which have fairly wide allowable temperature ranges might be used to supply the energy required for close control of other equipment and areas occupied by the crew. A variable-resistance thermal link would be required between the heat source and the item to be closely controlled.

The feasibility of this method of thermal control depends on a number of variables which are difficult to generalize such as equipment location, power dissipation, and power duty cycle. Consequently, it is not possible to conclude in a general way that such a system will or will not work. Such a conclusion must await an analytical study based on a particular vehicle design. If such an approach can be made to work it will have obvious advantages over the fluid circulation system.

In this study, no detailed analysis of any particular thermal control system was attempted. Based on the approximate expected loads, assuming no heat pump necessary, and averaging several possible vehicle configurations, the following table is applicable.

	Mass (kg)
Radiators	135
Circulating fluid	135
Insulation	45
Heat removal equipment	120
	435
Power requirement	1.6 kw (average)
	2.4 kw (peak)

The foregoing tabulation is based on current state-of-the-art and could probably be reduced with further development of surface coatings and variable resistance devices.

5.8 DIET AND METABOLISM

Diet requirements and energy expenditures are well documented for Earth living. Tables 5-8 through 5-11 are based on such data. The only space stress expected to have significant effect upon such values is weightlessness, the effects of which are uncertain but probably tend to decrease metabolic requirements.

The values shown in Tables 5-8 through 5-11 are based on the following assumptions:

- The sensible-latent split in Table 5-8 assumes subjects dressed in light clothing under indoor winter comfort conditions, i.e., about 24°C and 50 percent relative humidity. It does not assume wearing of an impermeable pressure suit.
- The amounts of protein and fat in Table 5-9 are 30 to 40 percent below U.S. middle class urban preferred values but healthier and well above the amounts required for nutrition. The balance of the diet is made up of carbohydrates since this foodstuff is processed most easily by the body and is not productive of nitrogenous wastes.
- The diet and metabolism determine the other values of Tables 5-9, 5-10, and 5-11 in accordance with relationships set forth in any standard human physiology text.

Table 5-8

ACTIVITY SPECTRUM AND METABOLISM

	Hours Per Day	Sensible (kcal/day)	Latent (kcal/day)	Total (kcal/day)
Sleep	8	400	140	540
Sitting up Resting	4	250	150	400
Light Work (Tailoring)	9.5	640	640	1,280
Medium Work (Carpentry)	2.5	200	400	600
		1,490	1,330	2,820

Table 5-9

METABOLIC CONSUMPTION AND PRODUCTION

Food	Amount (gm)	kc	O_2 Required cc (STP)	CO_2 Produced cc (STP)	H_2O Produced (gm)	Minerals, Vitamins, Cellulose Fibers (gm)	RQ
Protein	70	308	67,000	54,000	28.7	–	0.81
Fat	80	760	161,000	114,000	86.0	–	0.71
Carbohydrate	438	1,752	346,000	346,000	241.0	–	1.00
TOTAL	588	2,820	574,000	514,000	355.7	45	0.90
Total (lb)	1.30	–	1.82	2.23	0.78	0.10	–
(gm)	588	–	823	1,000	354	45	–

Table 5-10

WATER BALANCE (gm)

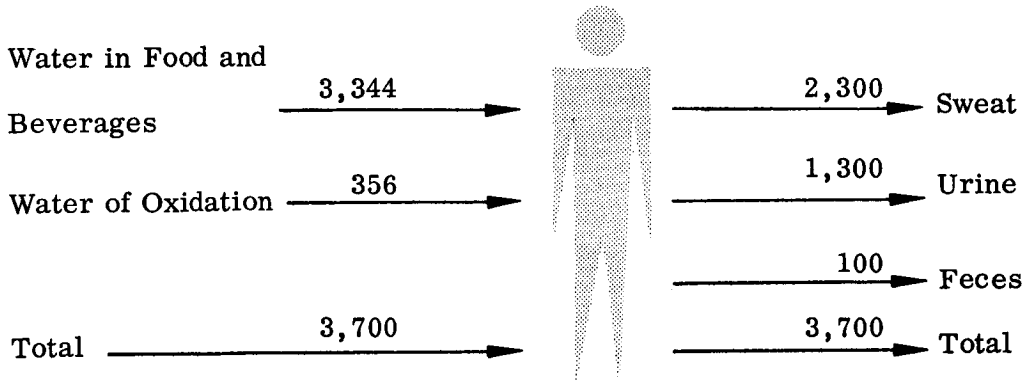
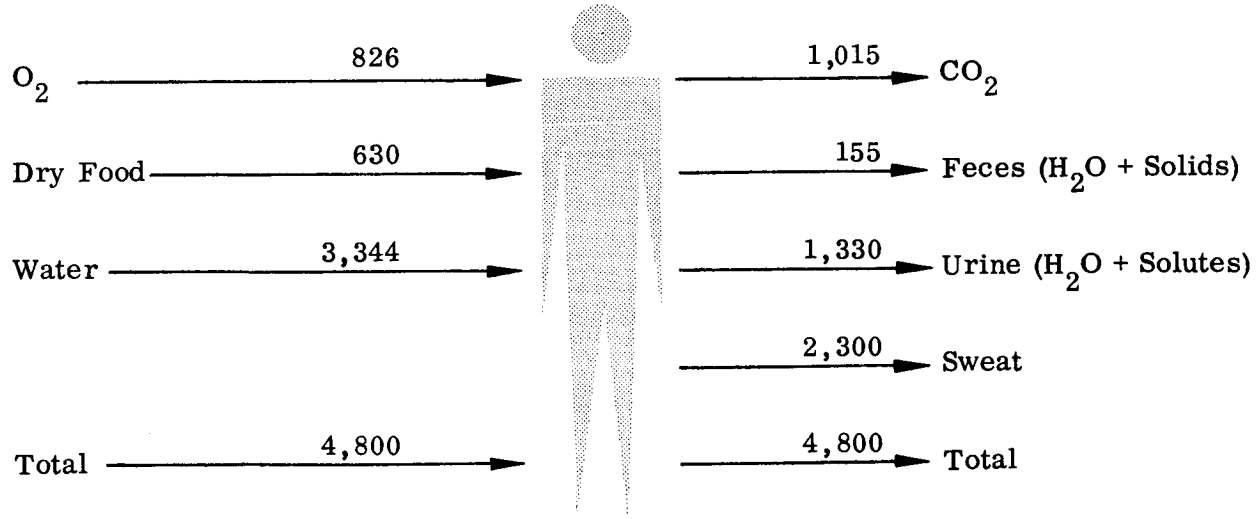


Table 5-11

MASS BALANCE (gm)



The diet selected is a compromise between health and eating enjoyment. It is highly probable that the 20 gm per day of fat of the average Japanese is healthier, but it would be difficult to satisfy American palates with such a diet.

The diet shown assumes stored food. In the case of biological regeneration it would probably not be possible to have as high a percentage of proteins in the diet. The algae tested so far show considerable latitude, however, in their ability to proliferate proteins and fats in various ratios from simple foodstuffs.

Individual variations from the quoted figures will be substantial — especially during weight loss or gain. The values shown are considered reasonable averages for the purpose of developing loads upon the system.

From Table 5-11, one can immediately size the open system requirements. Sixty grams are added to both the dry food and water values to allow for shelf spoilage and table waste. Container weights average about 10 percent of the contained dry food and about 20 percent of the contained water. Food "dried" by the freeze-dry technique actually has 2 to 3 percent water in it.

For purposes of taste, it has been stated, it would be desirable to have a portion of the diet not dehydrated. Hydrated food, however, carries a greater cost in refrigeration required to preserve it.

The following table shows the food and water — including container weights associated with an open system for the sample missions.

3 men — 365 days		3 men — 600 days
Dry food	830 kg	1310 kg
Water	4460	7350
Cooking equipment	20	30
Food storage	500	800
Total	5810 kg	9590 kg

The expected power consumption is 750 w average for food preparation and storage. The savings possible by utilizing physico-chemical and/or biological regeneration of wastes are discussed in the next two sections.

5.9 BIOLOGICAL REGENERATION

The minimum mission duration which makes profitable the use of biological regeneration has been estimated in the literature at anywhere from 21 to 1250 days. A great deal of publicity has been given experiments which succeeded in keeping mice alive for several days by absorbing the mouse-produced carbon dioxide and supplying the mouse with oxygen.

The fact is we are not yet able to specify an algae system in any detail. Many basic problems of algae metabolism remain to be worked out. As a simple gas exchange system where the algae harvest is dumped, the system offers no advantage – even theoretical – over physico-chemical systems. It is only for very advanced missions involving the necessity for more complete closure that algae systems look even theoretically rewarding. Complete closure means we must eat the algae or eat something that eats the algae. Aside from nutrition considerations, there are likely to be few volunteers to subsist for more than a year on a diet of pure or even largely algal composition until it can be prepared more tastefully.

Biological systems advocated at one time or another have included (besides algae) fungi, bacteria, moss, heather, higher plants, tissue cultures, arthropods, fish, higher vertebrates (e.g., cows) and symbiotic combinations of some or all of the above.

Animal "links" have value only for variety in the diet. Losses in the form of inedible horns, hoofs, etc., rise geometrically as more intermediates are added. Mosses have too little turnover to do the gas exchange job without a great mass of moss. Tissue cultures tax the most experienced biologists at keeping them alive in Earth-bound laboratories.

Higher plants require rather artistic handling, especially seed plants; many have seasonal and day-night cycling requirements and have an uncertain prognosis under zero g with water transfer, gas diffusion, and auxin system behavior difficult to predict.

Bacteria-algae systems have some advantages but aseptic algae systems seem to offer much more consistent results. Dr. Victoria Lynch of LMSC's Space Medicine Group has worked with such systems for some time. Dr. Lynch likens such combinations to the vintner's crops of wine. Some are excellent and others horrid.

The advantages of algae are the following: It can remove CO_2 from the atmosphere, it can produce O_2 and food from nothing but the CO_2 removed plus urine plus negligible trace amounts of minerals and possible one or more amino acids, it can process urine but requires only about 25 percent of the urine produced to react with carbon dioxide, it accepts feces as a nitrogen source but the feces darkens the mixture to the point where photosynthesis is greatly impaired, it can be automated, it does not require seasonal or day-night cycling.

Problems remaining to be solved include but are not limited to the following:

1. Matching stoichiometric relation of CO_2 and O_2.
2. Recycling period of the liquid phase possible without treatment.
3. Feeding to something beside "young growing rats" to determine nutrition and toxicity.
4. Palatability
5. Effects of ionizing radiation, weightlessness and other space stresses.
6. Filtration and treatment of urine necessary to prevent microbial contamination.

Based on current knowledge and techniques, the following values would apply to a three man algae system of 4 liters of algae per man:

Bulk Volume	13.5 m^3
Power	48 kw with artificial light 16 kw with natural light
Area of Exposure	170 m^2

In addition, equipment would be necessary for harvesting, cooling, mixing CO_2 and filtering urine.

It is the opinion of the Space Medicine Group of LMSC that a program costing some 30 to 40 million dollars would be necessary – if initiated very soon – to specify an algae system by 1966 and that this program would have to incorporate thorough investigation of basic phenomena to be successful.

5.10 PHYSICO-CHEMICAL REGENERATION

In order to aid the imagination in grasping the possibilities inherent in the regenerations of metabolic wastes, Fig. 5-14 is constructed. For convenience, the weights for a 600-day mission are marked.

The greatest saving is the recovery of atmospheric water. The fact that such water leaves high boiling point impurities behind upon evaporation and leaves many low boiling impurities behind upon re-condensation has led many workers to believe a simple water collection device coupled with the humidity control system, a charcoal (and possibly) a microbe filter will be sufficient to restore this water to potability. Some tests have shown no undesirable effects from drinking atmospheric water for up to 30 days with virtually no processing. The recovery of atmospheric water presents maximum savings for minimum efforts and will doubtlessly be utilized in missions of more than a few days duration.

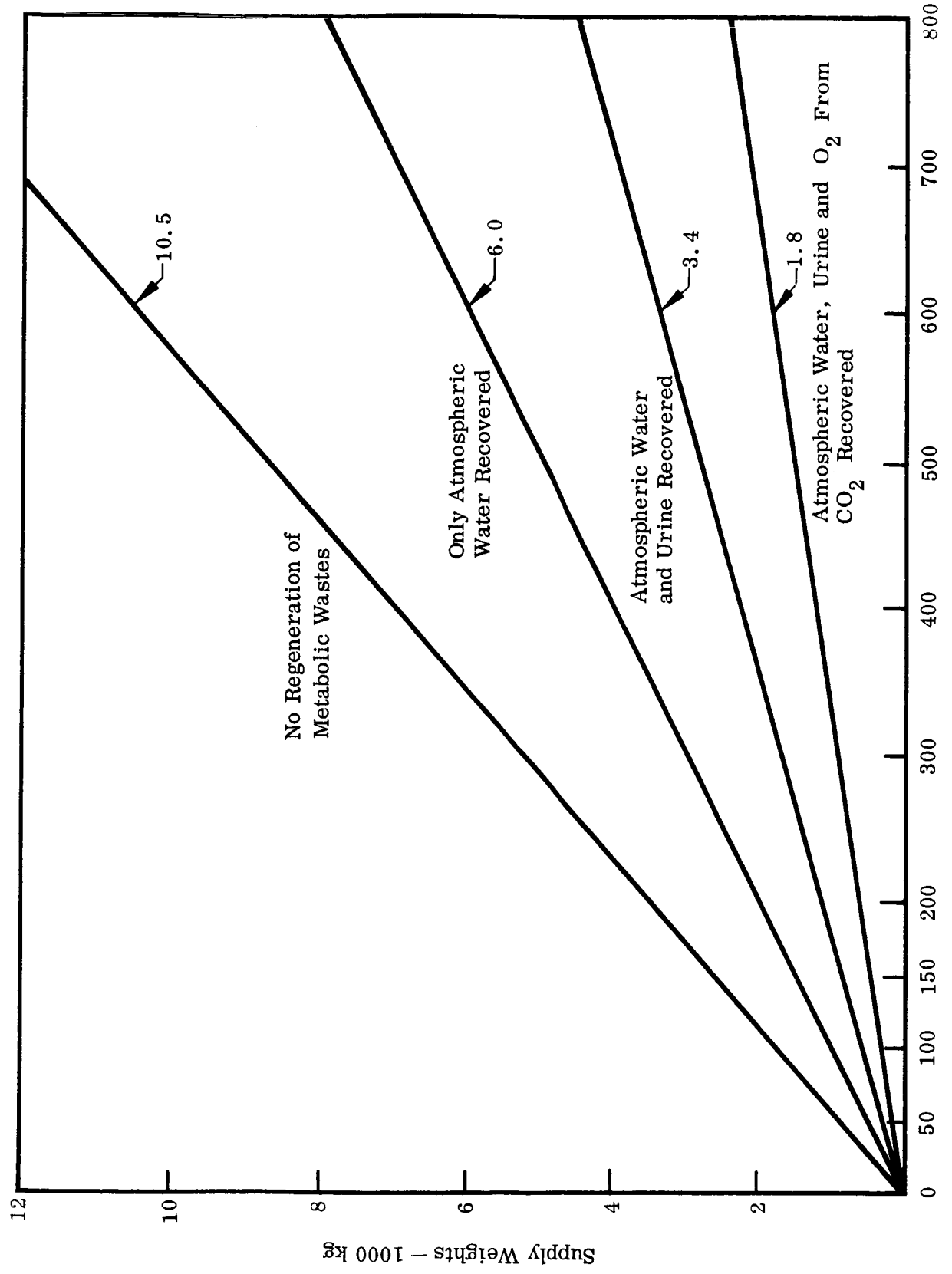


Fig. 5-14 Metabolic Supplies vs. Mission Duration for 3 Men. Metabolism of 2820 kcal day^{-1} Including Container Weights but Not Including Regeneration Equipment Weights or Power Penalities – O_2, H_2O, and Dry Food

The next greatest saving is the water from urine. The problem here is somewhat more formidable but a number of solutions seem feasible. Generally, it is desirable to use a high temperature distillation to destroy bacteria, and low temperature distillations to produce less ammonia.

The system favored at the moment by LMSC is the vapor-compression distillation method. The urine is evaporated in a distillation tank, and the resulting water vapor is compressed and passed through a condenser submerged in the evaporating liquid. The heat of evaporation is provided by the heats of condensation and compression. A chemical agent is added to the urine in the distillation tank to reduce odor, bacterial growth, and to minimize residue carryover. The condensed water vapor is passed through a series of filters before storage.

The recovered water is electrolyzed to provide: (1) Oxygen to meet metabolic and leakage requirements, and (2) hydrogen for carbon dioxide reduction. The recovered water is mixed with an electrolyte and pumped through an electrolytic cell, gas separators, and temperature control equipment. Hydrogen and oxygen separated from the electrolyte are stored in high-pressure storage tanks.

The smallest savings come from the recovery of oxygen from carbon dioxide. The problems here are an order of magnitude above those of urine distillation. No complete system has really been developed even in the laboratory. The high temperature associated with carbon dioxide reduction coupled with uncertainty in the development of the state of the art makes the recovery of carbon dioxide only about a 50 percent chance for a 1970 interplanetary mission. Several vendors have indicated confidence in their ability to deliver carbon dioxide reduction systems of the Sabatier type within two years from the initiation of a substantial development program. It is probable that such a development program would have to be very substantial in scope and intensity.

The type of system tentatively advocated by LMSC for early interplanetary flight is the following: Carbon dioxide reduction is accomplished in a Sabatier reactor to form

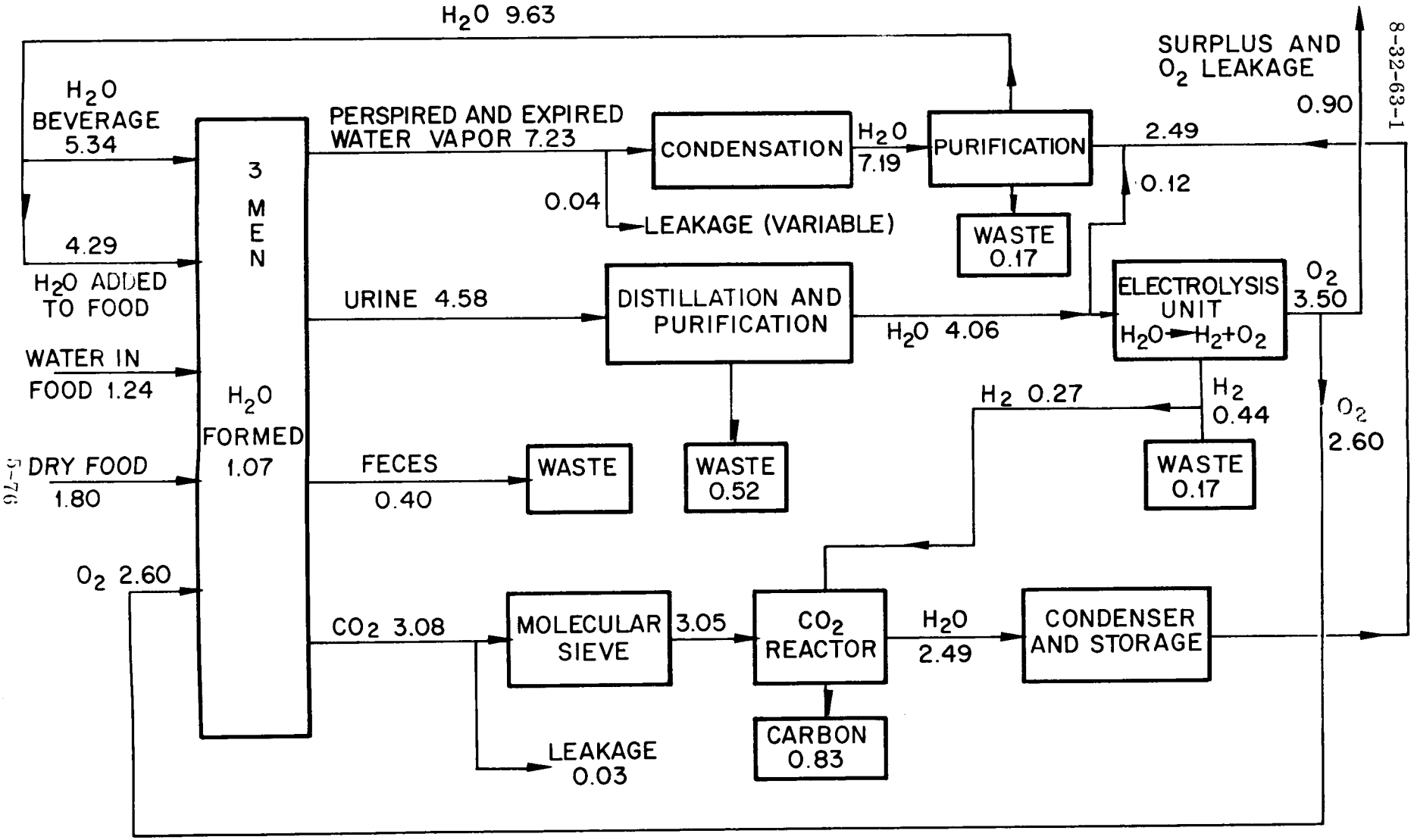
methane and water. Hydrogen stored during the electrolysis process and carbon dioxide stored during desorption of the carbon dioxide removal system are reacted over a catalyst at elevated temperatures. The resulting methane, water, and unreacted gases are cooled to remove the majority of the water vapor. The condensed water vapor is filtered and delivered to the cabin water supply system. With the Sabatier reactor high reduction efficiencies can be obtained with moderate temperatures.

The reduction of methane is accomplished in a high temperature reactor. The dehumidified exhaust gases from the Sabatier reactor are heated in a regenerative heat exchanger and passed over a catalyst. The catalyst is heated electrically to maintain the required reaction temperature. Carbon is deposited on the catalyst and the hot exhaust gases (mostly hydrogen) are passed through the regenerative heat exchanger to the inlet of the Sabatier reactor.

A formidable problem is the collection and concentration of carbon dioxide from the atmosphere and conveyance to the reactor. Although Hamilton Standard has worked on a system utilizing the silica gel molecular sieve system, it seems likely that freeze-out or electrodialysis methods will prove superior eventually. The latter require more work in the laboratory. The electrodialysis method is now being investigated by AiResearch and the freeze-out method by LMSC.

Figure 5-15 is a flow diagram for the type of system envisioned for early interplanetary flight. The values are commensurate with the assumptions of this study.

The methane reduction is a complicated step which saves only a relatively small amount of hydrogen. If the hydrogen were not recovered, however, hydrogen would have to be carried or manufactured. It would be desirable to avoid having to do either. The approximate weight for the recovery equipment as described is 150 kg. The average power required for the three man system is 1.7 kw. The amount of extra components, insulation, etc., necessary to provide the desired reliability is virtually impossible to predict without detailed analysis and probably more laboratory experience with these methods.



ALL QUANTITIES IN kg PER DAY

Fig. 5-15 Nearly Closed Life Suppot System

LOCKHEED MISSILES & SPACE COMPANY

5.11 WEIGHTLESSNESS, ARTIFICIAL g, AND CORIOLIS

Until man has endured weightlessness for at least 30 days it will be impossible to extrapolate to missions of one year and longer. So far, both Russian and American tests look favorable from the point of view of subjective sensation and performance.

Long term dangers envisaged include loss of muscle tonus in both involuntary and skeletal muscles, incapacitation of the cardiovascular system, decalcification of bone structures, and slowed down or modified cell replication.

It is possible to exercise at zero g using alternating accelerations and decelerations, stretching elastic bands, compressing springs, and just tensing and untensing the voluntary muscles. Probably enough of such activities would suffice to maintain at least voluntary muscle tonus. The question is how much of each day would have to be spent in such activities.

Since it is not clear at the moment whether or not the early interplanetary vehicle will require artificial g, a rotating vehicle was assumed for the major design work in this study. If rotation turns out to be unnecessary, the actual vehicle will be easier to construct.

Some ECS and life support equipment would be, however, more complicated in a weightless vehicle. It seems unwise to await the results of confirming experiments to begin considering the rotating vehicle design if the early 1970 deadline for flight is to be met.

In a rotating vehicle the problem of coriolis forces immediately appears. The problems associated with the design of a rotating vehicle to minimize such effects as visual problems, canal sickness, and locomotion problems are covered very well by B. J. Loret (Ref. 5-40).

The reasoning in that reference that leads to the conclusion that angular velocity should be kept below 0.4 radians sec^{-1} and that the induced gravity should be between 0.3 g and 0.85 g seems basically sound. It would be desirable to test further the necessity for not going over 0.4 radians sec^{-1} since a higher value would permit a shorter radius. The determining experiments for canal sickness carried out in Earth-bound centrifuges were not, of course, completely analagous to a space case because of the gravity vector.

Probably the two areas which require investigation most urgently with respect to interplanetary flight are long term weightlessness and solar flare phenomena.

5.12 METEORITIC PHENOMENA

5.12.1 Flux vs. Mass

In Fig. 5-16, Whipple's 1962 near-Earth meteoroid distribution data are compared with Whipple's 1957 and Watson's 1956 data. For a certain meteoroid flux, the meteoroid mass varies approximately 1 to 3 orders of magnitude depending upon which meteoroid distribution data are assumed.

Since the concentration of micro-meteoroids is influenced by the gravitational field, it will be reasonable to expect that the micro-meteoroid influx in deep space is less than that in the vicinity of the earth. When traveling in the asteroid belt located between Mars and Jupiter, it will be reasonable to expect an increase in the asteroidal meteoroids. The distribution of larger meteoroids of concern in shielding design for traveling from Earth to Venus, or to Mars, should not be significantly different from Whipple's near-Earth data.

5.12.2 Velocity vs. Mass

The theoretical meteoroid velocity in the vicinity of Earth can vary from 11 km sec^{-1} which is the low limit determined by Earth's graviational field, up to 72 km sec^{-1}

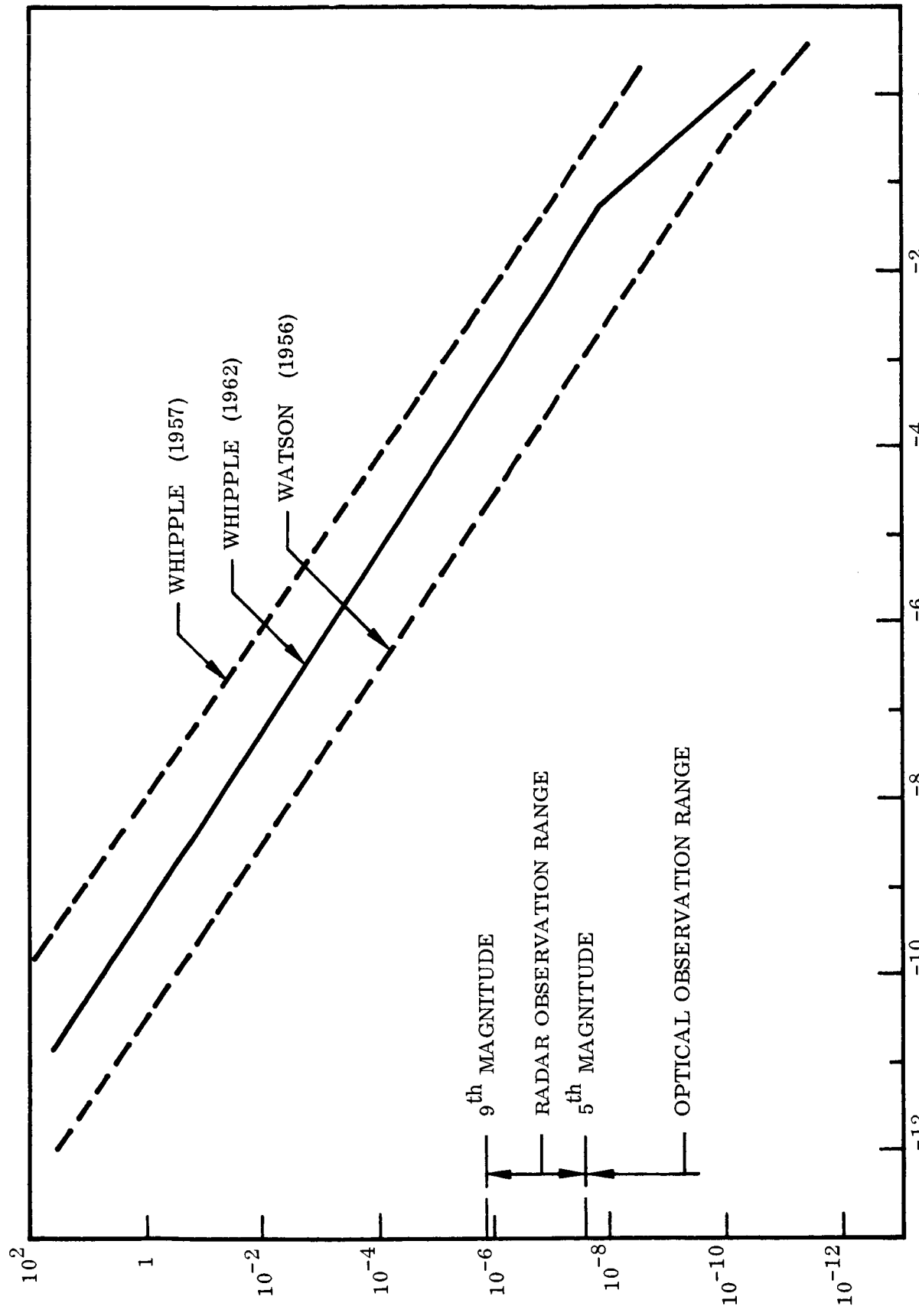


Fig. 5-16 Meteoroid Flux vs. Mass (In the Vicinity of Earth)

which is the maximum limit relative to Earth attainable at Earth's distance from the sun by a particle which is in the solar system. Whipple's estimated average meteoroid velocities vary from 15 km sec^{-1} to 28 km sec^{-1} for meteoroid visual magnitudes ranging from 0 to 25, with the higher mass having the higher velocity. The meteoroids in space on highly eccentric orbits around the sun can have velocities as high as 42.1 km sec^{-1} depending on whether the meteoroid collides head on with the interplanetary vehicle or catches up with the vehicle from the rear. A 30 km sec^{-1} meteoroid average velocity is used as a design basis for interplanetary operation. This is a relatively conservative assumption.

5.12.3 Density

Cometary meteoroids constitute about 90 percent of the total meteoroid influx. They are porous frangible and have a density of 0.05 gm cm^{-3}. The asteroidal meteoroids almost entirely account for the other 10 percent of the total meteoroid influx. The stoney asteroidal meteoroids have an average density of from 2.7 gm cm^{-3} to 3.5 gm cm^{-3}. For conservative design, a density of 3.5 gm cm^{-3} is assumed in shielding calculations for the interplanetary operations.

5.13.4 Hypervelocity Penetration

A variety of empirical and theoretical equations concerning the hypervelocity penetration can be expressed by

$$h = \gamma d \left(\frac{\rho_p}{\rho_t}\right)^{\phi} \left(\frac{v}{c}\right)^{\theta}$$

where

$$d = 2\left[\frac{3m}{4\pi\rho_p}\right]^{1/3}$$

expresses the diameter of the meteoroid in terms of its mass and density by assuming the meteoroid is spherical in shape. The symbols shown in these equations are tabulated below:

h	depth of meteoroid penetration in a semi-infinite target
γ	constant (varies with shielding material)
d	diameter of meteoroid
ρ_p	density of meteoroid
ρ_T	density of shielding material
V	velocity of meteoroid
C	sonic velocity in shielding material
ϕ, θ	constant (1/3 or 2/3)

Combining these equations, the meteoroid penetration depth can be expressed as a function of momentum of kinetic energy of the meteoroid, assuming the value θ to be 1/3 or 2/3 accordingly. Since there is a definite relationship between meteoroid mass, velocity and meteoroid flux ψ, the meteoroid penetration depth can be expressed directly as a function of meteoroid flux as

$$h = f(\psi)$$

For the same material, the shielding thickness to be just penetrated by a meteoroid will be 1.5 times thicker than the depth of penetration of a semi-infinite target. Single sheet aluminum shielding thickness required to prevent any penetration as a function of meteoroid flux is presented as Fig. 5-17, assuming the meteoroid velocity V to be 30 km sec^{-1}, meteoroid density ρ_p to be 3.5 gm cm^{-2} and Whipple's 1962 meteoroid mass-flux relationship.

The probability of no penetration is given by

$$p(o) = e^{-A \tau \psi}$$

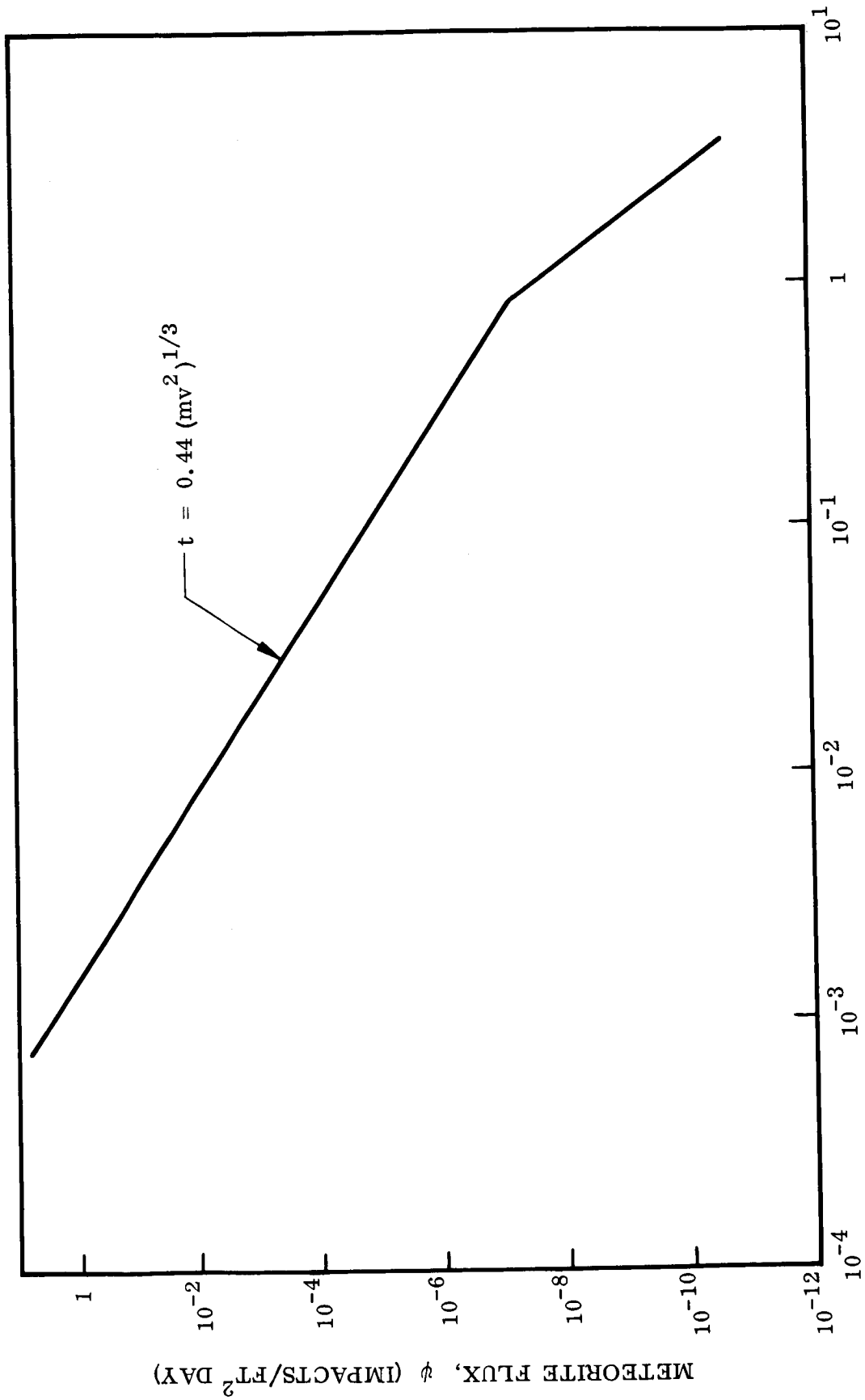


Fig. 5-17 Meteorite Flux Vs Single Sheet Aluminum Shielding Thickness

where

$p_{(o)}$	probability of no penetration
A	exposed area
τ	exposed time
ψ	meteoroid flux
e	base of napierian logarithms
ln	napierian logarithm of

For a mission time τ of 360 days, exposed area of 4.65×10^6 cm^2, the required single sheet thicknesses t associated with 90 percent, 99 percent, and 99.9 percent probabilities of no penetration are tabulated in the following table, which also shows the meteoroid diameters d corresponding to the penetrating fluxes.*

$p_{(o)}$	ψ	t	d
	p cm^{-2} day^{-1}	(cm)	(cm)
90 %	5.4×10^{-5}	2.54	0.23
99 %	6.0×10^{-6}	4.56	0.51
99.9%	6.0×10^{-7}	7.62	0.76

5.12.5 Bumper Design

Experimental results have shown, with an optimum bumper design, the weight saving over a single sheet shield can be as much as 66 percent to 80 percent. A 2.54 cm

*As this study went to press, current work indicated the momentum theory was, in fact, applicable and that the above thicknesses could be reduced by one half.

thick single sheet of shielding will thereby be reduced to 0.51 cm, i.e., 0.13-cm bumper with 0.38 shell. Theoretically, for the same material and total thickness, the greater the bumper spacing the lower the probability of penetration. The meteoroid bumper should not be so thin as to reduce its shattering effects and/or increase its fabrication and handling difficulties. With a constant bumper thickness, as the bumper spacing increases, the outside surface area will increase. The increased exposed surface area, in turn increases the probability of meteoroid penetration and the total weight. Bumper spacing of 2.54 to 5.08-cm is considered most practical from a design point of view.

The design approach of this preliminary investigation of the meteoroid protection for an interplanetary vehicle is purposely kept conservative where uncertainties exist. Hopefully, further research and actual deep space probes will provide information which will allow lighter weight shielding designs.

5.13 IONIZING RADIATION

It is expected that five types of ionizing radiation will constitute a hazard to manned interplanetary missions. These are cosmic primaries, solar flare protons, solar x-rays, and gamma and neutron radiation from nuclear propulsion engines and nuclear reactors supplying power for the operation of other systems.

The solar x-rays constitute a hazard only to crew members outside the vehicle in a space suit. The x-rays are not penetrating but are worthy of consideration to the extent of including a tin oxide layer or similar material inside the space suit to absorb these rays.

Nuclear propulsion engines will probably require 10,000 kg to 16,000 kg shielding to attenuate the neutron and gamma production to where the biological dose would be less than 10 rem. A very substantial amount of shielding is necessary, however, just to keep the propellant cool, and in some cases this amount is sufficient to provide effective

biological shielding. No intensive study was made of reactor shielding requirements. Methods of shielding propulsion reactors are relatively well understood. The same applies to the reactors used for vehicle power plants. In the design section, a calculation of a typical weight is given. The shielding required for such an application is a strong function of vehicle configuration.

Cosmic primaries will produce a dose of some 10 to 30 rads per year. The very high energies of these particles make shielding prohibitive. They are not expected to offer great danger except that a small portion of these particles are nucleons of atomic mass 12 and higher. These particles have, within a certain energy range, a very destructive way of being absorbed in tissue. One such particle can destroy a cylinder of tissue 1000 microns long and 20 microns in deameter by a "thindown" reaction.

The main radiation problem confronting manned interplanetary flight is the solar flare protons. These are streams of protons emitted by the sun during a (usually) optically observed flare. The unshielded dose from the largest of these events has been estimated at from 1000 to 8000 rads.

The proton producing flares may be roughly grouped into two catagories, relativistic (R) and non-relativistic (N-R). The relativistic flares produce protons with energies of several hundred mev and higher. There have been 7 to 9 of these — depending just how you count — in the last 21 years.

The non-relativistic flares occur about once a month during solar maximum and about once a year during solar minimum. Maxima (and minima) are about 11 years apart and the next maximum will come about 1969. The relativistic flares cannot be tied to a temporal cycle but show some indication that they occur between maxima and minima. The non-relativistic flares have protons with energies from 30 to some 300 Mev.

The terms relativistic and non-relativistic are somewhat arbitrary since all flares have different energy spectra, some steep and some relatively flat. The duration of such observable proton events is from 10 to 100 hours.

A question still unsettled — among many in this area — is the variation of dosage with radial distance from the Sun. The model that seems to best account for the observed phenomena would indicate about an inverse 2.5 power diminution. For conservatism, the inverse cube power is assumed to determine the Venus flux and the inverse square power to determine the Mars flux when extrapolating from Earth fluxes.

For this study it was desired to determine the probability of receiving a certain dose from solar flare protons as a function of mission duration and shielding thickness mainly, and to a certain extent as a function of mission trajectory and time of solar cycle. Several philosophical approaches are possible. One of the most obvious is to look at all missions within the last 21 years of the right length of time and calculate how many such missions would have received what dose. This should be done. If, however, one assumed that the occurrence is random, one can pick the mean number of days between events and simply calculate a Poisson distribution to see what percentage of the time a mission of N days would see M flares. The formula for this is

$$P_{(M)} = \frac{(N/D)^M}{M!} \left(\frac{1}{e}\right)^{(N/D)}$$

where

$P_{(M)}$	probability of exactly M events in N days
N	mission duration in days
D	average number of days between events
M	number of events

The above was computed separately for D = 1000 days (relativistic events), 365 days (non-relativistic events during solar minima), and 30 days (non-relativistic events during solar maxima.

The results are shown in Table 5-12.

Table 5-12
PROBABILITIES OF SOLAR PROTON EVENTS

	Nonrelativistic				Relativistic	
	Solar Max.		Solar Min.			
Probability	365 Days	600 Days	365 Days	600 Days	365 Days	600 Days
0.01	21	31	4	5	2	3
0.001	24	35	5	6	3	4
0.0001	27	38	6	8	4	5

At this point a completely unjustifiable assumption was made, i.e., that if there was P probability of A (N-R) flares and also P probability of B(R) flares, there was P probability of A(N-R) flares and B(R) flares. In fact, of course, the probability of both simultaneously is P^2, there are also other combinations with the probability P^2, however. There are a whole family of combinations of (A-X) (N-R) flares and (B + Y) (R) flares and also (A + X) (N-R) flares and (B - Y) (R) flares. Enough checking was done to assure that the method used was quite conservative.

The next question was what spectrum to assume for each flare. The simple but conservative approach used was that all (N-R) flares had the spectrum of the May, 1959 event as published in the LEM Work Statement, and that all (R) flares had the spectrum of the July, 1959 triple event as per Winkler's* data. The dose selected was 200 rads to the blood-forming organs which were assumed to be protected by 5 additional cm of tissue (water) relative to the surface dose.

On the basis of the above, Fig. 5-18 was drawn assuming no variation with radius from the Sun. Figure 5-19 was drawn using the same assumptions but assuming that the flux for the 600 day mission (Mars) was only 0.63 that of the comparable Earth flux and that the flux for the 365 day mission was 1.58 that of the comparable Earth flux.

*Private communication.

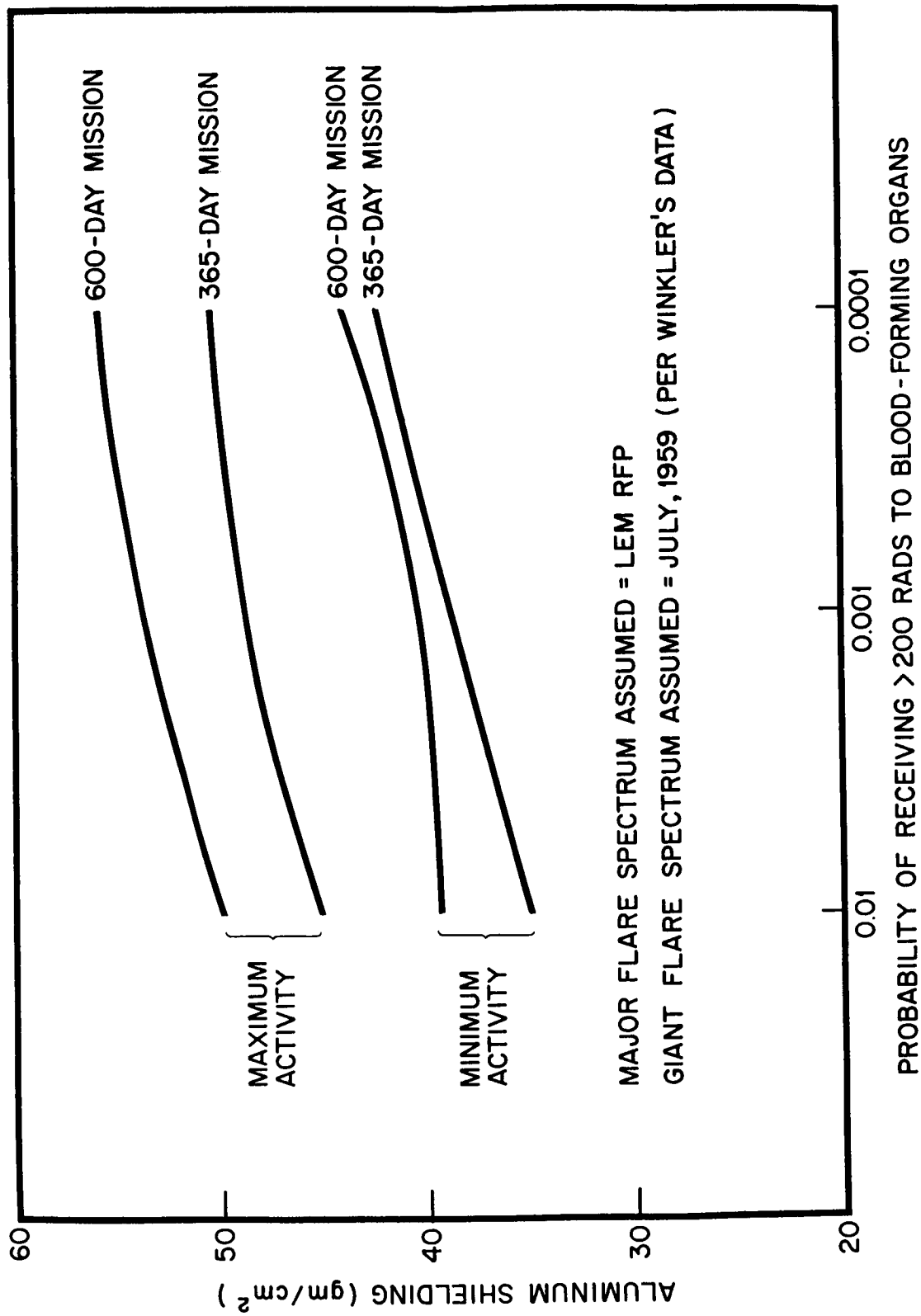


Fig. 5-18 Radiation Hazard

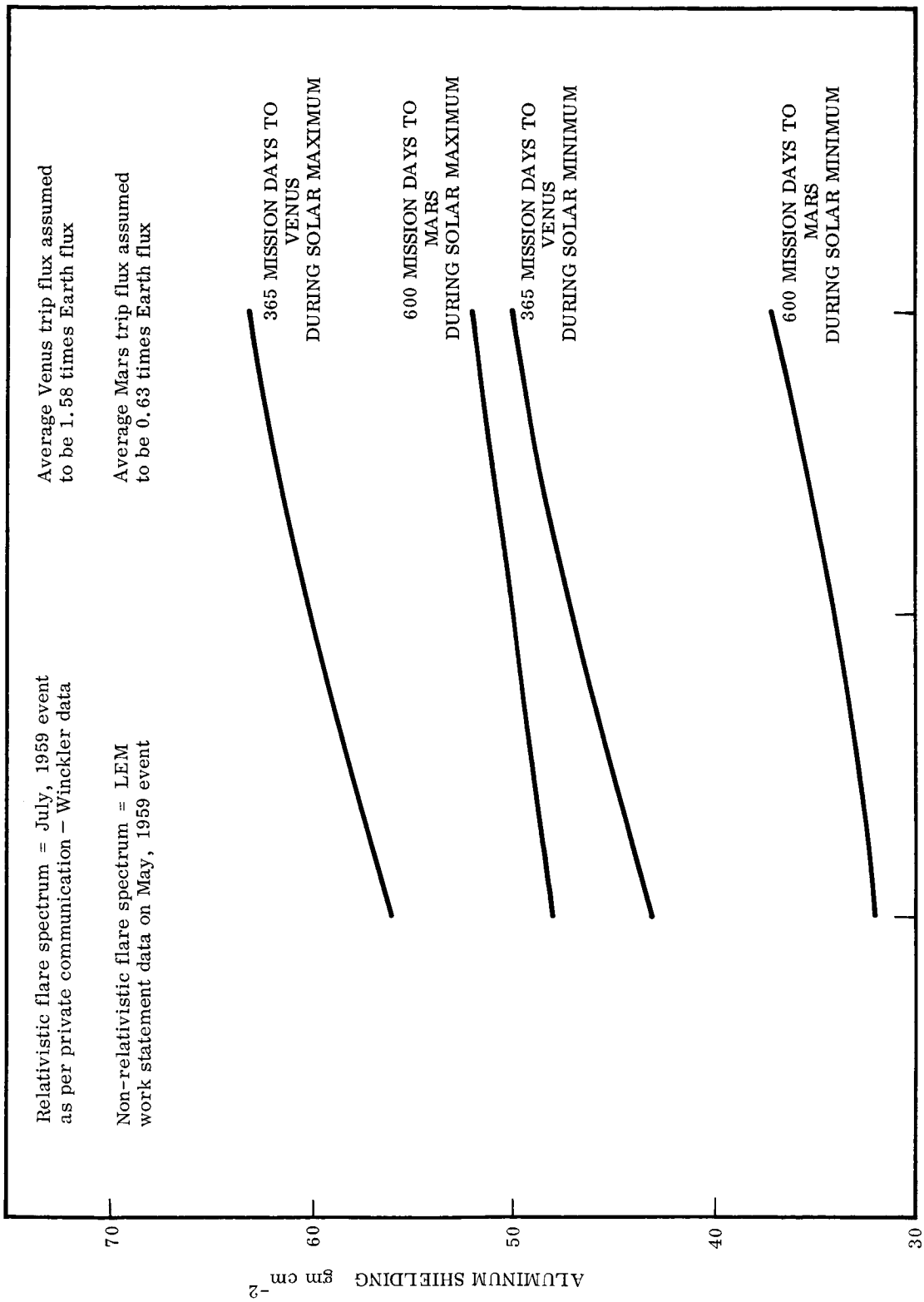


Fig. 5-19 Probability of Receiving > 200 Rads Aggregate to Blood-Forming Organs from Solar Flare Protons

Though not available when this work was done, the NLDB has a treatment of ERD (Equivalent Residual Dose) which purports to relate a chronic dose to an acute dose, i.e., the formula tells what the equivalent acute dose would be for a given chronic exposure. For 200 rads received in equal doses over a period of 600 days the equivalent acute dose was 14 rads or 21 rads if an assumed 0.1 rad per day from cosmic sources was added.

Some thought to the possibility of providing antibiotics, blood transfusions, and possibly even bone marrow transplants should be considered. Supplemental shielding for the eyes and possibly the spleen and/or bone marrow might be provided by shaped filled-bladder shields.

The biological effects of mixed radiation fields and long term low level exposures still need more investigation.

The shielding material considered in the study was aluminum. While water and polyethylene are somewhat, and hydrogen considerably more favorable on a gm cm^{-2} basis for shielding protons with minimal secondary production, geometry and structural factors favor aluminum. By geometry factor is meant the increase in total volume (and consequent mass) resulting from the use of a lower density material to provide a certain number of gm cm^{-2} of exposed surface area. For a spherical geometry, for instance, the following equation holds

$$M = \frac{4}{3}\pi\left[\frac{K^3}{\rho^2} + \frac{3K^2R}{\rho} + 3KR^2\right]$$

where

M total mass of shielding (gm)

K shielding required (gm cm^{-2})

R inside radius of shelter (cm)

ρ density of shielding material (gm cm^{-3})

Some idea of the effect of R upon the choice of shielding material is given by the following table

	Mass of Shield (gm)	
	R = 100 cm	R = 1000 cm
$K = 100\ g\ cm^{-2}$, $\rho = 3$	$4.11 \cdot 10^6$	$3.11 \cdot 10^8$
$K = 80\ g\ cm^{-2}$, $\rho = 1$	$4.83 \cdot 10^6$	$2.60 \cdot 10^8$
$K = 50\ g\ cm^{-2}$, $\rho = 1$	$21.50 \cdot 10^6$	$2.37 \cdot 10^8$

Since K is a function of the particular energy spectrum of the radiation flux against which one is trying to shield, it is difficult to generalize. K must also be determined considering secondary radiation production. It is apparent, however, that there is a definite limit to the savings available from going to lower K , lower ρ materials within the interesting range of R .

5.14 PRESSURE SUITS

It is assumed that very little use will be made of pressure suits outside the vehicle during fly-by missions. The main purpose of the pressure suit will be to provide a secondary emergency pressurization and thermal control system. Mobility problems are slowly being solved. The necessity for integration of the suit atmosphere with the cabin atmosphere, and the desirability of incorporation of some radiation protection features in suit design were mentioned. If shaped, filled bladders are used for supplemental partial body protection, these should be considered in the design of the pressure suit. It is expected that pressure suits including back-packs would weigh about 27 kg per man.

5.15 ACCELERATION STRESS

Ascent stresses will be well within permissible limits for reasons of propellant weight optimization. Reentry acceleration stresses will be the limiting factor it seems

tentatively, rather than the thermal pulse. Ten g is the design limit for brief reentry deceleration. This subject is probably the most thoroughly studied of space stresses and numerous articles have been published in Aerospace Medicine in the past 15 years. Again the NLDB is an excellent source of design limits. The FAA has evolved a number of restraint devices to moderate acceleration stress. The question of decreased ability to withstand acceleration stress following prolonged weightlessness was mentioned earlier.

5.16 SOUND AND VIBRATION CONTROL

The NLDB is again referenced for human tolerance levels. Ground testing of the vehicle will be necessary to determine the scope of the problem. High acoustical energy levels from motors will be experienced during take-off and during reentry from pressure fluctuations in the turbulent boundary layer. Tolerance levels are a function of frequency, amplitude, and duration.

High noise and vibration levels may weaken structure by resonance phenomena; switches may be thrown inadvertently and erroneous information may be sent to monitoring devices due to these phenomena.

5.17 WASTE HANDLING AND MICROBIAL CONTAMINATION

This topic was discussed in Empire Sterilization Requirements Status Report submitted earlier. Incineration of fecal waste would require about 1.2 kw average power consumption.

One of the main avowed goals of our space program is the investigation of extraterrestrial life forms. This topic is of interest, of course, for its own sake, but also as a possible source of information about the origin of all life.

Studies carried out at the Argonne National Laboratory, the School of Aviation Medicine, the University of California, and elsewhere have demonstrated the viability of Earth microbes in various space environments. In the light of this work, it becomes necessary to formulate sterilization concepts for spacecraft both going from and returning to Earth for three main reasons.

- To prevent the inadvertent "seeding" of life on an extraterrestrial body which would obscure subsequent exobiological studies
- To prevent a disastrous disturbance of the ecology of extraterrestrial bodies
- To prevent a disastrous disturbance of Earth's ecology including, perhaps, diseases of pandemic proportions

The use of utility water for cleaning, including weekly showers, would require about 200 kg of water plus about 1 kw per day for distillation. In a completely open system, this item could amount to 13,000 kg for a 600 day mission.

5.18 SENSORS AND WARNINGS

Some of the more important sensors and warnings needed — both visual and audio — are the following:

- O_2 partial pressure sensors
- N_2 partial pressure
- Total pressure sensors
- Humidity sensors
- CO_2 partial pressure sensors
- Flow rate meters
- Ionizing radiation monitors
- Radiator fluid leakage sensors
- Methane, ammonia, hydrogen, and possibly other containment concentration sensors
- Fire sensors
- Temperature monitors of sorbent beds, catalytic burners, cabin gas and others

Warnings are desirable to indicate the necessity for action in the presence of a malfunction or, where possible, an impending malfunction of any subsystem or component. Types of audio signals now in use include bells, buzzers, horns, sirens, and tones. Voice recordings are recommended.

5.19 CREW SUPPORT EQUIPMENT

This topic is defined to include the following:

Crew Support Equipment

	3 Men 365—600 Days Mass (kg)
Medical facilities	20.0
Fire equipment	10.0
Bedding, Clothing	15.0
Exercise and recreation equipment	20.0
Food preparation and eating equipment	5.0
TOTAL	70.0

Values are adopted principally from the Handbook of Astronautical Engineering, ed. by Heinz H. Koelle, 1st ed., McGraw-Hill, 1961.

5.20 RESEARCH AND DEVELOPMENT AREAS

The following list indicates the more important areas requiring research and development before a manned interplanetary mission is launched; a more accurate statement might be ... is launched by a booster expected to be available in 1970.

- Human Engineering
  - Task Analysis & Cabin Design
    - Normal Flight Functions
      - Flying
      - Housekeeping
      - Data Gathering & Processing

Emergency Modes

Man-Machine Division of Labor

Training and Selection for Exposure to Long-Term Confinement

Use of Drugs, Autohypnosis

- Atmosphere Selection and Gas Supply

  Long-Term Exposure to Exotic Environments

  Acclimatization

  Fire Control

  Leakage After Launch, Vacuum, Thermal Cycling, Etc.

  Partial Pressure Sensors

  Development of Emergency Decompression Procedures

- Carbon Dioxide Control

  Long-Term Exposure to 1 to 12 torr—During and Post Exposure

  Development of Electrodialysis and Freeze-Out Methods for Integration with CO_2 Reduction Devices

- Trace Contamination — Biological and Nonbiological Origin

  Cyclic Buildup for Particular Vehicle

  Toxicity

  Methods of Removal

- Heat and Humidity Control

  Transient Limits for Complex Thermal Inputs Especially With Other Stresses

  Variable Thermal Resistance Devices

  Utilization and Improvement of Superinsulation

  Develop Heat Pumps-Efficiency, Reliability, Zero g Capability

  Thermoelectric Cooling for Zero g Particularly for Low Power Penalty Applications

  Improve Water Separators for Zero g Applications

- Diet
  - Study Individual Needs of Prospective Crew
  - Study Nutrient Losses and Toxic Buildups in Closed Cycles
  - Zero g Preparation and Consumption Techniques
  - Long Term Dehydrated Storage, Maintaining Palatability

- Physico-Chemical Regeneration
  - Urine Regeneration
    - Long Term Reliability-Mechanical, Biochemical, & Microbiological
    - Integration With Vehicle – Particularly Heat Available & Power Penalties
  - Carbon Dioxide Reduction
    - Integration With CO_2 Removal Method & With Electrolytic Cell
      - Transfer of CO_2 to Reactor Storage
      - Transfer of H_2 to Reactor Storage
      - Purification & Concentration of Reactants
    - Flow of Reactants into Reactor
    - Catalyst Development – Preferential Reaction
    - Analysis & Development of Methane Pyrolizer
    - Byproduct Gas Build-Up
    - Study of High Temperature vs High Power, i.e., Safety vs Efficiency
    - Integrated Design

- Biological Regeneration
  - Matching of Stoichiometric Relations of CO_2 and O_2
  - Determination of Nutrition and Toxicity
  - Determination of How Much Recycling of the Liquid Phase Necessary
  - Diet Supplements Necessary-Amino Acids, Vitamins, and Minerals
  - Palatability
  - Zero g Problem of Gas Diffusion
  - Urine Filtering Necessary
  - Improve Action Spectrum

- Weightlessness, Artificial g, Coriolis
  - Long Term Physiological Effects of Weightlessness
  - Amelioration by Exposure to Partial g, for Part or Full Time
  - Amelioration by Exercise
  - Canal Sickness Limits in Gravity-Free Field
  - Crew Practice Under Simulated Flight Conditions

- Ionizing Radiation
  - Space Environment
    - Flare Frequency and Energy Spectrum-Time Dependence
    - Flare Flux Dependence Upon Distance From Sun
    - Approach to Probability of M Flares in N Days
    - 11 Year Cycle Reliability
    - Flare Predictability
    - Attenuation by Planetary Magnetic Fields and Atmospheres
  - Biological Effects
    - Long Term Exposure to Low Flux, High Energy Particles of $Z \geq 6$
    - Chronic Effects of High Dosage Over Extended Times
    - Mode of Interaction With Tissue of Particles of Energy > 500 Mev and Complex Radiations
  - Radiation Shielding
    - Interaction of Particles of Energy > 500 Mev Wtih Shielding Materials — Experimental and Analytical
    - Configuration Studies to Determine Amount of and Suitability of Otherwise Necessary Materials Available for Particular Missions
    - Use of Partial Body Shielding
    - Integrated Shielding Designs With Nuclear Propulsion and APU's
    - Radiation Monitoring Devices

- Meteoritic Phenomena
  - Determination of Deep Space and Planetary Vicinity Fluxes
  - Determination of Density and Velocity Spectrums

Determination of Penetration Mechanisms and Advantages of Double Wall Construction

Leak Detection and Repair Techniques

- Decompression and Pressure Suits

  Development of Mobility Under Internal Pressurization of 180 to 300 Torr at Reduced g

  Ionizing Radiation Resistance

  Thermal Control – High Weight of Convection vs Discomfort of Evaporative Cooling

  Development of Self-Sealing Suits

  Acclimatization Benefits and Procedures

- Acceleration Stress

  Fairly Well Delineated Except Wtih Respect to Combined Thermal, Pure O_2 Atmosphere, Prehistory of Reduced g, Hypoxia, and Decompression

- Sound and Vibration Control

  Long Term Resonance Phenomena

- Waste Handling and Sanitation

  Wet vs Dry Cleaning Procedures

  Sterilization of Wastes

  Dehydration & Incineration

- Sterilization of Probes for Flybys. Sterilization of Vehicle and Men Going to and Returning From Planetary Contacts. Determination of Probability of Contamination vs Method of Sterilization

- Sensors and Warnings

  Partial Pressure Sensors $-O_2, N_2$, CO_2, H_2O Trace Contaminations

- Crew Support Equipment

  Medical Facilities – Resuscitators, Diagnostic Computers, "Cyborgs"

  Fire Fighting Equipment Design

  Housekeeping, Exercise, and Recreation Equipment Design

- Emergency Mode Operation and Reliability

  Practice Under Simulated Emergency Conditions on the Ground and in Space

  Determination of Increases in Reliability of System From Modular Design, Back-Up and Redundant Systems, Repair Capability, Standardization of Parts

  Abort Procedures

- Test of Integrated System Under Simulated Flight Conditions on Ground and Actual Conditions in Space

Studies carried out by the Life Support Systems Research Group at LMSC during the last few years have repeatedly indicated the existence of an important gap in communication between physical, biological, and social scientists who are knowledgeable of the requirements of a man-supporting space system and the engineers responsible for the design of such a system.

In spite of the obvious importance of further basic experiments to determine more precisely the nature of the radiation and meteoritic environments, man and material responses to these environments, long term physiologic effects of weightlessness, and coriolis tolerances, the dissemination of extant knowledge in these and other fields is a problem of at least comparable magnitude.

The need for men or groups willing and able to undertake the unglamorous and sometimes thankless liaison activities between science and engineering is worthy of great emphasis. The development of such groups by NASA and industry could be of great importance to the Manned Space Program.

5.21 REFERENCES

5-1. T. C. Ruch and J. F. Fulton (Eds.), Medical Physiology and Biophysics, 18th ed., W. B. Saunders, 1960

5-2. A. Hurtado and R. T. Clark, Jr., "Parameters of Human Adaptation to Altitude," in Physics and Medicine of the Atmosphere and Space, edited by O. O. Benson, Jr., and H. Strughold, Wiley, New York, 1960

5-3. Aeromedical Laboratory, Handbook of Respiration, edited by D. S. Dittmer and R. M. Grebe, WADC TR-58-352, Aug 1958

5-4. H. Rahn and W. O. Fenn, A Graphical Analysis of the Respiratory Gas Exchange, The American Physiological Society, Washington, D.C., 1955

5-5. U. T. Slager, Space Medicine, Prentice-Hall, 1962

5-6. U. C. Luft, "Altitude Sickness," in Aerospace Medicine, edited by H. G. Armstrong, Williams and Wilkins, 1961

5-7. G. F. Gell, "Breathing Oxygen," in Aerospace Medicine, edited by H. G. Armstrong, Williams and Wilkins, 1961

5-8. B. Balke, Human Tolerances, Federal Aviation Agency, Civil Aeromedical Research Institute, Oklahoma City, Apr 1962

5-9. R. W. Bancroft, "Medical Aspects of Pressurized Equipment," in Aerospace Medicine, edited by H. G. Armstrong, Williams and Wilkins, 1961

5-10. U. C. Luft, "Physiological Limitations in Cabin Environments and Human Adaptations," in Physics and Medicine of the Upper Atmosphere, edited by C. S. White and O. O. Benson, Univ. of New Mexico Press, 1952

5-11. T. E. Morgan et al., "Observations in the SAM Two-Man Space Cabin Simulator, II. Biomedical Aspects," Aerospace Medical Journal, July 1961, pp. 591–602

5-12. R. P. Haviland, "Air for the Space Ship," Journal of Astronautics, Vol. 3, 1956, p. 31

5-13. J. H. Comroe, Jr., and R. D. Dripps, American Journal of Physiology, Vol. 142, 1944, pp. 700–707

5-14. W. O. Fenn et al., Am. Journal of Physiology, Vol. 146, 1946, p. 637

5-15. J. H. Comroe, Jr., et al., Fed. Proceedings, Vol. 9, 1950, p. 602

5-16. H. G. Clamann, "Decompression Sickness," in Aerospace Medicine, edited by H. G. Armstrong, Williams and Wilkins, 1961

5-17. R. S. Thomas and Y. S. Li, Extended Lunar Operations Feasibility Study, Second Quarter, 1962, TXA 1339/LMSC A051923, 25 June 1962

5-18. H. A. Klein, The Effects of Cabin Atmospheres on Combustion of Some Flammable Aircraft Materials, WADC TR 59-456, April 1960

5-19. J. L. Heldenbrand, "Selection of the Closed System Atmosphere," in Cloud Circuit Respiratory Systems Symposium, WADD TR 60-574, August 1960

5-20. Personal communication from F. Greene, Air Research, Los Angeles, Calif.

5-21. Garrett Corp. AiResearch Capabilities and Experience in the Field of Aerospace Cryogenics, Los Angeles, 1962

5-22. Garrett Corp., Cryogenic Propellant, Feed Systems for Electrothermal Engines, by J. R. Frey, J. S. Taylor, and G. A. Burgess, AE-1952-R, Nov 1961

5-23. C. S. Coe, et al., Atmospheric Control Systems for Space Vehicles, ASD-TDR-62-527, Jul 1962

5-24. C. S. Coe, J. Rousseau, and A. Shaffer, Analytical Methods for Space Vehicle Atmospheric Control Processes, Part II, ASD-TR-61-162, Jul 1962

5-25. K. E. Schaefer, "A Concept of Triple Tolerance Limits Based on Chronic Carbon Dioxide Toxicity Studies," Aerospace Medicine, Vol. 32, No. 3, 1961, pp. 197–204

5-26. Hamilton Standard, Carbon Dioxide Control Systems for Medium Duration Missions, HSER 2375, Windsor Locks, Conn., Feb 1961

5-27. Webb Associates, NASA Life Sciences Data Book, Yellow Springs, Ohio, Jun 1962

5-28. J. M. Smith, R. B. Jagow, and L. A. McKellar, "Thermal and Atmospheric Control for Manned Interplanetary Vehicles," (paper given at the Aeronautical Systems Div. Thermal and Atmospheric Control Symposium, Wright-Patterson AFB, 12-13 Feb 1963

5-29. W. G. Camack and D. K. Edwards, "Effect of Surface Thermal Radiation Characteristics on the Temperature Control Problem in Satellies," in Surface Effects on Spacecraft Materials, ed. F. J. Clauss, John Wiley & Sons, New York

5-30. L. A. McKellar, "Effects of Spacecraft Environment on Thermal Control Materials Characteristics," in Spacecraft Thermodynamics Symposium, ed. G. A. Etemad, Holden-Day, Inc., San Francisco, 1962, pp. 99–128

5-31. R. E. Gaumer and L. A. McKellar, Thermal Radiative Control Surfaces for Spacecraft, Lockheed Missiles & Space Co., LMSD 704014, Sunnyvale, Calif. Mar 1961

5-32. K. Goetzel and J. B. Singletary, Eds., Space Materials Handbook, Lockheed Missiles & Space Co., Sunnyvale, Calif. Jan 1962

5-33. F. S. Johnson, Ed., Satellite Environment Handbook, Stanford University Press, Stanford, California, 1961

5-34. R. E. Gaumer, F. J. Clauss, M. E. Siber, and C. C. Shaw, Materials Effects in Spacecraft Thermal Control, Lockheed Missiles & Space Co. LMSC 704019, Summyvale, Calif., Nov 1960

5-35. D. K. Bailey, "Time Variation of the Energy Spectrum of Solar Cosmic Rays in Relation to the Radiation Hazard in Space," Journal of Geophysical Research, Vol. 67, No. 1, Jan 1962

5-36. G. P. Kuiper, "Planetary Atmospheres and Their Origin," in The Atmospheres of the Earth and Planets, University of Chicago Press, Chicago, 1952, p. 308

5-37. W. M. Sinton and J. Strong, Astrophysical Journal, Vol 131, 1960, 470–490

5-38. T. M. Olcott and M. Ratner, "Analytical and Experimental Investigation of Self-Thermostatic Effects," Space Vehicle Thermal and Atmosphere Control Symposium, Wright-Patterson Air Force Base, Ohio, 12–18, Feb 1963

5-39. J. M. Smith, R. B. Jagow, and G. R. Werth, "Thermal and Atmospheric Control in Bioastronautic Systems," in Spacecraft Thermodynamics Symposium, ed. G. A. Etemad, Holden-Day, Inc., San Francisco, 1962

5-40. B. J. Loret, Optimization of Manual Orbital Satellites Vehicle Design With Respect to Artificial Gravity, ASD TR 61-688, Dec 1961

Section 6

GUIDANCE AND CONTROL

by

J. A. Carson

Section 6
GUIDANCE AND CONTROL

6.1 SUMMARY

To establish guidance techniques and requirements, the interplanetary mission has been divided into three phases; (1) injection, (2) midcourse, and (3) planet approach. The midcourse and planet approach phases are repeated on the return leg of the journey. Preceding sections have described feasible methods of obtaining guidance data by measurements made from the vehicle, a self contained system incorporating specific instruments has been defined, and an on-board guidance data-processing technique has been outlined. Trajectory corrections are assumed to be impulsive.

Guidance measurements for both the midcourse and planet approach phases are based on triangulation using optical angles and time. At least three angles and the time of measurement are required to establish a position fix. A minimum of two successive position fixes establish the required corrective impulse. Redundant data points are desirable to minimize random errors. For the midcourse phase, angles are measured between pairs of celestial bodies, at least one of which must be a planet or the Sun. As the target planet is approached,the scheme is shifted to one in which the angle subtended by the planet disc, and the angles between two stars and the planet center are measured. The vehicle trajectory may be computed directly from successive position fixes, using the equations of motion in a central force field. Linearized perturbation equations, however, appear to be sufficiently accurate for the midcourse phase, and reduce the time required to compute velocity corrections. Inertial guidance is used during boost to injection and for corrective thrust periods.

The selected guidance system includes star trackers, a field scanning telescope, an accurate time reference, an inertial platform with platform mounted accelerometers,

attitude control sensors and servos, and a computer. Total system estimated weight is 122 kg, volume 0.3 m^3, and maximum power requirement of 380 w. During quiescent periods, between navigation fixes, the guidance system power drain would be reduced to the order of 50 w. Addition of a manually operated space sextant would probably increase the weight by about 10 kg.

A number of important functions should be delegated to the human navigator. In addition to making manual sextant observations, the navigator may assist in automatic measurements by initiating navigation fix sequences and avoiding readings based on false targets. He will probably be required to make instrument substitutions and minor repairs to the system. He may also perform in-flight calibration of instruments using comparative checks or autocollimation techniques.

System performance evaluation is based on the integrated corrective impulse requirement, as well as the resulting position error at arrival. Error analyses indicate that a system of this type could provide a pericenter error on the order of ± 8 km at the target planet, and that an integrated corrective velocity impulse of less than 1000 m/sec would be required for an Earth-Mars round trip.

6.2 INTRODUCTION

A constantly increasing number of new techniques and instruments are being proposed for use in self-contained space navigation systems. Some of these advanced techniques, for example, "Mosaic Guidance" (Ref. 6-1, 6-2) are already available in working models but are limited by low resolution, poor sensitivity, and reliability problems. More exotic techniques include range rate measurement with template spectroscopy (Ref. 6-3), and optical angle rate sensing instruments. The availability of such techniques in the form of reliably operating navigation instruments is difficult to predict. The guidance system development in the following sections will, in general, rely on a more conservative extension of currently available techniques.

The missions used to define guidance requirements are manned trips to either Mars or Venus during the period of 1970–1975. Individual trips may be a pass near the target planet, or a stopover in a parking orbit. On return to Earth, atmospheric braking will be used to decelerate the spacecraft. The primary navigation equipment is to be self-contained within the spacecraft and capable of functioning without cooperative signals from external sources, once the spacecraft has been injected into the outward bound heliocentric orbit.

The study is divided into four parts; requirements, mechanization, guidance equations, and system physical characteristics. Midcourse and planet-approach guidance problems have been emphasized at the expense of ascent guidance. The latter is similar to ascent guidance requirements for current manned Earth orbit missions or the unmanned interplanetary probes, and has been treated extensively elsewhere.

6.3 NAVIGATION AND GUIDANCE ACCURACY REQUIREMENTS

6.3.1 Definition of the Problem

In order to develop guidance concepts and accuracy requirements, the spacecraft mission is divided into several phases, or parts, characterized by different guidance schemes and mechanizations. These phases are boost, or injection; midcourse, and terminal approach. On the round trip missions to which this study is directed, the midcourse and terminal approach phases are repeated on the return leg of the trip. Accuracy required of the navigation and guidance system is fixed by a compromise between the maximum permissible errors, and the maximum energy allowance for corrective maneuvers.

Trajectory errors in position and velocity are the combined results of factors such as uncertainties in the solar system dimensions, uncertainty in the propagation speed of electromagnetic energy, and stellar parallax due to the finite velocity of light, as well as guidance and control system performance. The following discussions deal

mainly with trajectory errors resulting from accuracy limitations of the guidance system. Stellar parallax due to changes in the vehicle position or vehicle velocity is a correctible bias error, provided the approximate velocity and position are known.

The approach adopted here is to demonstrate, through use of available error analysis results, the feasibility of mechanizing midcourse and approach guidance with self-contained equipment capable of meeting the accuracy requirements with sensibly small energy expenditures for corrective maneuvers.

6.3.2 Injection Errors

Boost phase guidance, resulting in velocity errors at the point of thrust termination, determines initial conditions for the midcourse flight phase. The most accurate inertial guidance systems, currently available, are capable of providing cutoff velocity errors of between 1 and 2 fps (Ref. 6-4). A convenient way of interpreting this error is available in the form of miss distance coefficients, which express the miss distance at the target planet, in terms of the thrust termination errors.

Error coefficients for Earth-Mars, and Earth-Venus flights have been published by a number of investigators, including Pitman (Ref. 6-4) and Kierstead (Ref. 6-5). Using a solar system model with circular coplaner planet orbits, Kierstead presents results for transfer-orbit central angles from 90 to 180 degrees. The Earth-Mars coefficients, reproduced in Fig. 6-1, show a range of values from 2000−7000 miles/ft/sec (10,600−37,000 km/m/sec) with the minimum value occurring at a 167-degree transfer angle, and the maximum at 180 degrees. The Earth-Venus error coefficients were found to be similar with the minimum error occurring at a transfer angle of 164 degrees. Calculation of these errors assumes the target planet to have zero mass. Both in-plane and out-of-plane velocity error components are included.

These error coefficients indicate that an injection velocity error of about 1 to 2 fps would be marginally adequate without midcourse guidance for a Mars or Venus flyby

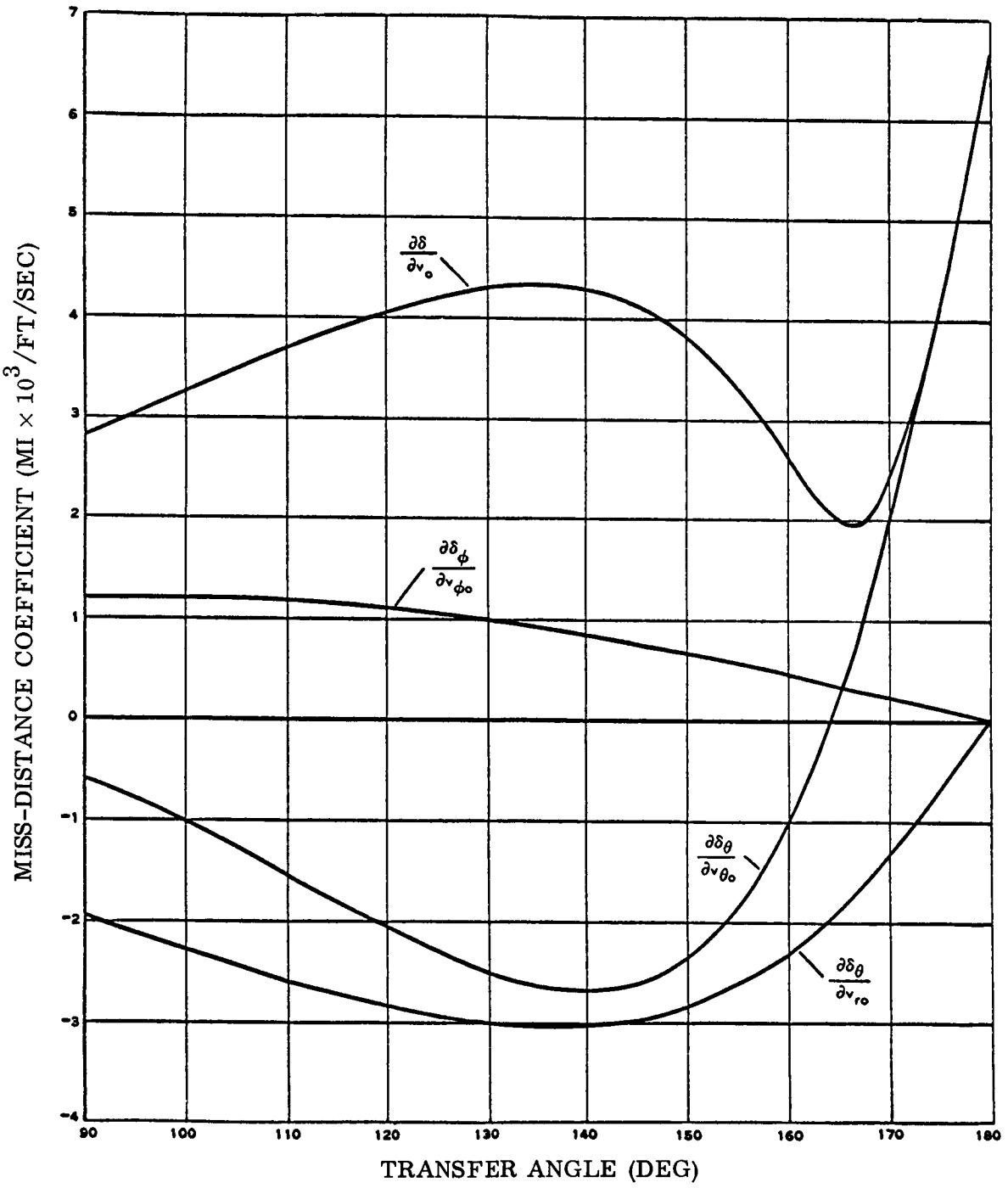


Fig. 6-1 Initial-to-Terminal Error Coefficients

provided optimum trajectories or transfer orbits are chosen and that a terminal correction is applied. The larger values, however, are excessive and this restriction on choice of transfer orbit is highly undesirable for manned trips. Earth-based tracking can be used to reduce these errors by a post injection command but an on-board midcourse guidance system will be needed after the Mars or Venus passage and will therefore be available on the outbound leg. The effect of injection velocity errors on midcourse position is shown in Fig. 6-2.

Data presented in Fig. 6-3 indicates the influence of injection velocity errors on the midcourse correction impulse for an Earth-Mars trip. This data is a result of the midcourse guidance study by Friedlander and Harry (Ref. 6-6) and the figures presented are based on statistical data adjustment scheme for eliminating or reducing random sighting errors. Instrument accuracy (sighting error) is treated parametrically with values of 10,. 40, and 120 sec of arc. The implication of this curve is that for a spacecraft equipped with midcourse guidance having an accuracy of 10 sec of arc, or better, the injection velocity accuracy requirements may be considerably relaxed without a severe increase in the midcourse corrective velocity. For example, if the injection velocity error is increased from 40 to 80 fps (12 to 25 m/sec), the total maximum ΔV increases from 150 to 250 fps (46 to 76 m/sec). Statistical median values are affected even less.

6.3.3 Midcourse Guidance Accuracy Requirements

In order to establish first order accuracy requirements for the on-board navigation equipment, the measurement techniques will be assumed to make use of optical star trackers, sextants, and star field scanning devices. Optical instruments appear the most promising for self-contained system on-board measurements by the early 1970's. Other possible techniques are discussed in the section on mechanization.

Results of the data adjustment and guidance logic techniques study by Friedlander (Ref. 6-6) are directly applicable to the determination of first order midcourse

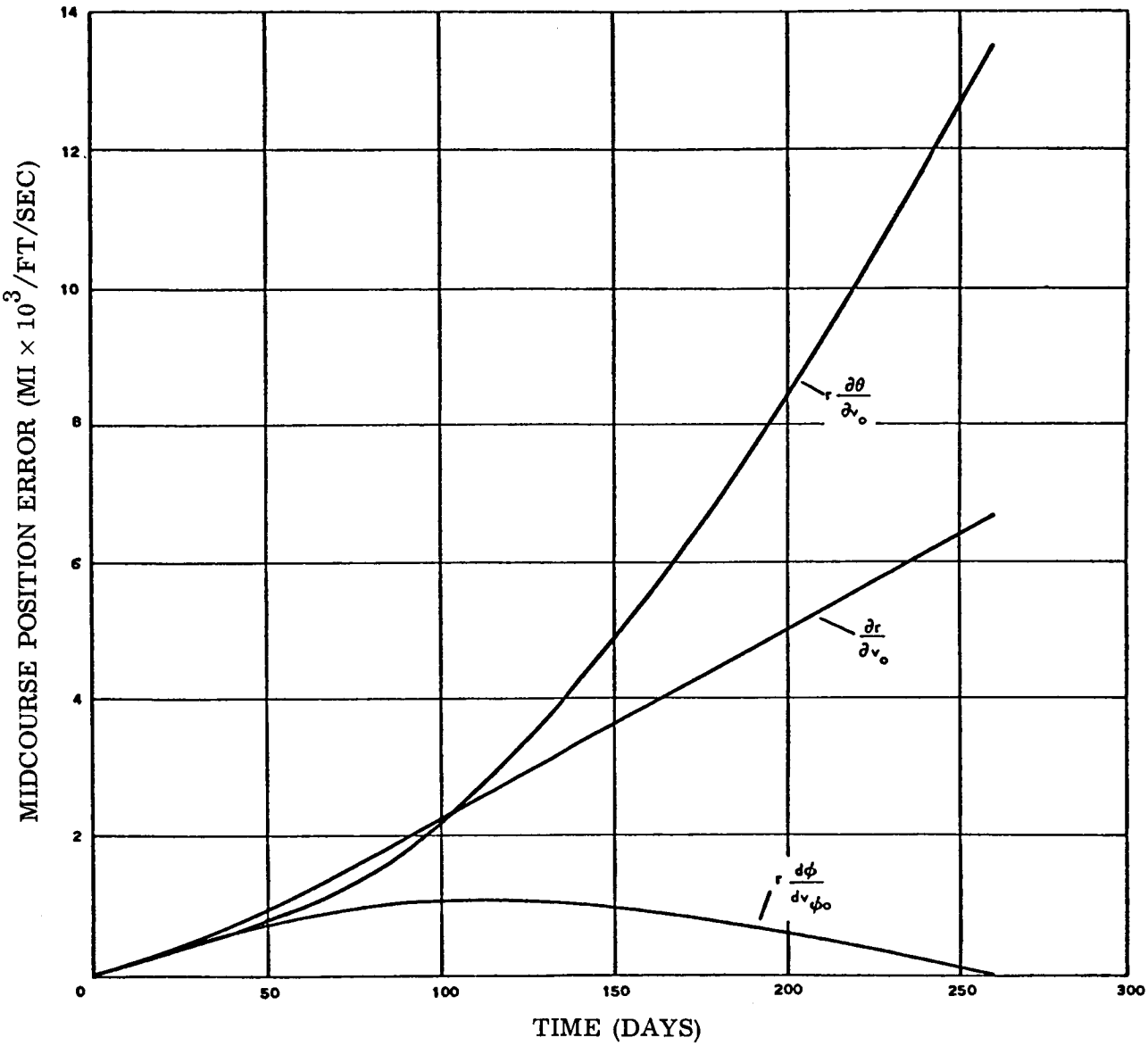


Fig. 6-2 Effect of Velocity Errors on Midcourse Position

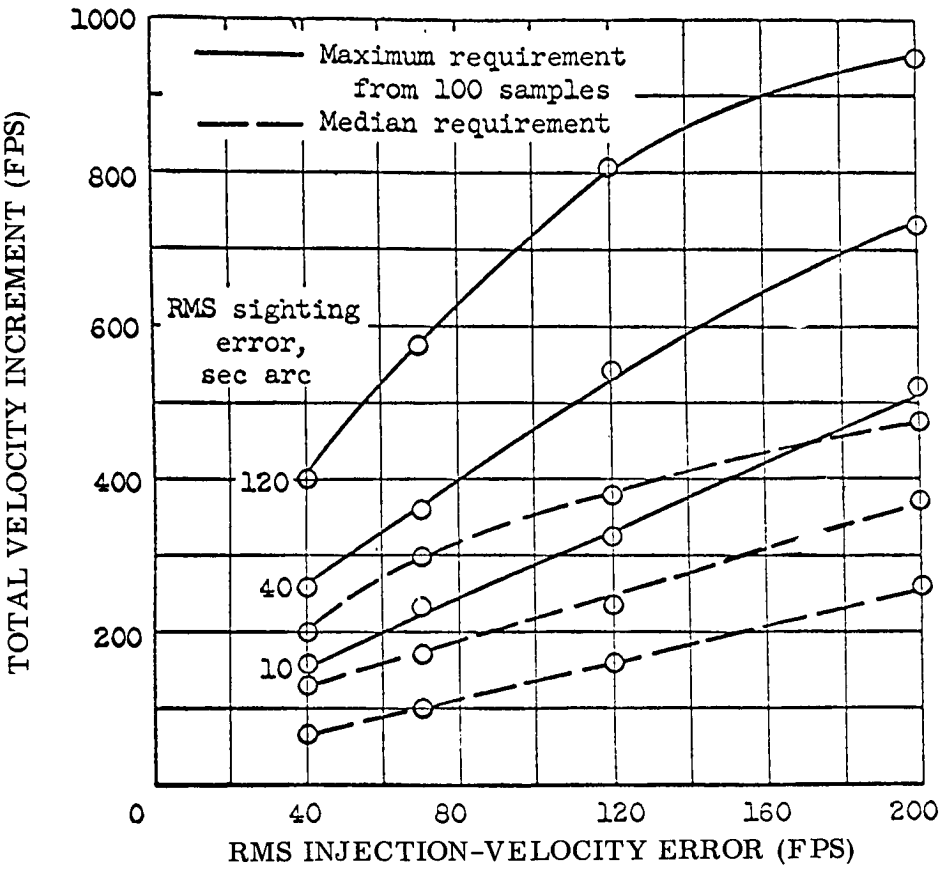


Fig. 6-3 Effect of Injection Velocity Error on Δv Requirements for Midcourse Correction (Ref. 6)

accuracy requirements. The effect of guidance accuracy on the system performance is interrelated to the number of corrections required, total-corrective velocity ΔV, and the initial condition velocity error (injection velocity error). For a 10-sec of arc (1σ, rms) sighting error, Friedlander and Harry simulated a Mars trip using statistical data smooting and a Monte Carlo random error injection scheme. Study results of error characteristic versus time are presented in Figs. 6-4 and 6-5. These figures illustrate that corrections based on fix data early in the trip are highly inaccurate and also that the data adjustment or smoothing technique provides a large improvement in the accuracy of a position fix. Figure 6-4 shows the rms error in determining or predicting the minimum pass distance at the target planet, neglecting planet gravity. This figure may be interpreted to mean that if a single correction, based upon on-board optical instruments, were applied ten days after departure from Earth, the vehicle would miss Mars by about 150,000 miles (240,000 km). Nine subsequent fixes ending at 180 days with velocity corrections interposed, reduce this error to about 600 miles (960 km). Velocity corrections in this model are made so that the corrective maneuver does not exceed the prediction uncertainty thus avoiding overcorrection, and using a velocity correction decision scheme with minimum and maximum ΔV limits of 10 fps and 1000 fps (3 mps and 10 mps) respectively. Table 6-1 presents a summary of the assumptions used for the simulation made to obtain the above results.

The measurement scheme for position determination used by Friedlander and Harry consists of optical observation of angles between three selected paris of celestial bodies, and a clock to indicate the reference time for the sightings. Reference bodies used in the simulated runs were the Sun, two stars, and a planet. The Sun was used in all measurements, and the planet (Mars or Earth) and stars varied to provide the best angle relationship for the planets; either Mars or Earth was used whichever was closest except when the Sun-planet angle was less than 15 degrees.

The miss distance obtained for 100 sample runs with this midcourse scheme, and a sighting error of 10 seconds of arc, had a median value of 600 miles (960 km) and a maximum of 2050 miles (3300 km) with a 90 percent probability of not exceeding

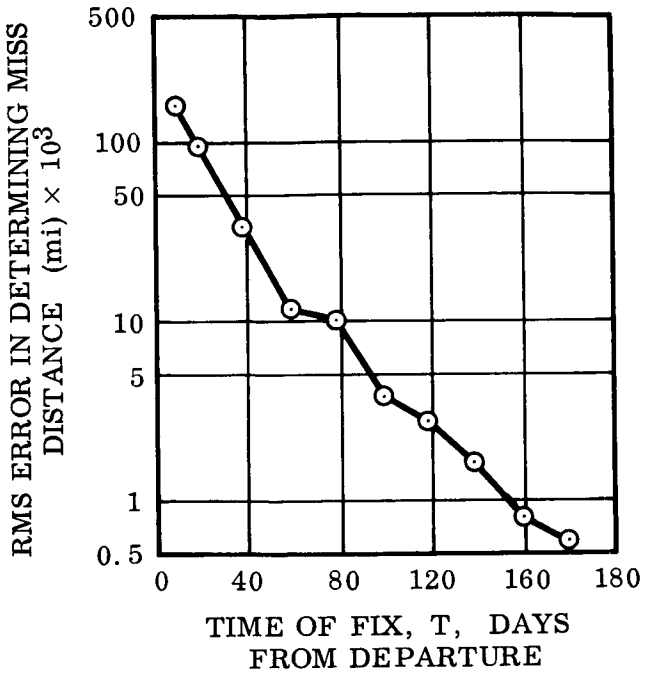


Fig. 6-4 Error Characteristic for Miss Distance. (Ref. 6-6)

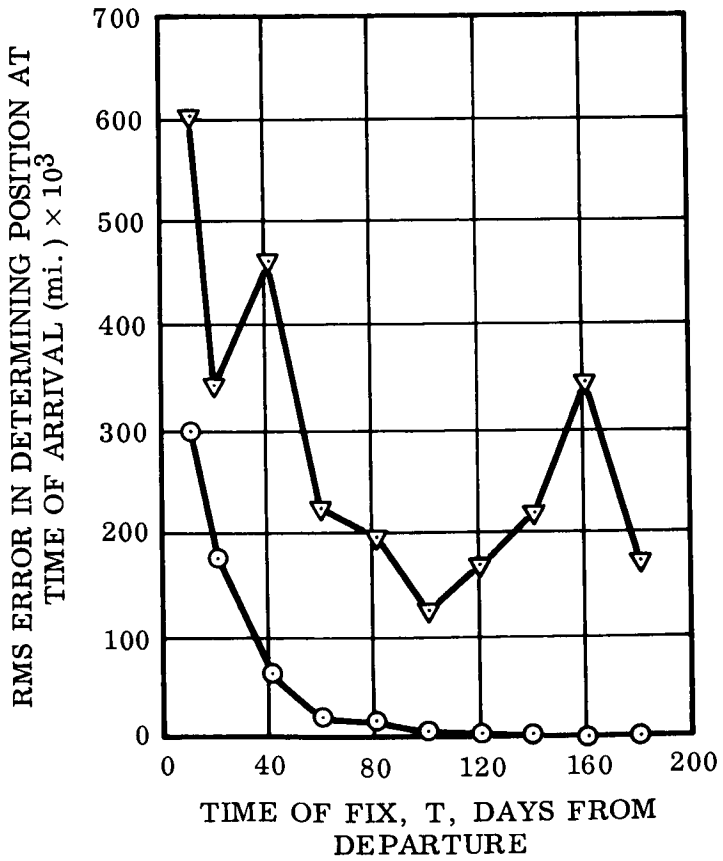


Fig. 6-5 Error Characteristic for Position Deviation at Arrival. (Ref. 6-6)

Table 6-1

VALUES ASSUMED IN REFERENCE CASE
FRIEDLANDER & HARRY (REF. 6-6)

	Parameter	Assumed Value
I	Reference Trajectory	
	Launch Data	13 Dec 1964
	Trip Time (days)	192.2
	Relative Velocity at Earth, (fps)	12,989 (3970 mps)
	Eccentricity	0.25404
	Semi-major axis, (AU)	1.3059
	Inclination to ecliptic, (deg)	0.556
	Relative velocity at Mars, (fps)	18,385 (5600 mps)
	Miss distance	0
II	Initial Conditions & Measurement Errors, σ, rms	
	Injection Velocity—x, y, z components (fps)	70 (21.4 mps)
	Angle Error, (sec arc)	10
	Clock Error, (%)	0.001
	ΔV Magnitude Error, (%)	0.1
	ΔV Direction Error, (sec arc)	20

1200 miles (1900 km). When the sighting error is increased to 40 sec of arc, results indicate a median miss distance of 1200 miles (1900 km) and a maximum of 4500 miles (7250 km). Thus it can be seen that the relationship between miss distance and sighting accuracy is not linear.

The way in which corrective velocity (ΔV) requirements for the sample cases were influenced by instrument sighting accuracy, and injection velocity errors, is shown in Fig. 6-3. These results demonstrate that only moderate values of total impulse

per unit mass are required for corrective maneuvers when a sighting error of 10 sec arc is available, even for large injection velocity errors. Maximum number of corrective impulses required for the total trip was six with a 10-sec arc sighting accuracy, and nine with a 40-sec arc sighting accuracy.

6.3.4 Planet Approach Guidance Accuracy

As the spacecraft approaches the target planet, either for flyby or atmospheric entry, the orbit is transposed from an elliptic heliocentric to a hyperbolic planet-centered trajectory. During the approach it is appropriate to make guidance measurements with respect to the target planet. Optical techniques will be assumed in order to determine the guidance accuracy requirements, although other instruments are available for implementing this phase of guidance. Choices exist between horizon scanner, and a field scanning telescope for measuring the angle subtended by the planet, and determining the geometric center of the planet disc for measuring the relative angles to other celestial bodies. It is not essential to specify which is used in determining the sighting accuracy requirements.

An analysis of guidance requirements for interplanetary vehicles approaching an entry corridor or grazing pass of a planet is described by Harry and Friedlander (Ref. 6-7). The simulated measurement scheme is based on a clock and optical instruments self-contained in the vehicle. Range to the planet is determined from optical measurement of the apparent diameter, and increments of vehicle rotation around the target planet are determined from measurements of the planet motion against the celestial sphere. The latter measurement may be obtained either by noting the time of occulation of selected stars by the planet, or by measuring the angle between the planet and any two stars. Cataloging of specific stars is unnecessary when a field scan telescope is used in the approach guidance scheme. The simulation assumes a vehicle computer programmed to compute two-body conic trajectories from the observed data.

Results of this study show that an instrument accuracy of 40 sec of arc rms provides a pericenter uncertainty of about ±5 miles (8 km). Improved instrument accuracy will not reduce the pericenter uncertainty to less than about ±2 miles (3.2 km) because of the influence of planet terrain errors, which are about 0.8 miles (1.3 km) rms.

Increasing the hyperbolic excess velocity from 16,000 to 50,000 fps (5.2 to 16.4 km/sec) roughly doubles the size of the smallest corridor that can be attained effeciently. Velocity increment requirements, due to approach guidance inaccuracies, vary from 200 to 1500 fps (65 to 500 mps) over the entry velocity range from 40,000 to 63,500 fps (13 to 21 km/sec) and instrument accuracy ranges from 40 sec of arc to 2 min of arc rms.

System tolerance to control errors in magnitude and direction of corrective impulse was found to be high, on the order of 10 percent and 0.1 radian rms respectively. The maximum number of impulse corrections required was six and the median number between three and four for 100 sample trips.

6.3.6 Summary of Guidance Accuracy Requirements

It is evident from the foregoing results that a midcourse selfcontained optical guidance system with angle determination errors of 10 sec arc or less can provide sufficient accuracy to meet the mission requirements of Mars and Venus trips and does not incur excessive corrective velocities. Use of a midcourse guidance system, in addition to improving the system reliability and accuracy, permits much larger injection velocity errors and permits a wider choice of potential transfer trajectories.

Results of the various approach guidance studies referenced demonstrate that, again using optical techniques, an angle measurement error of 40 sec arc is sufficient during the approach phase to meet the mission accuracy and corrective velocity requirements.

Table 6-2 summarizes the first order guidance accuracy and related corrective impulse requirements for midcourse and planetary approach phases.

Table 6-2

ESTIMATED GUIDANCE ACCURACY REQUIREMENTS AND RESULTING ERRORS
(Earth-Mars Trip Model Refs. 6-4, 6-6 and 6-7)

Injection Velocity

With Midcourse Guidance	70 fps rms (21.4 m/sec)
Without Midcourse Guidance	1−2 fps (0.3−0.6 m/sec)

Midcourse (Outbound)

Angle accuracy, 10 sec arc (Star Tracker)

10 position fixes

Max. ΔV = 235 fps (72 m/sec)

Max. error at Planet ~ 2000 miles (3200 km)

Planet Pass*

Angle accuracy, 40 sec arc (Wide field scan)

Passage error, ΔP ~ 5 miles (8 km)

Max. ΔV = 0.04 V_{esc} = 680 fps (208 m/sec)

Midcourse (Inbound)

Angle accuracy, 10 sec arc

(Approximately same as outbound)

Earth Approach for Reentry

Angle accuracy, - 40 sec arc (Wide field scan)

Perigee Error ΔP ~ 10 miles (16 km)

Max. ΔV = 0.4 V_{esc} = 1500 fps (460 m/sec)

---

*Instrument under development.

6.4 GUIDANCE MECHANIZATION

6.4.1 Sensing Techniques

Potentially useful data for determining the spacecraft trajectory include velocity, position, acceleration, and time. Fortunately, it is not necessary to measure all of these. For an unpowered vehicle in a known gravity field, the ephemeris may be determined from the position and velocity at a known time, or the position at two known times. In actual measurements it is necessary to obtain sufficient quantities of readings to apply a least squares method, or similar averaging techniques to minimize random errors.

Direct measurement of range and range rate with self-contained equipment does not appear promising for the midcourse flight phase. The application of template spectroscopy to measure velocity relative to natural electromagnetic radiation sources, such as the sun, is being investigated at the Franklin Institute (Ref. 6-3). This does not appear promising from the standpoint of sensitivity. Active radar ranging over interplanetary distances would require prohibitive power levels and equipment dimensions. The use of a vehicle transponder technique is planned for unmanned space missions, using the DSIF tracking stations.

Optical instruments for determination of angles between celestial bodies appear to be the most useful sensors for the midcourse flight phase. Position determination from a series of angle measurements reduces to the problem of finding the common intersection point of the surfaces defined by each angle. Individual measurements, angles or ranges, result in position loci of three basic types or shapes. Range from a given body places the position on the surface of a sphere; angle determination between a planet and a star places the position on the surface of a cone; and the loci of points determined by measuring the angle between two planets is the "Navoid" (Ref. 6-8). These surfaces are illustrated in Fig. 6-6. The Navoid is formed by rotating a circular arc about its chord. Spacecraft position is uniquely determined by a minimum

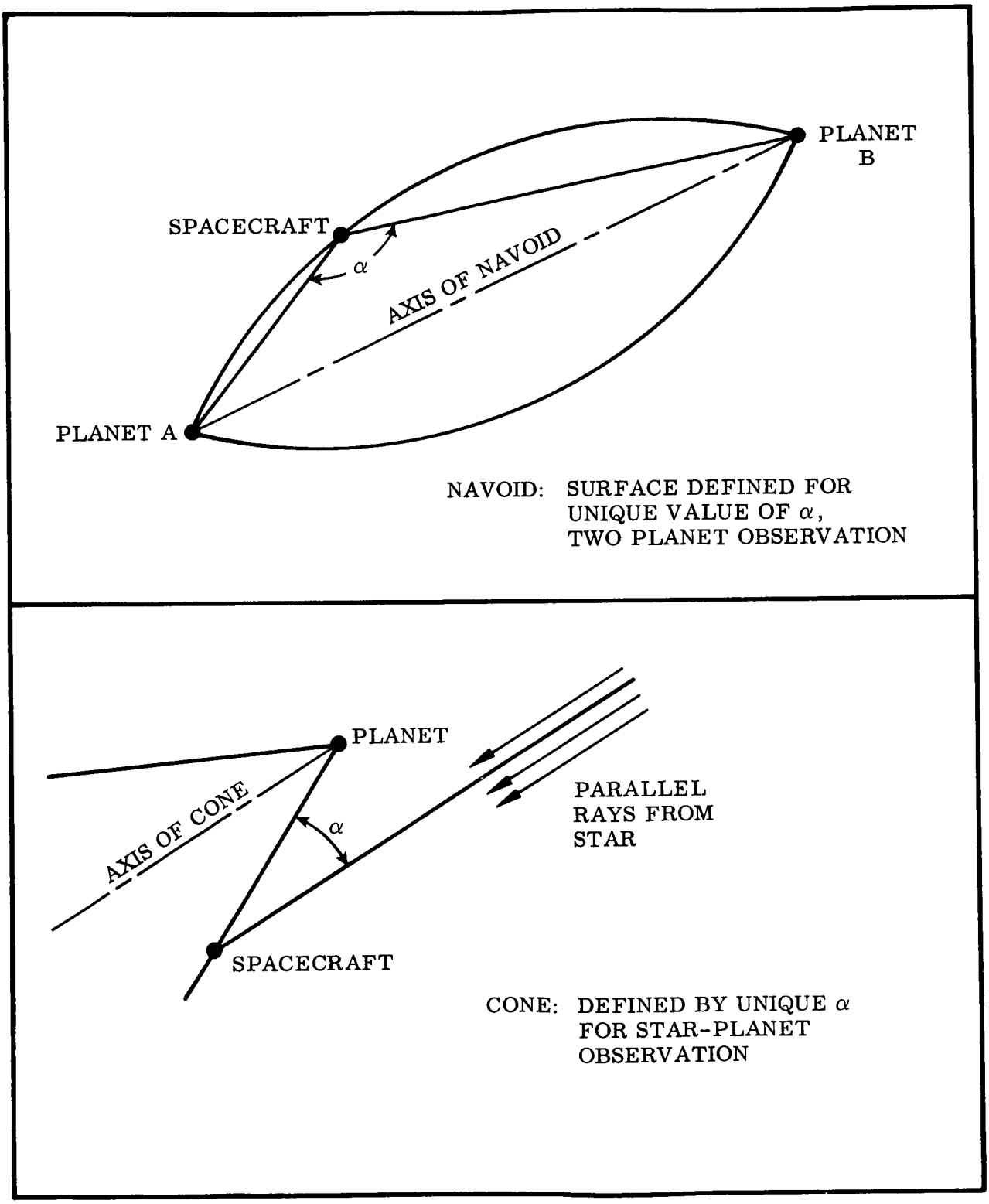


Fig. 6-6 Position Loci Determined by a Single Angle Measurement

of three measurements. When angle or range measurements are used with the linearized perturbation technique and a previously determined referenced trajectory, the region of interest on these surfaces is localized to that in the vicinity of the nominal trajectory. In this case the equations of the tangent planes or planes of measurement may be used, with a resultant simplification in the position determination calculation. These tangent planes may then be referred to as the "measurement planes." These angle measurements, plus the time when they were made, are easily transformed to a position fix as will be shown in Section 6.5.

Optical techniques for angle determination may be placed in the three categories: star trackers, sextants, and star field scanning instruments. Star trackers generally use an image nulling technique to determine when the reference star image is centered, and the reference angles are read from gimbal position sensors (Refs. 6-9, 6-10, and 6-11). Sextant instruments rely on a beam splitter and a rotating mirror so that the images of two stars are superimposed, and the angle read from the rotational position of the mirror. Star field scanners usually incorporate a fairly wide field of view optical system and an image scanning technique to record the positions of all bodies in the field of view. In this case the angle between two stars is determined by the linear separation of their images, and a knowledge of the optical magnification.

Image scanning and angle determination may be performed automatically through the use of vidicons, image orthicons, image dissector tubes, or solid state mosaics (Refs. 6-1, 6-2, and 6-12). As an alternative, manual determination of the reference angles may be made by photographically recording the field image and measuring star-planet separations on the resulting plate.

As the target planet is approached, and the planet dimensions become measurable, a stadiametric technique may be used to determine range from the planet center. The stadiametric range may be determined with apparent diameter measurements from a field scanning instrument, or with a set of three horizon sensing instruments which lock-on to the planet disc edge. The range, thus determined, two star-planet angles, and the time determines the position fix for the terminal approach guidance phase.

During corrective maneuvers when thrust is applied to the spacecraft, inertial instruments must be used for controlling the impulse direction and are also useful for determining engine cut-off.

6.4.2 Guidance Scheme and Mechanization

A functional diagram of the selected guidance and control system is shown in Fig. 6-7. Guidance sensors included consist of an inertial platform with accelerometers, star trackers, and a star field scanning telescope. Additional guidance data is provided from the time reference, command link receiver and the human navigator. This system is self-contained, except for the command link which is intended primarily for use in making the first correction at injection into the transfer orbit. The command link also provides an alternate mode of guidance which could be used if an emergency failure of the on-board instruments occurred. The human navigator also provides a redundancy to improve reliability. Recently published data from the X-15 program indicates that about 40 percent of the test flights could have failed destructively during reentry without the automatic-human redundant combination.

The system shown in Fig. 6-7 is based on mechanization requirements for both midcourse proper and terminal approach. The midcourse mechanization initiates operation immediately following booster cut-off. Ground-based tracking and computers of the DSIF, or a similar facility, provide a determination of the vehicle flight path or orbit, and compute the first corrective impulse (Ref. 6-13). Instructions for the first corrective impusle are then transmitted via the command link to the vehicle guidance computer.

Monitoring of the transfer orbit and subsequent midcourse corrections are based on the spacecraft optical sensors (automatic or manual) and computations carried out by the on-board computer. Angle determination with two gimbal-mounted starlock telescopes is the primary sensing technique proposed for use during this phase. Potentially useful reference bodies include stars having a visual magnitude of about 6 or brighter,

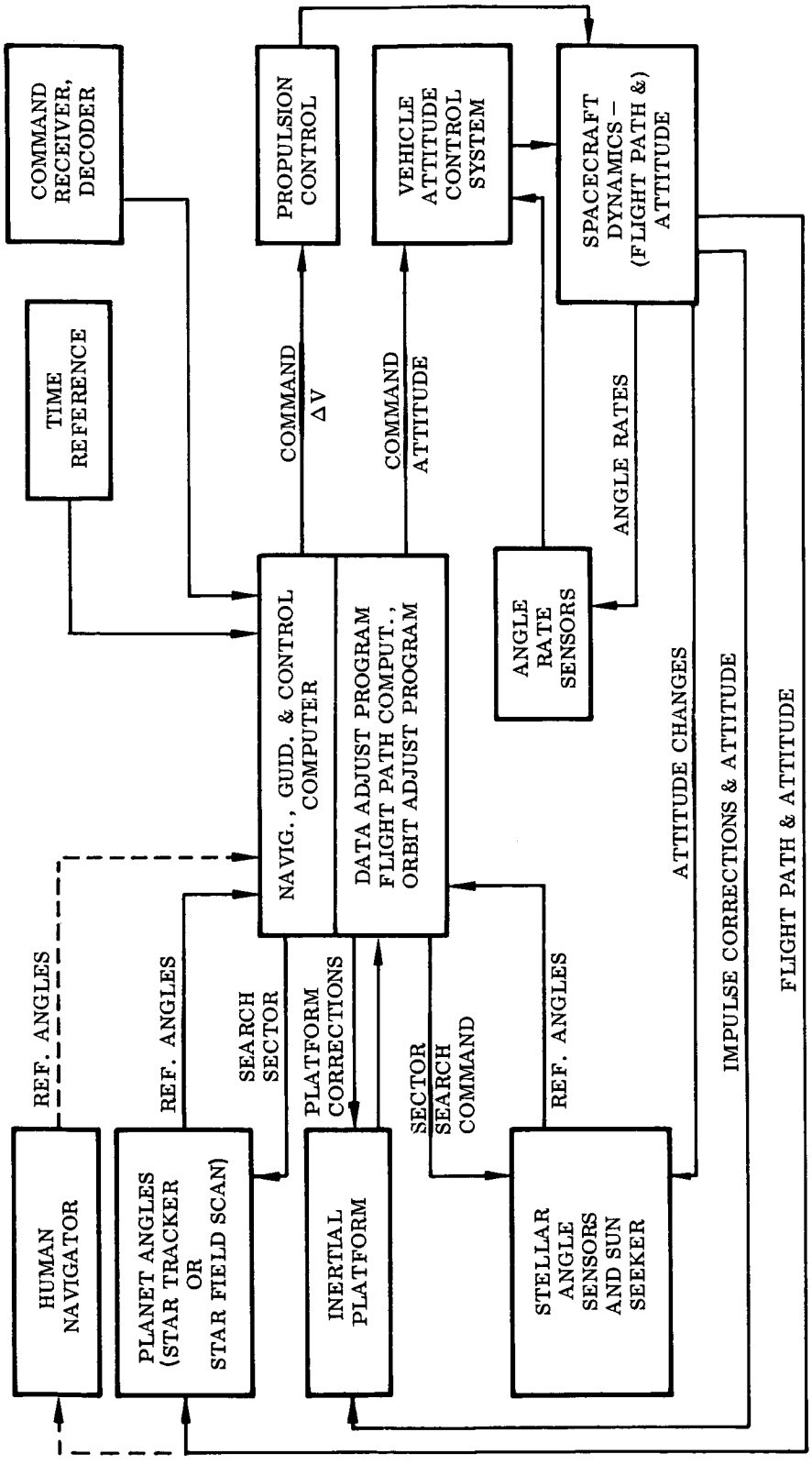
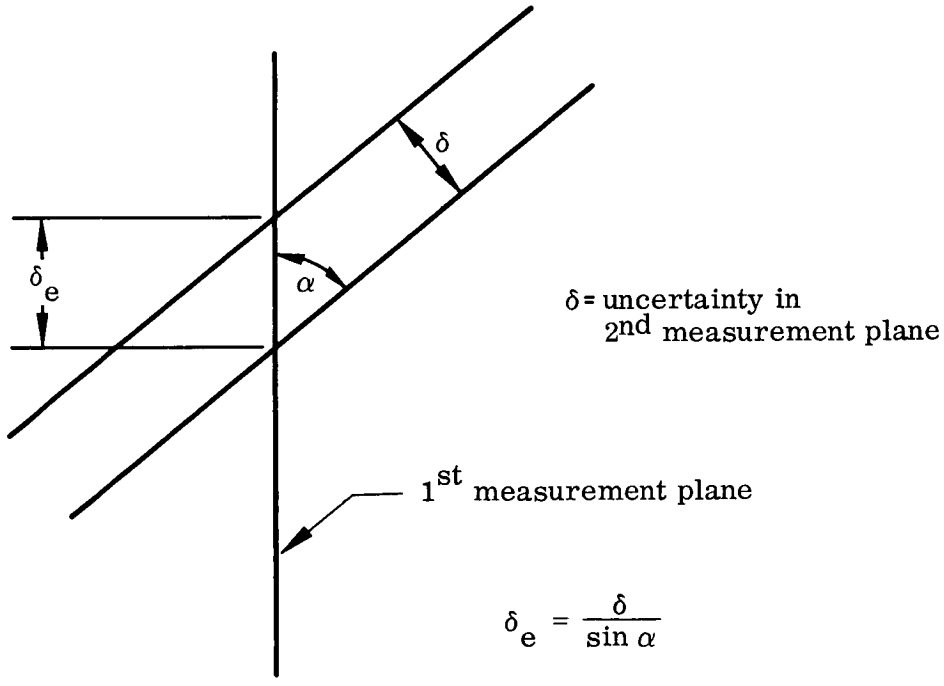


Fig. 6-7 Spacecraft G & C System for Performance Analysis

Earth, Mars, Venus, Jupiter, and any of the minor planets for which accurate ephemerides are obtainable. As previously demonstrated in the section on requirements, judicious selection of reference bodies is necessary because of the positional influence on the error. Choices of the reference bodies for use during various segments of the transfer orbit will be based on the specific mission, calendar date of launch, and particular orbit chosen.

For maximum accuracy the reference bodies should be chosen so that the measurement planes are mutually perpendicular, or nearly so, thus reducing the effective error. As shown in the sketch below, the effective error for two successive measurements is inversely proportional to the angle sine so that as $\alpha \rightarrow 90°$, $\delta_e \rightarrow \delta$



Capability of currently available automatic star-lock telescopes provides overall angular accuracies of about 8 to 10 sec of arc, rms, for example, see Ref. 6-11. Future instruments with improved gimbal position pick-offs may provide errors as

small as about 3 to 5 sec. Instruments of this type include a telescope mounted on servo-controlled gimbals and having optics which provide an angle of view of about 2 to 5 deg. An image modulating shutter, such as a rotating disc or vibrating reed, is generally provided near the plane of focus, to modulate the light falling on a photo-sensitive device. The gimbal seros drive the instrument to a null position determined by the optical-photo-electric sensor and angle position is read from the gimbal pick-offs. As an alternative mode of obtaining midcourse fixes, a manual or semi-automatic sextant is provided for use by the astronavigator. Such instruments are under development for the Apollo program and may provide accuracies on the order of 3 to 5 sec of arc. Manual readings of this type are, of course, obtained at much lower time rate than with the automatic star tracker thus limiting statistical data smoothing use. Use of a long focal length camera is another technique which may be used for manual fix data. Measurements are made directly on the photographic plate to determine reference planet locations on the celestial sphere. This method provides the greatest accuracy, about 0.5 to 1.0 sec of arc, but is also the most time consuming and requires storage and processing of photosensitive materials which are easily damaged by radiation.

During the terminal approach phase a star field scanning telescope with an acceptance angle of 12 to 15 degrees offers certain advantages over a star tracker or space sextant. Stadiametric measurements for range detection, required in the approach scheme, are more easily and rapidly obtained with the field scanner than with a star tracker. In addition, the same instrument provides angle measurements between the target planet and one or more reference stars. Angle determination with errors of 36 sec of arc, and a telescope acceptance angle of 15 deg, implies a scanning resolution of about 1500 television lines. Gimbal mounts are required for the field scan telescope but unlike the star tracker, angle measurements are determined by separation of points on the raster scan and are independent of gimbal pick-offs.

During the midcourse phase of a vehicle which provides gravity by rotation, optical guidance sensors must be isolated from the rotation by mounting on an inertially stabilized platform, or the vehicle rotation may be stopped to obtain readings.

An atomic resonance controlled oscillator (Atomichron) time reference provides high stability and accuracy for the position fixes. Time of the fix must be accurately measured whether angles are obtained manually or automatically. Midcourse-fix timing accuracy required is estimated as 0.001 percent (one part in 10^5) of the elapsed time, based on analyses of guidance requirements. The atomic resonance controlled oscillator is estimated to provide a long term error of less than one part in 10^8 and thus exceeds the requirement.

During periods of thrusting for corrective maneuvers, platform mounted accelerometers provide velocity change and thrust termination data to the computer. The platform also functions as an attitude reference during short periods when optical sensors are off target. During corrective maneuvers, the attitude and thrust vector directing should be maintained with an accuracy $\pm$ 0.10 deg, or better. During passive periods of free-fall, however, the vehicle attitude tolerance may be increased to the order of a degree thus reducing control torque generating power requirements. As a direct result of the ballistic missile effort, currently available stable platforms and inertial instruments meet the accuracy requirements. Developments during the 1963 to 1970 time period are not expected to have any large affect on inertial component weights or accuracies, but should yield significant gains in reliability for long term operation through the use of gas bearings or electrostatic suspension gyros.

6.4.3 Control Elements

Attitude and angle rate sensors are both used in the control system. Control system optical sensors are designed to have greater light sensitivity than guidance components, and do not require the extreme accuracy of the guidance sextant or star tracker. A sun seeker is selected as the basic optical attitude instrument. This instrument plus a low resolution star tracker comprises the minimal optical attitude sensor complement. An angle error of less than 0.01 deg is available in these instruments. During periods when they have lost their respective targets, or when new targets are to be acquired, the inertial platform will furnish a reference from which to program search procedures.

Inertial rate sensing instruments are included to provide damping and improve stability characteristics of the control systems during thrust maneuvers and when attitude changes are commanded. Integrated output of spring-mass angular accelerometers or pairs of linear accelerometers are better for this application than rate gyros because the latter instrument's rotating mass and bearings may impair long term reliability.

Control system amplifiers for the system will include variable gains and filter network switching to adapt for changes in vehicle weight and moments. In addition, the vehicle is assumed to have three modes of operation which may require separate control loops, depending on the degree of control adaptibility attainable. These three modes are : 1) Vehicle folded with thrust vector and roll control; 2) vehicle folded with three axis attitude control; and 3) vehicle extended and rotating with two axis attitude control and rate of spin control. Mode 3 of course is not used if a zero-g configuration is adopted.

Based on the foregoing consideration it appears that three control loops will be required for the three-axis attitude-control nozzles, two control loops for the thrust vector control actuators, and one control loop for the rate of spin. Thus, a total of six separate control loops will probably be needed.

During rotation of the spacecraft for gravity simulation the optical attitude sensors, like the navigation sensors, may also be platform mounted to keep them directed toward their respective reference points.

6.4.4 Computer

Primary sections of the computer are logic, memory or storage, programmer, and input-output buffers. The memory or storage section may be considered to consist of an internal and an external part. The interal portion is to provide rapid access and would contain information required by the program in operation. The external sections would provide additional large-volume storage.

The computer will probably be a general purpose type and will be used to perform the guidance computations on a time-sharing basis with other functions such as message decoding, and scientific data processing. The time required for guidance computations would probably not exceed a few minutes each day. If the linearized perturbation equations are used during the midcourse phase, for example, angle measurements taken with the vehicle sensors would be compared with pre-computed angles, and the difference multiplied by a precomputed matrix to determine the vehicle position relative to the reference trajectory. The velocity correction required is next determined by multiplying two successive position deviations by pre-computed matrices and taking the differences of the two products. Section 6.5 describes the equations and defines the required matrices for this technique. It is also possible to arrive at the required velocity correction from the angle deviations in a single step through the use of appropriate matrices.

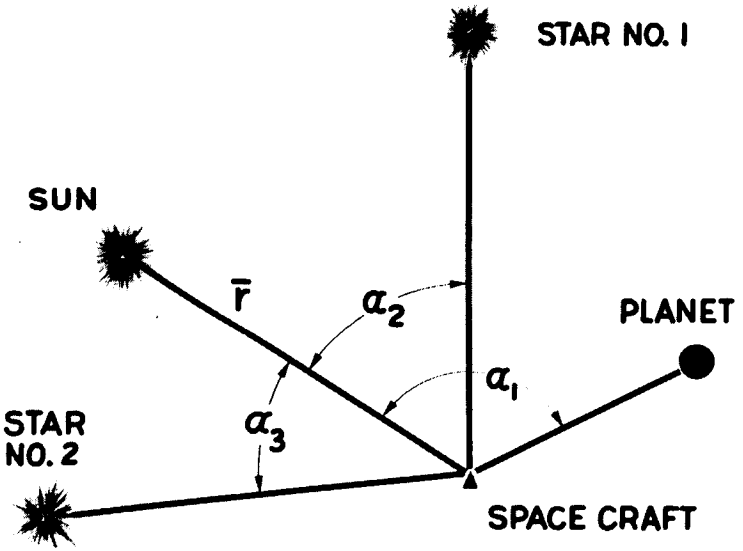
6.4.5 Integrated System Approach

Components of the midcourse guidance and control system are also suitable for the initial boost phase as well as for atmospheric reentry at return to Earth. During the boost phase the computer would be programmed with a suitable guidance scheme for steering and thrust cut-off determination, probably a path adaptive guidance scheme (see Ref. 6-14). Additional instruments required during this phase would be angle-of-attack and yaw meters and rate sensors located in the booster stages.

6.5 GUIDANCE ERROR EQUATIONS

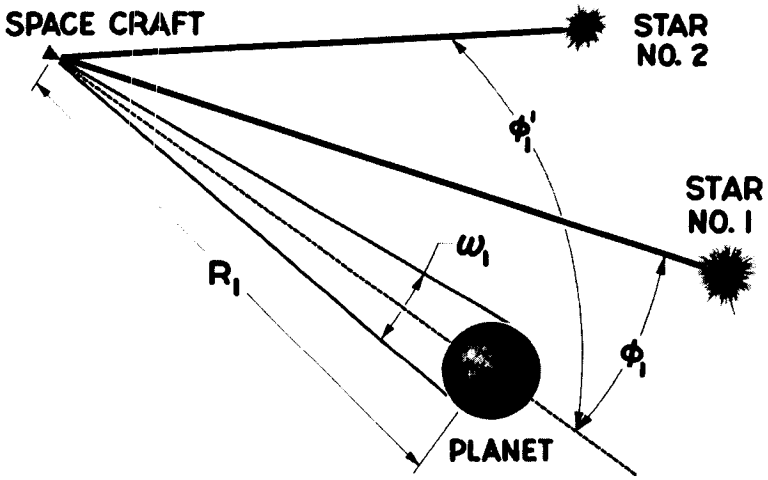
The general error equations for calculating corrective velocity impulses from the navigational fix data are presented for the midcourse phase. The measurement scheme uses the observed angles between three selected pairs of celestial bodies, and the determination of range by stadiametric means when in the vicinity of a planet (Fig. 6-8). Perturbation techniques are utilized, which implies that the approximate position, velocity and time are known. This restriction is reasonable since very large deviations from the nominal trajectory would probably be catastrophic.

MIDCOURSE POSITION FIX



MEASURING SCHEME USING TWO STARS, A PLANET, AND THE SUN TO DETERMINE SOLAR POSITION VECTOR $\bar{r}$. PLANET AND STARS USED WILL VARY DURING THE TRIP

PLANET APPROACH FIX



MEASURING SCHEME USING TWO STARS AND STADIOMETRIC PLANET RANGE

Fig. 6-8 Navigation Optical Sighting Geometry

In deriving linearized perturbation equations it is assumed that an ideal, or reference, trajectory has been selected, and that the difference between the actual vehicle position and the ideal position will remain small. Numerous references to the development of a linearized guidance theory appear in the literature; an excellent example is the MIT Instrument Laboratory Report (Ref. 6-15). Use of the small perturbation techniques and linearized equations provides a rapid means of reducing navigation fix data with the vehicle computer and reduces the ground computing load.

6.5.1 Linearized Equations

Let $\bar{r}_s$ (t) and $\bar{v}_s$ (t) be the actual position and velocity vectors of the vehicle at time t, given in inertial-heliocentric coordinates. Let $\bar{r}_o$ (t) and $\bar{v}_o$ (t) be the ideal position and velocity on the reference trajectory at the same instant. The deviations may then be written as

$$\delta\bar{r}(t) = \bar{r}_s(t) - \bar{r}_o(t) \tag{6-1}$$

$$\delta\bar{v}(t) = \bar{v}_s(t) - \bar{v}_o(t) \tag{6-2}$$

The equations of freefall in a gravity field are:

$$\frac{d\bar{r}}{dt} = \bar{v} \tag{6-3}$$

$$\frac{d\bar{v}}{dt} = \bar{g}(\bar{r},t) \tag{6-4}$$

where $\bar{g}(\bar{r},t)$ is the local gravitational acceleration due to the field.

Differentiating Eqs. (6-1) and (6-2) with respect to time, and substituting in Eqs. (6-3) and (6-4), we get:

$$\frac{d}{dt}\delta\bar{r}(t) = \bar{v}_s(t) - \bar{v}_o(t)$$

$$\frac{d}{dt}\delta\bar{v}(t) = \bar{g}(\bar{r}_s,t) - \bar{g}(\bar{r}_o,t)$$

Expanding $\bar{g}(\bar{r},t)$ in a Taylor series about $\bar{r}_o$ and neglecting higher order terms in $(\bar{r}_s - \bar{r}_o)$, results in

$$\bar{g}(\bar{r}_s,t) - \bar{g}(\bar{r}_o,t) = M_o(\bar{r}_o,t)\ \delta\bar{r}(t)$$

where M_o is the coefficient matrix whose elements are the partial derivative of the components of $\bar{g}(\bar{r}_o,t)$ with respect to the components of $\bar{r}_o(t)$.

$$M_o = \begin{bmatrix} \frac{\partial g_x}{\partial r_x} & \frac{\partial g_x}{\partial r_y} & \frac{\partial g_x}{\partial r_z} \\ \frac{\partial g_y}{\partial r_x} & \frac{\partial g_y}{\partial r_y} & \frac{\partial g_y}{\partial r_z} \\ \frac{\partial g_z}{\partial r_x} & \frac{\partial g_z}{\partial r_y} & \frac{\partial g_z}{\partial r_z} \end{bmatrix} \tag{6-5}$$

The linearized equations of perturbed motion may then be written

$$\frac{d}{dt}\ \delta\bar{r}(t) = \delta\bar{v}(t) \tag{6-6}$$

$$\frac{d}{dt}\ \delta\bar{v}(t) = M_o\ \delta\bar{r}(t) \tag{6-7}$$

Selecting appropriate boundary conditions, a solution to Eqs. (6-6) and (6-7) may be obtained. The special case considered here assumes that the initial perturbation is due only to errors in launch velocity $(\bar{v}_L)$ and that launch position at engine cutoff $(\bar{r}_L)$ is not in error, or that the position error is negligible.

$$\delta\bar{r}(t_L) = 0 \quad , \quad \delta\bar{v}(t_L) = \delta\bar{v}_L \tag{6-8}$$

For the planet intercept time t_A, it is assumed that position deviation at arrival is zero with any position errors removed by guidance maneuvers, but that the velocity at arrival ($\overline{v}_A$) is not constrained.

$$\delta\overline{r}\,(t_A) = 0 \; ; \; \delta\,\overline{v}(t_A) = \delta\,\overline{v}_A \tag{6-9}$$

Then for some time $t > t_L$, the position and velocity vectors, $\overline{r}_s(t)$ and $\overline{v}_s(t)$, are functions only of the departure velocity $\overline{v}(t_L)$. Performing a Taylor series expansion about the reference value $\overline{v}_o(t_L)$ with higher order terms neglected, we get

$$\delta\overline{r}(t) = R(t)\,\delta\overline{v}_L \tag{6-10}$$

$$\delta\overline{v}(t) = V(t)\,\delta\overline{v}_L \tag{6-11}$$

where $R(t)$ and $v(t)$ are coefficient matrices of partials with respect to v_L evaluated along the trajectory at time t.

Define

$$\nabla = \left(\frac{\partial}{\partial v_{L,x}} \; , \; \frac{\partial}{\partial v_{L,y}} \; , \; \frac{\partial}{\partial v_{L,z}} \right) \tag{6-12}$$

then

$$R(t) = \begin{bmatrix} \nabla\, r_x(t) \\ \nabla\, r_y(t) \\ \nabla\, r_z(t) \end{bmatrix} \quad , \quad V(t) = \begin{bmatrix} \nabla\, v_x(t) \\ \nabla\, v_y(t) \\ \nabla\, v_z(t) \end{bmatrix} \tag{6-13}$$

Substituting Eqs. (6-10) and (6-11) into (6-6) and (6-7)

$$\frac{dR}{dt}\,\delta\bar{v}_L = V\,\delta\bar{v}_L$$

$$\frac{dV}{dt}\,\delta\bar{v}_L = M_o\,R\,\delta\bar{v}_L$$

or

$$\frac{dR}{dt} = V \quad , \quad \text{and} \quad \frac{dV}{dt} = M_o\,R \tag{6-14}$$

From the boundary conditions of (6-8)

$$R(t_L) = 0 \;;\; V(t_L) = I \quad \text{(Unit matrix)} \tag{6-15}$$

Now using the terminal boundary conditions and working backwards from t_A to some point $t < t_A$, the position and velocity at t are a function only of $\bar{v}(t_A)$. The deviations for this case are written:

$$\delta\bar{r}(t) = R^*(t)\,\delta\bar{v}_A \tag{6-16}$$

$$\delta\bar{v}(t) = V^*(t)\,\delta\bar{v}_A \tag{6-17}$$

Then let the row vector ∇^* be defined

$$\nabla^* = \left(\frac{\partial}{\partial v_{A,x}} \;,\; \frac{\partial}{\partial v_{A,y}} \;,\; \frac{\partial}{\partial v_{A,z}}\right) \tag{6-18}$$

and

$$R^*(t) = \begin{bmatrix} \nabla^* r_x(t) \\ \nabla^* r_y(t) \\ \nabla^* r_z(t) \end{bmatrix} \quad , \quad V^*(t) = \begin{bmatrix} \nabla^* v_x(t) \\ \nabla^* v_y(t) \\ \nabla^* v_z(t) \end{bmatrix} \tag{6-19}$$

$$dR^*/dt = V^* \; ; \; dV^*/dt = M_o R^* \tag{6-20}$$

The boundary conditions require that

$$R^*(t_A) = 0 \; , \; V^*(t_A) = I \tag{6-21}$$

Equations (6-10) and (6-11) form one solution of the perturbed differential equations (6-6), (6-7), (6-16), and (6-17) form a second solution. The most general solution then to (6-6) and (6-7) is

$$\delta\bar{r}(t) = R(t)\,\bar{c} + R^*(t)\,\bar{c}^* \tag{6-22}$$

$$\delta\bar{v}(t) = V(t)\,\bar{c} + V^*(t)\,\bar{c}^* \tag{6-23}$$

where $\bar{c}$ and $\bar{c}^*$ are constant vectors over any interval of free-fall, i.e., they hold constant as long as no impulsive forces are applied. $\bar{c}$ and $\bar{c}^*$ may be determined from the boundary conditions. For the two body case Keplerian motion, the matrices R, V, R^*, and V^* can be obtained analytically.

6.5.2 Velocity Correction Determination

The following development is for fixed time of arrival guidance. It will be demonstrated that the velocity increment $\bar{v}(t)$ is required to correct position errors of two known position deviations along the trajectory.

Let $\bar{V}^*(t)$ be the velocity vector required at $\bar{r}(t)$ to intercept the target planet at t_A. Expanding $\bar{V}^*(t)$ in a Taylor series about the reference trajectory and neglecting terms higher than first order,

$$\bar{V}^*(t) = \bar{v}_o(t) + Q^*(\bar{r}_o, t)\,\delta\bar{r}(t) \tag{6-24}$$

where Q^* is a matrix of partial derivatives of the components of $\bar{V}^*(t)$ with respect to $\bar{r}(t)$ evaluated at $\bar{r}_o(t)$. The required velocity correction is then

$$\Delta\bar{v}(t) = \bar{V}^*(t) - \bar{v}(t) = Q^*\,\delta\bar{r}(t) - \delta\bar{v}(t) \tag{6-25}$$

The quantity $\delta\bar{v}(t)$ may be found from two successive position deviations. When t_n and t_{n-1} are substituted in Eq. (6-22), the resulting independent linear equation may be solved simultaneously for $\bar{c}$ and $\bar{c}^*$, which may then be substituted in (6-23). Denoting time dependent quantities with subscripts, for example $\delta\bar{r}(t_n) \equiv \delta\bar{r}_n$,

$$\bar{c}^* = \left(R_n^* - R_n R_{n-1}^{-1} R_{n-1}^*\right)^{-1} \left(\delta\bar{r}_n - R_n R_{n-1}^{-1} \delta\bar{r}_{n-1}\right)$$

$$\bar{c} = \left(R_n - R_n^* R_{n-1}^{*-1} R_{n-1}\right)^{-1} \left(\delta\bar{r}_n - R_n^* R_{n-1}^{*-1} \delta\bar{r}_{n-1}\right)$$

From the definition of Q^* and Eq. (6-13) it can be seen that

$$Q_n^* R_n^* = V_n^*$$

Substituting these results in (6-25) yields

$$\Delta v_n = H_n \delta\bar{r}_n - P_n \delta\bar{r}_{n-1} \tag{6-26}$$

where H_n and P_n are matrices which may be expressed in terms of R, v, R^* and V^* as follows

$$H_n = V_n^* R_n^{*-1} - V_n \left(R_n - R_n^* R_{n-1}^{*-1} R_{n-1}\right)^{-1} - V \left(R_n^* - R_n R_{n-1}^{-1} R_{n-1}^*\right)^{-1} \tag{6-27}$$

$$P_n = -V_n \left(R_n - R_n^* R_{n-1}^{*-1} R_{n-1}\right)^{-1} R_n^* R_{n-1}^{*-1} - V_n^* \left(R_n^* - R_n R_{n-1}^{-1} R_{n-1}^*\right)^{-1} R_n R_{n-1}^{-1} \tag{6-28}$$

The required velocity correction, $\Delta\bar{v}(t)$, at time t_n is expressed in Equation (6-26) as a function of the two successive position deviations $\delta\bar{r}_n$ and $\delta\bar{r}_n - 1$. The perturbation technique and Eq. (6-26) applies either to elliptic motion or hyperbolic motion and may also be used to compute velocity corrections during the terminal approach phase using pre-computed matrix coefficients.

6.5.3 Determining Position Deviations from Celestial Angle Measurements

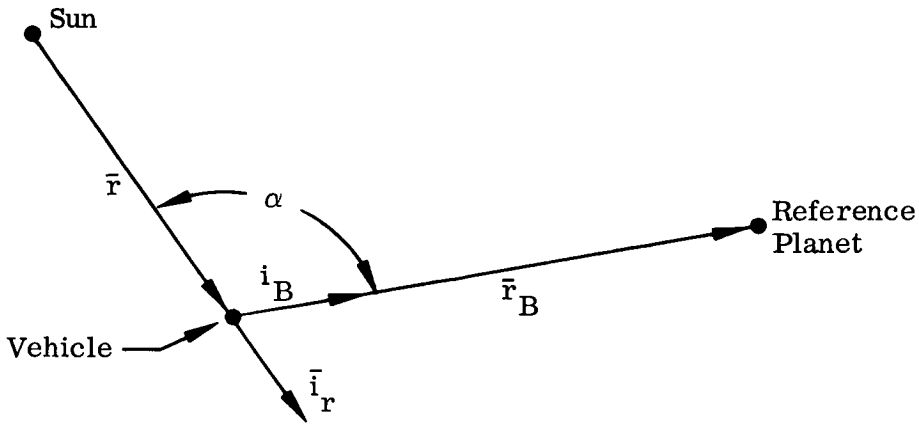
Let

$\bar{r}$ position vector of vehicle in inertial, heliocentric coordinates

$\bar{r}_B$ position vector of planet or reference star from the vehicle

α angle between $\bar{r}$ and $\bar{r}_B$

t time at which sighting is made



$\bar{i}_r$ and $\bar{i}_B$ are unit vectors along $\bar{r}$ and $\bar{r}_B$ respectively, and $\bar{r} \cdot \bar{r}_B = -rr_B \cos\alpha$ is the dot product.

Taking differentials of the dot product

$$\delta(\bar{r} \cdot \bar{r}_B) = \bar{r} \cdot \delta\bar{r}_B + \bar{r}_B \cdot \delta\bar{r} \qquad (6\text{-}29)$$

or

$$\delta(-r r_B \cos\alpha) = (r r_B \sin\alpha)\,\delta\alpha - (r_B \cos\alpha)\,\delta r - (r\cos\alpha)\,\delta r_B$$

$$= (r r_B \sin\alpha)\,\delta\alpha - r_B(\bar{i}_r \cdot \delta\bar{r})\cos\alpha - r(\bar{i}_B \cdot \delta\bar{r}_B)\cos\alpha$$

Note that $\delta\bar{r}_B = -\delta\bar{r}$. (6-30)

Combining Eqs. (6-29) and (6-30), and simplifying,

$$\delta\alpha = \left[\frac{1}{r\sin\alpha}(\bar{i}_B + \bar{i}_r\cos\alpha) - \frac{1}{r_B\sin\alpha}(\bar{i}_r + \bar{i}_B\cos\alpha)\right]\delta\bar{r} \qquad (6\text{-}31)$$

For any given time of fix t, and a known reference trajectory, the angle α and values in the brackets may be pre-calculated. $\delta\alpha$ is the difference between the measured and pre-determined values of α. The three spatial components of $\delta\bar{r}$ may then be determined using Eq. (6-31) and three independent angle measurements. When the reference body is a star, the value of $\bar{r}_B \to \infty$, and the second term within the brackets goes to zero. Then letting $\bar{u}$ represent the bracketed terms we may simplify the notation:

For sun-star measurements

$$\bar{u} = \left[\frac{1}{r\sin\alpha}(\bar{i}_s + \bar{i}_r\cos\alpha)\right] \qquad (6\text{-}32)$$

For sun-planet measurements

$$\bar{u} = \left[\frac{1}{r\sin\alpha}(\bar{i}_B + \bar{i}_r\cos\alpha) - \frac{1}{r_B\sin\alpha}(\bar{i}_r + \bar{i}_B\cos\alpha)\right] \qquad (6\text{-}33)$$

Equation (6-31) may now be expressed in matrix notation

$$\delta\bar{\alpha} = U\,\delta\bar{r} \qquad (6\text{-}34)$$

where $\delta\overline{\alpha}$ is a column vector, and U is a 3×3 matrix whose rows comprise the row vectors $\overline{u}_i$, for three measurements $\delta\alpha_i (i = 1, 2, 3)$.

Pre-multiplying (6-34) by the inverse of U, (valid if U is not singular)

$$\delta\overline{r} = U^{-1}\,\delta\overline{\alpha} \tag{6-35}$$

Influence of Measure Errors

Let

$\Delta\alpha_i$ error in measuring

Δt error in t (clock drift)

These are considered random errors with Gaussian distribution.

Then Δr the error in $\delta\overline{r}$ may be considered primarily due to the three major factors:

$\Delta\alpha_i$ the error in measuring α_i

Displacement of the planet between reference and actual sighting times, i.e., during Δt

Displacement of the vehicle during Δt

The component of $\Delta\overline{r}$, due to $\Delta\alpha_i$ may be determined directly from Eq. (6-35).

$$\Delta\overline{r}_i = U^{-1}\,\Delta\overline{\alpha} \tag{6-36}$$

The component of $\Delta\overline{r}_2$ due to planet motion during Δt is determined as follows:
Let α_3 = Sun-planet angle, then from (6-31)

$$-r\,r_B \cos\alpha_3 = \overline{r} \cdot \overline{r}_B$$

Taking differentials due to the planets motion and substituting $\delta \bar{r}_B = - \bar{v}_P \Delta t$, where $\bar{v}_P$ = planet velocity, we obtain

$$\delta\alpha_3 = \left[- \frac{1}{r_B \sin \alpha_3} (\bar{\imath}_r + \bar{\imath}_B \cos \alpha_3) \cdot \bar{v}_P \right] \Delta t \qquad (6\text{-}37)$$

Equation (6-37) expresses the deviation in α_3 caused by planet motion in the interval Δt . Using Eq. (6-35), the component $\Delta \bar{r}_2$ may be written in the general form

$$\Delta \bar{r}_2 = U^{-1} \bar{q} \Delta t \; ; \; \bar{q} \equiv \begin{Bmatrix} q_1 \\ q_2 \\ q_3 \end{Bmatrix} \qquad (6\text{-}38)$$

Where $q = q_2 = 0$ if α_1 , and α_2 are Sun-star angles, and q_3 is equal to the bracketed term in Eq. (6-37).

The component $\Delta \bar{r}_3$ due to vehicle motion during Δt is simply the product of vehicle velocity $\bar{v}$ and the clock error Δt .

$$\Delta \bar{r}_3 = - \bar{v} \Delta t \qquad (6\text{-}39)$$

The total error is the sum of equations (6-36), (6-38) and (6-39):

$$\Delta \bar{r} = U^{-1} \Delta \bar{\alpha} + (U^{-1} \bar{q} - \bar{v}) \Delta t \qquad (6\text{-}40)$$

The three planes defined by Eq. (6-37), relating angle deviations to position deviations, are termed planes of measurement. Minimum sensitivity of position error to errors in determining $\delta \bar{\alpha}$ is obtained if the three planes of measurement are mutually orthogonal. The criterion of approximate orthogonality should be applied in selecting the reference bodies for each preplanned position fix.

6.6 PHYSICAL CHARACTERISTICS

Components selected for mechanizing the guidance and control system represent a moderate extension of the current state of the art. Many of the system elements are currently available with performance equal to, or approaching, the system requirements.

Development during the intervening period to 1970, as indicated by industry predictions, will result in large reductions in weight and power requirements, and improved reliability of electronic components. Digital computers, for example, having the capability of present-day full-scale general purpose types, will be available in 1970 with a volume of only a few cubic feet (Kambatka Ref. 6-16). Optical-Mechanical elements, such as star trackers, will have weights and sizes comparable to present day advanced types, but with improved reliability and performance.

Estimates of weight, volume, and power requirements for the major elements are presented in Tables 6-3 and 6-4. These estimates are based on information gleaned from interviews with major component manufacturers, published projections by specialists in the component field, and from a knowledge of recent laboratory tests of experimental models.

Environmental control power requirements will depend on the location of the equipment in the spacecraft. Optical systems used in the star trackers may be designed to operate in the space vacuum but must be protected from temperature gradients which would result from exposure to direct solar radiation. Inertial instrument systems require temperature control within a few degrees, hermetically sealed inertial platforms require 100 to 150 w of heater power to maintain temperature. In addition, small amounts of make-up air would probably be required to compensate for leakage on the one- to two-year journey. For instruments installed in the crew compartment, the environmental control requirements are much easier to satisfy. An additional benefit derived fron in-cabin location of instruments is that maintenance, testing and calibration operations may be performed more frequently and with greater ease. Heat dissipated by electronic components, such as the central computer, could be utilized to augment the cabin heating system.

Table 6-3

GUIDANCE AND CONTROL PHYSICAL SYSTEM CHARACTERISTICS SUMMARY

(Estimated for 1970 State-of-the-Art)

	WEIGHT (kg)	VOLUME (m^3)	POWER (w)
TRAJECTORY DETERMINATION SYSTEM	65	0.14	200
Inertial Instruments, Optical Sensors, Atomic Resonance Time Reference and Associated Electronics			
ATTITUDE CONTROL SYSTEM	23	0.05	25
Inertial, Optical and Associated Electronics			
COMPUTER SYSTEM	32	0.10	150
Memory, Logic Elements and Input/Output			
COMMAND LINK RECEIVER AND TRANSLATION EQUIPMENT	2	7×10^{-3}	5
TOTALS	122	0.30	380

Notes: Environmental control equipment, attitude torquers, and power conversion equipment is not included.

Computer memory and clock are continuous; other items operated intermittently.

LOCKHEED MISSILES & SPACE COMPANY

Table 6-4

OPTICAL INSTRUMENT CHARACTERISTICS AND PERFORMANCE

Guidance & Control Optical Components	Image Detection	Output	Accuracy 1970	Instrument Application
Star Trackers Precision Gimbal Servos	Image Dissection Tube, or Vidicon	Gimbal Position	3 – 5 sec	Midcourse position and align inertial components
Field Scan Telescope Locking Gimbals	Vidicon or Mosaic	Image Scan Signal Analysis	10 sec	Planet approach position
Sun Tracker Locking Gimbals	Masked Photo Electric Cells	Angle Position Signal to Attitude Servo	30 – 50 sec	Vehicle coarse attitude references
Star & Planet Tracker, Locking Gimbals	Photo Multiplier or Image Dissection Tube	Angle Position Signal to Attitude Servo	30 – 50 sec	Vehicle coarse attitude references
Telescope-Camera (Manual oper'n.)	Photo Plates* or Electrostatic Film	Manual Measure of Solar System Bodies Positions on Star Field	1 sec or better	Manually operated midcourse position
Space Sextant (Semi-automatic)	Observer's Eye	Prism Angular Position Pick-off	3 – 5 sec	

*Requires special protection from radiation fogging.

Two manually operated instruments of particular interest for midcourse navigation are the sextant, and the star field camera. Use of these instruments requires a window in the crew compartment. Since the window forms part of the instrument optical system, the instrument would be constrained to rotate in a fixed gimbal system, and window distortion characteristics calibrated as a function of gimbal position. The sextant, or the camera, including gimbals and optics, but exclusive of the window, could be constructed with a weight of about 25 to 30 lb (11 to 14 kg).

Resolution of the sextant is limited by angle pick-offs used to determine the mirror position. The camera resolution, however, is limited by weight, due to the fact that for a given weight, the magnification (focal length) and lens diameter are constrained. Photography with large astronomical telescopes yields angle measurements (for star separation) accurate to the order of 0.005 sec of arc. With the spacecraft camera limited to about 25 to 30 lb (11 to 14 kg), an angle accuracy of 0.5 to 1.0 sec is likely.

The accurate time reference required for both navigation fixes and scientific observations utilizes an atomic resonance controlled oscillator. Some current models use rubidium vapor. The extremely accurate long term stability offered by these oscillators is illustrated by the performance characteristics of two types currently available, shown in Table 6-5.

6.7 REFERENCES TO SECTION 6

6-1. E. F. Lally and M. Pemberg, "A Survey of Advanced Mosaic Guidance" IAS Preprint No. 62-151, Presented at IAS National Summer Meeting, Los Angeles, 19—22 Jun 1962

6-2. Eugene Lally, "Mosaic Guidance for Interplanetary Travel," Astronautics, Vol. 7, No. 6, Jun 1962

6-3. R. G. Franklin, "The Study of Electromagnetic Techniques for Space Navigation," Franklin Institute, Navigation and Guidance Laboratory, 15 Nov 1961

Table 6-5

EXAMPLES OF TIME REFERENCE EQUIPMENT
(1962 State of the art)

Manufacturer	Type	Accuracy	Physical Specifications
Varian Associates (Model X-4700A)	Rubidium Vapor Frequency Standard	Stability: Long Term: $\pm 2 \times 10^{-10}$ (Any 90 day period) Short Term: $\pm 3 \times 10^{-11}$ (For one sec averaging time)	Total weight 95 lb (43 kg) 21 × 13 × 18 in. 2.9 ft^3 Output Frequency: 5 Mc, 1 Mc, and 100 kc
	Cost – $15,900	Ambient Temperature Range 15°C to 35°C	
STL Products (Model 1000A)	Rubidium Vapor Frequency Standard	Stability: Long Term: ±1 part in 10^{10} rms Short Term: ±2.5 parts in 10^{10} rms	Weight: 45 lb (20 kg) 9 × 9 × 17 in.
	Cost – $22,500	Accuracy: 1 part in 10^9 at all output frequencies	Power Requirement: 130-w max. (90-w continuous after warmup) Output Frequency: 4.996115 Mc, 5 Mc, 1 Mc, and 100 kc All outputs coherent

6-4. Inertial Guidance, Edited by George R. Pitman, Jr.

6-5. F. H. Kierstead, Jr., "Guidance Requirements for Interplanetary Flight," AAS Western National Meeting, Preprint No. 59-6, Aug 1959

6-6. Alan L. Friedlander, and David P. Harry III, "A Study of Statistical Data Adjustment and Logic Techniques as Applied to the Interplanetary Midcourse Guidance Problem," NASA Tech. Report R-113, 1961

6-7. David P. Harry III and Alan L. Friedlander, "An Analysis of Errors and Requirements of an Optical Guidance Technique for Approaches to Atmospheric Entry with Interplanetary Vehicles," NASA Tech. Report R-102, 1961

6-8. H. B. Haake and J. D. Welch, "A Self-Contained Interplanetary Navigator," IRE Transactions on Aerospace and Navigational Electronics, Mar 1961

6-9. Nortronics, "Space Navigation by Star and Planet Tracking Techniques," by F. Stevens, paper presented at IRE Fifth National Symposium on Space Electronics and Telemetry, Sep 1960

6-10. E. K. Sandeman, "Criterion for Angular Noise in Star-Lock Systems;" "FM Star-Lock System Using Mask with Linear Sectors;" and "FM Star-Lock System Using Mask with Spiral Sectors," IRE Transactions on Aerospace & Navigational Electronics, Mar 1962

6-11. General Electric Missile and Space Vehicle Dept., "A Precision Star Tracker for Space-Vehicle Attitude Control and Navigation," by D. R. McMorrow, C. A. Brownlee, Dardarian, and H. Schwartz; paper presented at American Rocket Society Conference on Guidance, Control, and Navigation, Stanford U., 7–9 Aug 1961

6-12. M. M. Birnbaum, P. M. Saloman, "The Astroguide – A Space Vehicle Navigation System," a paper presented at IRE National Convention, New York 26–29 Mar 1962

6-13. JPL Space Programs Summary, No. 37-16, Vol. III, "Deep Space Instrumentation Facility," 31 Jul 1962

6-14. George C. Marshall Space Flight Center, "The Path Adaptive Mode for Guiding Space Flight Vehicles," A paper presented by W. E. Miner and D. H. Schneider at ARS Guidance and Control Conference, Stanford U., 7–9 Aug 1961

6-15. "A Recoverable Interplanetary Space Probe, Vol. IV" Appendices, Rep. R-235, MIT, Jul 1959

6-16. J. V. Breakwell, "The Spacing of Corrective Thrusts in Interplanetary Navigation," AAS Preprint No. 60-76. Paper presented at the American Astronautical Society 3rd Annual Meeting, Seattle, Washington

Section 7

RECONNAISSANCE AND SCIENTIFIC INSTRUMENTATION

by

E. I. Curtis

Section 7
RECONNAISSANCE AND SCIENTIFIC INSTRUMENTATION

7.1 SCOPE AND SUMMARY

A preliminary feasibility-technique review was made of high-resolution optical reconnaissance from the manned Mars flyby vehicle. An in-house working report was prepared (Ref. 7-1) which dealt with that study, and added considerations and further study recommendations on other reconnaissance and scientific data collection requirements for both a manned flyby and an orbiting mission.

Pertinent sections of Ref. 7-1 are included here, reviewing methods applicable to reconnaissance in a manned Mars flyby mission. The special case selected for parametric treatment is that of extremely high-resolution optics, since this is at once the most productive and the most demanding reconnaissance function to be performed — with a good share of the design problems introduced by the dynamics of the trajectory itself. Feasibility is indicated.

The goal is to provide landing site detail of sufficient refinement to implement future precision manned landings. Both the vehicle large-payload capability and the man-implemented close planetary guidance contribute to this goal. Ground resolution capability as low as 5 ft (1.5 m) is sought. The closest and slowest feasible hyperbolic approach trajectory is selected as optimum for the mission, and variation of trajectory parameters examined for their effect on equipment design. Focal length, film resolution, stability requirements, light conditions, required film speed (ASA) ratings, varying frame rates, data collection and transmission rates are among the parameters explored in synthesizing a sample system to meet the stated performance requirements.

Other applicable techniques for reconnaissance and scientific data acquisition are reviewed briefly – both onboard the vehicle, and from a space-launched probe – as well as hypothetical sample payloads are provided. The Venus mission is, in general, excluded since permanent cloud cover may obscure the planet surface from onboard optical surveillance.

A number of the design problems presented by the flyby would be resolved if an orbiting vehicle were substituted. In addition, coverage would be improved. For comparative purposes, parametric values are presented for Mars orbital reconnaissance – both onboard and from probes. To contrast the two missions:

- The flyby, by its nature, is a limited reconnaissance tool. Limited in coverage to one swath per mission, it is also limited in design for high-resolution performance by the dynamics of the trajectory, by the continuous variation in sightline rotation rate and altitude above planet surface, and by the consequent variation in factors such as in frame, rate, and scale.
- The circular orbit, on the other hand, provides a superior reconnaissance platform; potentially stable, uniform in distance and speed of passage, capable of recording many swaths of planetary-surface for obtaining such information as detailed landing-site reconnaissance, and mapping. Its major problem is the potential superabundance of collectible data.

7.2 MISSION CONSIDERATIONS

The manned Mars flyby mission, projected for the 1971, or a later opposition, may serve either of two prime functions. First, it may provide landing-site reconnaissance and final environmental determination, in preparation for subsequent manned landing. To do this, the reconnaissance capability of this mission equipment must have as much or more resolution, coverage, flexibility, and data reliability as any carried by any preceding unmanned probes, flybys, orbiters, and landers such as Mariners and Voyagers. As illustrated in Fig. 7-1, onboard reconnaissance instrumentation may be supplemented by probes released from the manned craft.

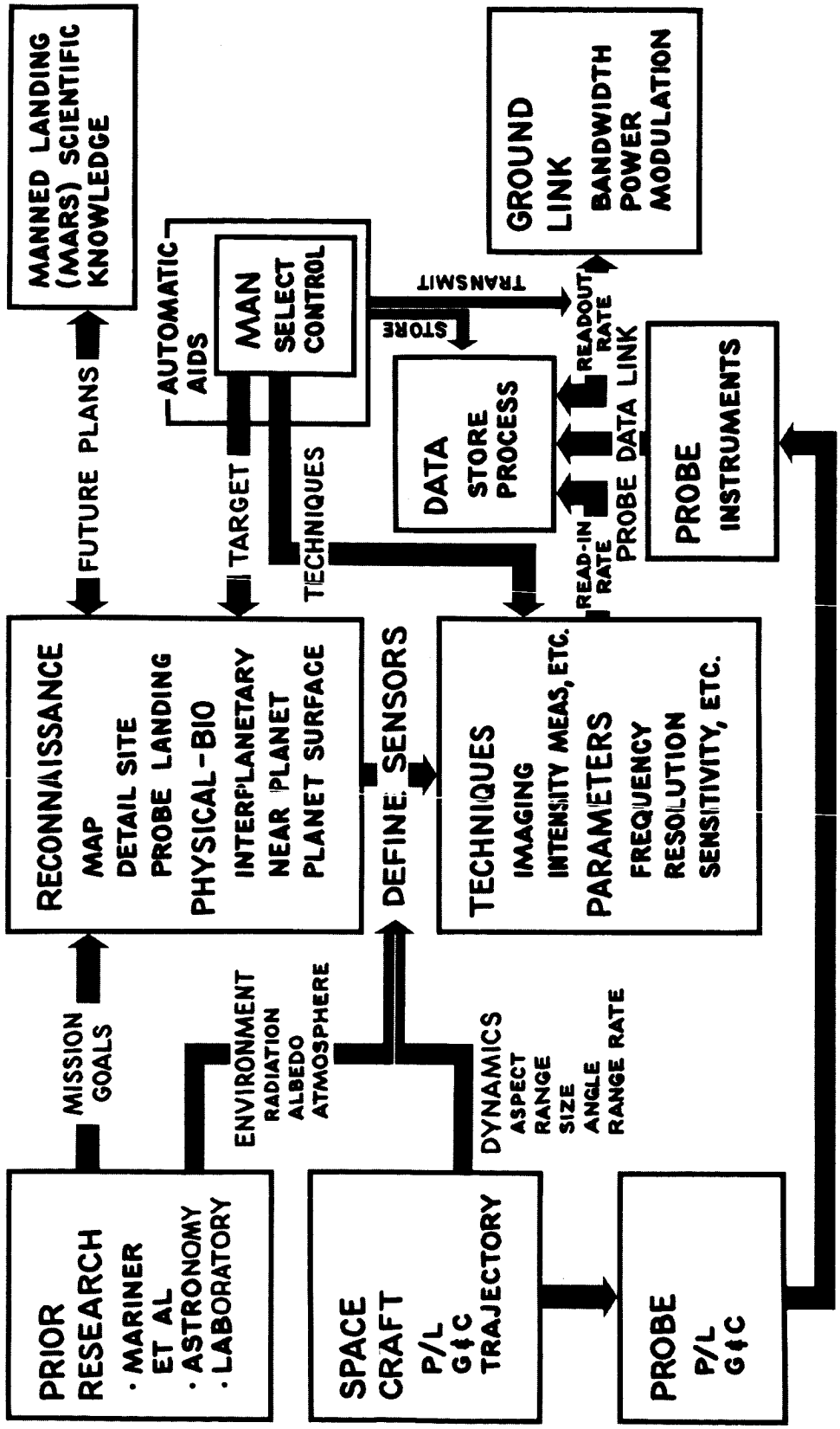


Fig. 7-1 The Manned Flyby Reconnaissance Role

Alternatively, the manned flyby may serve primarily as operational training for a later manned landing, with reconnaissance and other sensing instrumentation an incidental complement to the mission.

The extent to which the mission will compete with or surpass its unmanned predecessors as a reconnaissance tool is a function of the two principal factors of payload capability and the feasible closeness of planetary passage. As a preliminary estimate, an ultimate upper limit of several thousand pounds for reconnaissance equipment may be assumed. A reasonable lower-limit estimate might be several hundred pounds. Similarly, 250 nm (464 km) has been assigned as a mission goal for closeness of planetary passage at pericenter, with a ±10-mile (18.5 km) altitude accuracy assumed feasible.

The circa-1971, manned, Earth-returning flyby mission has several potential advantages as a reconnaissance mission:

- Targets will be carefully prechosen from prior data
- Sensing instrumentation, storage media, etc., may be designed solely to achieve optimum resolution, coverage, and accuracy, without primary concern for transmission methods and capabilities
- The onboard operator may aid guidance to the desired close planetary passage
- Direct visual observation by a trained observer may add reliability to the recorded reconnaissance data
- Some flexibility in the final choice of specific targets for detail reconnaissance may be provided by the presence of the onboard observer
- Compared to the unmanned lander, the flyby provides the potential for broader coverage at its highest resolution capability
- A superior instrumentation payload capability can generally be assumed

Note that, without the requisite payload capability, most of the prior advantage cited cannot be realized.

On the other hand, the manned flyby has several obvious disadvantages:

- Cost limits it to a one-shot or twin-shot mission
- Only one partial swath of the planet can be covered, compared to the multi-pass, long-term orbiter
- Compared to the orbiter, complex instrumentation is required to accomplish high-performance in the face of trajectory variations; and if optimum resolution is sought at all points of the approach trajectory, the recorded scale will vary continuously
- Compared again to the unmanned lander, distance handicaps its capability to resolve fine detail on the planet surface

Figure 7-2 summarizes the advantages and limitations of this mission.

7.3 POTENTIAL FUNCTIONS

7.3.1 Goals

The reconnaissance and data-gathering functions may be accomplished either by onboard equipment or by instrumentation of an unmanned probe to be launched toward the planet from the manned craft. Potential functions and methods available for comparative study and review are outlined below.

On-board Equipment Goals

- Detailed landing site reconnaissance – probably an order higher in ground resolution than achieved by earlier unmanned programs
- Mapping
- Weather and climate determination, e.g., cloud type and movement; heat balance between surface and atmosphere
- Detection of water and selected other elements
- Gravitation field measurement
- Magnetic field measurement
- Particle and radiation determination, interplanetary and planetary

MAJOR RECONNAISSANCE ADVANTAGES OF MANNED FLYBY (MARS)

Potential for:

FINE LANDING SITE DETAIL

- Large Optical Payload
- Man Guides Close Approach
  - Selects Reconnaissance Targets
  - Reviews & Analyzes Data
  - Selects Message Content

MAJOR LIMITATIONS

FLYBY VARIATIONS

In
- Range
- Range rate
- Angle rate
- Frame rate, etc.

LIMIT OPTIMUM SYSTEM DESIGN

ONLY 1 SWATHE per MISSION

Note: Orbiter is Superior as Reconnaissance Platform

Fig. 7-2 Advantages and Limitations of Mars Manned Flyby

Probe Functions

- Surface physical, chemical, and biological experiments
- Atmospheric measurement and particle count
- Closeup reconnaissance

7.3.2 Methods

The manned mission provides far greater flexibility than the unmanned mission in the design choice of reconnaissance methods to be used. The following outlines some indication of the range of choices.

Frequency Spectrum. There is no a priori restriction – except as the planetary environment may dictate – in the frequency choice of visual, infrared, or radar. The possibility of monochromatic optics, employing filters, is a potential aid to Mars surface coverage.

Optical Configuration. The choice may conceivably include any of the following:

Telescopes (choice of types)
Single pointing cameras
Rotating panoramic cameras (flight dynamics permitting)
Twin or trimetrogon mapping cameras
Spectrometers

Standard or Zoom Lens. Lens focal length may be held uniform to obtain optimum resolution in the near distance; or zoom techniques may be used to provide a uniform image scale at the sacrifice of near-planet resolution capability.

Data Handling. Methods of recording, processing, and display may range from standard film storage through such techniques as electrostatics, fiber optics, and TV; with a choice of compatible data processing and transmission techniques.

Infrared. Infrared configuration may include imaging, or intensity measurement, pointing or scanning, etc.

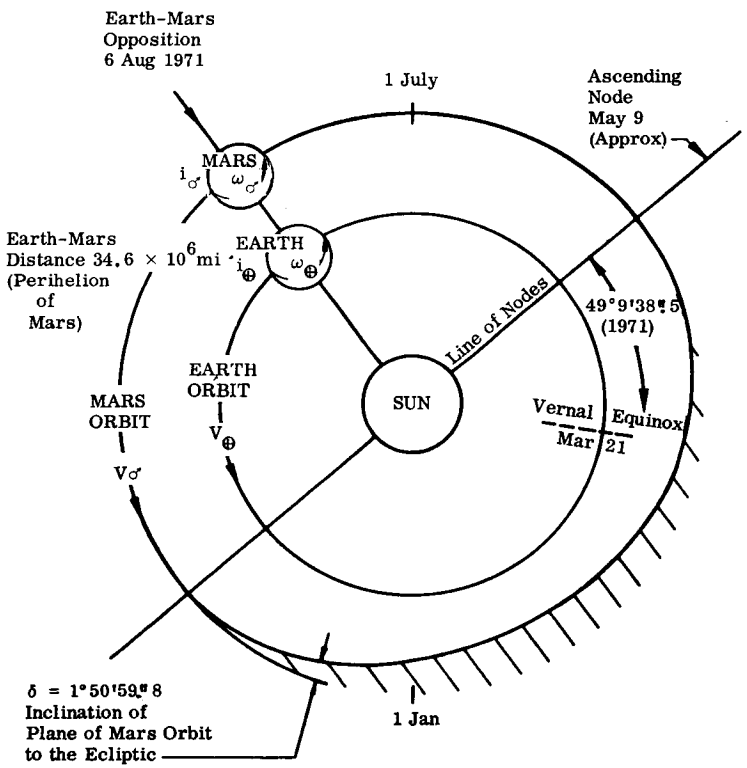
Radar. The utility of radar, either in the optical or R-F range, may be explored, particularly where the visual albedo is inadequate.

Since system constraints and reconnaissance capabilities are most critical for high-resolution optics, and since performance is closely related to the dynamics and geometry of the flyby, first consideration will be given to reviewing the factors affecting detailed landing-site reconnaissance.

7.4 TRAJECTORY CONSIDERATIONS

Trajectory considerations most pertinent to the reconnaissance problem are the choice of darkside or lightside planetary passage, as well as the range of distance and speed in the region of passage. (Lightside passage is the obvious choice for this report since optical techniques are under discussion.) A complete treatment of the mission environment would also relate planetary light conditions to the flight path, charting Sun angle of declination and planet latitude as functions of trajectory time and direction. However, for the purpose of this initial review, a representative set of Earth light data is converted to planetary use by the simple assumptions: (1) The level of Mars-to-Earth illumination is in inverse ratio to the squares of the planet orbital radii; and (2) That Mars surface reflectance is one-third that of Earth.

Reference data for the 1971 opposition year are presented in Fig. 7-3. Figure 7-4 shows the geometry of the reconnaissance portion of the mission — the hyperbolic approach and departure trajectory, along with a definition of the major elements to be resolved for the purposes of reconnaissance system design. Note that the major trajectory variables which affect the case are hyperbolic excess velocity, V_H and pericenter distance r_p, or similarly h_p, the vehicle height above Mars surface at periapsis.



	⊕ EARTH	♂ MARS
Orbital Data		
Orbital Period	$P_{\oplus}$ 365.26 da	$P_{\sigma'}$ 779.94 da
Rotation Period	$T_{\sigma'}$ $23^h37^m23^s$	$T_{\oplus}$ $23^h56^m4^s$
Mean Orbital Speed	$V_{\oplus}$ 16.06nm/sec	$V_{\sigma'}$ 13.01nm/sec
Rotation Speed	@ Approx 15 deg/hr	
Inclination Equator to Orbit Plane	$i_{\oplus}$ 23°.5	$i_{\sigma'}$ 24°
Physical Data		
Mean Radius ($R_{\oplus}$ = 3438 nm)	$R_{\oplus}$ 1	$R_{\sigma'}$ 0.523
Mass ($M_{\oplus}$ = 1.3173 × 10^{25} lb)	$M_{\oplus}$ 1	$M_{\sigma'}$ 0.1069
Mean Orbit Radius ($r_{\oplus}$ = 30.7 × 10^6 nm)	$r_{\oplus}$ 1	$n_{\sigma'}$ 1.524
Surface Gravity ($g_{\oplus}$ = 32.17 ft/sec^2)	$g_{\oplus}$ 1	$g_{\sigma'}$ 0.39
Surface Pressure ($p_{\oplus}$ = 78 cm Hg)	$P_{\oplus}$ 1	$p_{\sigma'}$ 0.08

Fig. 7-3 Earth/Mars Orbital Geometry and Physical Data (1971)

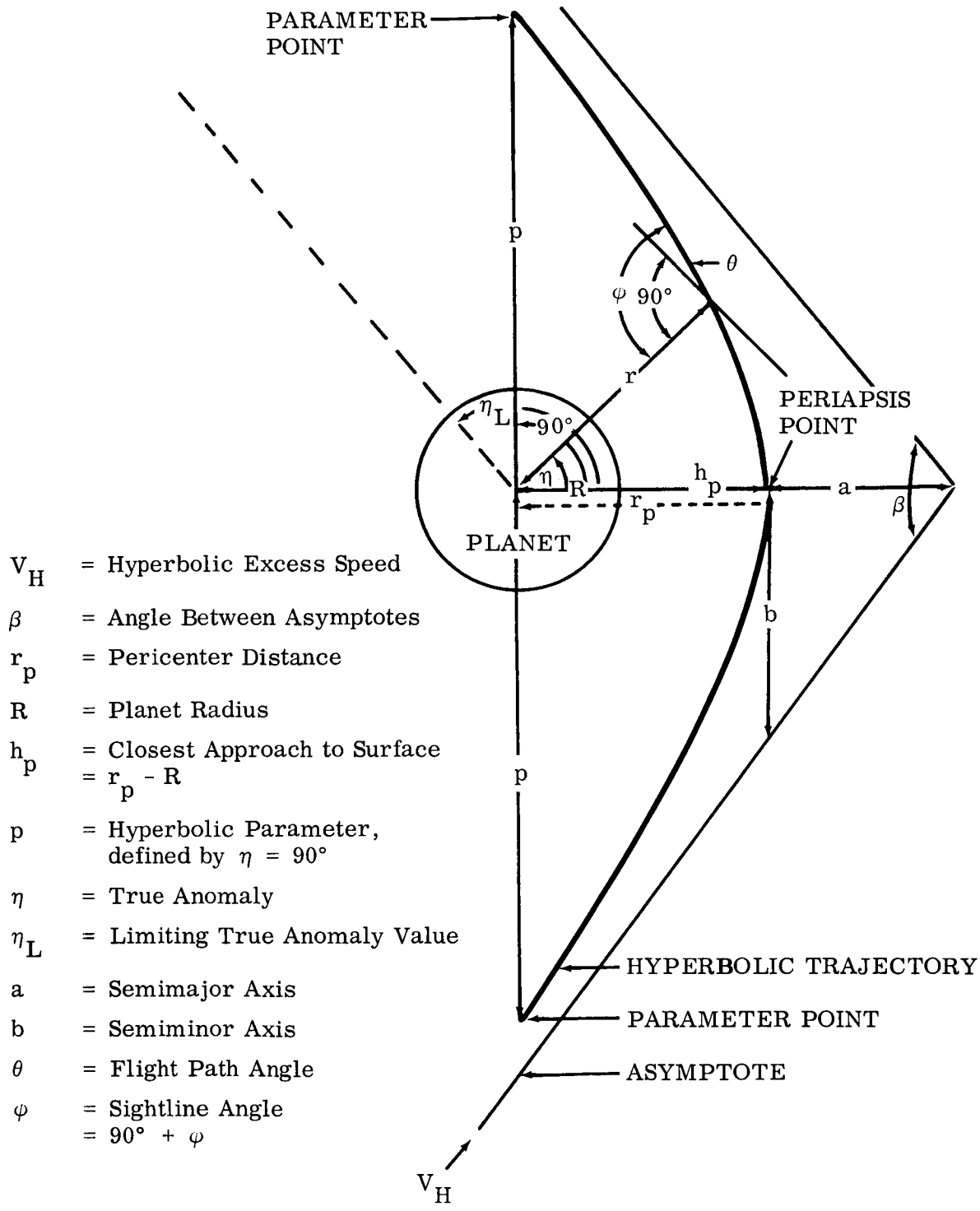


Fig. 7-4 Hyperbolic Approach-Departure Trajectory

As an example Fig. 7-5 shows the variation of true anomaly rotation rate with altitude for trajectories in which the hyperbolic excess velocity V_H equals 0.2 EMOS (Earth-mean-orbital-speed, $V_\oplus$. Figure 7-6 compares flight time between equivalent radial distances for trajectory families of V_H equals 0.2 and 0.3 $V_\oplus$ respectively. Other pertinent parameters are graphed in Ref. 7-1)

Review of these dynamic considerations, as well as the need for fine ground resolution, dictate the choice of the low, slow potentially feasible trajectory for the reconnaissance mission – i.e., the sample flight of hyperbolic excess velocity equal to 0.2 Earth-mean-orbital-speed and approaching within 250 nautical miles of the planet surface. In the next section, this trajectory will be employed in the synthesis of a sample high-resolution reconnaissance system.

7.5 HIGH RESOLUTION OPTICS

The large payload capability of the vehicle, the presence of the onboard operator to assist in guiding a near-planetary trajectory, and the physical returnability of the reconnaissance record all contribute to the mission potential for extremely high-resolution optical system performance.

A preliminary design goal of 5-ft (1.5 m) ground resolution will be assumed, along with an operational resolution capability (photographic) of 100 lines per millimeter, equivalent to 200 lines per millimeter TV resolution. Figure 7-7 illustrates related values for a sample high-resolution optical system meeting these goals, and the balance of this section outlines the tradeoffs which have been considered in constructing the system.

First, based on the trajectory considerations of Section 7.4, the optimum feasible flyby trajectory was selected, approaching within 250 nm (463 km) of the planet at periapsis. To facilitate discussion, the reconnaissance period is assumed to lie within the 105 min of flight time between the two parameter points. As illustrated in Fig. 7-7,

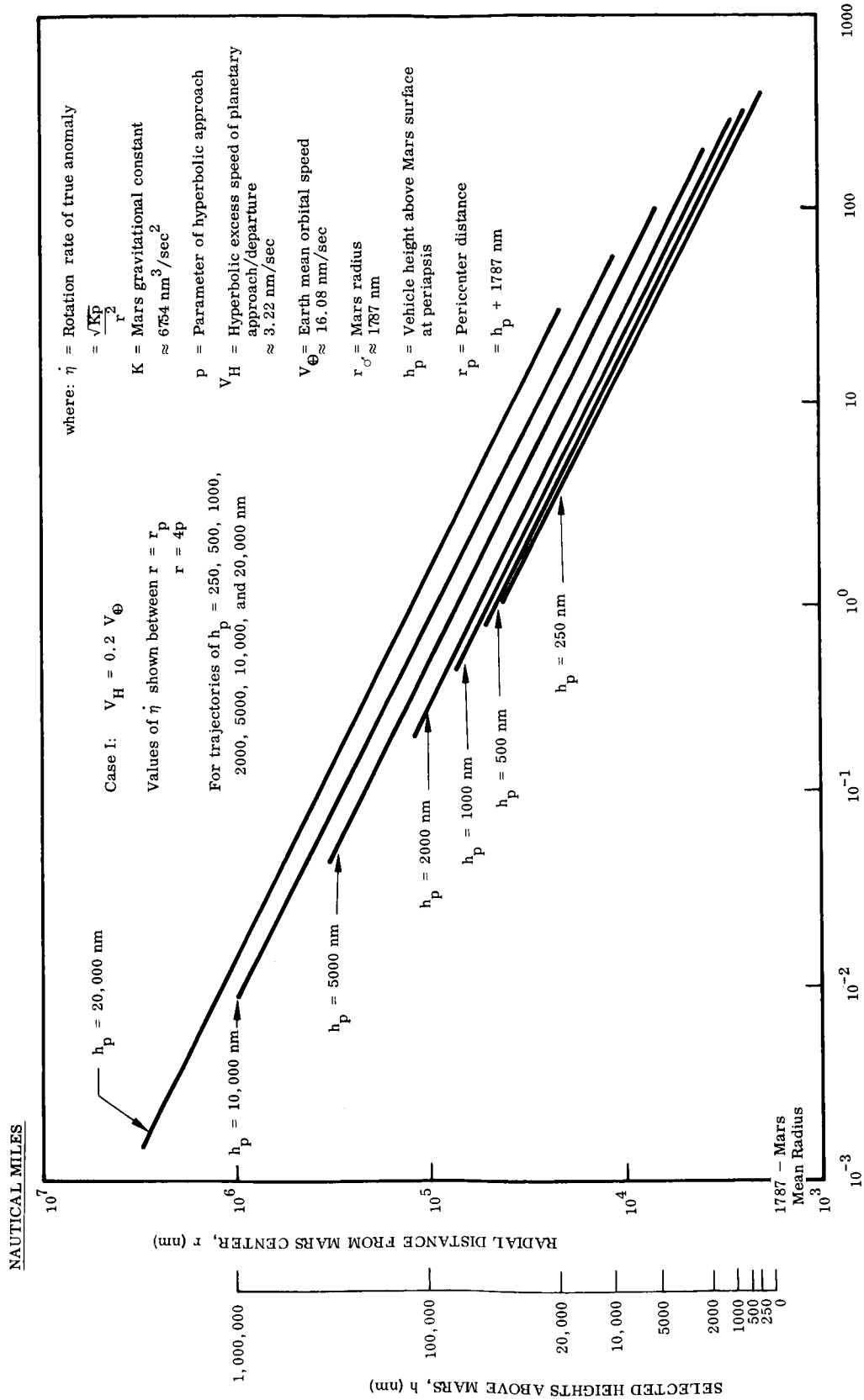


Fig. 7-5 Rotation Rate of True Anomaly vs. Radial Distance in Hyperbolic Approach to Mars as a Function of Periapsis Distance

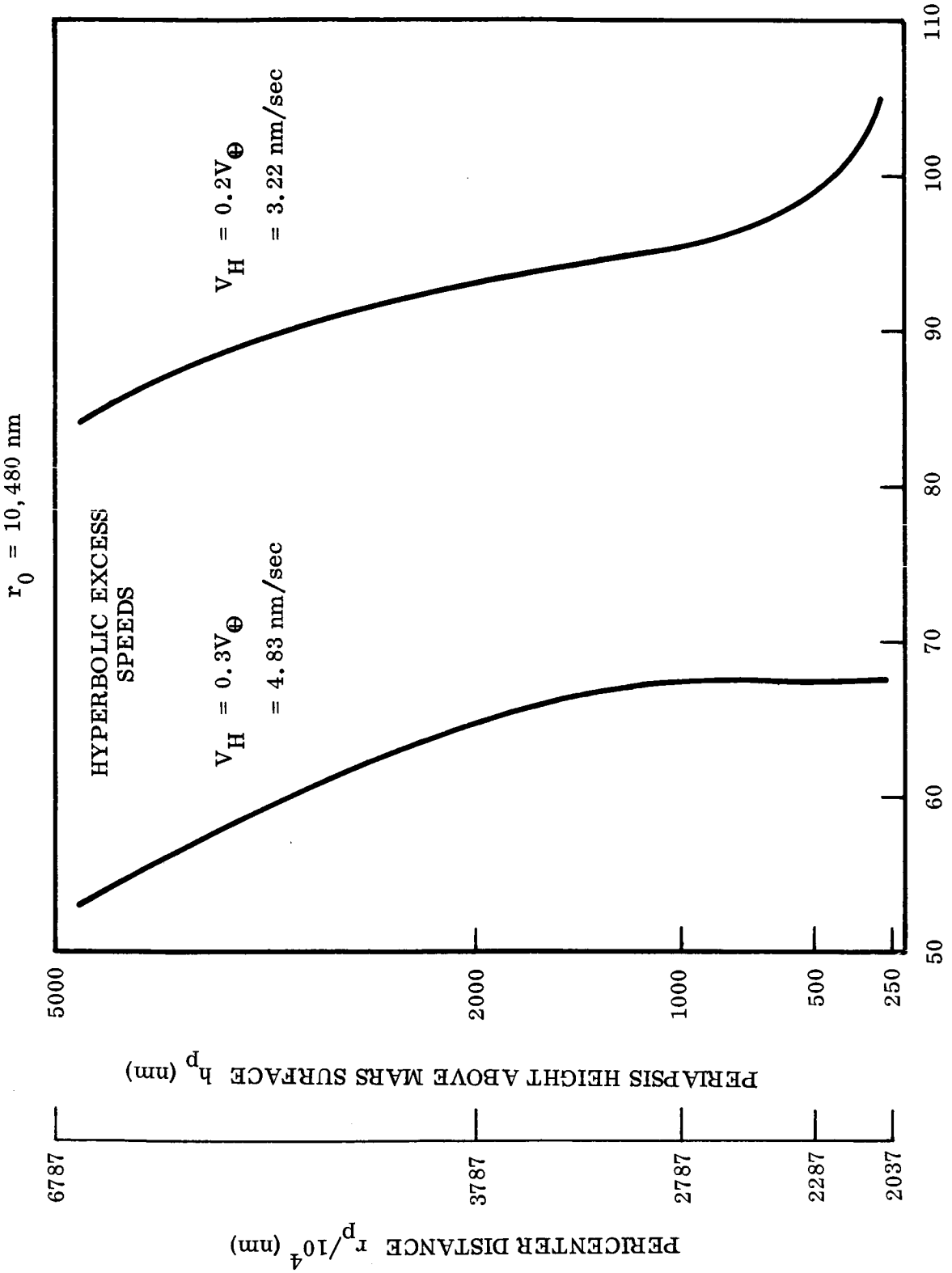
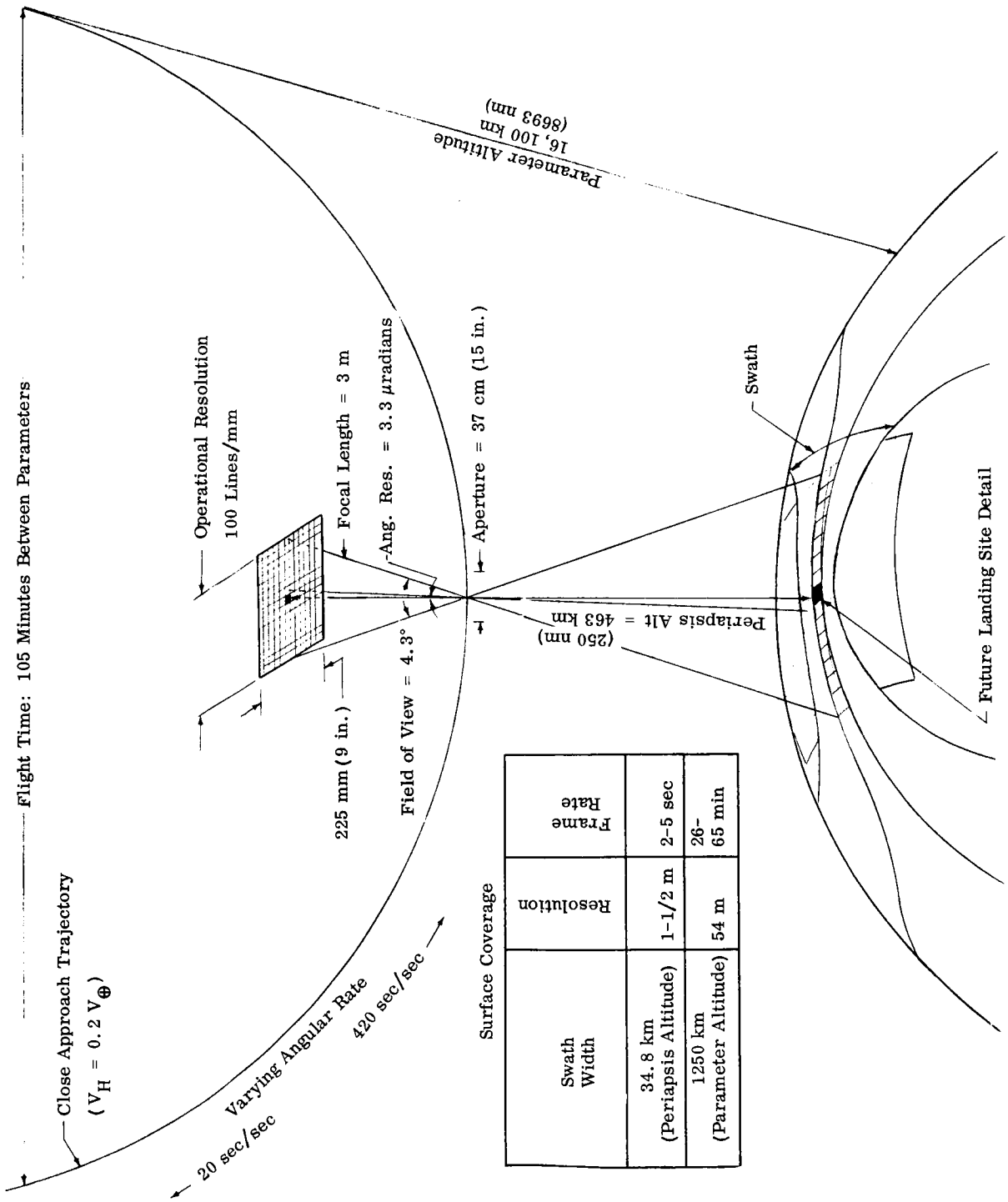


Fig. 7-6 Total Flight Time Between Equivalent Radial Distances from Mars Center as a Function of Periapsis Height, for Two Values of Hyperbolic Excess Speed



Surface Coverage

Swath Width	Resolution	Frame Rate
34.8 km (Periapsis Altitude)	1-1/2 m	2-5 sec
1250 km (Parameter Altitude)	54 m	26-65 min

Fig. 7-7 Sample High Resolution Optics

vehicle-to-planet distance is almost 9,000 nm ($\sim$ 16,000 km) at the parameter points of the approach and departure trajectory. The true anomaly rotation rate varies between 20″/sec at parameter and 420″/sec at periapsis.

In practice, design usually can best be optimized for a relatively narrow set of conditions, and some design compromise will probably be required to meet the broad range of operational conditions represented by the flyby trajectory.

Final design configuration may be based either on standard film techniques, electrostatic storage, or TV. However, for simplicity of discussion, the standard photographic method will be used for this initial quantitative treatment and tradeoffs evaluated considering such factors as reconnaissance altitude, coverage, ground resolution, focal length, stability, and illumination conditions.

7.5.1 Geometric Tradeoffs in Resolution

Ground resolution varies as a function of reconnaissance altitude, as well as of focal length and film resolution. Initially assuming a static system, the ground resolution may be computed by the simple geometry illustrated in Fig. 7-8. For example, at periapsis altitude h_p for the simplified static case noted, and assuming a film resolution capability of 100 lines per millimeter, i.e.,

$$x = 10^{-2}\ \text{mm} \approx 4 \times 10^{-4}\ \text{in.}$$

Focal Length, $F = 120$ in.(3m)

Film Width $X = 9$ in.(225 mm)

Altitude $H = h_p = 250$ nm (464 km)

Then, the overall field of view:

$$\Theta = 2 \tan^{-1}\left(\frac{9/2}{120}\right) = 4°.3$$

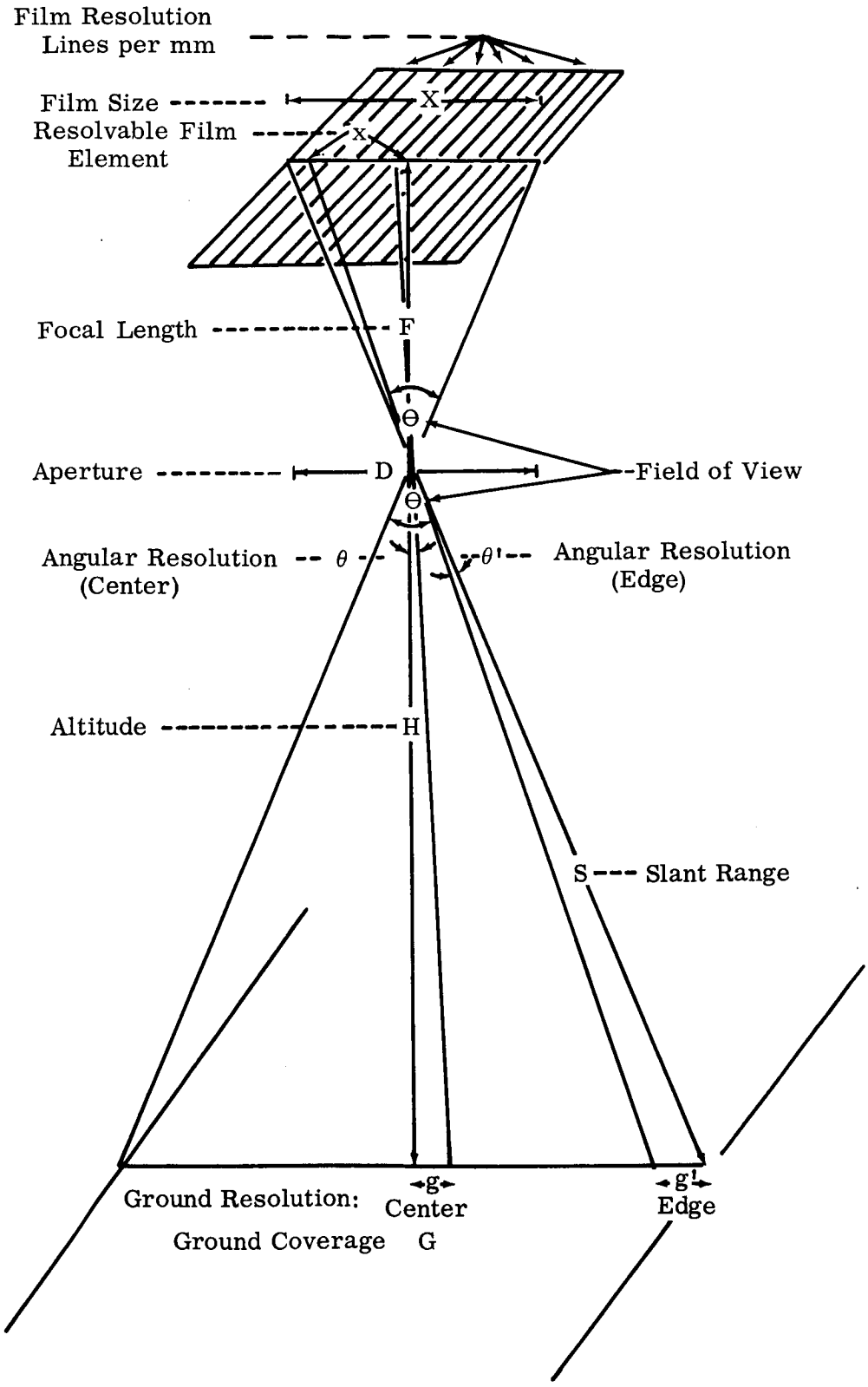


Fig. 7-8 Simplified Resolution Geometry

The overall width of ground coverage:

$$G = H\frac{X}{F} = 250 \times \frac{9}{120} = 18.75 \text{ nm } (34.8 \text{ km})$$

The ground resolution at the center of the field:

$$g = H\frac{x}{F} = 250 \times 6 \times 10^3 \times \frac{4 \times 10^{-4}}{120} = 5 \text{ ft } (1.5 \text{ m})$$

The angular resolution at the center of the field:

$$\theta = \frac{g}{H} = \frac{5}{250 \times 6 \times 10^3} = 3.3 \ \mu\text{rad} = 0.66'' \qquad (7\text{-}1)$$

The edge resolution in this case differs negligibly from the center since:

$$g' = g'' \quad \Theta/2 \approx 5.02 \text{ ft}$$

Similarly, since both resolution and coverage width vary linearly with altitude, at parameter altitude of approximately 9,000 nm (16,000 km), the ground resolution is 180 ft (54 m), and the width of the coverage swath is 675 nm (~ 1250 km).

7.5.2 Limiting Optical Resolution

In considering very long focal-length optics, particularly telescopes, the criterion must be applied of limiting optical resolution, established by the circle of diffraction. As illustrated in Fig. 7-9, the lens system is capable of resolving the overlap of one radius in adjacent circles of diffraction produced in light passage through the lens. Where a monochromatic, parallel beam of light from distant object O is diffracted by a slit or lens, it produces respectively a banded or circular interference pattern (light/dark) on the image plane.

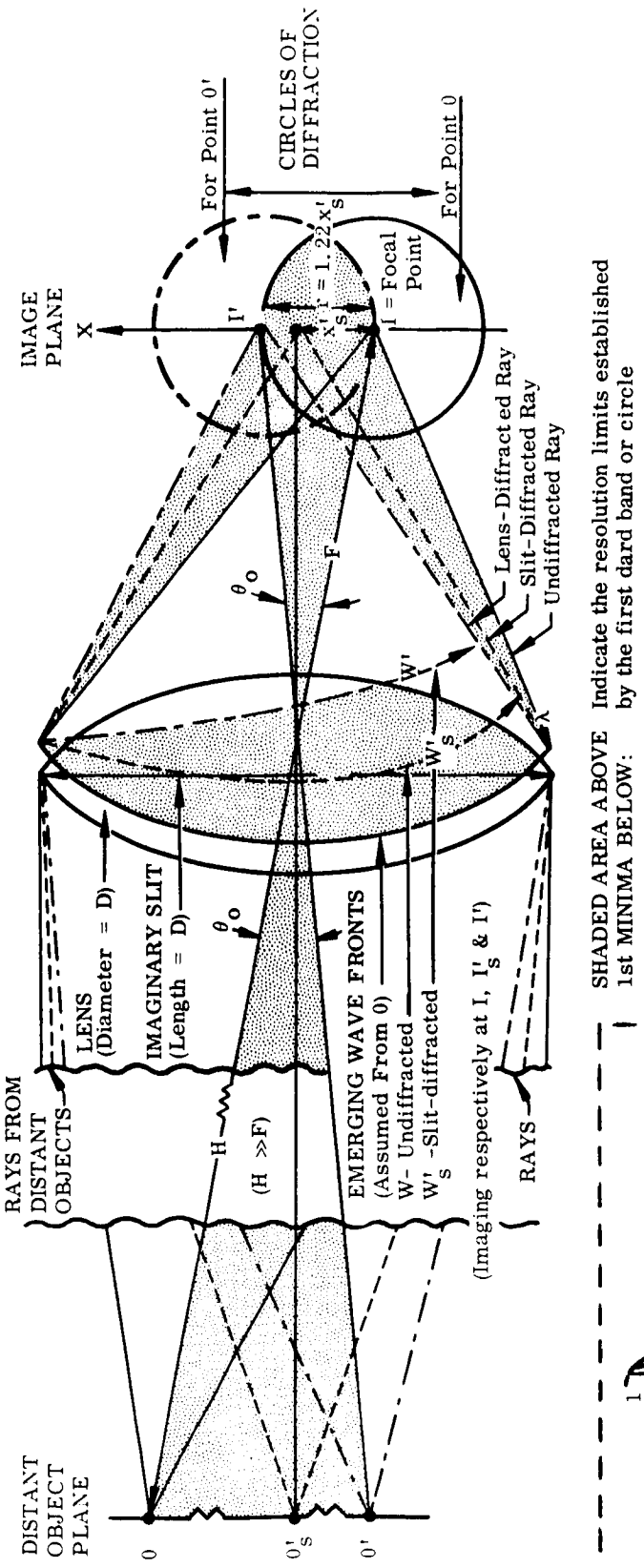


Fig. 7-9a Circle of Diffraction

Fig. 7-9b Image Intensity vs. Distance from Focal Point/Wavelength

In the case of the slit: When W'_s leads W by 1λ, light from the upper and lower half of the slit cancel each other, producing a dark spot at I'_s. Then, by similar triangles:

$$\frac{x'_s}{F} \approx \frac{\lambda}{D}$$

and O and O'_s are resolved.

In the case of the circular lens: The solid curve of Fig. 7-9b shows that, for light diffracted at a circular opening, the 1st minimum occurs at $x/\lambda = 1.220$; i.e., the radius of the circle of diffraction:

$$r = 1.220\,\lambda = 1.220\,x'_s$$

Also, the angular resolution limit:

$$\sin\theta_o \approx \theta_o \approx \frac{r}{F} \approx \frac{1.220\,x'_s}{F} \approx 1.220\,\frac{\lambda}{D}$$

indicating the resolvability of O and O'.

This resolving power θ_o is a function of wave length and may be computed as follows:

$$\theta_o = \frac{1.22\,\lambda}{D} \qquad (7\text{-}2)$$

where

λ wavelength of light

D diameter of lens aperture, as shown in Fig. 7-8.

For the median value of $\lambda = 5600$ A (green light)

$$\theta_o \approx \frac{27}{D}\ \mu\,\text{rad} \approx \frac{5.52''}{D} \qquad \text{where D is in inches.}$$

The focal length and diameter of an optical system are related by the f-number, defined as follows

$$f/No. = \frac{F}{D}$$

Thus, assuming a conservative value of f/8 for the 120-in. focal length of our example $\frac{F}{D} = 8$ and $D = \frac{120}{8} = 15$ in.(37.5 cm).

Hence, from Eq. (7-2)

$$\theta_o = \frac{5.52}{15} \approx 0.37 \text{ sec} \quad \text{or} \quad 1.8 \ \mu \text{ rad}$$

which is within the 3-μ rad capability specified in Eq. (7-1).

Also, this may be equated to an elemental ground blur

$$g_o = 1.8 \times 250 \times 6 \times 10^3 = 2.7 \text{ ft}$$

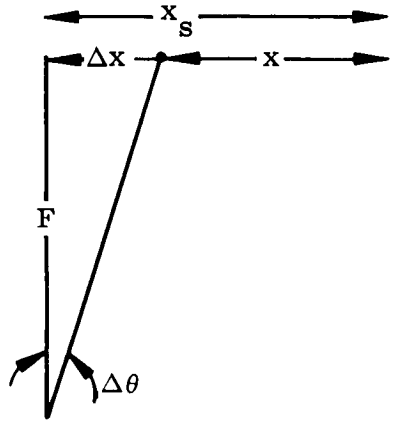
at 250 nm reconnaissance altitude.

7.5.3 Operational Resolution and Stability Requirements

The static film-lens resolution capability of a system may be degraded operationally by angular motion, as well as by distortion due to the transmission medium. We have already specified an operational resolution requirement x_s of 100 lines per mm for our system. Considering only the effects of angular motion, this capability may be achieved by assuming the following:

Required: $x_s = 100$ lines/mm

Given: Static Film Resolution $x = 115$ lines/mm
Frame time $t = 4$ millisec
Focal length $F = 120$ in. $= 3$ m



Then; permissible film travel during frame:

$$\Delta x = x_s - x = \frac{1}{100} - \frac{1}{115} = 1.3 \times 10^{-3} \text{ mm}$$

or, converting to the angle of travel

$$\Delta\theta = \frac{\Delta x}{F} = \frac{1.3 \times 10^{-3}}{3 \times 10^{3}} \approx 4 \times 10^{-4} \text{ millirad}$$

This imposes an angular stability requirement $\dot{\theta}$ on the system:

$$\dot{\theta} = \frac{\Delta\theta}{t} = \frac{4 \times 10^{-4} \text{ millirad}}{4 \times 10^{-3} \text{ sec}} = 0.1 \text{ millirad/sec}$$

7.5.4 Illumination Conditions and Film Speed Requirements

As indicated above, a short frame time of 4 millisec was chosen in order to ease the stability requirements on the vehicle system. Another limiting set of factors on high resolution photography, also associated with frame time, is that of illumination, reflectance and film speed (usually defined as ASA rating).

To test the feasibility of 4-millisec photography of Mars, a difficult set of light conditions (at Earth Lat. 60° N) where illumination data degrade to Mars conditions. Low-reflectance reconnaissance target and background were selected, respectively equivalent to dry concrete and soil or water.

The readily available basic Earth illumination data (per Ref. 4) were degraded to 1/2.25 the published values, corresponding to the ratio of the inverse squares of the planet orbital radii. Also, reflectances were degraded to 1/3 by use of the assumption current in the literature (Refs. 7-6, 7-7, and others) that reflectance on the Mars surface averages one-third that of Earth. Computation details are reviewed in Ref. 7-1.

The resulting film ASA rating requirements vary from 15, under the best light conditions, to 20,000 under the worst noted. The latter figure is probably currently attainable only by research films using direct positive processing.

7.5.5 Frame Rate

As illustrated in Fig. 7-7, the angular rate $\dot{\eta}$ of the true anomaly in the approach trajectory varies between periapsis and parameter point from 420 seconds-of-arc per second to 20 seconds-of-arc per second. Also, the coverage Θ_s provided on Mars surface by the 4.3° field of view of our system varies between 0.6 Mars degrees and 21.7 Mars degrees as height above the surface varies from 250 nm at periapsis to approximately 9,000 nm at parameter.

For continuous coverage of the reconnaissance swath, with no overlap of frames, the maximum frame rate N_o may be computed as follows:

At periapsis

$$N_o = \frac{\dot{\eta}}{\Theta_s} \frac{0.1165}{0.6°} \approx \text{one frame per 5 sec}$$

At parameter

$$N_o = \frac{\dot{\eta}}{\Theta_s} \frac{0.33}{21.7°} \approx \text{one frame per 65 min}$$

With 60 percent overlap, the frame rate is accelerated 2.5 times. Thus,

At periapsis

$$N_{60} = 2.5\, N_o \approx \text{one frame per 2 sec}$$

At parameter

$$N_{60} = 2.5\, N_o \approx \text{one frame per 26 min}$$

The computed values are summarized in Table 7-1.

Table 7-1
MAXIMUM FRAME RATE AT PERIAPSIS AND PARAMETER ALTITUDE

			Θ_s Mars°/Frame	Interval between Frames	
Altitude	nm	km	(Θ = 4.3°)	No Overlap	60% Overlap
Periapsis	250	463	.6°	5 sec	2 sec
Parameter	8693	16,100	21.7°	65 min	26 min

Integration of this continuously varying frame rate over the 105-minute reconnaissance period indicates a maximum limit of 100 frames required during the total flight between parameter points.

7.5.6 Total Data Bits

The computation of total data bits collectible per frame and per 105-minute flyby swath, as well as the associated bandwidth requirements, may be performed as follows, assuming:

Frame size $X = 225$ mm
Operational Resolution $= 100$ lines/mm
i.e. $x = .01$ mm
64 grey shades, requiring 6 bits for digital description
i.e. $s = 6$

Then the number of bits per frame:

$$b_1 = \frac{s X^2}{x^2} = \frac{6(225)^2}{(.01)^2} = 3 \times 10^9 \text{ bits/frame}$$

and the number of bits per 100 frames specified for the total mission:

$$b_{100} = 100\, b_1 = 3 \times 10^{11} \text{ bits/100 frames}$$

Total bits collected may be translated into transmission requirements by assumptions such as the following:

Operator selection ratio (Bits transmitted/bits collected)	$\sigma_o = 0.1$	
Transmission time	$T_t = 36$ days	$(8.64 \times 10^4$ sec/day)
Incremental bandwidth required	$w = 3$ cps/bit	

Then total bandwidth required:

$$W = \frac{\sigma_o\, b_{100}\, w}{T_t}$$

or

$$W = \frac{0.1 \times 3 \times 10^{11} \times 3}{36 \times 8.64 \times 10^4} = 30 \text{ kc for 36 days}$$

7.5.7 Data Handling

Analysis up to this point, while concerned mainly with the basic optical system, has employed optimum parameters which may be feasible using standard photographic film for storage. Alternative choices for data-handling and storage include electrostatic recording and TV. Relative advantages of the three techniques are reviewed in a qualitative way in Ref. 7-1. A signal disadvantage of standard film lies in the susceptibility of the unprocessed film to radiation fogging. Unfortuantely, this effect is intensified for high-speed film.

7.6 ADVANTAGES OF ORBITER FOR RECONNAISSANCE

While the instrumentation of a flyby reconnaissance system is a complex exercise in design ingenuity, the orbiting system presents a standard operational pattern for design optimization. This section will consider two possibilities:

- A manned system orbiting at 250-nm altitude above Mars with the high-resolution optics already described
- An unmanned probe released from the manned craft to orbit at 100-nm altitude, with the optical system reduced to provide equivalent performance capability at the lower altitude.

Comparing the orbiting reconnaissance system with the flyby, the following points are pertinent:

- The orbiter presents a considerable design advantage in the simplicity of uniform flight altitude, angular rate, and related operational conditions. Performance efficiency, reliability, and weight-saving are byproducts of this simplicity
- A uniform, standard, readily deciphered record is provided at uniform scale and coverage
- The potential volume of data collectible is enormous, requiring ingenuity in data-selection and handling techniques

7.6.1 The Manned, 250-nm Orbiter

Similarly to the system of Section 7.5, the 250-nm orbiter will be considered to be instrumented with a 120-in. focal-length camera, with a 4.3° field of view. The orbiter then records a uniform 5-ft ground resolution and approximately 19-mile-wide swath (0.6° of Mars surface) throughout the mission, in contrast to the 36-fold variation of the flyby between periapsis and parameter.

Computing the orbital period

$$T = \frac{2\pi r^{3/2}}{K^{1/2}} = 117 \text{ min, for 250-nm orbital altitude}$$

where

$K = 6754\ \text{nm}^3/\text{sec}^2$ = Mars gravitational constant

$r = R + h$ $\quad R$ = Mars Radius = 1787 nm

$\quad h$ = Orbital altitude above planet surface

This period is equivalent to a uniform angular rate of planetary passage of about 3 minutes-of-arc per second. The Mars sidereal day is $24^h37^m23^s$, or approximately 1477 minutes. Hence, there will be approximately 12.65 orbits per Mars day.

Since the width of surface coverage is 0.6° of Mars surface and each orbit crosses the equator twice, equivalent reconnaissance orbits required for adequate coverage (i.e., orbits assuming adequate light condition) may be obtained as follows.

For a polar orbit, (virtually complete planetary coverage):

$\frac{360°}{2 \times 0.6°}$ = 300 equivalent reconnaissance orbits, requiring about 24 equivalent days

For an orbit inclined 59 (coverage between 59°N and 59° S latitude):

$\frac{360°}{2 \times 0.6\ (\csc 59°)} = \frac{360°}{2 \times 0.7°}$ = 257 equivalent reconnaissance orbits, requiring about 20 equivalent days

Since adequate light conditions for photography will exist less than half the time, the actual number of days required for 300 equivalent reconnaissance orbits will be more than twice the equivalent days shown above.

As noted above, the potential abundance of reconnaissance data is a major system design problem. Table 7-2 indicates the maximum data rate, as well as film footage requirements, for high-resolution optics, assuming complete coverage. The figures for a single orbit are compared with the 105-minute flyby (with 60 percent overlap). As indicated, if the data collectible from a single equivalent orbit were to be transmitted in 36 days at 36-kc bandwidth, as assumed for the flyby – severely reduced data selection ratio would be required (bits transmitted/bits collected) ranging from 1.7 percent for no overlap, down to 0.7 percent for 60 percent overlap.

For complete planetary coverage by 300 equivalent orbits, assuming 100 days for transmission and a 1 percent data selection ratio, a bandwidth of approximately 1 Mc would be required. Film footage requirements would also be excessive, pointing again to the necessity for optimum data collection criteria.

7.6.2 Unmanned 100-nm Orbiter

A potential capability of the manned Mars flyby is that of launching an unmanned probe from the manned space vehicle into planetary orbit. If such a probe were orbited at 100-nautical-mile altitude and instrumented with a 48-in. focal-length camera and 9-in. format film, the performance capability in ground resolution and swath width would be equivalent to that previously noted for the 250-mile, 120-in. system.

The period of the 100-nm orbiter is approximately 105 minutes (about 14 orbits per Mars day), and the angular rate of planetary passage is about 3.5 minutes-of-arc per second. Reverting to Table 7-2 complete 300 equivalent-orbit coverage, transmitted within 100 days, would then require about 63 megacycles bandwidth. Any transmission selection ratio below unity would require ingenious pre-processing and comparison, since any data not transmitted would be lost. Hence, the problem of pre-selection of collected data is intensified for the unmanned orbiter.

Table 7-2

MAXIMUM DATA COLLECTION RATE AND TRANSMISSION BANDWIDTH REQUIREMENTS
HIGH-RESOLUTION ORBITER – (0.6° MARS SURFACE PER FRAME)

a. PER ORBIT

		No. of Frames	Ft. of Film	No. of Bits Collected	Selection Ratio Bits Transmitted/Collected	
Reference – 105-Min. Flyby (60% overlap)		100	75	3×10^{11}	10%	To Permit Transmission within 36 days at 30-kc bandwidth (3 cps/bit)
Orbiter	No overlap	600	450	1.8×10^{12}	1.7%	
Film	10 overlap	720	540	2.16×10^{12}	1.4%	
Coverage	60 overlap	1500	1125	4.5×10^{12}	.7%	

b. PER 300 EQUIVALENT RECONNAISSANCE ORBITS (Complete Coverage)

						Bandwidth Required to Permit Transmission Within 100 Days
Orbiter	No overlap	1.8×10^5	1.35×10^5	5.4×10^{14}	100%	62.6 mc
					1%	.63
Film	10 overlap	2.16×10^5	1.62×10^{15}	6.48×10^{14}	1%	.76 mc
Coverage	60 overlap	4.5×10^5	3.38×10^5	1.35×10^{15}	1%	1.58 mc

7.7 TOTAL FLYBY RECONNAISSANCE SYSTEM

The total reconnaissance system for the flyby mission may be instrumented by onboard equipment to obtain reconnaissance data over a wide range of the spectrum, as well as interplanetary and near-planet particle, field, and other physical data. In addition, one or more probes may be launched from the manned vehicle to orbit or land on the planet surface and transmit back atmospheric and planet-surface measurements. For the purpose of computing transmission requirements, it will be assumed here that the probes are launched in advance and transmit to the vehicle during the 105 minutes between parameter points on the hyperbolic approach-departure trajectory.

Figure 7-10 provides a resume of the capabilities, data volumes and total transmissior requirements of sample instrumentation, showing ground resolution capabilities down to 5 ft. Published data are included for comparison on the best resolution capabilities quoted for unmanned Mariner B. A summary weight-volume-power listing for the total equipment is given in Table 7-3.

7.7.1 Onboard Reconnaissance Instrumentation

Reconnaissance devices, as indicated in Fig. 7-10, may range from the extremely high-resolution optics already discussed, to medium-resolution stereo mapping, to lower-resolution cloud-cover and IR-imaging devices. Crude mapping of the radar reflectance of the planet terrain may also be indicated.

Table 7-4 lists a hypothetical equipment complement for such an onboard system, including the following:

(1) High Resolution Optics
   a) 120-in. focal-length, 4.3° field-of-view standard camera, as already described; or
   b) An electrostatic equivalent, somewhat reduced in capability and size.

Table 7-3

MANNED FLYBY POTENTIAL PAYLOAD RECONNAISSANCE & SCIENTIFIC INSTRUMENTATION

	WEIGHT (lb)	VOLUME (ft^3)	POWER (kw)
ON-BOARD RECONNAISSANCE SYSTEM Detail-Site Camera (120 in. F. L.) Stereo Mapper, IR Imaging, Radar + Processors, Displays, etc.	750–1250	31–37	3.3 (105 Min) (Mainly Radar)
ON-BOARD SCIENTIFIC INSTRUMENTS Interplanetary & Planetary Measure – Fields, Particles, Air (Growth from Mariner-Centaur Experiments + Display/ Analysis Aids for Manned Direction	450	17	0.2
ON-BOARD TOTAL	1200–1700	48–54	3.5 kw (peak)
PROBE INSTRUMENT SYSTEM TV, Weather, Gas, Radiation, Soil, Biological Tests + Beacon, Command Rcvr, Data Storage, Converters, Transmitter	210	8 cu ft	0.050 kw

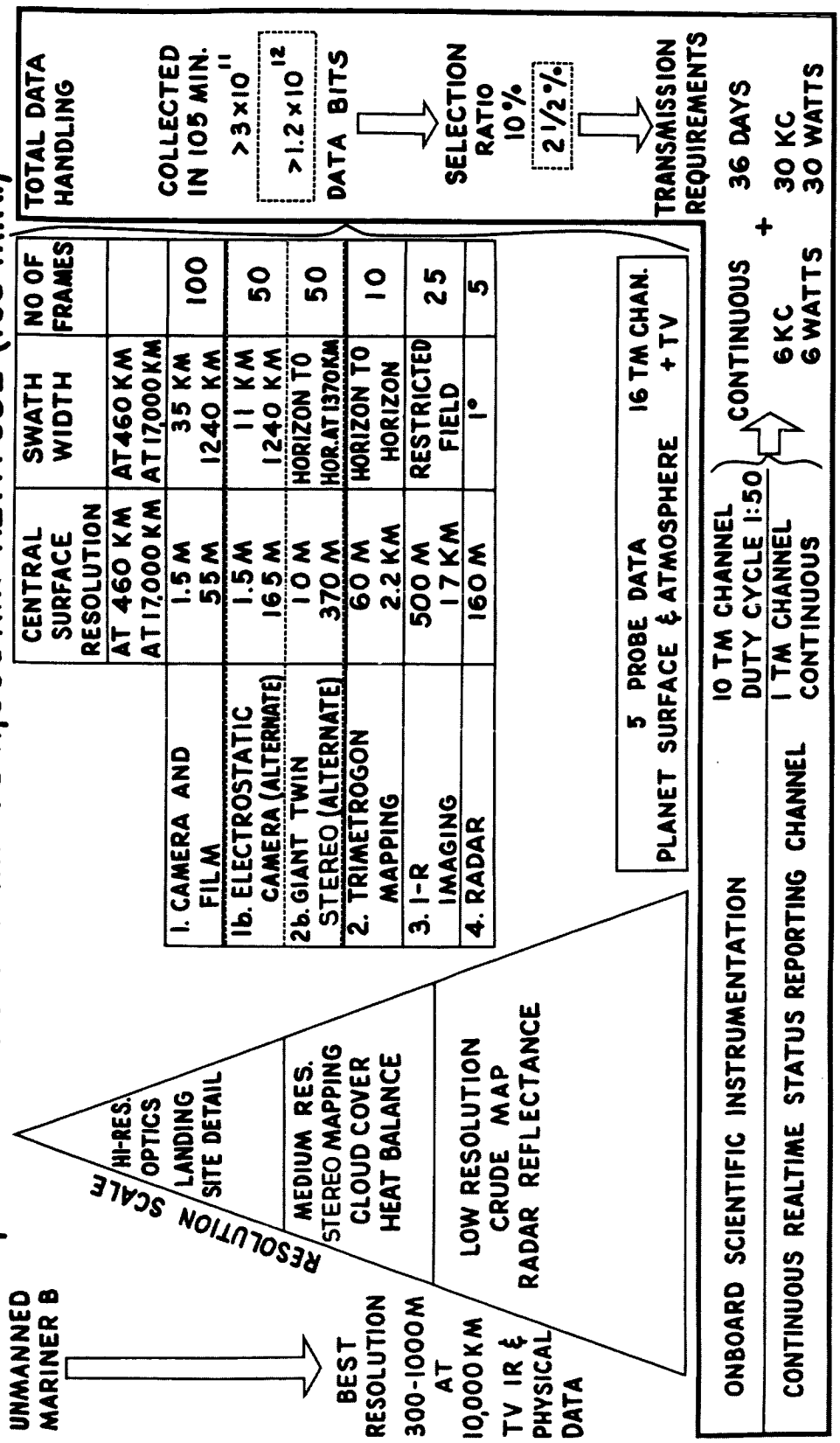


Fig. 7-10 Payload Performance Capability Manned Mars Flyby Reconnaissance

Table 7-4

MARS ONBOARD MANNED FLYBY HYPOTHETICAL RECONNAISSANCE SENSOR PACKAGE

PRIMARY ITEM & ALTERNATE		WT	VOL	During Operation Only POWER (w)
High-Resolution Camera (e.g., 120 in. FL)		600 – 1000 lb	25 ft^3	150 – 250
w/Processor, Display, Scanner		270 – 450 kg	0.71 m^3	
ALTERNATE				
Electrostatic Hi-Res Camera (Reduced Capability)		300 – 500 lb 140 – 230 kg	12.5 ft^3 0.35 m^3	250
Stereo Mapping Camera (TV)				
Small Monotrimetrogon (IR-Visual-UV)		35 lb 16 kg	1.5 ft^3 0.042 m^3	15
Giant Twin-Lens Stereo Mapper		300 lb	20 ft^3	150 – 250
w/Processor, Display, Scanner		140 kg	0.56	
I-R Imaging System		50 – 100 lb 25 – 45 kg	1.5 – 3 ft^3 0.042 – 0.084 m^3	75 – 125
Radar		65 lb 29 kg	2 ft^3 0.057 m^3	3000
TOTALS	Primary Package	750 – 1250 lb 340 – 565 kg	≈ 31 ft^3 0.88 m^3	≈ 3.3 kw
	Alternate Package	715 – 965 lb 325 – 440 kg	≈ 37 ft^3 1.05 m^3	≈ 3.6 kw

NOTE: Venus Onboard Package will supplant optics with greater radar coverage.

(2) Mapping Camera

a) A small stereo mapping TV set (e.g., a 3-in. focal-length trimetrogon camera), which may be equipped for alternate operation in the infra-red, visual, and ultraviolet range; or

b) A giant twin-lens stereo mapper (e.f., 18-in. focal length).

(3) IR. An IR imaging system, visualized here as a limited-field, pointing system. (The angular rate data previously derived for the flyby trajectory makes a scanning system impractical. However, this limitation would probably not apply to the orbiter.)

(4) Radar. A small radar set of moderate resolution capability (e.g., a coherent side-looker) is considered here to provide data on surface radar reflectance, which may be useful in future landing operations.

(Note: Instrumentation of a Venus mission, in which onboard optical reconnaissance has little application, would lean much more heavily on radar techniques.)

7.7.2 Onboard Scientific Instrumentation

Scientific instrumentation carried aboard the manned flyby vehicle would be designed to supplement and reinforce the data-collection capabilities of the various unmanned probes which precede it. Duplication of the unmanned experiments may or may not be indicated, depending on research goals and the potential value to the experiment of employing the services of the onboard observer.

Table 7-5 provides a hypothetical complement of scientific instrumentation for the flyby mission, representing essentially an extension of previously planned Mariner-Centaur experiments. Weight, volume, and power figures are guesstimates.

Table 7-5

MARS & VENUS ONBOARD MANNED FLYBY
HYPOTHETICAL SCIENTIFIC INSTRUMENT PACKAGE
(Extension of Mariner-Centaur)

Instrument	Weight (lb)	Weight (kg)	Volume (ft^3)	Volume (m^3)	Power (w)
I-R Spectrometer (Atmospheric Measure)	25	11.3	1	0.028	9
I-R Radiometer (Surface Heat Balance)	3	1.4	0.1	0.003	2.5
Microwave Radiometer (Surface Heat Balance)	31	14.1	1	0.028	6.4
UV Spectrometer	25	11.3	1	0.028	6
Trapped Radiation Detectors (Planet Radiation Belts)	3	1.4	0.1	0.003	0.5
Magnetometer (Interplanetary Fields)	11	5.0	0.4	0.011	8
Micrometeorite Detector (Interplanetary)	8	3.6	0.3	0.009	1
Cosmic Ray Spectrum Analyzer (Interplanetary)	18	8.2	0.7	0.020	2.5
Ion Chamber/Particle Flux Analyzer (Interplanetary Proton/Electron)	5	2.3	0.2	0.006	0.5
Proton Direction Monitors (Interplanetary)	7	3.2	0.2	0.006	1
Plasma Probes (Interplanetary)	28	12.7	1	0.028	5
UV Polarimeter (Atmospheric Scatter)	10	4.5	0.4	0.011	3
Faraday Cup (Interplanetary Electron/Proton)	3	1.4	0.1	0.003	3
Topside Sounder (Planet Ionosphere)	25	11.3	1	0.028	1
L-F Radio (Planet Radio Emission)	9	4.1	0.3	0.009	2
Phase-Locked Radio Receiver (Ionosphere & Interplanet Medium)	8	3.6	0.3	0.009	2
Stacked Crystal Spectrometer (Interplanetary Electron/Proton)	18	8.2	0.7	0.020	2.6
Extended Instrumentation, Display Analysis Aids (For Manned Direction)	213	96.6	8.2	0.223	150
TOTALS	450	204.2	17	0.481	210

7.7.3 Probe Instrumentation

Table 7-6 provides a list of potential experiments which might be performed by a landing probe on planetary atmosphere, soil, and possible biological material. A television camera is included, as well as required beacon, data link, storage and command receiver capability. As in the case of the onboard scientific instrumentation, any actual probe complement will be designed in liaison with the earlier data-gathering programs and with developed research needs. The sample table again represents an extension of planned Mariner B capabilities.

7.8 FUTURE RECONNAISSANCE/SCIENTIFIC STUDY REQUIREMENTS

This preliminary working report has established, tentatively, the feasibility of high-resolution optical reconnaissance for the Mars flyby mission. Further study is required to establish both mission requirements and applicable techniques to be considered in overall manned planetary reconnaissance and scientific data-gathering. Following is a partial list of pertinent study subjects.

(1) Mission Analysis – Reconnaissance

Liaison with cognizant agencies and continuing evaluation of the product of current space programs are needed to establish what is required of the manned planetary mission. (See also Item 6.) System studies must determine not only the feasibility of doing a particular job by the manned planetary route, but also that the goal cannot be accomplished more efficiently by other means.

(2) Light Conditions vs Trajectory

Accurate mission analysis, in the case of the flyby, can be implemented by charting the relationship of planetary light conditions to vehicle trajectory. This is a fair-sized effort and might be considered as an extension to the planetary trajectory work in process at LMSC under NASA contract.

The computation of light patterns for the orbital mission is a simpler matter.

Table 7-6

MANNED FLYBY MARS PROBE INSTRUMENTATION CANDIDATES
(After Mariner B)

INSTRUMENT	WT (LB)	(kg)	VOL (ft^3)	(m^3)	POWER (w)
Television	35	15.9	1.4	0.040	15
Weather Instruments (Temp, Press, Dens, Sound Vel)	5	2.3	0.2	0.006	0.5
Major Gas Measure (Specific gas quantities)	5	2.3	0.2	0.006	0.5
Gas Chromatograph (Total gas analysis)	17	7.7	0.7	0.020	2.5
Mass Spectrometer (Total gas analysis)	18	8.2	0.7	0.020	2.5
Organic chromatograph (Organic soil analysis)	15	6.8	0.5	0.014	0.5
Multivator (Electro-Optic Bio Measure)	15	6.8	0.5	0.014	0.5
Radiation Package (Near planet Measure)	5	2.3	0.2	0.006	0.5
Radioisotope Biochemistry (Metabolic process monitor)	15	6.8	0.6	0.017	0.5
Microscope (Detect microorganisms-Air/ Surface)	25	11.3	1	0.028	0.5
Macromolecule Analyzer (Detect complex molecules)	25	11.3	1	0.028	1
Beacon/Data Link/Command Rcvr (Data store, convert, transmit)	30	13.6	1	0.028	25
TOTALS	210	95.3	8	0.227	50

(3) Dark Side vs Light Side Trajectory Tradeoffs

(4) Flyby vs Orbiter Trade-offs

(5) Orbiter Reconnaissance Studies

(6) Data Selection Criteria

Studies are required both as to resolution requirements and methods of selecting reconnaissance targets. Appropriate liaison, again, is needed to permit planning of manned planetary reconnaissance and scientific work as an extension of current and future unmanned programs, as well as the work of Earth-based astronomical laboratories. (For example, the latter have already mapped Mars within an estimated probable error or only 1° or 60 kilometers on the planet surface. (Ref. 7-1)

(7) Implementation of Data Selection

Preliminary design consideration is required on methods of implementing data selection, both onboard aids to the operator and automatic techniques for probe use.

(8) Storage Techniques

Tradeoff studies are required on the alternative techniques of film, electrostatic, and TV for optical reconnaissance.

(9) Other Reconnaissance Elements

Specification of requirements and preliminary design are needed for the lower-resolution reconnaissance elements, including IR, radar, etc.

(10) Scientific Mission Analysis

Similarly to the studies of Item 1, scientific mission requirements must be defined to supplement earlier programs.

(11) Onboard Scientific Equipment

Preliminary design of the onboard scientific complement may follow the studies of Item 10.

(12) Probe Scientific Equipment

Preliminary design of the probe scientific complement is also required.

(13) Venus Mission

A separate approach is needed to review Venus mission reconnaissance-scientific requirements and applicable techniques. Radar is indicated for onboard work. The possibility may be explored of instrumenting a probe for potential surface photography below the cloud level.

(14) Probe Trajectory Dynamics

In line with the question of Venus photography by probe, alternative methods of probe launch require review, along with the associated probe trajectory dynamics. These relate to guidance and communications considerations, as well as to reconnaissance.

7.9 REFERENCES TO SECTION 7

7-1. E. I. Curtis, Reconnaissance/Scientific Instrumentation of a Manned Mars Fly-by, With Emphasis on High-Resolution Optics, LMSC AO 14294, 10 Jan 1963

7-2. J. F. McLaughlin, LMSC IDC, "Nominal Interplanetary Flyby Trips," 3 Jul 1962

7-3. Krafft Ehricke, Space Flight, Van Nostrand, 1960

7-4. U. S. Department of the Navy, Bureau of Ships, Report 374-1, Natural Illumination Charts, R&D Project NS 714-100, Sep 1952

7-5. Rudolph Penndorf, "Luminous Reflectance (Visual Albedo) of Natural Objects," Bulletin of the American Meteorological Society, V37, No. 4, pp. 142–144 Apr 1956

7-6. Payne-Gaposchkin, Astronomy, Prentice-Hall, 1955. C. F. Kuiper, Vaucouleurs, and general literature.

7-7. Gerard de Vaucouleurs, Physics of The Planet Mars, Faber & Faber Ltd., 1954

7-8. Gerard de Vaucouleurs, Aerographic Coordinates for 1958, USAF, AFCRL-818, Scientific Report No. 4, ARDC Contract AF 19(604)7461, Aug 1961

Section 8

POWER SYSTEMS

by

F. V. Bischof
G. E. Rich
C. M. Bennett

Section 8
POWER SYSTEMS

8.1 SUMMARY

LMSC studies on Early Manned Interplanetary Missions (EMPIRE) indicate that two types of space power systems are feasible. The two general classes that show promise of fulfilling the EMPIRE program requirements are the nuclear and the solar dynamic conversion systems. A general listing of the various space power systems which are currently funded by AEC, NASA and AF for development is presented in Table 8-1. Two of these power systems are attractive for the present conceptual designs of EMPIRE vehicles. The SNAP 2 nuclear reactor-turbogenerator system and the solar concentrator-turbogenerator system appear capable of producing the indicated power requirement of 5 to 6 kw(e)and can be installed on either the rotating or the zero-g class of configurations described in the next section of this report.

The currently estimated system weights for the 8 kw(e) version of SNAP 2 (unshielded value) and the 6-kw(e), biphenyl version of the Solar Dynamic system are 727 kg and 340 kg respectively. The respective radiator areas are 26 m^2 and 20.4 m^2. It will be noted that some of the values shown in Table 8-1 have changed from those previously presented. This is especially true for the nuclear systems. During this early study and development phase of these systems more changes are likely to occur. Both nuclear and solar power systems are described herein and the problems associated with incorporation into vehicle designs are discussed.

8.2 NUCLEAR POWER SYSTEMS

The nuclear power system being considered for the EMPIRE vehicles consists of a nuclear reactor heat source, a boiler superheater, a mercury turbine which drives

Table 8-1

PERFORMANCE OBJECTIVES FOR SPACE POWER SYSTEMS

Power Plant Designation	Power Output (kwe)	Energy Source	Type Energy Conversion	Total Weight (kg) Unshielded	Radiator Area (M^2)	Availability Operational Prototype *Satellite
Snap 10A	0.5	Nuclear Reactor	Thermoelectric (NaK)	320	5.9	1964*
Snap 2	4		Turbo-Alternator (NaK-Hg)	470	13	1965*
	8			727	26	Not currently sched. for flight test
Snap 8	30			1370	186	1967*
	60			2380	372	Not currently sched. for flight test
Snap 50	1,200		Turbo-Alternator (LiK)	4600	365	1970*
DCR 60	60		Thermionic	N.A.	N.A.	1967
Star-R	60		Thermionic	635	1.2	1967
Sunflower	3	Solar Concentration	Turbo-Alternator (Hg)	340	8.4	1965
Solar Dynamic	6		Turbo-Alternator (Biphenyl)	340	20.4	1965
Solar Dynamic	15		Turbo-Alternator (Rb)	450	7.4	1966
Solar Snap 8	30		Turbo-Alternator (Hg)	1135	56	1967
Steps	1		Thermionic	410	N.A.	1966

an alternator, and an integral radiator-condenser heat rejection system. It would be a modification of the system designated SNAP 2 which is scheduled for satellite flight test in 1965.

Figure 8-1 shows the reactor power plant installed on a rotating configuration, and Fig. 8-2 presents the same power plant located on a zero-g configuration.

Energy is produced in the nuclear reactor by the fission of U-235. A liquid metal (NaK) heat transfer fluid is circulated through the reactor core and mercury boiler by a rotating permanent magnet pump as shown in Fig. 8-3. The liquid mercury (Hg) is converted into superheated vapor which is expanded through the turbine. The resulting turbine mechanical power is converted to electrical power by the alternator. The mercury-vapor exhausted from the turbine is condensed and subcooled in the radiator condenser and the liquid Hg is pumped back to the boiler to repeat the cycle. Figure 8-4 is a schematic of the conventional SNAP 2 power system modified for use on the EMPIRE vehicle.

The unshielded radiation levels from the SNAP 2 reactor are based on this type of thermal reactor operating at a continuous output of 100 kw(t). The thermal output of this type reactor may be cycled to approximately one-half nominal power output by means of active reactivity control (manned). Cycling the reactor thermal output to correspond to EMPIRE vehicle/crew power demand is recommended as a technique to reduce total crew exposure to nuclear radiation, to reduce shield weight, and to increase the operational lifetime of energy conversion system components.

The biological shield recommended for the EMPIRE configuration is comprised of lead gamma shield and a lithium hydride neutron shield. Preliminary calculations, shown in Fig. 8-5 are based on a total integrated dose range of 5-20 R/yr at separation distances varying from 20 to 80 feet (6.1 to 24.4m.). The values shown in Fig. 8-5, however, are based upon the assumption of a shielding of 4π steradians in the vicinity of the reactor. The actual shielding weights incorporated into the vehicle concepts shown in the next section were based on specific configurations and involved shielding only the area subtended by the vehicle.

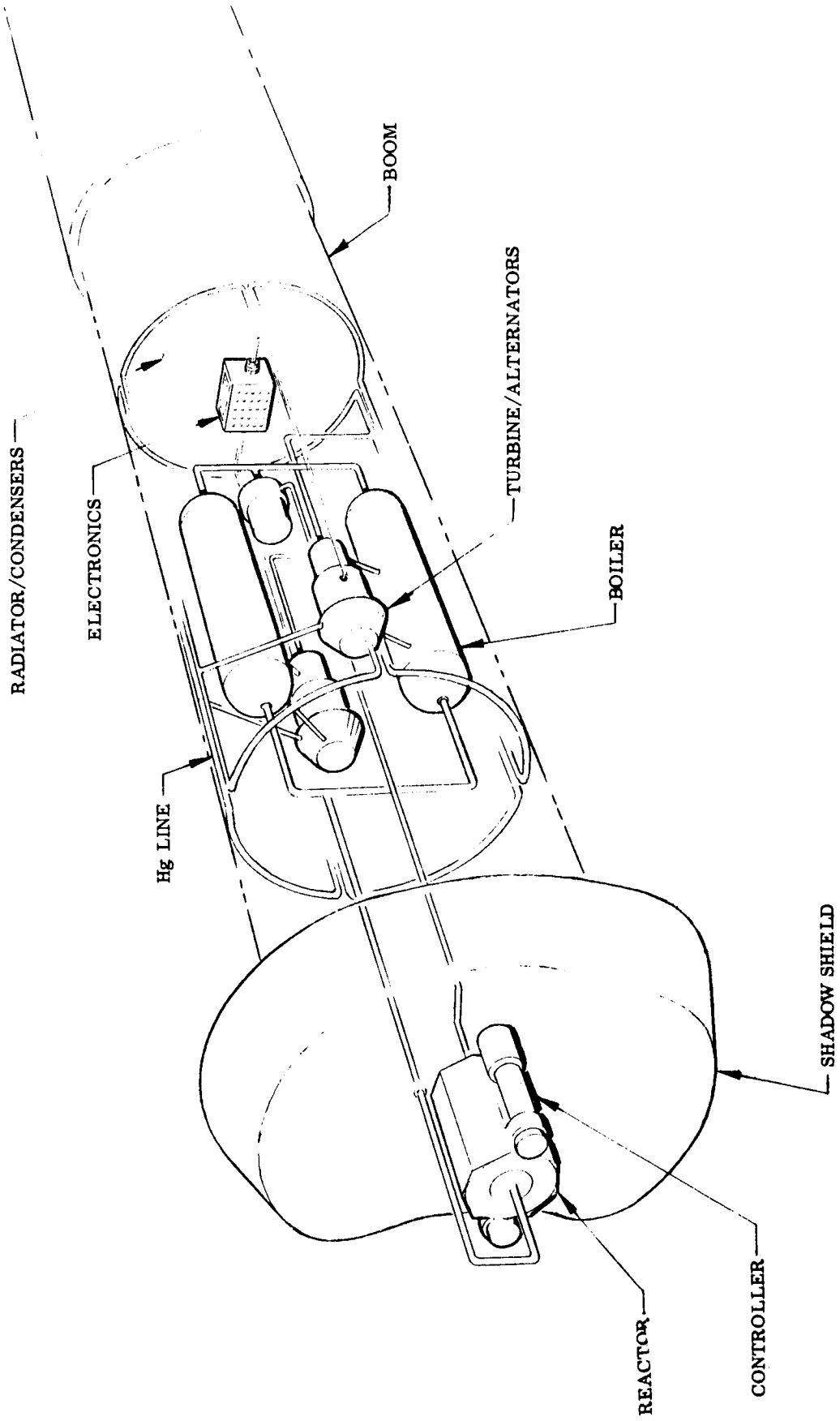


Fig. 8-1 Nuclear Power Plant – Rotating Vehicle Configuration

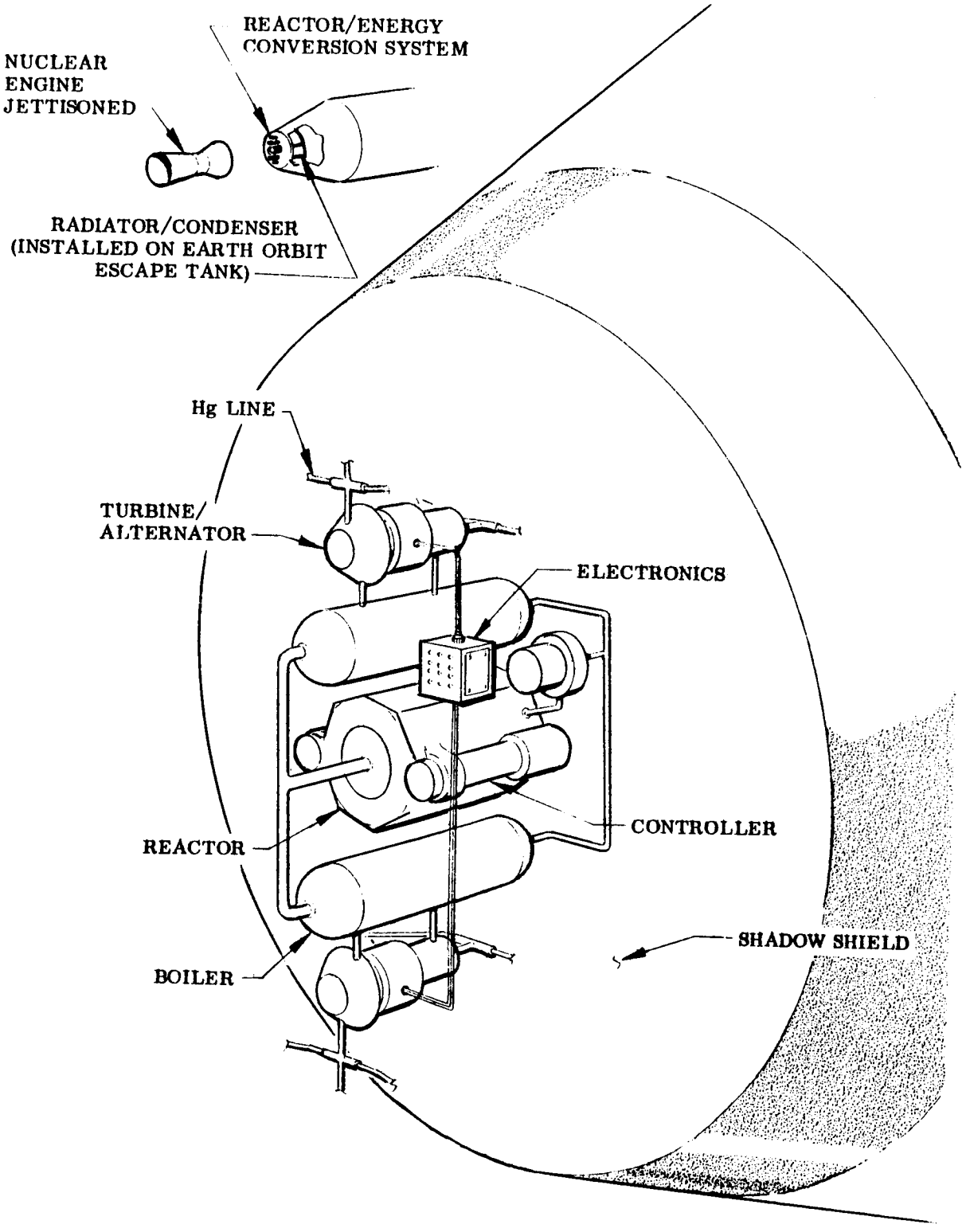


Fig. 8-2 Nuclear Power Plant – Zero G Vehicle Configuration

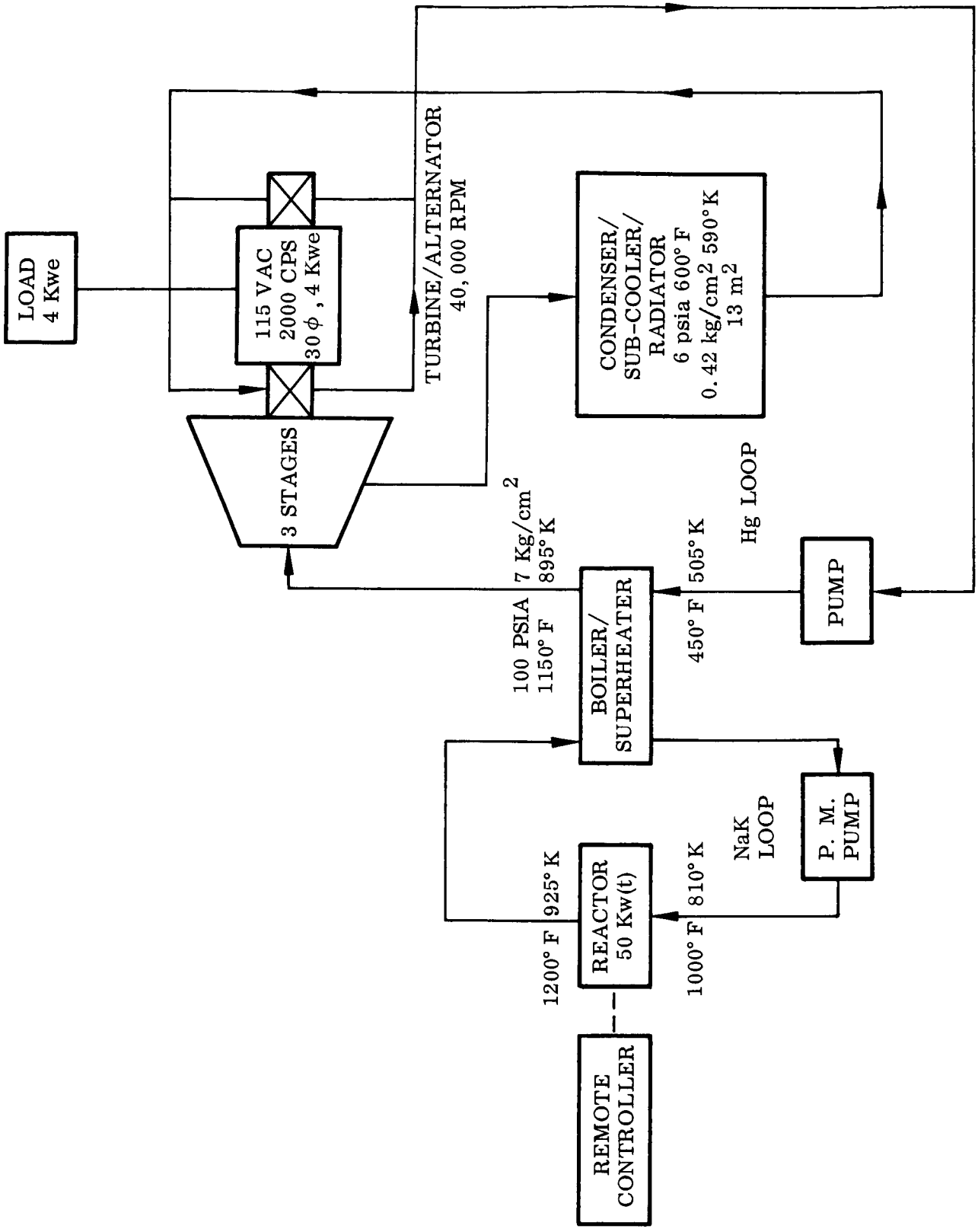


Fig. 8-3 SNAP 2 Flight System Schematic

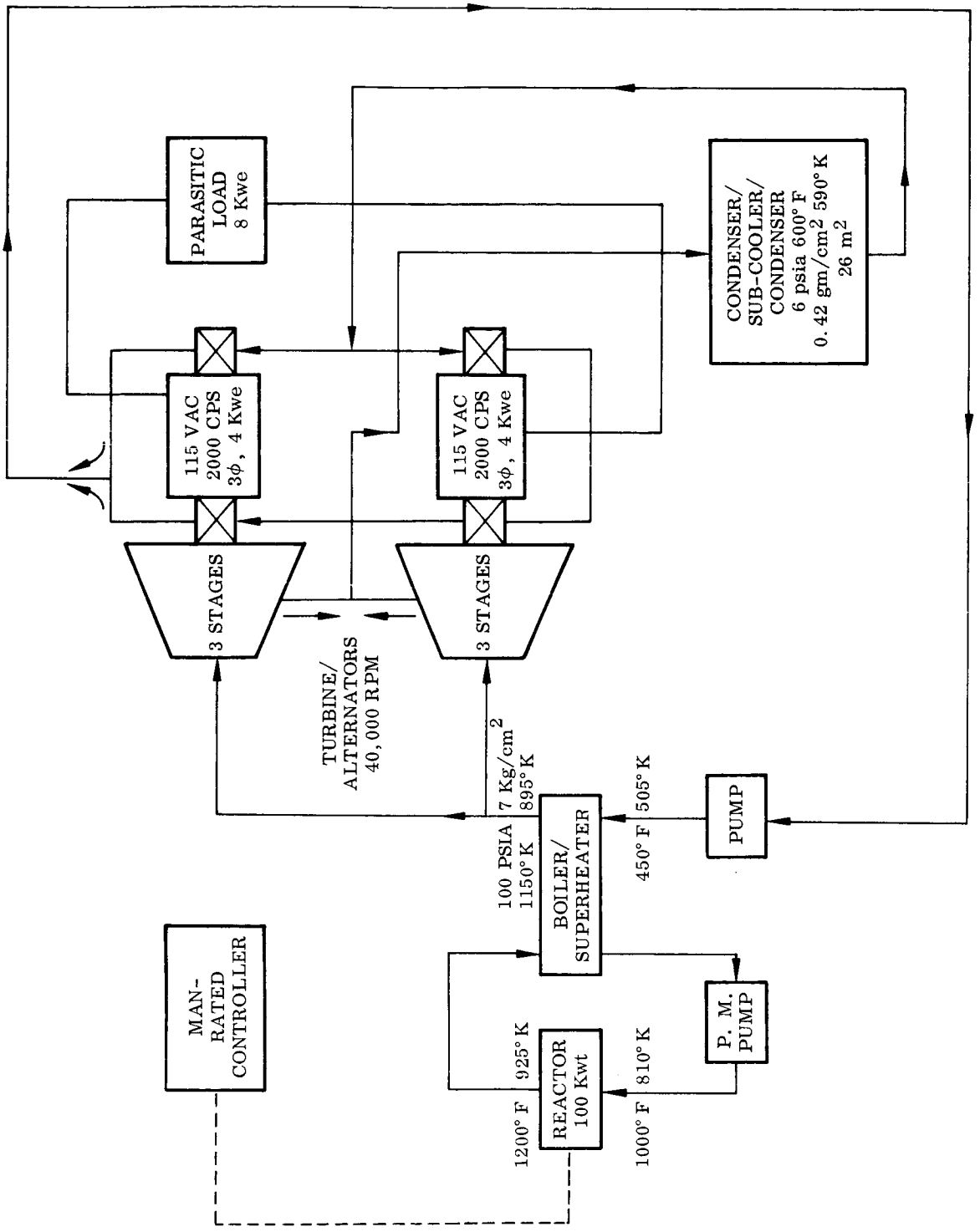


Fig. 8-4 Proposed 8 kw Power System Schematic

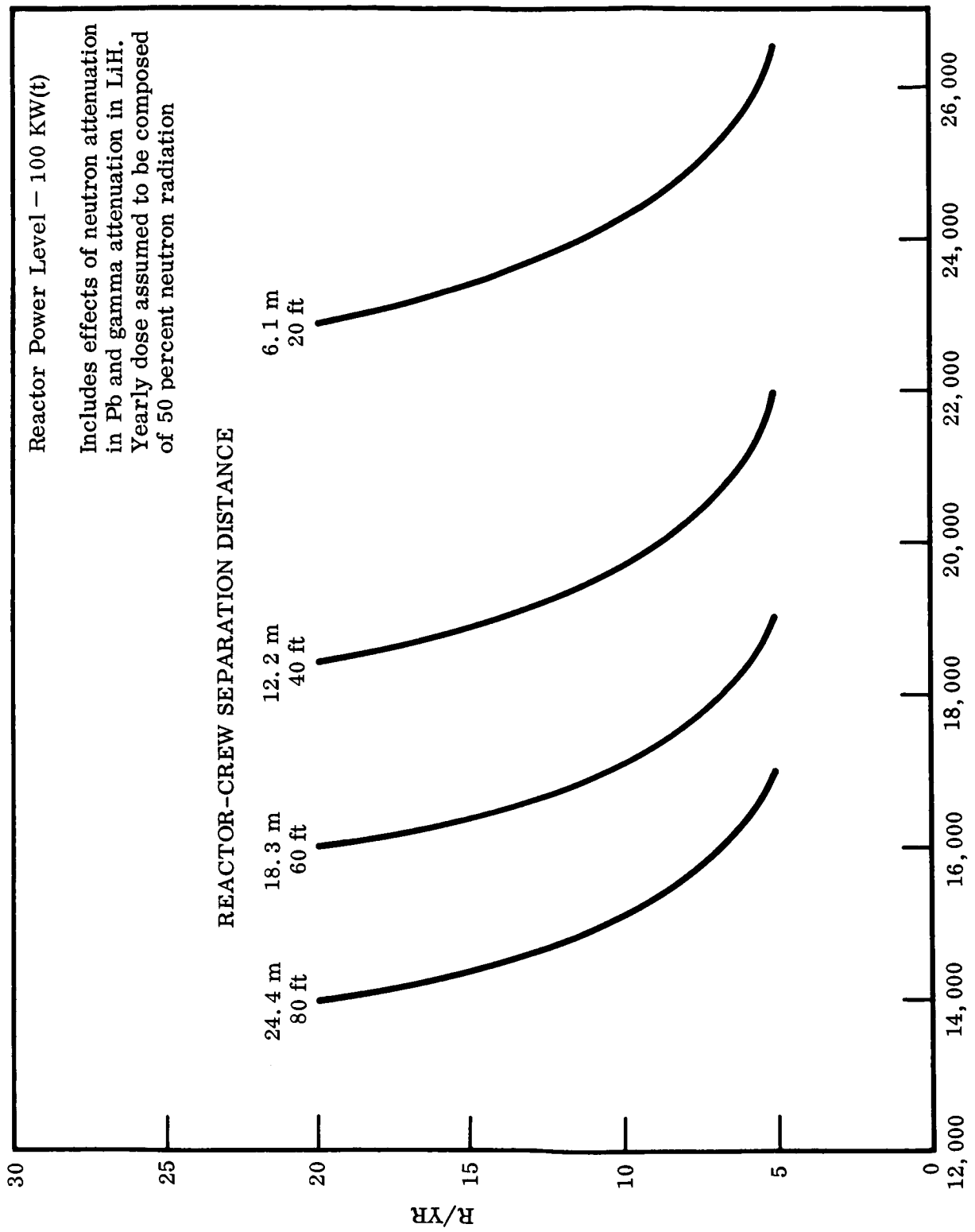


Fig. 8-5 4π Shield Weight vs. Total Integrated Dose and Separation Distance

The thickness of the lead gamma shadow shield which is adjacent to the reactor is approximately 25 cm. The lead shield weight could be reduced by 18 percent by substitution of depleted uranium for the lead. The lithium hydride neutron shadow shielding, which is adjacent to the gamma shield, is approximately 97 cm thick. The total shield thickness is therefore about 122 cm.

The volume of shadow shielding required for a given EMPIRE configuration could be approximated by subtending an angle from the outside diameter of the reactor to the projected dimensions of the nearest manned compartment.

Safety procedures for the handling of a nuclear power system during shipping, testing, and launch operations will be well developed under other contracts by the time EMPIRE vehicles are operational. Safety systems for launch aborts will be developed and range safety evaluation studies and analyses leading to operating and emergency procedures coordinated with cognizant agencies for approval, will be accomplished long before launching of an EMPIRE vehicle.

Some of the problems associated with a radiator-condenser of this type of power conversion will be discussed here. Condensation in the presence of a gravity gradient is a well established fact but for space applications where zero-g operations for prolonged time periods are a requirement, separation of vapor and condensate must be accomplished to prevent slugging and pump cavitation. Rotation of all or part of the space vehicle can provide a gravity gradient to overcome this difficulty.

Thermal control surfaces are required where rejection of heat from a spacecraft is involved. Major programs are now underway to develop thermal control surfaces for space radiators which are resistant to nuclear and ultraviolet radiation. At the condensing/subcooling temperatures, typical of SNAP 2 Rankine closed cycle radiator, two control surface properties are important. These are emissivity and solar absorbtivity. Energetic radiation has a degrading effect on thermal control surface materials properties. Nuclear radiation seriously degrades solar absorbtivity. However, the nuclear

radiation attenuation through the proposed EMPIRE biological shielding permits the use of contemporary thermal control surfaces.

Exposure to solar ultraviolet radiation, however, poses a problem. It may be assumed here that the technology of thermal control surfaces will have advanced sufficiently by the late 1960's to solve the problem.

Imperative for efficient performance of a solar-heated power system, is the orientation system which aligns the axis of the solar collector with the solar vector. The complexity of the system is dependent on the relative motion between the main vehicle and the space power system. The relative motion can vary from none, when the space power system is rigidly attached to the vehicle, to essentially unlimited, when the power system is linked to the vehicle only by electrical conduit. The Empire-type vehicle will probably require the solar concentrator to by suspended from at least a two degree-of-freedom universal joint.

The concentrator, requiring orientation accuracies of the order of ± 6 minutes of arc for efficient operation, could be sun oriented by means of electric drive motors and gears, along with the associated circuitry, sun sensing, and power amplification systems. An alternate approach could employ sensors and an active attitude control system mounted directly on a mechanically decoupled solar concentrator.

Results of studies currently conducted on the degree of degradation of concentrator optical characteristics are not yet available. Improved methods of coating the highly reflective mirror surface of the solar concentrator are being developed under contract. Several variables are involved in determining the magnitude of meteoroid protection required for solar mirrors: the mission duration, the meteoroid flux, velocity and density, and the meteoroid penetration parameters. More studies based on actual measurements by deep space probes will have to be carried out before any accurate design fixes for this problem can be established.

8.3 SOLAR DYNAMIC POWER SYSTEMS

The general solar-heated space power system configuration considered for EMPIRE missions is shown in Fig. 8-6. This system is a Rankine cycle machine, using either rubidium or biphenyl as the working fluid. It consists of four main components: (a) The paraboloidal concentrator (solar energy collector); (b) the heat receiver which is an integrated boiler and storage system; (c) the power conversion unit (turbogenerator); and (d) the heat rejection device, which is both a condenser and a radiator.

The working fluid is pumped through the boiler where solar energy absorbed in the cavity receiver raises its temperature to the boiling point, vaporizes and superheats it. The high temperature vapor is then expanded through the turbine which drives the alternator to produce electricity.

The energy content of the gas at the turbine exhaust is dissipated by radiation to space until the gas is completely condensed to liquid. The cycle is then repeated by pumping the liquid back to the boiler. Figure 8-7 shows a typical solar generator heat balance for the rubidium cycle. The specifications for a 6 kw solar-heated turbogenerator using rubidium and biphenyl as working fluids are compared in Table 8-2. Although the concentrator diameters and overall system weights are similar, the two systems vary widely in maximum operating temperatures and boiling pressure and also in the radiator area required to dispose of cycle waste heat.

Table 8-2
SOLAR DYNAMIC POWER SYSTEM

	Rubidium Cycle		Biphenyl Cycle	
Concentrator Diameter	8.7 m	(28.5 ft)	8.7 m	(28.5 ft)
Radiator Area	2.98 m^2	(32 ft^2)	20.4 m^2	(200 ft^2)
Max. Operating Temperature	1230°K	(1750°F)	645°K	(700°F)
Boiling Pressure	0.70 kg/cm^2	(10 psia)	7.7 kg/cm^2	(110 psia)
System Weight	345 kg	(760 lb)	340 kg	(750 lb)

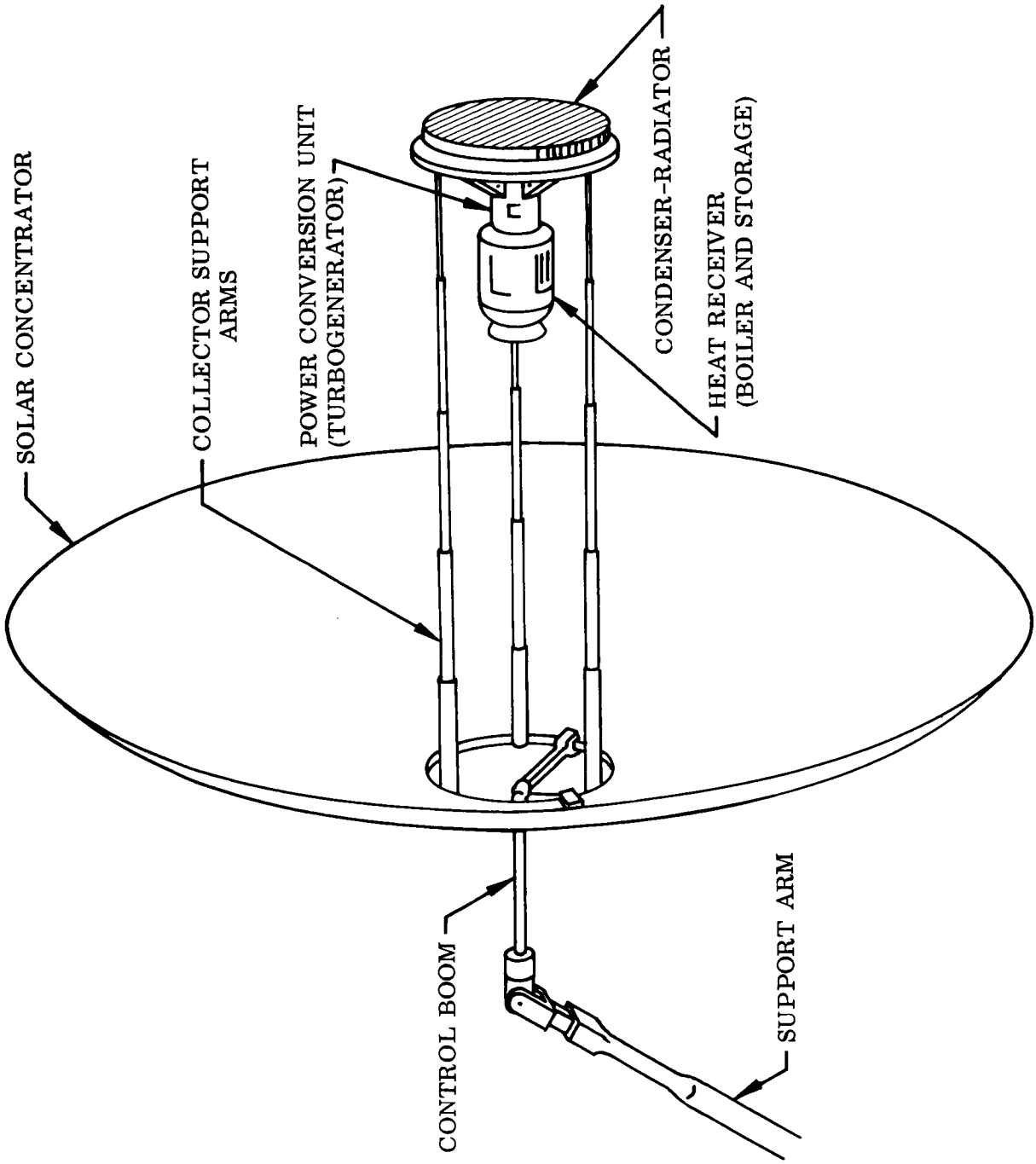


Fig. 8-6 Solar Space Power System

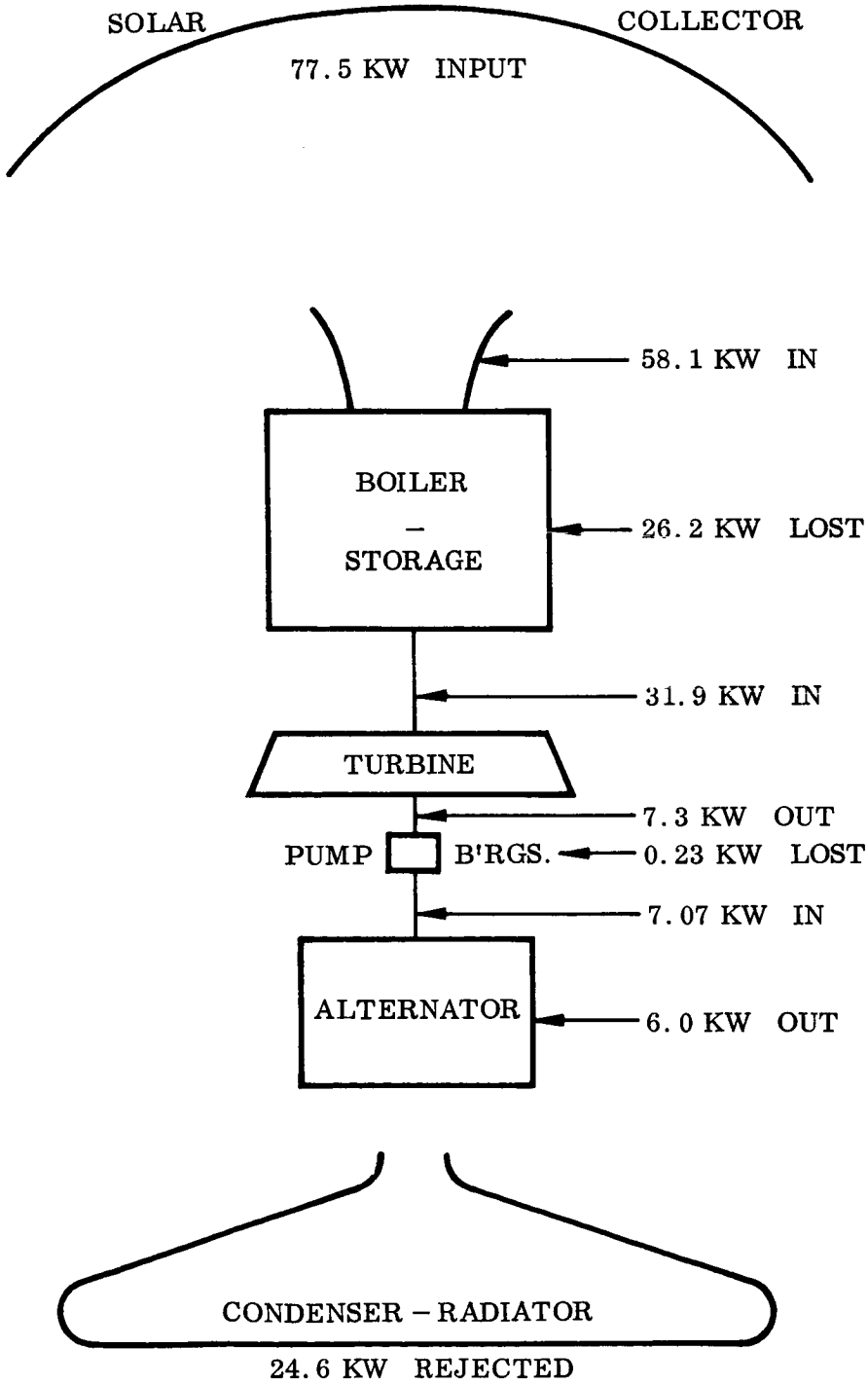


Fig. 8-7 Rubidium 6-kw Solar Turbogenerator

The radiator is a relatively heavy portion of the closed cycle space power plant, since its size and weight vary inversely with the fourth power of the radiator temperature. Therefore, to minimize radiator weight it is desirable to operate the radiator at as high a temperature as is feasible. However, cycle efficiency decreases as the ratio of radiator temperature to maximum cycle temperature increases. For this reason, the highest turbine inlet temperature compatible with the critical temperature of the fluid is selected. The critical temperatures of rubidium and biphenyl are 1940° (3032° F) at 196 kg/cm^2 (2790 psi), and 790° K (960° F) at 38.7 kg/cm^2 (551 psi) respectively.

Despite the fact that the size of the biphenyl loop radiator is 7 times that of the rubidium system, the system weights are almost equal since the low maximum operating temperature of the biphenyl system permits the use of lightweight materials, such as aluminum and magnesium, for fabrication of power unit and radiator components.

The use of solar-heated power systems on EMPIRE vehicles poses such problems as storage of the concentrator during launch, deployment and location of the solar power system after launch, accurate orientation of the concentrator during use, and degradation of the concentrator reflective surface by micrometeorites.

Two approaches to solar concentrator design are currently being pursued under funded contracts to determine which system is superior for launch, storage, deployment and erection: the inflatable-foam rigidized type or the rigid metal-petal foldable type. The former type, completely flexible before deployment, can be folded and stowed around the structural members and machinery. Its erection after deployment by pressure requires a foam generator and dispenser at the hub ring. The plastic foam rigidizes the aluminized Mylar skin, in a matter of 15 minutes, after which the complete envelope is depressurized and separated from the concentrator. The latter method requires an actuator system to move and lock the petals in position.

8.4 CONCLUSIONS

- Although both nuclear and solar power systems appear feasible for Empire missions, the Snap 2 mercury Rankine turbogenerator has been under development and hardware test for four years longer than either the rubidium or biphenyl cycles proposed for the solar concentrator system.
- The reactors for Snap 2 systems have been ground tested and will be flight tested within two years, whereas solar concentrator geometrical fabrication and optical accuracy methods have not advanced to the point where space test on a vehicle would prove profitable.
- Reliable and dependable deployment erection and orientation systems for large solar concentrators are still in the research and development stage and will be for several years to come. In addition, mechanical gimballing and drive systems for a large concentrator would drain some of the power output of the system.
- Protective coatings for the highly reflective surface of the paraboloidal dish must be developed to prevent degradation of the mirror over a long time from meteorite, ultraviolet ray and vacuum environments.
- The one real advantage that a solar power system has over the nuclear reactor system is the fact that no biological shield is required to protect personnel aboard the vehicle from neutron and gamma radiations emitted by the reactor. This given the solar system a slight weight advantage.

8.5 RECOMMENDATIONS

- Since the Empire program is only in the study phase, both solar and nuclear turboelectric systems should continue to be considered as power sources.
- Solar and nuclear power systems of the type discussed in this report should be investigated for 6 months to a year before making a final selection.
- As life support, scientific experimental objectives, and vehicle guidance, communication, and propulsion systems are more firmly defined, the Empire power requirements may reach the point (10 kw or greater) where solar concentrator power systems are no longer competitive with nuclear reactor power systems.

Section 9

VEHICLE CONCEPTS

by

J. Zoszak

Section 9
VEHICLE CONCEPTS

9.1 SUMMARY

Several spacecraft configurations were generated and evaluated for the early manned interplanetary flyby missions. These spacecraft were configured so that for minimum missions they could be launched with their 3-man crew by a single C-5 booster, erected and checked out on Earth orbit, then injected into the interplanetary orbit. The Apollo command module was used as one of the major components in the spacecraft and as the final Earth reentry body. The background of the manned spacecraft studies at LMSC, which includes the Military Test Space Station, Global Surveillance Space Station, and other inhouse studies, was utilized in the design and configuration of these spacecraft. Current state-of-the-art and projected Apollo technology were used throughout.

Of the configurations examined, the rotating (gravity) spacecraft received the major emphasis, primarily because of the considerations for man in the system. Flyby missions will require from 330 to 600 days and man may not survive in a zero-g field for this length of time. The exercises suggested for maintaining the body muscle tone may not contribute towards maintaining internal functions of the body. In addition to considerations for the crew, the mechanical systems are designed to operate in a gravity field, and such things as the circulation of air, and the separation of liquids and gases would present some problems in a zero-g field. The assumption was also made that if the more complex gravity spacecraft could be designed to meet the mission and booster requirements, then the zero-g configurations would not present additional problems except for the special treatment of fluid circulation.

The rotating spacecraft basically consists of two modules, the "command" and the "service" modules, which are connected by rigid structure and are rotated about a

central hub section. The command module is basically an Apollo command module and serves as the launch vehicle for the crew, as the command and control center for the spacecraft on orbit, and as the Earth reentry body. The service module serves as the crew's living and recreation area, and contains the primary life support equipment. These two modules are mounted opposite each other equidistant from the center of rotation to provide the crew in both modules with the same level of gravity. One crewman is stationed in the command module at all times, the other crewmen are in the service module either at work stations or in the rest area. The command module will have a retro-propulsion system or a drag brake assembly attached to it for providing the initial deceleration at Earth reentry. The total mass of this combination of command module and its braking unit is equal to the mass of the service module.

The hub section at the axis of rotation has the midcourse propulsion unit attached at one end, the power supply unit at the other, and has the solar flare shelter mounted inside. The midcourse propulsion system which provides all the midcourse trajectory corrections consists of the storable propellant, the tanks, and the engine with its controls. The power supply which furnished primary electric power for the entire spacecraft can be either the solar boiler or the nuclear reactor type. The former has a solar collector, about 9 m in diameter for the 8 kw system, which must be sun-oriented within close angular limits. The spacecraft itself is not restricted to such precise orientation so the entire solar power unit could be separated from the spacecraft except for power supply lines attached to the hub. This unit could have its own attitude control system to maintain the constant sun orientation, thus eliminating the need for applying a constant correction to change the attitude of the entire spacecraft in its orbit. Conversely, the nuclear power supply would be rigidly attached to the spacecraft and would not require constant corrections for solar orientation. This power supply would be mounted about 20 m from the occupied modules and have a radiation shield to keep the radiation dose within acceptable limits. Both the solar and nuclear power supplies have been incorporated into the configuration studies but a choice cannot be made between these two types of systems at this time.

A "storm cellar" shelter which protects the crew from solar flare protons is mounted in the hub. Shielding requirements are based on proton flux which varies with the

distance from the sun, and with the level of solar activity. For this study 56 gm/cm^2 of aluminum (20.3 cm of aluminum) is used as the shielding requirement. Weight considerations prohibit using this thickness for lining entire modules, therefore a minimum weight storm cellar shelter is used. This shelter is in the shape of a tent in which two men lie side by side at the base, the third man lies above the lower two. The shelter is mounted on rails in the hub and is rotated with respect to the spacecraft to put the shelter in a zero-g field. Flare activity lasts from hours to a day or two, and the crew should not be affected by the zero-g field for this short time. The weight of the aluminum storm cellar varies from about 13,000 to 17,000 lb (5,900 to 7,710 Kg) depending on the mission. A design study to integrate the food, water and equipment into a solar flare shelter in the service module showed that this equipment provided only 65 percent of the required shielding for only the sides of the shelter and had to be reinforced by aluminum plates. Additional plates, 20.3 cm thick were added at the top, bottom and both ends to complete the shelter. Total weight of this shelter is 19,000 lb (8,618 kg) as compared to 13,000 lb (5,897 kg) for the all-aluminum storm cellar.

The spacecraft has an 82 ft (25 m) spin radius to the floor of the modules. This radius was arbitrarily selected and is the result of using two sleeve extensions from each spoke. At this radius, and with a 0.4 rad/sec angular velocity, the crew experiences a 0.4 g level in the end modules. This combination of angular velocity and radius lies within the currently accepted "comfort zone" which is partly based on experimental data from centrifuge tests and the "slow-rotating-room" test where head movements and rotational rates were correlated relative to their effect on inner ear "canal sickness." Further tests of this type will have to be conducted on orbit to establish acceptable spin rates at various radii to verify present assumptions. Until such test results are available, the 0.4 rad/sec angular velocity will be assumed.

Several zero-g configurations were examined with both the solar and the nuclear power supply. In these spacecraft the crew is launched into orbit in the same type of command module as in the gravity spacecraft. On orbit this module is rotated 180 degrees and is secured to the service module which contains the life support equipment, the solar flare shelter, and the crew's living quarters.

A weight summary is included for three typical configurations for both a Mars and a Venus flyby. The typical 600 day Mars flyby requires more life support equipment than a typical 330 day Venus flyby. Solar flare shielding weight, however, is greater for the Venus flyby in which a higher proton flux is encountered when the spacecraft nears the sun. The sum of the weights of the life support system and the shielding are rather similar for the different configurations for both missions. The rotating spacecraft is about 12 percent heavier than the zero-g configuration. This is due to the added weight of the hub, spokes, additional midcourse propellant, and the interstage launch structure.

9.2 DISCUSSION

9.2.1 Missions

The spacecraft described herein are designed only for the early flyby missions – those missions in which the spacecraft passes within one or two radii of the planet's surface without orbiting that planet.

The selection of either Venus or Mars for the flyby missions will affect the spacecraft in the areas of life support and solar flare shielding. Life support system requirements are based on the length of trips. A typical 600 day Mars trip requires more life support equipment than a typical 330 day Venus mission. Solar flare shielding requirements are based on the proton flux which varies with the distance from the sun and the level of solar activity. A Venus mission would encounter a higher flux than a Mars mission and would therefore require more shielding.

9.2.2 General Assumptions and Requirements

The general assumptions and requirements considered in generating the configurations are listed below:

- 3 man crew
- Planetary flyby missions only

- Apollo command module integrated into spacecraft
- Shirt sleeve environment within spacecraft
- Launch pad emergency escape provisions
- Modular construction
- Semi-automatic erection of spacecraft on orbit
- Projected Apollo technology
- Meteoroid penetration protection
- Solar flare shielding for crew
- Midcourse correction capability
- Booster compatibility

9.2.3 Major Spacecraft Components

The spacecraft consists of the following major components: command module, service module, power supply, and midcourse propulsion system.

The command module is a modified Apollo command module with an internal volume of about 300 ft^3 (8.5 m^3). It serves in the following capacity:

- Launch vehicle for the crew
- Emergency escape vehicle during launch
- Earth reentry vehicle in any emergency from Earth orbit
- Command and control center for the spacecraft during the mission
- Earth reentry vehicle at completion of mission

The service module serves as the crew's living quarters as well as the dining and recreation area. Food, water, and life support equipment are located in this module which has an internal volume of about 4,000 ft^3 (113 m^3).

Primary electric power is supplied by the power supply unit which can be either a solar boiler type or a nuclear reactor type of unit.

Midcourse propulsion is the independent propulsion system which supplied all the midcourse trajectory corrections.

9.2.4 Gravity and Zero Gravity

At the present time it is impossible to evaluate man's capabilities, his physiological responses or his abilities to perform assigned tasks in a zero-g field, particularly over long periods of from 300 to 600 days. Numerous exercises have been proposed to maintain man's normal body-muscle tone in a zero-g field, however these exercises may not contribute towards maintaining the body's internal functions. For example, the cardiovascular system and the body cells may not function properly, the sinuses may not drain, and gases could build up within the alimentary canal and body cavities and create pain.

Man working in a zero-g field is out of his normal environment and, in general, he will require more time to perform his daily maintenance tasks under this new condition. Several training devices have been built which partially simulate four of the six degrees of freedom. These training aids familiarize the subject with the type of reaction he can expect as he applies forces in a zero-g field and will help him to reduce the time for completing tasks on orbit. Even with such training aids, and with the increased proficiency normally expected with time, it will take longer for man to complete his tasks in the new zero-g environment than it takes on Earth. For long interplanetary missions man should be able to work at maximum efficiency and under conditions approximating those he has experienced on Earth.

In addition to the consideration for the crew, the mechanical systems aboard the spacecraft would have to be modified to operate in a zero-g field if a non-rotating configuration is adopted. Loss of gravitational acceleration will affect such things as the circulation of air, the separation of liquids and gases, and the distillation of water. For these reasons and for those listed below, the rotating (gravity) spacecraft configuration received the major emphasis:

- More complex, requires balance of rotating masses
- Launch configuration requires additional fairings

- Heavier than zero-g configuration, more structure
- Alternate systems available for connecting rotating masses (cables or rigid structure)
- Life support and solar flare shielding masses vary with the mission selected, requiring special mass distribution considerations

Additionally, it was assumed that if the more complex rotating configuration could be designed to satisfy booster and mission requirements, then a simpler and lighter zero-g spacecraft would not present configuration difficulties.

9.2.5 Modular Arrangement

During the interplanetary mission the crew generally occupies both the command and the service modules. One crewman is stationed in the command center, the other crewmen are in the service module either at rest or at work stations. Since both modules are occupied they should be at the same distance from the center of rotation and have the same g-field. To achieve this, the modules can be attached together as a single unit counter-balanced by other major spacecraft components, or they can balance each other at opposite ends of interconnecting structure. The command module plus its retro-propulsion assembly weighs as much as the complete service module. Therefore the basic configuration was established with these modules opposite each other. Other alternatives for balancing present problems, i.e., using the empty injection booster for counterbalance. This increases the inert mass and therefore increases the midcourse propulsion requirements, the empty tank is not suitable for occupancy unless separate life support and thermal control equipment is provided, the large difference in the masses of rotating modules requires long separation distances to maintain reasonable g-level in the manned modules, and finally, the modules have to be reeled in before midcourse corrections can be applied if the great separation distance necessitates the use of flexible connectors as seems probable. The midcourse propulsion unit itself cannot be used as a counterbalance as its mass decreases with each correction.

9.2.6 Cable vs Rigid Attachment of Modules

The two modules can be connected by either a cable system or a rigid structure. The cable system is lighter, occupies less stowage space at launch, and permits very large spin radii. A normal six hour duty cycle in the command module requires accessibility between modules at least four times a day, in addition to any trips for servicing equipment. In a cable system, a pressurized shuttle would be required for transporting the crew plus any equipment between modules, otherwise the crew would have to use space suits and the air locks. A shuttle introduces its own problems; air would be lost at each coupling operation unless an air pump evacuated the lock each time, power is required to move the shuttle, mechanical problems arise as the shuttle mechanism operates over a guide system in a space environment where materials tend to "cold weld" and finally, a malfunction of the shuttle would endanger the success of the mission.

The spacecraft has to be despun and the modules reeled in before the thrust can be applied for midcourse corrections. Despinning a cable-connected system requires the simultaneous reeling-in of the end modules and the application of equal and opposite tangential forces at each module. Applying the force to only one module would cause the spacecraft to gyrate about some moving point within the system. If the outer modules in a rotating spacecraft are reeled in without despinning, the angular velocity increases because of the conservation of angular momentum. This increasing angular velocity at a decreasing spin radius has an adverse affect on the crew.

If the cable connected modules are despun first, they must next be brought together. This involves the following; the modules have to be accelerated towards each other, they have to move in a common plane and have an active attitude control system to maintain proper orientation relative to each other, they have to be decelerated prior to final contact, and finally the attaching structure has to be engaged and locked. This method of despinning increases the time and the crew's work load for this phase of the mission. The cable system therefore does not offer any advantages and is not considered applicable for this study.

Rigid connectors (spokes) between modules eliminate most of the problems inherent in the cable system. The spokes can be pressurized to allow unlimited access between modules, despinning the spacecraft does not require a configuration alteration, and the midcourse corrections can be made with the spokes extended. In addition, the rigid structure will dampen any oscillations which might be induced by crew movements or changes of equipment within the modules. The rigid system has several disadvantages; it is heavier than the cable system, it complicates the launch payload packaging, aerodynamic fairings are required at launch, and the spin radius is limited by the total system weight considerations, and by structural and mechanical problems.

9.3 CONFIGURATION DESCRIPTION

9.3.1 Rotating Spacecraft

The configuration receiving emphasis during this study period is shown in Fig. 9-1. The command module and service module are at opposite ends of a rigid interconnecting structure and rotate about a central hub section. The centrifugal force produced by this rotation acts outward, radially, and the crew within the modules experiences this force as "gravity." The hub at the center of rotation contains the heavy solar flare shelter, and has the midcourse propulsion unit attached at one end. The shelter and propulsion unit represent more than 30 percent of the total spacecraft weight, the exact proportion depending on the mission. By placing these components (plus the portion of the mission-dependent food and water supply, which is in excess of that needed for balancing the end modules) in the hub, the balance of the rotating masses will not be disturbed by variations in mission requirements. The primary power supply is attached at one end of the hub opposite the midcourse propulsion system. An air lock incorporated into the hub permits the crew to leave the spacecraft for external repairs or inspections.

This interplanetary configuration is "folded up" into the compact assembly on the launch booster shown in Fig. 9-2. The spokes are retracted to fit within the height of the payload envelope and are hinged at the hub and the service module.

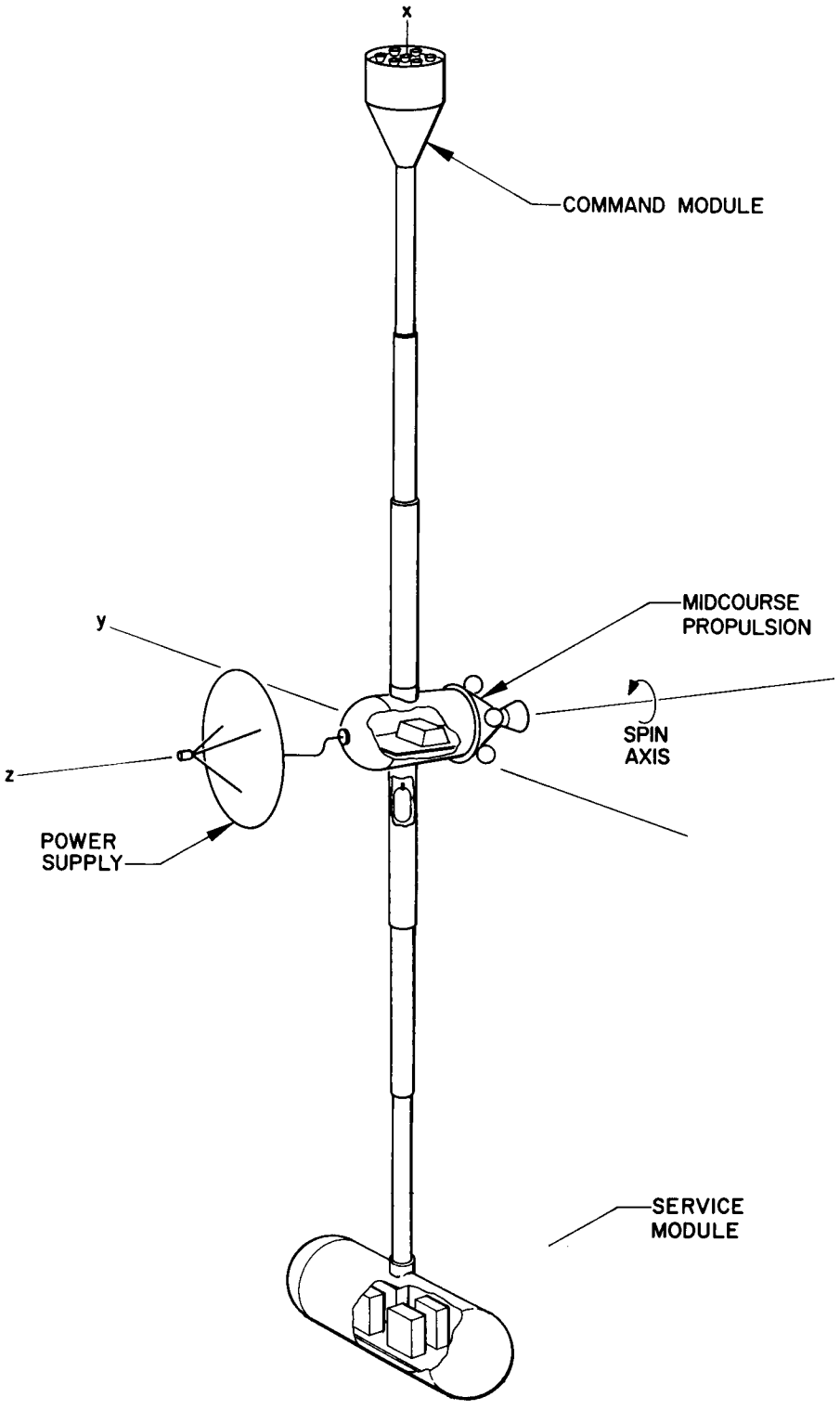


Fig. 9-1 Manned Interplanetary Spacecraft

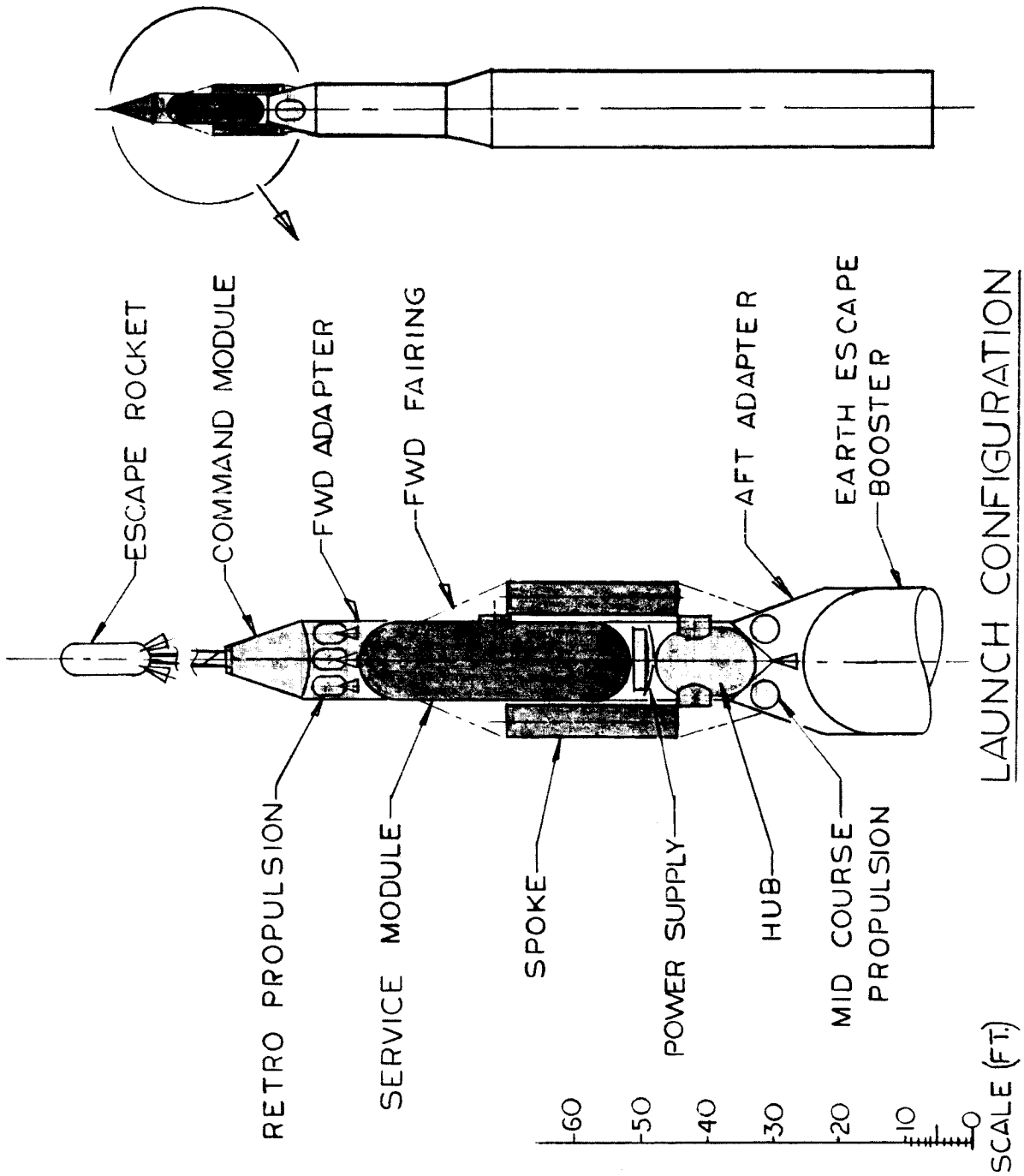


Fig. 9-2 Launch Configuration

The crew is launched into orbit in the command module at the forward end of the payload. An emergency escape rocket is attached to this module to pull it away from the remaining payload in the event of an abort situation. In a normal launch this rocket is jettisoned at the end of the first stage burnout. Interstage structure connects the modules and supports them on the booster during launch. The module walls act as their own launch support structure and do not require additional external structure.

Figures 9-3 and 9-4 show the sequence of events in Earth orbit for erecting the spacecraft. First the fairings and the interstage structure are jettisoned, the command module rotates 180 deg and is secured to the end of one spoke. This can be accomplished either by a cable system or with the attitude control system on the command module. Both spokes then rotate 90 deg and lock at the hub. A cable system can also be used to move the spokes and modules into position. All sub-systems within the spacecraft can then be checked out in orbit before proceeding with the interplanetary phase. The spacecraft is then oriented relative to the velocity vector and the Earth escape booster is operated to inject the spacecraft into the programmed heliocentric orbit. The spokes do not have to be folded for this injection phase as they are designed to withstand a 2-g burnout acceleration in the extended position. After booster burnout, the spokes are fully extended and locked in place, the solar power unit is extended and oriented, and the spacecraft spun up to the desired angular velocity.

When the spacecraft reaches the vicinity of the planet it may launch probes onto the surface or into orbit around that planet. During the Earth launch and orbit escape phases these probes can be mounted within the lower adapter between the hub and the injection booster as shown in Fig. 9-4. During the interplanetary phase these probes would be rotated about their forward attach points and would then be secured to the outside of the hub. Prior to launching of the probes, the spacecraft would be despun and oriented relative to the destination planet.

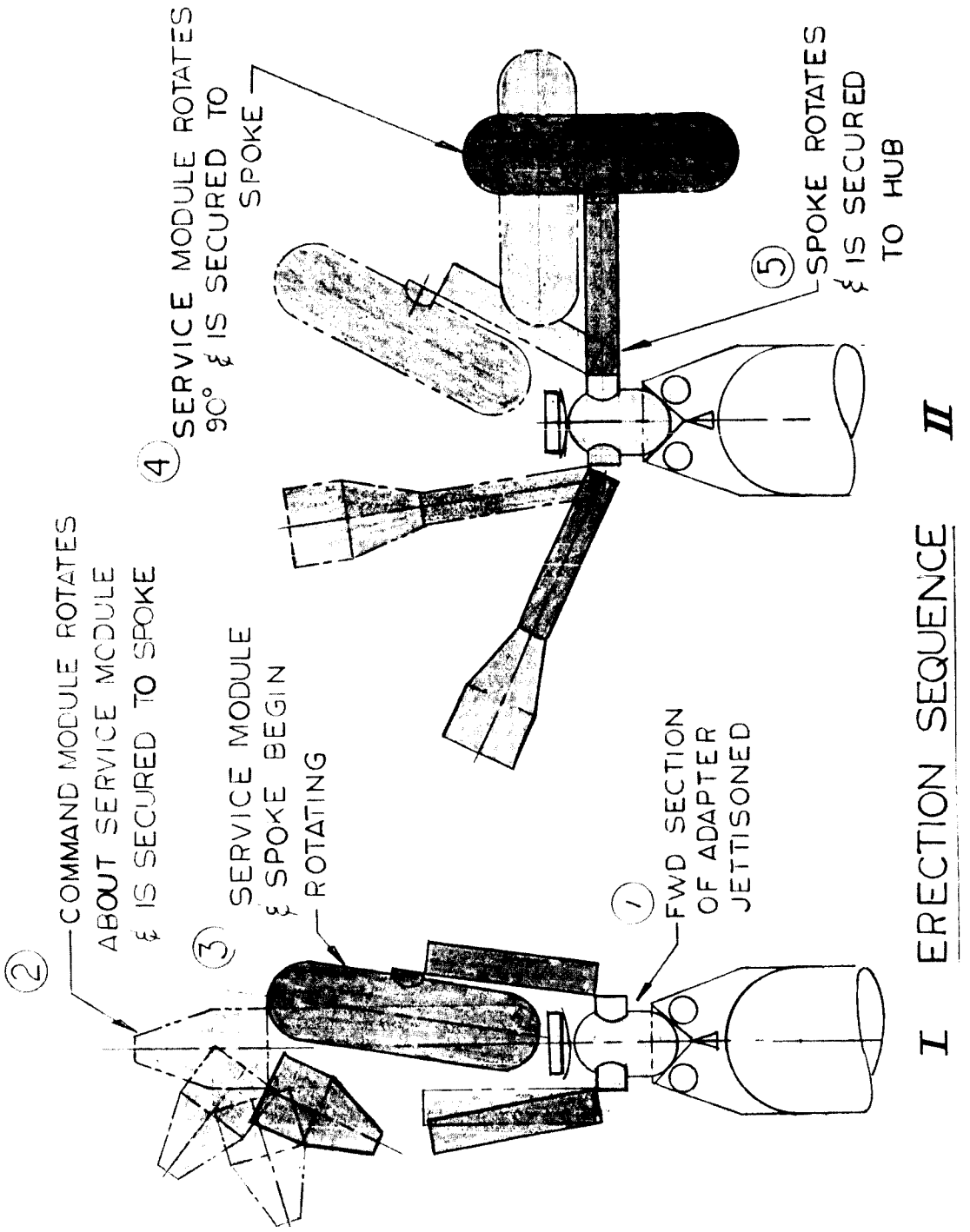


Fig. 9-3 Erection Sequence

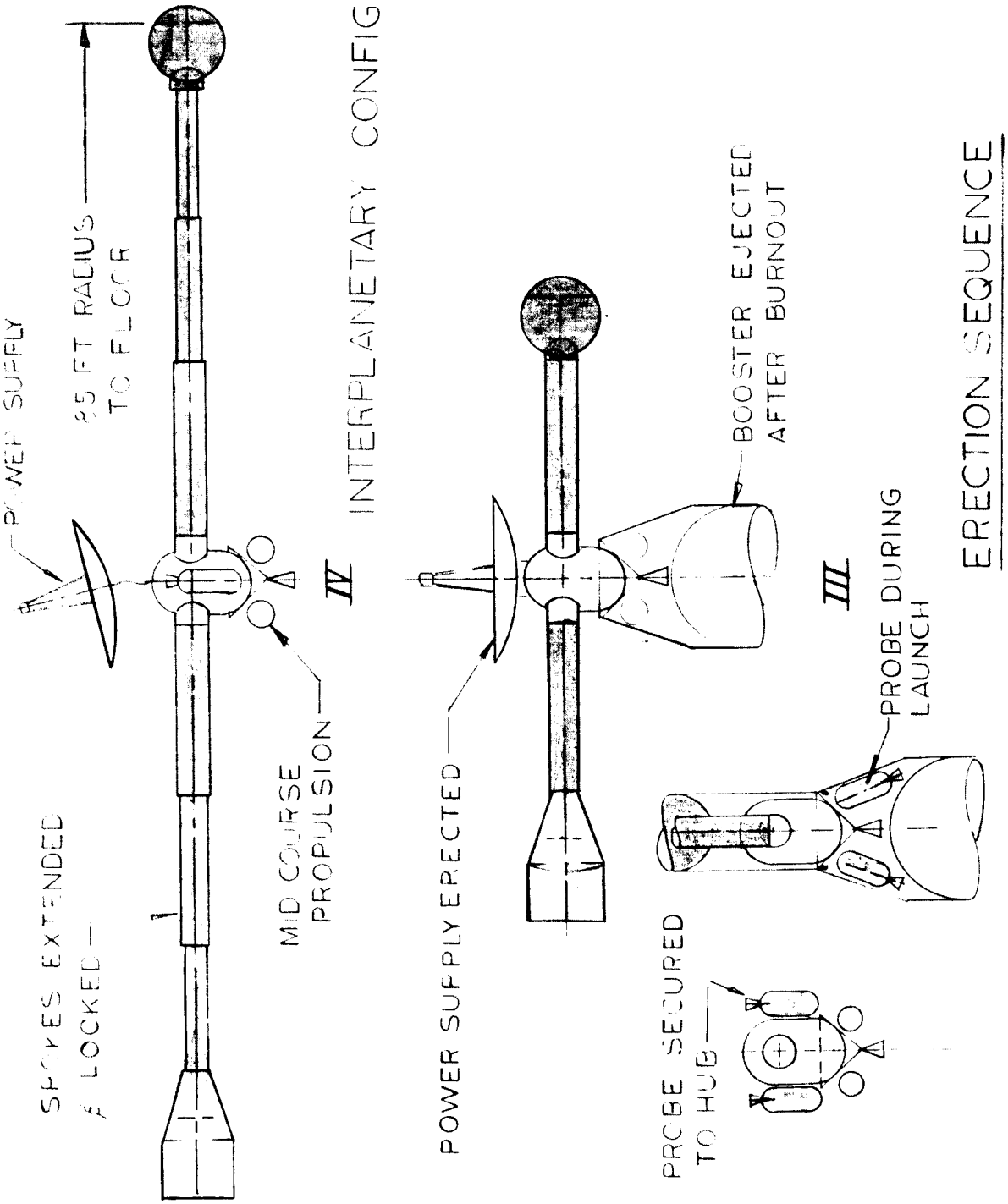


Fig. 9-4 Erection Sequence (Continued)

9.3.2 Power Supply

The power supply may be either a solar boiler or a nuclear reactor type of unit. The former has a solar collector, about 9 m in diameter for the 8 kw system, which focuses the sun's rays into a flux trap to heat a liquid system which drives the turbine-alternator. This unit generates the electric power for use in the spacecraft. At launch this assembly must be packaged into a compartment between modules, then on orbit these components must be deployed and positioned in a specific arrangement. The solar collector is the largest component to be deployed and erected, however the technique being developed by B. F. Goodrich for use in the Sundstrand solar power supply unit (Ref. 9-1) offers an attractive solution for packaging and deployment. This collector is formed on orbit by inflating a large balloon and rigidizing the lower section. The balloon is then severed, the upper section is ejected and the lower section remains as the solar collector.

The collector must be pointed towards the sun at all times within specified angular limits. If this unit were rigidly attached to the spacecraft then the entire craft would have to maintain this orientation towards the sun. This would mean an almost continuous changing of the craft's orientation in inertial space as it moves around the sun. For this reason the power supply unit is shown structurally detached from the craft and connected to the hub by power supply lines. Proper sun orientation could be maintained by an attitude control system mounted on the unit.

The solar boiler power supply has several advantages over the nuclear type; components can be repaired or replaced in space, the assembly is lighter since it doesn't require radiation shielding, and there is no radiation hazard.

A nuclear reactor type of power supply has to be placed at some large distance from the occupied modules, shielding added, and the assembly must be supported by structure capable of withstanding accelerations. The unit must be about 60 ft (18.3 m) from the modules to keep the radiation dose to an acceptable limit of 5 rem/year. Currently

there are no reactors available with the long life time requirements needed for the missions considered, but these units are being developed and should be available when required.

9.3.3 Midcourse Propulsion

The midcourse propulsion unit is attached to the center hub along the axis of rotation. A low thrust level of from 1/5- to 1/2-g is acceptable for the midcourse corrections which will permit the spokes to remain in the extended position during this thrust application. The unit consists of storable propellant, tanks, pressurization system, the engine and its controls and the supporting structure. Since propellant capacity is dependent on the mass to be accelerated it is important to minimize the interplanetary payload mass. At launch the engine is canted about 90 deg to reduce the height of the interstage structure, and it is repositioned after the Earth escape booster is jettisoned. The entire assembly is accessible during the mission to a crewman in a spacesuit.

9.3.4 Spin Radius and Coriolis Effects

One of the most critical considerations in human factors engineering in the design of rotating spacecraft is the complex dynamic environment to which a crewman is subjected as he moves within the rotating spacecraft. Normally man maintains a spatial orientation through the integration of information he receives from his sensory mechanism; his eyes, the vestibular organs in the inner ear and the mechanoreceptors in the muscles, tendons and joints of his body. The inner ear mechanism contains the otoliths and the semi-circular canals which operate on the inertia principle. As the crewman walks within a rotating spacecraft he is subjected to changing forces which also act on the inner ear mechanism. The normal relationship of what his eyes see, and what the inner ear and his mechanoreceptors feel on Earth will not be present in a rotating spacecraft. This will tend to cause disorientation and confusion. The cross coupling of forces due to spacecraft rotation coupled with head movements such as rotation, cocking of the head, or bending forward, all act on the vestibular mechanism.

These movements of the head, in and out of the plane of rotation, induce canal sickness which causes discomfort and degrades man's performance.

Many studies have been conducted in centrifuges to correlate head rotation rates with angular spin rates. Clark and Hardy (Ref. 9-2) have established an upper limit of 0.01 rad/sec for the angular velocity for a rotating spacecraft. If this limit is accepted then a 47.5 k spin radius is required to maintain a 0.5-g field. Experiments conducted at the Pensacola slow-rotating-room by Graybiel (Ref. 9-3) indicated that a higher value for the angular velocity may be permissible. B. J. Loret in a study of artificial gravity in rotating vehicles (Ref. 9-4) suggests that an upper limit of 0.4 rad/sec may be acceptable without inducing canal sickness. This limit of 0.4 rad/sec is a compromise between what is desirable from a human factors viewpoint and practical from an engineering standpoint.

In all centrifuge tests conducted on Earth, the subject initially has the force of gravity acting on the inner ear. As he beings to spin about the center axis of the centrifuge, he begins to experience radial and tangential acceleration in addition to the gravity accelerations. His response to head movements within this complex dynamic field on Earth will not be the same as when he is in orbit where this very large component of gravity is no longer present. Further tests will have to be conducted on Earth orbit to establish acceptable spin rate limits at various radii and to determine man's ability to learn to restrict his head movements in order to prevent canal sickness. Until such information is available, the limit of 0.4 rad/sec will be assumed.

With the 25 m radius shown for this spacecraft, and at the 0.4 rad/sec angular velocity, the crew experiences a 0.4-g field at the floor of the modules. This combination of radius and angular velocity lies within the physiological "comfort zone" for what is presently accepted as suitable for manned rotating spacecraft. To increase this to one full g at 0.4 rad/sec would require a 61 m spin radius, or 0.62 rad/sec at the 25 m radius. If spin radius is increased a total weight increase of 20 lb/ft (29.8 kg/m) is needed for increased spoke structure. The 25 m radius in this configuration was arbitrarily selected. It is the result of using two sleeve extensions from the spokes, and conceptually shows a method of providing long spin radii.

The walls of the service module and hub are constructed from double face sandwich structure for meteoroid penetration protection. Equipment is installed on each side of a center aisle in the service module (Fig. 9-5) and is mounted on tracks to permit access to the module walls as well as to the back of the equipment. The floor of the module is positioned to permit the most efficient man-equipment arrangement within the module diameter, and to allow a man to work on the lower surface of the module below the floor. With moveable equipment and removeable floors, the entire module wall surface is accessible. The long axis of the module is 90 degrees to the axis of rotation primarily because of the rotational stability requirements for the overall spacecraft configuration.

9.3.5 Radiation Shielding

The crew within the interplanetary spacecraft must be protected against solar flare radiation, predominantly solar flare protons, a major radiation problem in space. Figure 5-20 shows the shielding required for several missions and for several flare activity levels. For this study 56 gm/cm^2 of aluminum is used as the shielding requirement for the crew. This is equivalent to 20.3 cm of aluminum which is too thick from weight considerations to use for lining entire modules but feasible for local "storm cellar." This storm cellar is in the form of a tent with a trapezoidal cross section to minimize its weight. Two men lie side by side at the base of this trapezoid, the third man lies above the lower two. The shelter is long enough to permit all three occupants to stretch fully and is located in the hub where any changes in its mass requirements would not affect the balance of the end modules. The shelter is mounted on tracks within the hub. During an event when the shelter is occupied, it is rotated with respect to the spacecraft to put the occupants of the shelter in a zero-g field. An alternative of fixing the shelter to the hub might involve placement of the crew at a very short spin radius which would induce canal sickness. Despinning the entire spacecraft for each event has several disadvantages:

- Propellant is required for each despin, spinup cycle
- Relative frequency of events may make this undesirable from an operational standpoint

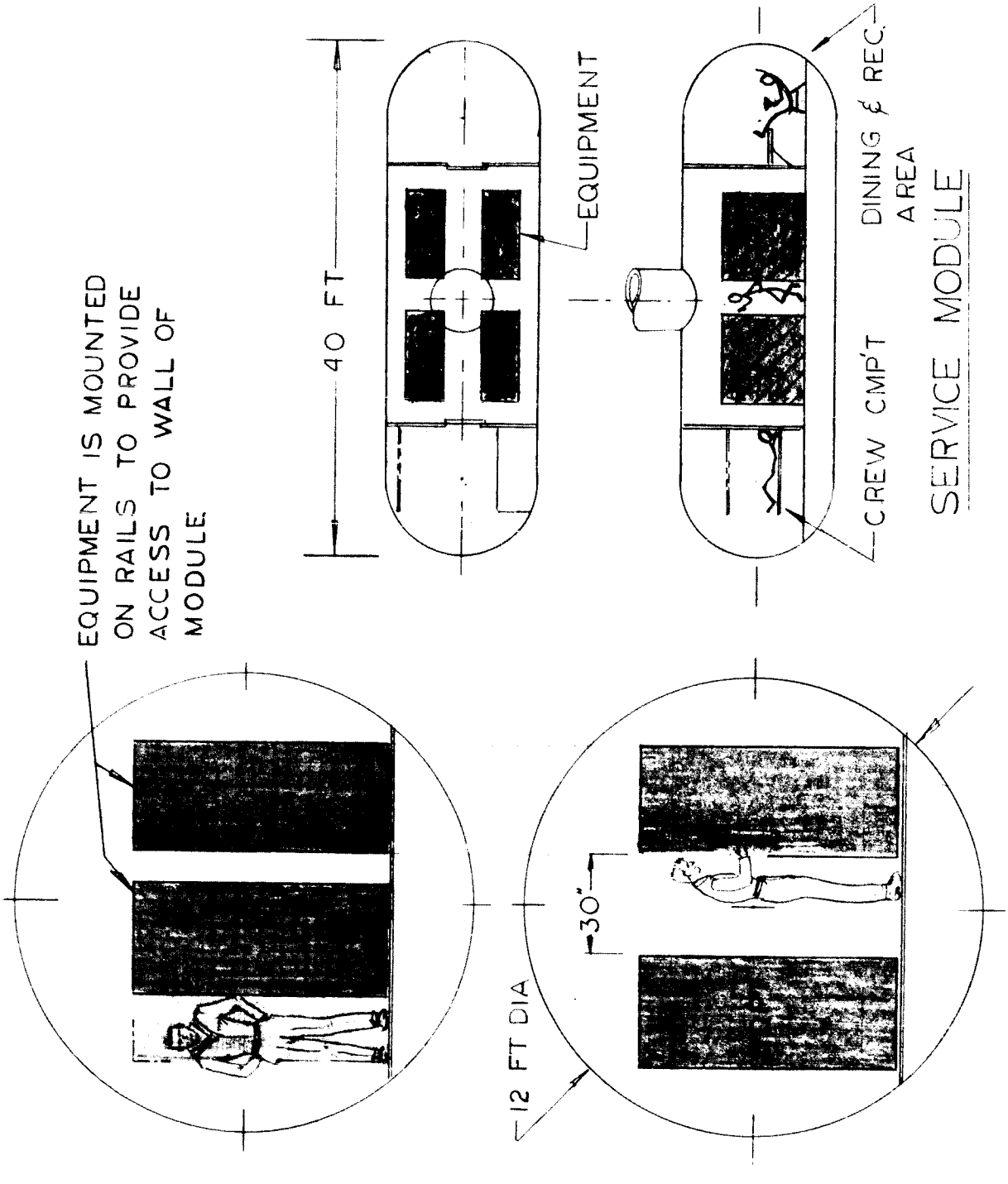


Fig. 9-5 Service Module

- Subsystems within the outer modules would have to function unattended in a zero-g field during this period
- Despinning requires time, during this period the crew might not be able to occupy the shelter

The shelter would normally have to be occupied for periods of from hours to perhaps a day or two, during events. Some events have lasted up to 3 or 4 days. In any case, zero-g occupancy of the shelter for these short periods should not adversely affect the crew.

The shelter is slab-sided and lies with its long axis 90 deg to the axis of rotation, within the hub. The crew has ample room within the shelter to wear spacesuits in case a sudden decompression should occur. An alternate provision to that of wearing spacesuits in the shelter is to build a pressure tight container around the shelter, within the hub. In this arrangement the crew would have enough room within the pressure vessel to don spacesuits if the hub structure were punctured while they were in the shelter.

Basic control and communications instrumentation is duplicated within the shelter for use during solar events. The crew can leave the shelter for short periods of time during the events without exceeding their allowable aggregate radiation dose.

A design study was made to integrate the food, water, and the life support equipment into a solar flare shelter within the service module. The available equipment and supplies provided only 37 gm/cm^2 protection at the sides of the shelter to which an additional 7.1 cm of aluminum was added bringing the total density up to the required 56 gm/cm^2. To complete this shelter a 20.3 cm aluminum plate was added on the top, bottom and at both ends. These plates overlap the equipment to maintain the required total density of the combined materials from every direction. For a 56 gm/cm^2 shield, 6,560 kg of aluminum is required in addition to the 2,040 kg of food, water, and equipment utilized as shielding as compared to 5,900 kg for the all-aluminum storm

cellar. If this composite shelter were placed within the service module the additional weight would almost double the weight of the service module and affect the balance of the rotating system.

In general, the shelter weight is dependent on 1) its volume and shape which determine its surface area, 2) on the density of the material used to enclose the shelter and 3) the effectiveness of the material as shielding (gram/cm^2). For attenuation of protons with minimum secondary production, low Z materials minimize shield mass per unit area. Hydrogen or materials with a large percent of hydrogen in their composition meet this requirement. However, because of the effect of shielded volume and shape on shielding surface area, the material should be as dense as possible, commensurate with effective shielding characteristics. This is because the denser the material, the more closely the centroid of its thickness approaches the minimum surface area of the shelter. For example, to provide a shield of 56 gm/cm^2, either 20.3 cm of aluminum, 53.3 cm of water or 61 cm of polyethylene may be used. These thicknesses placed over a 1.62 m diameter sphere would weigh 5,900 kg in aluminum, 7,940 kg in water, and 9,300 kg in polyethelyne. This indicates that the denser material, aluminum in this case, makes the lightest shelter.

9.3.6 Rotating Spacecraft Nuclear Power Supply

The rotating spacecraft (Fig. 9-6) has a nuclear reactor power supply mounted 80 ft (24.4 m) from the hub along the axis of rotation. The radiation shield is shaped to "shadow shield" the spacecraft, thus minimizing its weight. Radiation is limited to 5 rem/year in the modules, and the shield weight for this installation is 1088 kg. At launch, the reactor shield, radiators, and other components are stowed between modules. These are deployed in Earth orbit and secured to supporting structure which is able to sustain all Earth escape and midcourse accelerations.

The reactor and supporting structure could alternatively be mounted in the plane of rotation. This would displace the command module about 3.28 m from its present

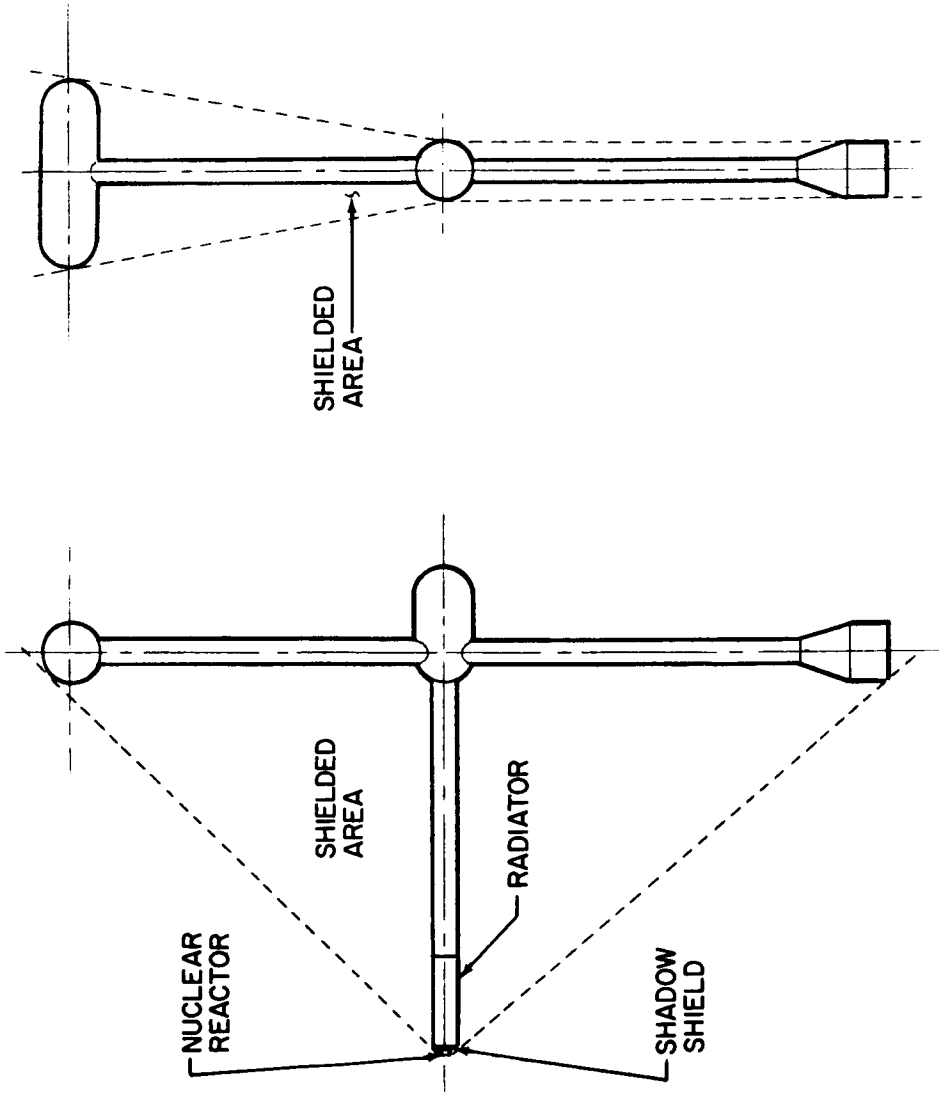


Fig. 9-6 Rotating Configuration Nuclear Power Supply

position, in the direction away from the reactor to maintain the center of rotation at the hub. The angle between the reactor and the service module would be 90 deg, the spin radius would remain at 25 m, and the crew would experience the same g-level in each module.

The rotational moment of inertia is increased in this arrangement and more propellant would be required for the spinup and despin operations. During the Earth escape and midcourse accelerations, the reactor support structure takes bending loads which suggests a supporting structure with some depth. At launch this support would be added externally to the other two external spokes. The shield weight would be about the same for both of these configurations.

9.4 ZERO-GRAVITY SPACECRAFT

Several zero-gravity spacecraft configurations were examined to determine the module arrangement and to establish weight saving possibilities. The primary difference here is in the internal arrangement of the service module. The lack of a gravitational field reduces the normal space a crewman needs for walking in the conventional upright manner. In a zero-g spacecraft the crewmen have the ability to move within the modules with the ease of a swimmer under water, and can orient themselves at any convenient position relative to the internal equipment. Bunks, tables, chairs and work stations do not require as much access and can be arranged in any number of positions within the modules irrespective of a common "floor." The long center aisle used in the g-configuration is changed into a center "tube" with the equipment surrounding it. Normal access is provided between the outer module wall and the equipment, as before. The resulting service module is shorter but larger in diameter than the g-module. Weight saving is realized in the elimination of spokes, hub, some inter-connecting structure and in reduction of midcourse propellant.

9.4.1 Zero-Gravity Configuration, Solar Power Supply

Two zero-g configurations are shown in Fig. 9-7. The crew is launched into orbit within the command module as before. In Earth orbit the command module with its

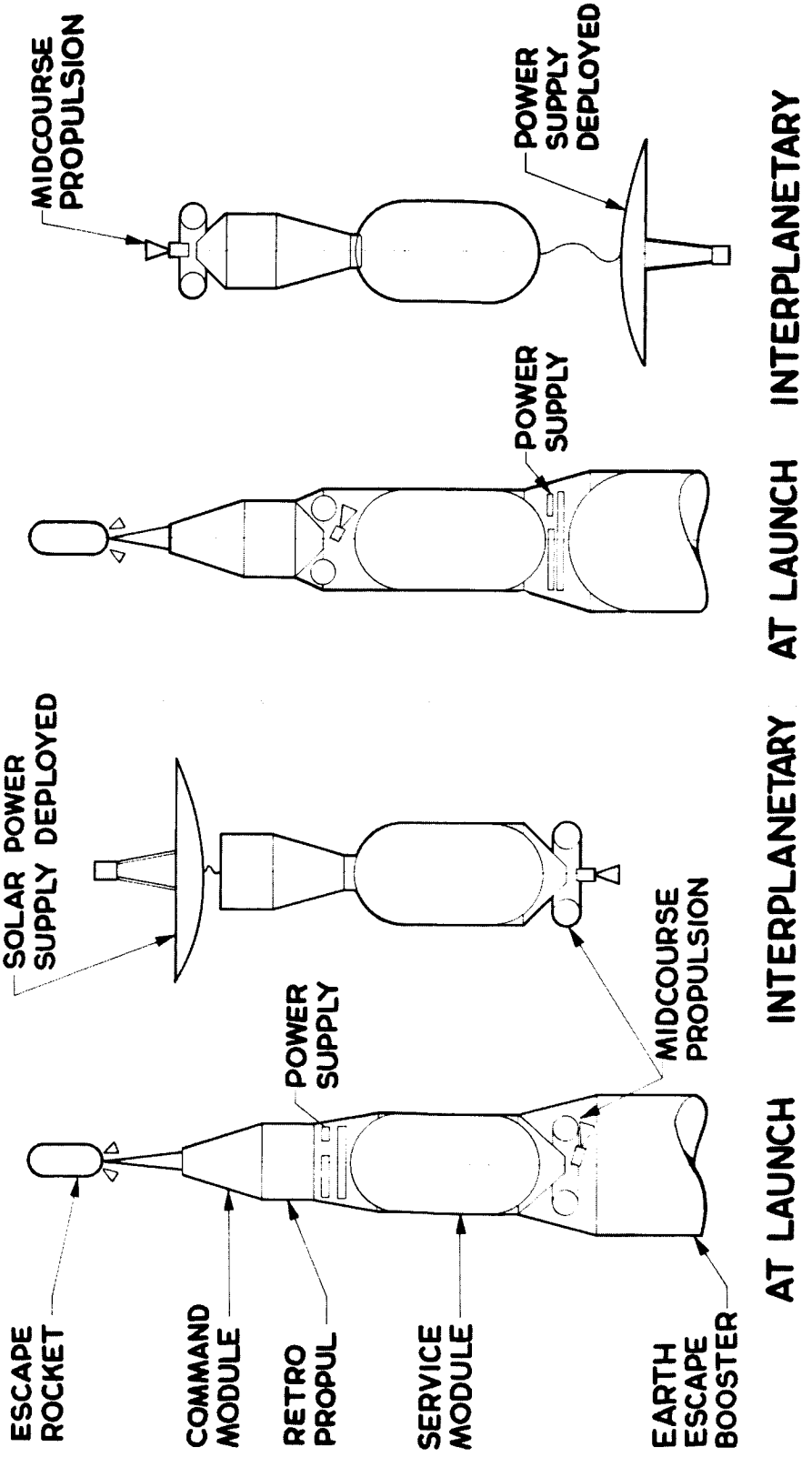


Fig. 9-7 Zero-G Configuration Solar Power Supply

attached unit of either the power supply or midcourse propulsion, is released from the service module, rotates 180 degrees and is secured to the service module. The crew now has direct access to this module which again contains all the life support equipment, crew's living quarters, and the solar flare shelter. Once the modules are secured, the solar power supply is deployed and oriented.

Two configurations are shown to illustrate the possible interchange of location of the power supply with the midcourse propulsion. There is no appreciable weight difference between these two configurations as the adapter weight and the lower interstage weight are similar. One disadvantage of the second configuration is that the Earth escape booster has to be jettisoned before the solar collector and power supply can be deployed, and this could only be accomplished after the craft has left Earth orbit.

9.4.2 Zero-Gravity Configuration, Nuclear Power Supply

In the configuration shown in Fig. 9-8 the nuclear power supply is mounted at the bottom of the propellant tank to take advantage of the tank length to keep the radiation dose to an acceptable minimum. In addition, all the plumbing and radiators are fixed in place on the booster, eliminating the need for erecting the power supply on orbit, thus reducing the possibility of leaks in the system. The shadow shield for this installation has to be large enough to shield the entire base of the empty tank, otherwise the radiation will be reflected and scattered forward into the crew compartment by the inside of the tank walls. The shield for this installation weighs about 4,400 lb (2,000 kg) but if the booster were replaced by a support structure of equal length the shield weight would be reduced to 1,350 lb (612 kg). The installation shown appears to be unacceptable from another standpoint if nuclear escape propulsion is used. The brief analysis made thus far indicates that the reactor of the nuclear stage booster would cause the multiplication of neutrons within the power supply reactor and raise its temperature to the melting point.

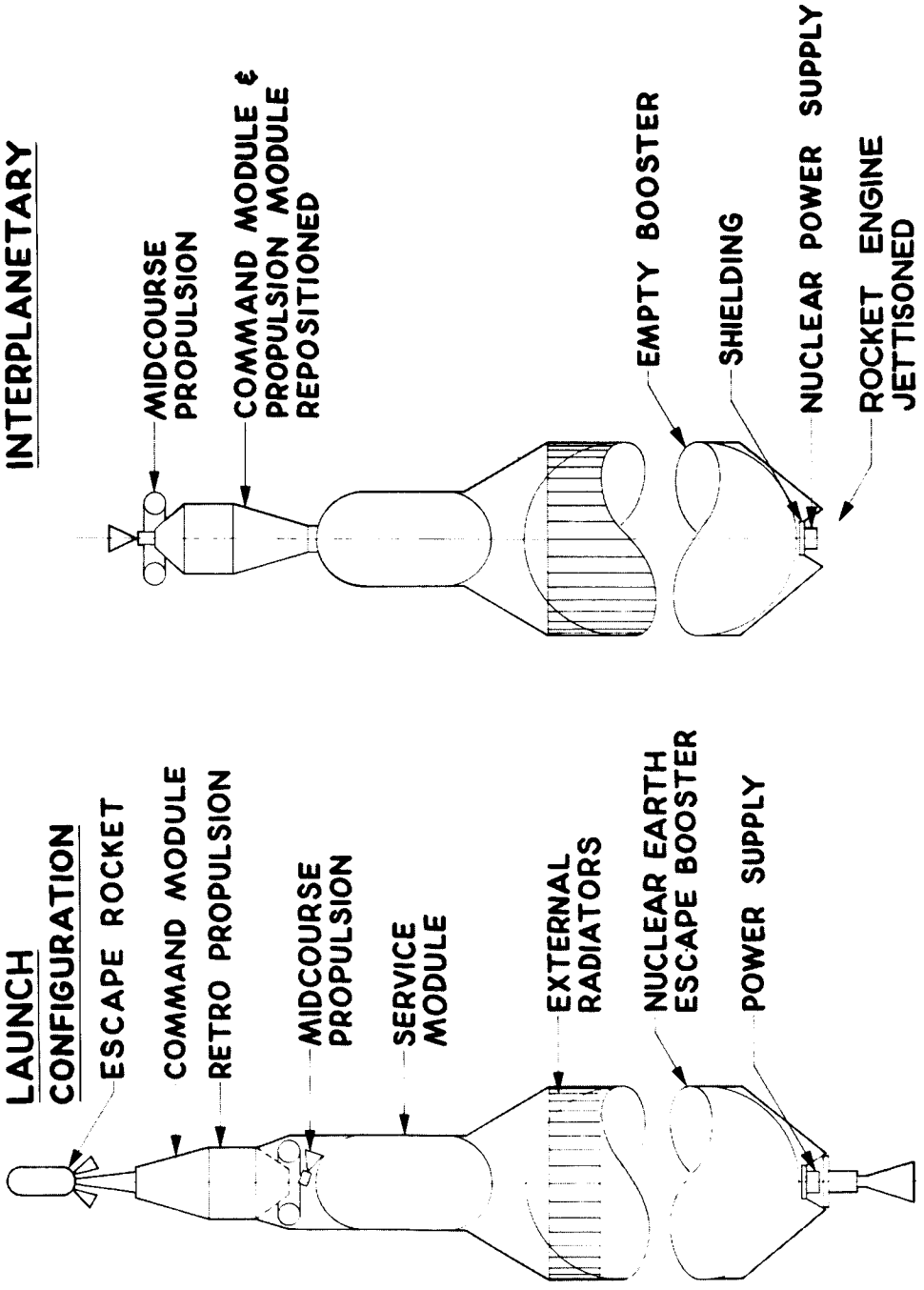


Fig. 9-8 Zero-G Configuration Nuclear Power Supply

9.5 SPACECRAFT WEIGHT SUMMARY

The weights for three spacecraft configurations are summarized in Table 9-1 for two general missions. The first column in each heading is for a 330-day Venus flyby, the second for a 600-day Mars flyby with the spacecraft assumed to be the same size for both missions. The weights listed are for the following configurations:

- Rotating configuration, solar power supply (Fig. 9-1)
- Zero-g configuration, solar power supply (Fig. 9-7)
- Zero-g configuration, nuclear power supply (Fig. 9-8)

There are several points to be noted in this weight summary. First, the weights of the life support system and the solar flare shelter vary significantly for the two missions but the sums of these subsystem weights are about equal. Next, the midcourse propulsion system weight varies depending on the total mass to be accelerated. For the zero-g nuclear power supply configuration the attached 13,600 kg inert injection booster has to be accelerated along with the spacecraft adding significantly to the midcourse propulsion weight. Finally, the total weight for any specific configuration does not vary more than about 2 percent between the two missions selected.

The weight difference of about 12 percent between the first two configurations represents the weight added for providing "gravity" in the spacecraft and is primarily due to the weight of the spokes, the hub, and the associated increase in midcourse propulsion.

9.6 STABILITY

The moments of inertia were calculated for the rotating spacecraft configuration based on general assumptions for distribution of mass within the modules. Dynamic studies indicate that a passive spin-stabilized spacecraft must be rotated about the axis of maximum moment of inertia. For the solar powered rotating configurations shown in Fig. 9-1, the moment of inertia about I_{zz}, the spin axis, is greater than the moment of inertia about the I_{yy} axis. The spacecraft is rotating about the axis of the maximum moment of inertia and satisfies the stability requirement.

Table 9-1

SPACECRAFT WEIGHT SUMMARY (KILOGRAMS)

	Rotating Configuration		Zero-g Configuration			
			Solar Power		Nuclear Power	
	♀	♂	♀	♂	♀	♂
Emergency Escape Rocket	4,535	4,535	4,535	4,535	4,535	4,535
Command Module	9,525	9,525	9,525	9,525	9,525	9,525
Service Module	2,950	2,950	2,270	2,720	2,270	2,720
Life Support	4,990	7,260	4,990	7,260	4,990	7,260
Power Supply	680	680	680	680	680	680
Hub and Spokes	3,630	3,630	–	–	–	–
Solar Flare Shelter	7,940	6,080	7,940	6,080	7,940	6,080
Midcourse Propulsion	7,875	8,010	7,210	7,300	9,840	9,980
Adapters and Fairings	1,725	1,730	1,790	1,880	1,810	1,905
Shield (Nuclear Power Supply)	–	–	–	–	2,220	2,220
Miscellaneous	1,360	1,360	1,135	1,135	1,135	1,135
TOTAL	45,210	45,760	40,075	41,115	44,945	46,040

♀ Venus flyby trip time, 330 days

♂ Mars flyby trip time, 600 days

The basic configuration can also be modified by replacing the solar-power supply with a nuclear reactor and placing this nuclear power supply with its shield in the plane of rotation. This arrangement would increase the moment of inertia about the spin axis and result in a more stable configuration with more pronounced differences between the moments of inertia about the three axes. In all of these configurations the moment of inertia about the I_{xx} axis is the smallest.

The change described above indicates a possible trend of modifications to the basic design concept for satisfying stability requirements.

9.7 REFERENCES TO SECTION 9

9-1. Sundstrand Aviation-Denver, a Division of Sundstrand Corp., Cryhocycle "R" Space Power Generation and Thermal Control Systems Demonstration, presented at Denver, Colorado, Apr 1962

9-2. C. C. Clark and J. D. Hardy, "Gravity Problems in Manned Space Stations," in the Proceedings of the Manned Space Stations Symposium, Institute of the Aeronautical Sciences, N. Y., N.Y.

9-3. A. Graybiel, et al., "Observation on Human Subjects Living in a 'Slow Rotation Room' for Periods of Two Days," A. M. A. Archives of Neurology, Vol 3, No. 55, 1960

9-4. B. J. Loret, "Optimization of Space Vehicle Design with Respect to Artificial Gravity," Aerospace Medical Association preprint, 9 Apr 1962

Section 10

DEVELOPMENT PLANNING

by

L. B. Stark

Section 10
DEVELOPMENT PLANNING

10.1 SUMMARY

The scope of the development planning activities was restricted to the consideration of early manned Venus flyby systems, utilizing a single Earth-launch mode of operation and considering no new launch vehicle technology beyond the Saturn C-5 program.

Planning objectives were centered on establishing development program requirements, preparing system development program plans, and identification of key development milestones and critical development problem areas.

The planning approach initially establishes basic premises and reviews factors in related national space programs that are applicable to the development programs for the selected early Venus flyby systems concepts. The significant aspects of related national space programs are discussed in detail for the categories including:

- Launch vehicles
- Spacecraft
- Support systems
- Facilities and logistics

Master development program plans were prepared in the form of integrated development schedules. Plans are presented and major features reviewed for early Venus flyby systems concepts utilizing an all-chemical propulsion, a single-launch mode, and one using a chemical launch vehicle with a nuclear upper stage based on an operational version of the basic NERVA nuclear rocket engine.

The program plans cover the interrelationship of major program areas, including launch vehicle requirements, spacecraft development, spaceborne subsystems, ground support and ground operating equipment, training and personnel, nuclear stage development, ground testing, and flight testing.

Major conclusions from the program planning viewpoint are presented in the form of key development milestones and their effects on program implementation. Comparative conclusions are presented on two alternatives involving the selection of operational nuclear-engine performance characteristics. Finally, significant effects of critical applied research and development problem areas are presented.

10.2 INTRODUCTION

The development planning task efforts during the first contract period were directed largely to the program requirements for manned Venus flyby systems utilizing all-chemical or chemical-and-NERVA technology nuclear vehicle propulsion systems.

Major objectives within the planning activities consisted of:

- Analysis and establishment of major development requirements
- Identification of critical development areas
- Preparation of integrated development program plans for two typical system concepts

A limited analysis was conducted to consider the relationship of advanced-nuclear-engine and advanced-launch vehicle systems to manned interplanetary missions systems concepts.

10.3 PLANNING PREMISES

The approach adopted in the development planning analysis was based on considerations relating the following major aspects of the interplanetary vehicle systems concepts:

- Premises defining propulsion and spacecraft technology
- Limitations due to selected mission requirements
- Related major national space programs

The final results in the form of development-program plans and assessment of key research and development requirements evolved from the integrated effects upon program planning of these major factors.

In conducting the planning analysis, the initial step consisted of the establishment of basic development planning premises. A separate group of premises were developed for each of the two systems concepts studied. These premise groups are discussed in the following sections.

10.3.1 Premises for Venus Flyby Chemical Propulsion

This system concept was based (for the purpose of generating a minimum development plan) on the utilization of a single launch to place the interplanetary spacecraft into Earth orbit and provide the capability for the escape stage to accomplish an early Venus flyby mission. All of the propulsion systems in the vehicle stages were assumed to be chemical systems, based on current technology and existing propulsion programs that do not require new research breakthroughs.

Summary of Major Premises

- Earliest operational capability consistent with utilization of current and firmly programmed launch vehicle, propulsion, and manned spacecraft technology
- Minimum-capacity spacecraft, with a crew size of three men and their requisite mission equipment
- Maximum utilization of current and approved programs technology, hardware, and facilities, encompassing the programs of: Saturn launch vehicles, lunar landing and Apollo spacecraft system, deep space instrumentation facility, integrated mission control center (NASA – Manned Spacecraft Center) and power systems development (SNAP programs and solar power systems)

- Accomplish the complete mission requirements with one launch (no rendezvous operations may be utilized). Mission requirements must be analysed more thoroughly before it can be determined whether even a Venus Flyby is possible with a single C-5 launch
- Spacecraft vehicle semi-automatically erectable in Earth orbit. It is mandatory that the crew supervise and exercise some manual control and assistance to ready the spacecraft for completion of the mission
- Overall requirements for providing the crew with solar flare shielding is provided by specific shielding material

10.3.2 Premises for Venus Flyby, Nuclear Upper Stage

The basis of this system concept is similar to that of the all-chemical propulsion system described in Section 2.1, in the study ground rule that requires this system to accomplish the mission with a single Earth launch, although the capability with a single C-5 launch is virtually assured. However, the major difference in this second concept is the requirement for a nuclear upper stage in the vehicle system, utilizing a nuclear engine based on NERVA nuclear propulsion system technology.

Summary of Major Premises

- The system must have the earliest operational capability, considering the combined requirements for launch vehicle, propulsion, manned spacecraft, and the operational qualification of the nuclear upper stage.
- Spacecraft capability for a crew of three, their requisite equipment and requirements for operating in the nuclear engine environmental conditions.
- Maximum utilization of current and approved programs technology, hardware, and facilities derived from the following programs: Saturn launch vehicles, lunar landing and Apollo spacecraft system, deep-space instrumentation facility, integrated mission control center (NASA – Manned Spacecraft Center) and power systems development (SNAP Programs and solar power systems)

- NERVA nuclear engine development will attain current RIFT Program objectives
- RIFT Program will complete flight testing in accordance with the current revised schedule (June 1969). This would result in a 7-year total span time for the overall Reactor-in-Flight-Test Program
- The nuclear upper stage for this early interplanetary vehicle system will evolve from the NERVA engine and RIFT vehicle technologies and program results
- The operational nuclear upper-stage development program will be initiated 4 years prior to the end of the RIFT program

10.4 RELATED NATIONAL SPACE PROGRAMS

In order to adequately define the major factors, which have been established to some extent by the planning premises that provide the basic elements for establishing development program plans, it is of major importance to designate specifically the areas of related national space programs that apply directly to the early manned interplanetary systems development.

These significant areas of national space programs can be most effectively related to manned interplanetary systems development by considering the following categories of systems and support activities.

Launch Vehicles. There are two programs in this category that would supply launch vehicles for the projected interplanetary systems development. The Saturn C-1B program would support early flight testing in Earth orbit of major elements for the interplanetary spacecraft. The Saturn C-5 program would provide launch vehicles for complete systems tests and the final flight testing phase involving simulated missions. In the case of the nuclear upper-stage system, Saturn C-5 also provides the launches for the stage operational capability qualification.

Spacecraft. The major contributing program is the Apollo spacecraft system. In particular, technology and design from the Apollo command and service modules will be applied to the interplanetary spacecraft command module development.

Launch Facilities. The basic facilities to provide launch center capability to all phases of the two development programs studied would be provided by the AMR Launch Complexes 37 and 39 derived from the overall Saturn Launch Vehicles Program. Requirements for modifications and time phasing into the interplanetary development programs will be indicated in the discussion of the development program plans.

Support Systems. The primary requirements for communications networks, ground telemetry installations, tracking, and data acquisition will be provided by the utilization of the deep space instrumentation facility and the global tracking network. It is considered that these capabilities will be available both from existing programs and the projected objectives of the Gemini, Apollo, and unmanned planetary probe programs.

Essential program requirements for a mission control center could be developed from the approved program for the integrated mission control center. The capabilities provided would cover central control displays, computer facilities, central communications, data handling, landing, and recovery control and basic simulation equipments.

Landing and Recovery Systems. The area and sites being developed to provide for the lunar program involving the landing of the Apollo command module would provide a basis for the requirements of the interplanetary mission. This is realistically based on the consideration that the reentry capsule for the two interplanetary systems studied consists of the command module of the integrated spacecraft. The derivation of this command module from the Apollo reentry module will provide basic compatibility with the usage of such landing facilities, with modifications considered in the development program plans.

10.5 MANNED INTERPLANETARY SYSTEM DEVELOPMENT PROGRAM PLANS

10.5.1 Program Plan – Early Venus Flyby – All-Chemical Propulsion

The master program plan for the development of a system for an early Venus Flyby based on all chemical propulsion systems is presented in Fig. 10-1.

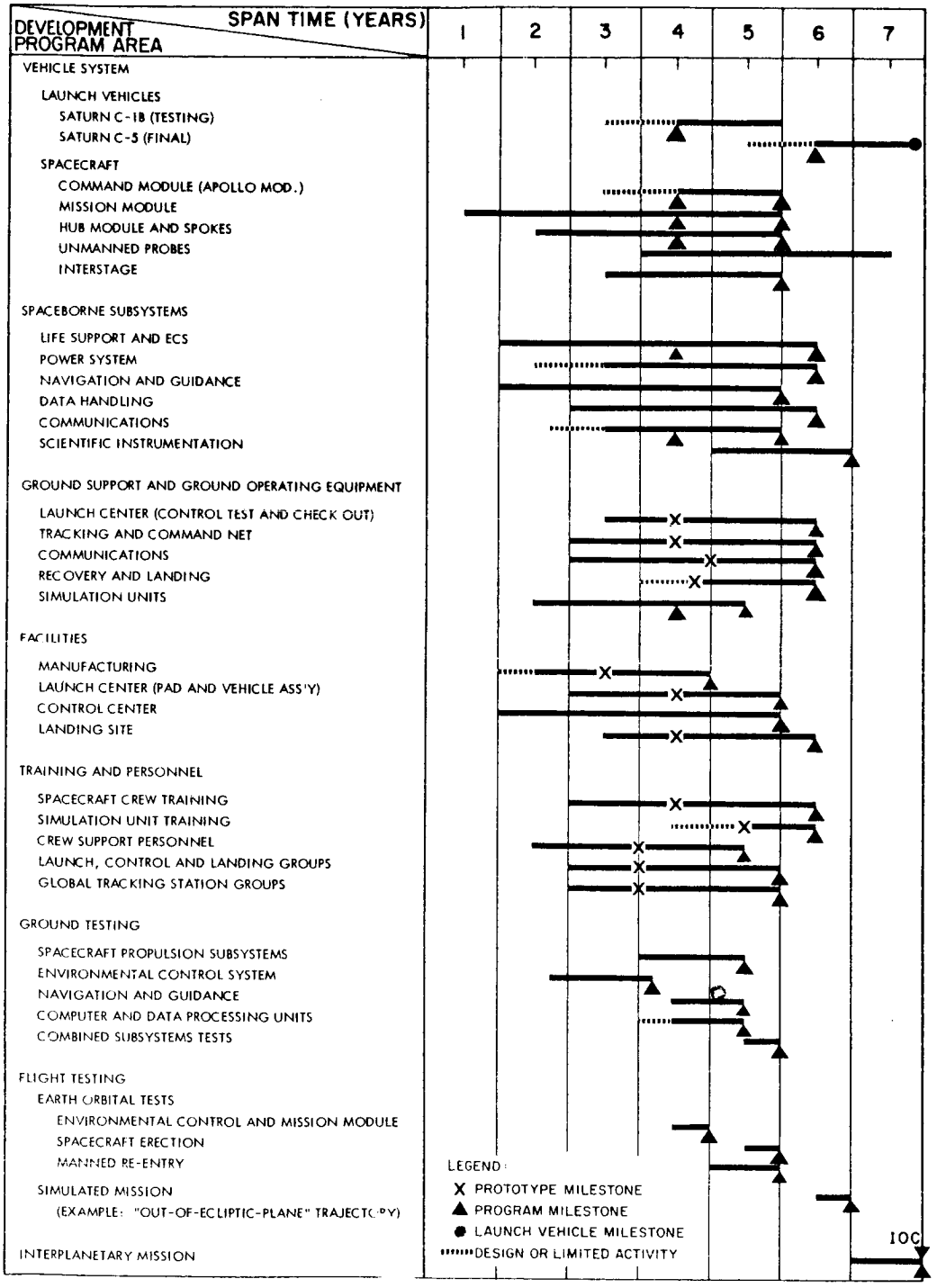


Fig. 10-1 Typical Early Venus Flyby – Single Launch Vehicle Development Program Plan

This development program plan was prepared by establishing the basic system development approach of qualifying the integrated system for operational capability by a flight test program with an initial phase accomplished by Earth orbital flight tests and a final phase of a simulated mission performed by a flight of six-month duration in a trajectory out of Earth's ecliptic plane.

The significant aspects of this plan can be most effectively presented by designating the key development areas and their related milestones.

Spacecraft Design and Development

- Command module – requires a 2-1/2 year span with completion up to final flight test 5 years after program start.
- Mission module – requires a 4-1/2 year span with completion up to final flight test 5 years after program start.

Spaceborne Subsystems Design, Development, and Testing

- Life support and environment control systems – require a 4-1/2 year span with completion 5-1/2 years after program start.
- Power system – one year preliminary requirements effort, 3-year span up to final flight test, with completion 5-1/2 years after program start.
- Navigation, guidance, and control – development up to final flight test required a 4-year span, with completion 5 years after program start.

Ground Support and Ground Operating Equipment

Basic requirements involve facilities additions and modifications and additions to existing equipment.

- Launch center – design and installation of changes in assembly launch control, checkout and systems test, and pad equipments. One-year span with completion for initial flight tests 4-1/2 years after program start. An additional two-year span with completion for final flight test 5-1/2 years after program start.

- Tracking and command net – design and installation of new and modified equipment at global tracking stations, mission control center, launch center and launch range stations. One and one-half year span with completion for initial flight tests 3-1/2 years after program start. An additional two-year span with completion for final flight test 5-1/2 years after program start.
- Landing and recovery – design, installation, preparation and operating tests involving equipment for utility services, local communications, and land and air transportation operating sites. One-year span with completion for initial flight tests 4 years after program start. A final span of 1-1/2 years with completion for final flight test 5-1/2 years after program start.

Facilities

These requirements include buildings, utilities, equipment for the functional needs and tooling for vehicle manufacturing and the launch center:

- Manufacturing for vehicles and subsystems – A span of 1-1/2 years with completion for initial ground testing 2-1/2 years after program start. Final readiness after an additional 1-1/2 years with completion 4 years after program start.
- Launch center – design and construction of modifications in and additions to assembly and control buildings and launch pads. One and one-half year span to completion for initial flight tests, 3-1/2 years after program start. A final span of 1-1/2 years for final flight test with completion 5 years after program start.

Ground Testing

This area involves the design and installation of special test equipment and the instrumentation and performance of the designated test categories.

- Spacecraft propulsion subsystems – static and vacuum firing tests of midcourse correction and attitude control units. One and one-half year span with completion for flight test installation 4-1/2 years after program start.

- Navigation and guidance subsystems – unit and combined equipment tests for qualification prior to combined subsystems testing. One-year span with completion for integration into final tests 4-1/2 years after program start.
- Combined subsystems tests – Final tests of fully integrated spacecraft subsystems for ground test qualification prior to final phase of the flight test program. Six-month span with completion 5 years after program start.

Flight Testing

The overall flight testing program is composed of two categories of tests, with three separate phases in the first group.

The first flight test category consists of Earth orbital tests, designed to qualify major elements of the interplanetary spacecraft. The separate steps in this group are:

Phase I: Prototype command and mission modules with Life Support and Environmental control subsystems (utilizes Saturn C-1B launches and a basic Apollo type reentry for return of the flight test crew).

Phase II: Spacecraft Erection – A command module and limited equipment mission module combined with hub module and spokes to verify spacecraft erection under mission Earth orbital conditions (a Saturn C-5 launch with the same Earth return as Phase I).

Phase III: Manned Reentry – The interplanetary spacecraft command module will be tested by three launches, with one un-manned and two manned flights. Provision of auxiliary propulsion will simulate the velocities and conditions encountered during actual mission Earth reentry and landing. (Saturn C-1B launches would be used.)

Phase I tests would be initiated 3-1/2 years after program start and completed in 6 months.

Phase II and III would be concurrently conducted during the fifth year of the program.

The second flight test category consists of a simulated mission, accomplished by launching a planned 6-month flight in a trajectory out of Earth's ecliptic plane. The system would be a complete duplication of an actual full scale mission, with the exception of limits on midcourse propulsion propellant quantity and would carry no unmanned probes. It would provide the potential option of a limited capability emergency abort propulsion system for the command module as a selective option of flight test planning.

This integrated development program plan would result in an initial operational capability for the system 7 years after program initiation. The final operational capability milestone is based on a normal funding and development schedule and assumes no major slippage of program milestones.

10.5.2 Program Plan for Venus Flyby, Nuclear Upper Stage

The master program plan for an early manned interplanetary system based on an all chemical propulsion, staged, Earth launch-to-orbit system, using a nuclear interplanetary injection stage, is shown in Fig. 10-2.

This development program plan was established based on an approach derived from two major considerations:

- The spacecraft design concept, spaceborne subsystems and Earth launch vehicle requirements are essentially the same as those in the single launch vehicle, all-chemical propulsion system discussed in Section 10.5.2. Facilities, support systems, and ground testing development requirements are expanded to accommodate the development requisites for the nuclear stage.
- The development of the nuclear stage, including operational nuclear engine development will be conducted concurrently with the spacecraft, subsystems, and support systems developments.

The major aspects of the development program are encompassed in the following program areas and key development milestones.

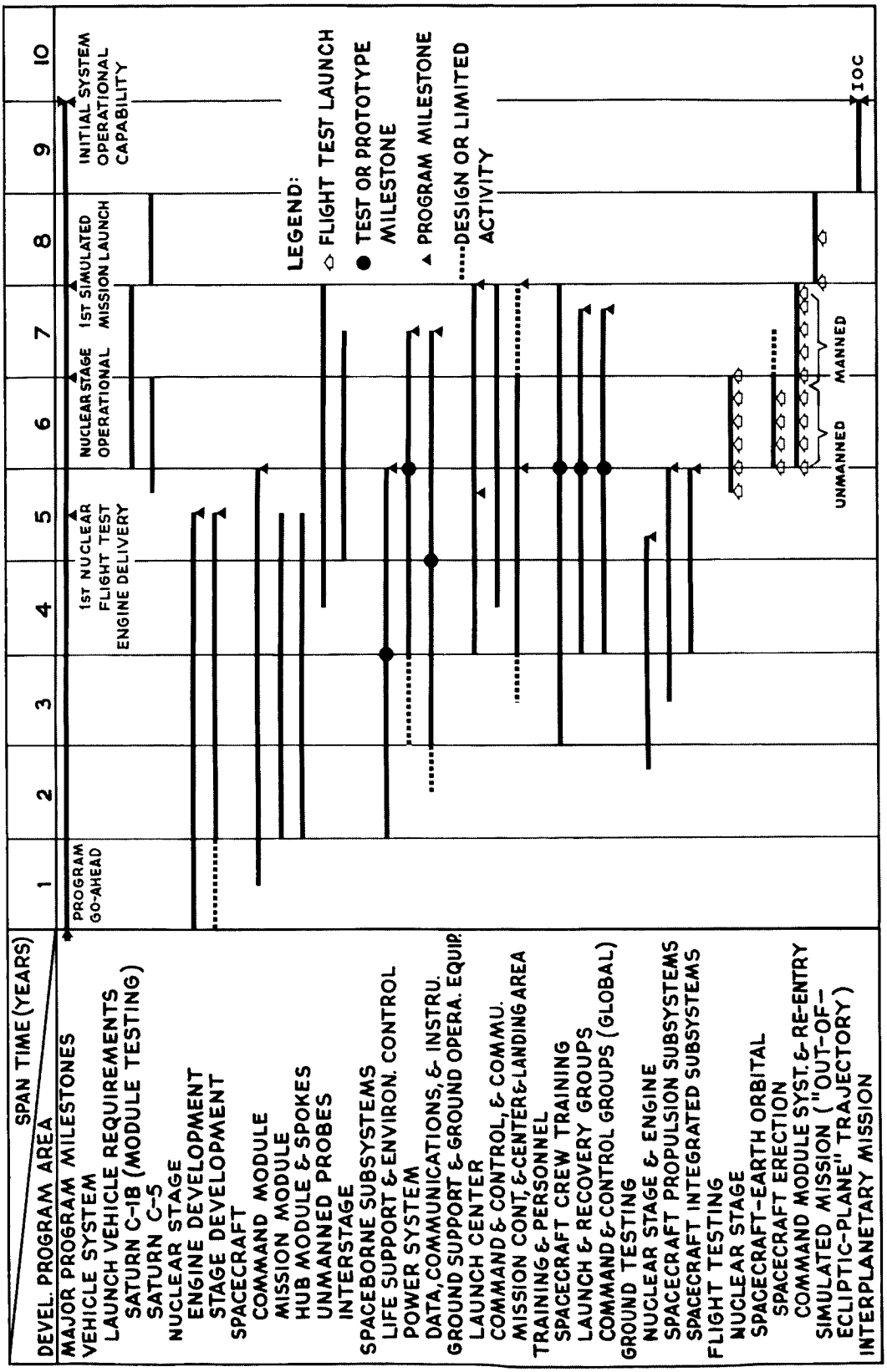


Fig. 10-2 Typical Venus Flyby – Nuclear Upper Stage System Development Program Plan

Group (A) Development Areas equivalent to those in the all-chemical propulsion system.

The program areas which have essentially the same development requirements and systems characteristics are:

- Spacecraft – development milestones range from 5 years after program start for the command module to 7 years for the unmanned probes.
- Spaceborne subsystems – completion of development ranges from 5 years for life support system to 6-1/2 years for data systems, after program start.
- Ground support and ground operating equipment – development milestones for completion up to final flight testing converge at 7 years after program start.

Group (B) Development Areas unique to the nuclear upper stage system

- Nuclear stage – with engine development starting at program go-ahead, completion up to delivery of the first flight test unit is required in 4-1/2 years.
- Ground testing program – engine and static test vehicle activities require a 2-1/2 year span with completion 4 years after program start.
- Launch center modifications – design and installation of safety and hazard control requirements, stage assembly area buildings and pad modifications. A 1-3/4 year span is required with readiness for delivery of first nuclear flight test stage 4-3/4 years after program start.

Group (C) System Flight Test Program

Phase I: Nuclear Stage Operational Qualification – A series of six Saturn C-5 launches into Earth orbit for nuclear engine re-start and engine burning time tests. The tests require 1-1/2 years and must be completed 6 years after program start.

Phase II: Spacecraft Earth Orbital Flight Qualification – A group of four flight tests for spacecraft erection and nine for crew modules and reentry tests are required (see Fig. 10-2 for time-phased schedule). The test flights are conducted concurrently in the sixth and seventh years of the program.

Phase III: Simulated Mission Flight Tests – These tests would be flown with systems duplicating an operational mission, with the exception of midcourse propulsion propellants being reduced and the elimination of unmanned probes. A planning option for limited capability abort propulsion on the command module could be considered in future hardware development planning.

Due to the limited prior history of the operational nuclear stage, two 6-month flight tests are programmed.

After completion of the foregoing developments, a period of one year was provided in the plan for design and equipment modifications evolving from flight test results and to provide for launch readiness of the first operational mission.

This course of development, based again on normal funding and scheduling, assuming no major slippages in key developments would provide a system initial operational capability 9 years after program initiation.

10.6 PROGRAM PLANNING CONCLUSIONS

The general conclusions derived from the development program planning are principally in the areas of critical system development requirements and areas that require additional analysis in future studies.

10.6.1 Major Development Aspects for Early Venus Flyby Systems

The most critical developments for the all-chemical system are the command module development, including completion of the manned reentry flight tests and the qualification of the spacecraft by the simulated mission flight test.

With respect to the nuclear upper stage engine system, the same critical requirements exist for the command module and simulated mission flight tests. In addition, the

ground testing of the operational nuclear engine and the completion of flight qualification tests of the nuclear stage are key pacing development milestones for the progress of the entire program.

10.6.2 Development of Operational Nuclear Engines

The selection of nuclear engine performance characteristics for the nuclear upper stage engine will have a critical effect on the projected time period of availability for this type of system. In Table 10-1, an overall summary is shown of program areas involved in the potential development of systems using two different types of nuclear engines, both derived from NERVA technology.

The single most significant factor revealed in this comparison is the projected availability of the higher powered nuclear engine approximately two years later than the lower powered engine. This estimate is based on current RIFT program projections of nuclear engine technology and the results of studies on Saturn D potential operational nuclear stages that were completed in the third quarter of 1962.

It should be emphasized that the time periods for the nuclear engine availabilities would have a direct influence on restricitng the type of mission available to the overall system.

10.6.3 Development Programs and Advanced Launch Vehicle Systems

In consideration of the time of availability restriction dependent on the type of nuclear engine selected, coupled with the Saturn C-5 launch vehicle, a major conclusion leading to increased system payload capability is noted. If it is desired to utilize an advanced launch vehicle capability for early manned missions prior to 1975, with or without nuclear upper stages, key decisions on the advanced launch vehicle program are required in the mid-1960's to identify and initiate development on long lead time applied to research and development.

Table 10-1

COMPARISON OF DEVELOPMENT PROGRAM REQUIREMENTS, INITIAL AND ADVANCED NUCLEAR ESCAPE STAGE SYSTEMS

Program Area / Types of Nuclear Stage	OPERATIONAL DEVELOPMENT OF EARLY NUCLEAR ENGINE	OPERATIONAL DEVELOPMENT ADVANCED NUCLEAR ENGINE
Spacecraft		
Command Module	Earth-Orbital Flight Test Program	Earth-Orbital Flight Test Program
Service Module	Life Support System & Power System	Life Support System, Auxiliary Power System, Shielding (for Nuclear Engine)
Reentry System Development Reauirements	Alternative A Design and Development of Retro-Propulsion; Ground Testing of Retro-Propulsion; Earth-Orbital Reentry Testing of Retro-Propulsion (with Command Module)	Alternative B Materials Development for Drag Brake; Structural and Thermal Ground Testing of Drag Brake Earth-Orbital Reentry testing of Drag Brake (with Manned Command Module)
Nuclear Stage		
Nuclear Engine Characteristics	Power Level: 1000−1500 Mw Life: 45 min to 1 hr	Power Level: 4000 Mw Life: 1 to 10 hr
Projected Engine Availability	1969 − 1970	1970 − 1972
Projected Stage Availability	1970 − 1972	1972 − 1974

A more detailed program planning analysis of this advanced launch vehicle aspect for early manned interplanetary systems is recommended as a key item in future studies.

10.6.4 Summary of Key System Research and Development Problem Areas

Although results in foregoing sections of this report have indicated some of the critical technical development problems, it would be well to emphasize in concluding the development planning discussion, that certain areas appear to be most critical, particularly from the standpoint of the reasonable successful progress of the programs presented in Figs. 10-1 and 10-2.

- Life Support System. Capability to qualify the command and mission modules in initial flight tests is wholly dependent on this area
- Environmental Control System. Capability to complete the Earth orbital flight test program is critically dependent on this area
- Navigation, Guidance, and Control. Initiation of the simulated mission flight testing is closely dependent on the earlier development milestones for these subsystems

Section 11

COST AND FUNDING SCHEDULE

by

S. M. Vuscovich

Section 11
COST AND FUNDING SCHEDULE

11.1 SUMMARY

A cost analysis of the Early Manned Interplanetary Mission concept has been conducted. Although this study was extremely cursory, it seems apparent that the cost will run between $1.4 and $1.9 billion (in 1962 dollars), depending upon the requirements for a nuclear upper stage. This cost is based on 10 interplanetary missions (5 to Venus and 5 to Mars) during the period 1970–1979. It must be emphasized that this estimate was developed from concept information only and design data required for a comprehensive cost analysis is unavailable at this time. However, it is expected that the estimates will be adequate for planning purposes.

11.2 ANALYSIS

Due to lack of definition numerous gross assumptions had to be made. It is anticipated that these assumptions will clarify most of the questions that may arise regarding the inclusions or exclusions of items in the estimate.

The assumptions are as follows:

General

- The manned space vehicle will weigh approximately 40 metric tons (88,000 pounds) including the command module which will be essentially an Apollo module
- The Apollo command module is developed and available for this program
- Two probes (Total Weight: 4.54 metric tons or 10,000 pounds) are required
- Mission requirements will be ten flights conducted during the calendar years 1970–79

- The Launch Vehicle will be either:
  - Three stage chemical Saturn C-5
  - Two stage chemical C-5 plus nuclear upper stage of 1500 – 4000 Mw power
- Facility requirements are limited to additional equipment and facilities peculiar to this program

Development

- Some of the systems development may be conducted in Earth orbital tests or on an existing space station in an Earth orbit. This will require launching of of equipment into orbit or to the station on Atlas type vehicles. Perhaps 10 flights would be made with life support, navigation, communication, etc. equipment aboard. The actual cost (if any) of conducting any experiments or tests (on a space station) is not included.
- Several flight tests of the drag brake will be conducted. This will entail flight of scale models by a solid fueled booster and accelerating the brake into the atmosphere to the required reentry speed of about 45,000 feet per second.
- No development cost of launch vehicles are to be included.
- Launch facilities may be used on a time sharing basis. Cost includes only special equipment or modifications required by the interplanetary mission payloads.
- Actual launch costs for the interplanetary missions are included.
- Development of the interplanetary vehicle will require the following:
  - Structure. Static and materials test and processing.
  - Electronics. Modify and package existing telemetering equipment.
  - Guidance equipment. Some guidance, navigation, and control equipment will require considerable development. Certain existing inertial and sensing components may be utilized but development will be necessary on computers, star field scanning, guidance and control for reentry, and for complete system integration.

- Communications and data handling equipment. Modify and package transreceivers, recorders, TV system, programmer, etc. Some development required due to the long distances involved.
- Life support and environmental control system. Although some components should be available, considerable development will be required.
- Power supply. Some components of either the solar array or the nuclear system will be available but considerable development to insure reliability will be required.
- Instrumentation. Modify and integrate sensors, monitors, pressure gauges, etc. from existing equipment.
- Mockups
- Non-flying prototype
- Simulators

The major items of cost associated with the above are:

- Design engineering
- Laboratory programs
- Systems test: component, subsystem and integrated systems
- Structural feasibility and materials analysis
- Static, dynamic, and environmental analysis
- Operational analysis and techniques
- Sub-contract coordination
- Program management
- Fabrication, assembly, installations and checkout
- Tool design, planning and manufacture
- Design, manufacture and checkout of test equipment
- Design and manufacture of ground handling equipment
- Manufacturing planning and production control
- Quality assurance
- Launch operations support
- Test requirements

- Data reduction
- Facility planning
- Applicable overhead

The development cost includes the first flyable vehicle.

Operational

- Modifications to the command module to satisfy the interplanetary mission requirements will be included.
- Initial investment includes "pay once" facilities and equipment required, such as assembly and checkout facilities peculiar to this program.
- Modifications to launch complex (umbilical, gantry, launch operations controls and electronics) completed on the development program may be used on the operational program.
- 20 flight crew members must be trained for a 5 year operational program.
- Launch facilities may be utilized on a time sharing basis. Cost will include only special equipment or modifications required for this program.
- Actual launch costs (assembly, checkout, fuel, pad refurbishment, range and tracking) are included.
- Cost of communications during missions will be shared.

The Major Items of Recurring Costs Include:

- Interplanetary vehicles (including 100% redundancy)
- Launch vehicles (including spares)
- Propellant
- Transportation
- Maintenance
- Range utilization
- Pad refurbishment
- Astronaut training
- Launch operations (personnel)

The launch vehicle estimate was derived from analysis of the schedule position on the learning curve during the year required by the interplanetary mission program. A 90 percent progress slope was assumed for all flight components.

No launch or vehicle reliabilities have been incorporated. However, spares amounting to 20 percent of the launch vehicles and 100 percent spares on the interplanetary vehicle have been included.

All costs are considered to be in 1962 dollars.

Lest it be inferred that the nuclear vehicle costs are substantially higher than the chemical launch vehicle costs, the following should be considered:

- The nuclear launch vehicle has a greater payload capability
- The chemical system will provide a marginal capability — it may not even be possible to carry any probes, or at best probes with a limited capability
- The Saturn chemical vehicle will be much further down the learning curve than the nuclear, resulting in a higher unit cost for the nuclear during the time period desired

In order to clarify the estimated cost of the NASA manned space flight program, the following data are supplied to put Apollo costs in better perspective for comparison with Empire cost estimates. The following information was derived from "NASA Authorization for Fiscal Year 1963, Hearings Before the Committee on Aeronautical and Space Sciences, U. S. Senate," June 1962, page 108.

Apollo Program:

1)	Budget request for 1963	$644 Million
2)	Total cost for Apollo Program including "capsule, service module and run out costs" for circumlunar and lunar flights	$1.5 Billion

Table 11-1

COST ESTIMATES FOR EARLY MANNED INTERPLANETARY MISSIONS CHEMICAL OR NUCLEAR UPPER STAGE

		Range (in millions)	
Development		$ 542	$ 560
Operating			
Initial Investment		50	60
Recurring		825	1293
	Total	$1417	$1913

Fiscal Year	Range (in millions)	
1964	$ 2	$ 2
5	12	12
6	36	36
7	81	100
8	148	169
9	160	190
70	122	200
1	115	190
2	110	170
3	105	155
4	102	140
5	97	126
6	91	115
7	86	106
8	76	100
9	64	90
80	8	10
1	1	1
2	1	1
Total	$1417	$1913

3) If facilities and launch vehicle costs are included the total increases to $2.5 Billion

Development costs of the propulsion systems (including those for Saturn and Nova, Gemini and Mercury) added to Apollo brings the total cost for successful lunar landing and return to: $15–20 Billion

It should be noted that the cost estimate of the interplanetary mission program ranges from 6.2 to 8.4 percent of the manned space flight program (using the $20 billion dollar estimate).

The budget request of 1963 for all manned space flight programs totals $2.26 billion. The estimate of yearly funds for the interplanetary missions program does not exceed 9 percent of this amount.